UNIVERSIDADE FEDERAL DO RIO GRANDE DO SUL
INSTITUTO DE GEOCIÊNCIAS
PROGRAMA DE PÓS-GRADUAÇÃO EM GEOCIÊNCIAS

CONTROLES DE PROVENIÊNCIA E QUALIDADE DE RESERVATÓRIO DA FORMAÇÃO BOTUCATU, CRETÁCEO DA BACIA DO PARANÁ

GABRIEL BERTOLINI

ORIENTADOR – Prof. Dr. Juliana Charão Marques
ORIENTADOR – Prof. Dr. Adrian John Hartley
CO-ORIENTADOR – Prof. Dr. José Carlos Frantz

Porto Alegre, 2020

UNIVERSIDADE FEDERAL DO RIO GRANDE DO SUL
INSTITUTO DE GEOCIÊNCIAS
PROGRAMA DE PÓS-GRADUAÇÃO EM GEOCIÊNCIAS

CONTROLES DE PROVENIÊNCIA E QUALIDADE DE RESERVATÓRIO DA FORMAÇÃO BOTUCATU, CRETÁCEO DA BACIA DO PARANÁ

GABRIEL BERTOLINI

ORIENTADOR – Profa. Dra. Juliana Charão Marques

ORIENTADOR – Prof. Dr. Adrian John Hartley

CO-ORIENTADOR – Prof. Dr. José Carlos Frantz

BANCA EXAMINADORA

Prof. Dr. Ernesto Luiz Correa Lavina - Universidade do Vale do Sinos

Prof. Dr. Marcus Vinicius Dorneles Remus - Universidade Federal do Rio Grande do Sul

Prof. Dr. Maximiliano Naipauer - Universidad de Buenos Aires

Tese de Doutorado apresentada como requisito parcial para a obtenção do Título de Doutor em Ciências.

Porto Alegre, 2020

CIP - Catalogação na Publicação

Bertolini, Gabriel
CONTROLES DE PROVENIÊNCIA E QUALIDADE DE RESERVATÓRIO DA FORMAÇÃO BOTUCATU, CRETÁCEO DA BACIA DO PARANÁ / Gabriel Bertolini. -- 2020.
256 f.
Orientadores: Juliana Charão Marques, Adrian John Hartley.

Coorientador: José Carlos Frantz.

Tese (Doutorado) -- Universidade Federal do Rio Grande do Sul, Instituto de Geociências, Programa de Pós-Graduação em Geociências, Porto Alegre, BR-RS, 2020.

1. Proveniência Sedimentar. 2. Qualidade de Reservatório. 3. Formação Botucatu. I. Charão Marques, Juliana, orient. II. Hartley, Adrian John, orient. III. Frantz, José Carlos, coorient. IV. Título.

Elaborada pelo Sistema de Geração Automática de Ficha Catalográfica da UFRGS com os dados fornecidos pelo(a) autor(a).

ÍNDICE

LISTA DE FIGURAS

LISTA DE TABELAS

RESUMO

Os depósitos vulcano-sedimentares do Cretáceo Inferior da Bacia do Paraná estão distribuídos ao longo de mais 1.000.000km^2, divididos entre Brasil, Argentina, Uruguai, Paraguai, Bolívia e Namíbia. Essa sucessão sedimentar é caracterizada por arenitos eólicos – com típica estratificação cruzada de grande porte – e derrames vulcânicos (básicos a ácidos), com estruturas variadas desde *pahoehoe*, *rubbly* e pacotes maciços. O *erg* Botucatu era caracterizado por um sistema saturado em areia ao longo de toda sua extensão, com uma regionalidade na direção predominante dos ventos, fruto do sistema climático monsonal atuante no mega-continente Gondwana. O repentino início do sistema vulcânico não desativou o colossal regime eólico, gerando uma série de pacotes eólicos preservados em períodos de quiescência vulcânica, denominados intratrap. A partir dessas premissas, a tese aborda, através de técnicas de proveniência e petrofísica, aspectos resultantes da interação entre os dois sistemas. O estudo *multiproxy* de proveniência (datação U-Pb em zircão detrítico, petrografia, minerais pesados e granulometria) visa a entender o preenchimento sedimentar do deserto, descrevendo tanto a variação pre- e sin- vulcânica (base e topo do deserto e intratraps) quanto a variação lateral do deserto. As áreas de estudo selecionadas se distribuem através de transectas ao longo das bordas Sul (Rio Grande do Sul e Uruguai), Nordeste (São Paulo e Minas Gerais) e noroeste (Mato Grosso e Mato Grosso do Sul) da bacia. O estudo de reservatório se propõe a entender os efeitos causados por rochas extrusivas em depósitos siliciclásticos síncronos, através de petrofísica e petrografia. Os atributos petrofísicos foram analisados ao longo de 5 testemunhos da região leste do Rio Grande do Sul e, posteriormente, foi realizada a caracterização diagenética dos intervalos afetados, através de estudo de petrografia. No que se refere ao estudo de proveniência, a composição dos arenitos eólicos apresenta variações sutis revelando uma associação entre os diversos embasamentos e as assinaturas de zircão detrítico. A região Sul, por exemplo, registra uma variação lateral na assinatura de zircão detrítico, apresentando um aumento na proporção de grãos >900Ma junto ao Uruguai, região com embasamento mais antigo (Rio de la Plata Craton). Ao norte da bacia, a assinatura da proveniência demonstra uma mudança da base do deserto para os depósitos *intratrap*. Entretanto, a predominante assinatura sedimentar policíclica, revelada pelo produto rico em quartzo e em minerais pesados resistatos (zircão,

turmalina e rutilo) indica que a própria Bacia do Paraná foi a fonte principal para o preenchimento do deserto. Além disso, respostas anômalas de minerais pesados foram encontradas isoladas, indicando inputs locais de sedimento. Para o estudo do impacto vulcânico nas propriedades de reservatório dos arenitos, os ensaios petrofísicos revelam uma diminuição na porosidade (16 a 5%) e um aumento da velocidade acústica (3000 para 5000 ms^{-1}) entre 0.1 e 1m do contato com os derrames de lava. Em detalhe, a análise petrográfica encontrou 2 caminhos digenéticos distintos formados em função da interação lava-sedimento: autigênese de fases ricas em Mg (Clorita e Dolomita) precoce relacionado ao sistema hidrotermal e dissolução química (microestilolitos em quartzo) precoce induzida por *overburden*. A limitada disseminação dos efeitos do sistema vulcânico (0.1 a 1m) nos arenitos pode auxiliar na compartimentalização do reservatório devido à redução de porosidade nas suas bordas, agindo como um selo. Em resumo, a tese apresenta os controles da proveniência sedimentar do deserto, demonstrando que: (1) o preenchimento sedimentar do *paleoerg* Botucatu foi predominantemente resultado do retrabalhamento da Bacia do Paraná; (2) variações anômalas de minerais pesados sugerem inputs sedimentares locais; (3) ainda que a sedimentação policíclica seja constante, variações laterais e estratigráficas ocorrem em ambas as margens. Adicionalmente, a tese destaca os efeitos de rochas extrusivas vulcânicas em reservatórios siliciclásticos, na qual se destacam: (1) porosidade e velocidade acústicas apresentam valores anômalos entre 0.1 e 1m do contato; (2) o processo digenético resultante da interação pode variar entre o domínio de sistemas hidrotermais ou soterramento precoce.

Palavras-chave: Proveniência Sedimentar; Formação Botucatu; Qualidade de Reservatório.

ABSTRACT

The volcano-sedimentary deposits from Early Cretaceous in Paraná Basin are distributed across more than 1,000,000 km^2, divided among Brazil, Argentina, Uruguay, Paraguay, Bolivia, and Namibia. The sedimentary succession is characterised by aeolian sandstones- with typical and widespread large-scale cross-bedding- and lava-flow packages (basic to acid compositions), with variable structures as pahoehoe, rubbly and massive flows. The Botucatu desert was a sand-saturated system across all its extension, with a regionality in the directions of the wind, due to the monsoon climate installed in Gondwana at the time. The sudden onset of the volcanic episode did not deactivate the overwhelm desertic system, generating a series of aeolian-packages preserved in volcanic quiescence period, denominated intratrap. Based on those premises, the thesis discusses the resulting in some aspects of the interaction of both systems, by using provenance and petrophysical techniques. The multiproxy provenance study (U-Pb dating in detrital zircons, petrography, heavy minerals and granulometry) seeks to understand the desert sedimentary filing, describing the sand composition variation from pre- to syn-vulcanic packages (from the base of desert to intratraps), as the lateral changes of the desert. The study areas are distributed in 3 transects in basin southern margin (Rio Grande do Sul state/Brazil and Uruguay) and NE and NW margins (Brazil central region). The reservoir study looks to the impact caused by the coeval volcanic system into the aeolian packages, utilising petrophysics and petrography. The petrophysical proprieties of volcano-sedimentary intervals from well-cores were analysed, with a posterior diagenetic characterisation on the affected intervals, via petrography. Regarding the provenance study, the sandstone composition presents subtle variations revealing a link with basement bounding sources and detrital zircons signatures. The southern region, for instance, registers a lateral change on detrital zircons spectra, presenting an increase of >900 Ma toward Uruguay, region with a predominant Orosirian-Rhyacian basement (Rio de la Plata Craton). On the other hand, the north margin registers a progressive shift in provenance from Botucatu base to intratrap deposits. However, the prevalent poly-cyclic sedimentary composition, revealed by the quartz-rich and resistates heavy minerals (zircon, tourmaline and rutile), indicates the Paraná Basin as the major source for the desert feeding. Besides, the isolated anomalous heavy mineral response suggests local sediment sources. Regarding the impact of the volcanic

activity into the sandstone reservoir proprieties, the petrophysical experiments show a decrease on porosity (av. 16 to 5%) and an increase of ultrasonic acoustic velocities (av. 3.0 to 5.0 kms^{-1}) from 0.1 to 1.0 m from lava-flows. In detail, the petrography found 2 distinct diagenetic pathways formed due to the lava-sediment interaction: early authigenic of Mg-rich phases – chlorite and dolomite- hydrothermally induced (type 1); and early chemical dissolution (quartz microstylolites) caused by lava overburden (type 2). The very local effect (up to 1 m), could act as a baffle to hydraulic circulation, working as a seal. In summary, the thesis presents the sedimentary controls of desert filing, demonstrating: (1) the grain-feeing of Botucatu paleoerg was predominantly resulted of Paraná Basin reworking; (2) the anomalous provenance compositions suggests local sedimentary inputs; (3) although the polycyclic sediment, lateral and upward stratigraphy occurs along the margins. Additionally, the thesis approaches the effects of extrusive volcanic rocks into a siliciclastic reservoir, founding that: (1) porosity and ultrasonic acoustic velocity present anomalous responses from 0.1 to 1m of lava contact; (2) diagenetic processes could vary from hydrothermal systems to lava overburden effects.

Palavras-chave: Sedimentary Provenance; Botucatu Formation; Reservoir quality.

AGRADECIMENTOS

Gostaria de agradecer a todos que me ajudaram durante os últimos anos. O doutorado foi, sem dúvida, a coisa mais difícil que fiz na minha vida e, por isso, sou incrivelmente grato.

Primeiramente, meu doutorado só pôde ser concluído devido ao apoio financeiro da Shell Brasil, através da legislação vigente de investimento em P&D via agência nacional do petróleo, gás natural e biocombustíveis (ANP) e do conselho nacional de pesquisas (CNPq) (bolsa numero 203786/2017-3), por meio do projeto “Sistemas Sedimentares BG05”. A tese foi construída em um esquema de dupla titulação entre a Universidade Federal do Rio Grande do Sul e Universidade de Aberdeen.

Em segundo lugar, agradeço aos orientadores Juliana Marques e Adrian Hartley pela supervisão. A Juliana, por me convidar para participar de um projeto tão fantástico e pela parceria para mais de 7.000 km de viagem de campo. Para Adrian, pelas revisões e ensinamentos. Aos meus coautores e aos funcionário e membros dos projetos de ambas universidades que ajudaram durante as viagens de campo, preparação de amostras e processos burocráticos, meus sinceros agradecimentos.

Por fim, sou muito grato a todos os meus amigos e colegas. Em particular a minha esposa e minha família por todo o apoio e amor. Um brinde a todos vocês!

CAPÍTULO 1 - INTRODUÇÃO

A interação entre sucessões sedimentares e vulcânicas em ambientes continentais tem sido amplamente documentada em bacias ao redor do mundo, desde Pré-Cambriano até a atualidade. Por exemplo, o carbonato-basáltico do Permiano no Grupo Zhesi (China), os depósitos fluviais de Mioceno do Columbia River (EUA), os sistemas de drenagem nos depósitos Devonianos do *Old Red Sandstones* (Hole et al., 2013; Ebinghaus et al., 2014; Chen et al., 2016;). Do ponto de vista de processos sedimentares, o início da atividade vulcânica pode desencadear modificações nos sistemas sedimentares associados. Por exemplo, o regime de drenagem relacionado à província ígnea Columbia River foi afetado por alterações topográficas geradas pela atividade vulcânica (Ebinghaus et al., 2014).

Adicionalmente, sucessões vulcano-sedimentares podem produzir targets econômicos, como, por exemplo, os plays de hidrocarbonetos da bacia de Shetland-Faroé ou os depósitos de sulfetados paleozoicos do Cinturão Piritoso Ibérico (Boulter et al., 2004; Schofield e Jolley, 2013). Devido à descobertas recentes, a indústria de petróleo e gás tem demonstrado cada vez mais interesse por sucessões vulcano sedimentares (por exemplo, pacotes fluviais intrabasálticos na Bacia de Faroé-Shetland; aeolianitos e basaltos intercalados no depósito de gás de Kudu na costa da Namíbia) (Schofield e Jolley, 2013; Stanistreet e Stollhofen, 1999). O intervalo Cretáceo da Bacia do Paraná apresenta potencial de avançar no entendimento dos controles sedimentológicos e de qualidade dos reservatórios relacionados a pacotes intercalados siciliclásticos e basálticos. A Bacia do Paraná se estende pelo Sudoeste do paleocontinente Gondwana no que hoje são os seguintes países: Brasil, Uruguai, Argentina e Namíbia (Fig. 1). O intervalo Cretáceo consiste no mega deserto Botucatu (> 1,0 milhão de km^2) (Fig. 1), posteriormente recoberto pela província ígnea Paraná-Etendeka, formando a Formação Serra Geral (Fig. 6), “congelando” as formas de leito eólicas *in situ*.

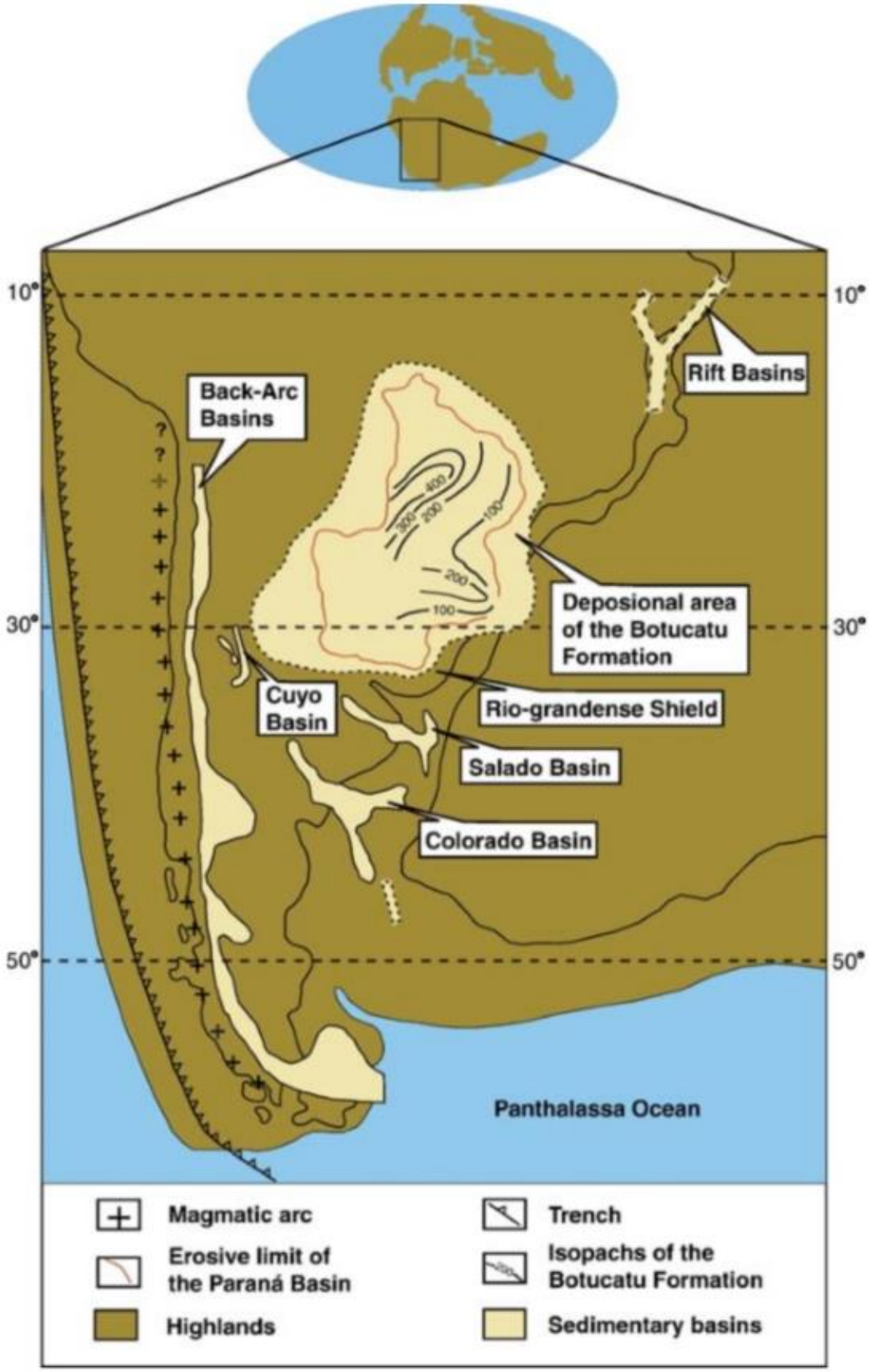

Figura 1 - Extensão do deserto de Botucatu no SO do paleocontinente Gondwana (extraído de Scherer e Goldberg, 2007).

Dentro do sistema Botucatu-Serra Geral, apesar da volumosa pilha vulcânica, o sistema eólico coexistiu com os derrames basálticos. Essa interação está amplamente evidenciada ao longo da bacia. Por exemplo, os pacotes eólicos “ensanduichados” entre os fluxos de lava, ilustrado, por exemplo, por marcas de fluxo dos derrames *pahoehoe* no dorso de dunas, que na época se encontravam inconsolidadas. A figura 2 mostra dois exemplos, nos municípios de Santo Antônio da Patrulha (RS) e Camapuã (MS), mais de mil km uns dos outros, ainda assim apresentando a mesma interação vulcano-sedimentar.

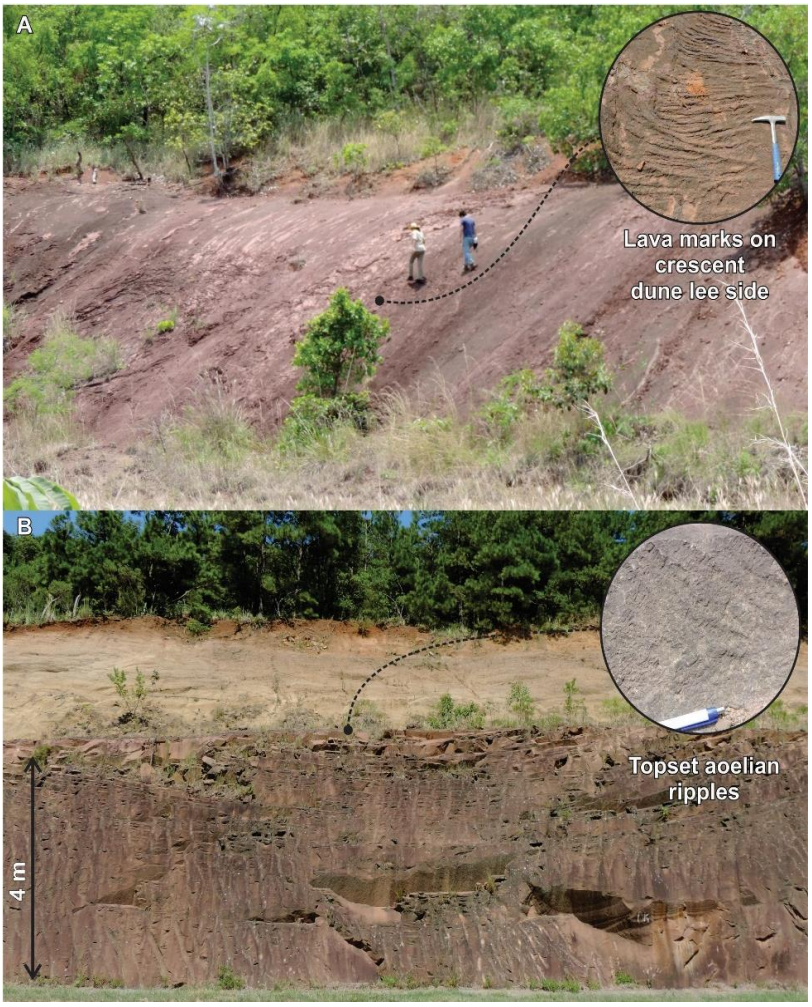

Figura 2 - Interações lava-sedimentos exibidas nas Formações Botucatu e Serra Geral. A imagem A mostra uma duna crescente *in situ* preservada pelo afogamento da forma de leito eólica pelo campo de lava, ilustrada pelas marcas de fluxo basáltico no arenito. A imagem B mostra a preservação de *wind ripples* no *topset* da duna recobertos de fluxos de lava *pahoehoe* compostos.

Além das questões relativas à sucessão vulcano-sedimentar, a dinâmica de preenchimento sedimentar no deserto do Botucatu também pode ser modificada por

processos basinais e desérticos. A composição da areia na Formação Botucatu se relaciona com aspectos como: reciclagem sedimentar dos intervalos pré-Cretáceos da Bacia do Paraná; possíveis variações nas fontes sedimentares controladas pelo embasamento complexo, bem como a variabilidade regional nas direções dos ventos (Fig. 1). A Formação Botucatu demonstra ser homogênea em toda a bacia, com pouca ou nenhuma variação de faciológica, sendo dominada por arenitos estratificados cruzados, formados por dunas e *draas* (Scherer, 2000; 2002). Dada a aparente uniformidade ao longo do deserto, faz-se necessária a aplicação de uma gama de técnicas diferentes para avaliar os papéis dos processos supracitados. A fim de estimar a influência do vulcanismo no suprimento e na composição de sedimentos e para verificar o potencial das diferentes áreas-fonte, foram utilizadas técnicas de proveniência *multiproxy*- datação U-Pb em zircão detrítico, análise de minerais pesados, análise petrográfica e análise granulométrica. Para entender o potencial de variabilidade lateral e estratigráfica na proveniência dos sedimentos, foram coletadas amostras ao longo das margens Sul e Norte da bacia, além dos intervalos pré e sin-vulcânicos (base e topo do deserto e arenitos *intratrap*).

Sob a ótica de reservatório, a Formação Botucatu Formação abriga uma das mais importantes fontes de água subterrânea da América do Sul- o Sistema Aquífero do Guarani- fato que ilustra a sua viabilidade como um análogo para reservatórios de petróleo e gás (Araújo et al., 1999). Portanto, os intervalos vulcano-sedimentares apresentam uma oportunidade de estudar a variabilidade diagenética e petrofísica gerada pelo vulcanismo síncrono a uma unidade siliciclástica. Caracterizar as propriedades físicas de rocha nos pacotes siliciclásticos através de experimentos petrofísicos e posterior identificação petrográfica dos processos digenéticos podem ser diretamente aplicados na compreensão e modelamento do efeito da atividade vulcânica nas propriedades de reservatório sedimentares.

1.1 Estrutura da tese

A tese está estruturada em 5 capítulos e 3 artigos científicos. A tese apresenta um capítulo introdutório (1. Introdução), um capítulo apresentando uma revisão bibliográfica dos temas abordados da tese (2.2 Estado da Arte), um capítulo descrevendo as técnicas aplicadas (3. Metodologia), um capítulo sintetizando e discutindo os resultados encontrados nos artigos (4. Resumo dos resultados) e, por

fim, um capítulo com as conclusões do trabalho (5. Conclusão). Os artigos científicos resultantes da pesquisa estão dispostos integralmente e com os pareceres de aceite ou submissão.

- Capítulo 1- Introdução
- Capítulo 2 - Estado da arte
- Capítulo 3 - Metodologia
- Capítulo 4 - Resumo dos resultados
- Capítulo 5 - Conclusões
- Artigo I (**Controls on Early Cretaceous desert sediment provenance in SW Gondwana, Botucatu Formation (Brazil and Uruguay**)
- Artigo II (**Provenance controls on Cretaceous aeolian sediment accumulation in Western Gondwana**)
- Artigo III (**The effect of basaltic lava flows on the petrophysical properties and diagenesis of interbedded aeolian sandstones: an example from the Cretaceous Paraná Basin, Brazil**)

O capítulo de introdução sintetiza a lógica da tese e a caracterização da questão científica. Os objetivos gerais da tese e questões científicas norteadoras do trabalho são descritos em "*1.2 Objetivos*".

O capítulo 2 resume o quadro geológico da Bacia do Paraná e das Formações Botucatu e Serra Geral (*2.1. Contexto Geológico Simplificado*), compila exemplos de sistemas desérticos atuais para demonstrar como os controles sedimentares podem ser explicados por estudos de proveniência (*1.2 Controles de proveniência em sistema desértico*) e discute a importância dos efeitos das rochas vulcânicas em processos diagenéticos em arenito e no seu impacto ao reservatório (*1.3 Impacto diagenético e de reservatório de rochas ígneas em depósitos siliciclásticos*).

O capítulo 3 apresenta uma breve descrição das metodologias aplicadas na tese: análise granulométrica, petrografia, análise de minerais pesados, geocronologia U-Pb em zircão detrítico, ensaios de velocidades acústicas e porosidade. As técnicas de proveniência são aplicadas diretamente nos artigos I e II, enquanto as técnicas de petrofísica são usadas no artigo III. Os subcapítulos abordam cada técnica,

apresentando uma visão geral de técnicas, procedimentos de preparação e análise de amostras e tratamento estatístico.

O capítulo 4 reúne os resultados e a discussão dos estudos apresentados nos artigos (I, II e III), apresentando uma visão geral de como os resultados originais da tese se encaixam na literatura científica.

O capítulo 5 compara as descobertas dos artigos aos objetivos de pesquisa e às questões científicas e apresenta futuras oportunidades de pesquisa sobre o tema.

Os artigos I, II e III compilam, apresentam e discutem os resultados encontrados na tese, na forma de artigos científicos. Estes artigos seguem a estrutura clássica de publicações geológicas, a qual consiste em um resumo, introdução, contexto geológico, metodologia, resultados, discussão, conclusão e referências.

O artigo I (*Controls on Early Cretaceous desert sediment provenance in SW Gondwana, Botucatu Formation (Brazil and Uruguay*)) apresenta o primeiro conjunto de dados de procedência *multiproxy* da Bacia do Paraná, no intervalo eólico cretáceo. O artigo discute a modificação do enchimento sedimentar na margem sul de Botucatu, mostrando uma variação lateral do zircão detrítico, minerais pesados, petrografia e granulometria correlacionada com as unidades subjacentes da Bacia do Paraná. O artigo se encontra publicado na revista *Sedimentology* (doi:10.1111/sed.12715) (QUALIS A1).

O artigo II (*Provenance controls on Cretaceous aeolian sediment accumulation in Western Gondwana*) descreve os dados de proveniência da margem norte de Botucatu, demonstrando uma composição lateral relativamente similar de NE a NW - porém apresentando ligeira variabilidade detrítica do zircão detrítico ao longo da evolução do deserto. Ambas as regiões apresentam composições de minerais pesados anômalas, indicando a presença de fontes sedimentares locais ao longo da margem da bacia. O artigo, atualmente, encontra-se em revisão na revista *Sedimentary Geology* (QUALIS A2).

O artigo III (*The effect of basaltic lava flows on the petrophysical properties and diagenesis of interbedded aeolian sandstones: an example from the Cretaceous Paraná Basin, Brazil*) investiga os efeitos vulcânicos em pacotes eólicos siliciclásticos intercamadados através de caracterização petrofísica e petrográfica. O estudo revela diminuição na porosidade e aumento na velocidade ultrassônica de 0,1 a 1 m para o contato com a lava, por devido a 2 tipos de alterações diagenéticas: (1) autigênese precoce de clorita e dolomita por processo hidrotermal e (2) compactação química em

grãos de quartzo por sobrecarga de lava. O artigo está atualmente submetido para a revista *Petroleum Geoscience* (QUALIS A2).

Os anexos I a VI compilam os dados das análises aplicadas na tese.

1.2 Objetivos

A tese tem dois objetivos gerais principais:

1. Compreender os controles de proveniência no deserto Cretáceo do Botucatu;

2. Determinar se, e como, as lavas básicas extrusivas afetaram a diagênese e propriedades dos reservatórios das unidades eólicas.

O primeiro objetivo aplica técnicas de proveniência para entender a composição sedimentar através da margem (variações laterais) e verticalmente através da estratigrafia (pré a sin-vulcânica). O objetivo pode ser respondido por três questões científicas diferentes:

1_A) O início do vulcanismo desencadeou mudanças ambientais que influenciaram a composição do sedimento?

O início repentino do vulcanismo da Formação Serra Geral pode causar mudanças ambientais na paleogeografia e paleotopografia dominantes no Cretáceo, levando a variações sedimentares no deserto do Botucatu. Para determinar isso, caracterizaremos a proveniência da Formação Botucatu da base ao topo do deserto e nos depósitos *intratraps* sobrejacentes.

1_B) O embasamento desempenha um papel importante no fornecimento de sedimento à bacia?

O deserto situava-se no coração do paleocontinente Gondwana, sobre uma infinidade de terrenos crustais, como: Cratons Amazônico e São Francisco (0,5 a 3,0 Ga) e faixas Brasília, Paraguai e Ribeira (500-800 Ma) na margem Norte, e Cratons do Rio da Plata (1,8-2,2 Ga) e Cinturão Dom Feliciano (500-900 Ma) na margem Sul. A bacia espalha-se sobre diversos terrenos geológicos diferentes, fato que poderia gerar viabilidade composicional dos sedimentos. Essas variações poderiam ser rastreadas usando assinaturas detríticas de zircão no *paleoerg*.

1C) O sistema de vento bimodal atuantes no deserto controlam composição dos sedimentos?

O deserto do Botucatu demonstra um domínio de vento bimodal, soprando na direção NE-E no Sul do *erg* e com uma direção de vento S-SE no Norte. A prevalência de terrenos antigos ao Norte, como o Craton da Amazônia (até 3,0 Ga), sugere a predominância de zircões antigos ao norte do deserto. Por outro lado, a região Sul é delimitada, principalmente, por cinturões Neoproterozóicos, que podem gerar populações de zircão detrítico distintas regionalmente, controladas pela direção dos ventos associados a variações no embasamento.

Os artigos I, "*Controls on Early Cretaceous desert sediment provenance in SW Gondwana, Botucatu Formation (Brazil and Uruguay)*", e II, "*Provenance controls on Cretaceous aeolian sediment accumulation in Western Gondwana*", apresentam os resultados e discussões dos dados, buscando responder às perguntas específicas apresentadas.

O segundo objetivo é investigar os impactos químicos e termais do vulcanismo na sucessão sedimentar. Esses intervalos foram caracterizados, aplicando ensaios petrofísicos e análises petrográficas, a fim de entender se, e como, as rochas extrusivas afetam a diagênese das unidades eólicas e se essas alterações modificam a qualidade dos reservatórios. Duas questões científicas orientam essa parte do estudo:

2A) Os pacotes basálticos produzem alterações diagenéticas através de autigênese ou compactação no arenito?

2B) A qualidade do reservatório da Formação Botucatu é afetada de alguma forma por possíveis alterações diagenéticas?

A seção "*2.3 Impacto diagenéticos e de reservatório de rochas ígneas em depósitos siliciclásticos*", mostra como a interação lava-sedimento pode levar ao desenvolvimento de um sistema hidrotermal ou levar a um aumento de compactação causada pelo *overburden* das lavas. Esses processos impactam diretamente a permeabilidade e a porosidade de uma rocha do reservatório, justificando o estudo.

O artigo III (*The effect of basaltic lava flows on the petrophysical properties and diagenesis of interbedded aeolian sandstones: an example from the Cretaceous Paraná Basin, Brazil*) aplica experimentos de velocidade acústica ultrassônica e porosidade e posterior caracterização petrográfica nos intervalos afetados. Foram

analisadas as alterações petrofísicas registradas próximas ao contato com a lava (1) e alterações diagenéticas responsáveis pelas alterações (2).

Em resumo, a tese procura responder a questões sedimentológicas e de qualidade de reservatórios relacionadas aos arenitos eólicos (Formação Botucatu) interacamadados com derrames de lava (Formação Serra Geral) do Período Cretáceo da Bacia do Paraná. O primeiro objetivo ("*Compreender os controles de proveniência no deserto Cretáceo do Botucatu*") examina a composição das areias do deserto. Os artigos I e II descrevem a análise de proveniência baseada em 3 transectas (margens Sul, Noroeste e Nordeste) examinando os arenitos pré-sin-vulcânicos, o efeito da regionalidade do regime de ventos e o efeito do embasamento na composição dos sedimentos. O segundo objetivo ("*Determinar se, e como, as lavas básicas extrusivas afetaram a diagênese e propriedades dos reservatórios das unidades eólicas*") aborda os processos diagenéticos e de qualidade reservatório a partir do contato lava-sedimento. O artigo III descreve a variabilidade petrofísica e petrográfica dentro da sucessão vulcano-sedimentar.

CAPÍTULO 2 - ESTADO DA ARTE

2.1 Contexto geológico simplificado

A tese aborda o Cretáceo Inferior da Bacia do Paraná na América do Sul - Brasil, Argentina, Uruguai, Paraguai e Bolívia. O intervalo apresenta duas unidades: os arenitos eólicos da Formação Botucatu e os basaltos continentais da Formação Serra Geral. A Bacia do Paraná é uma bacia intracratônica, registrando até 7 km de sedimentação do Ordoviciano ao Cretáceo. A bacia apresenta uma forma elipsoide alinhada em N-S, no centro-leste da América do Sul. As margens da bacia são controladas por uma elevação da crosta terrestre na margem leste e uma flexão litosférica a Oeste (Zannoto, 1993; Shiraiwa, 1994). O trabalho de Milani (1998) subdivide a bacia em 6 supersequências (no sentido de Vail, 1977): Rio Ivaí, Paraná, Gondwana I, Gondwana II, Gondwana III e Bauru (Fig. 3 e 4).

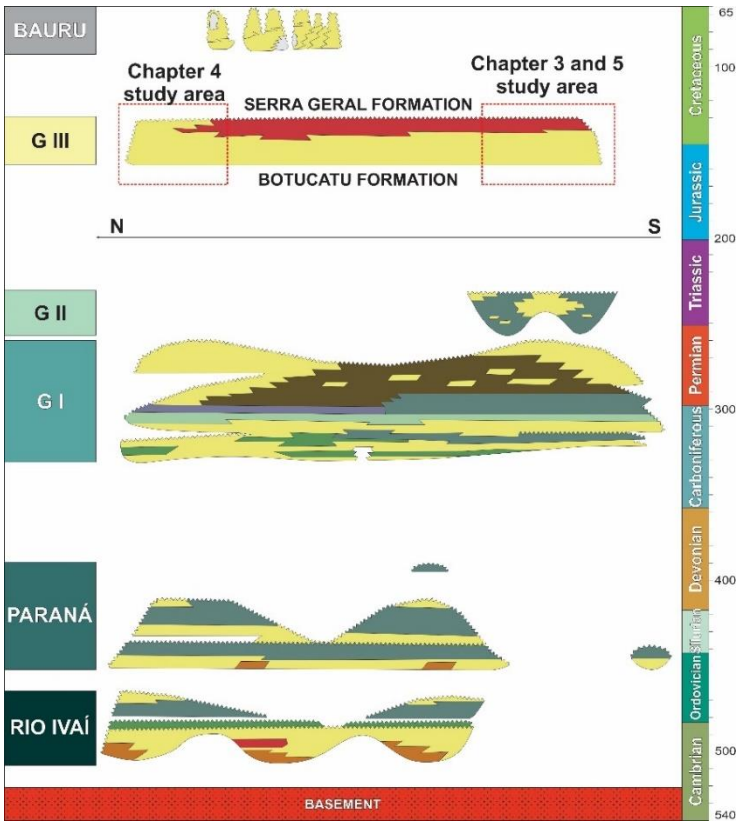

Figura 3 - Carta estratigráfica da Bacia do Paraná (Milani et al., 2007).

A supersequência de Rio Ivaí (Ordoviciano a Siluriano) inclui as formações Alto Garças, Iapó e Vila Maria (Assine et al., 1994), depositadas diretamente sobre o

embasamento. As unidades compreendem principalmente depósitos marinhos, com o primeiro ciclo transgressivo-regressivo na Bacia do Paraná. A supersequência Paraná (Devoniano) é dividida em duas unidades: os arenitos das Furnas e os pelitos das Formação Ponta Grossa. O período registra o segundo ciclo T-R na bacia, atingindo uma espessura máxima de 800m (Milani et al., 2007). A supersequência Gondwana I representa o intervalo mais espesso da bacia (até 2,5 km) durante o Carbonífero ao Triássico. As formações internas registram variações dramáticas sobre as condições climáticas, passando de pacotes glaciais carboníferos (Formação Itararé), sucessões de carvão no Permiano Inferior (Formações Rio Bonito e Palermo), ambientes marinhos regressivos no Permiano Médio a Superior (Irati, Serra Alta, Formações de Teresina e Rio do Rasto) até atingir o ambiente eólico no Triássico Inferior/Permiano (Formação Pirambóia) (França e Potter, 1998; Milani et al., 2007, Lavina, 1988). A supersequência Gondwana II (Triássico) ocorre localmente na parte Sul da bacia, relacionada a grábens distensivos. A unidade é caracterizada por argilitos lacustres e arenitos fluviais. A supersequência Gondwana III compreende os arenitos eólicos da Formação Botucatu e os vulcanitos bimodais da Formação Serra Geral. As unidades apresentam uma evolução parcialmente conjunta, evidenciada pelo interacamamento entre fluxos de lava e dunas eólicas, amplamente distribuídos pelo continente Gondwana. Por fim, a supersequência Bauru (Cretáceo Médio a Superior) é caracterizado por uma unidade suprabasáltica vulcano-sedimentar. O período foi tipificado por ambientes áridos e desérticos, sem continuidade em toda a bacia (Milani et al., 2007).

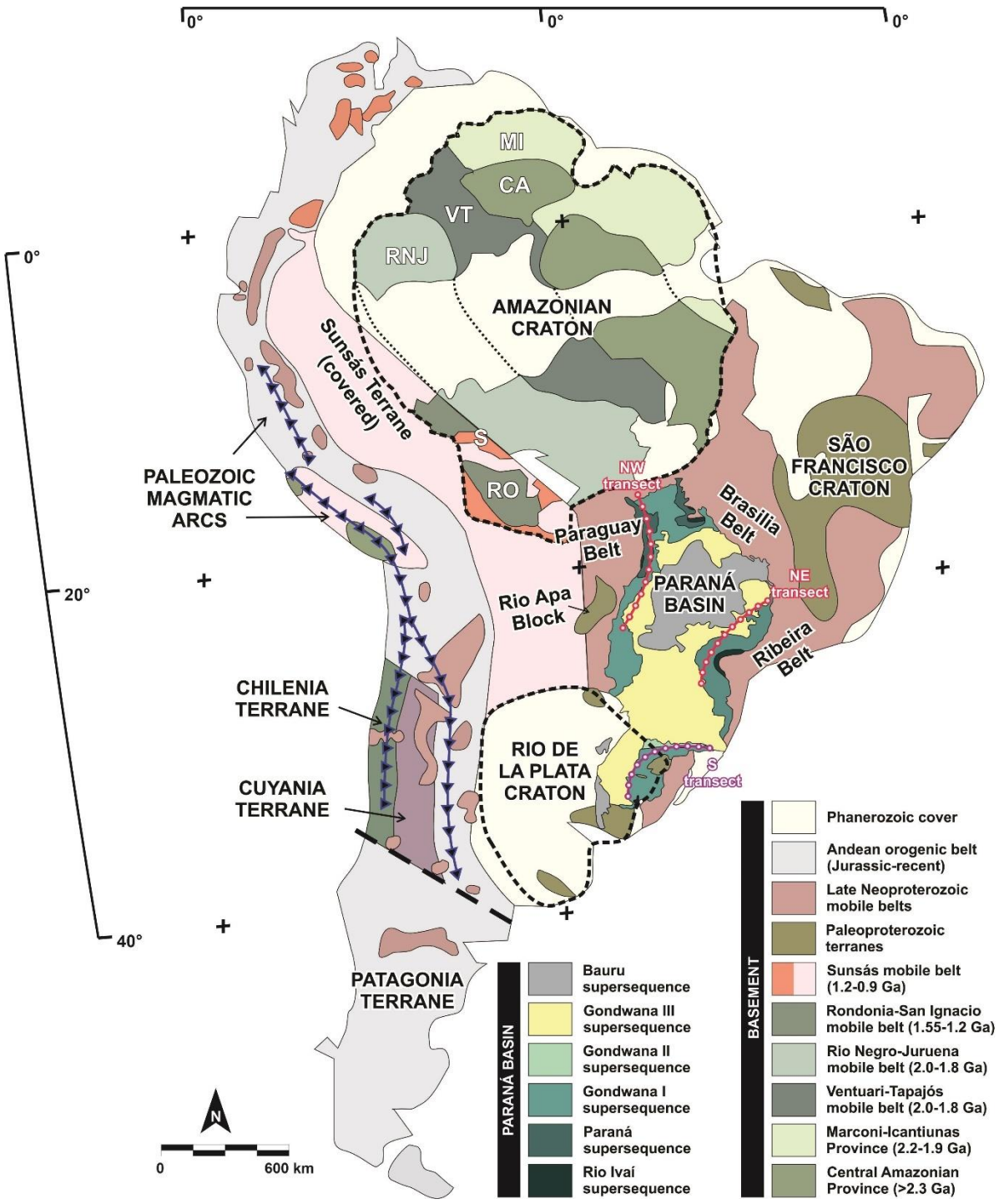

Figura 4 - Distribuição do embasamento e da Bacia do Paraná demonstrando as transectas estudadas (adaptado de Bahlburg et al., 2009).

A Formação Botucatu compreende pacote amalgamados de arenitos eólicos do início do Cretáceo da Bacia do Paraná. A unidade apresenta mais de 1.500.000 km^2 de campo de dunas contínuo (Almeida, 1954; Bigarella e Salamuni, 1961). A figura 4 mostra as áreas de exposição de Botucatu e os limites erosivos da bacia, porém depósitos associados também são descritos na Bolívia, no sul da Argentina e

na Namíbia (Scherer; Goldberg, 2007). A Formação Botucatu foi, primeiramente, descrita por Campos (1889), nomeada pelas colinas homônimas no estado de São Paulo, incluindo os pacotes Permianos da Formação Pirambóia. Posteriormente, em trabalhos das décadas de 50 e 60, Almeida (1954) e Bigarella (1967) identificam, formalmente, Botucatu como um gigantesco *erg* Jurássico-Cretáceo, mapeando as direções do vento no deserto desde o Mato Grosso até o Uruguai (Salamuni e Bigarrela, 1967). Schneider (1974) descreve a Formação Botucatu como arenitos eólicos bimodais avermelhados, finos a médios, bem arredondados.

A unidade apresenta uma espessura variável de 0 a 400, em média com 100m, atingindo 400m na região do Paraná (depocentro da bacia) (Scherer, 2000). Botucatu situa-se sobre um nível erosivo regional, em cima de diferentes unidades da Bacia do Paraná: Guará (Jurássico), Santa Maria (Triássico), Rio do Rasto (Permiano), Aquidauana (Permiano), Corumbataí (Permiano) e Furnas e Ponta Grossa (Devoniano) (Milani et al., 2007).

Scherer (2002) subdivide o registro sedimentar em 2 grupos: Unidade Genética Inferior e Unidades Genéticas Superiores. A Unidade Genética Inferior é composta por uma sequência espessa de arenitos com estratificação cruzada - formada por dunas crescentes e *draas* lineares. Localmente, também ocorrem rios efêmeros e lençóis de areia na base da unidade. A unidades genética superior está hospedada dentro dos fluxos de lava da Formação Serra Geral e são descritas como lentes finas (<3 m de espessura), interpretadas como lençóis de areia e lentes grossas (> 15 m), formadas por dunas crescentes. A Formação Botucatu não apresenta supersuperfícies, o que indica que todo registro sedimentar foi originado por um único *erg* (Scherer, 2000; 2002).

Bigarella e Salamuni (1961) apresentaram a primeira evidência de direção bimodal do vento no deserto, através da medição de milhares de paleocorrentes, mostrando a direção do vento para NE e E na margem sul e a direção do vento S-SE na margem norte. Scherer e Goldberg (2007) compararam a compilação de paleocorrentes com os padrões globais de circulação do vento no início do Cretáceo (Fig. 1), demonstrando que a regionalidade do vento era controlada por um clima de monção no supercontinente Gondwana. A zona de convergência intertropical (ITCZ) caiu cerca de 30o na direção ao Sul, justificando a existência de ventos alísios registrados no deserto Botucatu (Figura 4).

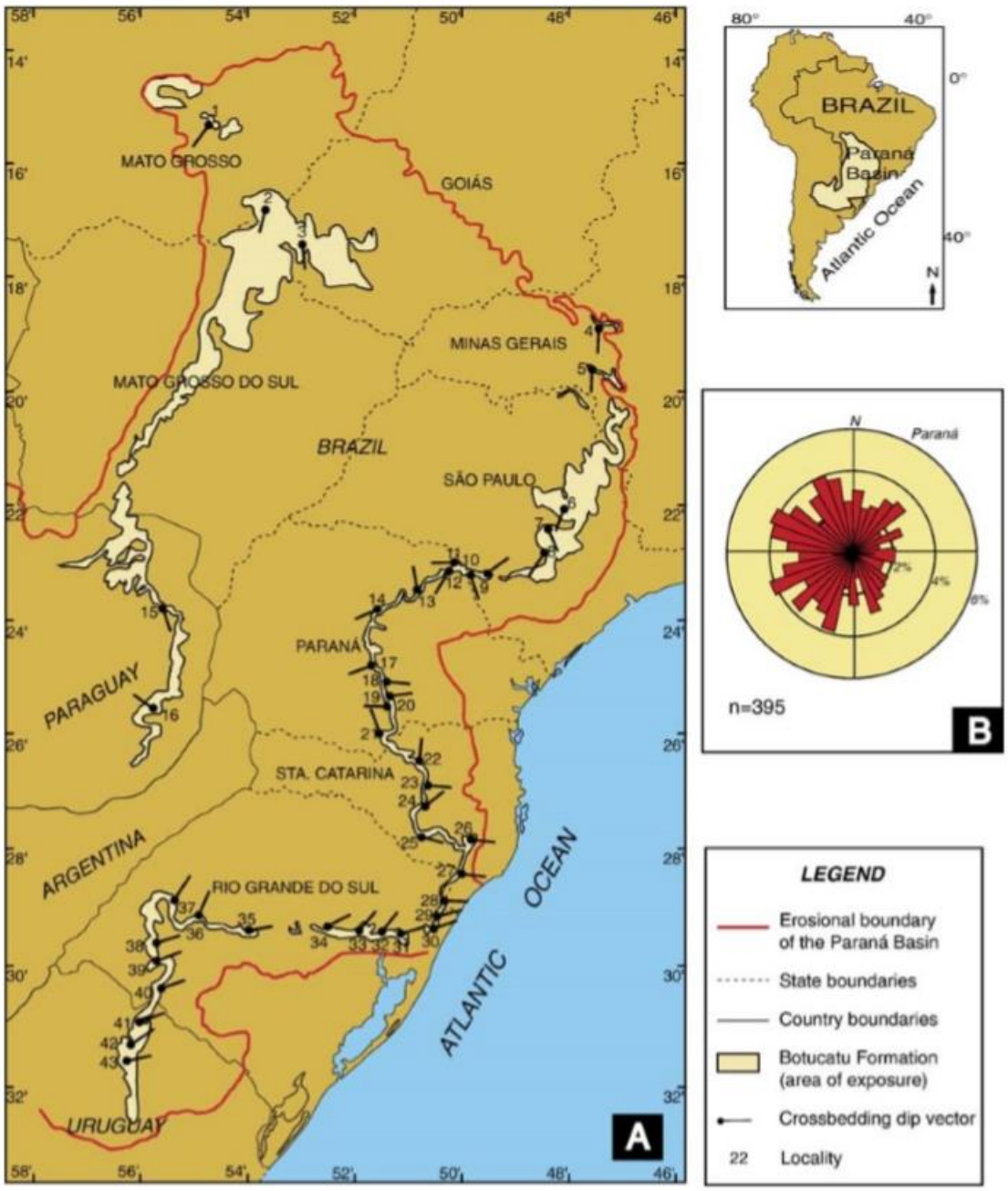

Figura 5 - Variação do paleovento ao longo da margem de Botucatu, mostrando direções de bento para NE-E e S-SO na região Norte (extraído de Scherer e Goldberg, 2007).

A Formação Serra Geral compreende os fluxos de lava subaéreos do Cretáceo Inferior na Bacia do Paraná. A unidade, juntamente com a unidade aos depósitos correspondentes do sudoeste africano - Etendeka lavas (Namíbia e Angola) - compõe a grande província ígnea do Paraná-Etendeka, um dos maiores episódios vulcânicos da Terra. A pilha vulcânica apresenta uma espessura média de 700m, chegando a 1750m no centro de distribuição da bacia (Piccirillo e Melfi, 1988), composta por basaltos, dacitos e riolitos. A idade do vulcanismo está restrita entre 135 e 131Ma (ver

Figura 6C), com estudos recentes com datação por U-Pb mostrando idades em torno de 134 Ma (Renne et al., 1992; Ernesto et al., 1999; Thiede e Vasconcelos, 2010; Pinto et al., 2011; Janasi et al., 2011). Os estudos de Peate (1992; 1997) apresenta uma classificação geoquímica formal para os tipos de lava, exibindo uma variação regional do teor de TiO_2, ilustrada na figura 6A. A região Sul apresenta os fluxos de lava mais antigos e é composta, principalmente, por unidades com baixo teor de TiO2: derrames básicos Gramado e Esmeralda e derrame ácido Palmas. Adicionalmente, ainda ocorre o tipo Urubici- alto teor de TiO2- de forma menos abundantes. Os vulcanitos do Norte são compostos, principalmente, por derrames básicos, com eventos ácidos locais. O tipo de magma de alto TiO_2 é subdividido nos tipos de magma Ribeira, Pitanga e Paranapanema.

As lavas extrusivas apresentam estilos de fluxo diferentes, conforme documentado recentemente por Waichel (2012), Barreto (2014) e Rossetti (2018), por exemplo: *pahoehoe* simples e composto, tipo *aa* brechado, fluxos de lixo para fluxos básicos e do tipo cúpula e fluxos tabulares para as rochas ácidas.

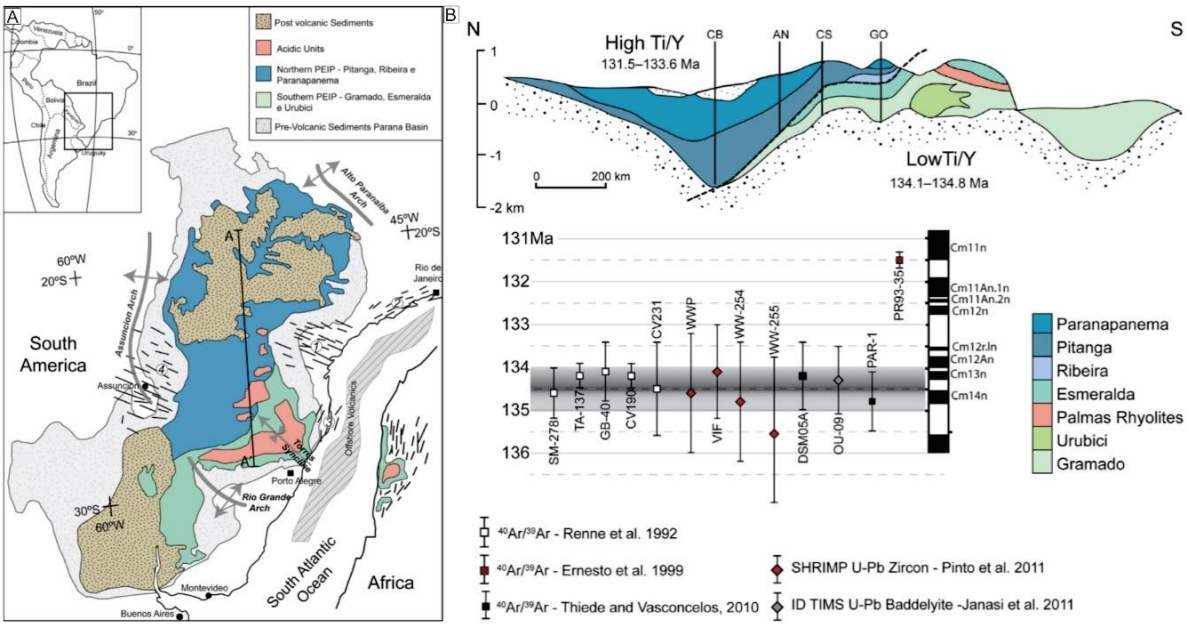

Figura 6 - A- Distribuição dos tipos de magma, enxames de diques e sedimentação pós-vulcânica na província ígnea Paraná-Etendeka (Formação Serra Geral na América do Sul e Etendeka no lado Africano); B- Estratigrafia vulcânica da Fm. Serra Geral mostrando a distribuição dos tipos de magma; C- Datações Ar/Ar e U-Pb encontrando idades entre 134-135 Ma para a unidade (Renne et al.,1992; Ernesto et al.,1999; Thiede e Vasconcelos, 2010; Pinto et al., 2011; Janasi et al., 2011).

2.2 Controles de proveniência em sistemas desérticos

Técnicas de proveniência têm se mostrado uma ferramenta poderosa no rastreamento de rotas de preenchimento sedimentar e *source-to-sink*. Eynatten e Dunkl (2012) definem como proveniência uma análise de fontes e processos aplicados a sedimentos pela caracterização desses produtos. O material detrítico é afetado pela litologia fonte, tectônica, climática e de transporte, resultando composições finais fruto desses processos. Técnicas como petrografia, análises geoquímicas e isotópicas são amplamente utilizadas nesse tipo de estudo. Análises de minerais pesados, tanto petrográficas quanto analíticas, são usadas extensivamente para estabelecer rochas-fonte, identificando rotas de sedimentos e avaliando alterações no transporte e na diagênese (Mange e Maurer, 1992). Para os possíveis efeitos de proveniência na dinâmica sedimentar e nos sistemas de alimentação de areia, apresentamos, a seguir, alguns exemplos de ambientes desérticos atuais: Deserto *Rub` al-Khali* (Saudita), *erg*s costeiros da costa da Namíbia e deserto *Taklamakan* (China). Esses sistemas desérticos aplicam técnicas de proveniência *multiproxy*, compostas por petrografia, análise de minerais pesados e geoquímica, zircão detrítico, para identificar a origem, rota e mistura de fontes de areia. Os estudos propõem soluções diferentes para o preenchimento sedimentar, aplicando proxies distintos.

O deserto de *Rub` al-Khali* é o maior deserto do mundo (mais de 650.000 km^2), localizado na Península Arábica. O *erg* apresenta indícios de reciclagem sedimentar massiva, registrando múltiplos ciclos de erosão e deposição dos sedimentos originados no Escudo da Arábia (Farrant et al., 2019, Garzanti et al., 2013 e 2016). Os estudos utilizam-se de razões de minerais pesados distintas - índice de rutilo-zircão ou Cr espinélio-zircão - geoquímica de concentrados minerais pesados e datação U-Pb de zircão detrítico para traçar as rotas sedimentares. Vários estudos revelam que a alimentação de Rub` al-Khali apresenta uma mistura de entradas fluviais, eólias e marinhas - ilustrada na figura 7 - apresentando o seguinte processo: (1) sedimentação das montanhas Zagros, realizada via Tigre-Eufrates com transporte marinho posterior pelo Golfo da Arábia e, finalmente, deflação eólica durante períodos marinhos *lowstand*; 2) transporte eólico pelos corredores das dunas *Dahna* e *Nafud*; (3) transporte fluvial quaternário e Miocênico das montanhas do escudo da Arábia e complexo ofiolítico *Hajar* (Farrant et al., 2019).

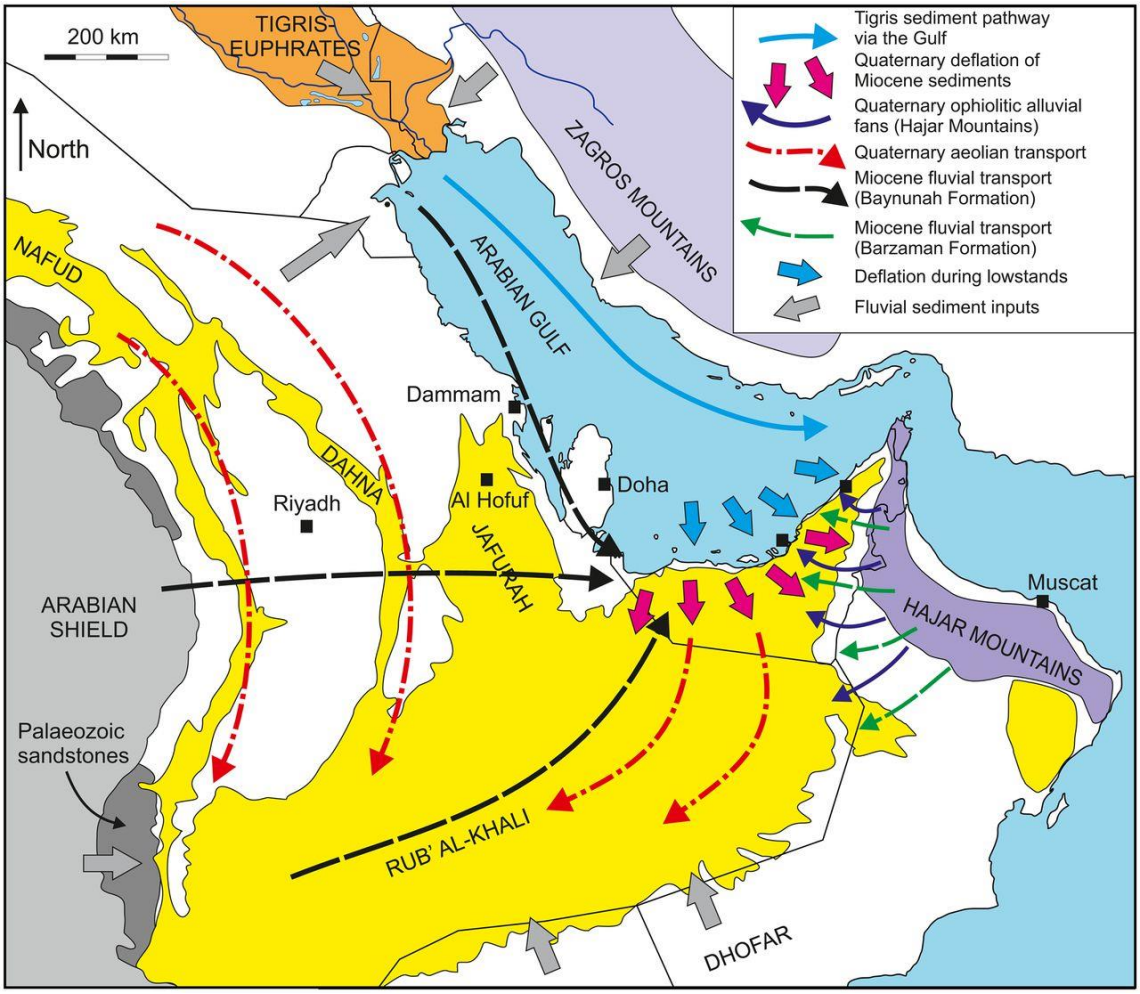

Figura 7 - Alimentação sedimentar complexa para o deserto Rub`al-Khali, registrando sedimentação proveniente do Rio Tigre-Eufrates (transporte fluvial, marítimo e finalmente por vento), deflação eólica (setas vermelhas) e transporte fluvio-eólico das montanhas do Escudo da Arábia e Hajar (extraído de Farrant et al., 2019).

O maior *erg* da China - o deserto de *Taklamakan* - está localizado na bacia de Tarim, com cerca de 15 km de espessura, em um ambiente geológico único, no sotavento da cadeia do Himalaia. O deserto inicia no Mioceno (Zheng et al., 2015), configurando a principal fonte de loess para o continente asiático. O *erg Taklamakan* apresenta altitude >1000m, delimitada pelas montanhas *Kunlun* e *Altun Shan* (Sul), *Tian Shan* (Norte) e *Pamir* (Oeste). A região apresenta sistemas de transporte diametrais: eólico (nordeste a sul) e fluvial (seguindo a topografia semicircular). Rittner (2016) aplica um estudo de procedência *multiproxy* na área, mostrando os *inputs* fluviais das montanhas a sudoeste (*Kunlun Shan* e *Pamirs* - Figura 8). O estudo utilizou ferramentas estatísticas de coordenação para identificar a prevalência de rios como sistema principal de distribuição de areia, com posterior retrabalho do vento.

As regiões costeiras do leste da África (Namib, baia Skeleton e Moçamedes) apresentam uma configuração climática hiperárida, ativa desde o Mioceno. Os desertos estão localizados sobre os orógenos dissecados Paleo- Neoproterozóicos (Namaqua e Damara) e sucessões sedimentares Cambrianas a Cretáceas que cobrem parcialmente o embasamento Precambriano. Estudos de proveniência (Vermeesch et al., 2013; Garzanti et al., 2015; Resentini et al., 2018) mostram que a ausência de intemperismo químico e drenagem fluvial eficaz em áreas do interior resulta em uma baixa contribuição de material continental para sedimentação do deserto. Os estudos demonstram que a alimentação sedimentar no deserto é um produto de um transporte de correntes costeiras originário da foz do rio Orange na Baía de Walvis (Fig. 8). Augita e pigeonita são trazidas pelo Rio Orange (extraído do intervalo vulcânico da Bacia do Karoo no Lesoto) e dispersadas na Costa da Namíbia. Os piroxênios encontrados no deserto apresentam assinatura compatível com as lavas do Karoo, excluindo fontes mais próximas do deserto (Garzanti et al., 2018).

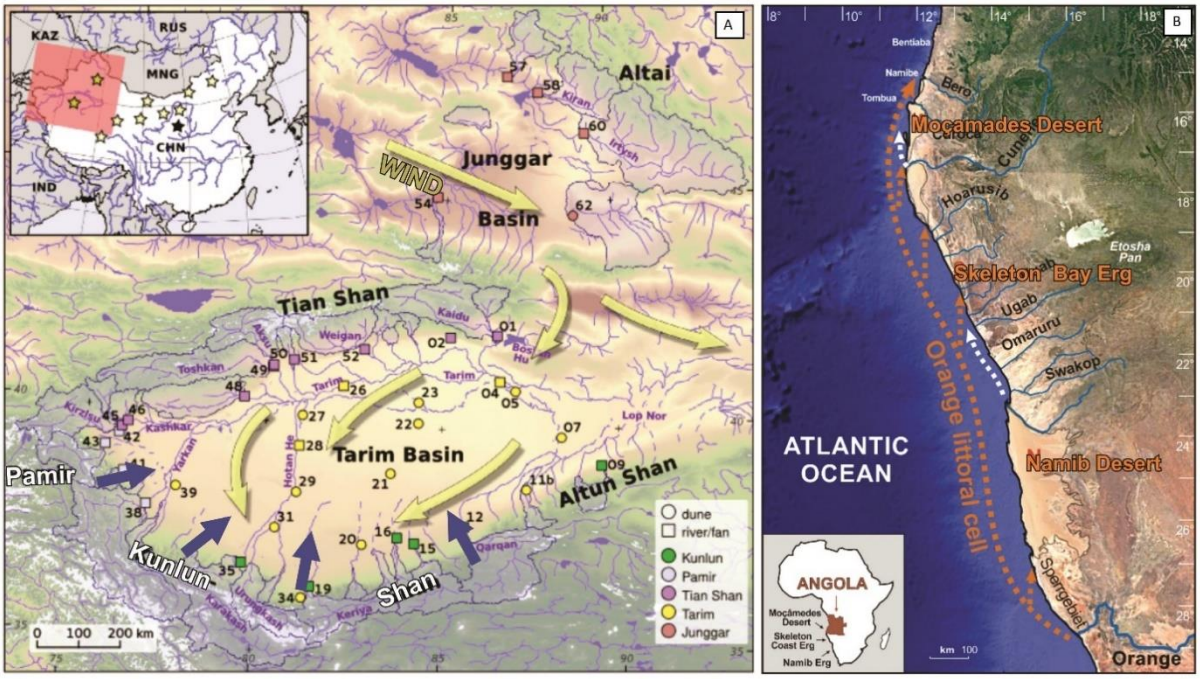

Figura 8 - A- Deserto Taklamakan com as setas azuis apontando a contribuição fluvial das montanhas a sul e sudeste; B- Sistema de alimentação do deserto da Namíbia caracterizada pelo transporte de sedimentos do rio Orange através de longshore currents da costa africana (adaptado de Rittner et al., 2016 e Garzanti et al., 2015).

Esses exemplos de sistemas modernos apresentam diferentes interações com os ambientes deposicionais adjacentes, como o preenchimento sedimentar

controlado pelos rios no deserto *Taklamakan*, marinho e fluvial para o deserto da Namíbia, e multisistemas como no deserto *Rub` al-Khali*. Análise de proveniência multiproxy revela vias sedimentares complexas, compostas por sistemas de geração de areia variados e processo de transporte particulares. Para sistemas eólicos antigos, os *ergs* Permiano-Jurássicos do Colorado Plateau (Fig. 9) compõem a sucessão mais bem estudada (Rahl et al., 2003; Dickinson; Gehrels, 2003) sob a ótica de proveniência. Os zircões detríticos dos grupos Jurássicos Glen Canyon e San Rafael (Dickinson e Gehrels, 2009) demonstram importante reciclagem sedimentar, através da dispersão de área por um sistema fluvial transcontinental atuante na Laurentia, associados a deflação eólica. Apesar do exemplo do platô do Colorado, unidades desérticas do registro geológico ainda carecem de estudos detalhados e compostos por diferentes técnicas, assim como aplicados nos ambientes modernos.

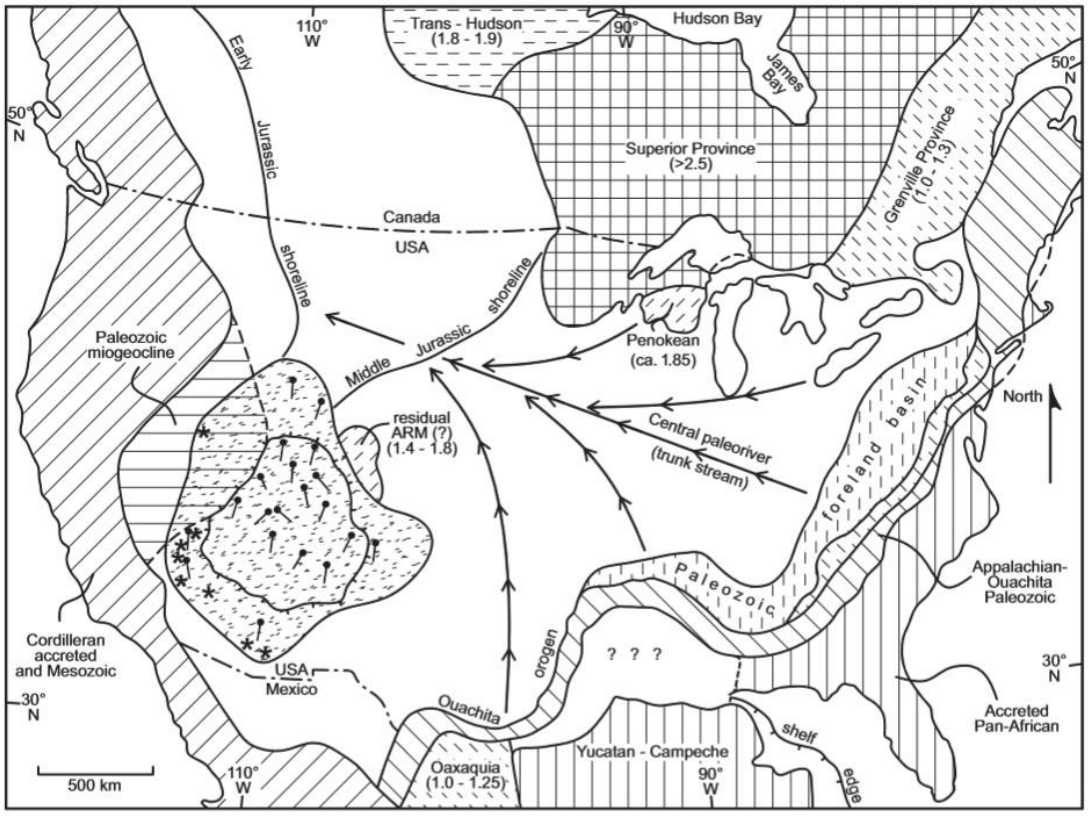

Figura 9 - Ergs Jurássicos do platô do Colorado controlados pelo transporte dos mega-rios, fluindo na direção SE-NO do paleocontinente Laurentia (extraído de Dickinson e Gehrels, 2009).

Os exemplos apresentados mostram a variabilidade do preenchimento sedimentar em desertos atuais e sua relevância para as areis dos *erg*. Além disso,

sistema eólico do passado (no registro) não foram estudados adequadamente por técnicas de proveniência. A caracterização da proveniência do deserto de Botucatu no Cretáceo contribui para a compreensão do enchimento sedimentar em deserto, em particular para os sistemas antigos. Compreender a dinâmica do deserto também melhora nossa compreensão das rotas e sistemas sedimentares do paleocontinente Gondwana. Além disso, os pacotes de sedimentos intercalados a lava podem ser aplicados para verificar possíveis modificações do regime sedimentar devido à natureza coeva dos sistemas vulcânico e eólico.

2.3 Impactos diagenéticos e de reservatório de rochas ígneas em depósitos siliciclásticos

Nos últimos anos, a crescente demanda global por recursos energéticos levaram a novas fronteiras na exploração de petróleo e gás, justificando os recentes estudos sobre sucessões vulcano-sedimentares. Essas sucessões podem gerar diferentes interações e, por consequência, possíveis impactos nas propriedades de reservatórios vulcânicos e sedimentares. Nosso foco de interesse, no entanto, são as alterações diagenéticas causadas pelos fluxos extrusivos de lava em uma unidade siliciclástica e o impacto resultante na sua capacidade como reservatório. As Formações interacamadadas Botucatu e Serra Geral apresentam uma oportunidade de estudo para entender os efeitos da lava básica nas propriedades de reservatório da unidade eólica. Estudos similares foram realizadas em unidades ao redor do mundo, procurando refinar esses processos. Por exemplo, as formações *Twyfelfountain* e Etendeka (Grove et al., 2017), *Wilhelmøya* em Svalbard (Haile et al., 2019) e *Maiden Creek Sill* (Wilson et al., 2019). Com o intuito de examinar os efeitos diagenéticos desencadeados pelas interações vulcano-sedimentares, expandimos a seguir esses estudos.

O estudo de Grove (2017) documenta a compartimentalização de reservatório gerado por diques básicos nas unidades eólicos de *Twyfelfountain*, na Namíbia. Os autores descrevem 3 estilos diagenéticos (ilustradas na Figura 10): (1) dunas tingidas de vermelho não apresentam fases autigênicas, representando a trajetória diagenética normal da unidade; (2) dunas esbranquiçadas devido à dissolução do revestimento de Fe nos grãos, com posterior autigênese abundante de minerais como calcita, caolinita e boemita; (3) alteração do contato “quente” restrita a 1m dos diques.

O fluxo de CO_2, Hs_2 e H_2- das águas subterrâneas hidrotermais é considerado a principal causa para o branqueamento (Figura 10). Haile (2019) demonstra as heterogeneidades causados pelo emplacement de sills nos sedimentos do Triássico-Jurássico de *Wilhelmøya* (Svalbard) (Diagênese normal vs. Diagênese hidrotermal (Fig. 10)). Os autores encontraram um sistema de convecção hidrotermal atingindo distâncias de até 65m do diabásio. O sistema hidrotermal promove o crescimento de calcita recristalizada, sericitização e albitização em feldspatos e neomorfismo de ilita fibrosa a partir de caulinita detrítica. As zonas de calcita hidrotermais criaram barreiras ao fluxo, afetando a porosidade e, consequentemente, a qualidade do reservatório apenas nesses domínios. O *emplacement* de sills do Paleógeno (Maiden Creek Sill) nos pacotes eólicos que compõem os arenitos da Formação Entrada (Utah) promove uma zona de cisalhamento sub-horizontal, resultando efeitos diagenéticos nos arenitos associados (Wilson et al., 2019). Faixas de deformação, estilolitos, cataclasitos e fragmentação da granulometria (Fig. 10F) e autigênese de calcita (Fig. 8F) promovem uma diminuição da porosidade (Fig. 10E e 10F).

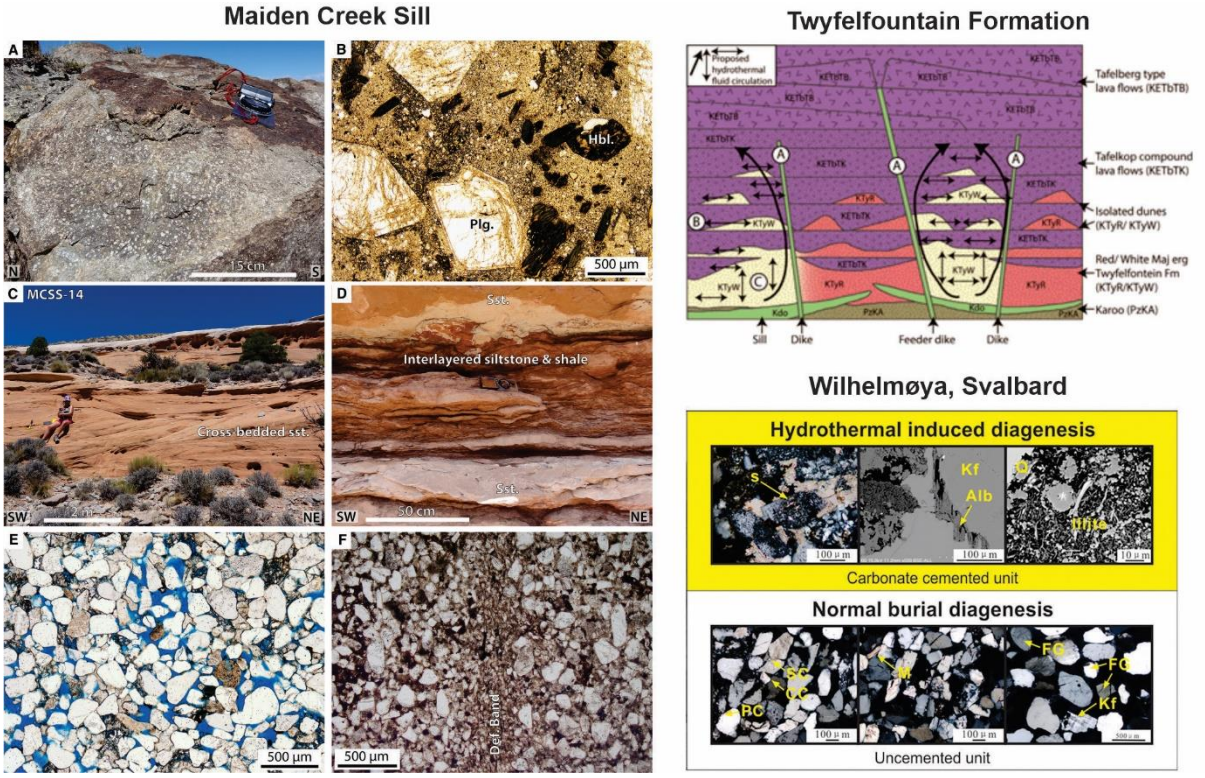

Figura 10 - Petrografia e efeitos hidrotermais em unidades siliciclásticas afetada por intrusões (adaptado de Grove et al., 2017; Haile et al., 2019; Wilson et al., 2019).

Em resumo, os estudos ilustram algumas formas nas quais arenitos são afetados por rochas ígneas associadas, podendo gerar variações positivas e negativas em suas propriedades de reservatório. No entanto, os exemplos também revelam que as interações podem variar de acordo com as particularidades de cada ambiente. Os efeitos hidrotermais parecem ser um processo importante, promovendo resultados relativamente opostos, como na dissolução dos revestimentos de grãos na Namíbia (positivo para o reservatório) ou crescimento autigênico nos exemplos de Svalbard e Utah (negativo ao reservatório). Além disso, deformações químicas e clásticas ocorrem no arenito Entrada e sugerem que a sobrecarga também pode impactar a diagênese diretamente e, finalmente, sua capacidade de reservatório. No entanto, os efeitos de unidades vulcânicas sobre a diagênese sedimentar e seu impacto nas características de reservatório ainda não foram totalmente compreendidos, justificando o estudo nas formações Botucatu e Serra Geral. Além disso, grande parte dos estudos aborda unidades intrusivas, com uma considerável lacuna na pesquisa sobre interações extrusivas de lava.

CAPÍTULO 3 - METODOLOGIA

3.1 Análise granulométrica

Rochas clásticas são compostas por grãos, com todos os tipos de tamanhos, formas e composições. Em termos de tamanho, as rochas siliciclásticas apresentam fragmentos de 4 m (ou mais) a menos de 0,2 um - rocha a argila. O tamanho de grão apresenta uma ampla gama de valores (pelo menos 7 ordens de magnitude), levando Krumbein (1934) a criar a notação *phi*, um logaritmo de base 2, calculado como:

$$\phi = log_2 S$$

Onde S é o tamanho do grão em milímetros. A Tabela 1 apresenta a correspondência da escala phi em milímetros e com a nomenclatura popular - a classificação de *Udden-Wentworth* (Wentworth, 1922). Os tamanhos de areia utilizados na tese seguem os intervalos propostos pela escala.

		US Standard sieve mesh	Millimeters		Phi (ϕ) units	Wentworth size class
GRAVEL			4096		−12	
			1024		−10	Boulder
			256	256	− 8	
			64	64	− 6	Cobble
			16		− 4	Pebble
		5	4	4	− 2	
		6	3.36		− 1.75	
		7	2.83		− 1.5	Granule
		8	2.38		− 1.25	
		10	2.00	2	− 1.0	
SAND		12	1.68		− 0.75	
		14	1.41		− 0.5	Very coarse sand
		16	1.19		− 0.25	
		18	1.00	1	0.0	
		20	0.84		0.25	
		25	0.71		0.5	Coarse sand
		30	0.59		0.75	
		35	0.50	½	1.0	
		40	0.42		1.25	
		45	0.35		1.5	Medium sand
		50	0.30		1.75	
		60	0.25	¼	2.0	
		70	0.210		2.25	
		80	0.177		2.5	Fine sand
		100	0.149		2.75	
		120	0.125	⅛	3.0	
		140	0.105		3.25	
		170	0.088		3.5	Very fine sand
		200	0.074		3.75	
		230	0.0625	1/16	4.0	
MUD	SILT	270	0.053		4.25	
		325	0.044		4.5	Coarse silt
			0.037		4.75	
			0.031	1/32	5.0	
			0.0156	1/64	6.0	Medium silt
			0.0078	1/128	7.0	Fine silt
			0.0039	1/256	8.0	Very fine silt
	CLAY		0.0020		9.0	
			0.00098		10.0	Clay
			0.00049		11.0	
			0.00024		12.0	
			0.00012		13.0	
			0.00006		14.0	

Tabela 1 - Tabela Udden-Wenworth de equivalência entre faixas de tamanho de grãos e unidade phi (Wenworth, 1922; extraído de Boggs e Boggs, 2009).

Para demonstrar a distribuição granulométrica de um determinado conjunto de dados estatísticos, são utilizados os seguintes conceitos estatísticos: modo (1), mediana (2), média (3), seleção (4), assimetria (skewness) (5) e curtose (Kurtosis) (6). A Figura 9 compila os atributos estatísticos de interesse na análise granulométrica. O modo do sedimento é o tamanho de grão mais frequente em um determinado grupo, representado pelo “pico” da distribuição de tamanho de grão. A mediana é o ponto médio entre os valores extremos (distribuição completa). A média aritmética é o tamanho médio dos grãos; no entanto, como os clastos individuais não

são medidos, uma média gráfica é usada (Figura 12). Seleção, curtose e assimetria avaliam a dispersão dos dados, descrevendo a distribuição do tamanho de grão.

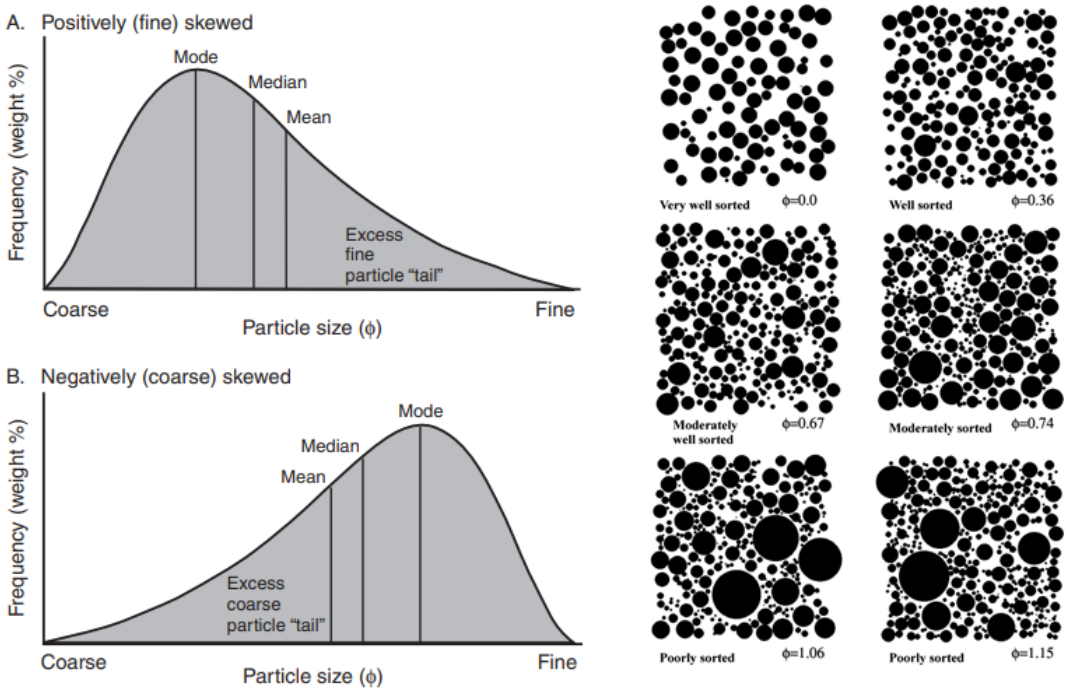

Figura 11 - Atributos estatísticos da distribuição granulométrica: modo, mediana, média, assimetria, curtose e classificação (extraídos de Boggs e Boggs, 2009 e de Jerram, 2001).

A seleção corresponde à dispersão em torno da média da amostra, matematicamente consiste no desvio padrão. A Figura 11 mostra uma visualização esquemática da classificação. A assimetria aborda a "cauda" da curva de distribuição, indicando se os dados são positivos (ricos em sedimentos grossos) ou negativos (ricos em sedimentos finos). A curtose descreve a forma das distribuições de distribuição- desde distribuições planas até picos.

Formulas for calculating grain size by

	the moment method	*graphical methods*
Mean (1st moment)	$\bar{x} = \frac{fm}{n}$	$M_z = \frac{16 + 50 + 84}{3}$
Standard deviation (2nd moment)	$= \sqrt{\frac{f(m \quad \bar{x})^2}{100}}$	$_i = \frac{84 \quad 16}{4} + \frac{95 \quad 5}{6.6}$
Skewness (3rd moment)	$Sk = \frac{f(m \quad \bar{x})^3}{100 \quad ^3}$	$SK_i = \frac{(84 + 16 \quad 2 \quad 50)}{2(84 \quad 16)} + \frac{(95 + 5 \quad 2 \quad 50)}{2(95 + 5)}$
Kurtosis (4th moment)	$K = \frac{f(m \quad \bar{x})^4}{100 \quad ^4}$	$K_G = \frac{(95 \quad 5)}{2.44(75 \quad 25)}$

f = Weight percent (frequency) in each grain-size grade present. m = Midpoint of each grain-size grade in phi values. n = Total number in sample; 100 when f is in percent.

Source: Folk, R. L. and W. C. Ward, 1957. Brazos River bar: A study in the significance of grain-size parameters: *J. Sediment. Petrol*, **27**, 3–26.

Figura 12 - Equações para cálculo de média, distribuição (desvio padrão), assimetria e curtose pelos métodos do momento e gráfico (extraído de Tucker, 2009).

Os atributos estatísticos podem ser calculados através de dois métodos: gráfico e de momentos. O método gráfico é mais adequado para distribuições sem intervalos fechados de tamanho grão e o método dos momentos para tamanho de grão definidos (Tucker, 2009). A figura 12 compila as equações para cada atributo e métodos de cálculo. Folk (1974) apresenta uma classificação descritiva (Tabela 2) para a classificação, assimetria e curtose, com base nos valores de *phi*.

Sorting (σ_1)		Skewness (SK_1)		Kurtosis (K_G)	
Very well sorted	<0.35	Very positively skewed	+0.3 to +1.0	Very platykurtic	<0.67
Well sorted	0.35–0.50	Positively skewed	+0.1 to +0.3	Platykurtic	0.67–0.90
Moderately well sorted	0.50–0.70	Symmetrical	+0.1 to −0.1	Mesokurtic	0.90–1.11
Moderately sorted	0.70–1.00	Negatively skewed	−0.1 to −0.3	Leptokurtic	1.11–1.50
Poorly sorted	1.00–2.00	Very negatively skewed	−0.3 to −1.0	Very leptokurtic	1.50–3.00
Very poorly sorted	2.00–4.00			Extremely leptokurtic	>3.00
Extremely poorly sorted	>4.00				

Tabela 2 - Classificação de seleção, curtose e assimetria de dados granulométricos usando valores *phi* (Folk, 1974; extraído de Tucker, 2009).

Os experimentos granulométricos usados nos artigos I e II aplicam a metodologia de peneiras (Krumbein e Pettijohn, 1961; Folk, 1974; Buller e McManus, 1979), com as seguintes etapas: cerca de 100g de amostra bruta é desagregada com pistilo emborrachado e almofariz, para evitar quebra de grãos (1); secagem da amostra em forno entre 60 e 80ºC por um dia inteiro (2); pesagem da amostra seca

(3); peneiração úmida para o intervalo selecionado - areia (tamanhos 0, 1, 2, 3 e 4 *phi*) (4); secagem de amostras ao forno (5); análise microscópica das frações grossas, verificando a existência de aglomerados de grãos e, caso necessário, re-desagregando a fração (6); pesagem de cada intervalo de areia individualmente (7); cálculo para atingir as proporções de cada classe granulométrica (8). A proporção da argila na amostra pode ser calculada; no entanto, as seções petrográficas não revelam matriz; portanto, o baixo conteúdo de material mais fino que o da areia, se trata de elementos não composicionais (exemplo: cimento). Para o artigo III, o tamanho do grão foi obtido através da medição dos eixos longos e curtos, individualmente para cada grão, e cálculo para obtenção de uma proporção. Os dados estatísticos foram tratados com a planilha *Excel* Gradistat (Blott e Pye, 2001).

3.2 Análise petrográfica

A análise petrográfica avalia os componentes presentes nas rochas sedimentares em lâminas petrográficas - através de microscópio óptico e microscópio eletrônico de varredura. Pelo menos 300 pontos foram contados em uma trama fixa, com passo definido, a fim de obter a proporção dos constituintes (Van der Plas e Tobi, 1965). Os elementos descritos são: minerais detríticos, porosidade, cimentos, tamanho de grão e morfologia. A fração mineral detrítica é composta por quartzo (mono-, poli-cristalino, deformado), feldspato (plagioclásio, ortoclasio e microclinio) e fragmentos líticos (plutônicos, vulcânicos, sedimentares e metamórficos). A Figura 13 ilustra a análise petrográfica, demonstrando a trama (linhas tracejadas em rosa), a identificação dos minerais no centro do reticulo (pontos coloridos), quantidade e tipo de contatos entre grãos, arredondamento e esfericidade (linhas tracejadas em azul e preto nas bordas dos minerais), medição de tamanho de grãos (eixo maior e menor), porosidade e interpretação das características diagenéticas.

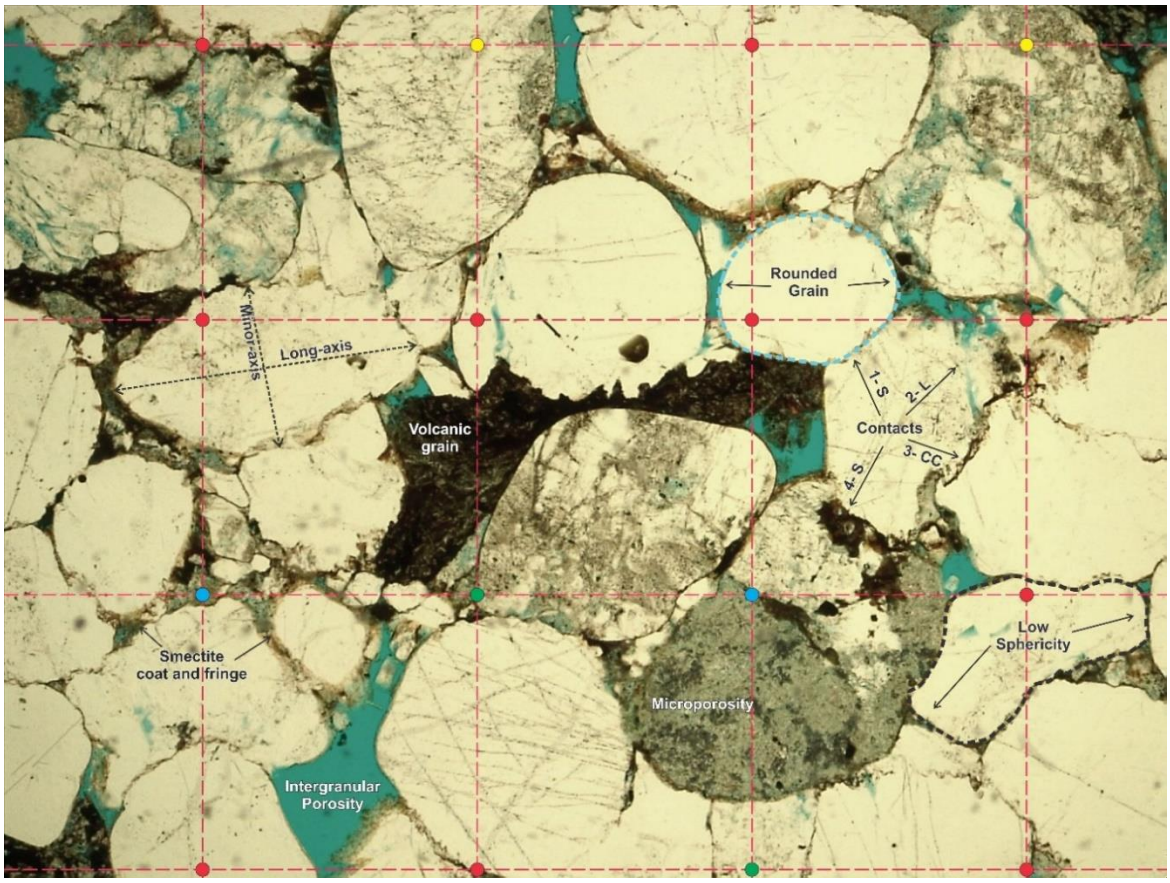

Figura 13 - Análise esquemática da petrografia, mostrando a grade da contagem, identificação de minerais e porosidade nos pontos coloridos, análise da morfologia dos grãos (grãos arredondados e pouco esféricos usados como exemplo) e identificação do estilo de cimentação. Pontos vermelhos - quartzo; Pontos amarelos - Feldspato; Pontos azuis - microporosidade.

A contagem foi feita aplicando o método de Gazzi & Dickinson (Ingersoll et al., 1984), consistindo na contagem dos fragmentos líticos como pontos mono-minerálicos para grãos de tamanho superior ao da areia muito fina (> 62,5 um). Por exemplo, um fragmento plutônico composto por quartzo e feldspato contará somente como mineral no centro do reticulo. O objetivo dessa técnica é eliminar o viés granulométrico na abundância de material líticos prevalentes em frações mais grossas. A técnica modal é usada para evitar a quebra lítica em grãos individuais e evitar o viés do tamanho dos grãos. Os dados de *petrografia* foram tratados como dados de classe de contagem de pontos no pacote *Provenance* rodados no software R (Vermeesch et al., 2016). O pacote *Provenance* foi utilizado para criar os gráficos ternários e as comparações estatísticas (gráficos MDS e PCA) apresentados nos artigos.

3.2.1 Classificação de arenitos

O estudo utiliza o esquema de classificação de arenito baseado no trabalho de Garzanti (2018; 2019) (Figura 14). A nomenclatura de arenito proposta por Garzanti (2018; 2019) aplica o diagrama QFL clássico (quartzo-feldspato-lítico), mas altera os nomes dos campos, evitando o uso de nomes genéticos ou abandonados, como, por exemplo, grauvacas e arcóseos. A Figura 14C mostra as 15 novas nomenclaturas, baseadas unicamente na abundância de componentes. Devido à composição rica em quartzo nas unidades de Botucatu, também aplicamos a nomenclatura da Figura 12D, adicionando mais campos.

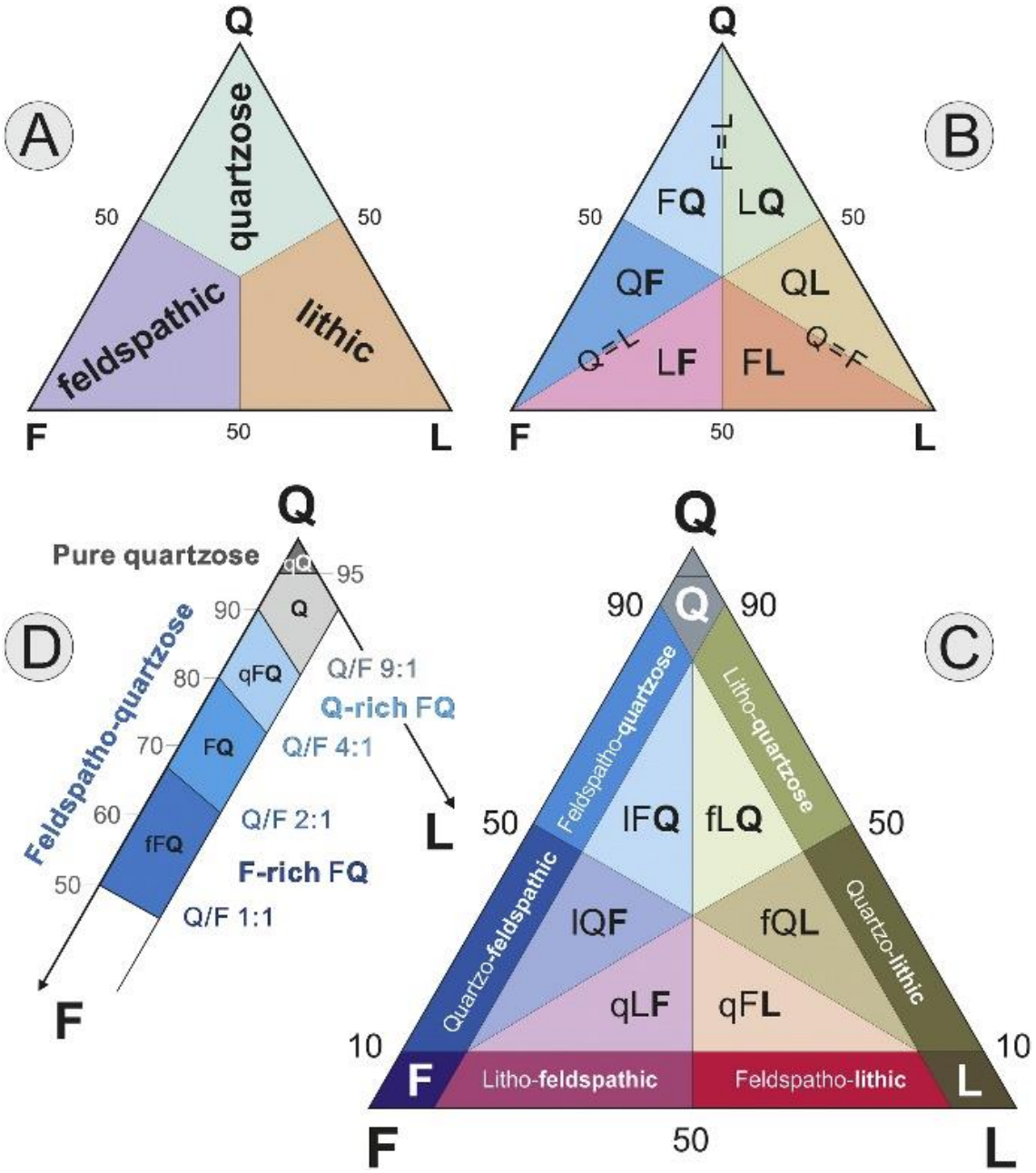

Figura 14 - Diagrama de classificação de arenitos usando o esquema de Garzanti (2018; 2019). Q = quartzoso (qQ = quartzoso purao); F = feldspático; L = lítico; QF = feldspato-quartzoso (QFA = rico em feldspato; qFQ = rico em quartzo); QF = quartzo-feldspático; LF = lito-feldspático; FL = feldspato-lítico; QV = quartzo-lítico; LQ = lito-quartzoso; QFQ = lito-feldspato-quartzose; lQF = lito-quartzo-feldspático; qLF = quartzo-litofeldspático; qFL = quartzo-feldspato-lítico; fQL = feldspato-quartzo-lítico; fLQ = feldspato-lito-quartzoso (extraído de Garzanti, 2019).

3.2.2 Morfologia de grãos

A morfologia e as texturas dos grãos foram descritas considerando o arredondamento dos grãos, a esfericidade e as relações de contorno dos grãos. O arredondamento descreve as arestas dos grãos, identificando os cantos como arredondados ou angulosos. A esfericidade mede a similaridade entre os grãos e uma esfera perfeita. Esses conceitos podem ser calculados, mas, para petrografia, utiliza-se a comparação visual, aplicando uma análise qualitativa (ver Figura 15A). A textura de uma rocha sedimentar reflete os processos de intemperismo, mineralogia inicial, rocha-fonte, transporte dos sedimentos e possíveis alterações digenéticas – como dissolução (Tucker, 2009). Pelo menos 200 grãos foram contados para avaliar a textura das amostras no artigo III. Os tipos de contatos de grãos estão relacionados a fábrica deposicional dos grãos somados aos efeitos de empacotamento constante causado pelo soterramento sedimentar. A figura 15B mostra os 5 tipos diferentes de contatos: flutuante, pontual, linear, côncavo-convexo e suturado. Atributos como porosidade e permeabilidade são controlados pelo empacotamento (Tucker, 2009). Portanto, foram contados 200 limites de grãos (quantos grãos estão em contato com o que está sob a mira) e o tipo de contato de grãos também.

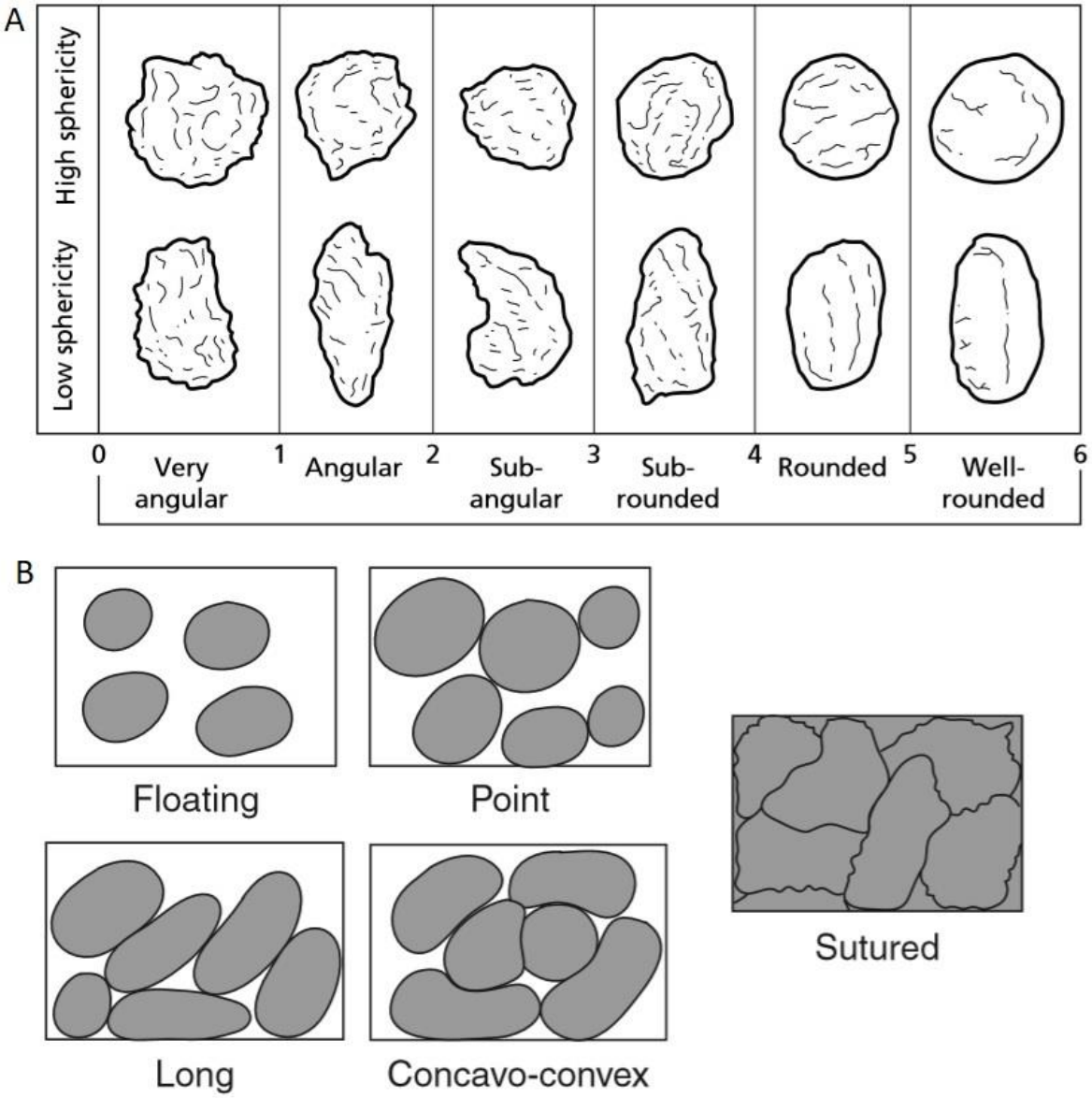

Figura 15 - Morfologia e fábrica de grãos detríticos ilustrando os tipos de esfericidade e arredondamento (A); os tipos de contatos de grãos - flutuante, pontual, longo (linear), côncavo-convexo e suturado (B) (adaptado de Taylor, 1950 e Boggs e Boggs, 2009).

3.2.3 Porosidade

Os poros correspondem à porção do volume total da rocha composta por material não sólido, como, por exemplo, ar, água ou hidrocarbonetos (Miliken e Curtis, 2016). A porosidade nas rochas pode ser dividida em dois tipos: primária e secundária. A porosidade primária é formada na deposição, podendo ser dividida em poros intergranulares (espaços em azul escuro nas Figuras 16A e B) ou poros intragranulares (poros localizados internamente aos grãos, como no círculo amarelo

da Figura 16C). A porosidade primária é a forma predominante de porosidade em arenitos e pelitos, mas é alterada pela compactação mecânica e química (Chester et al., 2004; Miliken; Curtis, 2016). A porosidade secundária é formada após a deposição, principalmente pela dissolução de grãos primários e ocasionais cimentos ou substituições de grãos (Miliken e Curtis, 2016; McBride, 1977; Pettijohn, 1941; Schmidt e Macdonald, 1979). A figura 16B ilustra a microporosidade relacionada diretamente com a fase autigênica (caulinita) e porosidade secundária formada em feldspato parcialmente dissolvido. A figura 16D apresenta porosidade móldica em carbonatos do tipo grainstone (Miliken e Choh, 2011).

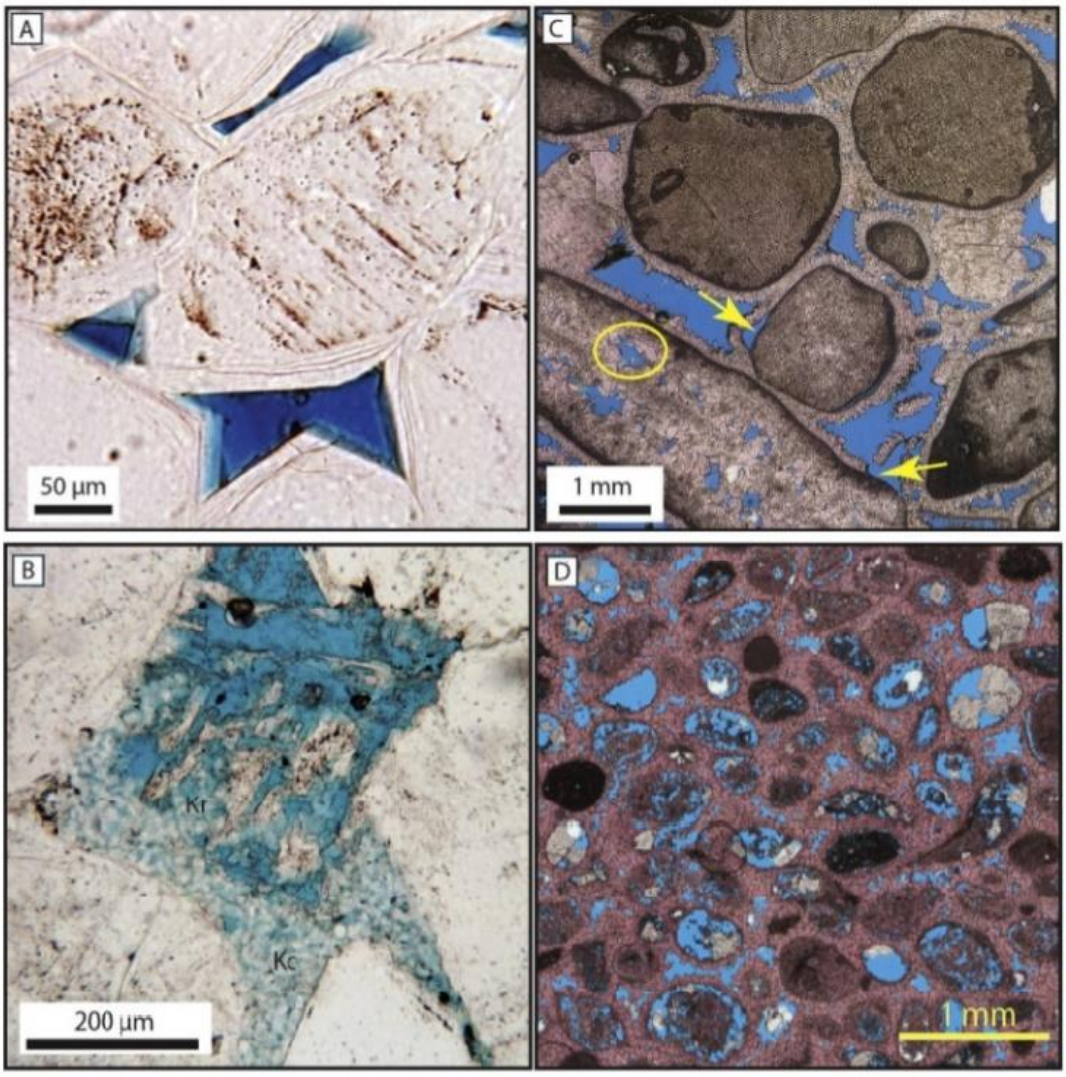

Figura 16 - Tipos de porosidade em lâminas petrográficas, mostrando porosidade primária intergranular em arenitos (A e C) e porosidade secundária dos tipos micro porosidade, móldica e intragranular (B e D) (adaptado de Miliken e Curtis, 2016).

3.2.4 Análise diagenética

A diagênese consiste nos processos físico, químico e biológico atuantes em rochas sedimentares após a deposição, envolvendo a interação da composição detrítica e da água intersticial dos poros, a fim de atingir um equilíbrio geoquímico (Curtis, 1977; Burley et al., 1985). O processo diagenético é dividido em três regimes, diretamente relacionados à evolução da bacia (Worden e Burely, 2003): eodiagênese (diagênese inicial), mesodiagênese (diagênese do soterramento) e telodiagênese (diagênese relacionado ao soerguimento) (Choquette e Pray, 1970; Schmidt e Macdonald 1979). A figura 17 ilustra o processo basinal responsável pelos regimes de diagênese. A eodiagênese ocorre em condições de superfície, fortemente afetada pelas condições geoquímicas ambientais. A temperatura varia de 30 a 70ºC e, dependendo da penetração do fluxo hidráulico meteórico da bacia, podendo ocorrer até 1 ou 2 km (Morad et al., 2000). A mesodiagênese inicia, no sentido de Morad (2000), após 1 a 2 km de soterramento e temperaturas acima de 30 a 70ºC. O limite entre a eodiagênese e a mesodiagênese nem sempre é claro, porém é caracterizado por uma transformação mineral controlada pelo soterramento (temperatura, pressão, litologia e fluidos basais), ao passo que a eodiagênese ocorre controlada pela presença de águas meteóricas superficiais (Worden e Burely, 2003). A telodiagênese começa após uma elevação basinal, re-expondo pacotes sedimentares soterrados às condições da superfície (Worden e Burley, 2003).

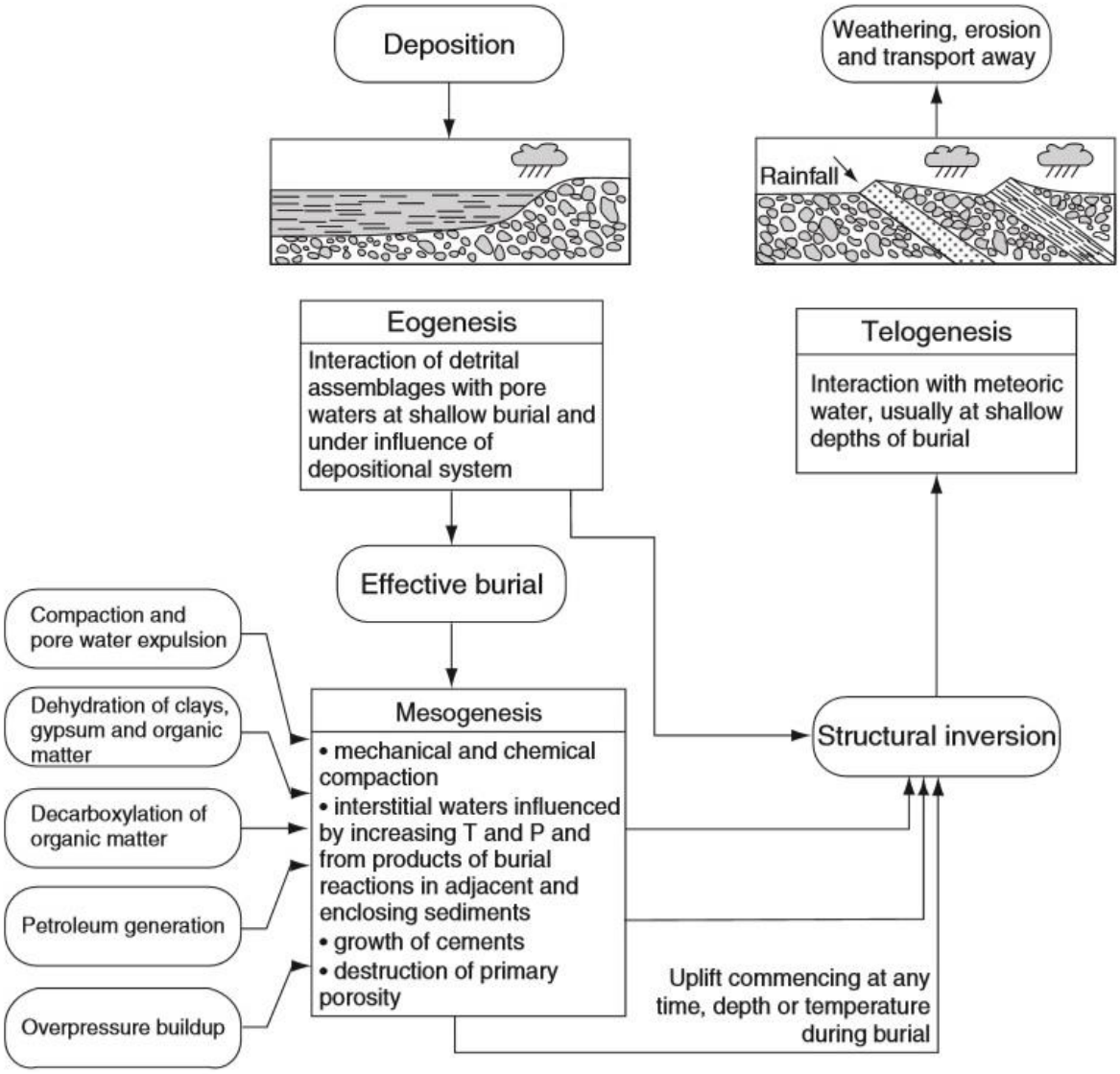

Figura 17 - Processos digenéticos e processos basinais (extraídos de Worden e Burley, 2003).

A figura 18 apresenta alguns exemplos de fases e texturas minerais de cimento. Os cimentos de quartzo e feldspato ocorrem tipicamente como sobrecrescimentos euédricos e sintaxiais (Fig. 18e) nas fases iniciais da diagênese (Worden e Burley, 2003). Minerais de preenchimento de poros como calcita e dolomita são comuns em condições áridas, como na área de estudo. Argilominerais, frequentemente, compõem os cimentos em arenitos - formados a partir da transformação de grãos detríticos (Fig. 18c) ou argilas filtradas mecanicamente por águas meteóricas (Fig. 168a). Os hábitos dos argilominerais variam de acordo com a mineralogia original e a química (Wilson; Pittman, 1977). Para avaliar a paragênese diagenética, é necessário identificar e quantificar fases e hábitos minerais (1),

estabelecer relações de crescimento entre os minerais, dissolução e empacotamento (2).

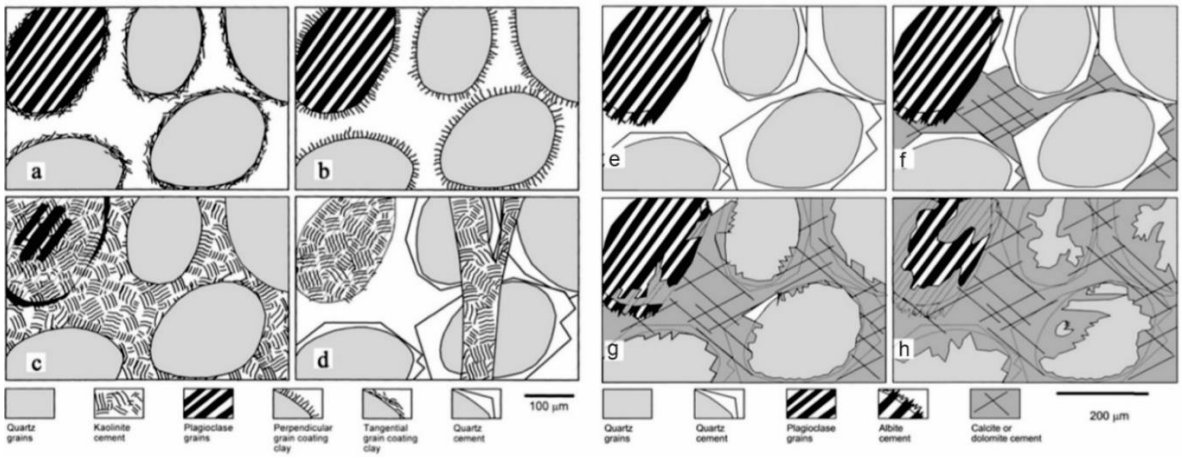

Figura 18 - Estilos de autigênese: a) revestimento de grãos por argilas infiltradas; b) revestimento de grãos por esmectitas perpendiculares, ilita e clorita; c) argilas preenchendo poros, substituindo o feldspato por caulinita; d) preenchimento de fraturas e caulinita substitutiva em grãos; e) sobrecrescimento de feldspato sintaxial e grão de quartzo; f) preenchimento de poros por calcita; g) sobrecrescimento de calcita em grãos; h) substituição extensiva de grãos por calcita (adaptado de Worden e Burley, 2003).

O processo de compactação consiste na redução de volume, causando a remoção da água intersticial dos poros em resposta a um aumento progressivo da compactação vertical com o constante soterramento (Worden e Burley, 2003). A compactação está diretamente relacionada à progressiva diminuição da porosidade e permeabilidade de rochas siliciclásticas. A compactação em arenitos ocorre por meio de rearranjo de grãos, fraturamento, deformação plástica (grãos dúcteis), dissolução (Worden; Burley, 2003). A figura 19 ilustra a transição do processo de compactação desde a deposição (contatos flutuantes ou pontuais), avançando para compactação mecânica durante os estágios iniciais do soterramento (contato linear e fraturamento) e, finalmente, atingindo dissolução química entre os grãos (contatos suturados e estilolitos).

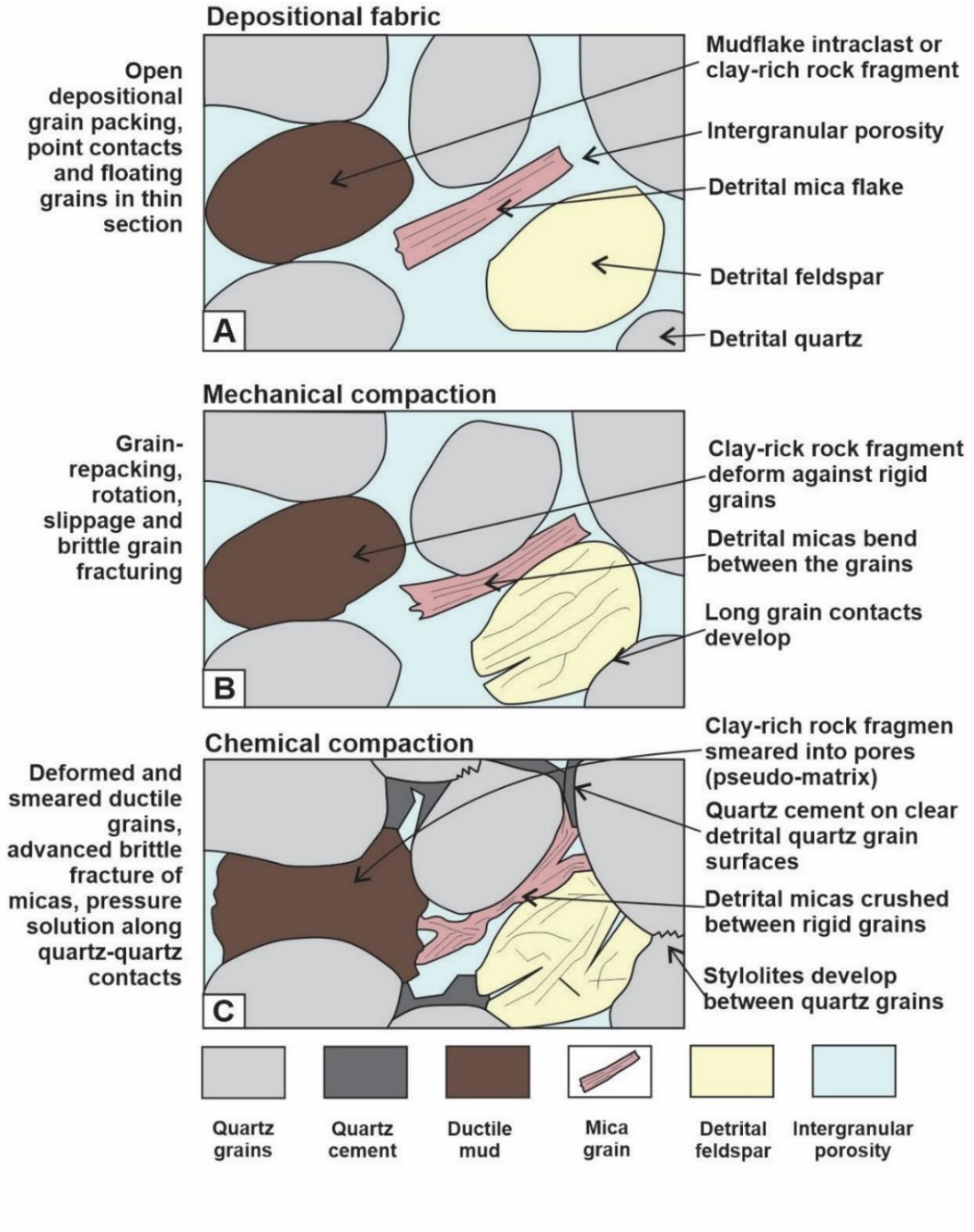

Figura 19 - Evolução de compactação por progressivo soterramento, ilustrando a transição entre um domínio de alta porosidade na deposição (a), diminuição da porosidade após a compactação mecânica inicial (teoricamente de 40% a 26%) (b) e a dissolução do contato com o grão (após 2000m de enterro) (c) (extraído de Worden e Burley, 2003).

3.3 Análise de minerais pesados

A análise de minerais pesados é uma ferramenta eficaz no entendimento da proveniência sedimentar, indicando a origem dos grãos através da associação à áreas-fonte (Morton e Hallsworth, 1999). A análise de minerais pesados é feita na fração mineral translúcida acima de 2,90 g/cm^3. Suas aplicações variam da correlação de reservatórios de hidrocarbonetos à caracterização e ao mapeamento de processos sedimentares (Morton e McGill, 2019, Garzati, 2007). A premissa da análise de minerais pesados consiste no entendimento de que o sedimento gerado por uma determinada área-fonte (associação litológica) produz uma assinatura mineral reconhecível (por exemplo, Cr-espinélios associados a ofiolitos ou anfibólios azuis em rochas formadas em altas pressões). Essas assinaturas podem ser rastreadas através de quantificação, geoquímica mineral ou geocronologia para traçar rotas e caminhos de sedimentação (*source to sink*). A figura 20 demonstra esse processo, no qual a erosão e o intemperismo nas áreas fontes produzem sedimentos, transportados por sistemas fluviais, finalmente depositados em uma bacia marinha.

Como ilustrado na figura 20, a assinatura da proveniência pode ser mascarada por diferentes graus de intemperismo (na fonte ou durante o transporte), abrasão e seleção hidrodinâmica e diagênese.

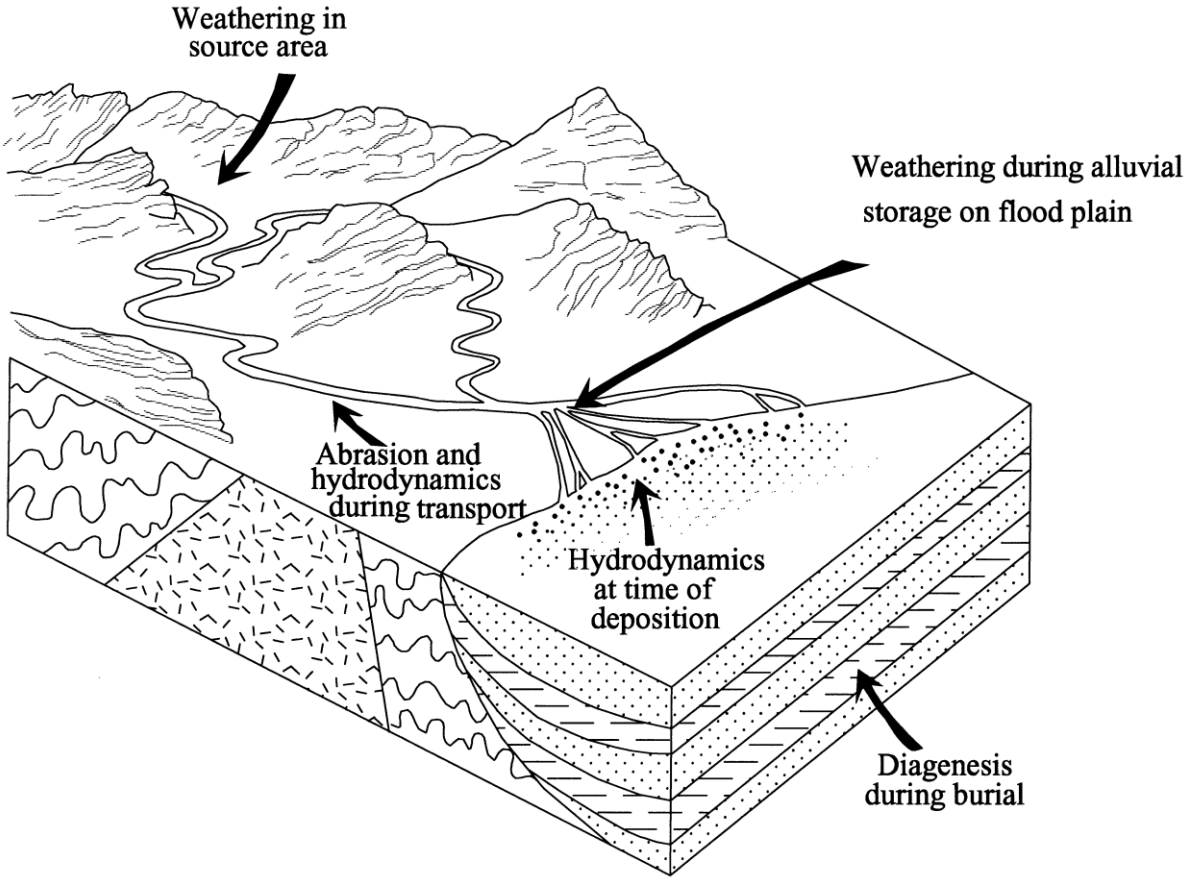

Figura 20 - Esquema source-to-sink sedimentar, composto por erosão nas áreas fontes, transporte e deposição em bacia (extraído de Morton e Hallsworth, 1994).

A seleção de grãos, abrasão mecânica e a dissolução podem ocorrer durante o transporte e devem ser avaliadas para caracterizar com precisão a assembleia mineral resultante. A tabela 3 apresenta uma ordem de estabilidade química para o processo de soterramento e intemperismo (Pettijohn, 1941; Pettijohn et al., 1973; Morton, 1985). No geral, os silicatos máficos (olivinas e piroxênios) são instáveis, ao passo que zircão, turmalina e rutilo são estáveis aos processos de alteração diagenética e dissolução superficial. Outros minerais, como apatita, são instáveis em condições superficiais ácidas, no entanto são estáveis ao processo de soterramento e diagênese.

A alta estabilidade da associação zircão-turmalina-rutilo, tanto quanto sob a perspectiva da abrasão física quanto para química, levou Hubert (1962) a criar o índice ZTR (soma dos totais de zircão, turmalina e zircão divididos pelo total de minerais translúcidos), fornecendo um valor numérico de maturidade mineralógica dos arenitos. Recentemente, Garzanti (2016) argumenta contra a validade do

conceito de maturidade, devido a sua direta relação com a petrologia original da rocha fonte, porém o índice ZTR ainda é válido como proxy de minerais pesados na identificação de reciclagem sedimentar.

ORDER OF PERSISTENCE Modified after Pettijohn (1941)	GENERALIZED ORDER OF CHEMICAL STABILITY Pettijohn et al. (1973),	Acid leaching (Morton 1985a)	Deep burial, saline or alkaline pore fluids, (Morton 1985a)
olivine sillimanite pyroxene sphene andalusite Ca-amphiboles glaucophane-riebeckite series epidote kyanite staurolite monazite xenotime apatite garnet zircon tourmaline rutile	very unstable olivine unstable hornblende actinolite augite diopside hypersthene andalusite moderately stable epidote kyanite garnet (iron-rich) sillimanite sphene zoisite stable apatite garnet (iron-poor) staurolite monazite ultrastable rutile zircon tourmaline anatase	olivine, pyroxene amphibole sphene apatite epidote, garnet chloritoid, spinel staurolite kyanite andalusite, sillimanite, tourmaline, rutile, zircon	olivine, pyroxene andalusite, sillimanite amphibole epidote sphene kynanite staurolite garnet* apatite*, chloritoid, spinel rutile, tourmaline, zircon * According to recent observations (MM) garnet and apatite appear to be more stable than chloritoid and spinel. The order of increasing stability from staurolite is therefore: staurolite chloritoid, spinel garnet apatite rutile, tourmaline, zircon

Tabela 3 - Tabela de estabilidade relativa de minerais pesados por Pettijohn (1941), Pettijohn et al. (1973) e Morton (1985). Morton (1985) demonstra a estabilidade diferente na dissolução ácida (durante transporte) e por alteração diagenética por soterramento.

No aspecto físico, os diferentes tamanhos, formas e densidades dos minerais pesados promovem modificações no arranjo das frações pesadas dentro da composição total dos sedimentos. A figura 21A demonstra o processo de equivalência de assentamento de grãos, no qual a mesma energia da corrente de tração arrasta diferentes tamanhos e formas de minerais, controlados pela sua densidade (Rubey, 1933). Por exemplo, correntes constantes de alta energia, como nas praias, podem gerar acumulações ricas em minerais pesados, denominados *placer*. O processo é controlado pelo arraste seletivo causado por diferenças de densidade e tamanho de minerais pesados e tectossilicatos, conforme ilustrado na Figura 21B (Garzanti et al., 2019).

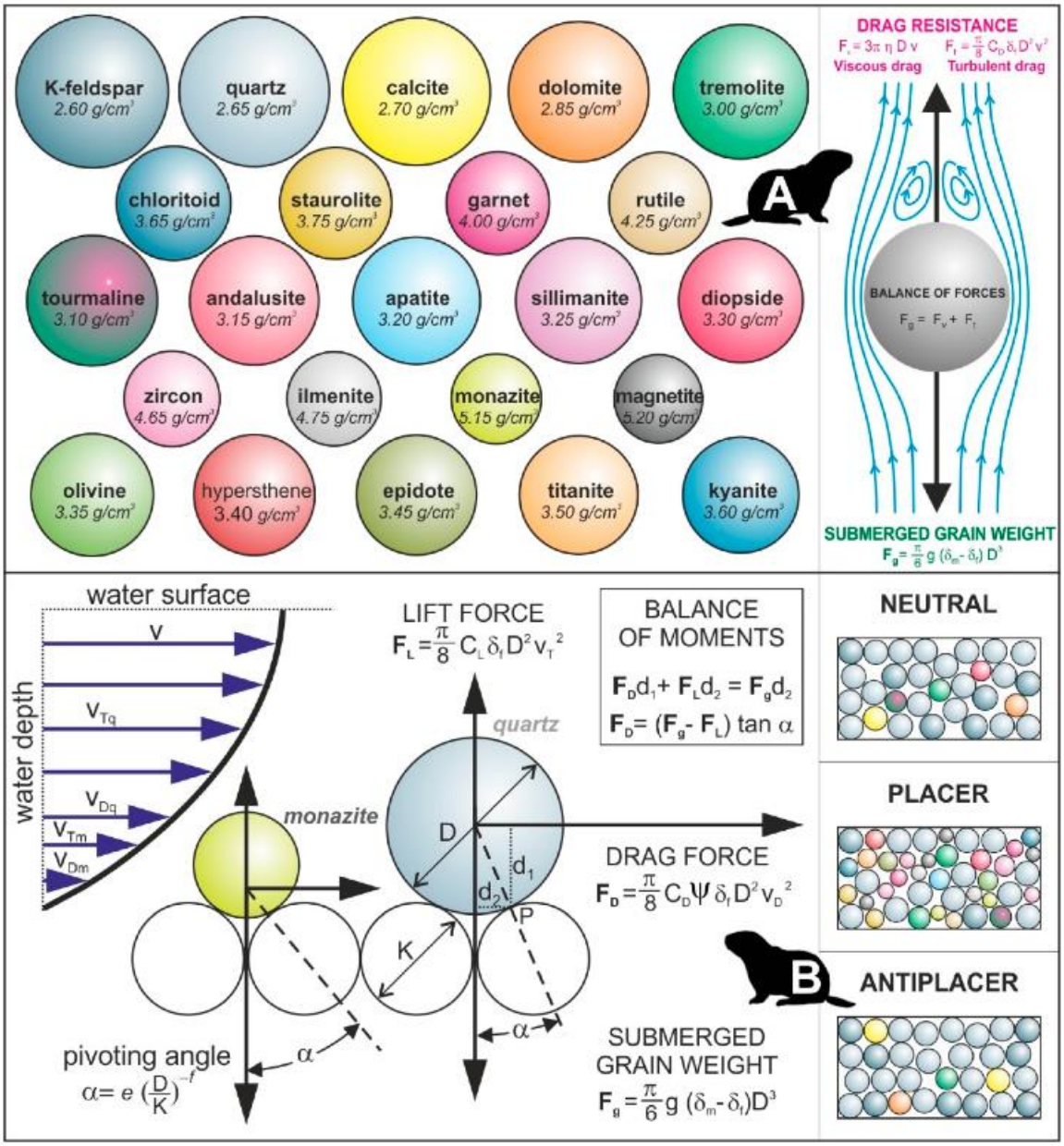

Figura 21 - Seleção hidráulica em rochas sedimentares. A- princípio de equivalência para arraste de grãos; B- arraste seletivo pode levar a concentração ou depleção de minerais pesados (extraída de Garzanti e Andó, 2019).

Foram utilizados entre 100 a 400g de arenitos na preparação de amostra. O processo consiste na: desagregação com pistilo de ponta de borracha para evitar a quebra dos grãos (1); retirada da fração areia muito fina (63 a 125 um) através de peneiramento (2); separação de minerais pesados através do uso de líquidos densos-bromofórmio (2,8 g/cm^3) (3); manufatura de lâminas com o uso de resina (Figura 22) (4). Pelo menos 150 grãos foram contados, aplicando o método *ribbon* (Mange e Maurer, 1992), que consiste na contagem de todos os grãos em uma área

determinada. Morton e Hallsworth (1994) sugerem o intervalo de areia muito fino, devido à representação eficiente das suítes minerais e à identificação mais fácil dos minerais (semelhante ao encontrado em lâminas petrográficas padrão de 30um).

Para auxiliar na identificação mineral, foram utilizados experimentos utilizando microscópio eletrônico de varredura no Laboratório de Geologia Isotópica (LGI) da Universidade Federal do Rio Grande do Sul. A análise utilizou interação backscaterring (identificando diferenças nas massas atômicas) e elétron secundário (observando a topografia dos grãos), com um JEOL 6610-LV com tensão de feixe de 15 kV e distância de trabalho de 12 mm.

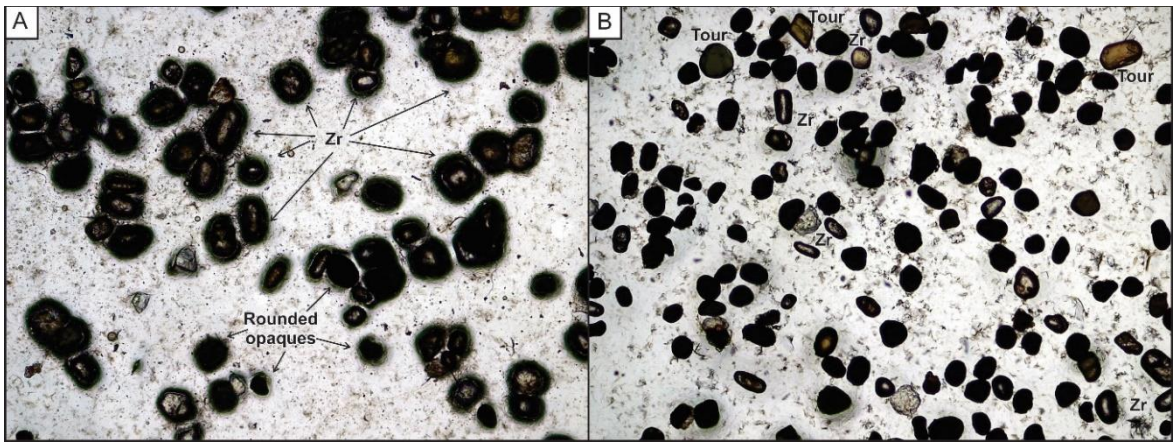

Figura 22 - Lâmina de minerais pesados.

As análises estatísticas foram realizadas no *software* R, através do pacote *Provenance* (Vermeesch et al., 2016). Os dados de minerais pesados foram tratados tanto como dados de contagem de pontos quanto dados composicionais. Os dados da contagem de pontos usam um teste qui-quadrado (Vermeesch, 2019), que diminui as incertezas intrínsecas ao processo de contagem. Devido aos valores 0 nos dados de contagem de pontos, o tratamento padrão *logratio* para dados de composição não é possível, por isso a conversão de dados de contagem para dados composicionais faz-se necessária. A vantagem da razão logarítmica para o tratamento estatístico é o uso da técnica de ordenação como análise de componentes principais, uma ferramenta poderosa na interpretação de proveniência. A tese utiliza a contagem de pontos com base na regressão qui-quadrado para gráficos ternários e intervalos de incerteza e dados de composição para *biplots* de análise de componentes principais.

3.4 Geocronologia U-Pb em zircão detrítico

A datação por U-Pb em zircão detrítico apresenta três fases de preparação da amostra: purificação do zircão detrítico (1); montagem e geração de imagens (2) e datação (3). A primeira etapa foi realizada no Laboratório de Geologia Isotópica (LGI) da Universidade Federal do Rio Grande do Sul (UFRGS). A purificação do zircão detrítico consiste em transformar a rocha consolidada (1-2 kg) em um único concentrado de grãos de zircão. Para isso, foram realizados os seguintes processos: limpeza de amostras (1); desagregação primária da amostra em britadeira mecânica (2); desagregação da amostra em moinho de placas (3); peneiramento da fração granulométrica menor que 300 um (4); pré-concentração de minerais pesados através de bateia (5); remoção de minerais magnéticos com imã de mão (6); remoção de minerais paramagnéticos usando separados isomagnético Frantz (até corrente de 1,8o) (7); concentração de minerais pesados via separação líquida densa (diod-metano> 3,3 g/cm³); microbateia com placa de Petri e álcool para purificação refinada (9). O processo pode variar dependendo da amostra original - por exemplo arenito friável pode não exigir desagregação inicial, ou a microbateia foi utilizada apenas em alguns casos para uma purificação definitiva do concentrado de zircão. Cuidados importantes são necessários nessa etapa para evitar a contaminação da amostra. Portanto, a limpeza do maquinário e vidraria é essencial para evitar contaminações.

A segunda e terceira etapas de geocronologia foram realizadas no Centro de Pesquisas Geocronológicas (CPGEO) da Universidade de São Paulo (USP). O segundo passo na geocronologia consiste na manufatura de mounts e na obtenção de imagens dos grãos, a fim de balizar a posterior datação. A metodologia para a fabricação dos *mounts* consiste em: montar, pelo menos, 200 zircões em uma fita dupla-face dentro do molde de 5 cm (1); despejar resina aquecida (80-100^{o}C) na peça fundida (2); polir e limpar com aparelhos ultrassônicos (3); Coating de Au ou C no mount e posterior imageamento - elétrons secundários e catodoluminescência em microscópio eletrônico (4); polir novamente, de forma suave, para remover e limpar o revestimento (5). O zircão, geralmente, apresenta históricos complexos de crescimento e reciclagem, portanto o imageamento por catodoluminescência (CL) é essencial para o posicionamento correto da ablação a laser. Além disso, fraturas e rachaduras cicatrizadas devem ser evitadas pelo acúmulo típico de Pb_{204}, prejudicial no cálculo de idades. A figura 23 mostra imagens de CL demonstrando o

posicionamento adequado da ablação a laser. Os disparos a laser foram feitos, preferencialmente, nas bordas dos grãos, adquirindo o último episódio de crescimento para cada história de zircão.

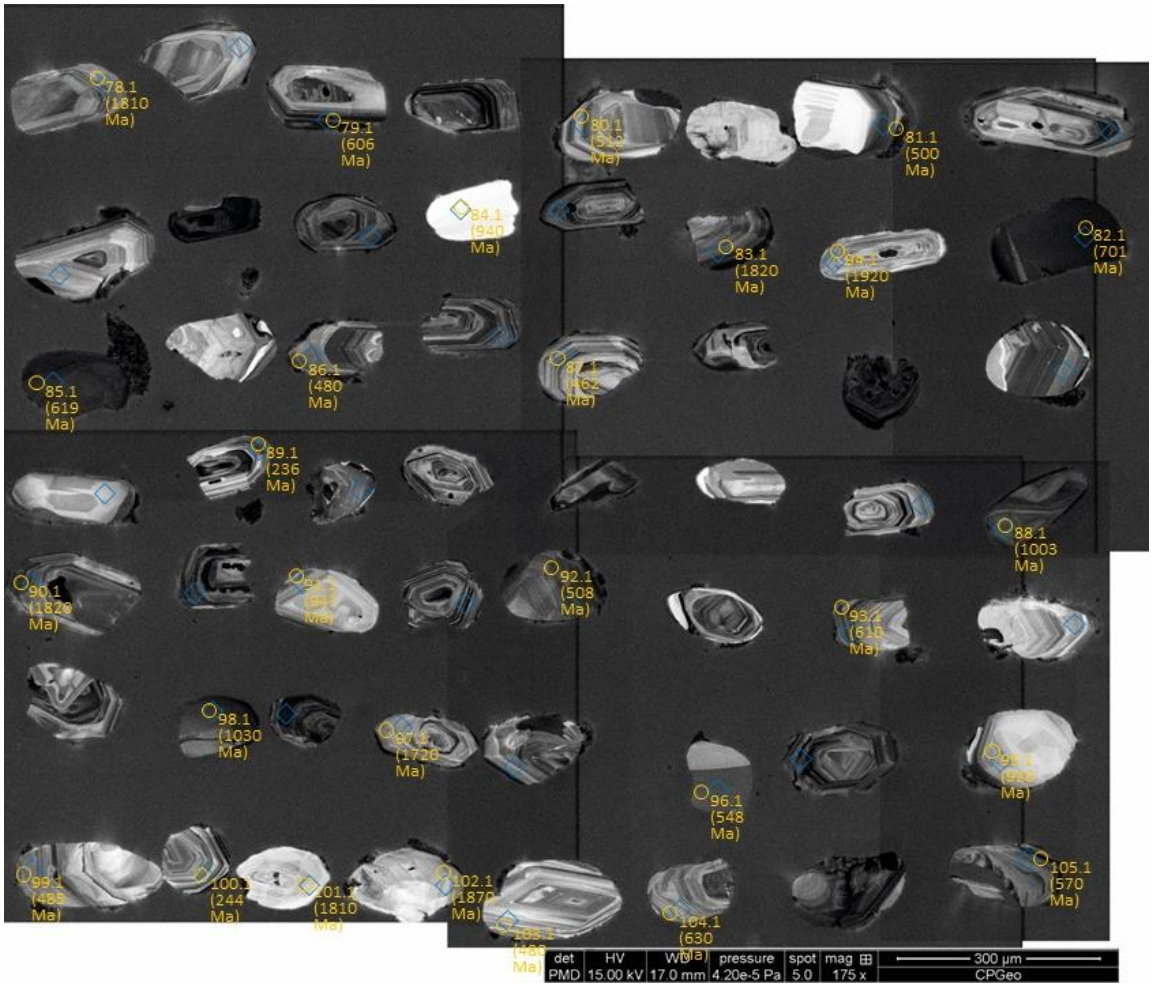

Figura 23 - Imagem de catodolumiscência de zircão detrítico, mostrando os spots selecionados para a abração (círculos amarelos) e idades resultantes.

A datação per se foi realizada utilizando o equipamento *Finnigan Netuno*, um espectrômetro de massa com coletores múltiplos e tocha de plasma de argônio como método de ionização (ICP) (Figura 242). A detecção de amostras ocorre em um aparelho de ablação a laser acoplado, *excimer* ArF laser. Atualmente, o LA-ICPMS é a técnica mais eficaz para a datação de grão único (rápida e barata), mas com maiores incertezas quanto à precisão e exatidão (1-2%) em relação a outros métodos, como SHRIMP ou ID-TIMS (Košler; Sylvester, 2003; Simonetti et al., 2005; Gehrels et al., 2008; Gehrels, 2011; Pullen et al., 2013).

Figura 24 - Equipamento LA-ICP-MS para datação U-Pb no CPGEO.

A geocronologia de urânio-tório-chumbo é frequentemente usada devido às suas três séries de decaimento independentes: $^{238}U \rightarrow {}^{206}Pb$ (meia-vida = 4,47Ga), $^{235}U \rightarrow {}^{207}Pb$ (meia-vida = 0,70 Ga) e $^{232}Th \rightarrow {}^{208}Pb$ (14,01 Ga) (Jaffey et al., 1971). A figura 25 mostra as proporções relativas para a série de 3 decaimentos, demonstrando os isótopos iniciais de Pb (denominados chumbo comum) e a abundância radiogênica.

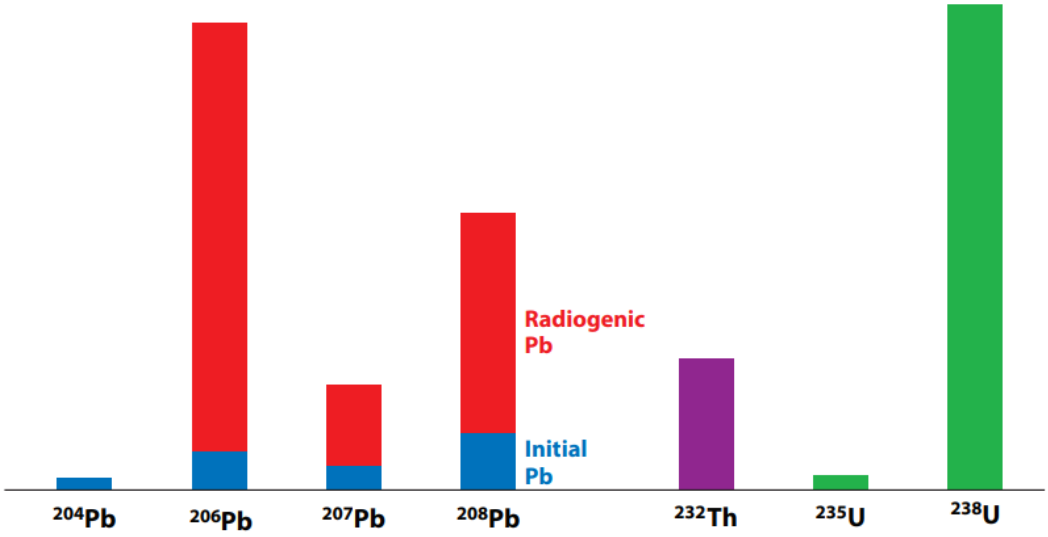

Figura 25- Abundância de isótopos de U-Th-Pb em zircão (extraído de Gehrels, 2014).

Em resumo, as idades são obtidas medindo as razões $^{206}Pb/^{238}U$, $^{206}Pb/^{207}Pb$ e $^{206}Pb/^{204}Pb$. O zircão apresenta uma quantidade variável de Th, de modo que o cronômetro $^{232}Th \rightarrow {}^{208}Pb$ não é tão confiável quanto as séries U-Pb. A relação 206Pb/204Pb é usada para rastrear o Pb comum. Devido à razão constante na natureza de $^{238}U/^{235}U$ (137,82 - Hiess et al., 2012), a razão de $^{206}Pb/^{207}Pb$ é medida em vez de $^{207}Pb/^{235}U$. O urânio e o chumbo tendem ao fracionamento durante a análise do espectrômetro de massa (devido a suas diferentes massas), no entanto a relação $^{206}Pb/^{238}U$ deve ser adquirida para a viabilidade do método. Para resolver isso, é utilizada uma técnica chamada bracketing de amostra padrão, que consiste em medir sistematicamente um zircão padrão, para adquirir um fator de correção de massa. A metodologia aplicada no CPGEO consiste em medir três vezes o padrão GJ-3 após seis grãos desconhecidos, para garantir a consistência dos dados da amostra. A ablação usa 5 mJ, 6 Hz e 29 µm de diâmetro durante 40s como condições analíticas. Um número de 70 a 100 zircões foram datados para cada amostra, com remoção de grãos alterados. A porcentagem máxima de ^{204}Pb é definida como 6% e a concordância entre as idades (porcentagem de similaridades da série de 2 decaimentos) é aceitável em mais ou menos 10%, comum em estudos de zircão detrítico (Gehrels, 2014). As idades de $^{207}Pb/^{206}Pb$ foram usadas para zircões com mais de 1,3 Ga e as idades de $^{206}Pb/^{238}U$ para grãos mais jovens (Cumming e Richards, 1975).

O tipo de dados resultantes da datação de zircão detrítico é considerado um dado distributivo por sua natureza variável contínua (Fedo et al., 2003; Vermeesch, 2019). As idades de U-Pb de zircão são tratadas com dois métodos estatísticos: estimador de densidades de kernel (KDE; Equação 1) e distribuição de idade cumulativa (CAD; Equação 2). Para a ordenação das amostras, é utilizado um dimensionamento multidimensional não-métrico (MDS), aplicando os conceitos de *Kolmogorov-Smirnov* e a estatística de estresse. As estatísticas aplicadas em zircão detrítico apresentadas nos artigos I e II aplicam o pacote *Provenance* (Vermeesch et al., 2016) no *software* R.

O KDE é uma técnica de estimativa para funções de densidade de probabilística (Silverman, 1986), gerada pela seguinte equação:

$$KDEx(t) = \frac{1}{n}\sum_{i=1}^{n} \mathrm{K(t|}x_i, \mathrm{bw)}$$

Onde o K é o kernel e o bw é a largura de banda. O kernel consiste na forma dos “picos”, na qual se utiliza a distribuição normal gaussiana - uma curva de sino. A seleção da largura de banda é um ponto crítico, como mostra Vermeesch (2012), sugerindo o uso do algoritmo de Botev (2010), como a seleção automática da largura de banda. A principal vantagem do KDE de outras funções de densidade é sua independência em relação ao tamanho da amostra (Vermeesch, 2012).

A densidade de idade cumulativa é uma função de etapa, estabelecendo uma classificação para as idades (Vermeesch, 2007, Anderson et al., 2019), evitando os efeitos de suavização gerados pela seleção de largura de banda no KDE. A fórmula CAD é:

$$CAD(t) = \frac{1}{n}\sum_{i=1}^{n} \mathrm{1(t} < t_i)/\mathrm{n}$$

O conjunto de dados MDS para zircão detrítico não é métrico, aplicando valores de dissimilaridades não euclidianos, através da mesma forma de variação ranqueada como no CAD. As diferenças das amostras são obtidas usando a distância *Kolmogorov-Sminof* (K-S), calculada como:

$$\delta = [i, j] = f(KS[i, j])$$

Onde KS [i, j] é a distância K-S em relação às amostras i e j usando a função de passo f como transformação monotônica. Em resumo, o teste K-S usa a diferença absoluta máxima entre 2 distribuições cumulativas (Vermeesch et al., 2016).

As três abordagens estatísticas diferentes têm vantagens e desvantagens, o KDE exibe os picos de idade claramente ao longo do eixo X (idades); no entanto, falha ao mostrar corretamente as diferenças entre amostras. O CAD ilustra as variações entre as amostras, usando distâncias K-S, embora o empilhamento de amostras em determinadas faixas de idade dificulte a correta interpretação. A técnica MDS apresenta um agrupamento de amostras, demonstrando o grau de dissimilaridade entre elas, mesmo para grandes conjuntos de dados, mas não fornece o elemento (no caso as idades) na qual as amostras se parecem. Portanto, as três técnicas são complementares e devem ser usadas para reconhecer adequadamente os padrões geológicos na datação por zircão detrítico.

3.5 Ensaio de velocidade acústica

Ondas acústicas ou sísmicas são ondas elásticas, classificadas entre os tipos P e S, causadas pela propagação da vibração mecânica (Yang e Wei, 2017). A onda P (primária ou longitudinal) é composta por uma série de dilatações e compressões e é, por definição, a onda sísmica mais rápida. A onda S (secundária ou cisalhamento) ocorre perpendicular à propagação da onda, mais lentamente em relação à onda P (Lowrie, 2019). As velocidades acústicas variam devido às propriedades elásticas e de densidade de um material sólido. O arenito permeável, por exemplo, apresenta valores que variam de 2500 e 4500 m/s (Yang; Wei, 2017). As propriedades físicas do arenito podem ser alteradas pelo processo diagenético, como cimentação ou empacotamento, assim a velocidade ultrassônica pode ser usada como proxy da variação do reservatório dentro de bacias sedimentares (Schon, 2015).

A metodologia do experimento de velocidade ultrassônica segue: medição da altura da amostra (8 a 10 vezes) (1); fixação da amostra no suporte do plugue entre os transdutores (diferentes para as ondas P e S) (2); identificação do tempo de atraso para a chegada da primeira onda no osciloscópio (3). A figura 26 ilustra o processo

de medição ultrassônica realizado no Laboratório de petrofísica e geomecânica da Universidade de Aberdeen (Departamento de Geologia e Geologia do Petróleo).

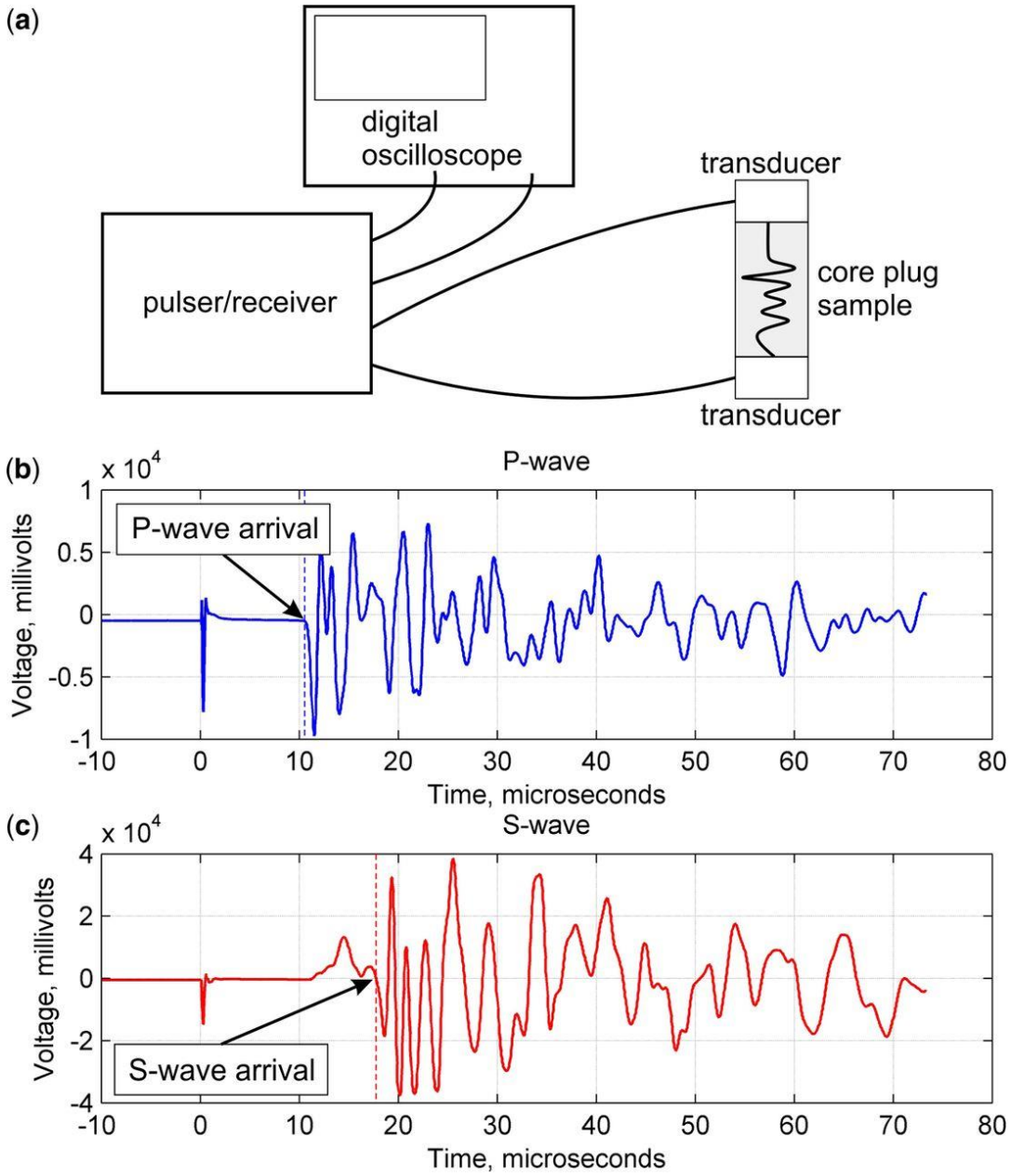

Figura 26 - Esquema de medição de velocidades ultrassônicas: a) trajetória do sinal do indutor para amostra retornando ao osciloscópio para análise de onda; b-c) identificação do atraso das ondas P e S (extraído de Healy et al., 2015).

A maior dificultada da técnica consiste na identificação adequada da chegada da onda S. A identificação da onda P é clara, conforme apresentado na Figura 26b, no entanto, a onda S induz uma onda P parasita que, por definição, é mais rápida que a onda S, resultando em uma sobreposição dos 2 tipos de ondas. A rotação do

transdutor (90º) ajuda a identificar adequadamente a onda S. A figura 26C mostra a assinatura característica da soma das fases das ondas P e S, inclinando a forma da onda. A técnica é repetida pelo menos três vezes para identificar adequadamente a onda S. A Figura 27 mostra as etapas para a medição da onda P em laboratório.

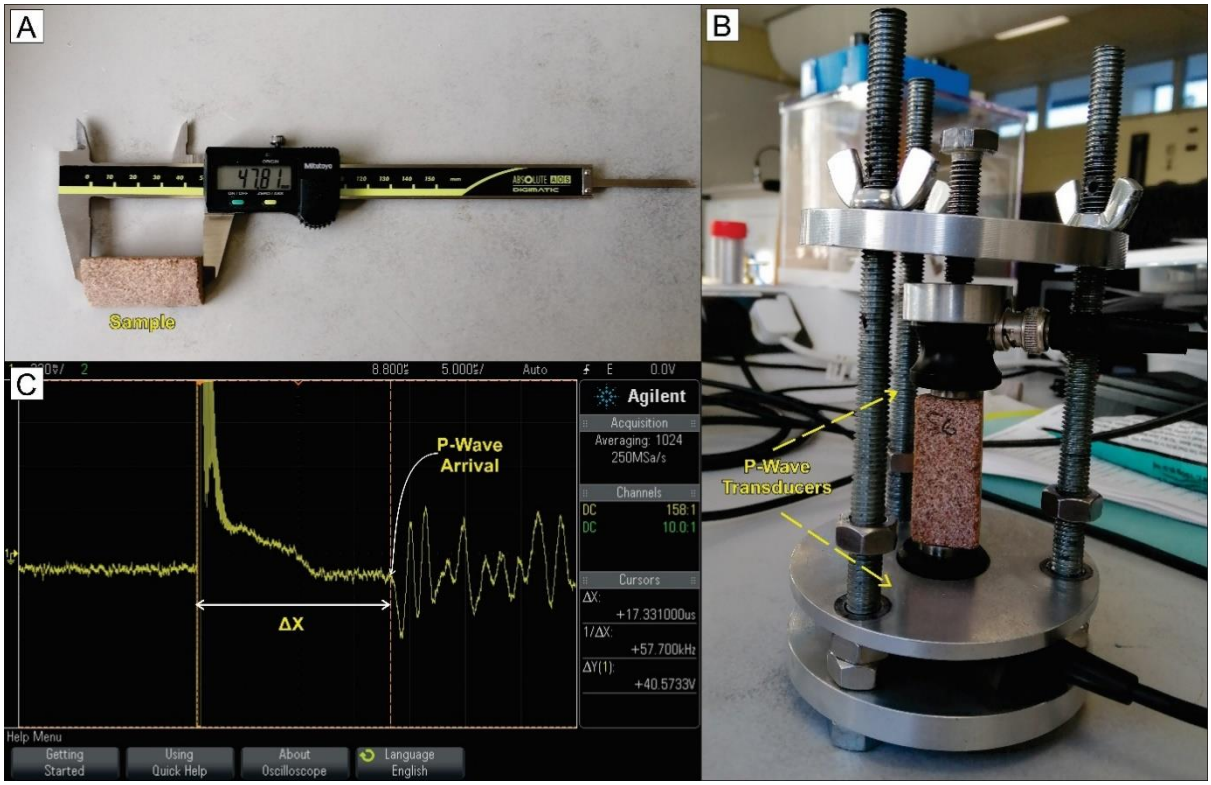

Figura 27 - Experimento de velocidade acústica ultrassônica. A- Medição do plugue com paquímetro digital; B- Porta amostra com transdutores na base e topo de amostras para medição de onda P; C- Medição do ΔX (tempo de atraso) no *software*.

3.6 Ensaio de porosidade

Os experimentos de porosidade foram realizados usando a técnica de Arquimedes, com base em seu princípio homônimo: “força de empuxo é igual ao peso do fluido”. Essa técnica foi utilizada devido aos pequenos plugues disponíveis, considerando que estes foram obtidos em poços da década 70, em programas de prospecção de carvão, gentilmente cedidos pela Companhia de Pesquisa em Recursos Minerais (CPRM). A metodologia aplicada consiste em: secagem dos plugues (forno entre 50-60ºC) por 4 a 6 horas (1); pesagem dos plugues secos em balança (escala de 0,1g), para obter a massa real da rocha (2); saturação dos poros com água destilada usando um esquema de bomba de vácuo (3 a 6h) (Fig. 28A) (3); pesagem do plug saturado submerso em água destilada - obtendo o peso submerso

(4); pesagem do plug saturado em agua, obtendo a massa da rocha saturada em água (Fig. 28B) (5). A maior dificuldade da técnica consiste na correta identificação da “molhabilidade” das superfícies dos plugues. A técnica necessita do peso da água nos poros da rocha e não da superfície, portanto qualquer gota de água superficial deve ser removida, porém é difícil estabelecer o grau de remoção da água, para não retirar a água dos poros. O artigo III mostra que a porosidade experimental foi correspondente à porosidade obtida pela petrografia, indicando a eficiência da técnica. A porosidade final foi obtida com a seguinte equação:

$$\phi = V \frac{\frac{W_{saturata} - W_{seca}}{\rho_{fluido}}}{\frac{W_{saturatea} - W_{submersa}}{\rho_{fluido}}}$$

Onde W é a massa do plugue (seco, saturado e submerso) e ρ é a densidade do fluido (água destilada = 1 g/cm^3).

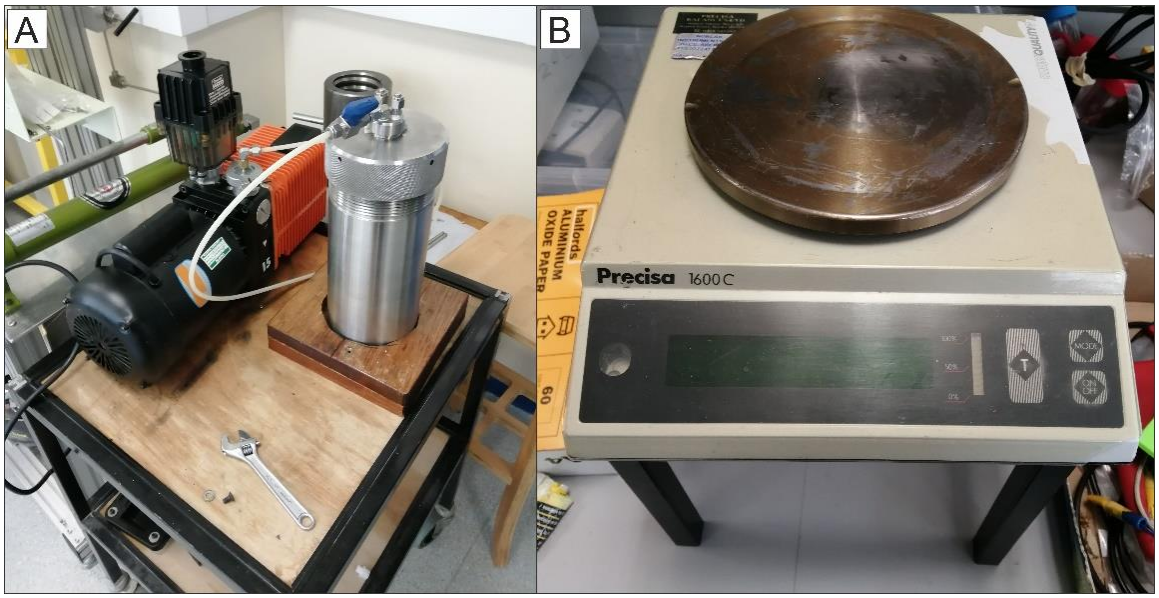

Figura 28 - Experimento físico para medição de porosidade em plugues A- Câmara acoplada a bomba à vácuo; B- Balança.

CAPÍTULO 4 - RESUMO DOS RESULTADOS

Esta tese apresenta uma ampla discussão sobre controles de proveniência de arenitos eólicos e qualidade de reservatórios de arenito eólico interacamadados com derrames basálticos. Os artigos I e II apresentam e discutem a variabilidade da proveniência- lateral e estratigráfica- do deserto do Botucatu. O artigo III documenta as modificações petrofísicas e petrográficas dos depósitos eólicos afetados pelos fluxos de lava síncronos, avaliando seu impacto nas propriedades de reservatório dos pacotes siliciclásticos.

Os depósitos eólicos na margem sul da bacia do Paraná durante a deposição de Botacatu apresentam uma composição média de $Qt_{89}F_8L_3$ e uma predominância de minerais pesados com alta resistência a alteração química e física (zircão-turmalina-rutilo) com uma composição média de ZTR_{84}. A margem Norte apresenta uma composição de sedimentos semelhante, composto por $Q_{91}F_6L_2$ e ZTR_{86}. Os dados da idade do zircão detrítico mostram que os zircões de idade Cambriana e Neoproterozoica são a principal contribuição sedimentar para o arenito Botucatu ao longo de toda a bacia, com contribuições subsidiárias de grãos com idade Toniano-Steniano e Orosiriano-Riaciano. Os grãos de idade permiana estão presentes ao longo de todo Botucatu, porém sua aparição na região norte está controlada a pacotes basais da bacia. As assembleias de minerais pesados revelam composições anômalas, caracterizadas por picos em granada, epidoto e apatita, sugerindo contribuições sedimentares locais. A região Sul apresenta uma variação lateral acentuada em todos os conjuntos de dados, com grãos mais grossos, quartzosos, grãos de zircão detríticos mais antigos (> 900 Ma), aumentando progressivamente no sentido oeste (Uruguai). Na margem Norte, não há alterações laterais consistentes, embora haja um aumento da idade Cambriana/ Neoproterozoica da base do deserto em direção aos pacotes *intratrap*. O atual estudo de proveniência da sucessão eólica de Botucatu fornece os primeiros conjuntos de dados de proveniência abrangente da Bacia do Paraná e contribui para nossa compreensão sobre os controles de proveniência e as rotas de sedimentos, bem como a reciclagem em sistemas sedimentares antigos, particularmente desertos. O grande conjunto de dados indica, em particular, que o sedimento de Botucatu é notavelmente similar, sob diversos aspectos, por milhares de quilômetros. A composição alta de quartzosa e rica em ZTR

demonstrou uma história policíclica para o sedimento, principalmente retrabalhada a partir das unidades subjacentes da Bacia do Paraná (ver Figura 9 do artigo I).

Ferramentas estatísticas foram usadas para extrair informações adicionais do conjunto de dados, demonstrando que, mesmo em uma unidade policíclica altamente retrabalhada, como o Botucatu, as ferramentas de proveniência podem ser usadas para fornecer um entendimento maior dos processos sedimentares. A variação lateral presente ao longo da margem sul demonstra a variabilidade nas composições sedimentares, indicando que o embasamento teve uma influência indireta na proveniência dos sedimentos. O plot MDS (Artigo I- Fig. 9) mostra que os pacotes *intratrap* e os sedimentos basais do deserto tendem a se agrupar separadamente, indicando uma mudança ascendente na composição - como um aumento nas idades Neoproterozoicas e uma diminuição nas idades Toniana-Steniano. Assim, a margem norte indica variações correlacionadas ao próprio processo de policíclico, possivelmente devido ao retrabalhamento de diferentes unidades antigas da Bacia do Paraná, de acordo com a evolução do deserto. O capítulo 2.1 ("*Controles de proveniência em sistemas desérticos*") apresenta exemplos de registros modernos e antigos do deserto, demonstrando como as ferramentas de proveniência podem identificar diferentes composições sedimentares relacionadas a diferentes processos sedimentares atuantes em desertos atuais e antigos. Alguns exemplos disso são o sistema fluvial transcontinental Jurássico do Colorado *Plateau* ou o sedimento do deserto da Namíbia sendo controlado pelas *long-shore currents* da costa Sudeste africana. Em comparação, o sistema eólico de Botucatu tem uma história policíclica relativamente simples, mas o conjunto de dados de proveniência mostra nuances e sutilezas que demonstram variabilidade interna nas areias da Bacia do Paraná.

O intemperismo e a alteração diagenética das composições de arenito são componentes importantes da análise de proveniência de unidades antigas e, sem entender seu impacto potencial, podem restringir a interpretação e limitar a importância dos estudos de proveniência. Os resultados dos artigos I e II demonstram como os arenitos intemperizados ainda podem registrar variações de composição, como observado pela presença de assembleias de minerais pesados anômalas. Além disso, a assinatura de zircão detrítico mostrou-se útil não apenas como parâmetro de idade para correlação com áreas-fonte, mas também como proxy para a mistura de diferentes fontes de sedimentos e alterações na proveniência. Os padrões de proveniência registrados em uma sucessão sedimentar derivada de retrabalhamento

basinal, como o arenito de Botucatu, indicam como as técnicas de proveniência com proxy múltiplo podem auxiliar no entendimento dos processos de geração, transporte e fornecimento de sedimentos para desertos antigos.

O artigo III ("*The effect of basaltic lava flows on the petrophysical properties and diagenesis of interbedded aeolian sandstones*") apresenta um estudo da diagênese e atributos petrofísicos de arenitos eólicos pré e sin-vulcânicos. Foram amostrados 72 plugues em 5 poços da região litorânea do estado do Rio Grande do Sul, que apresentam valores de porosidade entre 2 a 26% e velocidades acústicas de 2,8 a 5,0 kms^{-1}. Na zona de contato entre sedimento e lava (entre 0,1 a 1m), apresenta valores de porosidade entre 0 e 7% com velocidades ultrassônicas de 4,0 a 5,0 kms^{-1}. Em detalhes, as variações petrofísicas são explicadas por três estilos de diagênese: autigênese de fases ricas em Mg- dol (tipo 1); dissolução química precoce de grãos de quartzo (tipo 2); e cimentação poiquilotópica de calcita e esmectita por enchimento de poros (tipo 3). A área alterada diagenéticamente é restrita a distâncias inferiores a 1m do contato da lava do sedimento, sugerindo que o efeito pode não ser significativamente prejudicial ao análogo do reservatório eólico. As lavas da Serra Geral são caracterizadas por lavas fraturadas e vesiculadas, com altos valores de porosidade (até 30%); assim, uma vedação/ defletor adicional pode ser uma vantagem para um reservatório. Semelhanças podem ser traçadas entre as vias diagenéticas identificadas em Botucatu e outros estudos de interação sedimento-ígnea. Por exemplo, a diagênese de contato quente descrita por Grove et al. (2017) da Formação *Twyfelfontain* é semelhante a diagênese do tipo 1 no Botucatu. No estudo de um sistema hidrotérmico de Svalbard por Haile (2019) na Formação *Wilhelmøya*, também estão presentes semelhanças com a via diagênese do Tipo 1 em Botucatu, incluindo clorito autigênico, alteração dos feldspatos e dissolução do cimento carbonato. Por fim, a dissolução química associada à intrusão magmática descrita por Wilson et al. (2019) da Entrada Sandstone, é semelhante a diagênese tipo 2 do Botucatu - com estilolitos e contatos suturados. A comparação entre as relações extrusivas lava-sedimento descritas em Botucatu e os sistemas intrusivos documentados acima mostra que caminhos diagenéticos semelhantes ocorrem nas relações extrusivas e intrusivas de contato. Um novo aspecto do estudo é mostrar que rochas extrusivas podem promover alterações diagenéticas em estratos siliciclásticos, através de uma variedade de processos diferentes: (1) dissolução química do arenito causada pelo aumento da sobrecarga de estacas de lava; (2)

autigênese hidrotérmica produzida pela circulação das águas subterrâneas associada a temperaturas mais altas relacionadas à colocação de lava. As propriedades do reservatório são constantemente modificadas por facetas distintas da interação com a lava, ilustrando o efeito direto do vulcanismo na porosidade e permeabilidade na unidade siliciclástica. A tese demonstrou, com sucesso, que as lavas básicas da Formação Serra Geral impactaram diretamente a diagênese das unidades de arenito entrelaçadas, alterando localmente as propriedades do reservatório do arenito de Botucatu.

CAPÍTULO 5 - CONCLUSÕES

Os artigos I e II caracterizam e explicam as assinaturas de proveniência dos sedimentos fornecidos ao longo do *erg* Botucatu, buscando responder um dos objetivos gerais da tese: "*Compreender os controles de proveniência no deserto Cretáceo do Botucatu*". Para abordar adequadamente o objetivo, três questões científicas foram usadas, abordando controles de proveniência sob diferentes perspectivas.

O início do vulcanismo desencadeou mudanças ambientais que influenciam a composição do sedimento? - O estudo de proveniência ao longo da evolução estratigráfica da unidade apresenta diferentes resultados para as regiões Sul e Norte. A região Sul apresenta uma proveniência semelhante desde a base até aos pacotes eólicos intratrap. Em contraste, o Norte da Formação Botucatu mostra uma variação sutil e progressiva da proveniência da base do deserto até os depósitos *intratraps*. As alterações progressivas e não abruptas na proveniência demonstram que não há impacto ambiental significativo do vulcanismo na composição dos sedimentos. A variabilidade da proveniência é controlada principalmente pelo retrabalhamento intrabasinal das unidades sedimentares mais antigas, ao invés de um suprimento direto de sedimentos de primeiro ciclo trazidos pelo sistema eólico.

O embasamento desempenha um papel importante no fornecimento de sedimentos à bacia? - As assinaturas de zircão detrítico demonstram uma compatibilidade com os cinturões orogênicos Cambrianos-Neoproterozoicos do embasamento, espalhados ao longo da América do Sul, na qual a bacia se deposita. Sob esta ótica, as assinaturas de zircão detrítico são compatíveis as do embasamento, indicando que estes controlavam a composição dos sedimentos do deserto de Botucatu. No entanto, a natureza policíclica do sedimento sugere um efeito indireto desses terrenos, diluídos pela sedimentação Paleozoica-Mesozoica no SO do Gondwana. O sedimento policíclico no deserto do Botucatu sugere que sua areia foi derivada de unidades subjacentes da Bacia do Paraná. Ainda assim, os dados de proveniência da região Sul mostram variações no embasamento estão refletidas nas composições encontradas, como, por exemplo, o enriquecimento em grãos antigos (>900 Ma), quartzo e ZTR na região do Uruguai, compatível com o embasamento mais antigo – o Craton La Plata. O exemplo ilustra que unidades altamente

retrabalhadas podem conter assinaturas de seu material de origem, mesmo que isso tenha sido sujeito a vários ciclos de erosão e deposição em uma bacia sedimentar.

O sistema de vento bimodal atuantes no deserto controlam composição dos sedimentos? - Os dados de proveniência mostram uma composição notavelmente semelhante em toda a bacia, com arenitos ricos em quartzo e ZTR e assinaturas detríticas semelhantes. A comparação dos sistemas eólicos com as direções opostas do vento (margem sul e norte) deveria produzir composições identificáveis; no entanto, a ampla composição semelhante demonstra que o regime eólico não afetou a proveniência. No geral, o estudo revela que os controles de procedência em Botucatu são, principalmente, restritos à história de sedimentos policíclicos da Bacia do Paraná. As alterações de proveniência lateral e estratigráfica são sutis e estão correlacionadas com o retrabalho de unidades distintas da bacia, conforme mostrado no artigo I.

O segundo objetivo da tese, "**Determinar se, e como, as lavas básicas extrusivas afetaram a diagênese e, por consequência, as propriedades dos reservatórios das unidades eólicas**", avalia a variabilidade diagenética e de qualidade do reservatório no contato entre pacotes eólicos e de lava, pormenorizado no artigo III.

Os pacotes basálticos produzem alterações diagenéticas através de autigênese ou compactação no arenito? - A análise petrográfica demonstra a existência de 2 tipos de caminhos diagenéticos desencadeados a partir da atividade vulcânica. O tipo 1 apresenta dissolução química nos contatos de grãos, provavelmente associada à sobrecarga de basalto em arenitos. O tipo 2 revela um sistema hidrotermal responsável pela autigênese precoce de fases magnesianas - clorita e dolomita. Essa variabilidade diagenética gerada pela interação lava-sedimento ilustra o quanto estas interações podem ser.

A qualidade do reservatório da Formação Botucatu é afetada de alguma forma por possíveis alterações diagenéticas? - O conjunto de dados petrofísicos e petrográficos demonstram como a porosidade diminui perto do contato (até 1m). No entanto, a porosidade tende a apresentar valores típicos após as alterações diagenéticas, indicando que a zona afetada pode servir com selo ou barreira ao fluxo de fluidos.

Em síntese, o estudo do reservatório da Formação Botucatu pode ser um análogo valioso para as unidades em subsuperfície, demonstrando que rochas ígneas extrusivas afetam a qualidade do reservatório.

5.1 Potenciais estudos futuros

A tese aplicou várias técnicas para os estudos de proveniência e de qualidade de reservatório, resultando em possíveis novas oportunidades de pesquisa, buscando expandir nossa compreensão da área estudada. A variação de proveniência em Botucatu poderia ser refinada com um estudo mais amplo, por exemplo, na contraparte africana da bacia, podendo ser utilizada como comparação e ampliação da área estudada A Formação *Twyfelfountain* na Namíbia apresenta afloramentos excelentes de intervalos vulcano-sedimentares podendo ser um candidato válido para isso. Além disso, as partes do sul da América do Sul, em particular na Bacia Chaco-Paraná (Argentina), podem ser a chave para resolver a contribuição Jurássica encontrada.

Em termos de técnicas, análises geoquímicas adicionais podem auxiliar no entendimento das contribuições sedimentares locais - química mineral em granada, epidoto e turmalina, elementos traço e datação de U-Pb em apatita - são ferramentas poderosas de proveniência que seriam possivelmente interessantes na área de estudo. Devido à abundância de zircão em todo o conjunto de dados, a datação isotópica in situ de Lu-Hf pode ser aplicada para refinar os picos Neoproterozoico e Toniano-Steniano, estabelecendo as rochas-fontes para estes intervalos. Além disso, a geoquímica de elementos menores e de maiores em zircão pode ser útil para determinar fontes específicas.

No estudo de reservatório, análises petrofísicas adicionais e química mineral poderiam ser usadas para responder a mais perguntas. Devido ao pequeno tamanho dos plugues disponíveis, não foram realizadas experiências de permeabilidade. No futuro, análises de porosidade e permeabilidade conjuntas He produziriam uma caracterização refinada do reservatório. Outro estudo possível, consiste no entendimento dos reservatórios *intratrap* em escala de afloramento - verificando quão homogêneos são os atributos petrofísicos em um espaço tridimensional. Uma modelagem petrofísica, petrográfica e modelamento 3-D integrada dos corpos de areia pode ser usada como uma correlação com as unidades de subsuperfície. Na

perspectiva do processo, os efeitos hidrotermais e de deformação por sobrecarga litostática poderiam ser estudados em mais detalhe. Uma maneira possível é determinar com precisão as faixas de pressão-temperatura para cada geração de tipo de diagênese, aplicando ferramentas experimentais geoquímicas e físicas das rochas. Por exemplo, a análise geoquímica em clorita pode ser usada para adquirir a faixa de temperatura para o sistema hidrotérmico ou a análise isotópica por dolomita (C, O) gera os tipos de água subterrânea e a temperatura para a cristalização.

REFERÊNCIAS

Almeida, F. D. (1954). Botucatu, um deserto triássico da América do Sul. Notas Preliminares e Estudos da Divisão de Geologia e Mineralogia do DNPM, 86, 1-21.

Andersen, T., Elburg, M. A., & Magwaza, B. N. (2019). Sources of bias in detrital zircon geochronology: Discordance, concealed lead loss and common lead correction. Earth-Science Reviews, 102899.

Assine, M. L., Soares, P. C., & Milani, É. J. (1994). Sequências tectono-sedimentares mesopaleozóicas da Bacia do Paraná, Sul do Brasil. Revista Brasileira de Geociências, 24(2), 77-89.

Barreto, C. J. S., de Lima, E. F., Scherer, C. M., & Rossetti, L. D. M. M. (2014). Lithofacies analysis of basic lava flows of the Paraná igneous province in the south hinge of Torres Syncline, Southern Brazil. Journal of Volcanology and Geothermal Research, 285, 81-99.

Blott, S. J., & Pye, K. (2001). GRADISTAT: a grain size distribution and statistics package for the analysis of unconsolidated sediments. Earth surface processes and Landforms, 26(11), 1237-1248.

Boggs Jr, S., & Boggs, S. (2009). Petrology of sedimentary rocks. Cambridge university press.

Botev, Z. I., Grotowski, J. F., & Kroese, D. P. (2010). Kernel density estimation via diffusion. The annals of Statistics, 38(5), 2916-2957.

Bigarella, J. J., & Salamuni, R. (1961). Early Mesozoic wind patterns as suggested by dune bedding in the Botucatu Sandstone of Brazil and Uruguay. Geological Society of America Bulletin, 72(7), 1089-1105.

Buller, A. T., & McManus, J. (1979). Sediment sampling and analysis. Estuarine hydrography and sedimentation, 87-130.

Burley, S. D., Kantorowicz, J. D., & Waugh, B. (1985). Clastic diagenesis. Geological Society, London, Special Publications, 18(1), 189-226.

Campos, L. F. G. (1889) Seção geológica: São Paulo. Relatório de comunicação geográfica e geológica da província de São Paulo, p. 21-3.

Chester, J. S., Lenz, S. C., Chester, F. M., & Lang, R. A. (2004). Mechanisms of compaction of quartz sand at diagenetic conditions. Earth and Planetary Science Letters, 220(3-4), 435-451.

Choquette, P. W., & Pray, L. C. (1970). Geologic nomenclature and classification of porosity in sedimentary carbonates. AAPG bulletin, 54(2), 207-250.

Cumming, G. L., & Richards, J. R. (1975). Ore lead isotope ratios in a continuously changing Earth. Earth and Planetary Science Letters, 28(2), 155-171.

Curtis, C. D. (1977). Geochemistry: Sedimentary geochemistry: environments and processes dominated by involvement of an aqueous phase. Philosophical Transactions of the Royal Society of London. Series A, Mathematical and Physical Sciences, 286(1336), 353-372.

Dickinson, W. R., & Gehrels, G. E. (2009). U-Pb ages of detrital zircons in Jurassic eolian and associated sandstones of the Colorado Plateau: Evidence for transcontinental dispersal and intraregional recycling of sediment. Geological Society of America Bulletin, 121(3-4), 408-433.

Dickinson, W. R., & Gehrels, G. E. (2003). U–Pb ages of detrital zircons from Permian and Jurassic eolian sandstones of the Colorado Plateau, USA: paleogeographic implications. Sedimentary Geology, 163(1-2), 29-66.

Ernesto, M., Raposo, M. I. B., Marques, L. S., Renne, P. R., Diogo, L. A., & De Min, A. (1999). Paleomagnetism, geochemistry and 40Ar/39Ar dating of the North-eastern Paraná Magmatic Province: tectonic implications. Journal of Geodynamics, 28(4-5), 321-340.

Eynatten, H., & Dunkl, I. (2012). Assessing the sediment factory: the role of single grain analysis. Earth-Science Reviews, 115(1-2), 97-120.

Farrant, A. R., Mounteney, I., Burton, A., Thomas, R. J., Roberts, N. M., Knox, R. W., & Bide, T. (2019). Gone with the wind: dune provenance and sediment recycling in the northern Rub'al-Khali, United Arab Emirates. Journal of the Geological Society, 176(2), 269-283.

Fedo, C. M., Sircombe, K. N., & Rainbird, R. H. (2003). Detrital zircon analysis of the sedimentary record. Reviews in Mineralogy and Geochemistry, 53(1), 277-303.

Folk, R. L. (1974). Petrology of sedimentary rocks: Austin, Texas.

França, A. B., Araújo, L. M., Maynard, J. B., & Potter, P. E. (2003). Secondary porosity formed by deep meteoric leaching: Botucatu eolianite, southern South America. AAPG bulletin, 87(7), 1073-1082.

Garzanti, E., & Andò, S. (2019). Heavy Minerals for Junior Woodchucks. Minerals, 9(3), 148.

Garzanti, E., Vermeesch, P., Andò, S., Vezzoli, G., Valagussa, M., Allen, K., ... & Al-Juboury, A. I. (2013). Provenance and recycling of Arabian desert sand. Earth-Science Reviews, 120, 1-19.

Garzanti, E., Resentini, A., Andò, S., Vezzoli, G., Pereira, A., & Vermeesch, P. (2015). Physical controls on sand composition and relative durability of detrital minerals during ultra-long distance littoral and aeolian transport (Namibia and southern Angola). Sedimentology, 62(4), 971-996.

Garzanti, E., Dinis, P., Vermeesch, P., Andò, S., Hahn, A., Huvi, J., ... & Vezzoli, G. (2018). Sedimentary processes controlling ultralong cells of littoral transport: Placer formation and termination of the Orange sand highway in southern Angola. Sedimentology, 65(2), 431-460.

Garzanti, E. (2019). Petrographic classification of sand and sandstone. Earth-science reviews, 192, 545-563.

Garzanti, E., Dinis, P., Vermeesch, P., Andò, S., Hahn, A., Huvi, J., ... & Vezzoli, G. (2018). Dynamic uplift, recycling, and climate control on the petrology of passive-margin sand (Angola). Sedimentary geology, 375, 86-104.

Gehrels, G. E., Valencia, V. A., & Ruiz, J. (2008). Enhanced precision, accuracy, efficiency, and spatial resolution of U-Pb ages by laser ablation–multicollector–inductively coupled plasma–mass spectrometry. Geochemistry, Geophysics, Geosystems, 9(3).

Gehrels, G. E., Blakey, R., Karlstrom, K. E., Timmons, J. M., Dickinson, B., & Pecha, M. (2011). Detrital zircon U-Pb geochronology of Paleozoic strata in the Grand Canyon, Arizona. Lithosphere, 3(3), 183-200.

Gehrels, G. (2014). Detrital zircon U-Pb geochronology applied to tectonics. Annual Review of Earth and Planetary Sciences, 42, 127-149.

Grove, C., Jerram, D. A., Gluyas, J. G., & Brown, R. J. (2017). Sandstone diagenesis in sediment–lava sequences: exceptional examples of volcanically driven diagenetic compartmentalization in Dune Valley, Huab Outliers, NW Namibia. Journal of Sedimentary Research, 87(12), 1314-1335.

Haile, B. G., Czarniecka, U., Xi, K., Smyrak-Sikora, A., Jahren, J., Braathen, A., & Hellevang, H. (2019). Hydrothermally induced diagenesis: Evidence from shallow marine-deltaic sediments, Wilhelmøya, Svalbard. Geoscience Frontiers, 10(2), 629-649.

Healy, D., Neilson, J. E., Haines, T. J., Michie, E. A., Timms, N. E., & Wilson, M. E. (2015). An investigation of porosity–velocity relationships in faulted carbonates using outcrop analogues. Geological Society, London, Special Publications, 406(1), 261-280.

Hiess, J., Condon, D. J., McLean, N., & Noble, S. R. (2012). 238U/235U systematics in terrestrial uranium-bearing minerals. Science, 335(6076), 1610-1614.

Hubert, J. F. (1962). A zircon-tourmaline-rutile maturity index and the interdependence of the composition of heavy mineral assemblages with the gross composition and texture of sandstones. Journal of Sedimentary Research, 32(3), 440-450.

Hurst, A., Morton, A., Scott, A., Vigorito, M., & Frei, D. (2017). Heavy-Mineral Assemblages In Sandstone Intrusions: Panoche Giant Injection Complex, California, Journal of Sedimentary Research, 87(4), 388-405.

Ingersoll, R. V., Bullard, T. F., Ford, R. L., Grimm, J. P., Pickle, J. D., & Sares, S. W. (1984). The effect of grain size on detrital modes: a test of the Gazzi-Dickinson point-counting method. Journal of Sedimentary Research, 54(1), 103-116.

Jaffey, A. H., Flynn, K. F., Glendenin, L. E., Bentley, W. T., & Essling, A. M. (1971). Precision measurement of half-lives and specific activities of U 235 and U 238. Physical review C, 4(5), 1889.

de Assis Janasi, V., de Freitas, V. A., & Heaman, L. H. (2011). The onset of flood basalt volcanism, Northern Paraná Basin, Brazil: A precise U–Pb baddeleyite/zircon age for a Chapecó-type dacite. Earth and Planetary Science Letters, 302(1-2), 147-153.

Jerram, D. A. (2001). Visual comparators for degree of grain-size sorting in two and three-dimensions. Computers & geosciences, 27(4), 485-492.

Košler, J., & Sylvester, P. J. (2003). Present trends and the future of zircon in geochronology: laser ablation ICPMS. Reviews in mineralogy and geochemistry, 53(1), 243-275.

Krumbein, W. C. (1934). Size frequency distributions of sediments. Journal of sedimentary Research, 4(2), 65-77.

Lavina, E. L. The Passa Dois Group. In: International Gondwana Symposium: Field excursion guide book. São Paulo: Instituto de Geociências, p. 24-30. 1988.

Lowrie, W., & Fichtner, A. (2019). Fundamentals of geophysics. Cambridge university press.

Pettijohn, F. J. (1941). Persistence of heavy minerals and geologic age. The Journal of Geology, 49(6), 610-625.

Mange, M. A., & Maurer, H. (2012). Heavy minerals in colour. Springer Science & Business Media.

McBride, E. F., & EF, M. (1977). Secondary Porosity-Importance In Sandstone Reservoirs In Texas.

Milani, E. J.; Melo, J. H. G., Souza, P. A.; Fernandes, L. A.; França, A. B. (2007). Bacia do Paraná. In: Cartas Estratigráficas. Boletim de Geociências da Petrobras, Rio de Janeiro, v. 15, n. 2, p. 265-287.

Milani, E. J., Faccini, U. F., Scherer, C. M., Araújo, L. M. D., & Cupertino, J. A. (1998). Sequences and stratigraphic hierarchy of the Paraná Basin (Ordovician to Cretaceous), southern Brazil. Boletim IG-USP, 29, 125-173.

Milliken, K. L., & Choh, S. J. (2011). Carbonate petrology: An interactive petrography tutorial, v. 1.0. Discovery Series, Tulsa, Oklahoma, AAPG.

Milliken, K. L., & Curtis, M. E. (2016). Imaging pores in sedimentary rocks: foundation of porosity prediction. Marine and Petroleum Geology, 73, 590-608.

Morad, S., Ketzer, J. M., & De Ros, L. F. (2000). Spatial and temporal distribution of diagenetic alterations in siliciclastic rocks: implications for mass transfer in sedimentary basins. Sedimentology, 47, 95-120.

Morton, A. C. (1985). Heavy minerals in provenance studies. In Provenance of arenites (pp. 249-277). Springer, Dordrecht.

Morton, A. C., & Hallsworth, C. (1994). Identifying provenance-specific features of detrital heavy mineral assemblages in sandstones. Sedimentary Geology, 90(3-4), 241-256.

Morton, A. C., & Hallsworth, C. R. (1999). Processes controlling the composition of heavy mineral assemblages in sandstones. Sedimentary geology, 124(1-4), 3-29.

Morton, A., & McGill, P. (2018). Correlation of hydrocarbon reservoir sandstones using heavy mineral provenance signatures: Examples from the North Sea and adjacent areas. Minerals, 8(12), 564.

Peate, D. W. (1997). The Parana-Etendeka province. Geophysical Monograph-American Geophysical Union, 100, 217-246.

Peate, D. W., Hawkesworth, C. J., & Mantovani, M. S. (1992). Chemical stratigraphy of the Paraná lavas (South America): classification of magma types and their spatial distribution. Bulletin of Volcanology, 55(1-2), 119-139.

Pettijohn, F. J., Potter, P. E., & Siever, R. 1973, Sand and sandstone.

Piccirilo, E. M., & Melfi, A. J. (1988). The Mesozoic flood volcanism of the Paraná Basin. São Paulo: Universidade de São Paulo, Instituto Astronômico e Geofísico.Pinto et al., 2011

Pullen, A., Kapp, P., McCallister, A. T., Chang, H., Gehrels, G. E., Garzione, C. N., ... & Ding, L. (2011). Qaidam Basin and northern Tibetan Plateau as dust sources for the Chinese Loess Plateau and paleoclimatic implications. Geology, 39(11), 1031-1034.

Rahl, J. M., Reiners, P. W., Campbell, I. H., Nicolescu, S., & Allen, C. M. (2003). Combined single-grain (U-Th)/He and U/Pb dating of detrital zircons from the Navajo Sandstone, Utah. Geology, 31(9), 761-764.

Renne, P. R., Ernesto, M., Pacca, I. G., Coe, R. S., Glen, J. M., Prévot, M., & Perrin, M. (1992). The age of Paraná flood volcanism, rifting of Gondwanaland, and the Jurassic-Cretaceous boundary. Science, 258(5084), 975-979.

Resentini, A., AndÒ, S., & Garzanti, E. (2018). Quantifying roundness of detrital minerals by image analysis: Sediment transport, shape effects, and provenance implications. Journal of Sedimentary Research, 88(2), 276-289.

Rittner, M., Vermeesch, P., Carter, A., Bird, A., Stevens, T., Garzanti, E., ... & Lu, H. (2016). The provenance of Taklamakan desert sand. Earth and Planetary Science Letters, 437, 127-137.

Rossetti, L., Lima, E. F., Waichel, B. L., Hole, M. J., Simões, M. S., & Scherer, C. M. (2018). Lithostratigraphy and volcanology of the Serra Geral Group, Paraná-Etendeka Igneous Province in southern Brazil: Towards a formal stratigraphical framework. Journal of Volcanology and Geothermal Research, 355, 98-114.

Rubey, W. W. (1933). The size distribution of heavy minerals within a water-laid sandstone. Journal of Sedimentary Research, 3(1), 3-29.

Bigarella, J. J., Pinto, I. D., & Becker, R. D. (Eds.). (1967). Problems in Brazilian Gondwana Geology. Instituto de Geologia.

Scherer, C. M., & Goldberg, K. (2007). Palaeowind patterns during the latest Jurassic–earliest Cretaceous in Gondwana: evidence from aeolian cross-strata of the Botucatu Formation, Brazil. Palaeogeography, Palaeoclimatology, Palaeoecology, 250(1-4), 89-100.

Scherer, C. M. S. (2000). Eolian dunes of the Botucatu Formation (Cretaceous) in southernmost Brazil: morphology and origin. Sedimentary Geology, 137(1-2), 63-84.

Scherer, C. M. (2002). Preservation of aeolian genetic units by lava flows in the Lower Cretaceous of the Paraná Basin, southern Brazil. Sedimentology, 49(1), 97-116.

Schmidt, V., & Mcdonald, D. A. (1979). Texture and recognition of secondary porosity in sandstones.

Schneider, R. L., Muhlmann, H., Tommasi, E., Medeiros, R. A., Daemon, R. A., & Nogueira, A. A. (1974). Stratigraphic review of the Paraná Basin. In Proceedings of XXVIII Congress Brasileiro de Geologia (Vol. 1, pp. 41-65).

Schön, J. H. (2015). Physical properties of rocks: Fundamentals and principles of petrophysics. Elsevier.

Yang, S., & Wei, J. (2017). Fundamentals of petrophysics. Springer Berlin Heidelberg.

Shiraiwa, S. (1994). Flexura da litosfera continental sob os Andes Centrais e a origem da Bacia do Pantanal. 110f. Tese (Doutorado), Universidade de São Paulo, São Paulo.

Silverman, B. W. Apr. 1986. Density Estimation for Statistics and Data Analysis.

Simonetti, A., Heaman, L. M., Hartlaub, R. P., Creaser, R. A., MacHattie, T. G., & Böhm, C. (2005). U–Pb zircon dating by laser ablation-MC-ICP-MS using a new multiple ion counting Faraday collector array. Journal of Analytical Atomic Spectrometry, 20(8), 677-686.

Thiede, D. S., & Vasconcelos, P. M. (2010). Paraná flood basalts: rapid extrusion hypothesis confirmed by new 40Ar/39Ar results. Geology, 38(8), 747-750.

Tucker, M. E. (Ed.). (2009). Sedimentary petrology: an introduction to the origin of sedimentary rocks. John Wiley & Sons.

Vail, P. R. (1977). Seismic recognition of depositional facies on slopes and rises.

Van der Plas, L., & Tobi, A. C. (1965). A chart for judging the reliability of point counting results. American Journal of Science, 263(1), 87-90.

Vermeesch, P. (2007). Quantitative geomorphology of the White Mountains (California) using detrital apatite fission track thermochronology. Journal of Geophysical Research: Earth Surface, 112(F3).

Vermeesch, P. (2019). Exploratory Analysis of Provenance Data Using R and the Provenance Package. Minerals, 9(3), 193.

Vermeesch, P., Resentini, A., & Garzanti, E. (2016). An R package for statistical provenance analysis. Sedimentary Geology, 336, 14-25.

Vermeesch, P. (2012). On the visualisation of detrital age distributions. Chemical Geology, 312, 190-194.

Vermeesch, P. (2013). Multi-sample comparison of detrital age distributions. Chemical Geology, 341, 140-146.

Schneider, R. L., Muhlmann, H., Tommasi, E., Medeiros, R. A., Daemon, R. A., & Nogueira, A. A. (1974). Stratigraphic review of the Paraná Basin. In Proceedings of XXVIII Congress Brasileiro de Geologia (Vol. 1, pp. 41-65).

Waichel, B. L., de Lima, E. F., Viana, A. R., Scherer, C. M., Bueno, G. V., & Dutra, G. (2012). Stratigraphy and volcanic facies architecture of the Torres Syncline, Southern Brazil, and its role in understanding the Paraná–Etendeka Continental Flood Basalt Province. Journal of Volcanology and Geothermal Research, 215, 74-82.

Wilson, M.D. & Pittman, E.D. (1979) Authigenic clays in sandstones: recognition and influence on reservoir properties and palaeoenvironmental analysis. Journal of Sedimentary Petrology, 47, 3–31.

Simonetti, A., Heaman, L. M., Hartlaub, R. P., Creaser, R. A., MacHattie, T. G., & Böhm, C. (2005). U–Pb zircon dating by laser ablation-MC-ICP-MS using a new multiple ion counting Faraday collector array. Journal of Analytical Atomic Spectrometry, 20(8), 677-686.

Worden, R. H., & Burley, S. D. (2003). Sandstone diagenesis: the evolution of sand to stone. Sandstone diagenesis: Recent and ancient, 4, 3-44.

Zheng, H., Wei, X., Tada, R., Clift, P. D., Wang, B., Jourdan, F., ... & He, M. (2015). Late oligocene–early miocene birth of the Taklimakan Desert. Proceedings of the National Academy of Sciences, 112(25), 7662-7667.

ARTIGO I - CONTROLS ON EARLY CRETACEOUS DESERT SEDIMENT PROVENANCE IN SW GONDWANA, BOTUCATU FORMATION (BRAZIL AND URUGUAY)

Sedimentology / Accepted Articles

ORIGINAL ARTICLE

Controls on Early Cretaceous desert sediment provenance in south-west Gondwana, Botucatu Formation (Brazil and Uruguay)

Gabriel Bertolini, Juliana Marques, Adrian J. Hartley, Atila A.S. DaRosa, Claiton M. S.Scherer, Miguel A.S. Basei, José C. Frantz

First published:31 January 2020
https://doi.org/10.1111/sed.12715

Abstract

The Lower Cretaceous Botucatu Formation records the development of widespread dry–aeolian desert sedimentation throughout the Paraná Basin in south-west Gondwana. To reconstruct the provenance of the aeolian sediment, petrography, granulometric analysis, U-Pb detrital zircon ages have been determined from along the southern basin margin in Rio Grande do Sul state (southern Brazil) and Uruguay (Tacuarembó region). The dataset reveals a mean composition $Qt_{89}F_8L_3$, comprising very fine to medium-grained quartzose and feldspatho-quartzose framework. Heavy minerals analysis reveals an overall dominance of zircon, tourmaline and rutile grains (mean $ZTR_{0.84}$) with sporadic garnet, epidote and pyrolusite occurrences. The detrital zircon U-Pb ages are dominated by Cambrian to Neoproterozoic (515 to 650 Ma), Tonian Stenian (900 to 1250 Ma) and Orosirian to Rhyacian (1.8 to 2.2 Ga) material. The detrital zircon dataset demonstrates a significant lateral variation in sediment provenance: Cambrian to Neoproterozoic detrital zircons dominate in the east, while Tonian and Stenian and Orosirian to Rhyacian ages predominate in the west of the study area. Sandstones are quartz-rich with dominantly durable zircon, tourmaline and rutile heavy mineral suite, with subtle but statistically significant along-strike differences in heavy mineral populations and detrital mineralogy which are thought to record local sediment input points into the aeolian system. The similar age spectra of Botucatu desert with proximal Paraná Basin units, the

predominance of quartzose, and zircon, tourmaline and rutile components, suggests that recycling is the mechanism responsible for the erg feeding.

Supporting Information

Filename	Description
sed12715-sup-0001-SupinfoS1.pdf PDF document, 77.4 KB	SupinfoS1
sed12715-sup-0002-SupinfoS2.pdf PDF document, 218.1 KB	SupinfoS2
sed12715-sup-0003-SupinfoS3.pdf PDF document, 67.3 KB	SupinfoS3
sed12715-sup-0004-SupinfoS4.pdf PDF document, 475.9 KB	SupinfoS4

Please note: The publisher is not responsible for the content or functionality of any supporting information supplied by the authors. Any queries (other than missing content) should be directed to the corresponding author for the article.

CONTROLS ON EARLY CRETACEOUS DESERT SEDIMENT PROVENANCE IN SOUTH-WEST GONDWANA, BOTUCATU FORMATION (BRAZIL AND URUGUAY)

Bertolini, G.[1,2,*], Marques, J.C. [1], Hartley, A.J.[2], Da-Rosa, A.A.S.[3], Scherer, C.M.S.[1], Basei, M.A.S[4], Frantz, J.C.[1],

[1] Universidade Federal do Rio Grande do Sul
[2] University of Aberdeen
[3] Universidade Federal de Santa Maria
[4] Universidade de São Paulo

* **Corresponding author** (e-mail: gabertol@gmail.com)

Abstract: The Lower Cretaceous Botucatu Formation records the development of widespread dry-aeolian desert sedimentation throughout the Paraná Basin in SW Gondwana. To reconstruct the provenance of the aeolian sediment, petrography, granulometric analysis and U-Pb detrital zircon have been determined from along the southern basin margin in Rio Grande do Sul state (S Brazil) and Uruguay (Tacuarembó region). The dataset reveals a mean $Qt_{89}F_8L_3$, comprising very-fine to medium grained quartozose and feldspathatho-quartzose framework. Heavy mineral analysis reveals an overall dominance of zircon, tourmaline and rutile grains (mean ZTR_{84}) with sporadic garnet, epidote and pyrolusite occurrences. The detrital zircon U-Pb ages are dominated by Cambrian to Neoproterozoic (515-650 Ma), Tonian to Stenian (900-1250 Ma) and Orosirian to Rhyacian (1.8-2.2 Ga) material. The detrital zircon dataset demonstrates a significant lateral variation in sediment provenance: Cambrian to Neoproterozoic detrital zircons dominate in the east, while Tonian and Stenian and Orosirian to Rhyacian ages predominate in the west of the study area. Sandstones are quartz-rich with dominantly durable ZTR heavy mineral suite, with subtle but statistically significant along strike differences in heavy mineral populations and detrital mineralogy which are thought to record local sediment input points into the aeolian system. The similar age spectra of Botucatu desert with proximal Paraná Basin units, the predominance of quartzose and ZTR components, suggests that recycling is the mechanism responsible for sediment supply to the Botucatu erg.

Keywords: Botucatu desert, Cretaceous Paraná Basin, desert accumulation, detrital zircon, heavy minerals, provenance analysis.

1. INTRODUCTION

Determining the origin and transport paths of sediment in aeolian systems is important for understanding how and why large accumulations of aeolian sediment are developed and preserved (Dickinson and Gehrels, 2003; Rahl *et al.*, 2003). Provenance studies of dune field sediment supply and erg sand-delivery systems reveal a range of desert sand supply mechanisms. For example sands in the Namib Desert are sourced by longshore drift from the Orange River delta (Garzanti *et al.*, 2014), sands in the Taklamakan Desert are supplied by fluvial systems draining the surrounding mountain ranges (Rittner *et al.*, 2016), and the Rub` Al Khali erg (Arabian Desert) is derived from a mix of sand sources including aeolian transport and deflation as well as fluvial, alluvial and coastal inputs (Farrant et al., 2019). In the rock record, a study of the Jurassic ergs of the Colorado Plateau was able to reconstruct a transcontinental SE-NW paleoriver and paleowind system responsible for transportation and dispersal of sediment in Laurentia (Dickinson and Gehrels, 2009). When studying the sedimentary record however, it is often difficult to properly reconstruct aeolian sediment supply systems due to the incompleteness of the succession and post-depositional diagenetic modification of the original mineralogy (McBride, 1985; Cardenas *et al.*, 2019). As a consequence, with the exception of the Permian-Jurassic Colorado Plateau ergs (Dickinson and Gehrels, 2003; 2009 and 2010; Rahl *et al*. 2003), there is a lack of studies that address the reconstruction of sediment source terranes, sediment pathways, sediment mixing, recycling and transport distance in ancient large-scale ergs. To address this gap, we have undertaken a provenance analysis of the Botucatu Formation, a Cretaceous aeolian unit deposited across SW Gondwana.

The Cretaceous Botucatu dune field extended continuously across 1.5 million km^2 of the interior of the SW Gondwana Supercontinent and represents part of what was probably the most voluminous continuous dune field in Earth history (Scherer and Goldberg, 2007; Fig. 1). The Botucatu sand sea forms part of the intracratonic Paraná Basin-fill succession and represents the last phase of sedimentation in the Paraná Basin prior to break-up of the South American and African continents. The Paraná Basin developed across a wide range of different pre-Mesozoic basement terranes (Paleoproteorozoic to Cambrian) with differing ages and compositions. Consequently, when combined with previous work on paleowind directions, it should be possible to distinguish different provenance signatures in the Botucatu Formation. Previous studies of the formation (e.g. Bigarella and Salamuni, 1961) show that coarser sediment prevails in the southern part of the basin suggesting input from the south. In addition, the close proximity of the Botucatu to basement highs (e.g. the Rio-Grandense and Uruguayan Shields), may allow establishment of a direct source-to-sink connection. Sediment provenance studies from the southern part of the basin will therefore be important in reconstructing sediment routing systems, understanding controls on sediment supply and assessing the potential for first cycle input direct from basement terranes.

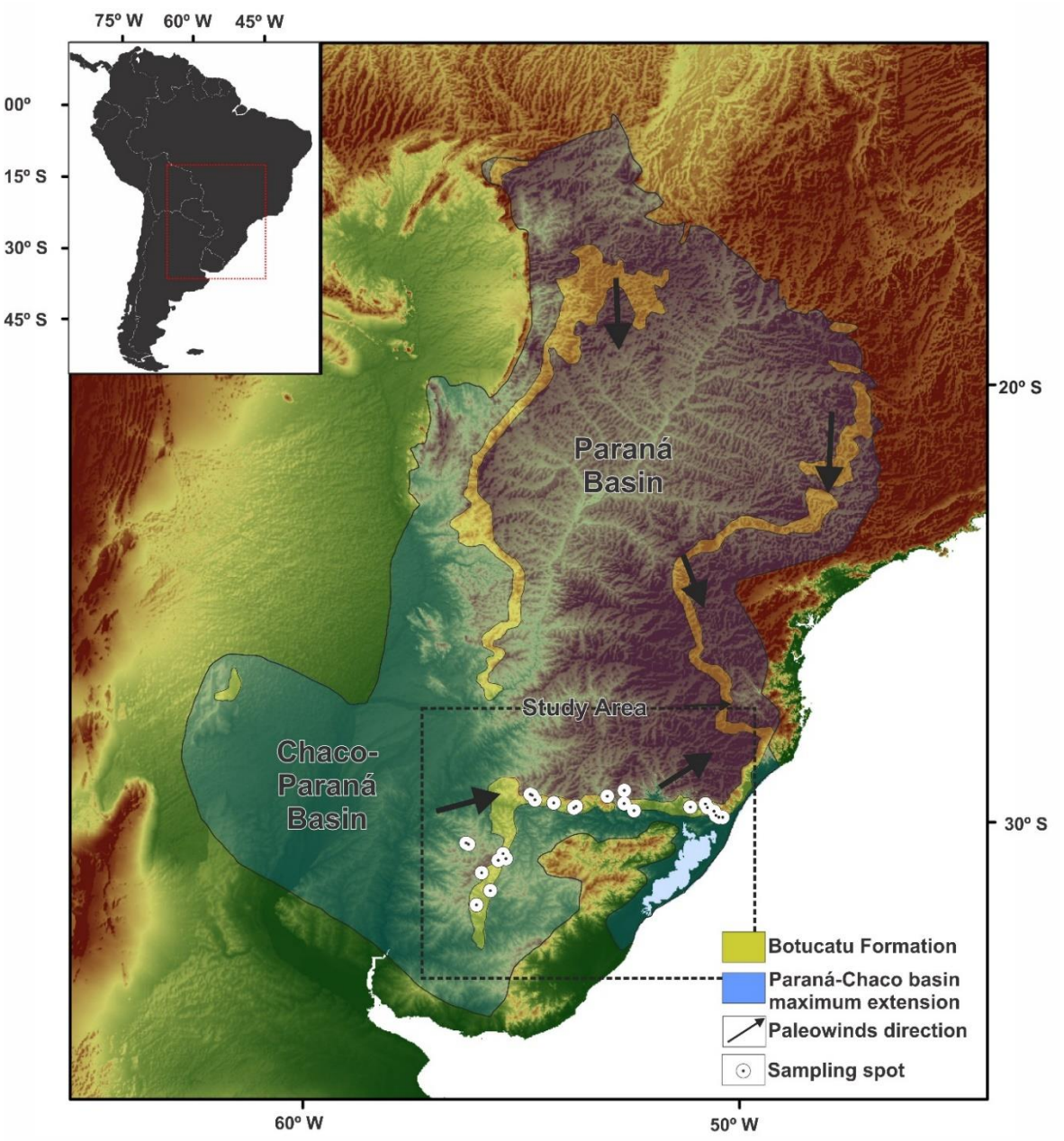

Figure 1- Botucatu desert extent in South America within the Paraná and Chaco-Paraná Basins with sample locations. The desert had a bimodal wind pattern, with southerly directions in low latitudes and NE-E directions in the study (Scherer, 2000; Scherer and Goldberg, 2007).

The primary objective of this study is to constrain and clarify the nature of the sediment source for the Botucatu dunes along a transect of the southern Paraná Basin margin (SE Brazil and Uruguay). Due to the continental scale of the aeolian system, the Botucatu Formation covers a number of distinct geologic terranes providing a wide range of potential sediment source areas and pathways. Provenance analysis utilizing

U-Pb detrital zircon geochronology, heavy mineral analysis, petrography, and granulometric analysis has been undertaken to ascertain if significant variations in sediment provenance signatures across the southern basin margin can be identified.

2. GEOLOGIC CONTEXT

The Botucatu Formation forms part of the intracratonic Paraná Basin fill succession - an 8 km thick (Zálan et al., 1990) sedimentary-magmatic package of Late Ordovician to Early Cretaceous age (Fig. 2). In the south (Brazil, Argentina, Paraguay), the basin-fill is divided into six supersequences (Milani *et al.*, 1998): Rio Ivaí (Ordovician-Silurian), Paraná (Devonian), Gondwana I (Carboniferous-Lower-Triassic), Gondwana II (Triassic), Gondwana III (Early Jurassic to Lower Cretaceous) and Bauru (Early Cretaceous). The Rio Ivaí, Paraná and Gondwana I supersequences represent marine and shoreline deposits. The Gondwana II, Gondwana III, and Bauru supersequences comprise terrestrial sediments and associated volcanic strata. The Botucatu Formation and the Serra Geral Formation form part of the Gondwana III supersequence, also known as the São Bento Group (Schneider *et al.*, 1973). The Botucatu paleoerg is overlain by 700-1700m of lava-flows from the Paraná-Etendeka Large Igneous Province (Serra Geral Formation). Interbedded basaltic lava flows and aeolian sediments indicate co-existence between, and a transition from, aeolian sedimentation to lava emplacement (Scherer, 2002).

The age of the top of the Botucatu Formation is constrained by overlying lavas of the Serra Geral Formation, which have yielded ages of 134.5 Ma ± 0.5 Ma (Valagininan) by Ar/Ar (Whole-rock grains/ plagioclase) and U-Pb methods (Zircon and Badeleeite) (Ernesto *et al.,* 1999; Thiede and Vasconcelos, 2010; Pinto *et al.,* 2011, Janasi *et al.,* 2011; Rossetti *et al.,* 2018, Baksi, 2018). The determination of the onset

of Botucatu deposition is imprecise due a lack of dated interbedded volcanics and/or palaeontological constraints. The Botucatu Formation overlies the Upper Jurassic Guará and Batovi Member (Soto and Perea, 2008; Perea *et al.,* 2009; Francischini *et al.,* 2015), suggesting an earliest Cretaceous age (Berriasian to Valanginian) for paleoerg accumulation.

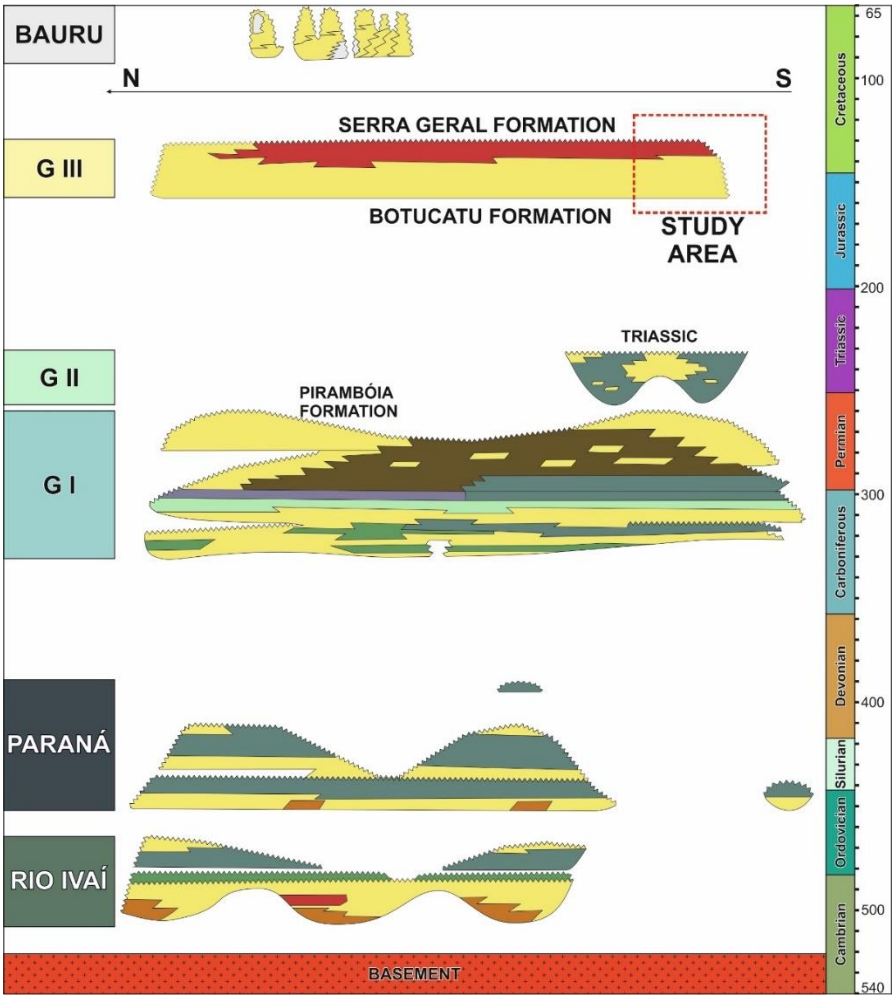

Figure 2 - Paraná Basin stratigraphic chart with the 6 Supersequences: Rio Ivaí, Paraná, Gondwana I, Gondwana II, Gondwana III, Bauru (Milani, 2007).

The study area is located along the southern margin of the Paraná Basin, in Rio Grande do Sul State (Brazil) and Central Uruguay. In Uruguay, the Botucatu Formation is equivalent to the Rivera Member of the Tacuarembó Formation (Amarante *et al.*, 2019). The Botucatu Formation also has equivalent units in Argentina

(San Cristobal Formation), Paraguay (Missiones Formation), Bolivia (Ichoa Formation) and Namibia (Twyfelfontain Formation) (Scherer and Goldberg, 2007). Outcrops in Rio Grande do Sul State and Uruguay likely represent the upwind margin of the erg as illustrated by: (i) variations in thickness from 0 to 100 m along the southern margin to up to 400 m thickness in the basin center (Milani *et al.*,1998), and (ii) paleocurrent data demonstrating a consistent NE/E paleowind direction along the southern basin margin (Scherer and Goldberg, 2007; Fig. 1).

Scherer (2000) described 4 facies across the southern Botucatu margin: thick large-scale trough cross-stratification; large-scale planar cross-stratification; medium-scale trough cross-stratification and low-angle cross-stratification. The relatively monotonous and simple sedimentary facies are controlled by dune morphology, illustrating a consistent predominance of crescentic dunes and linear draa bedforms. The Botucatu is considered to represent a dry-aeolian system (*sensu* Havholm and Kocurek, 1994), indicated by the absence of deposits or sedimentary features such as wet interdune deposits or adhesion structures generated by water-table or flooded/wet interdune areas.

In the study area, the Botucatu Formation overlies 3 distinct units of the Gondwana I and II supersequences of the Paraná Basin-fill: (i) the Jurassic Guará Formation and Batovi Member of Tacuarembo Formation (Uruguay) in the west; (ii) the Triassic Caturrita Formation in the central region and (iii) the Permian to Jurassic Pirambóia Formation in the east. The Guará Formation (Batovi Member) is an Upper Jurassic fluvial-aeolian unit, comprising a S-SW directed distributive fluvial system and small to medium size dunes (Scherer and Lavina, 2006; Amarante *et al.*, 2019). The Triassic Caturrita Formation comprises amalgamated sandstones intercalated with siltstones that represent high energy, low sinuosity river deposits (Zerfass *et al.*, 2003;

Jenisch *et al.,* 2017). The Permian Pirambóia Formation is a wet aeolian system, composed of red fine-to coarse sandstones (Dias and Scherer, 2008).

The Paraná Basin basement framework comprises a series of complex Cambrian to Paleoproterozoic rocks forming the following terranes (from East to West): Dom Feliciano Belt, Tacuarambó Terrane (Sul-Rio-Grandense Shield), Nico Pérez and Piedras Altas Terranes (Uruguayan Shield). For simplification, the overall crustal framework displays a distribution of Neoproterozoic ages in the East (Dom Feliciano Belt) and Paleoproterozoic age terranes in the West (Tacuarembó, Nico Pérez and Tacurambó Terranes) (Fig. 11). The Dom Feliciano Belt forms part of the Central-to-East Rio-Grandense Shield and includes 3 main orogenic events: Passinho (0.9 – 0.86 Ga), São Gabriel (0.77 – 0.68 Ga) and Dom Feliciano (0.65 – 0.54 Ga) (Philip *et al.*, 2016). Additionally, the Dom Feliciano terrane includes a Neoproterozoic-Cambrian volcano-sedimentary succession (Camaqua Basin) and a Neoproterozoic metamorphic syn-collision belt (Porongos Belt) (Höfig *et al.*, 2018; Janikian *et al.*, 2012). The granitic-gneissic Tacuarembó, Piedras Altas and Nico Perez Terranes are located on the Western Sul-Rio-Grandense and Uruguayan Shields. These terranes yield Orosirian to Archean ages, with peaks from 1.8 to 2.2 Ga (Oyhantçabal *et al.*, 2018a and 2018b).

3. MATERIALS AND METHODS

To constrain the provenance of the Botucatu sandstones in the southwestern part of the Paraná Basin, sedimentary petrography, heavy mineral analysis, grain size analysis and detrital zircon geochronology were undertaken. Twenty-one samples (Fig. 1) were collected along the southern margin of the basin from sandstones at the base and top of the formation together with sandstones from within the Serra Geral

Formation lavas (Intratrap sandstones) to observe possible lateral and chronological changes in provenance signal. In the studied area, the Botucatu Formation outcrop ranges from 0.5 to 30 m in thickness and mostly comprises fine to medium sand. The predominant sedimentary facies are large-scale cross-beds, with occasional low-angle-beds, trough cross-bed sets and locally massive sandstones. Scherer (2000) considered these facies to represent parts of aeolian dune morphologies (simple to compound crescentic dunes and complex linear *draas*) with very local ephemeral fluvial stream deposits. Table 3 documents the sedimentary facies as well as the sample number, location, stratigraphic level (base, top and interbedded), and the provenance techniques performed. The samples were collected mostly form large scale cross- and trough-stratified sandstones (Ste), with some from low-angle stratified (Sle) and massive sandstones (Sm). Figure 3 shows the 11 studied profiles (based on Scherer, 2000) and the position of each sample within the stratigraphy.

Table 1 - Sample locations by stratigraphic position and location. Heavy Mineral (HM); Bulk Petrography (BP); Detrital Zircon (DZ); Granulometric Analysis (GR).

Sample Code	Facies Code	Stratigraphic Level	Coordinates Lat/Long	Region Sampled	Provenance Techniques			
					BP	DZ	HM	GR
PB-01	Sle	Base	-50.482903/-29.886139	East	X			
PB-02A	Ste	Top	-50.395787/-29.877412	East	X	X	X	X
PB-02C	Sm	Intratrap	-50.395787/-29.877412	East	X	X		
PB-03	Ste	Top	-50.529168/-29.830188	East	X			
PB-09	Ste	Top	-50.577807/-29.743651	East	X		X	X
PB-18	Ste	Top	-52.414231/-29.726391	East	X	X	X	X
PB-31B	Ste	Intratrap	-51.131414/-29.632367	East		X	X	X
PB-19	Sm	Intratrap	-52.634681/-29.55371	Central	X			
PB-20	Sm	Intratrap	-52.638663/-29.261931	Central	X		X	X
PB-21	Ste	Top	-52.631227/-29.566123	Central	X		X	X
PB-22	Ste	Intratrap	-53.0209/-29.406328	Central	X	X	X	X
PB-23	Ste	Base	-54.68608/-29.481004	Central	X	X	X	X
PB-24	Ste	Top	-54.749004/-29.365739	Central		X	X	X
PB-29	Ste	Intratrap	-54.764559/-29.36278	Centra	X			
PB-04	Sm	Base	-55.412019/-30.717301	West	X		X	X
PB-10	Ste	Base	-55.72246/-31.564436	West	X	X	X	X
PB-11	Ste	Top	-55.897349/-31.147843	West		X	X	X
PB-12	Ste	Intratrap	-55.913833/-31.142028	West		X	X	X
PB-14	Sle	Top	-56.216685/-30.486345	West			X	X
PB-16	Ste	Top	-55.517067/-30.852035	West	X			
PB-17	Ste	Base	-55.349101/-30.82337	West	X			

Sample preparation was undertaken separately for each analysis. For granulometric and heavy mineral analysis, disaggregation was carefully undertaken with a rubber point pestle and mortar to avoid grain breakage. For geochronological studies sample disaggregation was carried out using a mechanical jaw crusher (when necessary) and a plate mill.

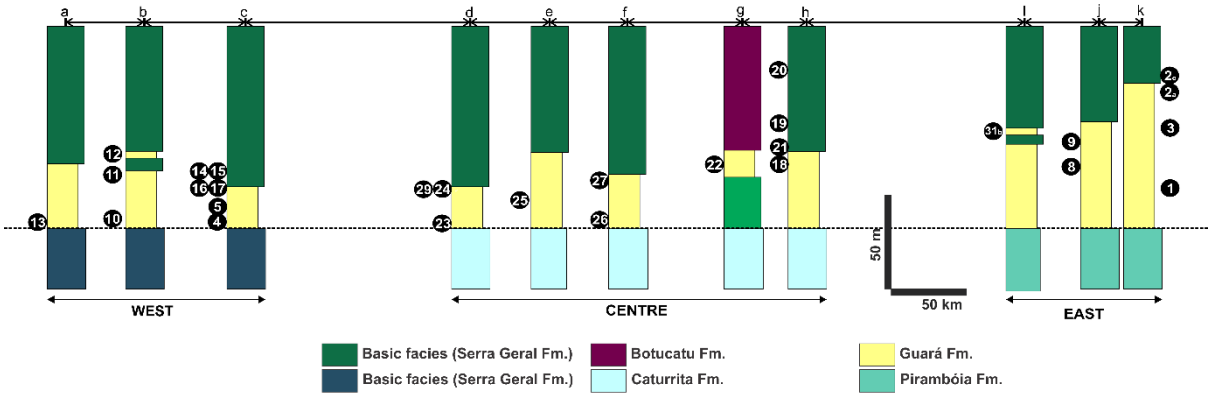

Figure 3 - Sedimentary profiles (Adapted from Scherer 2000) with the stratigraphic position of the sampling where the leters a-k refers to the profile locations a- Tacuarembó (Uy); b- Tranqueras (Uy); c- Santana do Livramento (Br); d- Jaguari (Br); e- Sao Pedro do Sul (Br); f- Santa Maria (Br); g- Sobradinho (Br); h- Herveiras (Br); i- Ivoti (Br); j- Santo Antônio da Patrulha (Br); k- Osório (Br)

Nineteen petrographic thin sections were described and subject to point counting (300 points/sample) using the Gazzi and Dickinson method (Ingersoll *et al.,*1984). The results are displayed following the scheme of Garzanti (2018) (Fig. 4).

Grain size analyses were undertaken on fourteen samples, with 100g of each sandstone. The process consisted of sample cleaning (removal of external exposed surfaces), disaggregation, drying and sieving. The petrographic data reveal no silt sized grain-size, justifying the sand-class interval measuring (63-125 µm, 125-250 µm, 250-500 µm, 500-1000 µm). Samples were weighed after each step and the difference recalculated and assigned to each respective grain size proportion.

Between 150 to 400g of fourteen samples were selected for heavy mineral analysis. Samples were dried and sieved (63-125 µm) following the grain-size window interval of Morton and Hallsworth (1994) via dense liquid separation (Bromoform -2.80 g/mL). The mainly fine sand sediment framework composition of the Botucatu Formation is compatible with hydraulic equivalence of heavy mineral assemblage, ruling out significant hydraulic sorting bias effects (e.g. Morton and Hallsworth, 1994; Hurst *et al.*, 2017).

Heavy mineral concentrates were mounted on petrographic slides, with identification of 150 translucent minerals using the ribbon technique following the method of Mange and Maurer (2012). A complementary elemental analysis was undertaken with an energy-dispersive X-ray spectrometer (EDS) on a scanning electron microscope (SEM) to aid with heavy mineral identification. The analysis was carried out at the Universidade Federal do Rio Grande do Sul using a Jeol 6610-LV (15 kV beam voltage and 12mm working distance).

Detrital zircon grains were analyzed from 10 samples for U-Pb at University of São Paulo, using a Finnigan Neptune mass spectrometer and an excimer ArF laser (λ=193nm) ablation system. The laser ablation multi-collector inductively coupled plasma mass spectrometry (LA-MC-ICP-MS) uses 5 mJ, 6 Hz and 29 μm diameter beam as analytical conditions. The $^{207}Pb/^{206}Pb$ ages were used for zircons older than 1.3 Ga and the $^{206}Pb/^{238}U$ ages for younger grains. The discordance tolerance is 10%, values above this limit were dismissed. The parameters used are discussed in Sato *et al.* (2011).

The GRADISTAT software (Blott and Pye, 2001) was used for statistical analysis and to determine sediment distribution. The Provenance R Package (Vermeesch *et al.,* 2016) was used to run the cumulative age densities (CAD), kernel densities estimators and Multidimensional Scaling (MDS) plots.

4. RESULTS

Petrography reveals a mean composition of $Qt_{89}F_8L_3$, compositionally classified (Garzanti, 2018) as pure-quartzose (PB-04, -23), quartzose (PB-01, -03, -10, -16, -17, -18, -19, -21, -22, -24, -29A) and quartz-rich feldspatho-quartzose (PB-2A, -2C, -09, -20) (Fig. 4) sandstones. Monocrystalline quartz is predominant (93 to 100%) over

polycrystalline quartz. K-feldspar is most frequent over plagioclase (mean 70%), however center region samples show an increase in plagioclase (60 to 70%). The lithic fragment distribution (Fig. 4) shows both igneous (felsic plutonic) and volcanic (basaltic lathwork to glassy trachyte) fragments. In the eastern and central regions moderately sorted fine sand predominates with poorly sorted medium sand in the west.

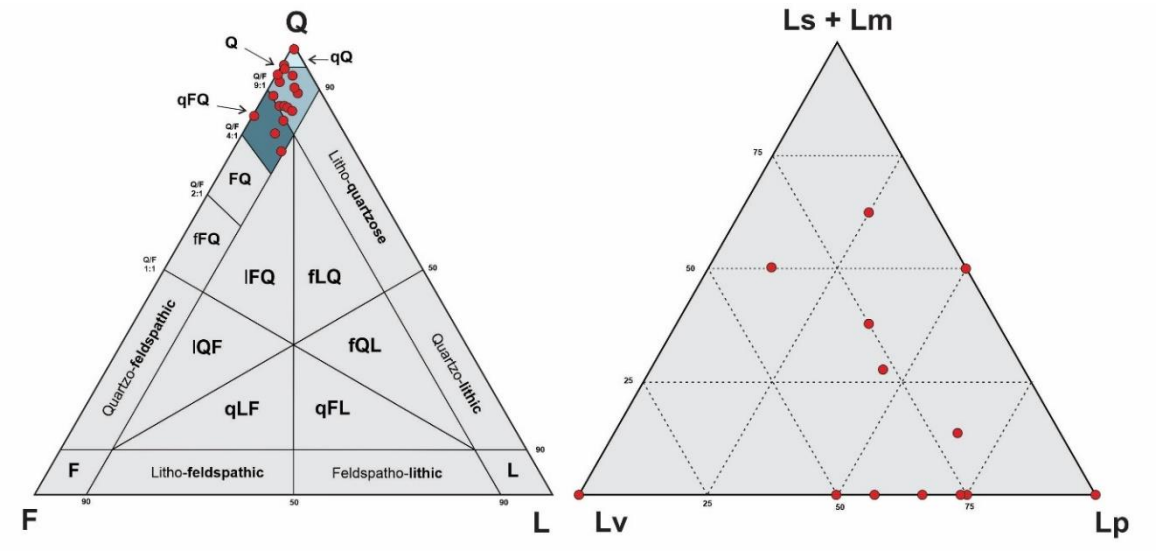

Figure 4 - Sandstones classification scheme (Garzanti 2018) and lithics plot. Samples point to quartzose and felsic plutonic compositions. (Q- Total quartz; F – K-feldspar and plagioclase; L- total lithics; Lv- volcanic rock fragments; Lp – Plutonic lithics; Lm and Ls- metamorphic and sedimentary lithics; qQ- pure-quartzose; Q- Quartzose; qFQ- quartz-rich feldspatho-Quartzose).

The heavy mineral population of the 21 studied samples comprises 14 mineral species, with a dominant signal from resistant species - zircon, rutile, and tourmaline. Local occurrences of anomalously high amounts of garnet, epidote, pyrolusite and apatite and a few grains of other species such as alumino-silicates (kyanite, andalusite or sillimanite), spinel, corundum, monazite, fluorite, xenotime, sulfides (cassiterite and pyrite) are also recorded. Figure 5 shows the heavy mineral assemblage distribution across the studied region, illustrating the high ZTR and very-local occurrences of garnet, epidote and pyrolusite. The heavy mineral analysis presents a mean $ZTR_{0.84}$, ranging from 33.5-to 99.4% and is characterized by the predominance of zircon,

reaching almost 98% in sample PB-24. The area contains zircons that display different levels of roundness, varying from rounded oval grains to elongate bi-pyramidal prismatic grains. Samples PB-2A, -31B, -20 show peaks in Fe-garnet and epidote and sample PB-09 contains a high abundance of pyrolusite.

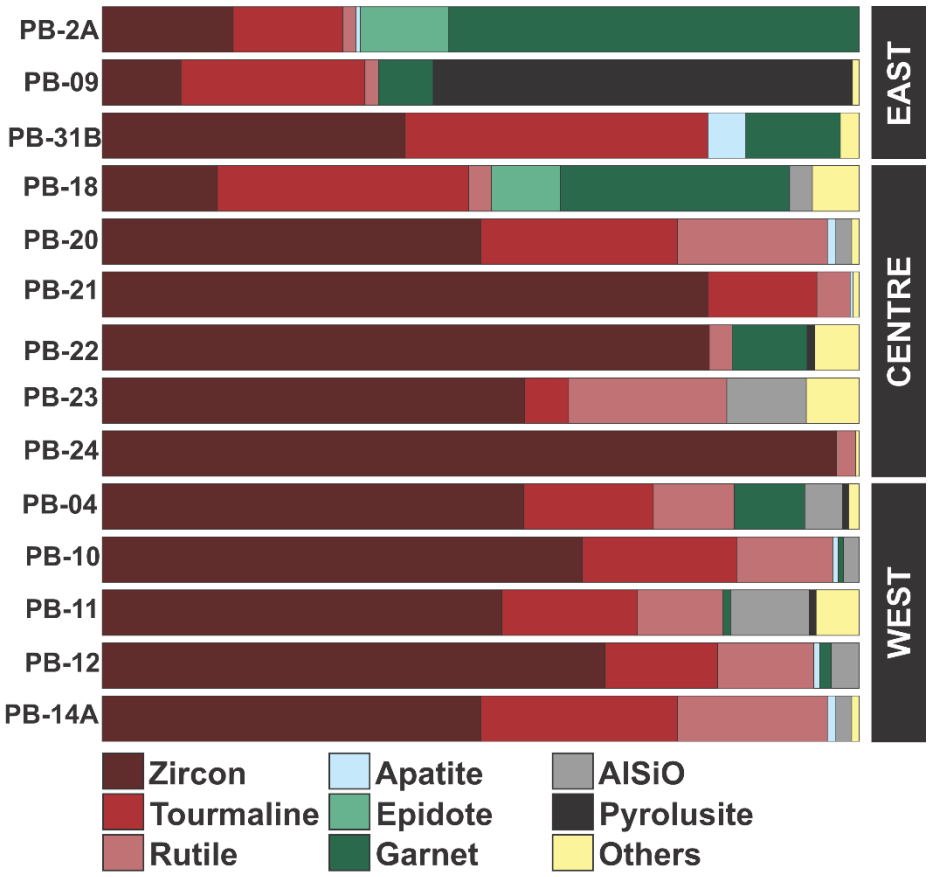

Figure 5 - Heavy mineral suites distribution across the regions, with prevalent zircon, tourmaline and rutile (ZTR) assemblage.

Detrital zircon age spectra display a complex signature, with ages ranging from 155 Ma to 3290 Ma. The wide age distribution reflects the complex geologic history of the basement rocks and potential recycling from older sedimentary units. In order to track possible sediment pathways using the detrital zircon (DZ) record, the ages were separated into 7 groups that correspond to significant crustal construction periods in South America (Bahlburg *et al.,* 2009): Late Paleozoic to Mesozoic (Gondwanides Cycle), Devonian to Cambrian (Famatian Cycle), Cambrian to Neoproterozoic

(Brasiliano/ Pampean/ Pan-African cycles), Tonian to Stenian (Grenvilian Cycle), Mid-Mesoproterozoic to Statherian, Orosirian to Rhyacian and Neo- to Paleoarchean (Fig. 6).

The detrital zircon data indicate that Early Neoproterozoic to Cambrian ages (515-650 Ma) are the main contributor to the DZ population with Late Paleozoic to Mid Mesozoic (150-359 Ma), Tonian-Stenian (0.9 – 1.25 Ga) and Orosirian to Rhyiacian ages (1.8- 2.25 Ga) forming subsidiary contributions. The detrital zircon signal appears to be relatively homogeneous but grouping the samples by region reveals a transitional signature across the southern margin of the Botucatu desert, with increasing Cambrian to Neoproterozoic ages (31.6 to 52.5%) and a decrease in ages older than 900 Ma towards the East.

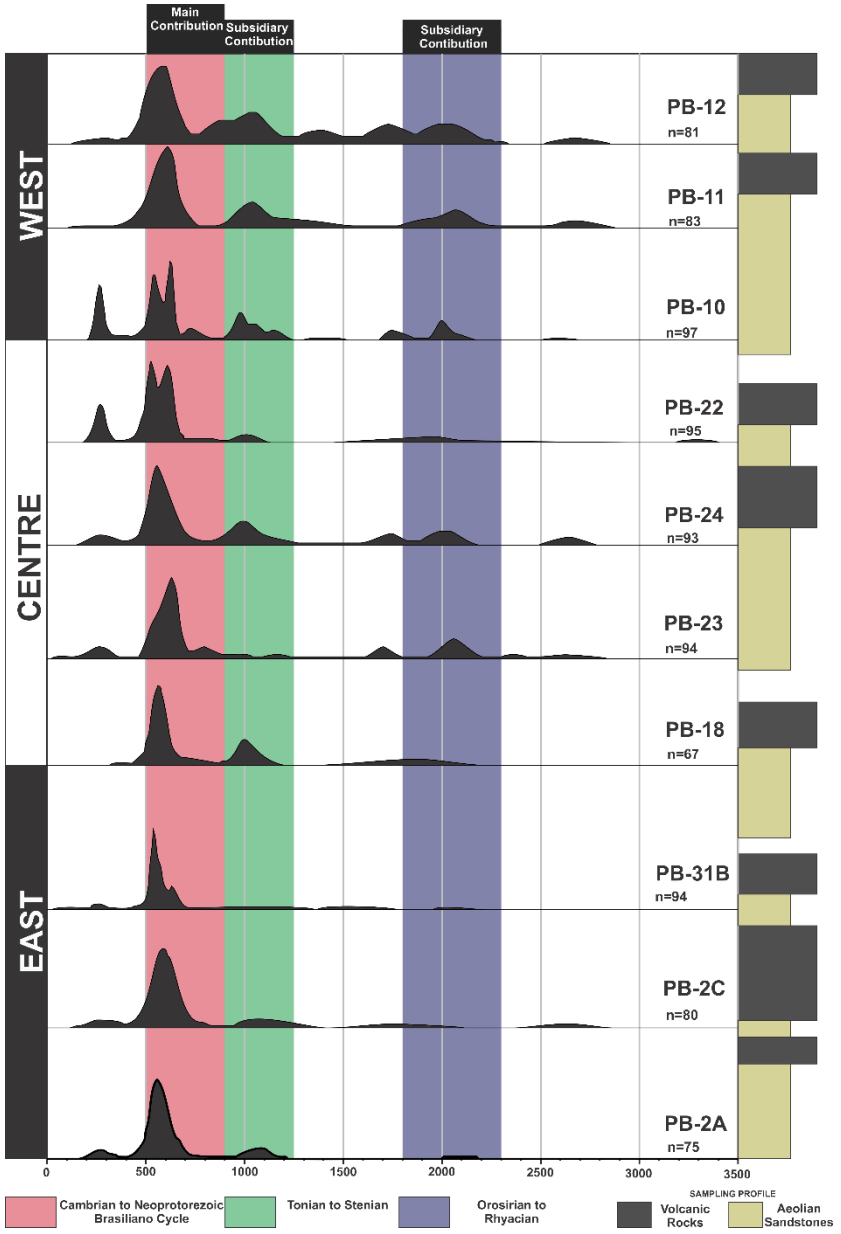

Figure 6 - Normalized probability density plots located on the schematic stratigraphic profile. The colored areas demonstrate the most prominent age intervals.

The geographic location of each sample and a compilation of the different dataset types are illustrated in Figure 7. U-Pb detrital zircon ages are plotted using a probability density plot, the bulk petrography, heavy mineral, and granulometric analyses are illustrated using pie charts. The sampling level in the stratigraphy and location relative to the Serra Geral lavas are also shown in Figure 3. The provenance dataset reveals a lateral variation described in further detail below.

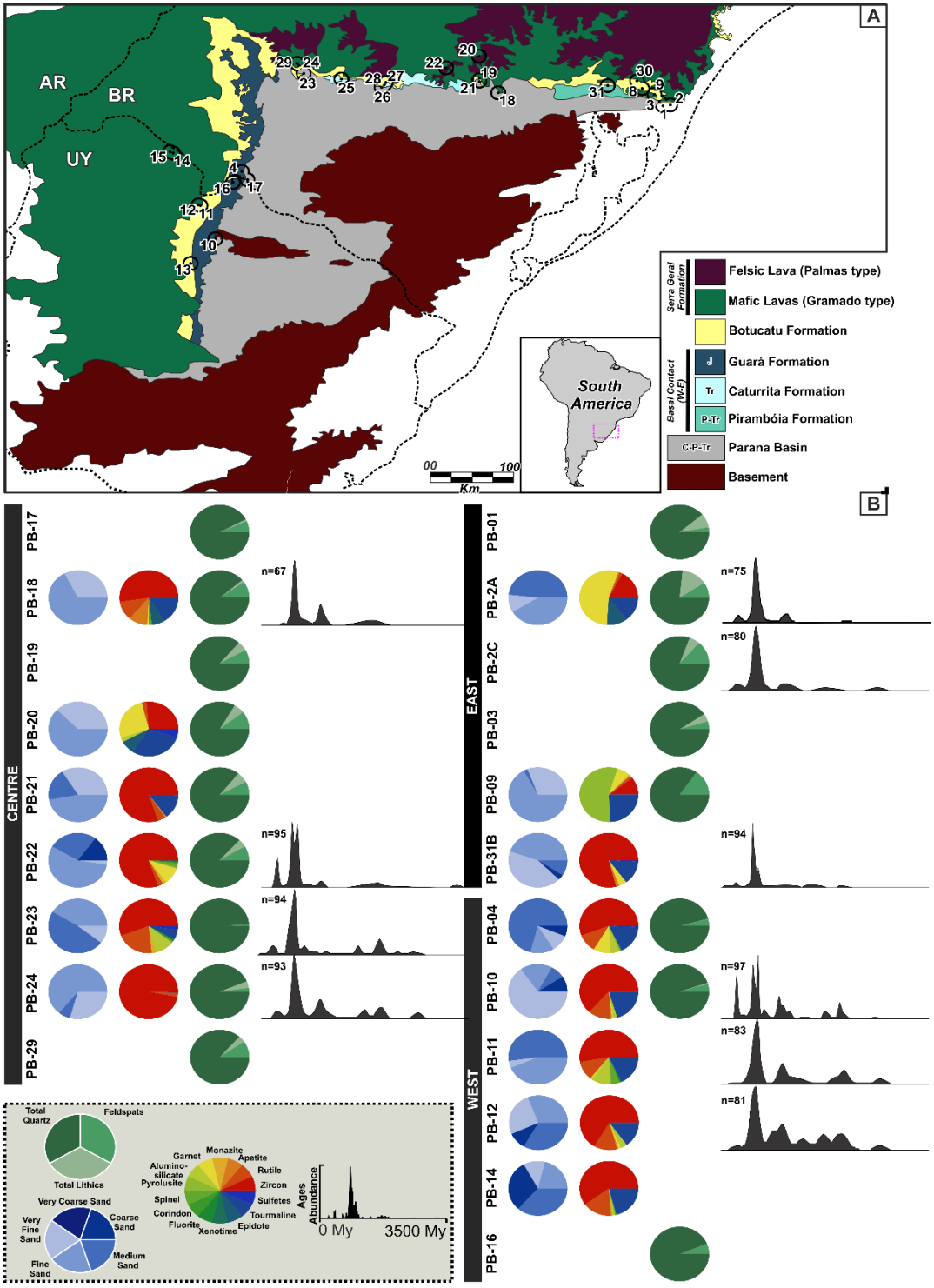

Figure 7- Geologic map (adapted from Wildner et al. 2006) with the sampling spots; B - Provenance data compilation.

4.1 Eastern Region

Three sections were sampled in the eastern region: Santo Antônio da Patrulha (PB-03 and -09), Osório (PB-01, -02A, -02C) and Ivoti (PB-31B) (see Figure 3). Bulk petrography shows a mean composition of $Qt_{85}F_{11}L_4$, with a relative change in feldspar content (5 to 15%). The granulometric analysis reveals a unimodal distribution, fine-sand, moderately (PB-02A, PB-31B) to moderately well sorted (PB-09). The heavy mineral analyses (Fig. 5) revealed that samples PB-02A and -31B contain 54.3% and 12.5% of almandine respectively, PB-02A contains 11.5% epidote and sample PB-20 comprises 55.4% pyrolusite. Detrital zircon dating reveals an age signature ranging for 155 Ma to 3231 Ma, with main peaks in the Late Paleozoic to Mid Mesozoic (11%), Neoproterozoic to Cambrian (52%) and Tonian to Stenian (10%). Eastern region samples show a significant upward increase in the proportion of C-NP zircons from 49% at the base (PB-02A) to 72% in interbedded sandstones (PB-31B) at the top of the Botucatu Formation.

4.2 Central Region

The central portion samples were collected from 5 sections (Fig. 3): Jaguari (PB-23, -24, -23), Sao Pedro do Sul (PB-25), Santa Maria (PB-26, -27), Sobradinho (PB-22) and Herveiras (PB-18, -21, -19, -20). Petrography reveals a mean composition of $Qt_{89}F_7L_3$, classified as quartz-enriched feldspatho-quartzose and quartzose sandstones. Bulk petrography shows total quartz varying from 83 to 99%, feldspars from 0 to 10% and total lithics from 0 to 6%. Grain-size analysis reveals a unimodal distribution, moderately well (PB-18, -20, -24) to moderately sorted (PB-21, -22, -23), fine-sand to medium-sand (PB-23). Heavy mineral analysis (Fig. 5) shows a

variable ZTR value, ranging from 51.5 to 99.5%, with a garnet peak (30.3%) occurring in sample PB-20. Samples 18, 21, 22, 23 and 24 have high zircon, tourmaline and rutile (ZTR) values, reaching >95% zircon in sample 24. Fe- garnet and epidote are observed in sample 20 (>35%). Detrital zircon ages range from 174 Ma to 3290 Ma, including Early Neoproterozoic to Cambrian (41 %), Tonian - Stenian (12 %) and Orosirian-Rhyacian (10%) peaks.

4.3 Western Region

Seven samples were taken from the western part of the study area from 3 sections (Fig. 5): Tacurambó (PB-13), Tranqueras (PB-10, -11, -12) and Santana do Livramento (PB- 4, -5, -14, -15, -16, -17) in Uruguay and Brazil. Petrographically the samples have a predominantly quartzose composition (mean $Qt_{94}F_5L_0$). The granulometric analysis shows unimodal sorting, moderate-well (PB-11), moderately (PB-04, -10) to poorly sorted (PB-12, -14A), medium- (PB-04, -11, -14A) to fine sand (PB-10, -12).). Heavy mineral analysis (Fig. 5) reveals high ZTR concentration (83 to 96%) with zircons dominant. The region has a higher than average rutile content (13%) contrasting with a mean of 5% from other regions. Al-Si polymorphs (mean 5%) appear consistently in the west but only occur occasionally in the east and central regions. Garnet (Fe-Almandine) appears only in sample PB-04. Detrital zircon grains from samples PB-10, PB-11, and PB-12 display ages ranging from 155 Ma to 2717 Ma, with mainly Early Neoproterozoic to Cambrian (32%), Tonian to Stenian (18%) and Orosirian to Rhyacian (14%) peaks.

5. DISCUSSION

5.1 Lateral variations

The detrital zircon geochronology dataset illustrates that Cambrian-Neoproterozoic (C-NP) aged zircons form the main component of the population with the Tonian-Stenian (0.9-1.25 Ga) and Orosirian-Rhyacian (1.80-2.25 Ga) providing subsidiary contributions in all regions. More detailed analysis allows lateral variations in age groups can be distinguished. Variations in detrital zircon age distributions across the regions are compiled in Table 4 and demonstrate a relative increase in C-NP ages in the eastern region, with a predominance of >900 Ma grains in the western region. The central region is transitional between both regions containing intermediate values in all age periods.

Table 2 - Detrital zircon age proportions from the southern margin of the Botucatu Fm. organized by regions. The data show an overall increase in>900 Ma ages to the west and Brasiliano peak to the east.

Event	Time Interval (Ga)	%		
		East	Center	West
Late Paleozoic to Mid Mesozoic	0.150-0.359	11.027	9.695	9.294
Early Famatian (Ordovician-Silurian)	0.359-0.515	8.365	6.648	5.948
Early Neoproterozoic to Cambrian Ages (Late Brasiliano)	0.515-0.650	52.471	40.720	31.599
Early Brasiliano	0.650-0.900	9.886	9.418	7.807
Tonian-Stenian Ages (Grenvillian Cycle)	0.900-1.250	9.886	11.634	18.216
Mid-Mesoproterozoic to Statherian ages	1.250-1.800	3.422	6.648	9.665
Orosirian to Rhyacian ages	1.800-2.200	2.662	9.695	12.639
Neo- to Paleoarchean	2.200-3.400	2.281	5.540	4.833

The lateral variations described above are likely to be related to changes in either basement units immediately adjacent to the outcrop or to recycling of underlying sedimentary successions or a combination of both. These variations are also expressed in Figure 8 as cumulative density plots (A) and multidimensional scaling

plots (B). The CDP demonstrates that the C-NP is the most variable detrital zircon age group from east to west, with almost 20% variation, whilst the MDS plots illustrate the transitional characteristics of the lateral changes. The average compositional dataset (granulometry, petrography and heavy minerals) also displays a lateral modification from West to East. The petrography shows an increase of lithics and feldspar over quartz components ($Q_{94\text{-}5}F_{5\text{-}10}L_{0\text{-}5}$), and the granulometry demonstrates a medium to very fine sand transition. The heavy mineral data presents an increase of the mean ZTR from 80 to 89% (East to West). The western region also shows an increase of Al-Si minerals, suggesting greater influence of metamorphic sources.

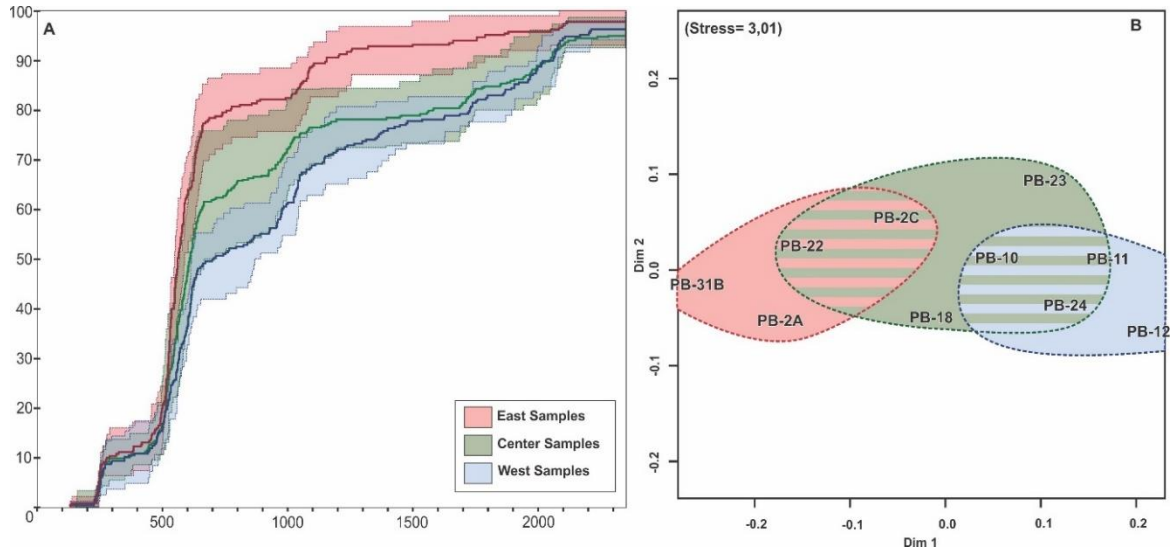

Figure 8 - Cumulative probability plot (A) and MDS plots (B) illustrating the lateral variability of detrital zircon U-Pb ages. Western region is enriched in older ages (>1.25 Ga) whilst the eastern region isdominated by Early Brasiliano ages (515-620 Ma). The central portion of the basin is transitional between the two. The bold central lines in plot A correspond to the sum of values for each region.

In the study area, the Paraná Basin is developed above a basement composed of Neoarchean to Cambrian rocks. The contact between basement and basin-fill occurs beneath Permian units (Itararé and Rio Bonito Formations), as such there is no direct contact between basement and the Botucatu Formation. In addition, the basal contact of the Botucatu changes laterally, from the Upper Jurassic Guará Formation/ Rivera Member (West), Triassic Caturrita Formation (Central) and Permian

Pirambóia Formation (East). No detrital zircon age data are available from these underlying units, so it is not possible to ascertain if zircons were derived directly from these strata. Zircon ages from the underlying basement also show distinct age domains across the margin. The Rio-Grandense and Uruguayan Shields, contain zircon populations of 500 – 900 Ma (Cambrian- Neoproterozoic contribution) and 1250-3400 Ma (including Orosirian-Rhiacian subsidiary contribution) (Philip *et al.,* 2016). Tectonic domains such as the Piedras Altas, Nico Pérez and Tacuarembó terranes, yielded multiple Neoproterozoic to Neoarchean ages, but overall ages are composed predominantly of >1.25 Ga rocks (Oyhantçabal *et al.,* 2012; Santos *et al.,* 2003; Oriolo *et al.,* 2016). The Dom Feliciano Belt in Rio Grande do Sul State and the coastal region of Uruguay comprises a Cambrian to Neoproterozoic granite-gneissic orogenic belt (Philip *et al.,* 2016, Basei *et al.,* 2008). The progressive upward increase in C-NP ages in the Eastern region (48.8% to 71.6%) could indicate increased direct input from these source terrains at this location.

A lack of direct first cycle input into the majority of the Botacatu Formation is indicated by the limited presence of detrital zircon grains of Jurassic age (180-155 Ma). These grains occur only in the extreme west of the Botucatu exposure (Central Argentina) where they are considered to be derived directly from the Andean magmatic arc (Peri et al. 2016). The Tonian-Stenian ages (Grenvilian Cycle) are not present in basement terranes close to the study area and could indicate an original source in areas such as the Sierra Pampeanas (Argentina) and Natal-Namaqua Belt (SW Africa) (Rapela *et al.,* 2010; Casquet *et al.,* 2008; Bial *et al.,* 2015).The relative increase in zircons derived from strata that yielded Tonian-Stenian ages in the western region together with the prevailing NE wind pattern could indicate that first-cycle grains were derived from the SW Gondwana margin terranes (Sierra Pampeanas). Canile *et*

al. (2016) show that juvenile zircons (Positive ƐHf) from the Natal-Namaqua belt (in present day Namibia and South Africa) are present in older Paraná Basin units, demonstrating the existence of previous recycling. The Tonian-Stenian age signature probably records the presence of recycled grains from a mixture of Natal-Namaqua Belt and Western Sierra Pampeanas sources.

5.2 Sedimentary Recycling

U-Pb detrital zircon dating is a useful tool that allows the resulting age spectra from a sedimentary rock to be linked potentially to an original sediment source (Gehrels, 2014). However, due to the resistance of zircon to transport, burial and even metamorphic events, detrital zircon age spectra commonly include grains recycled from older strata such that the final detrital zircon age spectra within a sedimentary rock represent a composite of original and recycled material (Dickinson and Gehrels, 2009; Hadlari *et al.*, 2015). As a consequence, if solely utilizing the detrital zircon dataset it is a virtually impossible to establish if the age peaks in the Botucatu are derived directly from basement (1st cycle sediment) or by multiple phases of deposition and reworking (poly-cycling sediment). By combining the detrital zircon data with petrographic and heavy mineral data it is possible to more precisely determine the sediment origin. The petrographic and heavy mineral dataset shows a highly quartzose and ZTR-rich composition. A quartzose sedimentary factory requires multiple steps of diagenesis, weathering and recycling in order to obtain a pure-quartzose and high ZTR end-member (e.g Congo River sediment described by Garzanti *et al.*, (2019), suggesting that Botucatu sediment has a predominant poly-cyclic history. To understand the polycyclic sediment history of the Botucatu sediment and its relationship with Paraná Basin Carboniferous-Jurassic units, we compare the

detrital zircon data presented here, with other datasets from older strata in the southern Paraná Basin.

Cumulative age density and multidimensional scaling biplots (Figs 9A and B) are utilized to assess and compare the DZ populations present in the Carboniferous Itararé Group (Rio do Sul Fm.), Carboniferous-Permian Guatá (Palermo, Sideropólis, Paraguacu and Triunfo Fms.), Permian Passa Dois Group (Irati, Serra Alta, Teresina, Morro Pelado and Serrinha Fms.), Triassic Santa Maria formation (Santa Maria and Santa Catarina region- based on Canile *et al.*, 2016; Philip *et al.*, 2018). The MDS biplot (Fig. 9A) shows a distribution of units enriched in Paleoproterozoic sources (Rio Bonito and Palermo Formation), Permian-Triassic ages (Irati, Serra Alta, Teresina Formation), Cambrian-Neoproterozoic ages (Triassic and Eastern Botucatu) and a zone of mixed ages (Center, West, N Botucatu, Itaré, Serrinha, Triunfo Formations) can be defined. The MDS shows that the Late Carboniferous-Early Permian units (Rio Bonito and Palermo Formations) corresponds to a western Botucatu signature, suggesting that these units were the primary source.

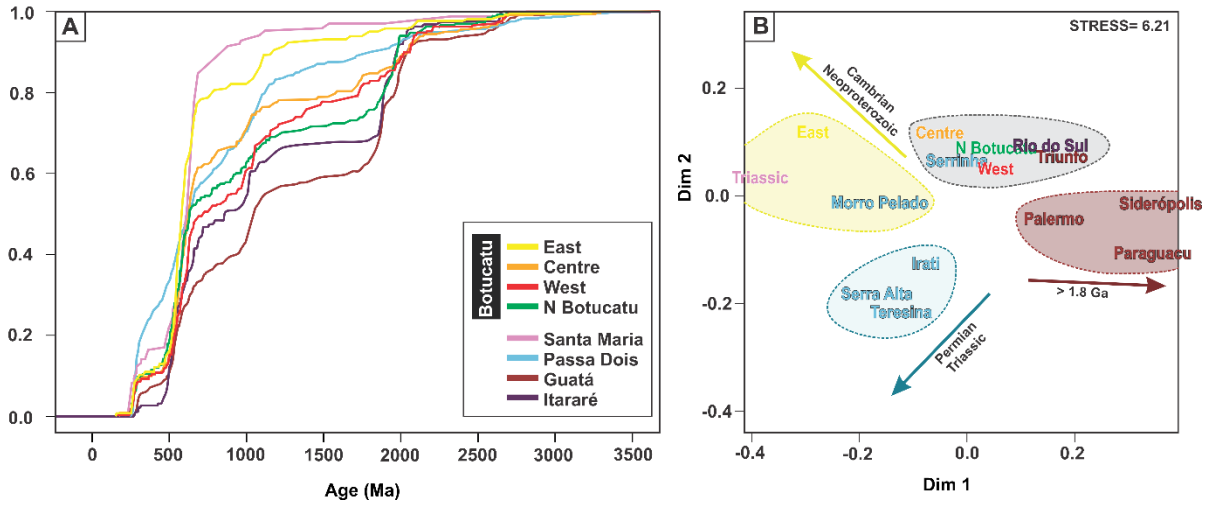

Figure 9 - Paraná Basin polycyclic nature revealed by CAD (A) and MDS plots (B), demonstrating an overlapping of detrital zircon ages from Carboniferous to Cretaceous strata (data from Canile et al., 2016; Phillip et al., 2018).

The conglomeratic end-member of the Triassic unit (Santa Cruz Sequence - Philip *et al.*, 2018) contains an assemblage enriched in Cambrian-Neoproterozoic ages, whilst finer grained components display a complex Permian to Paleoproterozoic age distribution. The similarity between the conglomerate end-members (Triassic) and eastern Botucatu samples (MDS and CAD) suggests that eastern Botucatu samples contain a relatively smaller amount of recycled material in comparison to central/west samples, especially in intratrap (PB-31B) samples.

5.3. Controls on Heavy Mineral Assemblages

The MDS biplot of the heavy mineral (Fig. 10) data defines two distinct clusters: (i) a well-defined group, referred to here as the average Botucatu composition and (ii) isolated samples referred to as local detrital component. The average Botucatu composition includes the majority of studied samples and has a mean composition of $ZTR_{0.9}$, with samples distributed throughout the basin, irrespective of stratigraphic level (basal, top or interbedded sandstone) or the sampling region (west, center or east). The local detrital component has a mean composition of $ZTR_{0.6}$ related primarily to peaks of Fe-Garnet, epidote, and Mn oxides (samples PB -31B, -20, -2A, -09). Fe-Garnet and epidote are common heavy mineral constituents, although pyrolusite is infrequent. Mn oxides are common in Serra Geral lavas, and its presence in the Botucatu indicates an authigenic phase. The heavy mineral and petrographic composition of the Botucatu Formation is considered to be representative of the original sediment source composition with little subsequent modification by burial diagenesis and weathering the reasons for which are discussed below.

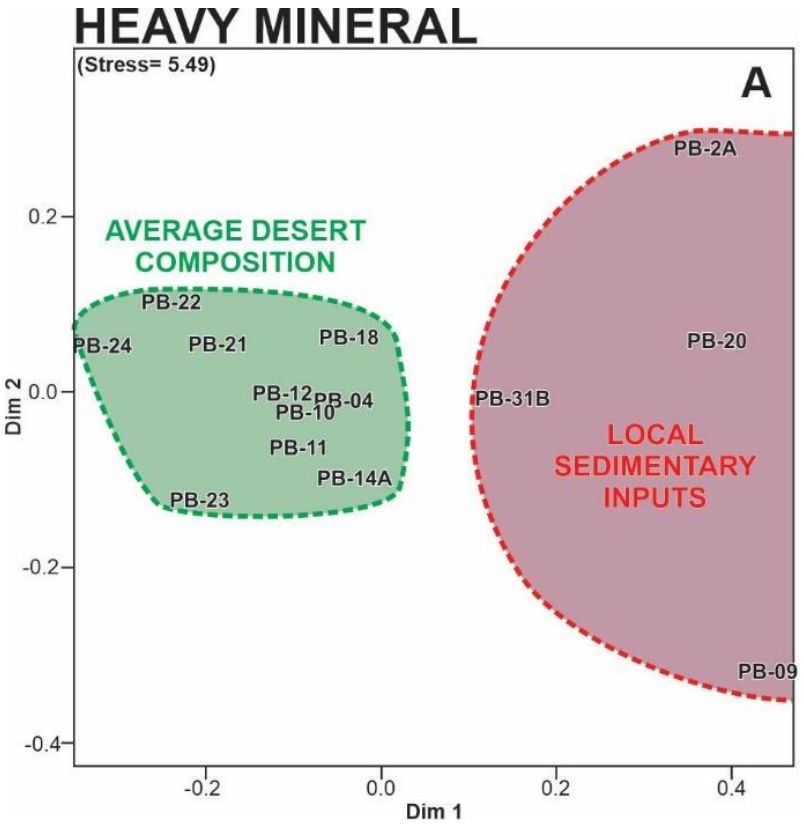

Figure 10 - MDS biplot on heavy mineral dataset demonstrates an average composition (ZTR-rich) and local detrital input (garnet, epidote and pyrolusite).

Morton and Halllsworth (2007) described the effects of burial related dissolution on heavy mineral assemblages. They demonstrated that epidote and garnet remain stable until respectively 1.0 and 3.5 km in the North Sea Basin. Andò (2012) in a study of cores from Bengal Bay showed that the progressive dissolution of amphibole occurred at burial depths of up to 1.5 km and for epidote at depths of up to 2.5 km, transitioning to a garnet and ZTR assemblage below 2.5. km depth. The Botucatu burial history suggests relatively shallow burial of up to 1.5 km in the basin depocenter in the north (Milani, 2007). The thinner lava-pile and absence of upper-basalt sedimentary deposits along the southern margin, points to a relatively shallower burial depth of 700-800 m (lava-pile thickness in south). Limited burial suggests that the presence of garnet and epidote is not controlled by burial related dissolution but likely due to provenance controls.

The common presence of micro- and moldic porosity (on lithics and feldspars) and feldspar dissolution may suggest a degree of surface weathering altering the composition on outcrops. However, França *et al.* (2003) describes feldspar dissolution in well cores, such that the process also occurs at depth. The sampling occurs mostly on road-side outcrops in similar climatic condition (humid and hot) across the studied area. If differential dissolution was the driving mechanism to generate local compositional variations, intermediate of heavy minerals assemblages would also be expected with highly weathered/dissolved garnet and epidotes in ZTR enriched samples, which does not occur. Thus, the local variations apparently are not controlled by differential surface weathering, indicating the heavy mineral and petrographic changes are depositional.

Reconstructions of desert depositional systems (e.g. Pye and Tsoar, 2008) illustrate the coexistence of different depositional environments such as rivers, alluvial fans and deltas that could provide sediment for a dune field. An erg margin, as in the study area, is prone to different styles of interaction between depositional systems, particularly at the fluvial-aeolian interface (Al-Masrahy and Mountney, 2015). Whilst there are very few preserved records of waterlain deposits in the dry-aeolian Botucatu system, fluvial input is likely to have occurred around the erg margins with subsequent aeolian reworking removing that sedimentary signature. Provenance studies from present day deserts such as Taklamakann (Rittner *et al.,* 2016), Arabia (Garzanti *et al.,* 2013) and Namibia (Garzanti *et al.,* 2012), demonstrate that shifts in provenance can be correlated with fluvial, alluvial fan or deltaic inputs. The localized heavy mineral peaks (Fig. 5) concomitant with increase in quartz content suggests a point-sourced alluvial system reworked laterally by aeolian processes. Aeolian systems promote an

increase in grain roundness, but at the same time maintain stable heavy mineral proportions (Resentini *et al.*, 2018).

6. MULTISCALE DESERT FILLING

Despite the similarities in the petrographic, heavy mineral and detrital zircon compositions, subtle differences are present in the dataset, indicating the presence of additional controls on sandstone composition. The data set reveals two important characteristics: (i) lateral variations in detrital zircon age spectra and (ii) differences in heavy mineral and petrographic data that suggest local sediment input points. The lateral provenance variations (5.1) are illustrated on Figure 11, demonstrating that the detrital zircon, granulometry, petrography and heavy mineral assemblages change from East to West. Additionally, the figure shows the underlying units (Paraná Basin) and basement terranes that compose the Sul-Rio-Grandense and Uruguayan shields.

As discussed in 5.2, the detrital zircon composition of Botucatu and Paraná Basin units display a statistical similarity, suggesting that underlying units provided the last sediment source for the Botucatu Desert. Figure 11 displays the overlap of the lateral variations and underlying units of Botucatu (Guará Fm., Santa Maria Fm., and Pirambóia Fm.) suggesting these units as the most feasible sediment source. Furthermore, Figure 11 illustrates how ultimately the basement age framework contributes to the lateral detrital zircon variation. The prevalent >900 Ma terranes in the West (Tacuarembó, Nico Perez and Piedras Altas) contrasting with the C-Np ages at East (Dom Feliciano Belt) probably contributed with Ordovician to Jurassic Paraná Basin filling, later being rework for Botucatu. The grain-size, heavy mineral and petrography partly support the lateral changes in the detrital zircon population, supporting the notion that reworking of Paraná underlying rocks was the main reason

for the lateral variation. The large-scale control (up to 600km margin) shows that aeolian processes were not able to completely homogenize the overall composition of the sand supplied to the Botucatu erg.

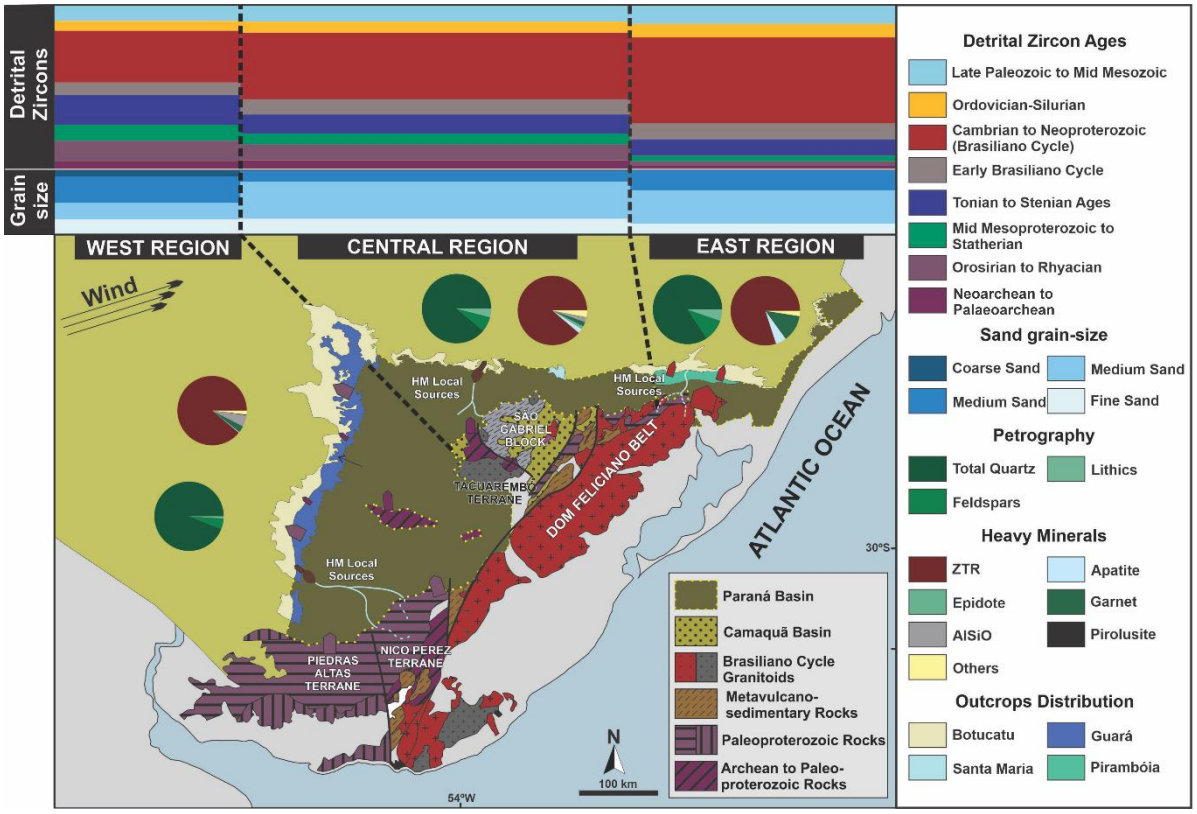

Figure 11 - Source-to-sink map demonstrating the impact of surrounding basement and external sources on the Botucatu DZ composition. Pie-charts displays the mean petrography and heavy mineral compositions, mirroring a lateral variation with DZ and granulometric data. At local level, fluvial inputs generate heavy mineral anomalous compositions. Data for the basement are from Saalman *et al.* (2011) and the desert extent is from Scherer and Goldberg (2007)

The anomalous heavy mineral values characterize local sedimentary input, however, is not clear if this input was sourced directly from basement material, reworked from older, underlying sedimentary successions or combination of both. Figure 11 illustrates the fluvial systems draining Paraná Basin units and possible basement terranes. The evidence for local sediment input supports the idea of a

number of distinct sediment pathways into the Botucatu erg, resulting in distinct, identifiable compositional signatures.

7. CONCLUSIONS

A provenance analysis of the aeolian sediments of the Botucatu Formation along the southern margin of the Paraná Basin has been undertaken to provide insights into depositional controls. The provenance dataset of detrital zircon U-Pb dating, heavy mineral analysis, petrography and granulometric analysis using multi-statistical tools (multidimensional scaling, cumulative density plot, and density plots) indicate that:

- Cambrian to Neoproterozoic ages (515-650 Ma) are the main detrital zircon component, with subsidiary contributions from Orosirian to Rhyacian (1.8-2.2 Ga) and Tonian to Stenian ages (0.9-0.125 Ga);

- A progressive lateral change in detrital zircon ages together with changes in the underlying basin stratigraphy and basement domains suggests a polycyclic provenance;

- Eastern region records an upward increase of Cambrian to Neoproterozoic detrital zircons, central and western regions show no significant changes;

- There is a progressive downwind decrease in grain size from medium to very fine sand over a distance of 600 km from downwind;

- An average quartz-ZTR enriched composition predominates along the southern Botucatu margin, variations allow recognition of local sediment input points within an otherwise homogenous aeolian system which likely relate to local fluvial systems developed along the erg margin.

8. ACKNOWLEDGMENTS

The authors gratefully acknowledge support from Shell Brasil through the 'BG05: UoA-UFRGS-SWB Sedimentary Basins' project at UFRGS and the strategic importance given by ANP through the R&D levy regulation. We also thank Conselho Nacional de Desenvolvimento Científico e Tecnológico (CNPq) by the financial support (grant 203786/2017-3). The authors would like to thank Renan Guilherme de Souza and Adriano Reis for help in Tacuarembó/Uy Field Trip. This work is part of the current dual-degree Ph.D. from Gabriel Bertolini at Universidade Federal do Rio Grande do Sul and University of Aberdeen.

9. REFERENCES

Al-Masrahy, M. A. and Mountney, N. P. (2015) A classification scheme for fluvial-aeolian system interaction in desert-margin settings. *Aeolian Research*, 17, 67-88.

Amarante, F. B., Scherer, C. M. S., Aguilar C. A. G., Reis, A. D., Mesa, V. and Souto, M. (2019). Fluvial-eolian deposits of the Tacuarembó Formation (Norte Basin - Uruguay): Depositional models and stratigraphic succession. *J. S. Am. Earth Sci.*, 90, 355–376.

Andò, S., Garzanti, E., Padoan, M., and Limonta, M. (2012). Corrosion of heavy minerals during weathering and diagenesis: A catalog for optical analysis. *Sed. Geol.*, 280, 165-178.

Bahlburg, H., Vervoort, J. D., Du Frane, S. A., Bock, B., Augustsson, C. and Reimann, C. (2009). Timing of crust formation and recycling in accretionary orogens: Insights learned from the western margin of South America. *Earth-Sci. Rev.*, 97(1-4), 215-241.

Baksi, A. K. (2018). Paraná flood basalt volcanism primarily limited to~ 1 Myr beginning at 135 Ma: New 40Ar/39Ar ages for rocks from Rio Grande do Sul, and critical evaluation of published radiometric data. *J. Volcanol. Geoth. Res.*, 355, 66-77.

Basei, M. A. S., Frimmel, H. E., Nutman, A. P., and Preciozzi, F. (2008). West Gondwana amalgamation based on detrital zircon ages from Neoproterozoic Ribeira and Dom Feliciano belts of South America and comparison with coeval sequences from SW Africa. *Geological Society*, London, Special Publications, 294(1), 239-256.

Bial, J., Buettner, S. H., Schenk, V. and Appel, P. (2015). The long-term high-temperature history of the central Namaqua Metamorphic Complex: Evidence for a Mesoproterozoic continental back-arc in southern Africa. *Precambrian Res.*, 268, 243-278.

Bigarella, J. J., and Salamuni, R. (1961). Early Mesozoic wind patterns as suggested by dune bedding in the Botucatu Sandstone of Brazil and Uruguay. *Geological Society of America Bulletin*, 72(7), 1089-1105.

Blott, S. J. and Pye, K. (2001). GRADISTAT: a grain size distribution and statistics package for the analysis of unconsolidated sediments. *Earth Surf. Proc. Land.*, 26(11), 1237-1248.

Canile, F. M., Babinski, M. and Rocha-Campos, A. C. (2016). Evolution of the Carboniferous-Early Cretaceous units of Paraná Basin from provenance studies based on U-Pb, Hf and O isotopes from detrital zircons. *Gondwana Res.*, 40, 142-169.

Cardenas, B. T., Kocurek, G., Mohrig, D., Swanson, T., Hughes, C. M., and Brothers, S. C. (2019). Preservation of Autogenic Processes and Allogenic Forcings in Set-Scale Aeolian Architecture II: The Scour-and-Fill Dominated Jurassic Page Sandstone, Arizona, USA. *J. Sed. Res*., 89(8), 741-760.

Casquet, C., Pankhurst, R. J., Rapela, C. W., Galindo, C., Fanning, C. M., Chiaradia, M., Baldo, E., González-Casado, J. M. and Dahlquist, J. A. (2008). The Mesoproterozoic Maz terrane in the Western Sierras Pampeanas, Argentina, equivalent to the Arequipa-Antofalla block of southern Peru: Implications for West Gondwana margin evolution. *Gondwana Research*, 13(2), 163-175.

Dias, K. D. N. and Scherer, C. M. (2008). Cross-bedding set thickness and stratigraphic architecture of aeolian systems: an example from the Upper Permian Pirambóia Formation (Paraná Basin), southern Brazil. *J. S. Am. Earth Sci.*, 25(3), 405-415.

Dickinson, W. R. and Gehrels, G. E. (2003). U–Pb ages of detrital zircons from Permian and Jurassic eolian sandstones of the Colorado Plateau, USA: paleogeographic implications. *Sed. Geol.*, 163(1-2), 29-66.

Dickinson, W. R., and Gehrels, G. E. (2010). Insights into North American paleogeography and paleotectonics from U–Pb ages of detrital zircons in Mesozoic strata of the Colorado Plateau, USA. *International Journal of Earth Sciences*, 99(6), 1247-1265.

Dickinson, W. R., and Gehrels, G. E. (2009). U-Pb ages of detrital zircons in Jurassic eolian and associated sandstones of the Colorado Plateau: Evidence for transcontinental dispersal and intraregional recycling of sediment. *Geological Society of America Bulletin*, 121(3-4), 408-433.

Dickinson, W. R. (1985). Interpreting provenance relations from detrital modes of sandstones. In.: *Provenance of arenites* (pp. 333-361). Springer, Dordrecht.

Ernesto, M., Raposo, M. I. B., Marques, L. S., Renne, P. R., Diogo, L. A., and De Min, A. (1999). Paleomagnetism, geochemistry and 40Ar/39Ar dating of the North-eastern Paraná Magmatic Province: tectonic implications. *Journal of Geodynamics*, 28(4-5), 321-340.

Farrant, A. R., Mounteney, I., Burton, A., Thomas, R. J., Roberts, N. M., Knox, R. W., and Bide, T. (2019). Gone with the wind: dune provenance and sediment recycling in the northern Rub'al-Khali, United Arab Emirates. *Journal of the Geological Society*, 176(2), 269-283.

França, A. B., Araújo, L. M., Maynard, J. B. and Potter, P. E. (2003). Secondary porosity formed by deep meteoric leaching: Botucatu eolianite, southern South America. *AAPG bulletin*, 87(7), 1073-1082.

Francischini, H., Dentzien–Dias, P. C., Fernandes, M. A. and Schultz, C. L. (2015). Dinosaur ichnofauna of the Upper Jurassic/Lower Cretaceous of the Paraná Basin (Brazil and Uruguay). *J. S. Am. Earth Sci.*, 63, 180-190.

Garzanti, E., Vermeesch, P., Vezzoli, G., Andò, S., Botti, E., Limonta, M., Dinis, P., Hahn, A., Baudet, D., De Grave, J. and Yaya, N. K. (2019). Congo River sand and the equatorial quartz factory. *Earth-Science Reviews*, 102918.

Garzanti, E., Vermeesch, P., Padoan, M., Resentini, A., Vezzoli, G., and Andò, S. (2014). Provenance of passive-margin sand (Southern Africa). *The Journal of Geology*, 122(1), 17-42.

Garzanti, E., Vermeesch, P., Andò, S., Vezzoli, G., Valagussa, M., Allen, K., Kadi, K.A. and Al-Juboury, A.I. (2013). Provenance and recycling of Arabian desert sand. *Earth-Sci. Rev.*, 120, 1-19.

Garzanti, E., Andò, S., Vezzoli, G., Lustrino, M., Boni, M. and Vermeesch, P. (2012). Petrology of the Namib Sand Sea: long-distance transport and compositional variability in the wind-displaced Orange Delta. *Earth-Sci. Rev.*, 112(3-4), 173-189.

Garzanti, E., Dinis, P., Vermeesch, P., Andò, S., Hahn, A., Huvi, J Limonta, M., Padoan, M., Resentini, A., Rittner, M. and Vezzoli, G. (2018). Dynamic uplift, recycling, and climate control on the petrology of passive-margin sand (Angola). *Sed. Geo.*, 375, 86-104.

Gehrels, G. (2014). Detrital zircon U-Pb geochronology applied to tectonics. *Annual Review of Earth and Planetary Sciences*, 42, 127-149.

Havholm, K. G., and Kocurek, G. (1994). Factors controlling aeolian sequence stratigraphy: clues from super bounding surface features in the Middle Jurassic Page Sandstone. *Sedimentology*, 41(5), 913-934.

Höfig, D. F., Marques, J. C., Basei, M. A. S., Giusti, R. O., Kohlrausch, C., and Frantz, J. C. (2018). Detrital zircon geochronology (U-Pb LA-ICP-MS) of syn-orogenic basins in SW Gondwana: New insights into the Cryogenian-Ediacaran of Porongos Complex, Dom Feliciano Belt, southern Brazil. *Precambrian Research*, 306, 189-208.

Hurst, A., Morton, A., Scott, A., Vigorito, M., and Frei, D. (2017). Heavy-Mineral Assemblages In.: Sandstone Intrusions: Panoche Giant Injection Complex, California. *J. Sed. Res.*, 87(4), 388-405.

Ingersoll, R. V., Bullard, T. F., Ford, R. L., Grimm, J. P., Pickle, J. D. and Sares, S. W. (1984) The effect of grain size on detrital modes: a test of the Gazzi-Dickinson point-counting method. *J. Sed. Res.*, 54(1), 103-116.

Janasi, V. A., Freitas, V. A. and Heaman, L. H. (2011). The onset of flood basalt volcanism, Northern Paraná Basin, Brazil: A precise U–Pb baddeleyite/zircon age for a Chapecó-type dacite. *Earth Planet. Sci. Lett.*, 302(1-2), 147-153.

Janikian, L., de Almeida, R. P., Fragoso-Cesar, A. R. S., de Souza Martins, V. T., Dantas, E. L., Tohver, E., and D'Agrella-Filho, M. S. (2012). Ages (U–Pb SHRIMP and LA ICPMS) and stratigraphic evolution of the Neoproterozoic volcano-sedimentary successions from the extensional Camaquã Basin, Southern Brazil. *Gondwana Res.*, 21(2-3), 466-482.

Jenisch, A. G., Lehn, I., Gallego, O. F., Monferran, M. D., Horodyski, R. S. and Faccini, U. F. (2017). Stratigraphic distribution, taphonomy and paleoenvironments of Spinicaudata in the Triassic and Jurassic of the Paraná Basin. *J. S. Am. Earth Sci.*, 80, 569-588.

Mange, M. A., and Maurer, H (2012). *Heavy minerals in colour*. Springer Science & Business Media.

Mcbride, E. F. (1985). Diagenetic processes that affect provenance determinations in sandstone. In.: *Provenance of arenites* (pp. 95-113). Springer, Dordrecht.

Milani, E. J., Melo, J. H. G., Souza, P. A., Fernandes, L. A. and França, A. B (2007). Bacia do Paraná. *Boletim de Geociências Petrobrás*, 15 (2), 265-287.

Milani, E. J., Faccini, U. F., Scherer, C. M. S., Araújo, L. M. and Cupertino, L. M. (1998). Sequences and stratigraphic hierarchy of the Paraná Basin (Ordovician to Cretaceous), Southern Brazil. Bol. IG USP, Série Científica, 29, 125-173.

Morton, A. C. and Hallsworth, C. (2007). Stability of detrital heavy minerals during burial diagenesis. *Developments in Sedimentology*, 58, 215-245.

Morton, A. C., and Hallsworth, C. (1994). Identifying provenance-specific features of detrital heavy mineral assemblages in sandstones. *Sed. Geol*, 90(3-4), 241-256.

Oriolo, S., Oyhantçabal, P., Basei, M.A., Wemmer, K. and Siegesmund, S. (2016). The Nico Pérez Terrane (Uruguay): from Archean crustal growth and connections

with the Congo Craton to late Neoproterozoic accretion to the Río de la Plata Craton. *Precambrian Res.*, 280, 147-160.

Oyhantçabal, P., Oriolo, S., Philipp, R. P., Wemmer, K. and Siegesmund, S. (2018a). The Nico Pérez Terrane of Uruguay and Southeastern Brazil. In *Geology of Southwest Gondwana* (pp. 161-188). Springer, Cham.

Oyhantçabal, P., Cingolani, C. A., Wemmer, K., and Siegesmund, S. (2018b). The Río de la Plata craton of Argentina and Uruguay. In.: *Geology of Southwest Gondwana* (pp. 89-105). Springer, Cham.

Oyhantçabal, P., Wagner-Eimer, M., Wemmer, K., Schulz, B., Frei, R. and Siegesmund, S. (2012). Paleo-and Neoproterozoic magmatic and tectonometamorphic evolution of the Isla Cristalina de Rivera (Nico Pérez Terrane, Uruguay). *International Journal of Earth Sciences*, 101(7), 1745-1762.

Perea, D., Soto, M., Veroslavsky, G., Martínez, S. and Ubilla, M. (2009). A Late Jurassic fossil assemblage in Gondwana: biostratigraphy and correlations of the Tacuarembó Formation, Parana Basin, Uruguay. *J. S. Am. Earth Sci.,* 28(2), 168-179.

Peri, V. G., Naipauer, M., Pimentel, M. and Barcelona, H. (2016). Eolian deposits of the shouthwestern margin of the Botucatú paleoerg: reconstruction of the Gondwana landscape in central northern Argentina. *Sed. Geol.*, 339, 234-257.

Philipp, R. P., Schultz, C. L., Kloss, H. P., Horn, B. L., Soares, M. B., and Basei, M. A. (2018). Middle Triassic SW Gondwana paleogeography and sedimentary dispersal revealed by integration of stratigraphy and U-Pb zircon analysis: the Santa Cruz Sequence, Paraná Basin, Brazil. *J. S. Am. Earth Sci.*, 88, 216-237.

Philipp, R. P., Pimentel, M. M. and Chemale Jr, F. (2016) Tectonic evolution of the Dom Feliciano Belt in Southern Brazil: geological relationships and U-Pb geochronology. *Brazilian Journal of Geology*, 46, 83-104.
Pinto, V. M., Hartmann, L. A., Santos, J. O. S., McNaughton, N. J., and Wildner, W. (2011). Zircon U–Pb geochronology from the Paraná bimodal volcanic province support a brief eruptive cycle at~ 135 Ma. *Chemical Geology*, 281(1-2), 93-102.

Pye, K., and Tsoar, H. (2008). Aeolian sand and sand dunes. Springer Science & Business Media.

Rahl, J. M., Reiners, P. W., Campbell, I. H., Nicolescu, S., and Allen, C. M. (2003). Combined single-grain (U-Th)/He and U/Pb dating of detrital zircons from the Navajo Sandstone, Utah. *Geology*, 31(9), 761-764.

Rapela, C. W., Pankhurst, R. J., Casquet, C., Baldo, E., Galindo, C., Fanning, C. M. and Dahlquist, J. M. (2010). The Western Sierras Pampeanas: Protracted Grenville-age history (1330-1030 Ma) of intra-oceanic arcs, subduction–accretion at continental-edge and AMCG intraplate magmatism. *J. S. Am. Earth Sci.*, 29(1), 105-127.

Resentini, A., Andó, S., and Garzanti, E. (2018). Quantifying roundness of detrital minerals by image analysis: Sediment transport, shape effects, and provenance implications. *J. Sed. Res.*, 88(2), 276-289.

Rittner, M., Vermeesch, P., Carter, A., Bird, A., Stevens, T., Garzanti, E., Andò, S., Vezzoli, G., Dutt, R., Xu, Z. and Lu, H. (2016). The provenance of Taklamakan desert sand. *Earth Planet. Sci. Lett.*, 437, 127-137.

Rossetti, L., Lima, E. F., Waichel, B. L., Hole, M. J., Simões, M. S., and Scherer, C. M.S. (2018). Lithostratigraphy and volcanology of the Serra Geral Group, Paraná-Etendeka Igneous Province in southern Brazil: Towards a formal stratigraphical framework. *J. Volcanol. Geoth. Res.*, 355, 98-114.

Saalmann, K., Gerdes, A., Lahaye, Y., Hartmann, L. A., Remus, M. V. D., and Läufer, A. (2011) Multiple accretion at the eastern margin of the Rio de la Plata craton: the prolonged Brasiliano orogeny in southernmost Brazil. *International Journal of Earth Sciences*, 100(2-3), 355-378.

Santos, J. O. S., Hartmann, L. A., Bossi, J., Campal, N., Schipilov, A., Piñeyro, D. and McNaughton, N. J. (2003). Duration of the Trans-Amazonian Cycle and its correlation within South America based on U-Pb SHRIMP geochronology of the La Plata Craton, Uruguay. *Int. Geol. Rev.*, 45(1), 27-48.

Sato, K., Basei, M. A. S., Ferreira, C. M., Sproesser, W. M., Vlach, S. R. F., Ivanuch, W. and Onoi, A. T. (2011). U-Th-Pb analyses by excimer laser ablation/ ICP-MS on MG Brazilian xenotime. *Goldschmidt Conference Abstracts*. Miner Mag 1801.

Scherer, C. M. and Goldberg, K. (2007). Palaeowind patterns during the latest Jurassic–earliest Cretaceous in Gondwana: Evidence from aeolian cross-strata of the Botucatu Formation, Brazil. *Palaeogeogr. Palaeoclimatol. Palaeoecol.*, 250(1-4), 89-100.

Scherer, C. M. and Lavina, E. L. (2006). Stratigraphic evolution of a fluvial–eolian succession: the example of the Upper Jurassic-Lower Cretaceous Guará and Botucatu formations, Paraná Basin, Southernmost Brazil. *Gondwana Research*, 9(4), 475-484.

Scherer, C. M. S. (2000). Eolian dunes of the Botucatu Formation (Cretaceous) in southernmost Brazil: morphology and origin. *Sed. Geol.*, 137(1-2), 63-84.

Scherer, C. M. S. (2002). Preservation of aeolian genetic units by lava flows in the Lower Cretaceous of the Paraná Basin, southern Brazil. *Sedimentology*, 49(1), 97-116.

Schneider, R. L., Muhlmann, H., Tommasi, E., Medeiros, R. A., Daemon, R. F. and Nogueira, A. A. (1973). Revisão estratigráfica de Bacia do Paraná An. XXVIII Congr. Bras. Geol., Soc. Bras. Geol., 1, pp. 41-65.

Soto, M. and Perea, D. (2008). A ceratosaurid (Dinosauria, theropoda) from the late Jurassic-Early Cretaceous of Uruguay. *Journal of Vertebrate Paleontolology*, 28(2), 439-444.

Thiede, D. S., and Vasconcelos, P. M. (2010). Paraná flood basalts: rapid extrusion hypothesis confirmed by new 40Ar/39Ar results. *Geology*, 38(8), 747-750.

Vermeesch, P., Resentini, A. and Garzanti, E. (2016) An R package for statistical provenance analysis. *Sed. Geol.*, 336, 14-25.

Wildner, W., Ramgrab, G. E., Lopes, R. C. and Iglesias, C. M. F. (2006). Mapa geológico do Estado do Rio Grande do Sul, Escala 1:750.000. CPRM - Companhia de Pesquisa de Recursos Minerais, Porto Alegre.

Zalán, P. V., Wolff, S. J. C. J., Conceição, J. D. J., Marques, A., Astolfi, M. A. M., Vieira, I. S., Appi, V. T. and Zanotto, O. A. (1990). Bacia do Paraná. *Origem e evolução das bacias sedimentares*, pp.135-168.

Zerfass, H., Lavina, E. L., Schultz, C. L., Garcia, A. J. V., Faccini, U. F. and Chemale Jr, F. (2003). Sequence stratigraphy of continental Triassic strata of Southernmost Brazil: a contribution to Southwestern Gondwana palaeogeography and palaeoclimate. *Sed. Geol.*, 161(1-2), 85-105.

ARTIGO II - PROVENANCE CONTROLS ON CRETACEOUS AEOLIAN SEDIMENT ACCUMULATION IN WESTERN GONDWANA

From: Sedimentary Geology
Sent: 05 March 2020 05:15
To: gabertol@gmail.com; gabertol@terra.com.br
Subject: SEDGEO7652 - Notice of manuscript number

*** Automated email sent by the system ***

Dear Mr. Bertolini,

Your submission entitled "Provenance controls on cretaceous aeolian sediment accumulation in Western Gondwana" has been assigned the following manuscript number: SEDGEO7652.

Your paper will be considered as belonging to the category Research Paper. Please contact us if this is not correct.

You will be able to check on the progress of your paper by logging on https://ees.elsevier.com/sedgeo/ as Author.

Thank you for submitting your work to this journal.

Kind regards,

Sedimentary Geology

PROVENANCE CONTROLS ON CRETACEOUS AEOLIAN SEDIMENT ACCUMULATION IN WESTERN GONDWANA

Bertolini, G.[1,2,*], Marques, J.C[1]., Hartley, A.J.[2], Basei, M.A.S[3], Frantz, J.C.[1], Santos, P.R.[3]

[1] Universidade Federal do Rio Grande do Sul
[2] University of Aberdeen
[3] Universidade de São Paulo

* **Corresponding author** (e-mail: gabertol@gmail.com)

Abstract: The Early Cretaceous Botucatu Formation comprises a dry-aeolian system developed in western Gondwana and preserved within the Paraná Basin of central Brazil. Multiproxy provenance analysis (detrital zircon U-Pb dating, heavy mineral, petrographic and granulometric analysis) was undertaken across two 500 km transects (NW and NE) along the northern margin of the Paraná Basin. To assess the provenance variation within the aeolian stratigraphy, samples were taken from the base and top of the Botucatu Formation and from sandstones interbedded with volcanics in the overlying Serra Geral Formation. Granulometric analysis shows a mean fine to very-fine sand. The bulk petrography shows an average composition of $Q_{91}F_6L_2$ and, and heavy mineral analysis shows a mean of 86% of zircon-tourmaline-rutile, demonstrating the overall polycyclic nature of the sediment. The discrete occurrence of garnet, apatite and epidote indicates local sediment input points, providing indirect evidence for point-sourced fluvial input into an overall dry aeolian system. Detrital zircon U-Pb LA-ICP-MS dating demonstrates a dominant Cambrian to Neoproterozoic (520-750 Ma) population with subsidiary Tonian-Stenian (0.9-1.2 Ga) and Orosirian-Rhyacian (1.9-2.3 Ga) contributions. Statistical plots illustrate the detrital zircon age variability- recording an upward decrease in the age proportion of Permian and Tonian-Stenian populations and an increase of Cambrian-Neoproterozoic dates towards the top. Botucatu sands registers a polycyclic history, however the age proportion variations, such as the Cambrian-Neoproterozoic increase in NE, suggests a stronger impact of the Ribeira Belt granites in NE region, while in the NW region a mixture of Paraguay Belt, Rio Apa and Amazonian Craton sources is envisaged.

1. INTRODUCTION

Western Gondwana was dominated by an extensive arid region during the Early Cretaceous, with development of a continuous, laterally extensive dune field (Scherer, 2000), referred to as the Botucatu Desert. The Botacatu Formation and its equivalents cover the present-day territories of Brazil (central to south), Uruguay, Argentina, Paraguay and Namibia (Scherer & Goldberg, 2007). Early Cretaceous desert development in Gondwana was controlled primarily by the landmass configuration, wind circulation patterns, location of orogenic massifs and oceanic currents (Livingstone and Warren, 2019). Modern sand-sea analogues, such as the Rub`al Khali, Kalahari and Sahara, shows complex sediment supply systems with a number of different coexisting depositional environments (Goudie, 2004; Garzanti *et al.*, 2013 and 2014), which should be similar for the ancient Botucatu sand sea. Provenance studies have been used to characterize sedimentary transport routes and source-to-sink paths, including the impact of basement terrains on supplying sediment to aeolian systems (Dickinson and Gehrels, 2003; Rahl *et al.*, 2003; Garzanti et al., 2016; Rittner et al., 2016; Farrant et al., 2019). These studies reveal that even subtle variations in sands compositions can be traced back to ergs depositional process. The Paraná Basin developed across a number of cratonic terranes and orogenic belts related to the Brasiliano - Pan African cycles (Bahlburg *et al.*, 2009; Zalán *et al.*, 1990). The Archean to Neoproterozoic bounding basement ultimately sourced the sediment for the Paraná Basin, however the low sedimentary input and the complex erosive/deposition history during basin evolution may have resulted in complex intrabasinal reworking dominating over first cycle derived material in supplying sediment to the basin. To understand the relationship between desert sediment generation and basement terrane composition, we evaluated variations in sediment

provenance across >1000km along the northern outcrop of the Botucatu Formation. This work addresses vertical and lateral changes in the northern Botucatu Formation derivation through the application of multi-provenance techniques including U-Pb LA-ICP-MS dating on detrital zircon (DZ), heavy mineral analysis, petrography and granulometric analysis.

2.GEOLOGIC SETTING

The present-day geological configuration of Central Brazil comprises a number of amalgamated orogenic belts including the Amazonian, Rio Apa, Paranapanema and Sao Francisco Cratons (Almeida 1981) covered by Paleozoic-Mesozoic sediments of the Paraná Basin. The 8 km thick Ordovician to Cretaceous depositional record ot the Paraná Basin consists of 6 supersequences (Fig.1) (Zalán, 1990; Milani, 2007). The basin has a complex fill history, broadly transitioning from marine successions during three cycles (Rio Ivaí, Paraná and Gondwana I supersequences) to continental deposition (Gondwana II Gondwana III, Bauru) (Milani *et al.*, 1998) (Figure 1). The Botucatu Formation and overlying lavas of the Serra Geral Formation (Paraná-Etendeka large igneous province) comprise part of the Gondwana III supersequence (Milani *et al.*, 1998). In the northern part of the basin, the Permian fluvial-aeolian Pirambóia Formation is present beneath the Botucatu Formation, in contrast to the Triassic-Jurassic sediments that underlie the Botucatu in the southern Paraná Basin.

During the Early Cretaceous, the Paraná Basin occupied an extensive area of SW Gondwana (Scherer, 2000 and 2002; Scherer and Lavina, 2006; Milani *et al.*,1998). Deposition of the Botucatu Formation records the onset of sedimentation in the basin following a ca. 100 Ma hiatus (Milani *et al.*, 1998). The Botucatu Formation occupies an area of $1.5x10^6$ km^2, with a thickness between 0 and 400m. In the study

area, along the northern basin margin, the formation ranges from 200 m thick in the northeast to 400m in the northwest (Milani *et al.*, 1998). Botucatu sediments are considered to represent a dry aeolian system, marked by the absence of interdune deposits. In some areas, occurrences of small fluvial deposits (ephemeral streams) have been documented (Scherer 2000, Scherer and Lavina, 2006 and Moraes and Seer, 2017). Paleowind patterns in the northern part of the Botucatu outcrop belt are to the south (Scherer and Goldberg, 2007).

An important characteristic of the Botucatu Formation is the relationship with the overlying lava flows of the Serra Geral Formation (Paraná-Etendeka LIP). This interaction produces widespread occurrences of *in situ* dunes preserved by and interbedded with lava flows. U-Pb and Ar-Ar dating of the Serra Geral Formation constrains the end of Botucatu deposition as being Valanginian in age (ca. 134 Ma) (Ernesto *et al.*,1999; Thiede and Vasconcelos, 2010; Pinto *et al.*, 2011; Janasi *et al.*, 2011, Baksi, 2018).

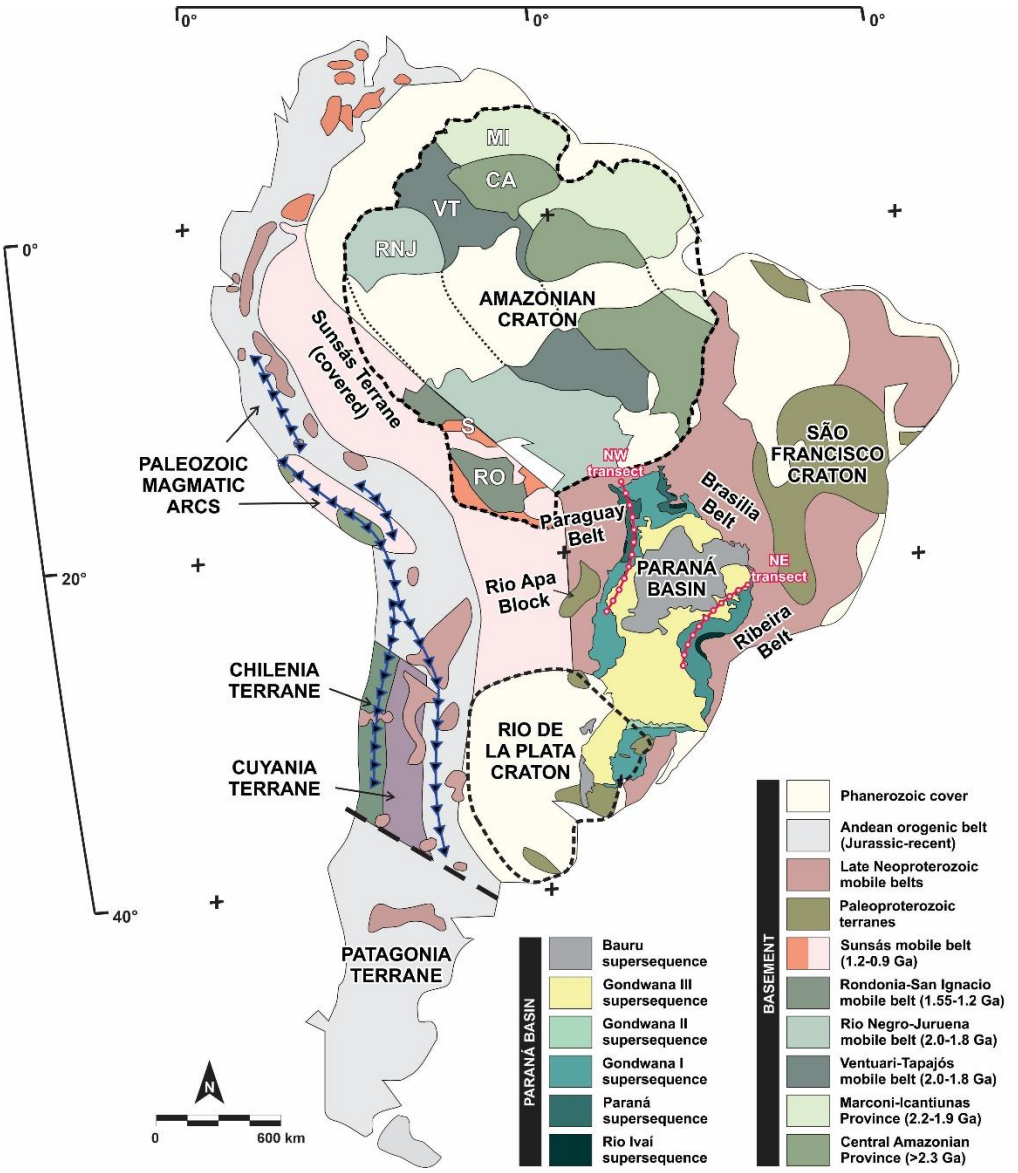

Figure 1 - Geological distribution of basement rocks showing Paraná Basin supercycles and the basement units across South-America continent (Adapted from Bahlburg et al., 2009 and Milani, 1998). The studied area is illustred by the pink-line NE and NW transects.

The Paraná basin basement rocks are composed of the Brasilia and Ribeira belts (Northeastern margin) and the Paraguay Belt and the Rio Apa and Amazonian Cratons (Northwestern margin) (Fig. 1A). The Ribeira Belt comprises Neoproterozoic metasedimentary rocks (840-565 Ma), magmatic arcs (840-605Ma), syn-to-late collisional granite-gneisses (605-480 Ma) and a Meso-Paleoproterozoic basement (1.9-2.8 Ga) (Heilbron *et al.*, 2000, 2004 and 2008). West of and adjacent to the

Ribeira Belt, the Southern Brasilia Belt includes a series of Neoproterozoic metasedimentary successions (Araxá and Canastra Groups) and the Goiás Magmatic arc (900-650 Ma) (Valeriano, 2017, Pimentel *et al.*,1991; Pimentel and Fuck, 1994; Gioia,1997; Motta-Araújo, Pimentel and Armstrong, 2003; Laux *et al.*, 2004). The Paraguay Belt corresponds to an Ediacaran – Cryogenian metasedimentary succession, with limited associated Cambrian magmatic rocks (Sao Vicente Granite (490-510 Ma)) (Nogueira *et al.*, 2007; McGee *et al.*, 2012). The multiphase Amazonian Craton comprises multiple NW-SE trending accreted arcs: Central Amazon Province (2.5-3.0 Ga), Maroni-Itacaiunas (2.45-1.95 Ga), Ventuari-Tapajós (2.0-1.8 Ga), Rio-Negro-Juruena (1.82-1.60 Ga), Rondonia-San Ignacio (1.59-1.30Ga) and Sunsás (1.20-0.95 Ga) provinces. The Rio Apa Craton comprises an Orosirian-Statherian continental terrane, considered a southern extension of the Amazonian Craton (a dispersed fragment of the Ventuari-Tapajós province) (Faleiros *et al.*, 2016).

3. METHODOLOGY

To determine possible lateral and chronological changes in provenance within the Botucatu sandstones in the northern Paraná Basin, sedimentary petrography, heavy mineral analysis, grain size analysis and detrital zircon geochronology has been undertaken. Twenty sandstone samples (Fig. 5) were collected along the northern basin margin from the base and top of the formation, together with sandstones from within the Serra Geral lavas (Intratrap sandstones). Samples were collected from the NE and NW flanks of the Paraná Basin in the west-central and southeast regions of Brazil (Fig. 3 and 4). Table 1 presents the samples with the facies code, stratigraphic level (base, top and interbedded), coordinates, region location and the provenance techniques applied.

Nineteen petrographic thin-sections were subject to point count analysis (300 points/sample) using the Gazzi & Dickinson method (Ingersoll *et al.*, 1984). The results are displayed in compositional ternary diagrams (Fig. 2 - Garzanti, 2018).

Table 1 - Sampling list with the provenance techniques. BP- Bulk petrography; DZ- Detrital Zircon U-Pb dating; HM- Heavy mineral and GR- Granulometric analysis.

Sample Code	Facies Code	Stratigraphic Level	Coordinates Lat/Long	Region Sampled	Provenance Techniques			
					BP	DZ	HM	GR
PB-32	Ste	Base	-48.36 / -22.94	NE region		X	X	X
PB-33	Ste	Top	-48.41 / -22.88			X	X	X
PB-34	Ste	Top	-49.47 / -23.31			X	X	X
PB-35	Ste	Base	-49.47 / -23.32			X	X	X
PB-36	Ste	Intratrap	-47.91 / -22.47		X	X	X	X
PB-37	Ste	Base	-48.08 / -21.82		X	X		X
PB-38	Ste	Base	-47.42 / -20.16		X	X	X	X
PB-39	Ste	Top	-47.44/ -20.13		X	X	X	X
PB-40	Ste	Intratrap	-47.47/ -20.11		X	X	X	X
PB-41	Sm	Intratrap	-48.27/ -18.78		X	X	X	X
PB-44	Ste	Base	-54.04 / -19.54	NW region	X	X		X
PB-46	Ste	Base	-54.11 / -19.48				X	X
PB-47	Ste	Top	-54.38 / -19.30		X	X	X	X
PB-48	Ste	Base	-54.79 / -19.08				X	X
PB-49	Ste	Top	-53.68 / -18.15				X	X
PB-50	Ste	Base	-53.68 / -18.15		X	X		X
PB-51	Ste	Top	-53.70 / -18.13		X	X	X	X
PB-52	Ste	Top	-53.67 / -18.39		X		X	X
PB-56	Ste	Base	-55.84 / -15.38		X	X	X	X
PB-59	Ste	Top	-55.84 / -15.37		X	X	X	

Sixteen samples were selected for heavy mineral analysis, with approximately 400g from each being prepared for analysis. Samples were dried and sieved (63-125 μm), and the heavy fraction was separated using bromoform (2.80 g/mL). Heavy mineral concentrates were mounted on petrographic slides, with subsequent identification of 150 translucent minerals using the ribbon technique following the method of Mange and Maurer (1992). Sixteen samples were dated using U-Pb on detrital zircon grains at Centro de Pesquisas Geocronológicas at the University of São

Paulo, using a Finnigan Neptune mass spectrometer and an excimer ArF laser ablation system (λ=193nm). The analytical settings used for the laser ablation multi-collector inductively coupled plasma mass spectrometer (LA-MC-ICP-MS) were 5 mJ pulse energy, 6 Hz pulse rate and a 29 μm diameter beam. The $^{207}Pb/^{206}Pb$ isotopic ratios were used to date zircons older than 1.3 Ga and the $^{206}Pb/^{238}U$ ratios were used for younger grains. The discordance tolerance is 10%, and values above this limit were dismissed. The analytic configuration for the U-Pb dating is discussed in Sato et al. (2011).

Grain size analysis was undertaken on 19 samples, with 100g of each sandstone dried, cleaned and sieved over a range of class sizes (63–125 μm, 125–250 μm, 250–500 μm, 500–1000 μm). Samples were weighed after each step and the difference recalculated and assigned to each respective grain size proportion. The GRADISTAT software (Blott and Pye, 2001) was used for statistical analysis and to determine sediment distribution. The Provenance R Package (Veermesch *et al.*, 2016) was used to produce the probability density plots and Multidimensional Scaling plots.

4.RESULTS

The petrographic analyses for all the studied samples demonstrate an overall quartzose composition with a mean $Q_{91}F_6L_2$. Lithics are largely low-grade metamorphic grains, comprising 77% of the lithic fraction. K-feldspar dominates the feldspar component. Sample PB-44 shows the only major variation, with a strong input of metamorphic and volcanic grains (up to 20%) (Fig. 2). Petrographic data classify the rocks as pure-quartzose (PB-37, -38, -39, -49, -59), quartzose (PB-31, -47, -50, -51, -52, -55, -56), quartz—rich feldspatho quartzose (PB-, -40, -59) and litho-quartzose (PB-44).

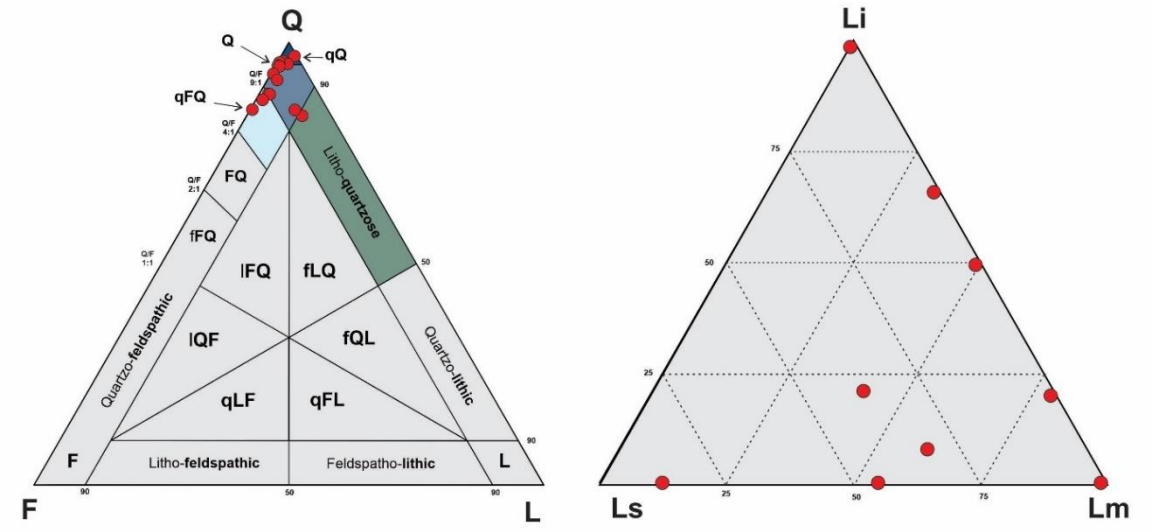

Figure 2 - Framework composition shows a predominant quartzose sediment *(A)* and metamorphic lithic grains *(B)* (Garzanti, 2018) Q-Quartz- F- Feldspars; L- lithics; Ls- Sedimentary lithics; Lm- Metamorphic lithics and Li-Igneus lithics

Heavy mineral analysis reveals a predominance of opaque (71.7%) over translucent minerals (28.3%), with the NW region generally enriched relative to the NE (64.5 - 78.1%). Samples PB-49 and 51 from the NW do show anomalously lower percentages of opaque minerals however (23.9 and 42.5%). The opaque mineral population also shows variations in shape, with highly angular grains apparently related to post-depositional processes, and rounded grains produced through sedimentary abrasion. The main minerals include zircon, tourmaline, rutile, apatite, garnet, epidote, with accessory titanite, hornblende, augite, aluminosilicates, spinel, chlorite, muscovite, monazite, and staurolite. Zircons show a wide range of topology from oval rounded to euhedral prismatic grains. Tourmaline grains display a variety of colours, with mostly rounded tabular to prismatic shapes. Garnet grains occur primarily as angular fragments to etched prisms. Apatite and epidote occur as short prisms with rounded to sub-rounded form. Other minerals, such as hornblende and pyroxene (augite), are mostly highly weathered forming prismatic subangular grains. The overall zircon-tourmaline-rutile (ZTR) index is 86%, with variations through stratigraphic levels

from the base (87.4%), top (73.05%) and interbedded (93.16%). Despite the predominance of a ZTR composition of up to 80%, some minerals such as garnet (30.4% in PB-54), epidote (60.8% in PB-32) and apatite (40.4% in PB-32) dominate locally.

U-Pb dating of detrital zircons from both the NE and NW regions reveals a range of ages from 186 Ma to 3468 Ma. Data are grouped by age peaks (Figures 3 and 4) and related to the major tectonic divisions of the basement framework of Western Gondwana (Bahlburg et al. 2009) which include: Late Paleozoic to Mid Mesozoic (150-359 Ma), Ordovician-Silurian (359-520Ma), Cambrian to Neoproterozoic (520-720 Ma), Early Neoproterozoic (750-900 Ma), Tonian to Stenian (900-1200 Ma), Mid to Early Mesoproterozoic (1.2-1.6 Ga), Late Paleoproterozoic (1.6-1.9 Ga), Orosirian to Rhyacian (1.9-2.3 Ga) and Siderian to Archean (2.3-3.8 Ga). The dominant signature within the studied samples comprise Cambrian to Neoprotorozoic ages (C-Np) (520-750Ma) making up between ca. 35 to 49% of the DZ proportion. Orosirian to Rhyacian ages (O-R)(1.9-2.3 Ga) and Tonian to Stenian ages (T-S)(900-1200 Ma) comprise 10-14% and 21-11% of the DZ population respectively. Permian (PB-38 and -44) and Late Paleoproterozoic (PB-51, -38 and -32) ages also form important contributions locally. Figures 3 and 4 show the normalized probability density plots, constructed with a kernel density estimator (Veermesch, 2016), illustrating the age peaks for both the NE and NW regions.

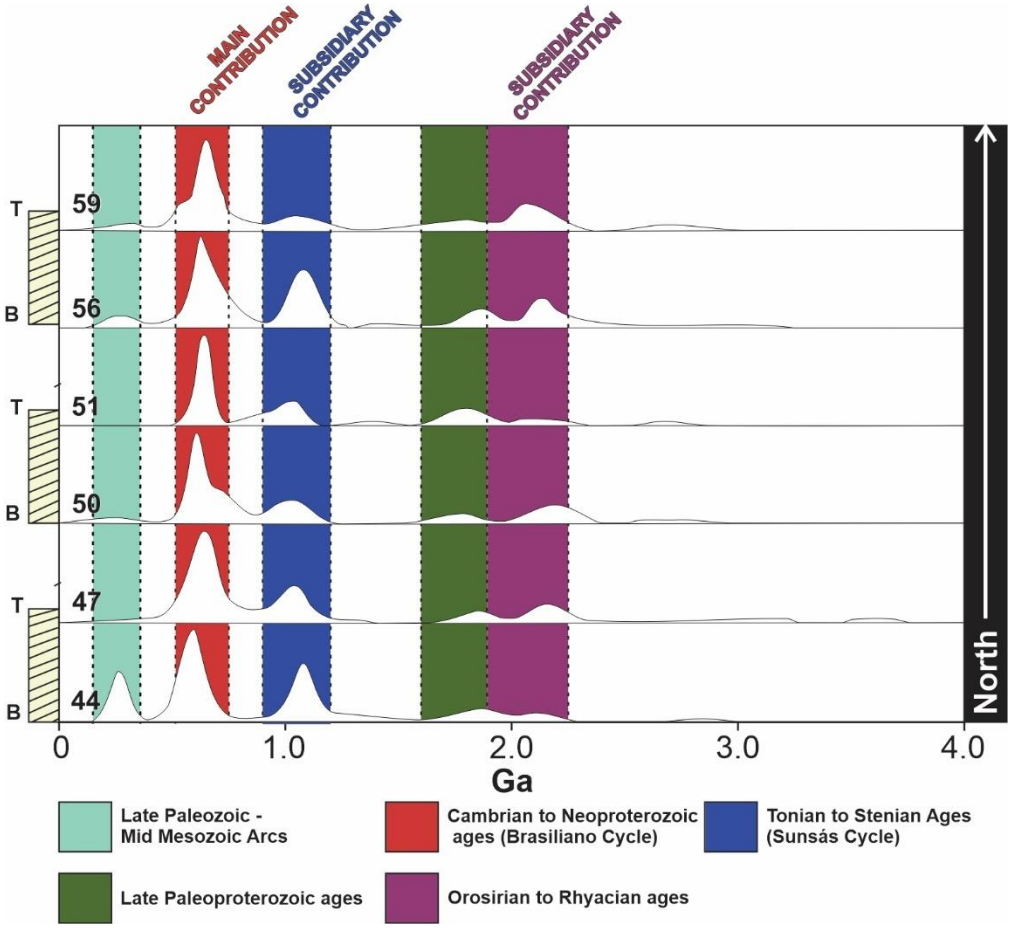

Figure 3 - Detrital zircon KDE plots revealing a Cambrian-Neoproterozoic and Tonian-Stenian prevalent contribution on NW region. The simplified profiles (yellow cross-stratified sandstones) demonstrates the sampling position, where B- Basal desert and T-Top desert

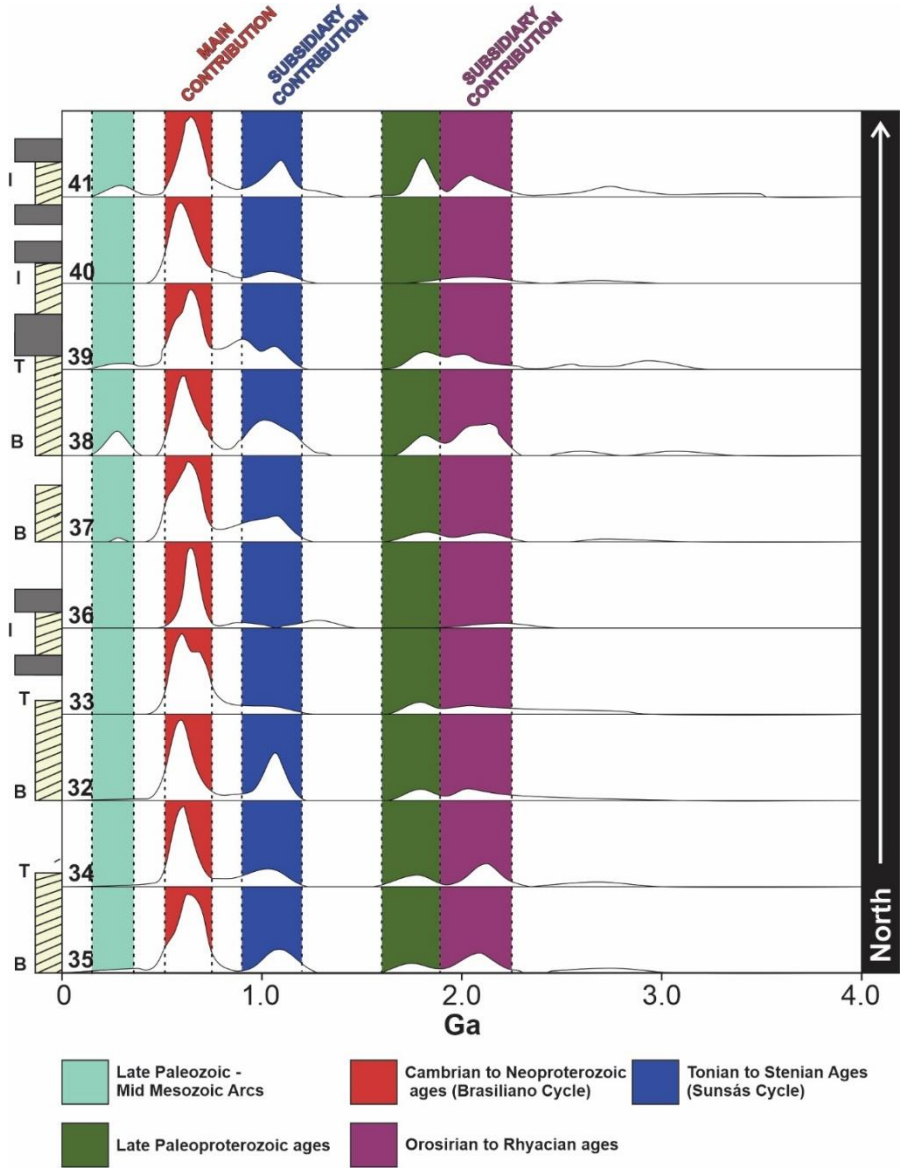

Figure 4 - Detrital zircon contribution displays the Cambrian-Neoproterozoic and Tonian-Stenian ages in NE region. The simplified profiles (yellow cross-stratified sandstones and gray lava packages) demonstrates the sampling position, where B- Basal desert, T-Top desert, and I-Intratrap bed

The provenance dataset is plotted in Figure 5, showing the spatial distribution of the samples and graphical representations of the results from the analyses of each sample. Petrography, heavy minerals and granulometry data are illustrated via pie charts, and the detrital zircon U-Pb dating in kernel density estimators.

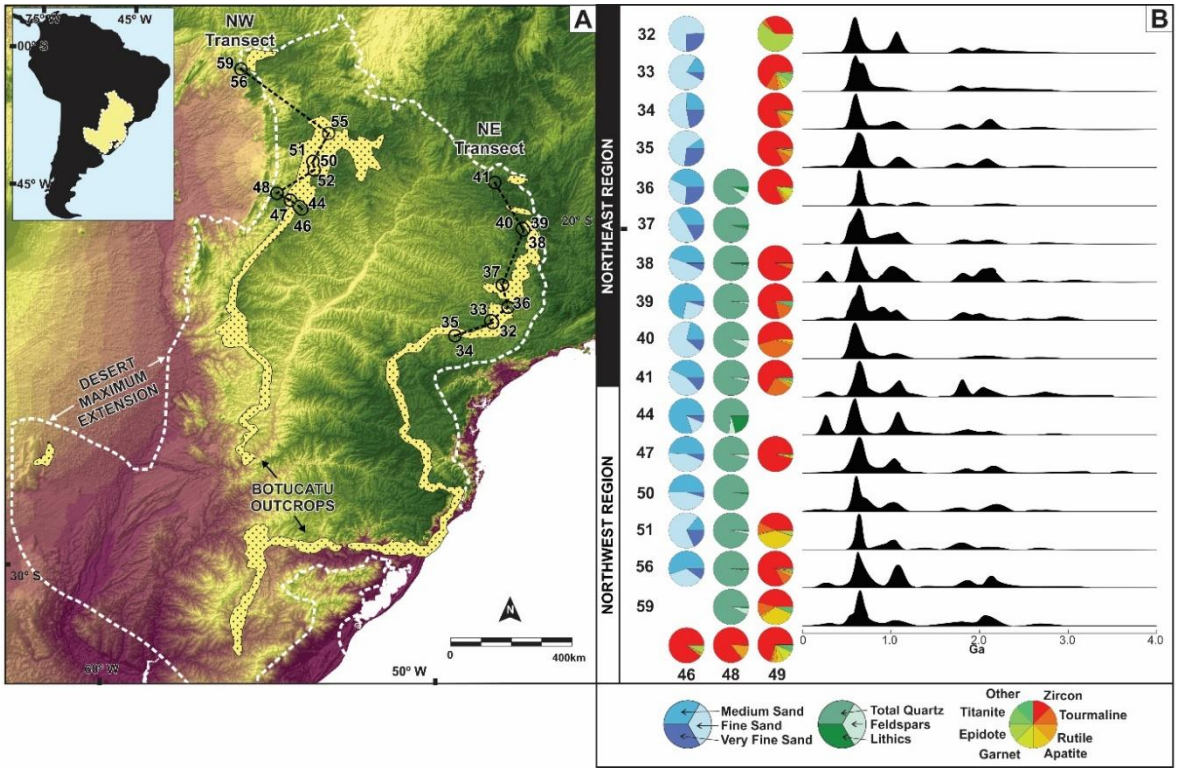

Figure 5 - Data compilation with the geographical location of each sample (A) and the granulometry (Blue tones), petrography (green tones), heavy mineral (Colourful) and DZ data for the samples across the basi *showing the provenance data variability.* Detrital zircon data are represented in probability cumulative plots with KDE estimators (Veermesch, 2016). Paleowinds and outrcrops obtained in Scherer 2000 and Scherer and Goldberg 2007).

4.1 Summary of data for the Northeast Region

Samples PB-32 to 41 were collected from the NE Paraná basin outcrops at the margins of the Serra do Mar, where the mean Botucatu Formation thickness is 200m. The geochronological data reveal a variation in ages, ranging from 248 Ma to 3257 Ma. Bulk petrography indicates a mean composition of $Q_{91}F_8L_1$, with samples classified as quartz-rich feldspatho-quartzose, quartzose and pure-quartzose sandstones. Heavy mineral species include zircon, tourmaline, rutile, apatite, garnet, epidote, titanite, hornblende, spinel, and non-discriminated opaque minerals. Heavy mineral ratios have an average ZTR_{87}, with sample PB-32 being unusual with a ZTR_{39} and the remaining samples having overall ZTR values of ZTR_{80}. Opaque to translucent mineral ratios vary from 2.07 (PB-32) to 10.67 (PB-39), illustrating the predominance

of opaque grains. Granulometric analysis shows a unimodal fine-sand grain size, except for PB-39 (medium sand), moderately (PB-34, -36, -37, -41) to moderately well sorted (PB-32, -33, -35, -38, -39, -40), with variable distributions: mesokurtic (PB-32, -37, -39), leptokurtic (PB-33, -34, -35) and platykurtic (Pb-36, -38,-41) with predominant symmetrical (PB-33, -34, -35, -37, -38, -40, -41) and fine- (PB-32, -36) to very-fine skewness (PB-39).

4.2 Summary of data for the Northwest Region

The Northwest region is exposed in Mato Grosso do Sul and Mato Grosso states, in the center-west region of Brazil where the Botucatu Formation is up to 400m thick. The geochronological analysis shows an age range from ca. 186 Ma to ca. 3468 Ma, with a mean ZTR_{80} with the opaque to translucent mineral ratio varying from 0.74 (PB-51) to 4.95 (PB-54). Heavy mineral species include zircon, tourmaline, rutile, apatite, garnet, epidote, titanite, hornblende, muscovite, monazite, staurolite and non-discriminated opaque minerals. The bulk petrography reveals a mean composition of $Q_{91}F_6L_3$, indicating predominantly quartz-sandstones, except sample PB-44 which contains up to 20% lithics. The grain-size analysis reveals a predominance of unimodal fine sand, with only sample PB-44 presenting a peak of medium sand, moderately (PB-46, -49, -52, -56) to moderately well sorted (PB-44, -47, -48, -50, -51). The samples distributions are mesokurtic (PB-46), leptokurtic (PB-44, -51) and mainly platykurtic (PB-47, -48, -49, -50, -52), with symmetrical (PB-46, -47, -49, -50, -51) to fine- (PB-52, -56) very-fine (PB-44) and coarse skewness (PB-48).

5. DETRITAL ZIRCON VARIATIONS

The DZ compositions show a consistently dominant Cambrian-Neoproterozoic contribution with subsidiary Tonian-Stenian and Orosirian-Rhyacian contributions in both the NW and NE regions. Despite similar overall contributions, there are subtle variations both laterally and vertically within the stratigraphy. When DZ population data are compiled by stratigraphic position a number of possible trends can be identified (Fig. 3 and 4). For example, from the base of the Botucatu to the sandstones interbedded with the lavas, the Late Paleozoic to Mid-Mesozoic DZ population shows a decrease from 8.0 to 2.4 in the NW, the Tonian-Stenian population decreases from 19.5 to 11.5% in the NE and 21.2 to 14.4 % in the NW region. The Cambrian to Neoproterozoic population increases from 39.1 to 49.1% in the NE and from 34.7 to 39.2% in the NW region. Table 2 demonstrates the age proportions from the DZ populations and tectonic events of comparable age occurring in W Gondwana.

Table 2 - Age proportions for the detrital zircon data from the compiled data for each region and stratigraphic level.

Event	Time Interval (Ma)		NE			NW	
			Base	Top	Intratrap	Base	Top
Late Paleozoic to Mid Mesozoic	150	359	3.8	2.0	1.7	8.0	2.4
Early Famatian (Ordovician-Silurian)	359	520	4.4	3.5	4.7	4.0	5.3
Cambrian to Neoproterozoic	520	650	39.1	44.1	49.1	34.7	39.2
Early Neoproterozoic	650	900	6.2	8.7	5.6	4.0	6.2
Tonian to Stenian	900	1200	19.5	11.0	11.5	21.2	14.4
Mid-Early Mesoproterozoic	1200	1550	0.6	0.4	4.7	3.3	3.8
Late Paleoproterozoic	1550	1800	8.0	9.4	6.4	8.0	7.7
Orosirian to Rhyacian	1800	2200	13.0	12.2	10.3	12.0	14.4
Siderian to Archean	2200	3800	5.3	8.7	6.0	4.7	6.7

The Late Paleozoic to Mid Mesozoic population is mostly represented by Permian ages (ca. 260 Ma) which occur more frequently in the NW region. Normalized

probability plots (Figs. 4 and 5) illustrate that the Permian contribution is particularly prevalent in basal samples such as PB-38, -44, and -56, comprising 14.6 % in sample 44. Previous studies of the Botucatu Formation in the southern region (Bertolini *et al.*, 2020; Canile *et al.*, 2016) show a higher proportion, and a homogeneous population (both laterally and stratigraphically), of Permian grains (ca 10%). In contrast, on the extreme western border of the Botucatu Formation in Argentina Peri *et al.* (2016) demonstrates an absence of Permian grains. The Permian contribution is normally interpreted as representing the recycling of Choiyoy Volcanic Group ash fall layers deposited in the underlying Paraná Basin units as Rio Bonito, Irati, Teresina and Serrinha Formations (Rocha-Campos *et al.*, 2011; Canile *et al.*, 2016). However, the ash fall deposits are prevalent in the southern Parana Basin (Rio Grande do Sul State and Uruguay) (Matos *et al.*, 2001; Rocha-Campos *et al.*, 2019; Guerra-Sommer *et al.*, 2008a, 2008b; Mori *et al.*, 2012; Cagliari *et al.*, 2016, Santos *et al.*, 2006). The lack of ash fall deposits within underlying units in the northern basin region suggests that the northern Permian age-zircons may have been derived from the southern region. In addition, the increase in preserved sediment thickness in the northern area of the basin, particularly in the NW region, suggests that a possible depocentre located in this area could provide a sink for sediment transferred northwards. Differently, Bertolini (2020) shows the compositional overlapping of underlying Paraná Basin units with lateral variations within Botucatu, suggesting that the erratic Permian age contribution, may be generated by differential unroofing of underlying units.

The T-S detrital zircon population is similar at the base of the Botucatu Formation in both the NE and NW regions (Fig. 8), and ranges between 20 and 22% decreasing upwards to between 11 to 14% at the top. The Sunsás Belt of the Amazonian craton (Fig. 9) is the most feasible source for T-S aged zircons. However,

the lack of a progressive increase in T-S ages in the NW towards the Sunsás Belt suggests that sourcing of zircons directly from the belt did not occur during the Cretaceous, pointing to a Paraná Basin polycyclic sediment derivation. The regional upward decrease across the 1000km transect indicates a regional change in the supply of T-S aged zircons to the basin. The C-Np aged zircons form the dominant population in the Botucatu Formation, most likely due to the predominance of Brasiliano Cycle orogenic material forming the northern Paraná Basin margin. Both the NE and NW regions show a slight increase in C-Np sourced zircons towards the top of the formation.

Analysis of the multidimensional scaling plot (Fig. 6) indicates the presence of 2 distinct DZ groups: a central sample cluster, and anomalous sample signatures. The central core is composed of samples PB-33, -32, -37, -34, -38, -41, -35, -39 (NE region) and PB-59, -56, -50, -47 (NW region). This cluster illustrates the similarity of the DZ compositions, regardless of spatial distribution and stratigraphic position. The NW region shows smaller variation compared to the NE region.

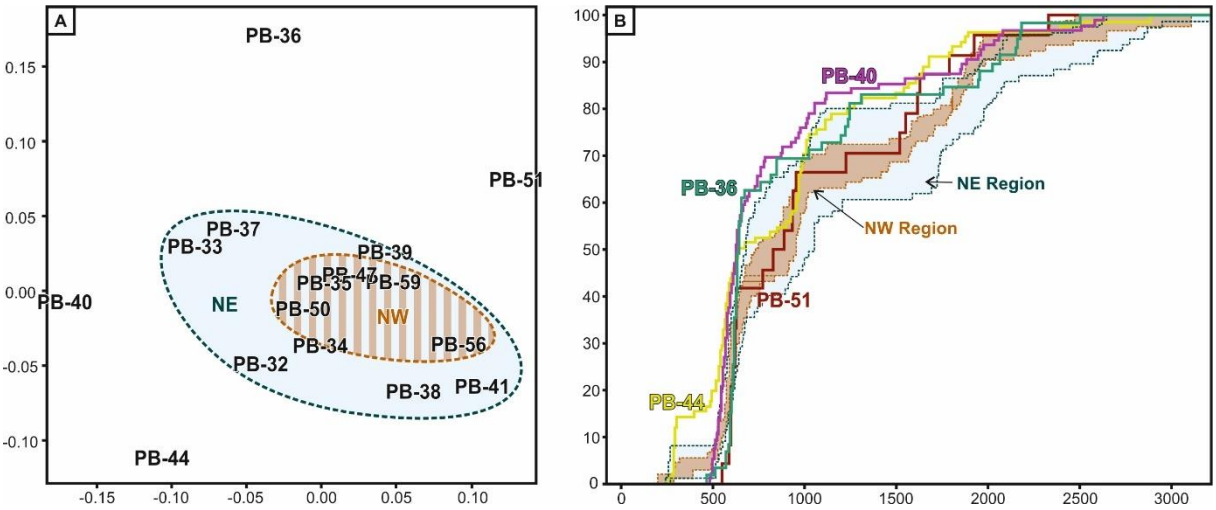

Figure 6 - A- MDS plot (K-S test) showing the overall similar behaviour on NW region compared to NE region, and the anomalous composition on PB-36, -40, -44 and -51. B- Cumulative Probability plot showing the slight variations in C-Np ages for PB-36 and 40, Permian in PB-44 and Statherian ages in PB-51.

Samples PB-36, -40 in the NE region and PB-44, -51 in the NW region show significant differences compared to the central homogeneous DZ signature. Samples 40 and 36 correspond to interbedded sandstones, deposited after the onset of volcanism, and are dominated by Cambrian to Neoproterozoic zircons (56.2 and 59.3% respectively), suggesting a possible increase in the Brasiliano source material. Samples 51 and 44 from the NW region also display anomalous petrographic and heavy mineral compositions. PB-44 has a larger component of metamorphic and volcanic lithic grains (up to 20%), while PB-51 shows a peak in apatite, reaching 40.4% (further discussed in section 7). PB-51 has a relative increase in Statherian ages (6.1 to 16.6%) and PB-44 shows an increase in Paleozoic and Mesozoic ages (14.3% to 1.1%) and Tonian-Stenian ages (24.2% to 17.9%) compared with samples of the same profile (PB-50 and PB-47). In summary, in the NE region, DZ age variations are stratigraphically controlled, whereas in the NW region anomalies are associated with variations in mineral composition (bulk and heavy minerals).

6. DISCUSSION

Potential present-day analogues for the Botucatu desert are located in intracontinental, cratonic lowlands, such as Australia, the Arabian Peninsula and Africa (Hesse, 2019). These modern sand seas show a clear relationship between major long-distance sediment transport systems (fluvial and marine) and their upland basement sources. Rub`Al Khali detritus is carried via the Euphrates-Tigris-Karun fluvial system from the Anatolia Plateau and Zagros Mountains and then transferred to the Arabian Shield by the Shamal winds (Garzanti *et al.*, 2017; 2013). Subtle variations in provenance, similar to those recorded in the Botucatu, occur in the

Taklamakan Desert and are related to aeolian reworking of fluvial sediment derived from drainage systems in the Kunlun Shan and Pamir mountain ranges (Rittner *et al.*, 2016). The quartzose sands of the Kalahari Desert were mostly derived from deflation and reworking of the paleo-Kunene, -Zambezi and -Okavango river sediment during drier seasons (Shaw and Goudie, 2002; Garzanti *et al.*, 2014). Whilst no fluvial deposits have been recognised from the Lower Cretaceous of the Paraná Basin, it is possible that fluvial and/or older deposits exposed along the northern basin margin have been reworked. Following deposition of the Gondwana I sequence in the Northern Paraná Basin from the late Permian to the Cretaceous, the basin was dominated by erosion and/or non-deposition within an overall endorheic setting, with sediment effectively trapped inside this anorogenic topographic lowland (Milani *et al.*, 1998 and Milani, 2007). The similar DZ compositions present for more than 1000km along the northern basin margin suggests limited supply of 1st cycle material to the Botucatu Formation, indicating that sediment was mostly derived from within the Paraná Basin. However, the subtle changes in DZ compositions suggest some local variations in sediment movement within the basin. The variation in Permian-grains is taken to relate to the recycling of volcanic material from the southern basin region, suggesting a south to north directed detrital sediment transport path. The modern-day analogues documented above show similar features where a fluvial system is responsible for the transfer of extrabasinal material into the central part of the aeolian system. The occurrence of DZ outliers in the NW region (PB-44 and -51) that also show related petrographic and HM variations could indicate a proximal source area in the NW region. Other evidence for local sediment input is recorded by the increase in the C-Np population at the top and within the interbedded sandstones in the NE region which likely reflects input from Brasiliano granitoids, which are particularly common in

the Ribeira Belt (Heilborn *et al.*,2017), the eastern bounding basement terrane of the Paraná Basin. The upward decrease in the T-S population may also record evidence for Paraná Basin sediment reworking, particularly in the basal packages. The upward variation in provenance is illustrated in Figure 7, displaying the detrital zircon variations of Permian, Cambrian to Neoproterozoic, Tonian-Stenian and Orosirian-Rhyacian age intervals. Furthermore, the plot in Figure 7 aggregates the detrital zircon, granulometry and petrography data using the 3-way MDS method (Vermeesch *et al.*, 2016) which shows a transitional provenance signature, marked by the clear intratap and basal Botucatu domain, with the top Botucatu desert having intermediary signatures. However, the polycyclicity may simply indicate the unroofing of older Paraná-Basin units, generating a progressive change in provenance.

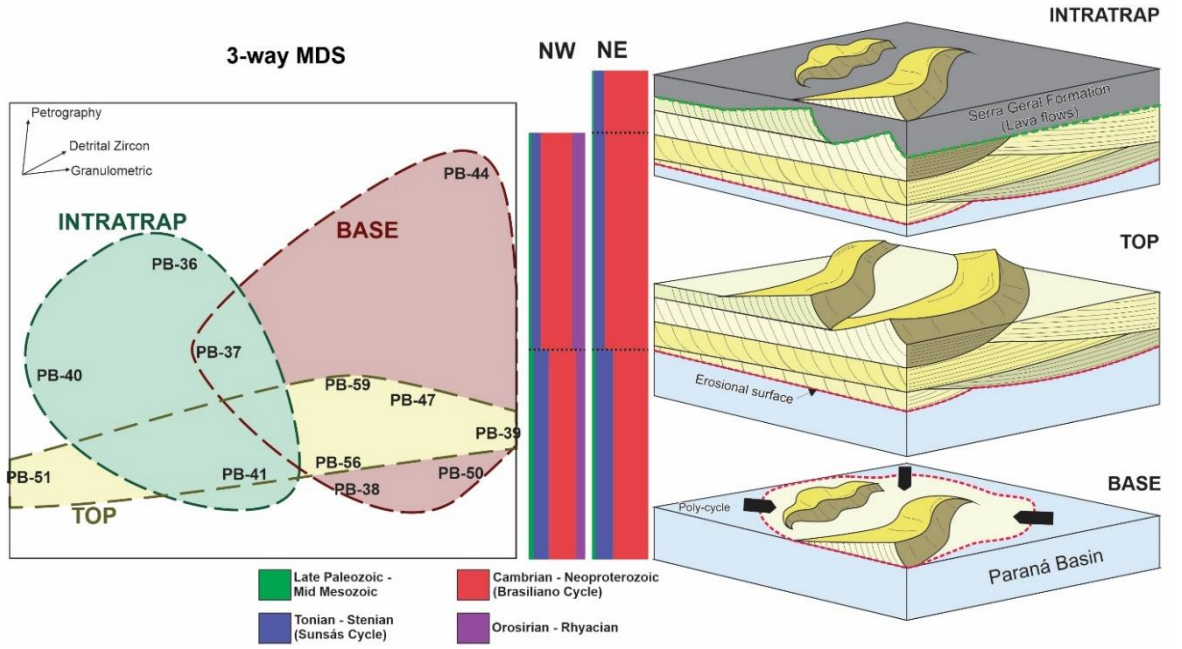

Figure 7 - Upward desert variation illustrated on detrital zircon ages proportion and 3-way MDS plot. The basal and intratrap beds presents a variation both on detrital zircons ages groups also in the 3-way MDS plot, with top desert present a transitional register.

6.1 Tracking sediment sources

The Northern Paraná Basin straddles the contact between the major terranes that comprise the W Gondwana crustal framework, the Amazonian, Sao Francisco (W Congo), Rio Apa and Paranapanema cratons (Almeida, 1981). The amalgamation of these cratonic pieces generated a wide, multiphase Neoproterozoic orogenic belt that forms the actual geomorphological margin of the northern Paraná Basin. The orogenic belt is divided, from NE to NW, into Ribeira, Southern Brasilia and Paraguay (Valeriano, 2017; Heilbron *et al.*, 2017; Faleiros *et al.*, 2016, Teixeira *et al.*, 2019, Roverato *et al., 2019*, Degler et al., 2017). Each area has a distinctive history and chronostratigraphic record, with ages ranging from Neoproterozoic to Archean. The broad age ranges in adjacent terranes together with probable reworking within the basin-fill means that establishing clear sediment pathways for each DZ age peak is not possible. However, the subtle variations present within the Botucatu may suggest that the bounding terranes contributed, at least partly, directly into the basin.

Figure 8 shows a comparison of KDE plots between the basal to interbedded Botucatu Formation DZ data and the metasedimentary units, magmatic phases (collisional granite-gneisses and volcanic arcs) and Paleoproterozoic basement of the Ribeira and Brasilia Belts. These data reveal the relative absence of Tonian and Stenian ages, supporting the reworked nature of this population. The increase in C-Np ages as well , particularly the increase in the interbedded packages, suggests a possible direct contribution of Ribeira Belt Granitoids into the basin-fill, specifically the I-III phase of the syn-collisional granitoids (Heilborn *et al.*, 2017) and Socorro, Serra da Bolivia, Rio Negro and Serra da Prata magmatic arcs (Heilborn *et al.*, 2017).

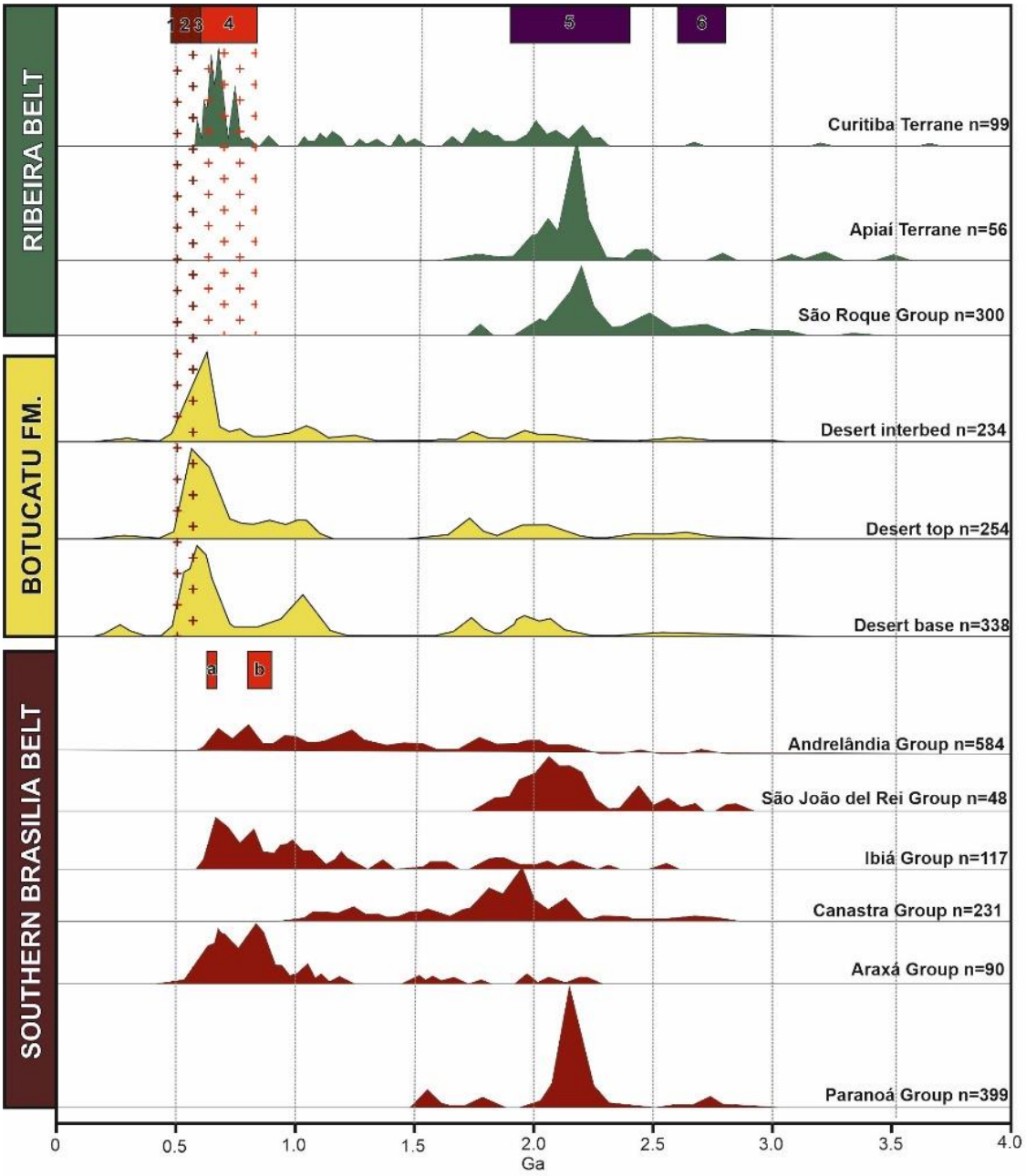

Figure 8 - Normalized probability plots illustrating the I-II syn-collision Granitoids (Ribeira Belt) as sources to the main sedimentary contribution in upward succession in NE region. The absence of Tonian-Stenian sources around Botucatu, indicate desert reworking as the main mechanism of sediment. 1- III Late-collision granitoids; 2- III Late-collision granitoids, 3- III Late-collision granitoids; 4 – Magmatic arcs; 5- Basement; 6 – Basement. Adapted from Campanha et al.,2009 and references (Basei et al. 2008; Siga Jr. et al., 2012, Henrique-Pinto et al., 2015, Valladares et al., 2004, Rodrigues et al., 2012, Piuzana et al., 2003, Matteini et al., 2012, Fruggis, 2018, Heilborn et al., 2017).

Figure 9 compares the KDE plots of the Botucatu Formation (Base and Top) with the Paraguay Belt, Rio Apa Terrane and magmatic events within the Amazonian craton. The increase in C-Np ages suggests an input from the Ediacaran Guaicurus

Formation Group (Paraguay Belt), while the up to 1.9 Ga ages (Orosirian-Rhyacian and Archean ages) suggests Rio Apa Terrane and Amazonian (Maroni-Icantiunas and Ventuari-Tapajós province) contributions in the upper part. The Sunsás Belt (0.9 to 1.2 Ga) is the most probable source for the Tonian-Stenian population.

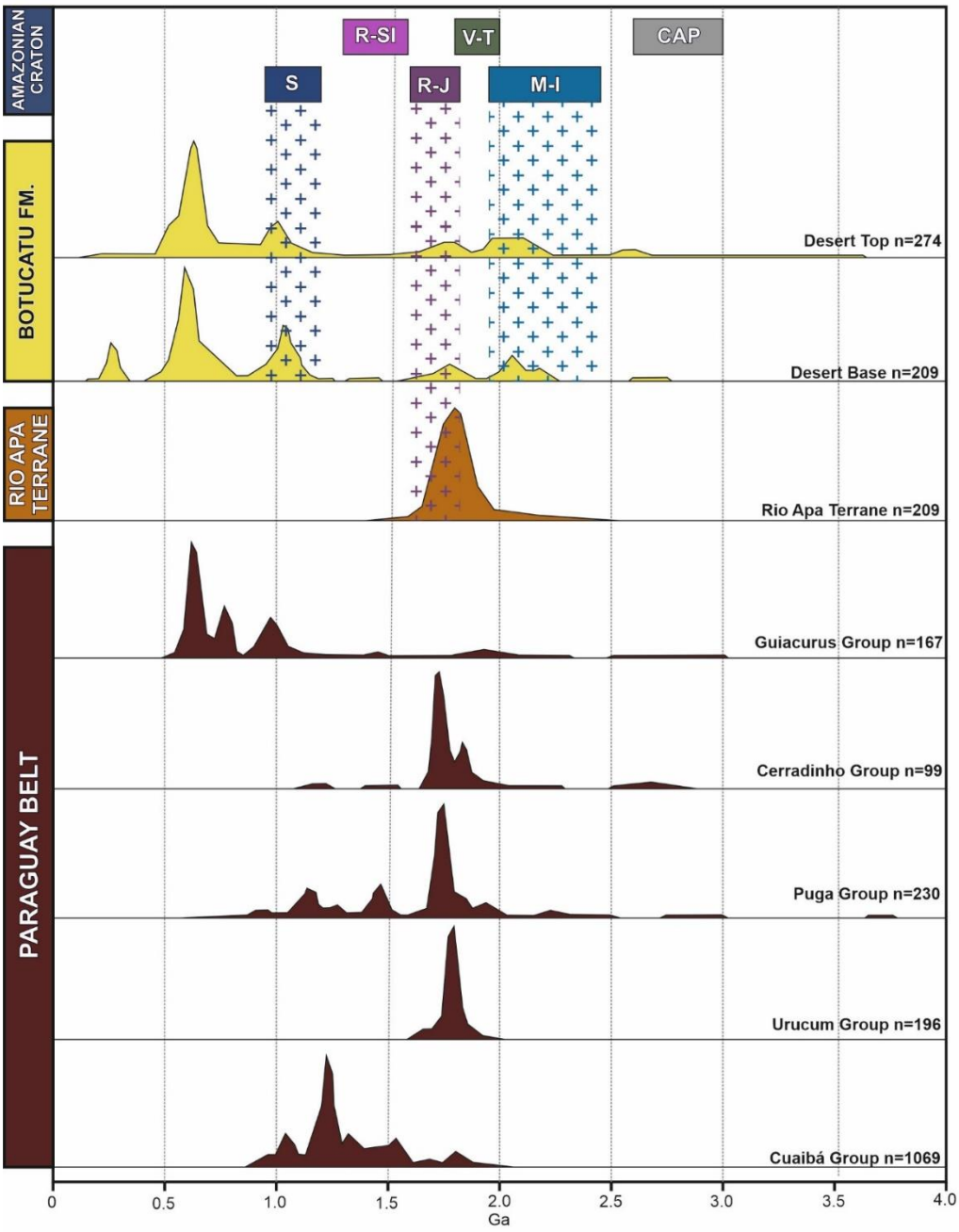

Figure 9 - Normalized probability plots showing the Rio-Apa Terrane and Rio Negro-Juruena Province as upward sources of O-R ages of Botucatu in NW. The increase on C-Np ages may indicate a contribution from Guaicurus Group in Paraguay Belt. Sunsás Terrane might provide a Tonian-Stenian age for the desert. However, the relative homogeneity on these ages indicates an intrabasinal rework. S- Sunsás Belt; R-SI- Rondonia-San Ignacio Provence; R-J- Rio Negro-Juruena Province; V-T- Ventuari-Tapajós Province; Maroni-Icantiunas Province; CAP- Central Amazonian Province. Paraguay and Rio Apa data obtained on McGee 2018).

The sediment trackway proposed in Figure 10 is based on the data acquired in each region, showing the Paraná Basin supplied by the age-compatible bounding terranes that ultimately filled the Botucatu Desert. The Ribeira belt, particularly the Ediacaran granitoids, is likely the most important source of sediment, with an upward increase in input in the NE region. Metasedimentary successions from the Ribeira (Curitiba and Apiai terranes and Sao Roque Group) and Brasilia Belts (Andrelandia, Sao Joa del Rei, Ibiá, Canastra, Araxá and Paranoá Groups) apparently were not prevalent in the Botucatu age composition, as shown by the KDE plots (Fig. 8). The multiphase Brasiliano orogeny (Ribeira and Brasilia Belts), comprises collisional granitoids and magmatic arcs from 480 to 840Ma (Heilbron *et al.*, 2017) resulting in a broad dispersion of ages in the Cambrian-Neoproterozoic interval of the Botucatu Formation (ca. 490 to 630 Ma). Figure 8 reveals an enrichment in grains of Early Cambrian age (490-520Ma) at the Botucatu base, with a progressive increase of Neoproterozoic-aged grains toward the top (550-630Ma). In the Ribeira belt, this age interval coincides with the post-collisional granites (480-510 Ma) of the Oriental Terrane, and the III phase of collisional granitoids (510-535 Ma) from the Occidental, Paraíba do Sul-Embu, and Oriental Terranes. The signatures of the II and I collisional granitoids (Occidental, Paraiba do Sul-Embú and Oriental Terranes) tend to increase toward the top/intratrap desert, suggesting a progressive increase in material supplied from proximal terranes (Ocidental and Paraiba do Sul-Embú) relative to the more distal Ribeira Belt (Oriental Terrane).

The O-R and Neoarchean age increase suggests a greater input from the Amazonian (Rio Negro and Juruena and Maroni-Icantiunas Provinces) and Rio Apa Terranes. The Cambrian-Neoproterozoic ages, in contrast to the NE region, display a more restricted peak (ca. 630 Ma). The Paraguay Belt is mostly a metasedimentary

succession, without the widespread granitogenesis of the Cambrian-Neoproterozoic Ribeira Belt. The metasedimentary units in the Paraguay Belt, such as the Guaicurus Formation show a similar range (Figure 9), indicating that this unit may have been the predominant source of sediment supplied to the NW Botucatu region.

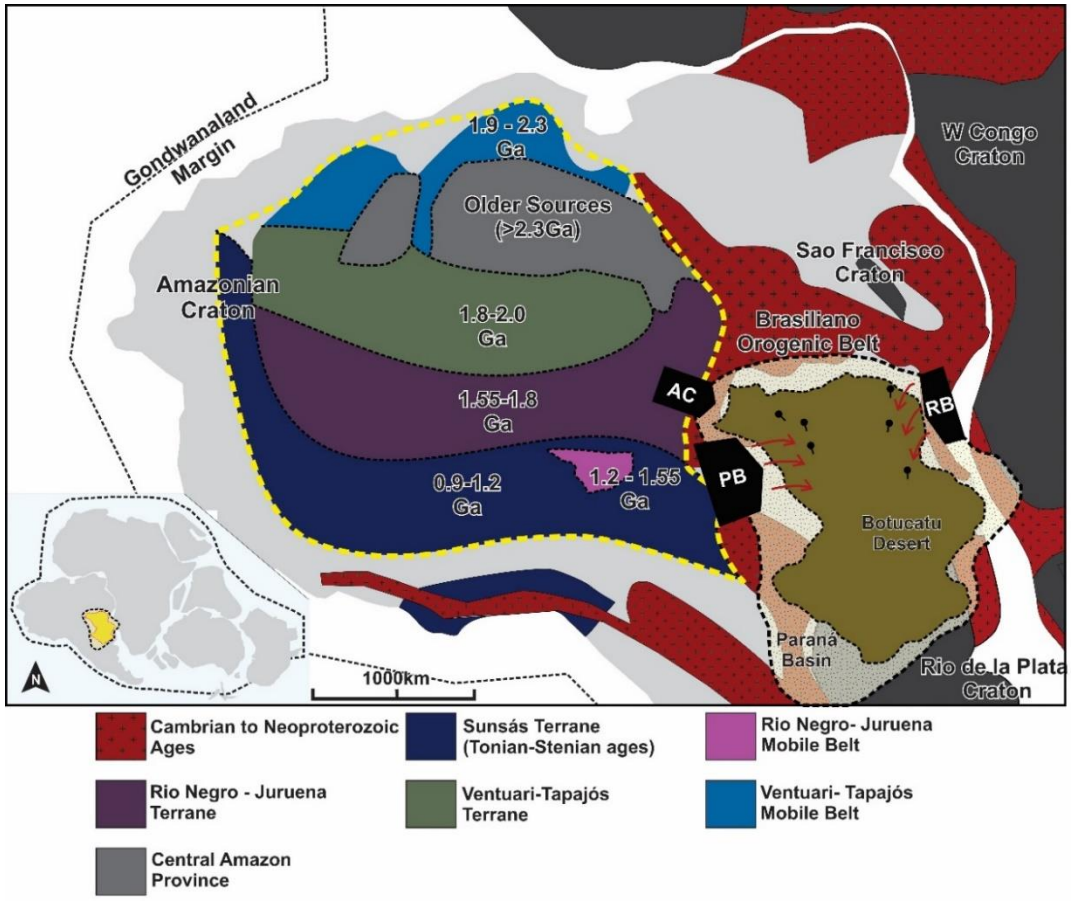

Figure 10 - Sediment pathway on a W Gondwana tectono-stratigraphic configuration. NW region registers an enhance in Cratonic ages, especially from the Rio Negro-Juruena/Maroni-Icantiunas Provinces, and Rio Apa Cratons. The NE region register an enhance in C-Np ages, characterizing an increasing of Ribeira Belt sources (Brasiliano Granitoids).

6.2. Local sediment inputs

The heavy mineral analysis reveals a predominant ZTR enriched composition (up to 90%), indicating a polycyclic sedimentary system. Figure 11 presents a multidimensional scaling (MDS) plot showing a central zone, clustering most samples, and an outer region containing samples with anomalous HM compositions. The central region, with mean $ZTR_{94,}$ represents an average desert composition. Samples PB-54,

-32, -49, -51 and -59 demonstrate slight variations, illustrated by the occurrence of garnet, apatite, and epidote without any apparent sedimentologic variation in paleocurrents, facies or granulometry. These samples characterize outlier inputs located on the external part of the MDS, presenting a mean ZTR_{55}. The outlier compositions, with mean ZTR_{55} and distinct HM occurrences compared to the predominant ZTR_{94} enriched background, indicate the existence of local sedimentary inputs into the desert. The study of Bertolini (2020) demonstrated a similar behaviour in the southern part of the Paraná Basin, suggesting the occurrence of similar processes across the entire basin, as illustrated by the appearances of garnet, epidote and pyrolusite outliers over the predominantly high ZTR values.

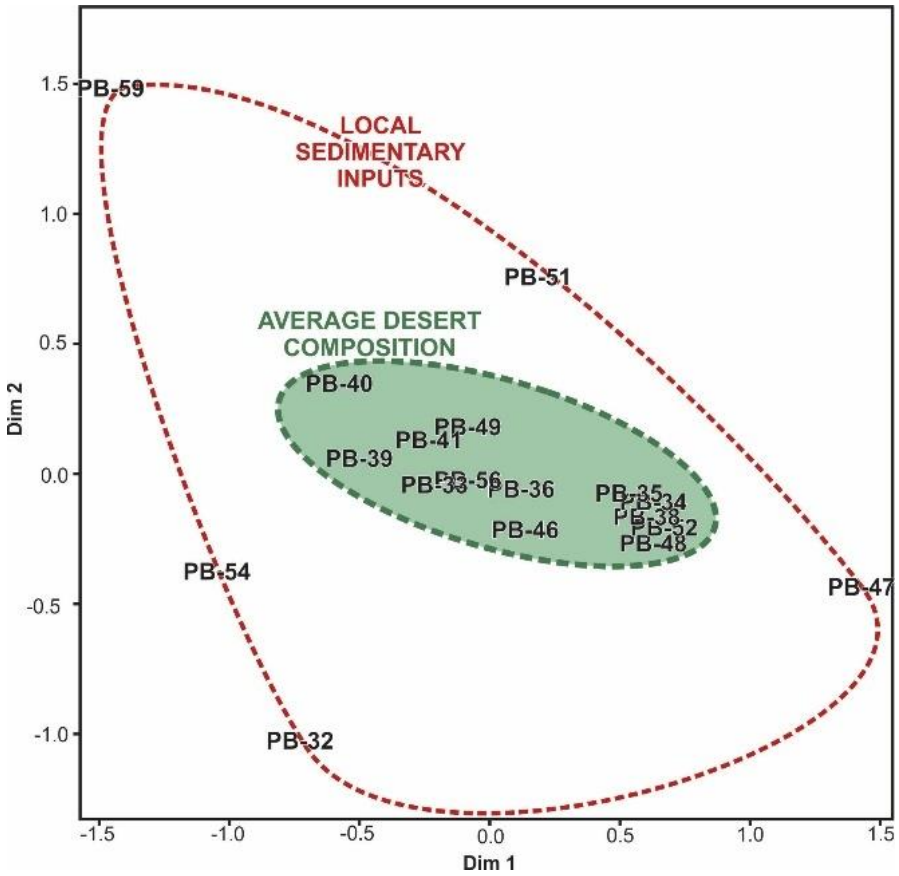

Figure 11 - Multidimensional Scaling plot of heavy minerals demonstrating the internal grouping of the high ZTR compositions and demonstrating the existence of outliers (PB-47, -51, -59, -54, -32).

The Botucatu Desert is considered to be an excellent example of a dry sand-sea due to the predominance of dry-aeolian strata (cross-bedded dune deposits (Mountney, 2006)) over rare ephemeral stream packages, and absent interdune sets (Scherer, 2000 and 2002). On the northern border, localized sedimentological and paleontological finds may suggest aeolian interaction with waterlain conditions. The Botucatu succession contains silicified coniferous tree trunks within coarse sandstones along the extreme northeast border at the PB-41 sampling site (Pires *et al.*, 2011). Pires (2011) suggests that the tree-ring pattern of the coniferous species was drought generated and compatible with areas located adjacent to a desert. Moraes and Seer (2018) show the coexistence of lacustrine environments within the Serra Geral lava flows, indicating the existence of a wetter environment in that region. In Sao Paulo State, where sample 37 was collected, several records of dinosaur trackways have been described (Fernandes et al., 1988, Fernandes et al., 1990, Leonardi, 1980, Leonardi, 1981, Leonardi and Godoy, 1980, Leonardi and Oliveira, 1990, Leonardi *et al.*, 2007, Francischini et al., 2015). The presence of theropod, sauropod and ornithopod footprints indicates an environment capable of sustaining large vertebrates, suggesting at least some seasonal water input. These studies indicate the coeval development of waterlain deposits during, or associated with, desert development, regardless of the direct presence of fluvial deposits in the vast majority of the Botucatu Formation.

The only direct record of ephemeral streams is from Scherer (2000), who described a few small packages (5-30cm) at the base of the Formation along the SW margin. The heavy mineral input signature, described here, suggests a relationship between fluvial and aeolian systems, even without the preservation of waterlain deposits. Maroulis *et al.* (2007) demonstrated an interrelationship between fluvial

channels and aeolian activity in the Lake Eyre Basin (SW Australia), revealing the capacity of the wind system to partially rework the floodplain. Figure 12 shows a model for the input of ephemeral stream sediments into a desert, which are then partially-to-completely reworked by wind activity. The local sediment inputs are probably not the major source of the desert sediment, resulting in a progressive dilution of this composition towards the average desert composition. A similar situation occurs in the Rub`al Khali sand sea, with a dominant contribution from Paleozoic Sandstones derived from the Yemen and Oman Uplands, but with local basement contributions from local catchments (Garzanti *et al.*, 2012; 2013 and Stone *et al.*, 2013). The heavy mineral variations found in the Botucatu desert suggest that the average desert composition is probably related to the huge amount of sand available within the Paraná basin, whilst local sedimentary inputs can be correlated to catchment contributions along the desert margin.

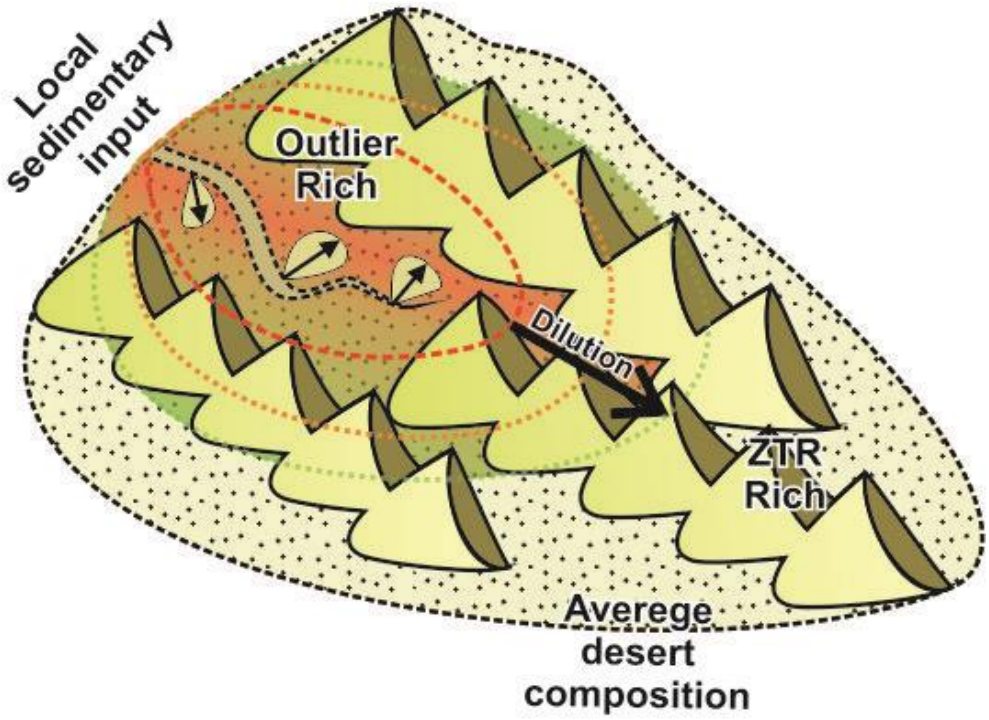

Figure 12 - Local sedimentary input model of sediment distribution, demonstrating the punctual characteristic of the heavy mineral peaks by the sediment dilution under the overwhelming high ZTR, the average desert composition.

7. CONCLUSIONS

The multiproxy provenance analysis of the Botucatu Formation along the northern Parana basin margin demonstrates the dominance of polycyclic sediment supply signature across a vast desert area (>1000km) as well as within the paleoerg stratigraphy. The detrital zircon U-Pb dating, heavy mineral, granulometric and petrographic data, coupled with statistical analysis, reveals further variations within its spatial and stratigraphic history:

- Botucatu Desert quartzose- and ZTR-rich ($Q_{91}F_6L_2$ and $ZTR_{0.86}$) compositions demonstrate a polycyclic sediment derived from the Paraná basin;
- Major detrital zircon contribution of Cambrian to Neoproterozoic (520-750Ma) grains with subsidiary Tonian to Stenian (0.9-1.2G) and Orosirian to Rhyacian (1.9 – 2.3 Ga) contribution;
- MDS plot demonstrates a clustering of samples with variations in the interbedded sandstones PB-36, -40 in the NE region and in PB-44,-51 in the NW region.
- DZ reveals a slight upward decrease in T-S and Permian ages across the basin, and an increase in C-Np through to the interbedded lava-sandstone unt, which may indicate an unroofing of underlying basin units;
- The increase of Cambrian to Neoproterozoic ages in the NE region suggests the Ribeira Belt (collisional granitogenesis and magmatic arcs) as the main protosource toward the top;
-In the NW region, the increase of C-Np and Orosirian to Archean ages (Up to 1.9 Ga), indicates a mixed contribution from Paraguay, Rio Apa, and Amazonian Craton protosources;

- MDS plot for heavy minerals (Fig 11) reveals a grouping of similar compositions (average desert composition) and outlier populations, suggesting local sediment inputs to the aeolian system.

8. ACKNOWLEDGEMENTS

The authors gratefully acknowledge support from Shell Brasil through the 'BG05: UoA-UFRGS-SWB Sedimentary Basins' project at UFRGS and the strategic importance given by ANP through the R&D levy regulation. We also thank Conselho Nacional de Desenvolvimento Científico e Tecnológico (CNPq) by the financial support (grant 203786/2017-3). The authors would like to thank Dr. Deborah Mendes for field trip assistance. This work is part of the current dual-degree Ph.D. from Gabriel Bertolini at Universidade Federal do Rio Grande do Sul and University of Aberdeen.

9. REFERENCES

Almeida, F.F.M., Hasui, Y., de Brito Neves, B.B. and Fuck, R.A., 1981. Brazilian structural provinces: an introduction. Earth-Science Reviews, 17(1-2), pp.1-29.

Bahlburg, H., Vervoort, J.D., Du Frane, S.A., Bock, B., Augustsson, C. and Reimann, C., 2009. Timing of crust formation and recycling in accretionary orogens: Insights learned from the western margin of South America. Earth-Science Reviews, 97(1-4), pp.215-241.

Baksi, A. K. (2018). Paraná flood basalt volcanism primarily limited to~ 1 Myr beginning at 135 Ma: New 40Ar/39Ar ages for rocks from Rio Grande do Sul, and critical evaluation of published radiometric data. J. Volcanol. Geoth. Res., 355, 66-77.

Basei, M.A.S., Frimmel, H.E., Nutman, A.P. and Preciozzi, F., 2008. West Gondwana amalgamation based on detrital zircon ages from Neoproterozoic Ribeira and Dom Feliciano belts of South America and comparison with coeval sequences from SW Africa. Geological Society, London, Special Publications, 294(1), pp.239-256.

Bertolini, G., Marques, J.C., Hartley, A.J., da Rosa, A.A.S. Scherer, C., Basei, M.A.A.S., Frantz, J.C. and, 2017, (2020). Controls on Early Cretaceous desert

sediment provenance in SW Gondwana, Botucatu Formation (Brazil and Uruguay). Sedimentology (In press).

Blott, S.J. and Pye, K., 2001. GRADISTAT: a grain size distribution and statistics package for the analysis of unconsolidated sediments. Earth surface processes and Landforms, 26(11), pp.1237-1248.

Cagliari, J., Philipp, R.P., Buso, V.V., Netto, R.G., Hillebrand, P.K., da Cunha Lopes,R., Basei, M.A.S. and Faccini, U.F., 2016. Age constraints of the glaciation in the Paraná Basin: evidence from new U–Pb dates. Journal of the Geological Society, 173(6), pp.871-874.

Campanha, G.A.D.C., Faleiros, F.M., Cawood, P.A., Cabrita, D.I.G., Ribeiro, B.V. and Basei, M.A.S., 2019. The Tonian Embu Complex in the Ribeira Belt (Brazil): revision, depositional age and setting in Rodinia and West Gondwana. Precambrian Research, 320, pp.31-45.

Canile, F.M., Babinski, M. and Rocha-Campos, A.C., 2016. Evolution of the Carboniferous-Early Cretaceous units of Paraná Basin from provenance studies based on U-Pb, Hf and O isotopes from detrital zircons. Gondwana Research, 40, pp.142-169.

Valeriano, C.V., 2017. The Southern Brasília Belt. In São Francisco Craton, Eastern Brazil (pp. 189-203). Springer, Cham.

Dickinson, W.R. and Gehrels, G.E., 2003. U–Pb ages of detrital zircons from Permian and Jurassic eolian sandstones of the Colorado Plateau, USA: paleogeographic implications. *Sedimentary Geology*, *163*(1-2), pp.29-66.

Teixeira, W., Hamilton, M. A., Girardi, V. A., Faleiros, F. M., & Ernst, R. E. (2019). U-Pb baddeleyite ages of key dyke swarms in the Amazonian Craton (Carajás/Rio Maria and Rio Apa areas): Tectonic implications for events at 1880, 1110 Ma, 535 Ma and 200 Ma. Precambrian Research, 329, 138-155.

Milani, J.H.G. Melo, P.A. Souza, L.A. Fernandes, A.B. França. Bacia do Paraná. Bol. Geociências Petrobrás, 15 (2) (2007), pp. 265-287

Ernesto, M., Raposo, M.I.B., Marques, L.S., Renne, P.R., Diogo, L.A. and De Min, A., 1999. Paleomagnetism, geochemistry and 40Ar/39Ar dating of the North-eastern Paraná Magmatic Province: tectonic implications. Journal of Geodynamics, 28(4-5), pp.321-340.

Faleiros, F.M., Pavan, M., Remédio, M.J., Rodrigues, J.B., Almeida, V.V., Caltabeloti, F.P., Pinto, L.G.R., Oliveira, A.A., de Azevedo, E.P. and Costa, V.S., 2016. Zircon U–Pb ages of rocks from the Rio Apa Cratonic Terrane (Mato Grosso do Sul, Brazil): New insights for its connection with the Amazonian Craton in pre-Gondwana times. Gondwana Research, 34, pp.187-204.

Fernandes, A.C.S., Carvalho, I.S. and Netto, R.G., 1990. Icnofósseis de invertebrados da Formação Botucatu, São Paulo (Brasil). Anais da Academia brasileira de Ciências, 62(1), pp.45-49.

Folk, R.L., 1980. Petrology of sedimentary rocks. Hemphill Publishing Company.

Francischini, H., Dentzien–Dias, P.C., Fernandes, M.A. and Schultz, C.L., 2015. Dinosaur ichnofauna of the Upper Jurassic/Lower Cretaceous of the Paraná Basin (Brazil and Uruguay). Journal of South American Earth Sciences, 63, pp.180-190.

Frugis, G.L., Neto, M.D.C.C. and Lima, R.B., 2018. Eastern Paranapanema and southern São Francisco orogenic margins: Records of enduring Neoproterozoic oceanic convergence and collision in the southern Brasília Orogen. Precambrian Research, 308, pp.35-57.

Garzanti, E., Vermeesch, P., Andò, S., Vezzoli, G., Valagussa, M., Allen, K., Kadi, K.A. and Al-Juboury, A.I., 2013. Provenance and recycling of Arabian desert sand. Earth-Science Reviews, 120, pp.1-19.
Garzanti, E., Vermeesch, P., Padoan, M., Resentini, A., Vezzoli, G. and Andò, S., 2014. Provenance of passive-margin sand (Southern Africa). The Journal of Geology, 122(1), pp.17-42.

Gioia, S.M.C., 1997. Preparação da Metodologia Sm–Nd para Datação de Amostras Geológicas e sua Aplicação em Rochas das Áreas de Firminópolis, Fazenda Nova e Americano do Brasil. Universidade de Brasília, Dissertação de Mestrado, p. 100.

Guerra-Sommer, M., Cazzulo-Klepzig, M., Formoso, M.L.L., Menegat, R. and Fo, J.G.M., 2008. U–Pb dating of tonstein layers from a coal succession of the southern Paraná Basin (Brazil): a new geochronological approach. Gondwana Research, 14(3), pp.474-482.

Guerra-Sommer, M., Cazzulo-Klepzig, M., Menegat, R., Formoso, M.L.L., Basei, M.Â.S., Barboza, E.G. and Simas, M.W., 2008. Geochronological data from the Faxinal coal succession, southern Paraná Basin, Brazil: a preliminary approach combining radiometric U-Pb dating and palynostratigraphy. Journal of South American Earth Sciences, 25(2), pp.246-256.

Heilbron, M., Mohriak, W.U., Valeriano, C.M., Milani, E.J., Almeida, J. and Tupinambá, M., 2000. From collision to extension: the roots of the southeastern continental margin of Brazil. Geophysical Monograph-American Geophysical Union, 115, pp.1-32.

Heilbron, M., Pedrosa-Soares, A.C., Campos Neto, M.D.C., Silva, L.D., Trouw, R.A.J. and Janasi, V.D.A., 2004. Província Mantiqueira. Geologia do continente sul-americano: evolução da obra de Fernando Flávio Marques de Almeida, pp.203-235.

Heilbron, M., Ribeiro, A., Valeriano, C.M., Paciullo, F.V., Almeida, J.C.H., Trouw, R.J.A., Tupinambá, M. and Silva, L.E., 2017. The Ribeira Belt. In São Francisco Craton, Eastern Brazil (pp. 277-302). Springer, Cham.

Heilbron, M., Valeriano, C.D.M., Tassinari, C.C.G., Almeida, J., Tupinamba, M., Siga, O. and Trouw, R., 2008. Correlation of Neoproterozoic terranes between the Ribeira Belt, SE Brazil and its African counterpart: comparative tectonic evolution and open questions. Geological Society, London, Special Publications, 294(1), pp.211-237.

Henrique-Pinto, R., Janasi, V.D.A., Vasconcellos, A.C.B.C., Sawyer, E.W., Barnes, S.J., Basei, M.A. and Tassinari, C.C., 2015. Zircon provenance in meta-sandstones of the São Roque Domain: Implications for the Proterozoic evolution of the Ribeira Belt, SE Brazil. Precambrian Research, 256, pp.271-288.

Ingersoll, R.V., Bullard, T.F., Ford, R.L., Grimm, J.P., Pickle, J.D. and Sares, S.W., 1984. The effect of grain size on detrital modes: a test of the Gazzi-Dickinson point-counting method. Journal of Sedimentary Research, 54(1), pp.103-116.

Janasi, V.A., Freitas, V.A. and Heaman, L.H., 2011. The onset of flood basalt volcanism, Northern Paraná Basin, Brazil: A precise U–Pb baddeleyite/zircon age for a Chapecó-type dacite. Earth and Planetary Science Letters, 302(1-2), pp.147-153.

Laux, J.H., Pimentel, M.M., Dantas, E.L., Armstrong, R., Armele, A. and Nilson, A.A., 2004. Mafic magmatism associated with the Goiás magmatic arc in the Anicuns region, Goiás, central Brazil: Sm–Nd isotopes and new ID-TIMS and SHIMP U–Pb data. Journal of South American Earth Sciences, 16(7), pp.599-614.

Leonardi, G. and de Oliveira, F.H., 1990. A revision of the Triassic and Jurassic tetrapod footprints of Argentina and a new approach on the age and meaning of the Botucatu Formation footprints (Brazil) Revista Brasileira de Geociências, 20(1-4), pp.216-229.

Leonardi, G., & Godoy, L. C. (1980). Novas pistas de tetrápodes da Formação Botucatu no Estado de São Paulo. *Congr. Bras. Geol*, *31*, 3080-3089.

Leonardi, G., 1980. On the discovery of an abundant ichno-fauna (vertebrates and invertebrates) in the botucatu formation ss in araraquara, sao-paulo, brazil. Anais da Academia Brasileira de Ciências, 52(3), pp.559-567.

Leonardi, G., Carvalho, I.D. and Fernandes, M.A., 2007. The desert ichnofauna from Botucatu Formation (Upper Jurassic-Lower Cretaceous), Brazil. Paleontologia: cenários de vida, 1, pp.371-383.

Livingstone, I. and Warren, A., 2019. Aeolian Geomorphology: A New Introduction. Wiley-Blackwell. pp10-440.

M.M. Pimentel, R.A. Fuck, 1994. Geocronologia Rb–Sr da porção sudeste do maciço de Goiás. Revista Brasileira de Geociências, 24 (2), pp. 104-111

Mange, M.A. and Maurer, H.F.W., 1992. Heavy mineral in colour. pp.1-147.

Maroulis, J.C., Nanson, G.C., Price, D.M. and Pietsch, T., 2007. Aeolian–fluvial interaction and climate change: source-bordering dune development over the past~

100 ka on Cooper Creek, central Australia. Quaternary Science Reviews, 26(3-4), pp.386-404.

Matos, S.L.F., Yamamoto, J.K., Riccomini, C., Hachiro, J. and Tassinari, C.C.G., 2001. Absolute dating of Permian ash-fall in the Rio Bonito formation, Paraná Basin, Brazil. Gondwana Research, 4(3), pp.421-426.

Matteini, M., Dantas, E.L., Pimentel, M.M., de Alvarenga, C.J.S. and Dardenne, M.A., 2012. U–Pb and Hf isotope study on detrital zircons from the Paranoá Group, Brasília Belt Brazil: Constraints on depositional age at Mesoproterozoic–Neoproterozoic transition and tectono-magmatic events in the São Francisco craton. Precambrian Research, 206, pp.168-181.

McGee, B., Babinski, M., Trindade, R. and Collins, A.S., 2018. Tracing final Gondwana assembly: Age and provenance of key stratigraphic units in the southern Paraguay Belt, Brazil. Precambrian Research, 307, pp.1-33.

McGee, B., Collins, A.S. and Trindade, R.I., 2012. G'day Gondwana—the final accretion of a supercontinent: U–Pb ages from the post-orogenic São Vicente Granite, northern Paraguay Belt, Brazil. Gondwana Research, 21(2-3), pp.316-322.

McGee, B., Collins, A.S., Trindade, R.I. and Payne, J., 2015. Age and provenance of the Cryogenian to Cambrian passive margin to foreland basin sequence of the northern Paraguay Belt, Brazil. Bulletin, 127(1-2), pp.76-86.

Milani, E.J., Faccini, U.F., Scherer, C.M., Araújo, L.M.D. and Cupertino, J.A., 1998. Sequences and stratigraphic hierarchy of the Paraná Basin (Ordovician to Cretaceous), southern Brazil. Boletim IG-USP, 29, pp.125-173.

Moore, G.T., Hayashida, D.N., Ross, C.A. and Jacobson, S.R., 1992. Paleoclimate of the Kimmeridgian/Tithonian (Late Jurassic) world: I. Results using a general circulation model. Palaeogeography, Palaeoclimatology, Palaeoecology, 93(1-2), pp.113-150.

Moraes, L.C. and Seer, H.J., 2018. Pillow lavas and fluvio-lacustrine deposits in the northeast of Paraná Continental Magmatic Province, Brazil. Journal of Volcanology and Geothermal Research, 355, pp.78-86.

Mori, A.L.O., de Souza, P.A., Marques, J.C. and da Cunha Lopes, R., 2012. A new U–Pb zircon age dating and palynological data from a Lower Permian section of the southernmost Paraná Basin, Brazil: biochronostratigraphical and geochronological implications for Gondwanan correlations. Gondwana Research, 21(2-3), pp.654-669.

Motta-Araújo, J.G., Pimentel, M.M. and Armstrong, R., 2003. U-Pb ages, Sm-Nd isotopes and structural analysis of the Moiporá-Novo Brasil shear sone system: the limits between the Neoproterozoic Goiás Magmatic Arc and the Archean Uvá Complex, Tocantins Province, Central Brazil. In South Am. Symp. Isotope Geology (Vol. 4, pp. 221-224).

Nogueira, A.C., Riccomini, C., Sial, A.N., Moura, C.A., Trindade, R.I. and Fairchild, T.R., 2007. Carbon and strontium isotope fluctuations and paleoceanographic changes in the late Neoproterozoic Araras carbonate platform, southern Amazon craton, Brazil. Chemical Geology, 237(1-2), pp.168-190.

Peri, V.G., Naipauer, M., Pimentel, M. and Barcelona, H., 2016. Eolian deposits of the southwestern margin of the Botucatú paleoerg: Reconstruction of the Gondwana landscape in Central Northern Argentina. Sedimentary Geology, 339, pp.234-257.

Pimentel, M.M., Heaman, L. and Fuck, R.A., 1991. Zircon and sphene U-Pb geochronology of Upper Proterozoic volcanic-arc rock units from southwestern Goiás, central Brazil. Journal of South American Earth Sciences, 4(4), pp.295-305.

Pinto, V.M., Hartmann, L.A., Santos, J.O.S., McNaughton, N.J. and Wildner, W., 2011. Zircon U–Pb geochronology from the Paraná bimodal volcanic province support a brief eruptive cycle at~ 135 Ma. Chemical Geology, 281(1-2), pp.93-102.

Pires, E.F., Guerra-Sommer, M., dos Santos Scherer, C.M., dos Santos, A.R. and Cardoso, E., 2011. Early Cretaceous coniferous woods from a paleoerg (Paraná Basin, Brazil). Journal of South American Earth Sciences, 32(1), pp.96-109.

Piuzana, D., Pimentel, M.M., Fuck, R.A. and Armstrong, R., 2003. SHRIMP U–Pb and Sm–Nd data for the Araxá Group and associated magmatic rocks: constraints for the age of sedimentation and geodynamic context of the southern Brasılia Belt, central Brazil. Precambrian Research, 125(1-2), pp.139-160.

Rahl, J.M., Reiners, P.W., Campbell, I.H., Nicolescu, S. and Allen, C.M., 2003. Combined single-grain (U-Th)/He and U/Pb dating of detrital zircons from the Navajo Sandstone, Utah. *Geology*, *31*(9), pp.761-764.

Rittner, M., Vermeesch, P., Carter, A., Bird, A., Stevens, T., Garzanti, E., Andò, S., Vezzoli, G., Dutt, R., Xu, Z. and Lu, H., 2016. The provenance of Taklamakan desert sand. Earth and Planetary Science Letters, 437, pp.127-137.

Rocha-Campos, A.C., Basei, M.A., Nutman, A.P., Kleiman, L.E., Varela, R., Llambias, E., Canile, F.M. and Da Rosa, O.D.C., 2011. 30 million years of Permian volcanism recorded in the Choiyoi igneous province (W Argentina) and their source for younger ash fall deposits in the Paraná Basin: SHRIMP U–Pb zircon geochronology evidence. Gondwana Research, 19(2), pp.509-523.

Rocha-Campos, A.C., Basei, M.A.S., Nutman, A.P., Santos, P.R., Passarelli, C.R., Canile, F.M., Rosa, O.C.R., Fernandes, M.T., Santa Ana, H. and Veroslavsky, G., 2019. U-Pb Zircon Dating of Ash Fall Deposits from the Paleozoic Paraná Basin of Brazil and Uruguay: A Reevaluation of the Stratigraphic Correlations. The Journal of Geology, 127(2), pp.167-182.

Rodrigues, J.B., Pimentel, M.M., Buhn, B., Matteini, M., Dardenne, M.A., Alvarenga, C.J.S. and Armstrong, R.A., 2012. Provenance of the Vazante Group: new U–Pb, Sm–Nd, Lu–Hf isotopic data and implications for the tectonic evolution of the Neoproterozoic Brasília Belt. Gondwana Research, 21(2-3), pp.439-450.

Rossetti, L., Lima, E.F., Waichel, B.L., Hole, M.J., Simões, M.S. and Scherer, C.M., 2018. Lithostratigraphy and volcanology of the Serra Geral Group, Paraná-Etendeka Igneous Province in southern Brazil: Towards a formal stratigraphical framework. Journal of Volcanology and Geothermal Research, 355, pp.98-114.

Sato K, Basei MAS, Ferreira CM, Sproesser WM, Vlach SRF, Ivanuch W, Onoi AT (2011) U–Th–Pb analyses by excimer laser ablation/ ICP-MS on MG Brazilian xenotime. Goldschmidt Conference Abstracts. Miner Mag 1801.

Scherer, C.M. and Goldberg, K., 2007. Palaeowind patterns during the latest Jurassic–earliest Cretaceous in Gondwana: Evidence from aeolian cross-strata of the Botucatu Formation, Brazil. Palaeogeography, Palaeoclimatology, Palaeoecology, 250(1-4), pp.89-100.

Scherer, C.M., 2002. Preservation of aeolian genetic units by lava flows in the Lower Cretaceous of the Paraná Basin, southern Brazil. Sedimentology, 49(1), pp.97-116.

Scherer, C.M.S., 2000. Eolian dunes of the Botucatu Formation (Cretaceous) in southernmost Brazil: morphology and origin. Sedimentary Geology, 137(1-2), pp.63-84.

Shaw, A.I. and Goudie, A.S., 2002. Geomorphological evidence for the extension of the Mega-Kalahari into south-central Angola. South African Geographical Journal, 84(2), pp.182-194.

Siga Junior, O. ; Campanha, G. A. C. ; Faleiros, F. M. ; Basei, M. A. S.; Sato, K. ; Dantas, E. and McReath I. 2012. Detrital Zircon U-Pb and Hafnio Geochronology from the Capiru and Turvo-Cajati Formations (S-SE BRAZIL): Tectonic Implications. In: VIII South American Symposium on Isotope Geology – SSAGI, 2012, Colombia. Summaries. Colombia, 2012.

Stone, A.E.C., 2013. Age and dynamics of the Namib Sand Sea: a review of chronological evidence and possible landscape development models. Journal of African Earth Sciences, 82, pp.70-87.

Thiede, D.S. and Vasconcelos, P.M., 2010. Paraná flood basalts: rapid extrusion hypothesis confirmed by new 40Ar/39Ar results. Geology, 38(8), pp.747-750.

Valladares, C.S., Machado, N., Heilbron, M. and Gauthier, G., 2004. Ages of detrital zircon from siliciclastic successions south of the São Francisco Craton, Brazil: implications for the evolution of Proterozoic basins. Gondwana Research, 7(4), pp.913-921.

Vermeesch, P., Resentini, A. and Garzanti, E., 2016. An R package for statistical provenance analysis. Sedimentary Geology, 336, pp.14-25.

Zalán, P.V., Wolff, S.J.C.J., Conceição, J.D.J., Marques, A., Astolfi, M.A.M., Vieira, I.S., Appi, V.T. and Zanotto, O.A., 1990. Bacia do Paraná. *Origem e evolução das bacias sedimentares*, pp.135-168.

ARTIGO III – THE EFFECT OF BASALTIC LAVA FLOWS ON THE PETROPHYSICAL PROPERTIES AND DIAGENESIS OF INTERBEDDED AEOLIAN SANDSTONES: AN EXAMPLE FROM THE CRETACEOUS PARANÁ BASIN, BRAZIL

From: Petroleum Geoscience
Sent: 16 March 2020 20:36
To: Gabriel Bertolini
Subject: A manuscript number has been assigned to The effects of basaltic lava flows on the petrophysical properties and diagenesis of interbedded aeolian sandstones: an example from the Cretaceous Paraná Basin, Brazil

Dear Mr. Bertolini,

Your submission entitled "The effects of basaltic lava flows on the petrophysical properties and diagenesis of interbedded aeolian sandstones: an example from the Cretaceous Paraná Basin, Brazil" has been been assigned the following manuscript number: petgeo2020-036.

You will be able to check on the progress of your paper by logging on to Editorial Manager as an author.
The URL is https://www.editorialmanager.com/petgeo/.

Thank you for submitting your work to this journal.

Kind regards,

Petroleum Geoscience Editorial Office

THE EFFECTS OF BASALTIC LAVA FLOWS ON THE PETROPHYSICAL PROPERTIES AND DIAGENESIS OF INTERBEDDED AEOLIAN SANDSTONES: AN EXAMPLE FROM THE CRETACEOUS PARANÁ BASIN, BRAZIL

Bertolini, G.[1,2,*], Hartley, A.J.[1], Marques, J.C[2]., Healy, D.[1], Frantz, J.C.[2]

[1] University of Aberdeen

[2] Universidade Federal do Rio Grande do Sul

* **Corresponding author** (e-mail: gabertol@gmail.com)

Abstract: An analysis of the petrophysical and diagenetic effects of the emplacement of basaltic lava flows (Serra Geral Formation) on interbedded aeolian sandstones (Botucatu Formation) has been undertaken on subsurface datasets in the Parana Basin, Brazil. From 0.1 to 1 m from the contact zone higher P-wave velocities are recorded (Av. 3759.3 ms^{-1}) than in areas (av. 3376.8 ms^{-1}) > 1 m away from the contact, whilst porosity presents a 6.5% average near the contact (0.1 to 1 m), to mean 10.7% >1 m away from the contact. The petrographic evaluation describes two diagenetic pathways responsible for modification of the rock-physics: early cementation (Type 1) and early packing (Type 2). Type 1 is represented by early Mg-rich authigenic phases chlorite and dolomite and is probably related to a hydrothermal system. Type 2 is characterized by early packing causing microstylolites and sutured grain contacts, indicating temperatures between 70-100° C, suggesting the lava overburden associated with the basalt emplacement as the main mechanism for chemical dissolution. Within the sandstones diagenesis associated with volcanism results in decreased porosity and increased acoustic velocities. At the sandstone-lava contact the increased impact of cementation (0.1 to 1 m) may be useful from a reservoir perspective, as a potential fluid seal/barrier. The lava-induced diagenetic effects may form a baffle or seal to fluids around the margins of the sandstone bodies. Therefore, whilst diagenesis associated with lava emplacement may hinder reservoir quality around the margins of sandstone bodies, good reservoir properties may be preserved within these large sandstone bodies.

1. INTRODUCTION

Siliciclastic diagenesis is controlled by several processes within sedimentary basins such as sediment composition, deposition and burial conditions (Morad et al., 2000; Morada et al., 2010). However, multiple additional factors can also affect the burial history of sedimentary basins and affect and altering a standard/expected diagenetic evolution- for instance, chemical, thermal and deformation process can be generated in basins by intrusion emplacement, salt deformation, basin inversion or organic sediment maturation. One aspect that may be overlooked when considering the diagenetic history of a basin is the potential impact of coeval igneous activity on potential reservoir development. Understanding the diagenetic effects associated with lava-sediment interaction may clarify the impact of hydrothermal activity on authigenic and dissolution processes in interbedded sandstone bodies and the role that increased overburden may have on grain-packing. Moreover, the presence of igneous strata within sedimentary basins is often a challenge for hydrocarbon exploration and production as it may adversely affect maturation, seal and reservoir understanding as well as the direct impact it may have through hydrothermal and grain packing effects on reservoir quality (Schofield et al., 2015, Angkasa et al., 2017, Haile et al., 2019).

Hydrocarbons are produced from a wide range of basins that contain interbedded volcanics including Faroe-Shetland Basin (Schofield & Jolley, 2013, Hardman et al., 2019), the Campos, Santos and Neuquen Basins in South America (Alves et al., 2015, Rabbel et al., 2018), Bight, Otway, Bass, Gippsland and Sorrell basins in SW Australia (Holford et al, 2013), Voring Basin in Norway (Omosanya et al., 2017) and understanding the impact of volcanism on reservoir development has direct implications for both exploration and production. However, most studies to date are concerned with the impact of intrusive igneous rocks on the sedimentary

succession (Mckinley et al., 2001, Ahmed, 2002, Ochoa et al., 2007, González-Acebrón et al., 2011, Grove, 2017, Holford et al., 2013, Haile et al., 2019) with only limited consideration of the impact of extrusive igneous activity on reservoir properties. As a consequence, understanding the diagenetic effects associated with extrusive volcanism on porous sandstone, and its impact on reservoir properties is important for new frontier plays in volcano-sedimentary successions. The interbedded nature of the continental flood basalts and aeolian erg deposits from the Cretaceous interval of the Paraná Basin, Brazil represent an excellent opportunity to evaluate the impact and magnitude of the diagenetic effects in sandstones associated with interbedded basaltic lava flows. This study addresses this issue and utilises petrophysical analysis of sub-surface cores, via ultrasonic acoustic velocities and porosity measurements in 5 wells, with petrographic analysis constraining diagenetic variations across basalt-sandstone contacts.

2. GEOLOGIC CONTEXT

The Paraná Basin occupies present day Brazil, Paraguay, Argentina, Uruguay and Namibia and developed across western Gondwana. It contains 7,000 m of sediment ranging from Ordovician to Cretaceous in age. This intracontinental basin is subdivided into 6 major sequences: Rio Ivaí (Ordovician), Paraná (Devonian), Gondwana I (Carboniferous-Permian), Gondwana 2 (Triassic), Gondwana III (Early Cretaceous) and Bauru (Mid- to Late Cretaceous) (Milani et al., 2007) (Fig. 1). The supersequence stratigraphy and distribution is illustrated in Figure 1. The Gondwana III succession consists of a volcano-sedimentary interval composed of the aeolian Botucatu Formation and the continental flood basalts of the Serra Geral Formation and which form the subject of this study.

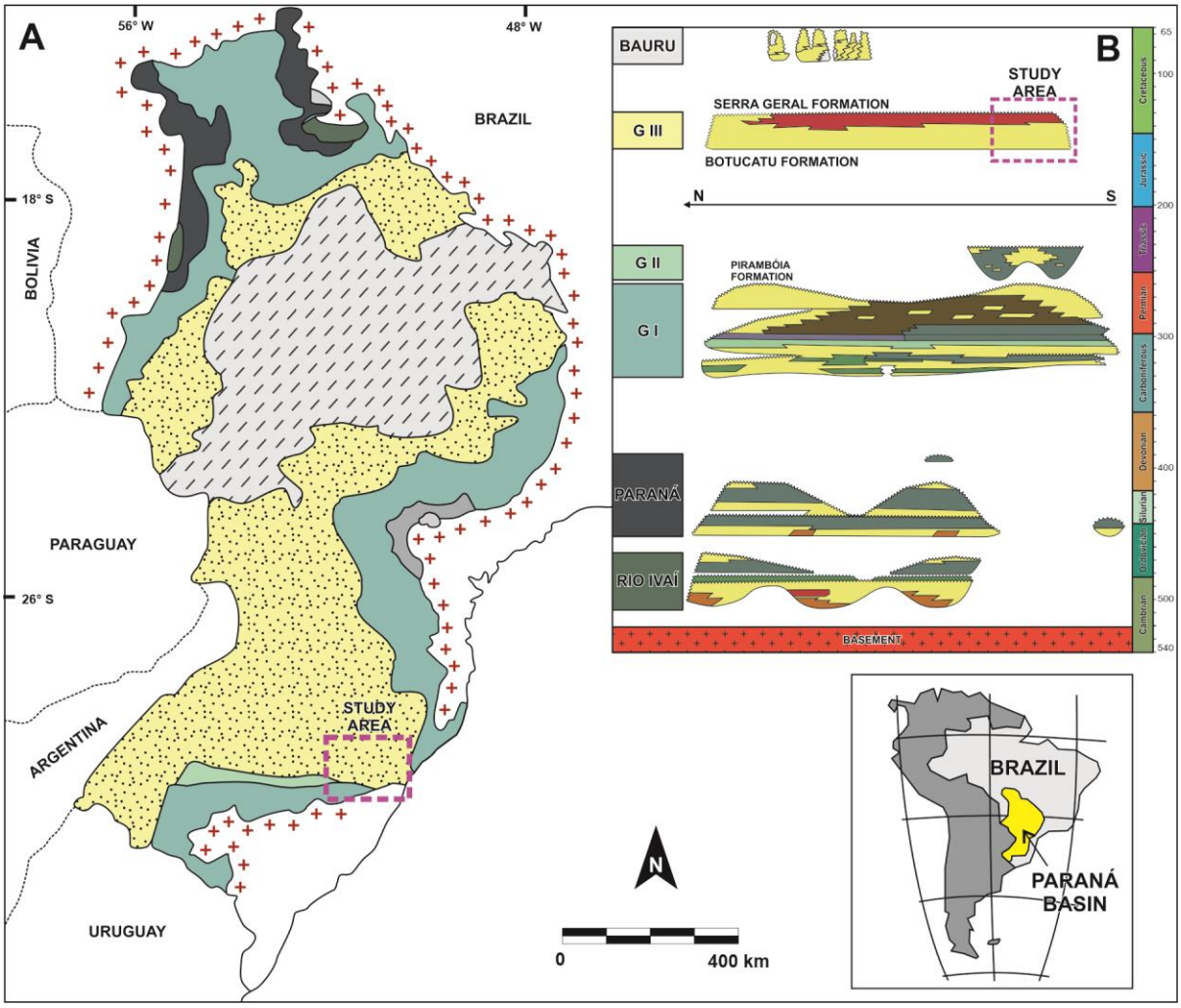

Figure 1 - (A) Paraná Basin supersequences distribution and (B) stratigraphic chart. The studied area is located in SE region (Adapted from Milani et al., 2007; Milani & Ramos, 1998).

The studied area contains a 0 to 100m thick aeolian interval and 700-800 m thick volcanic pile. The Botucatu Formation is the main pre-volcanic aeolian unit, comprising cross-stratified sandstones (large-scale; through; mid-scale and low-angle) representing dune and draa bed-form development (Scherer, 2000). The overlying interbedded sandstone and lava interval comprises two sandstone types in the SE Paraná Basin: major and minor sandstone bodies (Scherer, 2002). Major sandstone bodies are composed of lenses up to 15 m thick and hundreds of meters in extent, interpreted as residual deposits of migrating dunes. The minor sandstone

bodies form thinner packages (smaller than 3 m thick) and are restricted laterally, extending for a maximum of 20 m. Scherer (2002) defines thin horizontal laminated (wind-ripple dominated) packages as dry sand sheet deposits. Preservation of top sets, lava-rope marks and striations in interbedded sandstones demonstrates the coeval character of lava-sedimentation. The onset of volcanic activity occurred around 135 Ma (Ernesto et al., 1999; Thiede & Vasconcelos, 2010; Pinto et al., 2011; Janasi et al., 2011; Baksi, 2018).

Petrographically, Gesicki (2007) described the Botucatu Fm. as a moderate to well sorted fine to medium sand, (Folk, 1968), with a quartzose to sub-arkose bulk composition. The following diagenetic history was identified by Gesicki (2007): iron coating grain adhesion (1); clay infiltration on vadose zone (2); smectite neoformation on clay coatings in eodiagenetic conditions (3); quartz and K-feldspar authigenesis under mesodiagenetic conditions (4); interstitial calcite in mesodiagenesis (5); dissolution of lithic and feldspathic framework generating secondary porosity during telodiagenetic conditions (6); amorphous silica (opal) neoformation in telodiagenesis (7). Hirata (2011) showed that authigenic effects do not negatively impact porosity in well cores from the Sao Paulo region (av. porosity 19.5%), with only limited calcite cementation. França (2003) illustrated the effects of meteoric water dissolution on feldspars and calcite/dolomite leaching in shallow aquifer. Additional data on porosity are provided for the Botucatu as it forms part of a major hydrogeological system in South America referred to as the Guarani Aquifer System. The Botucatu aquifer has a mean thickness of 138 m (0 to 484 m), porosity from 17 to 30% and a mean permeability of 8.7 mD, (Araujo et al., 1999).

Rossetti et al. (2019) studied the petrophysical signature of the Serra Geral pahoehoe and rubbly basalts and interbedded sandstones from outcrops. Stratified

sandstones have a small degree of cementation, display a mean porosity of 22.4% (9.3–34.2), mean permeability of 448.4 mD (39.71–1115.3), and mean Vp and Vs of 3.1 and 1.9 km s^{-1}. The massive sandstone contains some intervals with silicic cementation, with a mean porosity of 16.3% (3.5 to 28.4%), mean permeability of 18.0 mD (0 to 77 mD), and ultrasonic velocities of 3.4 and 2.3 km s^{-1}. Porosity and ultrasonic values are similar among the 2 types of sandstones, although silicified massive sandstones have lower porosity (< 5%) and permeability (<1 mD) values.

For the Serra Geral Formation the lava flows are bimodal in composition with basic flows - basalts to andesites - and silicic flows - dacite and rhyolites. The silicic units occur only in the upper part of the volcanic pile. (Peate et al., 1992 and 1997). In the studied area, the onset of volcanism is represented by basic flows characterized by a total average thickness of 200 m composed of inflated sheet-like lobes, ponded lavas and compound pahoehoe flows (Rosseti et al., 2018). The upper part of the lava-pile stratigraphy displays up to 500 m of basaltic andesites, described as rubbly sheet-like lavas (Rosseti et al., 2018). Petrophysically the Serra Geral lavas display porosities ranging from 0.03 to 28.4%; permeabilities between 0.001 to 415.7 mD and ultrasonic velocities from 1.8 to 5.9 km s^{-1} (Rosseti et al., 2019). Higher porosity values are associated with vesiculation patterns occurring at the top and base of lava-flows and brecciation at the top of rubbly flows. Permeability values in lavas are usually low, however the intricate fracture pattern has a positive effect increasing the permeability.

3. METHODOLOGY

Five wells from the SE region of the Paraná Basin, Rio Grande do Sul State (South Brazil) coastal area- Osório and Santo Antonio da Patrulha cities were studied. A quarter of 8 cm diameter cores were sampled in 4 wells (TG-27, TG-100, TG-179,

and TG-227) from Companhia de Pesquisa em Recursos Minerais (CPRM) and 1 (CBM-100F) in cores in UFRGS. Samples were taken from the lava-sandstone contact and immediately adjacent to it in order to assess any changes with distance away from the contact. Seventy-two samples were collected for petrophysical characterization (ultrasonic and porosity attributes) and subsequent petrographic studies.

The petrophysical analysis was undertaken in the Rock Physics & Geomechanics Laboratory at the University of Aberdeen. The ultrasonic velocity measurement uses the pulse transmission technique (Birch, 1960), consisting of measuring the wave delay time (in microseconds) of a parallel transmitter and receiver. A synthetic wave signal is generated and sent through the core plug, recorded on an oscilloscope allowing identification of the wave arrival time. The set-up measures the P- and S-waves, using as parameters a 60 dB gain and a voltage of 900 V. To avoid errors on wave arrival identification, the resulting velocity consists of a mean of 3 measurements. For further details on wave type identification and methodology see Healy et al. (2015). Due to the small size of the available samples, the porosity measurements were carried out using the Archimedes method. The method consists of weighing dry, fluid-saturated, and suspended in fluid samples to obtain the density and, ultimately, the porosity. The following methodology was applied: plug drying at 40-50^{o} C in an oven for 2-3 h (1); dry-plug weigh 3-4 times in a 0.1 g scale (2); plug saturation with distilled water by vacuum pumping a sealed cylinder for 2 to 5 h (3); plug weighing suspended in distilled water (4); saturated plug weighing (5).

Twenty-one thin sections were made and focussed on intervals with distinct petrophysical values to examine possible effects of volcanic activity on sandstone reservoir characterisation. For each section, petrographic analysis included counts of

>300 grains and the Gazzi-Dickinson method were utilised (Ingersoll et al., 1984). The framework mineralogy, type of porosity, authigenic phases and habits, grain-size, rounding and sphericity and fabric contacts were determined. The bulk framework consists of quartz (monocrystalline, polycrystalline, and deformed quartz), feldspar (plagioclase, orthoclase, and microcline), and lithic fragments (metamorphic, plutonic, volcanic and sedimentary), and results are presented as ternary plots (Garzanti, 2018). Sandstones ternary plots and coordination techniques (principal component analysis (see Veermesch et al. (2016) for details) were performed on the Provenance package on R software (Vermeesch et al., 2016). The authigenic components were counted and described under scanning electron microscopy and cathodoluminescence. The SEM study was undertaken in the Aberdeen Centre for Electron, Analysis and Characterization (ACEMAC) laboratory, using a Carl Zeiss SEM 300VP with coupled NanoAnalysis Xmax80 EDS detector and Deben Centaurus CL detector. For grain-size, 200 grains were measured under an optical microscope along both major and minor axes, and the statistical distribution was obtained with the Gradistat Software (Blott and Pye, 2001). The grain-shape was described by counting 200 grains, evaluating the grain rounding using 4 simple groups: angular, sub-angular, sub-rounded and rounded-, with grain sphericity in 2 groups: high and low. Fabric contacts were evaluated by counting the number and type of contacts a specific grain had with each adjacent grain for at least 200 grains. The contact type consists of floating (no contacts with any grains), point, linear, concave-convex and sutured.

4. RESULTS

4.1 Petrophysics

Sampled intervals for the 5 wells range from 18 to 100 m in thickness with porosity and the acoustic velocities of 72 samples measured across these intervals. Results are shown in Table 1 with mean, maximum, and minimum values for each well. Ultrasonic acoustic velocities for the whole dataset have a mean P-wave velocity of 3472 m/s (1711 to 4966 m/s) and mean S-wave velocity of 2710 m/s (1657 to 3919 m/s). Porosity values range from 0 to 17% (av. 9.7%) and density ranges from 1.9 to 3.0 g/cm^3 (mean 2.2 g/cm^3). Figure 2 plots the petrophysical data of all the wells, showing the stratigraphic variations on the data.

Well		**TG-27**	**TG-100**	**TG-179**	**TG-227**	**CBM-100TF**	**Sum**
n		11	17	19	14	11	72
Vp (m/s)	Max	4612.5	4811.2	4795.9	4585.5	4965.9	4965.9
	Min	2452.7	2945.8	2713.2	3351.6	1710.6	1710.6
	Mean	**3501.8**	**3311.9**	**3855.3**	**3855.3**	**3438.7**	**3472.4**
Vs (m/s)	Max	4612.5	4811.2	4795.9	4585.5	4965.9	4965.9
	Min	1656.6	2010.1	2206.8	2039.2	2482.8	1656.6
	Mean	**2712.9**	**2501.8**	**2886.3**	**2886.3**	**2971.7**	**2710.4**
Porosity (%)	Max	17.3	14.5	17.1	16.6	16.9	17.3
	Min	0.2	1.9	0.0	5.3	6.1	0.0
	Mean	**9.4**	**8.0**	**11.3**	**11.3**	**12.4**	**9.7**
Density (g/cm^3)	Max	2.8	2.8	3.0	2.7	2.4	3.0
	Min	1.9	2.0	1.9	2.0	1.9	1.9
	Mean	**2.4**	**2.3**	**2.1**	**1.8**	**1.8**	**2.2**

Table 1 - Well cores petrophysics data; Acoustic velocities P- and S-wave, porosity and rock bulk density.

The wells show distinct arrangements of volcanic and sedimentary packages. Well TG-27 comprises two sampled intervals. The first is composed of 8 m of interbedded sandstone (denominated intratrap packages), and the second of layers of sandstone (20 cm) and basalt (2.4 m) and sandstone (4 m). Wells TG-100 and -227 display a simpler stratigraphy composed of large, stacked aeolian beds (40 and 90 m) between lava sheets. The TG-179 and CBM-100UF cores display a similar stratigraphy with intratrap sandstones in between lava packages, with thicker lava packages in the CBM well.

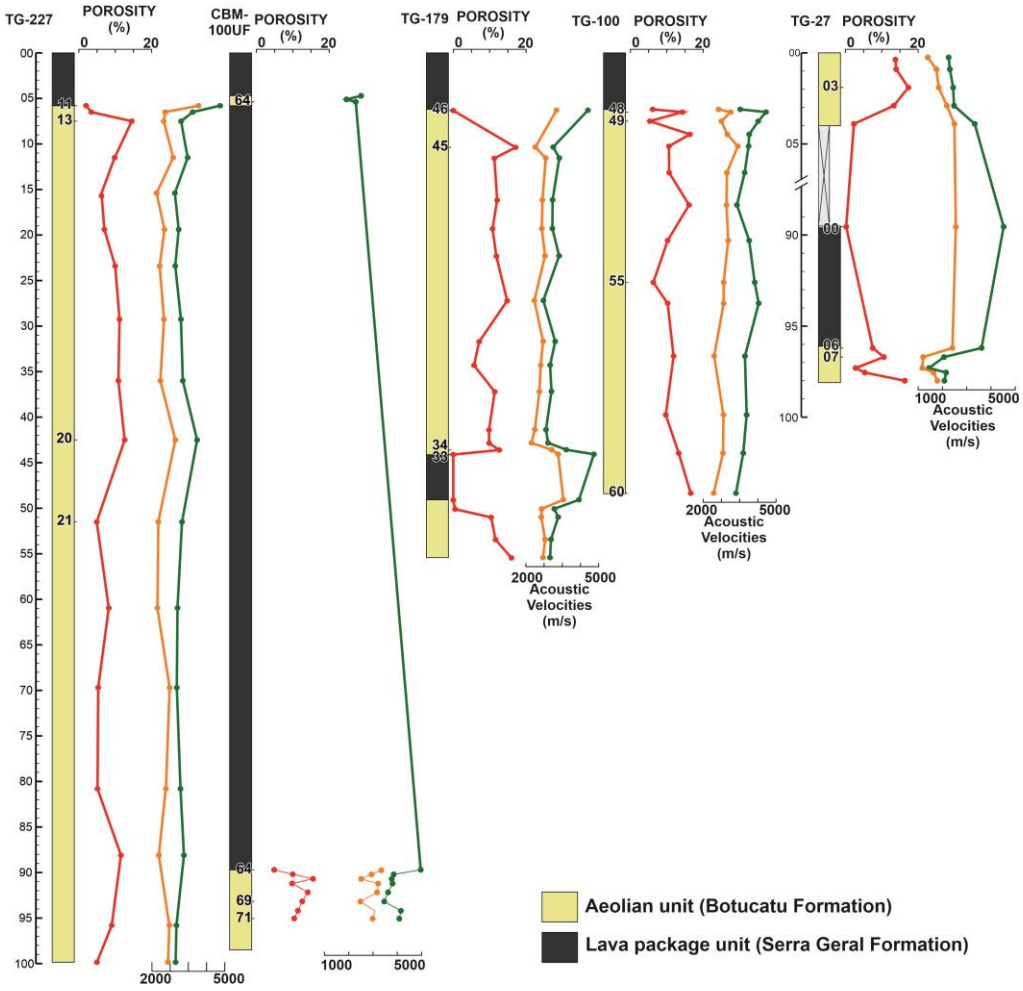

Figure 2 - Well core with the petrophysics dataset plotted of the distinct petrophysical facies. Thin sections position are marked with black numbers on the profiles.

Relatively homogeneous low acoustic velocities and high porosities can be seen throughout the wells (Fig. 3 and Fig. 13), except at the basalt/sandstone contact zones. Near lava contacts, acoustic velocity values record an increase and are associated with a decrease in porosity (at both the top and base of flows). Figure 3A shows the Vs and Vp data for all wells, demonstrating a coupled increase in Vs and Vp data, with most Vp data occurring between 3000 and 4000, with Vs data between 2000 and 3000. The porosity vs acoustic velocity plot (Fig. 3B) shows an inverse relationship between Vp (and consequently Vs). In all wells it is possible to observe, even near the contact, some scattering of the petrophysical response. This variation shows the existence of a distinct process occurring near the contact and accounts for the scatter in the linear models on plots 3A and 3B.

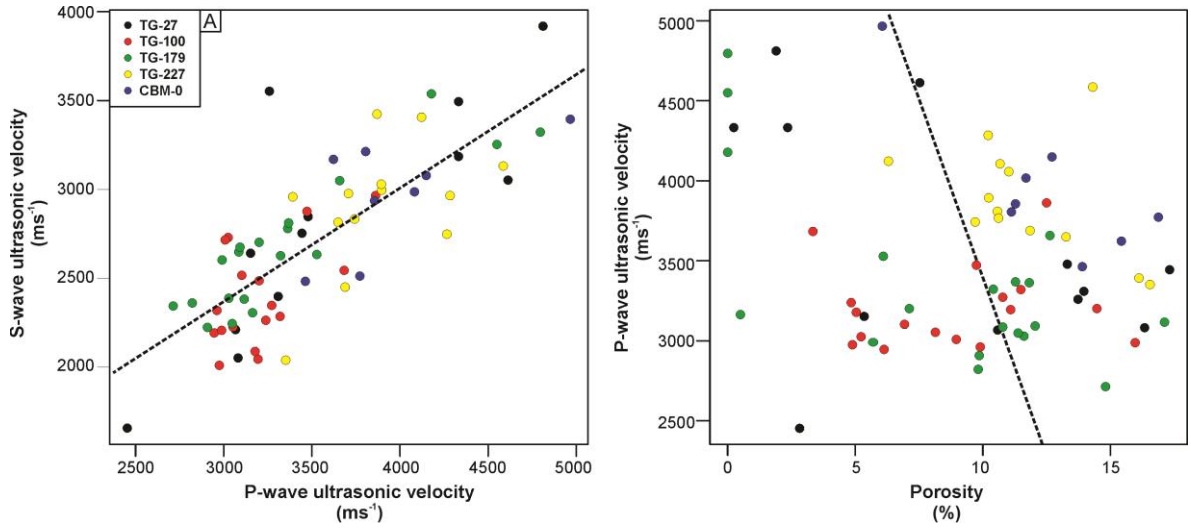

Figure 3- (A) P- and S-wave velocities distribution (B) and porosity and p-wave velocity.

4.2 Petrography

The framework composition of the Botucatu Formation is $Q_{65}F_{25}L_{10}$ and is shown in Figure 4A. The sandstones are litho-feldspatho-quartzose (lFQ), feldspar-rich feldspatho-quartzose (fFQ), feldspatho-quartzose (FQ) and quartz-rich feldspatho-quartzose (qFQ) sandstones (naming scheme follows that of Garzanti, 2018). The detrital quartz grains comprise homogeneous quartz from 64.1 to 97.3%

(av. 89.5%), deformed quartz 2.0 to 35.9% (av. 9.7%), and polycrystalline quartz from 0 to 3.1% (av. 0.9%). The feldspar detrital component includes plagioclase from 19.1 to 62.3% (av. 41.2%), microcline 26.4 to 70.2% (av. 50.9%) and orthoclase 0 to 21.1% (av. 7.9%) (Fig. 4B). The lithic components comprise 0 to 26.3% metamorphic grains (av. 8.6%), 47.4 to 84.6% plutonic grains (av. 66.7%), 7.7 to 41.4% volcanic grains (av. 20.8%) and 0 to 11.1% sedimentary grains (av. 3.9 %) (Fig. 4C). The plutonic content is composed of granitic material, the volcanic grains are composed of basic lavas (i.e., basaltic). The metamorphic grains are composed of low-grade banded micaceous-quartz-feldspathic rocks and meta-granites. The sedimentary grains are composed of sandstones. Felsic plutonic rocks are the predominant lithic material with subordinate volcanic grains. Heavy mineral grains include garnet, tourmaline, zircon and oxides.

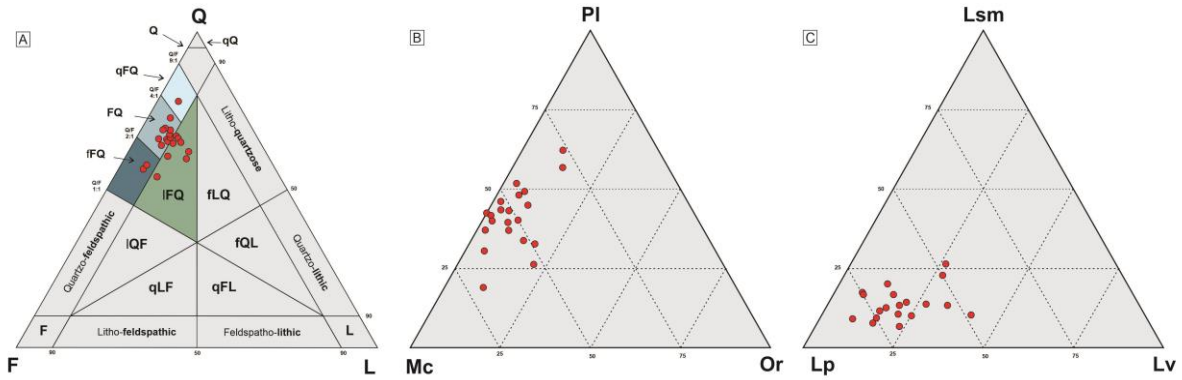

Figure 4- (A) Sandstone classification scheme (Garzanti, 2018) showing a feldspatho-quartzose to lithic-feldspato quartzose composition ; (B) Feldspar mineral ternary plot displays the similar microcline and plagioclase composition; (C) lithic ternary plot drawing the felsic plutonic lithic fragments composition (C). F- Feldspar; Q-Total Quartz; L- Lithics; Mc- Microcline; Or- Orthoclase; Pl- Plagioclase; Lp- Plutonic fragment; Lsm- Sedimentary and metamorphic fragments; Lv- Volcanic fragments.

In terms of sediment characteristics, the Botucatu samples have a predominantly unimodal distribution (71%) with some bimodal samples (29%). The grain sorting ranges from poor to moderate. For bimodal samples the thin section is taken from wind-ripple laminae such that the overall sorting values for the section are low. The sandstones comprise silt to very coarse grade material including fine sand (57%), medium sand (38%), and coarse sand (5%). It includes rounded grains 14 to 40% (R_{25}), sub-rounded grains 24 to 57% (SR_{466}), sub-angular grains 8.8 to 34.1% (SA_{21}), and angular grains 1 to 24% (A_9) (Fig. 5A). Cylindricity analysis indicates 21 to 46% of grains have high cylindricity (H_{31}) with 54 to 78% (L_{69}) having low cylindricity. Overall, the Botucatu sandstones are poor- to moderately sorted, medium to fine gained, sub- to well-rounded with regular cylindricity grain shapes (Fig. 5A and 5B). Grain contact types include float, point, linear (plane), concave-convex, and sutured. Figure 5A demonstrates the variability in the data, with a predominance of linear contacts, concave-convex contacts, with an occasional increase in sutured contacts (up to 26%). Point contacts are mostly associated with thicker laminae where displacive calcite growth occurs.

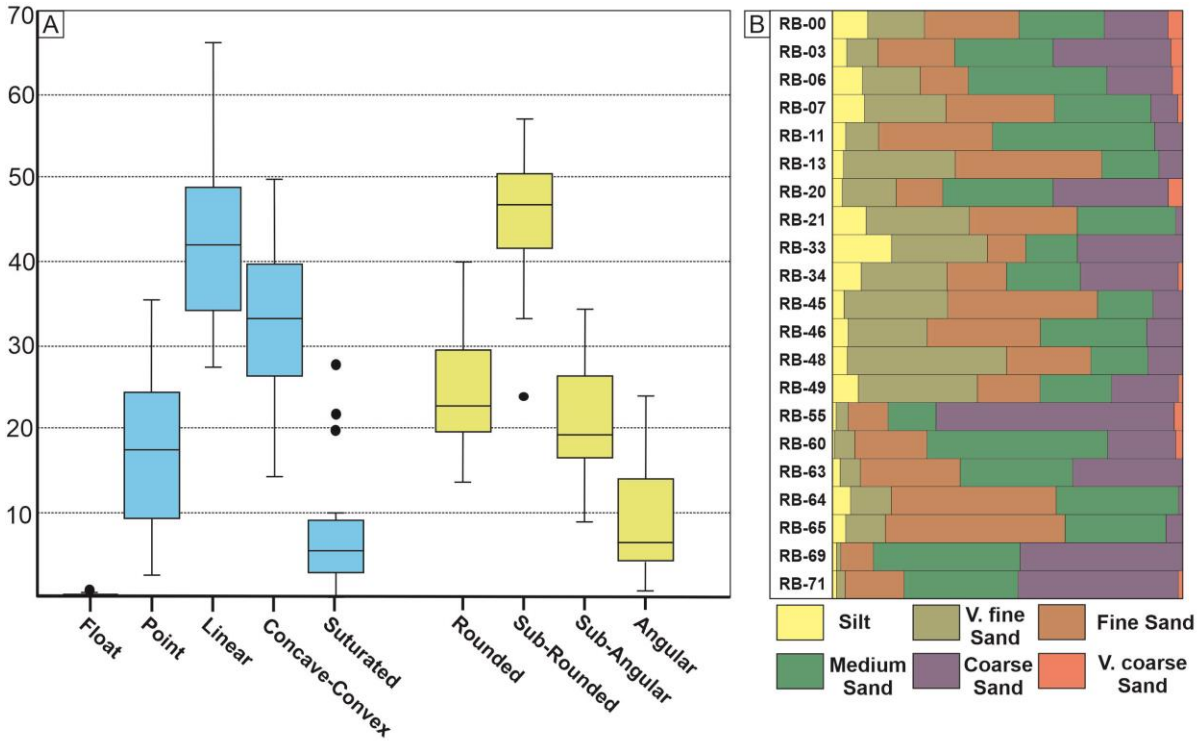

Figure 5- Granulometric characteristics of the aeolian Botucatu Sandstones; Blue box-Packing assessment demonstrating the overall medium packing (Linear predominance) with occasional peaks in sutured grains (black dots outliers). ; Yellow box- Roundness box-plot demonstrating the tendency toward high roundness in the aeolian system (Sub- and Rounded grains); C- Grain-size classes from the samples, illustrating poor-moderate sorting, as well as bimodal characteristics (RB-06,-20,-33,-34,-49).

The Botucatu sandstones have primary intergranular porosity that ranges from 0 to 16% (av. 8.7), moldic porosity from 0 to 2.2 (av. 2.2%) and intragranular porosity from 0.3 to 6.6% (av. 3.0). The total porosity ranges from 0.3 to 21.1% (av. 11.6%) and is mostly of the primary intergranular type. Dissolution is common, especially feldspar where moldic and intragranular secondary porosity is developed. The intergranular volume (IGV) has values ranging from 12.9 to 31.7% (av. 22.3%). Figure 6A displays a positive correlation between primary pore space and rock sorting, illustrating tendency towards porosity reduction in poorly sorted samples. The Houseknecht diagram (Fig. 6B) demonstrates that cementation is the main control on porosity loss.

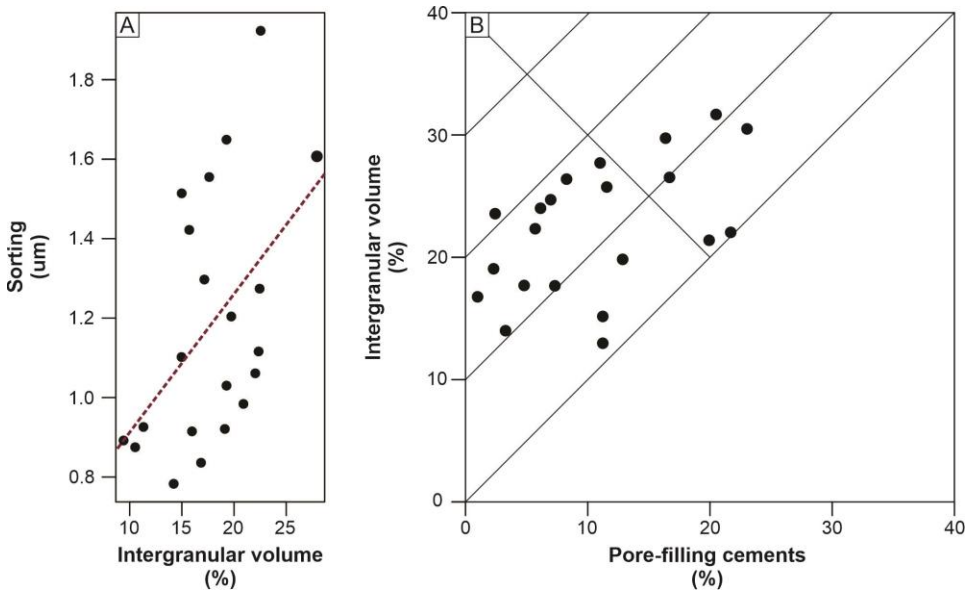

Figure 6 - Houseknecht Diagram demonstrating the tendency over compaction as a mechanism of porosity destruction. IGV- Intergranular volume (%) (Sum of primary porosity and pore filled cements).

The Botucatu sandstone samples contain between 1 and 23.1% (av. 10.7%) authigenic minerals include ten cement types: K-feldspar (0 to 2.2 %), quartz (0 to 7.9%), calcite (0 to 13.4%), dolomite (0 to 18.7%), smectite (0 to 6.3%), chlorite (0 to 20%), heulandite (0 to 8.1%), gypsum (trace), titanite (trace) and apatite (trace). K-feldspar, quartz, calcite, smectite and chlorite occur more frequently, while the other constituents are uncommon but representative.

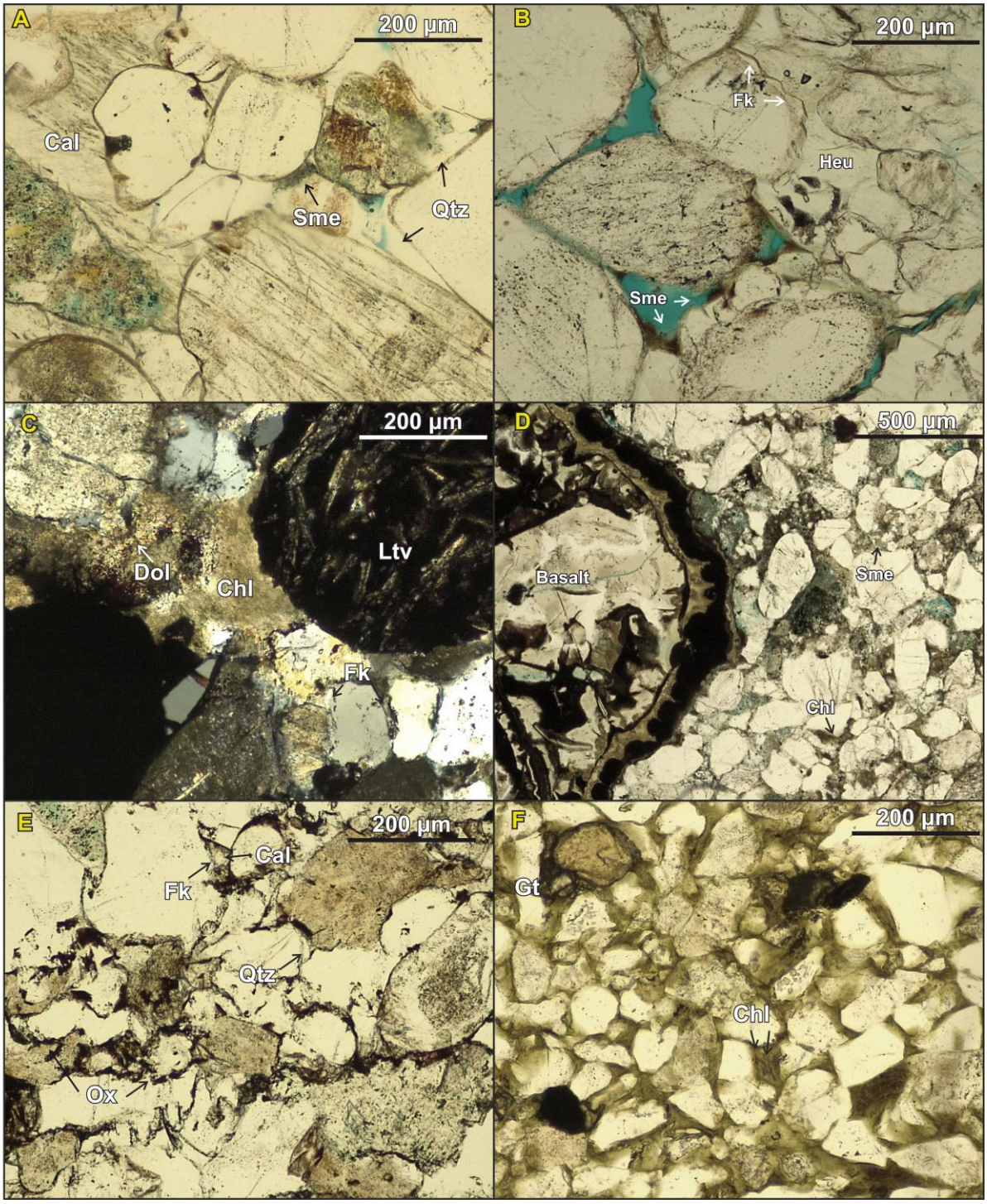

Figure 7- (A) Early quartz cement and poikilotopic calcite (Low packing) and post-burial smectite fringes; (B) Euhedral syntaxial feldspar, poikilotopic heulandite and smectite fringes; (C) Diagenetic signature near contact, early feldspar pore and overgrowth, fine dolomite cements and late chlorite pore filling; (D) Lava-sediment contact showing chlorite and smectite fringes and pore filling; (E) Highly packed samples with microstylolites (sutured contacts) with early feldspar and quartz overgrowth and post-burial calcite pore-filling; (F) Complete chlorite pore filing; Qtz-Quartz; Cal- Calcite; Sme- Smectite; Fk- K-Feldspar; Heu- Heulandite; Dol- Dolomite; Chl- Chlorite; Ltv- Lithic volcanic fragment; Ox- Fe Oxide; Gt- Garnet grain; Tour- Tourmaline grain.

K-feldspar occurs as euhedral syntaxial overgrowths, directly on quartz and feldspar constituents, in both sandstones affected and unaffected by volcanic packages (Figure 7B, C and 8A-D). Quartz cement occurs as syntaxial overgrowths, with euhedral shapes in less compacted samples (Fig. 7B) and as a post-burial pore fill (Fig. 7E). Quartz cement is present most commonly adjacent to the volcanic contact. Calcite cement occurs primarily as poikilotopic crystals, particularly in coarser grained laminae, (Fig. 7A and 8B) EDS and cathodoluminescence analysis demonstrate a homogeneous composition in the poikilotopic bands. Dolomite occurs locally adjacent to the volcanic contact as fine, pore-filling crystals (Fig. 7C and fig. 8C-D). Smectite cements are the most common clay mineral especially in samples unaffected by volcanic activity. Smectite occurs mostly as post-burial fringes (Figures 7A-B-D and 8A), and locally as cutans. Chlorite cement is the predominant clay mineral in near-contact sandstones. Chlorite occurs as post-burial pore-lining and pore-filling coats (Fig. 7C-F and 8C-D). Chlorite shows an increase in Mg from pore-lining to stacked- pore filling (Fig. 7F and 8F). Heulandite occurs as pre-burial poikilotopic cement in one sample (RB-63) and occurs in an interbedded sandstone (Fig. 7B). Accessory cements – apatite, titanite- were identified in SEM analysis (Fig. 8E-F), occurring as rims and pore-filling cementing locally, related to lithic material.

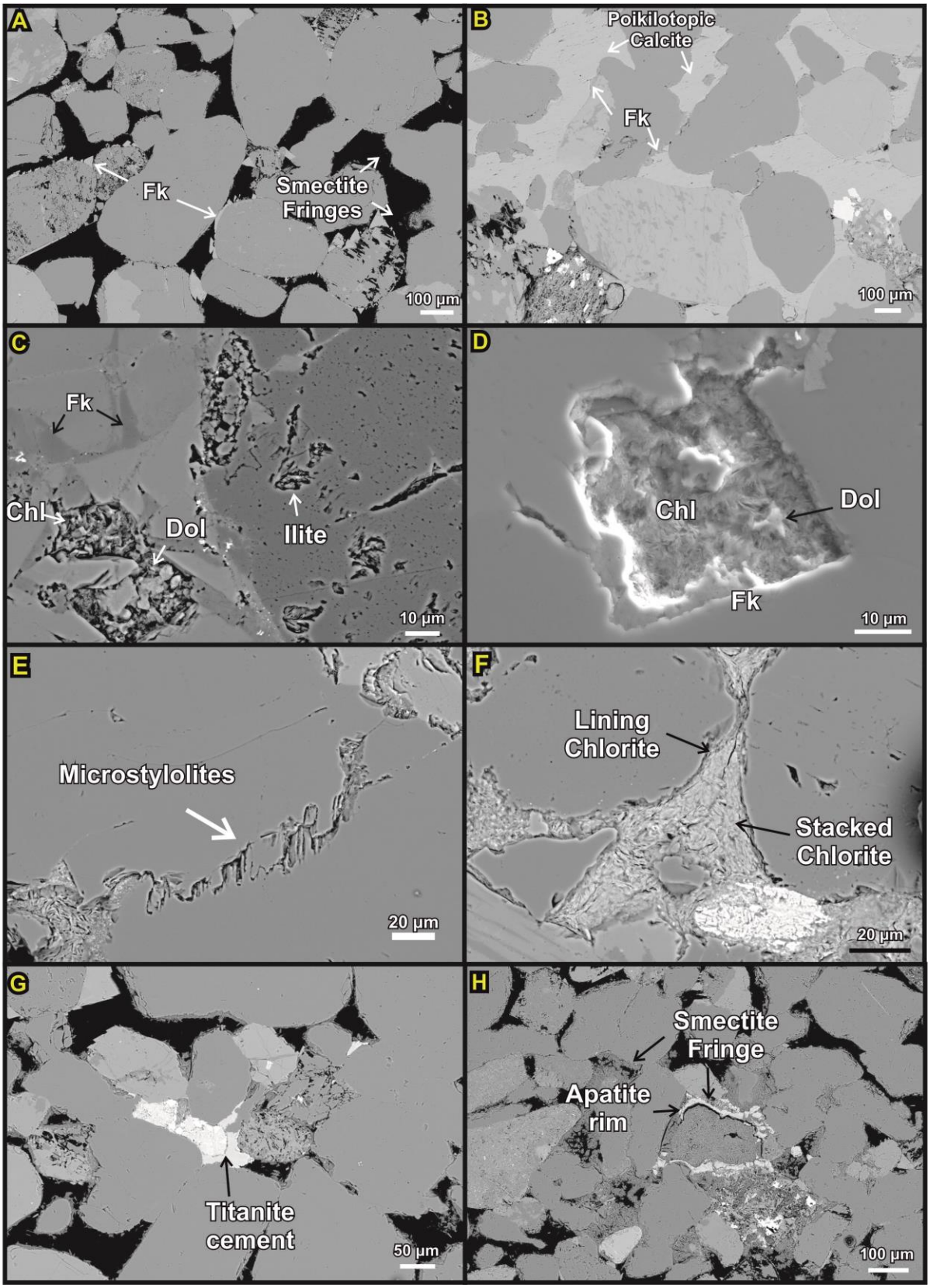

Figure 8- Petrography features in SEM: (A) Euhedral feldspar and smectite fringes; (B) Early K-feldspar overgrowth and displacive poikilotopic calcite ; (C-D) Chlorite and dolomite authigenesis near the contact; (E) Sutured contacts; (F) Two chlorite phases-lining and pore-filling (Mg-rich); (G-H) Accessory cements, titanite and apatite, related with lithic fragments. Fk- Feldspar; Chl- Chlorite; Dol- Dolomite.

5. DIAGENESIS

The petrographic and petrophysical examination of the dataset reveals 3 distinct types of diagenesis that correlate strongly with overlying lava packages. Types 1 and 2 demonstrate mineralogic and textural alterations related to the lava-contact environment, while type 3 shows no effects of volcanism with aeolian sediment displaying an overall shallow burial diagenetic pathway.

Type 1 is characterized by strong chloritization, smectite and Mg-carbonate cements. The presence of early chlorite and dolomite suggest a chemical interaction between lava and sediment, with an important influx of Mg from the basic lavas to the porous sedimentary system. Figures 8C, D and F illustrate aspects of the diagenetic processes, with feldspar overgrowths, fine dolomite and chlorite cements. Figure 8F demonstrates complex chlorite pore-filling, composed by 2 events (lining and pore-filling chlorite).

Type 2 is present a higher compaction, demonstrated by an average 23.0% of sutured contacts against the 7.0% elsewhere (Fig. 5), with concave-convex and sutured contacts (microstylolites) indicating localized chemical dissolution. The sutured contacts frequently occur among quartz, while feldspar and lithics grains are broken. The packing occurs early in the diagenetic history, with later pore-filling quartz, calcite and chlorite. Figure 7 illustrates the intensive packing with Fe oxide and stylolite bands. Figures 7 and 8 show the sutured contacts in detail with Fe oxide layers between grains.

Type 3 comprises an early poikilotopic cement, mostly calcite, but with local heulandite and anhydrite. This early cementation occurs usually in the coarser grained laminae, rarely occupying thinner bands where authigenic clays are most frequent,

particularly smectite fringes. Type 3 presents features characteristic of aeolian environment- such as poikilotopic calcite on coarser laminae and smectite clays in thinner bands- suggesting that this type corresponds to a zone without any volcanic effects.

Types 1 and 2 are restricted to the contacts between aeolian sandstone and lava, indicating that the lava-sediment interaction produces distinct diagenetic effects. Type 3 shows no influence of volcanic activity, recording typical aeolian environment diagenesis. Figure 9 presents a primary component plot using the petrographic data - authigenic-phases, porosity and sutured contacts - displaying a similar trend as observed petrographic examination. The plot demonstrates the grouping of petrographic elements according to diagenesis type, for instance the key element of type 3 diagenesis – the poikilotopic cements (calcite, heulandite and gypsum)- tends to behave similarly, validating the qualitative interpretation.

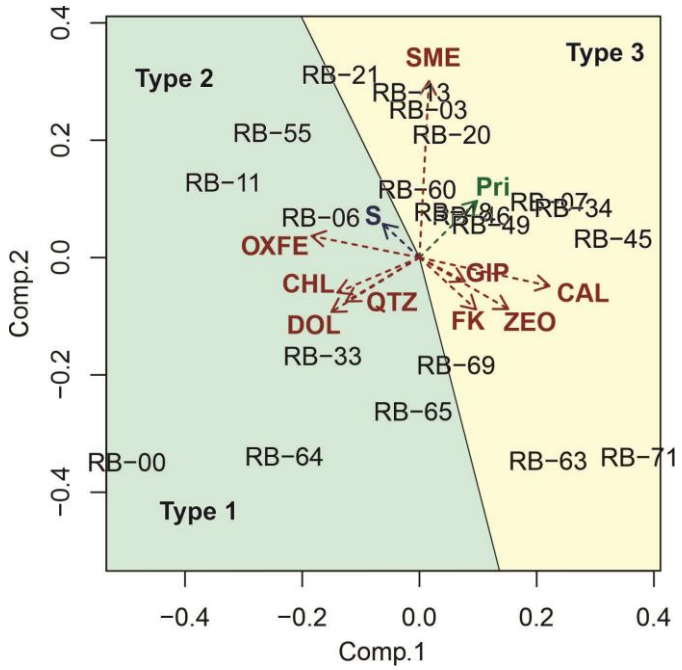

Figure 9- Primary component analysis of petrographic elements demonstrating the styles of diagenesis. Authigenic phases: SME-Smectite; GIP- Gypsum; FK- Potassium Feldspar; CAL-Calcite; ZEO- Zeolite; QTZ- Quartz; CHL- Chlorite; OXFE- Iron oxide; PRI- Primary porosity; S-Sutured grain contacts.

Overall, types 1 and 3 show low grain contact dissolution and limited evidence for chemical burial and differ from type 2 which displays abundant grain contact dissolution features. Post dissolution processes caused by weathering, increase the secondary porosity in all samples, but more frequently in type 3. Figure 10 shows a model for each style of diagenesis, indicating the characteristics features for each type.

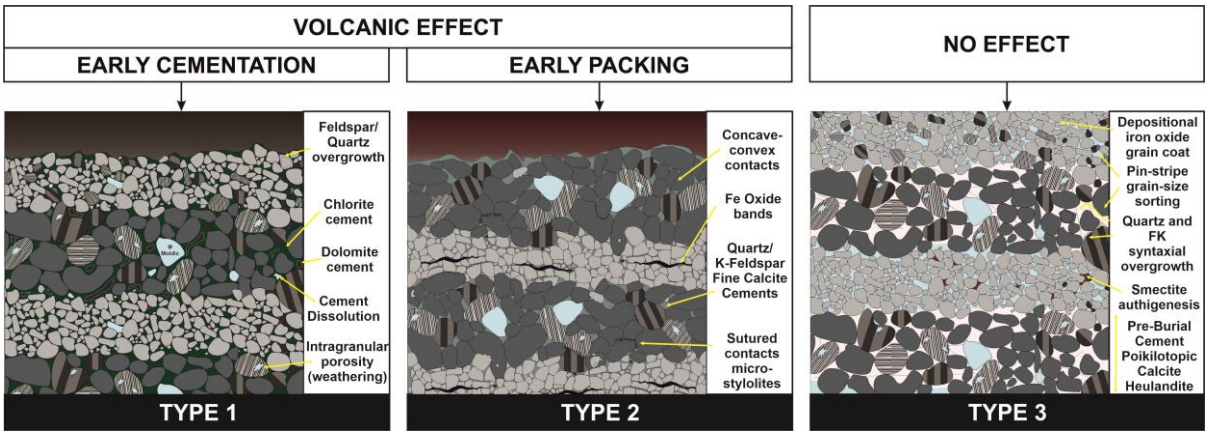

Figure 10 - Diagenetic pathways in the Botucatu Formation; Type 1 – early Mg-rich authigenesis; Type 2- Early chemical dissolution process-; Type 3 – Early poikolotopic calcite and smectite cementation.

5.1 Paragenetic evolution

The paragenetic sequence for each type differs, although early feldspar cementation and late feldspar dissolution caused by weathering are common to all 3 types. Type 1 displays the following paragenetic sequence: (i) early feldspar and quartz cementation; (ii) dolomite pore-filling; (iii) chlorite lining and pore-filling cement; (iv) secondary porosity induced by weathering. Type 2 is defined by: (i) early feldspar and quartz cementation; (ii) early mechanical (broken grains) and dissolution compaction (micro-stylolites) processes; (iii) fine calcite and quartz pore-filling

cementation; (iv) secondary porosity induced by weathering. Type 3 comprises the following paragenesis: (i) early feldspar and quartz cementation; (ii) poikilotopic cement (calcite, heulandite, and anhydrite); (iii) mechanical compaction (iv) smectite fringes; (v) secondary porosity induced by weathering. Figure 11 synthesizes the paragenetic evolution for all 3 types.

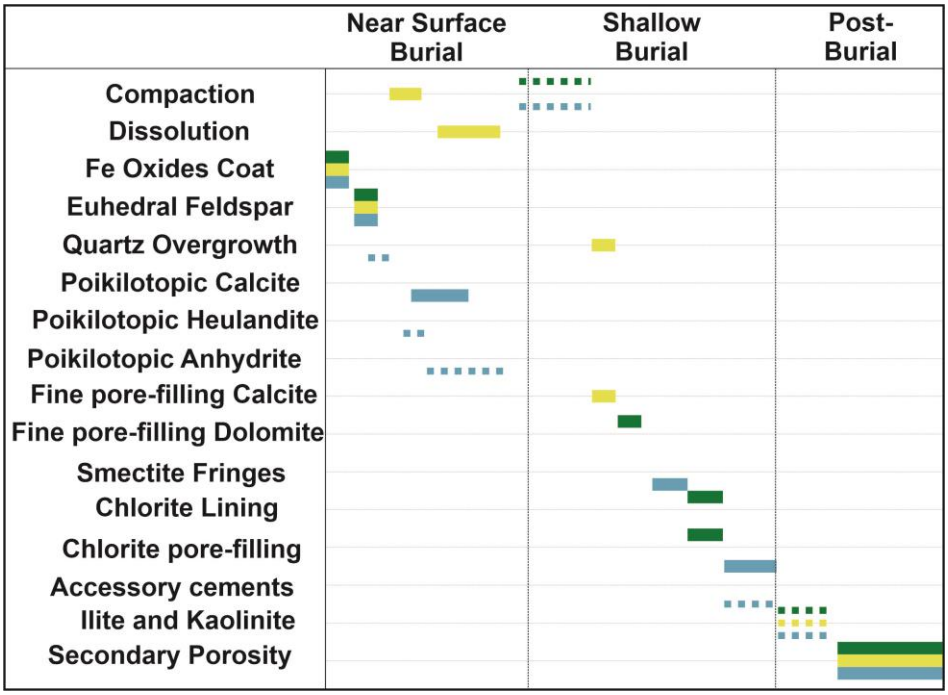

Figure 11 - Paragenesis chart for diagenetic events for each type. Green bar- Type 1; Yellow bar- Type 2; Blue bar- Type 3.

Fe-oxides and clay coatings occur frequently in the Botucatu sandstones and are considered typical of continental sediments (red beds) due to clay adhesion and subsequent iron-oxide precipitation in an aeolian environment (Walker, 1979, Wilson, 1992). Euhedral K-feldspar forms a fine rhomb habit to pore-filling cement (Figs. 8A-B) and is widespread in all samples. K-feldspar authigenesis also occurs as feldspar grain overgrowths, mostly in coarser grained zones. K-Feldspar occurs in all 3 types of diagenesis, indicating early authigenesis common to all types. The early cement occurrence suggests precipitation at shallow burial depths, with high activity of alkalis

and silica in intrapore waters (De Ros et al., 1994; Maraschin et al., 2004). Early K-feldspar authigenesis is commonly associated with humid-environments (Maraschin et al., 2004 and Anjos et al., 2000), in contrast to the mainly arid environment envisaged for the Botucatu. Gesicki (2007) suggests that hydrothermal fluids associated with the Serra Geral Formation lavas could provide the source for alkali-silica enriched interstitial pore-waters responsible for the cement. Volcanic induced hydrothermal activity is considered the primary mechanism responsible for the early feldspar phase in the Botucatu formation.

Quartz overgrowths are less abundant than K-Feldspar, but similarly occur relatively early in the diagenetic history. Quartz cementation is usually controlled by depth and temperature, and associated with grain dissolution (Bjørlykke, 1999). The existence of shallow dissolution processes associated with volcanism (Type 2), may account for the silica required for quartz overgrowths, particularly as pore-filling quartz is a common Type 2 constituent.

Pre-burial cementation of poikilotopic minerals (calcite, heulandite, and anhydrite) is common in Type 3, especially calcite. SEM images (Backscatter and cathodolumiscence) reveal homogenous Fe-poor calcite, predominant in coarser grained laminae. The low mechanical packing present in the grain framework affected by the poikilotopic cement, suggests an eodiagenetic character, mostly controlled by environmental conditions. Anhydrite appears rarely as a pore-filling/poikilotopic cement and is restricted exclusively to coarser laminae. Anhydrite and gypsum minerals are not frequent due to dissolution, however De Ros (1998) demonstrated the existence of gypsum crystal imprints in the Botucatu, indicating the common existence of this mineral in the unit. Sediments deposited in hot, arid regions with low rainfall and high rates of evaporation commonly contain carbonate and gypsum (and

anhydrite) cements (Worden & Burley, 2003, Henares et al., 2014, Wright et al, 1992). Heulandite displays similar characteristics to calcite and anhydrite; however it is restricted exclusively to intratrap sandstones packages (RB-63). Vavra (1989) shows that the authigenesis of heulandite, laumontite, and prehnite in the Triassic Fremouw and Falla Formations, result from rock-fluid interactions driven by heat from a diabase intrusion. Zeolite minerals are common as fracture fills in the Serra Geral units (Murata et al., 1987), indicating post-volcanic zeolite growth. The Corda Formation (Parnaiba Basin) (Rabelo,2019) displays a similar feature with poikilotopic zeolite in interbedded sandstones and lava flows. Rabelo (2019) suggests that ion release from weathered basalts is the main mechanism in the generation of massive zeolite bearing sandstones in the Parnaiba Basin. In the Botucatu, the zeolite cement appears to be relatively early as indicated by floating grain contacts and differs from cementation Types 1 and 2. The absence of mechanical compaction suggests that zeolite cementation occurs shortly after lava extrusion and is likely derived from fluids associated with the volcanics. Dolomite authigenesis is common in aeolian systems, especially related to brines in sabkhas and other evaporitic settings (Rossel, 1982; Pye and Krinsley, 1986; Davies, 1997). However, the dolomite cementation occurs exclusively at the lava-contact, suggesting it is related to lava emplacement.

Clay minerals include smectite and chlorite. Smectite is common in Type 3 and occurs inside thinner sand laminae as fringes and disconnected fringes. The smectite forms after an initial mechanical packing increase, marked by filling in intergranular pores. Smectite growth is controlled by depositional and diagenetic factors (McKinley, 1999), with detrital material and environmental conditions affecting the clay morphology and appearance. Smectite coats in eogenetic conditions suggest continental environments subject to evaporation (Hover et al., 1999; Pozo & Casas,

1999). Chlorite which occurs as grain rims is usually related to mesogenetic conditions due to a progressive increase in pressure, temperature and changes in water chemistry (Worden & Morad, 2009). Continuous burial results in transformation of metastable phases into chlorite, requiring transformation from a previous clay mineral species (Worden & Morad, 2009; Beaufort, 2015). Type 1 displays a pervasive chloritization process, with smaller occurrences in type 2. Smectite transitions to chlorite under mesodiagenetic conditions, however apparently the distribution of chlorite is pervasive and restricted to the contact zone while the smectite is predominant in thinner laminae. The shallow burial of the Botucatu Fm. and the absence of chlorite outside 0.1 to 1 m suggest that hydrothermal fluids were responsible for the Mg-rich cements (such as chlorite and dolomite), especially in Type 2 examples. Accessory authigenic phases such as apatite and titanite rims were identified via SEM. Liu (2019) describes apatite and Ce-apatite authigenesis as related to hydrothermal fluids induced by intermediate-felsic magma intrusion in the Xihu Depression (East China Sea), and may support a hydrothermal origin for these mineral phases.

5.2 Diagenetic Models

Cementation Types 1 and 2 show how synchronous volcano-sedimentary activity may lead to discrete diagenetic pathways. Type 1 shows the Mg-rich authigenic minerals, chlorite and dolomite, while Type 2 displays chemical compaction as indicated by microstylolites.

Figure 12 displays a model for Type 1 diagenesis, with smaller lava packages sealing the lava contact with the generation of fluid circulation near the contacts at both the base and top of the lava, creating conditions for dolomite and chlorite authigenesis. Chlorite is common as a hydrothermal alteration product of igneous

rocks (Beaufort, 2015). Hydrothermal systems (sensu Machel & Lonnee, 2002) display an anomalously higher temperature relative to the burial conditions to which the basin is subjected. The Type 1 cementation style is characterised by a typical deep-burial clay mineral (chlorite) in relative shallow burial conditions (less than 1km), suggesting that hydrothermal fluids strongly influenced Type 1 cementation. For chlorite and dolomite authigenesis, the Mg- ion could be derived from mafic lithic fragments and detrital clays. The dolomite cement is restricted to the contact zone, whilst calcite is predominant elsewhere. The typical early calcite poikilotopic cement (Type 3), is not present in types 1 and 2, suggesting calcite dissolution and later recrystallization as dolomite or direct dolomite growth. For chlorite, common smectite could be a source; however, the smectite volume should not be enough to generate the pore-filling chlorite found in type 1 examples. Furthermore, lithic detritus is not abundant (mean 10%) and is composed mostly of felsic plutonic material (Fig. 4A). The Serra Geral lavas are candidates for supplying the Mg for chlorite and dolomite, contributing not only the chemical ions but the hydrothermal system as well. Mg-chlorites in hydrothermal systems form under temperatures ranging from 100 to 300^{o}C (Beufort, 2015), significantly higher than the shallow burial conditions that the Botucatu has been subjected to.

The key feature of the Type 2 cementation is the microstylolites, with a mean of 26% sutured grain contacts, indicative of dissolution process (chemical compaction) near the lava contacts. Compaction and mineralogy control quartz dissolution which usually occurs at burial depths of 2 to 3 km (Bjørlykke, 1999). Burial of the Botucatu is less than 1km in the study area, and the dissolution is restricted to the lava sediment contact suggesting a volcanic influence/control. Figure 12 presents a model for Type 2 diagenesis, with thicker volcanic packages between the aeolian units generating

significant overburden pressure on underlying sandstones. Typical temperatures for quartz dissolution are 70-100° C (Bjørlykke, 1999). A similar process occurs in the Entrada sandstone on the Colorado Plateau, associated with igneous intrusions, where Wilson (2019) describes stylolites within a 5 m thick aeolian sandstones horizon associated with shallow intrusions.

Two mechanisms are considered responsible for chemical dissolution of sandstones - a stress independent phenomena generated by illite-mica grain coats (Bjorkum, 1996; Bjorkum & Nadeu, 1999) and a stress induced compaction represented by intergranular pressure-solution (Osborne & Swarbrick, 1999; Sheldon et al., 2003; Stricker et al., 2016). The presence of chemical dissolution processes only at some lava-sediment contacts, suggests that grain coats were not an important factor in the Botucatu- considering that grain coating occurs indiscriminately. In addition, Figure 12 shows that thicker lava packages tend to show more chemical dissolution. Therefore, the difference between Types 1 and 2 may be directly controlled by the differential effective stress generated by the variable lava thicknesses on top of the aeolian sandstones. If the lava overburden is capable of promoting early compaction as in type 2, any potential hydrothermal system may have been baffled or nullified due to the permeability and porosity loss.

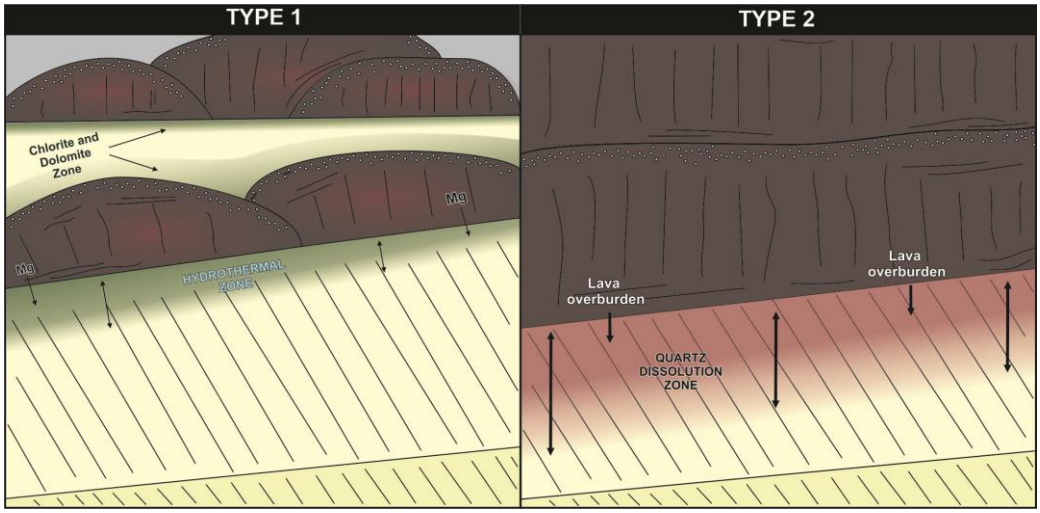

Figure 12- Model for diagenetic transformation of type 1 – Hydrothermal system generated by lava-fluid interaction inducing an early Mg-rich authigenesis; type 2- Lava overburden produce an increase on effective stress and temperature causing chemical dissolution.

6. RESERVOIR IMPLICATIONS

The volcanic-related diagenetic effects produced by the lava-field interbedded with the aeolian sandstones of the Botucatu Formation tends to reduce porosity and increase ultrasonic velocities. Table 2 compiles the petrophysical attributes and petrographic appearance for each diagenetic style (Types 1-3). In general, Types 1 and 2 show low porosity values, low permeability (low connectivity between the pores), and high acoustic velocitiy values in comparison to Type 3. Types 1 and 2 have higher mean velocitiy values then Type 3 (up to 1000 m/s difference), with Type 2 having notably higher Vs values. Type 3 has higher porosity values, but occasional pervasive calcite cementation also generates low values. The permeability of Type 3 may be affected by the occasional predominant calcite, but the intergranular porosity shows good connectivity. Types 1 and 2 display recognizable petrophysical attributes (Table 2), with up to 4000 ms^{-1} P-wave velocities, 2800 ms^{-1} S-wave velocity, and 6%

porosity. Type 3 shows 3500 and 2700 ms^{-1} P- and S-waves, respectively, and at least 12% porosity.

	Petrography	Porosity			Permeability*	Ultrasonic velocities		Grain packing					Main diagenetic features
		Experiment	Primary	Secondary		Vp	Vs	F	P	L	CC	S	
Type 1		2.6	1.8	2.5	Bad	4580.2	3289.8	0.7	27.7	38.7	27.3	5.5	Chlorite, dolomite and feldspar cementing
Type 2		4.0	1.8	1.0	Bad	4888.6	3656.8	0.0	9.2	22.8	47.3	20.7	Quartz dissolution (CC and sutured contacts)
Type 3		10.6	10.8	3.3	Regular to good	3622.0	2568.4	0.2	16.9	44.3	32.3	6.3	Poilotopic calcite and smectite pore-filling cements

Table 2- Summary of diagenetic types and petrophysical attributes.

Figures 13A suggests that towards the lava contact porosity values tend to decrease. However, the process is not linear, forming separate clusters, as illustrated on plot 13B, that shows a wider range of variation in P-wave velocity values near contact, while it tends to be more restricted around 3000 ms^{-1} elsewhere. The P-waves extreme values (4000 to 5000 m/s) tends to be next to the lava (0.1 m), while the low porosity values (<5%) occur mostly from 0.1 to 1 m away. This response indicates a heterogeneous effect of the volcanic packages over the siliciclastic unit.

Considering that the thicker lava packages should provide more heat into the sedimentary pile, the plots 13C and D normalizes the distance to the lava by the size of the volcanic package. The plots 13C and D shows the increase of Vp and decrease

of porosity to smaller ratio values. The plot suggests that the diagenetic alteration is not controlled exclusively by the distance to lava, but also by the lava thickness, justifying the existence of low velocity near the contact. As overall behaviour, the petrophysical data shows a heterogenous response near the contact, with a slight tendency toward porosity diminishing and acoustic velocity increase from 0.1 to 1m of the contact, but also presenting higher porosity values in the affected area. However, the petrographic data (Fig.14) presents clearer porosity changes near the contact.

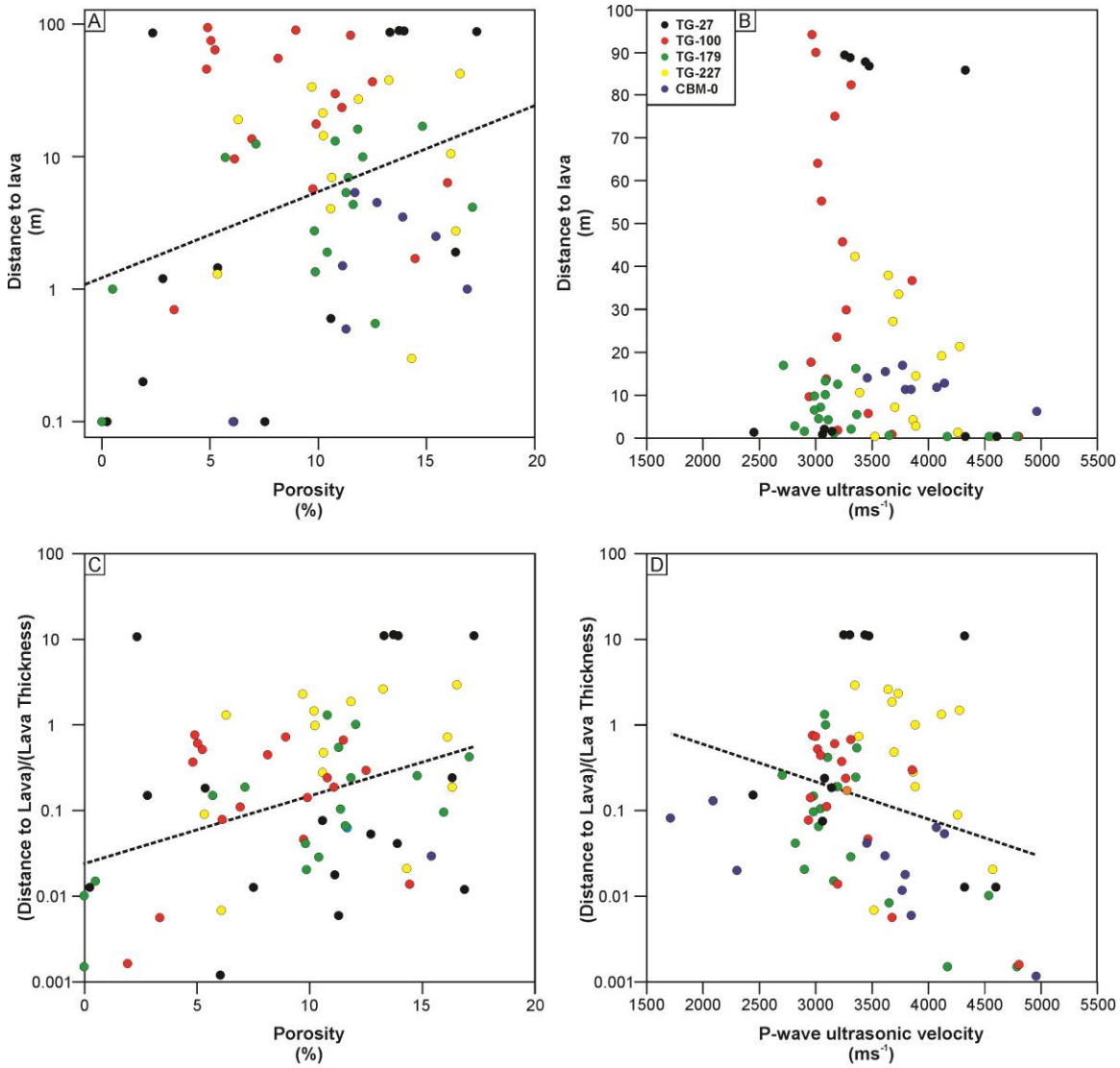

Figure 13-(A-B) Petrophysical variation (porosity and P-wave velocity) controlled by lava distance; (C-D) lava distance normalized by lava thickness.

Types 1 and 2, are associated with extensive porosity reduction and are detrimental to the reservoir system; however, Figure 13 illustrates that the effects are restricted to within 0.1 to 1 m of the contact suggesting this feature could be a fluid seal. Permeability data from intrabasaltic sandstones reported by Rosseti (2019) have low values (100 to 0.1 mD) supporting this interpretation. The anomalously low values that are not related to the contact zones can be explained by the normal aeolian permeability heterogeneity Kv/Kh (Howell & Mountney, 2001), by weathering cement dissolution or by the lava thickness (Fig. 13C). Furthermore, common poikilotopic minerals are relatively frequent in thicker laminae, so the low porosities may reflect these features.

The high ultrasonic velocities of Types 1 and 2 (Vp up to 5000 m/s) overlap values of volcanic facies of Serra Geral formation (Rossetti et al., 2019). The contrast between zones with high and low ultrasonic velocities may lead to false interpretations of seismic data during reservoir evaluation and modelling phase. Watson (2019) discussed how acoustic impedance variations in volcanic rocks from the Bass Basin (SE Australia), result in miss-prediction of igneous bodies during pre-drill phases. The data from the Botucatu shows that these miss-interpretations could also happen between highly cemented sandstones, poorly cemented sandstone and basaltic lavas.

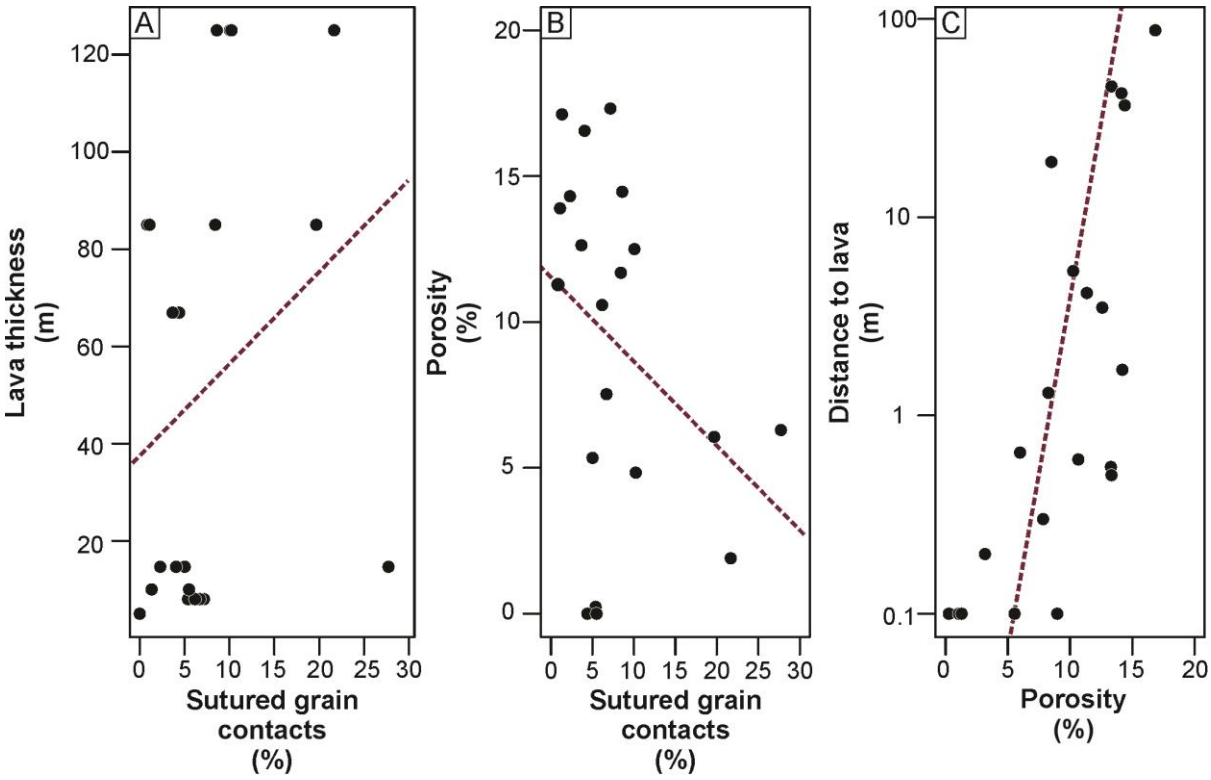

Figure 14 - (A) Relationship of chemical dissolution (Sutured grain contacts) with porosity (B) and lava sheets thickness; (C) The porosity on petrography presents a positive correlation from the distance to lava and the porosity.

Figure 14 demonstrates the relationship between size and thickness of lava packages with grain contacts and porosity. The larger lava thickness partially explains the increase in sutured grain contacts (Fig. 14A), generated by increased lava overburden. The sutured contacts and porosity, show a clear negative correlation, demonstrating how the increase in compaction diminishes pore size (Fig. 14B). In the petrographic dataset, the porosity shows a clearer trend of decreasing towards the lava contact, in comparison with the petrophysical data (Fig. 14C). The petrographic dataset illustrates more clearly than petrophysical data, the porosity diminishing near the contact, and reiterate the lava thickness impact on diagenesis.

7. CONCLUSIONS

Petrophysical and petrographic studies were undertaken on sandstones beneath, and interbedded with basaltic lava flows from the Cretaceous Botucatu (sandstone) and Serra Geral (lavas) in the Paraná Basin. The objective was to understand if and how effusive volcanic rocks promote alteration of reservoir proprieties. Ultrasonic and porosity values were measured for 72 plugs from 5 wells and petrography from the intervals near the lava-sediment contacts was described, revealing:

- Petrophysical data shows that the zone affected by lava ranges from 0.1 to 1m to the lava contact;
- P- wave velocities show higher values, between 4000 and 5000 ms^{-1} within 1 m of the contact and 2500 and 4000 ms^{-1} outside the volcanic affected area;
- Porosity presents average 6.5% within 1 m of the contact and 10.7% in the non-affected zone;
- The contact zone shows 2 types of diagenesis- early Mg-rich authigenesis and early packing and chemical dissolution;
- Mg-chlorite and dolomite pore-filling suggests a hydrothermal system on Type 1;
- Type 2 displays microstylolites, and sutured contacts correlated with thicker lava packages indicates the lava overburden as a mechanism of diagenesis;
- The variability of lava packages thickness appears to affect the diagenetic effects, partially justifying anomalous velocity and porosity values near to contact;

- The low porosity near the contact may promote an additional seal to a possible reservoir in a volcano-sedimentary play.

8. ACKNOWLEDGMENTS

The authors gratefully acknowledge support from Shell Brasil through the 'BG05: UoA-UFRGS-SWB Sedimentary Basins' project at UFRGS and the strategic importance given by ANP through the R&D levy regulation. We also thank Conselho Nacional de Desenvolvimento Científico e Tecnológico (CNPq) by the financial support (grant 203786/2017-3). The authors would like to thank Companhia de Recursos Minerais (CPRM) and to Prof. Wolfgang Kalkreuth for the core plugs. This work is a part of the current Ph.D. thesis from Gabriel Bertolini at the University of Aberdeen, and Universidade Federal do Rio Grande do Sul.

9. REFERENCES

Ahmed, W. 2002. Effects of heat-flow and hydrothermal fluids from volcanic intrusions on authigenic mineralization in sandstone formations. *Bulletin of the Chemical Society of Ethiopia*, **16(1)**, 37-52.

Alves, T.M., Omosanya, & K., Gowling, P., 2015. Volume rendering of enigmatic high amplitude anomalies in southeast Brazil: a workflow to distinguish lithologic features from fluid accumulations. *Interpretation*, **3(2)**, A1-A14.

Angkasa, S.S., Jerram, D.A., Millett, J.M., Svensen, H.H., Planke, S., Taylor, R.A., Schofield, N. and Howell, J. (2017). Mafic intrusions, hydrothermal venting, and the basalt-sediment transition: Linking onshore and offshore examples from the North Atlantic igneous province. *Interpretation*, **5(3)**, SK83-SK101.

Anjos, S. M. C.; De Ros, L. F.; Souza, R. S.; Silva, C. M. A.; & Sombra, C. 2000. Depositional and diagenetic controls on the reservoir quality of Lower Cretaceous Pendencia sandstones, Potiguar rift basin, Brazil. AAPG Bulletin, **84(17)**, 19-1742.

Baksi, A. K. 2018. Paraná flood basalt volcanism primarily limited to~ 1 Myr beginning at 135 Ma: New 40Ar/39Ar ages for rocks from Rio Grande do Sul, and critical evaluation of published radiometric data. *Journal of Volcanology and Geothermal Research*, **355**, 66-77.

Beaufort, D., Rigault, C., Billon, S., Billault, V., Inoue, A., Inoué, S., & Patrier, P. 2015. Chlorite and chloritization processes through mixed-layer mineral series in low-temperature geological systems–a review. *Clay minerals*, **50(4)**, 497-523.

Birch, F. 1960. The velocity of compressional waves in rocks to 10 kilobars: 1. *Journal of Geophysical Research*, **65**, 1083-1102.

Bjorkum, P.A., 1996. How important is pressure in causing dissolution of quartz in sandstones?. *Journal of Sedimentary Research*, **66**, 147-154.

Bjørlykke, K. 1999. An overview of factors controlling rates of compaction, fluid generation and flow in sedimentary basins. *Growth, dissolution and pattern formation in geosystems*. Springer, Dordrecht, 381-404

Blott, S.J. & Pye, K. 2001. GRADISTAT: a grain size distribution and statistics package for the analysis of unconsolidated sediments. *Earth Surface Processes and Landforms*, **26(11)**, 1237-1248.

Davies, G. R. 1997. Aeolian sedimentation and bypass, Triassic of Western Canada. *Bulletin of Canadian Petroleum Geology*, **45(4)**, 624-642.

De Ros, L. F. 1998. Heterogeneous generation and evolution of diagenetic quartzarenites in the Silurian-Devonian Furnas Formation of the Paraná Basin, southern Brazil. *Sedimentary Geology*, **116(1-2)**, 99-128.

De Ros, L. F.; Sgarbi, G. N. C.; & Morad, S. 1994. Multiple authigenesis of K-feldspar in sandstones: evidence from the Cretaceous Areado Formation, Sao Francisco Basin, central Brazil. *Journal Sedimentary Res*earch, **64**, 778-787.

Ernesto, M., Raposo, M. I. B., Marques, L. S., Renne, P. R., Diogo, L. A., & De Min, A. 1999. Paleomagnetism, geochemistry and 40Ar/39Ar dating of the North-eastern Paraná Magmatic Province: tectonic implications. *Journal of Geodynamics*, **28(4-5)**, 321-340.

Folk, R. L. 1968. Petrology of sedimentary rocks: Hemphill's. *Austin, Texas*, **170**.

França, A. B., Araújo, L. M., Maynard, J. B., & Potter, P. E. 2003. Secondary porosity formed by deep meteoric leaching: Botucatu eolianite, southern South America. *AAPG bulletin*, **87(7)**, 1073-1082.

Garzanti, E. 2018. Petrographic classification of sand and sandstone. *Earth-science reviews*, 192, pp.545-563.

Gesicki, A. L. D., 2007. Evolução diagenética das formações Pirambóia e Botucatu (Sistema Aqüífero Guarani) no Estado de São Paulo. São Paulo, PhD thesis, University of São Paulo, Brazil.

González-Acebrón, L., Goldstein, R. H., Mas, R., & Arribas, J. 2011. Criteria for recognition of localization and timing of multiple events of hydrothermal alteration in sandstones illustrated by petrographic, fluid inclusion, and isotopic analysis of the Tera Group, Northern Spain. *International Journal of Earth Sciences*, **100(8)**, 1811-1826.

Grove, C. 2013. Submarine hydrothermal vent complexes in the Paleocene of the Faroe-Shetland Basin: Insights from three-dimensional seismic and petrographical data. *Geology*, **41(1)**, 71-74.

Grove, C., Jerram, D. A., Gluyas, J. G., & Brown, R. J. 2017. Sandstone diagenesis in sediment–lava sequences: exceptional examples of volcanically driven diagenetic compartmentalization in Dune Valley, Huab Outliers, NW Namibia. *Journal of Sedimentary Research*, *87*(12), 1314-1335.

Haile, B. G., Czarniecka, U., Xi, K., Smyrak-Sikora, A., Jahren, J., Braathen, A., & Hellevang, H. 2019. Hydrothermally induced diagenesis: Evidence from shallow marine-deltaic sediments, Wilhelmøya, Svalbard. *Geoscience Frontiers*, **10(2)**, 629-649.

Hardman, J., Schofield, N., Jolley, D., Hartley, A., Holford, S., & Watson, D. 2019. Controls on the distribution of volcanism and intra-basaltic sediments in the Cambo–Rosebank region, West of Shetland. *Petroleum Geoscience*, *25*(1), 71-89.

Healy, D., Neilson, J. E., Haines, T. J., Michie, E. A., Timms, N. E., & Wilson, M. E. 2015. An investigation of porosity–velocity relationships in faulted carbonates using outcrop analogues. *Geological Society, London, Special Publications*, **406(1)**, 261-280.

Henares, S., Bloemsma, M. R., Donselaar, M. E., Mijnlieff, H. F., Redjosentono, A. E., Veldkamp, H. G., & Weltje, G. J. (2014). The role of detrital anhydrite in diagenesis of aeolian sandstones (Upper Rotliegend, The Netherlands): Implications for reservoir-quality prediction. *Sedimentary Geology*, **314**, 60-74.

Hirata, R., Gesicki, A., Sracek, O., Bertolo, R., Giannini, P. C., & Aravena, R. 2011. Relation between sedimentary framework and hydrogeology in the Guarani Aquifer System in São Paulo state, Brazil. *Journal of South American Earth Sciences*, **31(4)**, 444-456.

Holford, S. P., Schofield, N., Jackson, C. L., Magee, C., Green, P. F., & Duddy, I. R. 2013. Impacts of igneous intrusions on source reservoir potential in prospective sedimentary basins along the western Australian continental margin. In: *The Sedimentary Basins of Western Australia IV* (Ed. by M.Keep & S.J.Moss), Proceedings of the Petroleum Exploration Society of Australia Symposium, Perth, WA.

Hover, V. C., Walter, L. M., Peacor, D. R., & Martini, A. M. 1999. Mg-smectite authigenesis in a marine evaporative environment, Salina Ometepec, Baja California. *Clays and Clay Minerals*, **47(3)**, 252-268.

Howell, J., & Mountney, N. 2001. Aeolian grain flow architecture: hard data for reservoir models and implications for red bed sequence stratigraphy. *Petroleum Geoscience*, **7(1)**, 51-56

Ingersoll, R. V., Bullard, T. F., Ford, R. L., Grimm, J. P., Pickle, J. D. & Sares, S. W. 1984. The effect of grain size on detrital modes: a test of the Gazzi-Dickinson point-counting method. *Journal of Sedimentary Research*, **54(1)**, 103-116.

Janasi, V. A., Freitas, V. A. & Heaman, L. H. (2011) The onset of flood basalt volcanism, Northern Paraná Basin, Brazil: A precise U–Pb baddeleyite/zircon age for a Chapecó-type dacite. *Earth Planetary Science Letters*, **302(1-2)**, 147-153.

Araújo, L.M., França, A.B. and Potter, P.E., 1999. Hydrogeology of the Mercosul aquifer system in the Paraná and Chaco-Paraná Basins, South America, and

comparison with the Navajo-Nugget aquifer system, USA. *Hydrogeology Journal*, 7(3), pp.317-336.

Liu, Y., Jin, S. D., Cao, Q., & Zhou, W. 2019. Tertiary hydrothermal activity and its effect on reservoir properties in the Xihu Depression, East China Sea. *Petroleum Science*, **16(1)**, 14-31.

Machel, H. G., & Lonnee, J. 2002. Hydrothermal dolomite—A product of poor definition and imagination. *Sedimentary Geology*, **152(3-4)**, 163-171.

Maraschin, A. J., Mizusaki, A. M. P., & De Ros, L. F. 2004. Near-surface K-feldspar precipitation in Cretaceous sandstones from the Potiguar Basin, Northeastern Brazil. *The Journal of Geology*, **112(3)**, 317-334.

McKinley, J. M., Worden, R. H., & Ruffell, A. H. 1999. Smectite in sandstones: a review of the controls on occurrence and behaviour during diagenesis. *Clay mineral cements in sandstones*, 109-128.

Mckinley, J. M., Worden, R. H., & Ruffell, A. H. 2001. Contact diagenesis: The effect of an intrusion on reservoir quality in the Triassic Sherwood Sandstone Group, Northern Ireland. *Journal of Sedimentary Research*, **71(3)**, 484-495.

Milani, E.J. and Ramos, V.A., 1998. Orogenias paleozóicas no domínio sul-ocidental do Gondwana e os ciclos de subsidência da Bacia do Paraná. *Revista Brasileira de Geociências*, **28(4)**, pp.473-484.

Milani, E.J., Melo, J.H.G., Souza, P.A., Fernandes, L.A. and França, A.B. 2007. Bacia do Paraná. *Boletim de Geociências Petrobrás*, **15(2)**, 265-287.

Morad, S., Al-Ramadan, K., Ketzer, J. M., & De Ros, L. F. 2010. The impact of diagenesis on the heterogeneity of sandstone reservoirs: A review of the role of depositional facies and sequence stratigraphy. *AAPG bulletin*, **94(8)**, 1267-1309.

Morad, S., Ketzer, J. M., & De Ros, L. F. 2000. Spatial and temporal distribution of diagenetic alterations in siliciclastic rocks: implications for mass transfer in sedimentary basins. *Sedimentology*, **47**, 95-120.

Murata, K. J., Formoso, M. L., & Roisenberg, A. 1987. Distribution of zeolites in lavas of southeastern Parana Basin, state of Rio Grande do Sul, Brazil. *The Journal of Geology*, **95(4)**, 455-467.

Ochoa, M., Arribas, J., Mas, R., & Goldstein, R. H. 2007. Destruction of a fluvial reservoir by hydrothermal activity (Cameros Basin, Spain). *Sedimentary Geology*, **202(1-2)**, 158-173.

Omosanya, K. O., Johansen, S. E., Eruteya, O. E., & Waldmann, N. 2017. Forced folding and complex overburden deformation associated with magmatic intrusion in the Vøring Basin, offshore Norway. *Tectonophysics*, **706**, 14-34.

Osborne, M.J. & Swarbrick, R.E. 1999. Diagenesis in North Sea HPHT clastic reservoirs: Consequences for porosity and overpressure prediction. *Marine and Petroleum Geology*, **16**, 337-353.

Peate, D. W. 1997. The Paraná-Etendeka province. *Geophysical Monograph-American Geophysical Union*, **100**, 217-246.

Peate, D. W., Hawkesworth, C. J., & Mantovani, M. S. 1992. Chemical stratigraphy of the Paraná lavas (South America): classification of magma types and their spatial distribution. *Bulletin of Volcanology*, **55(1-2)**, 119-139.

Pinto, V. M., Hartmann, L. A., Santos, J. O. S., McNaughton, N. J., and Wildner, W. 2011 Zircon U–Pb geochronology from the Paraná bimodal volcanic province support a brief eruptive cycle at~ 135 Ma. *Chemical Geology*, **281(1-2)**, 93-102.

Pozo, M. & Casas, J. 1999 Origin of kerolite and associated Mg clays in palustrine-lacustrine environments. The Esquivias deposit (Neogene Madrid Basin, Spain). *Clay Mineral.*, **34**, 395–418.

Pye, K. & Krinsley, D.H. 1986. Microfabric, mineralogy and early diagenetic history of the Whitby Mudstone Formation (Toarcian), Cleveland Basin, UK. *Geological Magazine*, 123(3), pp.191-203.

Rabbel, O., Galland, O., Mair, K., Lecomte, I., Senger, K., Spacapan, J.B. and Manceda, R., 2018. From field analogues to realistic seismic modelling: a case study of an oil-producing andesitic sill complex in the Neuquén Basin, Argentina. *Journal of the Geological Society*, **175(4)**, pp.580-593.

Rabelo, C. E. N., Cardoso, A. R., Nogueira, A. C. R., Soares, J. L., & Góes, A. M. 2019. Genesis of poikilotopic zeolite in aeolianites: An example from the Parnaíba Basin, NE Brazil. *Sedimentary Geology*, **385**, 61-78.

Rossel, N.C. (1982) Clay mineral diagenesis in Rotliegend aeolian sandstones of the southern North Sea. *Clay Minerals*, **17**, 69–77

Rossetti, L. M., Healy, D., Hole, M. J., Millett, J. M., de Lima, E. F., Jerram, D. A., & Rossetti, M. M. 2019. Evaluating petrophysical properties of volcano-sedimentary sequences: A case study in the Paraná-Etendeka Large Igneous Province. *Marine and Petroleum Geology*, **102**, 638-656.

Foster, S., Hirata, R., Vidal, A., Schmidt, G. and Garduño, H., 2009. The Guarani Aquifer initiative—towards realistic groundwater management in a transboundary context. World Bank.

Scherer, C. M. & Goldberg, K. 2007. Palaeowind patterns during the latest Jurassic–earliest Cretaceous in Gondwana: Evidence from aeolian cross-strata of the Botucatu Formation, Brazil. *Palaeogeography, Palaeoclimatology, Palaeoecology.*, **250(1-4)**, 89-100.

Scherer, C. M. S. 2000. Eolian dunes of the Botucatu Formation (Cretaceous) in southernmost Brazil: morphology and origin. *Sedimentary Geology*, **137(1-2)**, 63-84.

Scherer, C. M. S. 2002. Preservation of aeolian genetic units by lava flows in the Lower Cretaceous of the Paraná Basin, southern Brazil. *Sedimentology*, **49(1)**, 97-116.

Schofield, N., Holford, S., Millett, J., Brown, D., Jolley, D., Passey, S.R., Muirhead, D., Grove, C., Magee, C., Murray, J. and Hole, M., 20172015. Regional magma plumbing and emplacement mechanisms of the Faroe–Shetland Sill Complex: implications for magma transport and petroleum systems within sedimentary basins. *Basin Research*, **29**, 41-63.

Sheldon, H.A., Wheeler, J., Worden, R.H., Cheadle, M.J., 2003. An analysis of the roles of stress, temperature, and pH in chemical compaction of sandstones. *Journal of Sedimentary Research*, **73**, 64-71

Stricker, S., Jones, S. J. & Grant, N. T., 2016. Importance of vertical effective stress for reservoir quality in the Skagerrak Formation, Central Graben, North Sea. *Marine and Petroleum Geology*, **78**, 895-909.

Thiede, D. S. & Vasconcelos, P. M. 2010. Paraná flood basalts: rapid extrusion hypothesis confirmed by new 40Ar/39Ar results. *Geology*, **38(8)**, 747-750.

Vavra, C. L. 1989. Mineral reactions and controls on zeolite-facies alteration in sandstone of the central Transantarctic Mountains, Antarctica. *Journal of Sedimentary Research*, **59(5)**, 688-703.

Vermeesch, P., Resentini, A. & Garzanti, E. 2016. An R package for statistical provenance analysis. *Sedimentary Geology.*, **336**, 14-25

Walker, T. R. 1979. Red color in dune sand. *A Study of Giobbi Sand*, pp.61-61.

Wilson, P. I., McCaffrey, K. J., & Holdsworth, R. E. 2019. Magma-driven accommodation structures formed during sill emplacement at shallow crustal depths: The Maiden Creek sill, Henry Mountains, Utah. *Geosphere*, **15(4)**, pp.1368-1392.

Wilson, M. D., 1992. Inherited Grain-Rimming Clays in Sandstones from Eolian and Shelf Environments: their Origin and Control on Reservoir Properties. In: Houseknecht, D.W. and Pittman E.D., eds. Origin, diagenesis, and petrophysics of clay minerals in sandstones: SEPM Special Publication 47, p. 209–225.

Worden, R. H., & Burley, S. D. 2003. Sandstone diagenesis: the evolution of sand to stone. *Sandstone Diagenesis: Recent and Ancient*, **4**, 3-44.

Worden, R., & Morad, S. (Eds.). 2009. *Clay mineral cements in sandstones* (Vol. 19). John Wiley & Sons.

Wright, V. P., Sloan, R. J., Garces, B. V. & Garvie, L. A. J., 1992. Groundwater ferricretes from the Silurian of Ireland and Permian of the Spanish Pyrenees. *Sedimentary Geology*, **77**, 37-49.

ANEXO I - DADOS DE PETROGRAFIA

	Sample	Total	Quartz		Feldspars		Lithics					HM	Porosity			Cements					
			Mono-	Poli-	FK	Plagioclase	Not identified	Sedimentary	Vulcanic	Igneous	Metamorphic	Zircon	Intergranular	Moldic	Intragranular	Iron Oxide Coat	Infiltred Clay	Kaolinite	Opal	Sme	Zeolite
1	PB-01	310	228	0	9	3	11	0	2	2	0	0	16	22	0	0	0	17	0	0	0
2	PB-2A	303	199	4	19	18	6	0	5	14	0	0	30	4	0	0	0	4	0	0	0
3	PB-2C	303	244	0	20	21	3	0	3	10	2	0	0	0	0	0	0	0	0	0	0
4	PB-03	302	216	16	12	0	4	2	1	2	3	0	9	27	0	0	0	2	8	0	0
5	PB-04	304	221	1	9	0	1	0	0	0	0	0	37	27	0	8	0	0	0	0	0
6	PB-09	303	221	0	17	23	0	0	0	0	0	0	42	0	0	0	0	0	0	0	0
7	PB-10	304	235	2	7	4	0	0	2	0	0	0	42	12	0	0	0	0	0	0	0
8	PB-16	306	223	0	10	5	0	0	0	0	0	0	59	3	0	2	0	4	0	0	0
9	PB-17	300	235	1	7	10	0	0	1	2	0	0	36	4	0	0	0	4	0	0	0
10	PB-18	300	227	2	10	15	0	2	0	2	0	0	38	0	0	4	0	0	0	0	0
11	PB-19	302	192	2	6	12	6	0	3	4	0	0	0	0	0	0	0	0	77	0	0
12	PB-20	308	176	0	20	2	2	0	3	5	3	0	0	0	0	10	0	5	82	0	0
13	PB-21	300	197	2	13	5	7	0	2	3	3	0	31	3	0	7	0	27	0	0	0
14	PB-22	301	215	1	19	2	4	2	3	1	2	0	30	4	0	1	0	0	0	17	0
15	PB-23	301	238	0	1	0	0	0	0	1	0	0	26	1	0	1	0	9	24	0	0
16	PB-24	304	235	3	6	1	5	0	2	2	0	0	33	12	0	2	0	1	0	2	0
17	PB-29A	306	196	3	19	3	1	0	2	6	0	0	0	0	0	0	0	0	76	0	0
18	PB-36	326	202	0	25	2	0	0	2	5	1	0	0	0	0	0	0	0	0	0	6
19	PB-37	310	224	0	0	1	0	0	0	0	6	0	14	1	0	0	0	10	10	1	0
20	PB-38	332	212	0	23	0	0	0	0	0	5	0	68	21	0	1	0	0	0	2	0
21	PB-39	315	234	0	10	0	0	0	0	0	1	0	53	2	1	6	0	5	5	3	0
22	PB-40	317	219	0	38	0	0	0	0	0	1	0	34	21	0	0	0	0	0	4	0
23	PB-41	316	252	2	12	0	0	2	0	0	1	0	29	5	1	7	0	0	0	5	0
24	PB-44	319	188	4	12	1	0	2	7	1	16	0	50	19	0	2	0	9	9	6	0
25	PB-47	318	197	0	14	0	0	0	0	0	1	0	95	0	0	1	2	0	0	7	0
26	PB-49	329	214	4	3	3	0	0	0	0	5	1	85	6	0	0	0	0	0	8	0

27	PB-50	313	250	2	28	0	0	0	0	4	5	0	11	0	0	0	0	0	0	9	0
28	PB-51	325	220	0	8	3	0	0	0	0	1	0	81	2	0	0	0	0	0	10	0
29	PB-52	334	239	0	17	0	0	1	0	0	4	0	53	7	0	2	0	0	0	11	0
30	PB-55	324	182	2	14	0	0	4	7	0	8	0	29	0	0	18	0	0	0	12	0
31	PB-56	322	229	0	15	0	0	2	0	0	0	0	42	1	0	16	0	4	4	13	0
32	PB-59	326	205	0	6	1	0	1	0	0	1	0	97	1	0	0	0	0	0	14	0

ANEXO II - DADOS DE MINERAIS PESADOS

Sample	Zircon	Tourmaline	Rutile	Apatite	Epidote	Garnet	AlSiO	Pyrolusite	Spinel	Corundum	Fluorite	Xenotime	Sulfides	Monazite	Titanite	Hornblende	Piroxene	Chlorite	Muscovite	Staurolite	Total
PB-2A	30	25	3	1	20	94	0	0	0	0	0	0	0	0	0	0	0	0	0	0	173
PB-04	78	24	15	0	0	13	7	1	1	0	0	0	1	0	0	0	0	0	0	0	140
PB-09	23	54	4	0	0	16	0	123	0	0	0	0	0	2	0	0	0	0	0	0	222
PB-10	90	29	18	1	0	1	3	0	0	0	0	0	0	0	0	0	0	0	0	0	142
PB-11	56	19	12	0	0	1	11	1	5	0	1	0	0	0	0	0	0	0	0	0	106
PB-12	89	20	17	1	0	2	5	0	0	0	0	0	0	0	0	0	0	0	0	0	134
PB-14A	48	25	19	1	0	0	2	0	1	0	0	0	0	0	0	0	0	0	0	0	96
PB-18	65	20	14	13	9	1	0	0	2	0	0	0	0	0	0	0	0	0	0	0	124
PB-20	5	11	1	0	3	10	1	0	0	0	0	0	2	0	0	0	0	0	0	0	33
PB-21	200	36	11	1	0	0	0	0	0	0	0	0	1	1	0	0	0	0	0	0	250
PB-22	81	0	3	0	0	10	0	1	2	1	0	1	0	2	0	0	0	0	0	0	101
PB-23	48	5	18	0	0	0	9	0	1	0	1	0	2	2	0	0	0	0	0	0	86
PB-24	192	0	5	0	0	0	0	0	0	0	0	0	1	0	0	0	0	0	0	0	198
PB-31B	16	16	0	2	0	5	0	0	0	0	0	0	1	0	0	0	0	0	0	0	40
PB-32	79	9	1	0	138	0	0	0	0	0	0	0	0	0	0	0	0	0	0	0	227
PB-33	91	16	6	0	7	5	0	0	0	0	0	0	0	0	10	0	1	1	0	0	137
PB-34	194	16	18	0	9	1	0	0	0	0	0	0	0	0	0	0	1	0	0	0	239
PB-35	180	18	13	0	3	1	0	0	0	0	0	0	0	0	1	0	0	0	0	0	216
PB-36	126	4	5	3	1	13	0	0	0	0	0	0	0	0	0	1	0	0	0	0	153
PB-38	196	12	0	0	0	0	0	0	0	0	0	0	0	0	0	0	0	0	0	0	208
PB-39	73	15	0	0	0	0	0	0	0	0	0	0	0	0	0	5	0	0	0	0	93
PB-40	71	52	3	4	0	0	0	0	0	0	0	0	0	0	0	0	0	0	0	0	130
PB-41	94	33	6	0	0	3	0	0	1	0	0	0	0	0	0	0	4	0	0	0	141
PB-46	125	1	3	0	10	1	0	0	0	0	0	0	0	0	0	0	0	0	0	0	140
PB-47	400	0	0	8	8	0	0	0	0	0	0	0	0	0	1	0	0	0	0	0	417
PB-48	184	2	28	0	0	1	0	0	0	0	0	0	0	0	0	0	0	0	0	0	215
PB-49	98	3	7	8	0	14	0	0	0	0	0	0	0	2	3	0	2	1	2	0	140
PB-51	104	26	3	99	11	1	1	0	0	0	0	0	0	0	0	0	0	0	0	0	245

PB-52	203	2	7	0	0	0	3	0	0	0	0	0	0	0	3	0	0	0	0	0	218
PB-54	62	1	0	5	27	42	0	0	0	0	0	0	0	0	1	0	0	0	0	0	138
PB-56	105	12	5	1	2	0	2	0	0	0	0	0	0	0	0	0	0	0	0	0	127
PB-59	22	6	1	16	0	0	0	0	0	0	0	0	0	0	0	1	0	1	0	1	48

ANEXO III - DADOS GRANULOMÉTRICOS

	ϕ scale	0.0	1.0	2.0	3.0	4.0	
	Class size	Very Coarse Sand	Coarse Sand	Medium Sand	Fine Sand	Very Fine Sand	Total
1.0	PB-2AA	0.0	0.0	48.2	41.3	10.5	100.0
2.0	PB-04	0.0	6.2	70.9	13.0	9.9	100.0
3.0	PB-09	0.0	0.0	2.2	67.0	30.8	100.0
4.0	PB-10	0.0	9.2	8.0	17.5	65.2	100.0
5.0	PB-11	0.0	0.0	52.2	43.6	4.2	100.0
6.0	PB-12	0.0	9.9	33.4	31.0	25.8	100.0
7.0	PB-14A	0.0	30.3	36.7	21.2	11.8	100.0
8.0	PB-18	0.0	0.0	0.0	67.5	32.5	100.0
9.0	PB-20	0.0	0.0	0.0	62.4	37.6	100.0
10.0	PB-21	0.0	0.0	18.9	47.1	34.0	100.0
11.0	PB-22	0.0	14.8	26.7	55.8	2.6	100.0
12.0	PB-23	0.0	0.0	48.2	41.3	10.5	100.0
13.0	PB-24	0.0	0.0	6.6	64.1	29.3	100.0
14.0	PB-31B	0.0	3.2	43.0	44.7	9.2	100.0
15.0	PB-32	0.0	0.0	0.6	74.1	25.3	100.0
16.0	PB-33	0.0	0.0	16.0	76.1	7.9	100.0
17.0	PB-34	0.0	0.0	24.7	53.2	22.1	100.0
18.0	PB-35	0.0	0.0	9.7	63.3	27.0	100.0
19.0	PB-36	0.0	0.0	42.9	31.1	26.1	100.0
20.0	PB-37	0.0	0.0	34.5	48.3	17.2	100.0
21.0	PB-38	0.0	0.0	44.4	48.3	7.2	100.0
22.0	PB-39	0.0	0.0	71.7	23.7	4.7	100.0
23.0	PB-40	0.0	0.0	21.3	67.3	11.4	100.0
24.0	PB-41	0.0	0.0	42.0	45.1	12.9	100.0
25.0	PB-44	0.0	0.0	80.5	13.3	6.3	100.0
26.0	PB-46	0.0	0.0	10.3	50.9	38.8	100.0
27.0	PB-47	0.0	0.0	49.0	44.5	6.5	100.0
28.0	PB-48	0.0	0.0	32.1	63.0	4.9	100.0
29.0	PB-49	0.0	0.0	45.7	46.7	7.6	100.0
30.0	PB-50	0.0	0.0	50.0	45.5	4.5	100.0
31.0	PB-51	0.0	0.0	14.2	67.7	18.1	100.0
32.0	PB-52	0.0	0.0	49.6	41.3	9.0	100.0
33.0	PB-56	0.0	0.0	55.3	34.7	10.0	100.0

ANEXO IV - DADOS U-PB EM ZIRCÃO DETRÍTICO

		RATIOS																AGES							
Sample	Spot	207/235	1sigma	206/238	1 sigma	coef. corr	238/206	1 sigma	207/206	1 sigma	208/206	1 sigma	Total Pb (%)	Pb rad (ppm)	Th (ppm)	U (ppm)	Th/U	T206/238	1 sigma	T207/235	1 sigma	T207/206	1 sigma	Conc. 206/238	Conc. 206/238 - 207/206
PB 23	13.1	0.3176	0.0087	0.0445	0.0005	0.71	22.4654	0.2476	0.0517	0.0015	0.2151	0.0071	0.29	51.5	474.2	805.7	0.589	280.7	3	280.1	6.7	274.3	67.9	100	102
PB 23	41.1	0.35	0.049	0.045	0.0012	0.44	22.2183	0.5912	0.0564	0.0088	0.3036	0.025	1.47	5.7	65.9	83.4	0.791	283.8	7.4	304.7	36.8	468.3	338.6	93	60
PB 23	15.1	0.3422	0.0384	0.045	0.0016	0.51	22.2131	0.7841	0.0551	0.0075	0.4041	0.028	0.9	6.2	90.1	84.8	1.063	283.9	9.8	298.8	28.3	417.4	274.6	94	68
PB 23	49.1	0.3499	0.0139	0.0462	0.0007	0.26	21.6532	0.3313	0.0549	0.0026	0.1779	0.0113	0.36	17.7	173.7	275.6	0.63	291	4.4	304.6	10.5	410	102.2	95	70
PB 23	2.1	0.6922	0.0184	0.0854	0.0009	0.02	11.7121	0.1186	0.0588	0.0016	0.2153	0.0048	0.09	54.7	257.6	439.9	0.586	528.2	5.1	534.1	11.1	559.5	59.2	98	94
PB 23	68.1	0.6986	0.017	0.0857	0.0009	0.06	11.675	0.1284	0.0592	0.0015	0.0887	0.0046	0.16	24.9	50.8	224.2	0.227	529.8	5.6	538	10.2	572.9	55	98	92
PB 23	46.1	0.7074	0.0261	0.087	0.001	0.43	11.4891	0.1325	0.0589	0.0023	0.1776	0.0069	0.22	28.2	115.5	241.5	0.478	538	6	543.2	15.7	565.2	85.9	99	95
PB 23	65.1	0.709	0.0127	0.0873	0.0008	0.78	11.4494	0.1076	0.0589	0.001	0.0017	0.0017	0.13	59.2	1.8	567.4	0.003	539.8	4.9	544.2	7.6	562.6	38	99	95
PB 23	55.1	0.699	0.0121	0.0876	0.0008	0.9	11.4185	0.1049	0.0579	0.001	0.0147	0.0016	0.05	130	47.5	1255	0.038	541.2	4.8	538.2	7.2	525.4	36.6	100	103
PB 23	52.1	0.7414	0.0199	0.0876	0.0011	0.45	11.4126	0.1411	0.0614	0.0018	0.1492	0.0054	0.25	23.9	73.5	202.9	0.362	541.5	6.4	563.2	11.6	652.3	63.5	96	83
PB 23	79.1	0.7114	0.0219	0.0877	0.0011	0.48	11.4026	0.1425	0.0588	0.0019	0.1602	0.0243	0.28	31.4	66.8	269.6	0.248	541.9	6.5	545.6	13	561	71.3	99	96
PB 23	38.1	0.7236	0.0387	0.0897	0.0012	0.35	11.1533	0.1552	0.0585	0.0033	0.4006	0.0139	0.34	18.5	139.4	129.2	1.079	553.5	7.4	552.8	22.1	549.9	119.9	100	100
PB 23	6.1	0.7493	0.029	0.0906	0.0012	0.01	11.0391	0.1464	0.06	0.0025	0.2714	0.0071	0.19	26.6	147.3	197.7	0.745	559	7.1	567.8	16.8	603.2	90.6	98	92
PB 23	22.1	0.7632	0.026	0.0932	0.0013	0.04	10.729	0.1467	0.0594	0.0023	0.106	0.0053	0.28	24.7	59	204	0.289	574.5	7.5	575.9	15	581.4	83.8	99	98
PB 23	64.1	0.7562	0.015	0.0935	0.0009	0.85	10.7001	0.1053	0.0587	0.0011	0.057	0.0187	0.1	48.8	85.2	400	0.213	576	5.4	571.8	8.6	555.4	42.1	100	103
PB 23	5.1	0.7853	0.0223	0.094	0.001	0.82	10.6389	0.1129	0.0606	0.0018	0.0391	0.004	0.1	45.3	35	391.7	0.089	579.1	5.9	588.5	12.7	624.9	63.2	98	92
PB 23	7.1	0.806	0.0284	0.0951	0.0012	0.67	10.5179	0.132	0.0615	0.0023	0.1403	0.0055	0.2	28.4	79.8	214.5	0.372	585.5	7	600.2	16.1	656.2	83.7	97	89
PB 23	92.1	0.8026	0.022	0.0958	0.0009	0.38	10.4348	0.1017	0.0607	0.0017	0.1236	0.0035	0.15	40.3	97.6	309.5	0.315	589.9	5.5	598.3	12.4	630	62.4	98	93
PB 23	72.1	0.7926	0.0189	0.0965	0.0011	0.01	10.3634	0.1132	0.0596	0.0015	0.241	0.0041	0.24	29.5	155.4	213.6	0.727	593.8	6.2	592.6	10.8	588.1	53.8	100	100
PB 23	66.1	0.8097	0.0192	0.0967	0.001	0.29	10.3435	0.1116	0.0607	0.0015	0.2595	0.0052	0.17	30.7	145.7	213.4	0.683	594.9	6.1	602.3	10.8	630.1	52.2	98	94
PB 23	57.1	0.8023	0.0208	0.0968	0.0012	0.01	10.3306	0.1244	0.0601	0.0017	0.3242	0.038	0.19	36.8	231.2	256.9	0.9	595.6	6.8	598.1	11.7	607.6	59.8	99	98
PB 23	27.1	0.8672	0.0455	0.0972	0.0013	0.01	10.283	0.1354	0.0647	0.0037	0.2435	0.0132	0.35	16.2	71.3	113.6	0.628	598.3	7.5	634	24.9	763.8	125	94	78
PB 23	23.1	0.8063	0.0196	0.0978	0.001	0.76	10.2266	0.1079	0.0598	0.0015	0.0048	0.0025	0.14	46.5	1.8	397.7	0.005	601.4	6.1	600.4	10.9	596.5	54.9	100	100
PB 23	74.1	0.7984	0.0138	0.0978	0.0009	0.59	10.2245	0.096	0.0592	0.001	0.062	0.0018	0.07	123	151	982.9	0.154	601.5	5.4	595.9	7.7	574.7	35	100	104
PB 23	51.1	0.8015	0.0137	0.0979	0.0009	0.99	10.2137	0.0931	0.0594	0.001	0.0524	0.0407	1.15	115	80.7	962	0.084	602.1	5.2	597.7	7.8	580.8	36.9	100	103
PB 23	96.1	0.8488	0.047	0.1006	0.0016	0.02	9.9367	0.1585	0.0612	0.0038	0.4158	0.0132	0.4	17.4	108.6	103.9	1.045	618.1	9.4	624	25.8	645.2	131.5	99	95
PB 23	1.1	0.8667	0.0278	0.1015	0.0012	0.01	9.8531	0.1153	0.0619	0.0021	0.0895	0.0044	0.16	32.2	60.4	242	0.25	623.1	7	633.8	15.1	671.9	72.3	98	92
PB 23	50.1	0.8862	0.0414	0.1015	0.0019	0.32	9.8539	0.184	0.0633	0.0035	0.2801	0.0193	0.49	12.3	58.4	75.6	0.772	623.1	11.1	644.3	21.4	719.5	106.8	96	86
PB 23	85.1	0.9741	0.0596	0.103	0.002	0.01	9.7049	0.1846	0.0686	0.0046	0.2568	0.0308	0.35	16.3	71.1	102	0.697	632.2	11.4	690.6	30.7	885.6	147.2	91	71
PB 23	90.1	0.8765	0.0231	0.1034	0.001	0.63	9.6744	0.0927	0.0615	0.0017	0.0733	0.0031	0.16	39.9	45.9	291.8	0.157	634.1	5.8	639.1	12.4	656.7	57.8	99	96
PB 23	30.1	0.8969	0.0382	0.1037	0.0012	0.57	9.6462	0.1133	0.0627	0.0029	0.1445	0.0525	0.17	37.7	43.1	266.1	0.162	635.9	7.1	650.1	20.4	699.6	96.6	97	90
PB 23	32.1	0.8894	0.0302	0.1044	0.0011	0.29	9.5804	0.1018	0.0618	0.0022	0.3529	0.0092	0.21	33.4	198.8	201.3	0.988	640	6.5	646.1	16	667.2	74.1	99	95
PB 23	61.1	0.8995	0.0283	0.1044	0.0013	0.18	9.5814	0.1213	0.0625	0.002	0.3823	0.0409	0.4	13.3	61.8	85.5	0.723	640	7.7	651.4	14.7	691.4	68.2	98	92
PB 23	67.1	0.8955	0.0392	0.1052	0.0017	0.54	9.5055	0.1492	0.0617	0.003	0.151	0.0152	0.58	9	25	64.4	0.388	644.8	9.6	649.3	21.1	665	107.3	99	96
PB 23	62.1	1.0169	0.0456	0.1059	0.0018	0.02	9.4443	0.1599	0.0697	0.0035	0.1883	0.0212	0.66	7.9	24.3	52.3	0.465	648.8	10.4	712.3	23.1	918.1	110.1	91	70
PB 23	93.1	0.9104	0.0337	0.1059	0.0013	0.54	9.4404	0.1134	0.0623	0.0025	0.3948	0.0081	0.23	25.9	143.1	151.9	0.942	649.1	7.4	657.3	17.6	685.6	82.7	98	94
PB 23	80.1	0.8963	0.0269	0.106	0.0013	0.11	9.4348	0.1169	0.0613	0.0019	0.2671	0.0058	0.23	30.7	118	188.6	0.626	649.4	7.6	649.7	14.2	650.9	65.4	99	99
PB 23	76.1	0.9176	0.0223	0.1069	0.0012	0.33	9.3502	0.1033	0.0622	0.0015	0.0308	0.0032	0.15	39.9	21.6	291.2	0.074	655	6.9	661.1	11.7	681.8	52.7	99	96
PB 23	43.1	0.9241	0.0369	0.107	0.0013	0.01	9.3461	0.1145	0.0626	0.0026	0.2242	0.0064	0.26	22.3	98.1	148.8	0.659	655.3	7.6	664.5	19.4	696.1	89.2	98	94
PB 23	31.1	0.9176	0.0646	0.1071	0.0016	0.6	9.3414	0.1437	0.0622	0.0048	0.6316	0.0204	1.78	13.7	121.2	69.8	1.737	655.6	9.6	661.1	34	679.9	161.5	99	96
PB 23	95.1	0.9039	0.0336	0.1079	0.0013	0.43	9.2677	0.1114	0.0608	0.0024	0.1538	0.007	0.24	22.9	87.8	154.1	0.569	660.5	7.5	653.8	18	630.6	87.3	101	104
PB 23	60.1	0.9353	0.0243	0.1081	0.0013	0.32	9.2523	0.1119	0.0628	0.0018	0.2112	0.018	0.33	22.8	75.4	153.7	0.49	661.6	7.6	670.4	12.8	700.1	60.4	98	94
PB 23	73.1	0.9078	0.0303	0.1089	0.0014	0.31	9.1833	0.1206	0.0605	0.0021	0.3617	0.007	0.43	28	154.1	160	0.963	666.3	8.3	655.9	15.8	620.1	74.1	101	107

PB 23	89.1	1.1841	0.0323	0.1299	0.0013	0.29	7.699	0.0764	0.0661	0.0019	0.252	0.0042	0.26	41.3	135.8	216.6	0.627	787.2	7.4	793.2	14.9	810.1	58.5	99	97
PB 23	56.1	1.2376	0.0349	0.1316	0.0017	0.4	7.5994	0.101	0.0682	0.0021	0.2422	0.0063	0.26	23.3	78.1	122.5	0.637	796.9	10	817.8	15.9	875	64.7	97	91
PB 23	39.1	1.1928	0.0228	0.1325	0.0012	0.48	7.5477	0.0661	0.0653	0.0012	0.1677	0.0021	0.05	112	301.6	623	0.484	802.1	6.6	797.2	10.6	783.8	38.3	100	102
PB 23	88.1	1.2214	0.0244	0.1341	0.0011	0.8	7.4548	0.0607	0.066	0.0013	0.248	0.0051	0.06	92.5	472.5	468.7	1.008	811.5	6.2	810.4	11.3	807.6	41.9	100	100
PB 23	58.1	4.0578	0.084	0.2842	0.0033	0.62	3.519	0.0406	0.1036	0.0022	0.1497	0.0136	0.12	43.2	37	110.7	0.334	1612	16.5	1646	16.7	1689	39.7	97	95
PB 23	12.1	4.1806	0.1106	0.2856	0.0034	0.58	3.5014	0.0422	0.1062	0.003	0.1251	0.0052	0.17	28.1	27.1	72.4	0.374	1620	17.2	1670	21.4	1735	52.3	96	93
PB 23	17.1	4.1812	0.0955	0.2911	0.0035	0.11	3.4351	0.0418	0.1042	0.0026	0.0825	0.0039	0.32	33.9	20.9	86.4	0.242	1647	17.7	1670	18.7	1700	46.8	98	96
PB 23	82.1	6.686	0.1078	0.3821	0.0038	0.01	2.6168	0.0259	0.1269	0.0019	0.1238	0.0035	0.09	71.4	42.3	131.1	0.323	2086	17.6	2071	14.2	2055	26.7	100	101
PB 23	94.1	6.6899	0.1196	0.3837	0.0032	0.01	2.6063	0.0217	0.1265	0.0022	0.1235	0.0035	0.09	71.9	43.2	135.5	0.319	2094	14.9	2071	15.7	2049	30.4	101	102
PB 23	34.1	6.9371	0.1228	0.3887	0.0036	0.7	2.5726	0.0236	0.1294	0.0023	0.3901	0.0039	0.1	74.1	119.9	112.5	1.066	2117	16.5	2103	15.8	2090	31.6	100	101
PB 23	47.1	6.8622	0.1151	0.3903	0.0034	0.97	2.5621	0.0226	0.1275	0.002	0.1349	0.0033	0.16	82	72.7	153.4	0.474	2124	16	2094	14.9	2064	27.4	101	102
PB 23	59.1	0.9496	0.0219	0.1105	0.0012	0.63	9.0524	0.1009	0.0623	0.0015	0.1059	0.0054	0.22	32.1	61	231	0.264	675.5	7.2	677.9	11.5	685.9	52.1	99	98
PB 23	70.1	0.843	0.0373	0.0997	0.0016	0.39	10.0329	0.1574	0.0613	0.003	0.1937	0.0131	0.66	8.8	31.8	62.5	0.509	612.5	9.2	620.8	20.6	651.3	103.3	98	94
PB 23	86.1	0.8669	0.0347	0.0999	0.0013	0.01	10.012	0.1294	0.063	0.0027	0.2354	0.0109	0.29	20.9	83.1	143.9	0.577	613.7	7.5	633.9	18.8	706.6	93.1	96	86
PB 23	84.1	0.9009	0.0821	0.1027	0.0028	0.28	9.7338	0.2656	0.0636	0.0069	0.2666	0.0535	1.28	5.8	23.6	36.7	0.641	630.4	16.4	652.2	43.7	728.4	219.4	96	86
PB 23	9.1	0.9502	0.0773	0.1029	0.0028	0.28	9.7169	0.2623	0.067	0.0063	0.29	0.025	0.43	8.7	47.3	56	0.844	631.5	16.2	678.2	42.3	836.7	209.1	93	75
PB 23	36.1	0.7595	0.057	0.0897	0.0014	0.19	11.144	0.1785	0.0614	0.005	0.0837	0.0487	0.68	8.8	12.5	81.4	0.153	554	8.5	573.7	32.6	652.7	168.9	96	84
PB 23	33.1	0.677	0.0231	0.0841	0.0009	0.47	11.8908	0.123	0.0584	0.0021	0.2142	0.01	0.16	32.5	152.5	268.3	0.568	520.5	5.2	525	14	544.3	78.1	99	95
PB 23	45.1	0.9429	0.1562	0.1104	0.0036	0.15	9.0592	0.2964	0.062	0.0115	0.5035	0.1317	0.59	9.4	55.6	51.9	1.072	675	21	674.4	73.5	672.6	309.4	100	100
PB 23	35.1	1.0213	0.0314	0.1162	0.0012	0.75	8.6089	0.0875	0.0638	0.0021	0.0645	0.0182	0.12	48.4	29.4	344.8	0.085	708.4	6.8	714.5	15.8	733.8	67.9	99	96
PB 23	91.1	1.1709	0.0695	0.1261	0.0023	0.09	7.9305	0.1438	0.0673	0.0046	0.1402	0.0188	0.66	9.8	20.9	58	0.361	765.5	13.1	787.1	31.9	848.5	134	97	90
PB 23	77.1	1.3645	0.151	0.1381	0.0049	0.58	7.2423	0.2556	0.0717	0.0091	0.2483	0.0438	2.62	4.6	12.1	21.8	0.557	833.8	27.8	873.8	62.2	976.7	248.7	95	85
PB 23	11.1	0.6422	0.0364	0.0813	0.0014	0.4	12.2927	0.2132	0.0573	0.0037	0.46	0.0698	1.52	12.1	84.1	92.4	0.911	504.2	8.4	503.7	22.7	501.4	139.2	100	100
PB 23	83.1	1.5468	0.0301	0.1566	0.0016	0.9	6.3876	0.0648	0.0717	0.0014	0.1221	0.0044	0.11	61.5	88.7	293.5	0.302	937.6	8.9	949.2	12.1	976.2	39.9	98	96
PB 23	16.1	1.5774	0.0513	0.1588	0.0023	0.33	6.299	0.0905	0.0721	0.0028	0.1431	0.0213	1.14	21.5	35.7	98.1	0.363	949.9	12.7	961.3	20.8	987.7	81	98	96
PB 23	26.1	1.8992	0.0561	0.1786	0.0019	0.14	5.5992	0.0597	0.0771	0.0024	0.103	0.0058	0.22	27.3	31.3	115.2	0.271	1059	10.4	1081	19.7	1124	62.4	98	94
PB 23	10.1	2.2566	0.0682	0.199	0.0025	0.61	5.0251	0.0624	0.0822	0.0027	0.128	0.0048	0.38	26.4	37.1	100.3	0.37	1170	13.3	1199	21.3	1251	65.5	97	93
PB 23	87.1	2.3341	0.0649	0.2051	0.0023	0.01	4.8763	0.0538	0.0825	0.0024	0.118	0.0077	0.24	26.1	28.1	93.2	0.302	1203	12.1	1223	19.8	1259	57.7	98	95
PB 23	44.1	7.1956	0.1222	0.4009	0.0036	0.51	2.4944	0.0222	0.1302	0.0021	0.0901	0.006	0.08	101	52.7	190.7	0.276	2173	16.5	2136	15.1	2100	27.6	101	103
PB 23	40.1	7.4597	0.1215	0.4041	0.0035	0.01	2.4746	0.0215	0.1339	0.002	0.0666	0.0012	0.09	117	50.9	218.9	0.233	2188	16.1	2168	14.6	2150	26.1	100	101
PB 23	54.1	7.2794	0.1253	0.4071	0.004	0.72	2.4565	0.0244	0.1297	0.0022	0.0574	0.0024	0.1	79.8	33.1	146.7	0.225	2202	18.6	2146	15.3	2094	29.3	102	105
PB 23	42.1	7.4019	0.1325	0.4107	0.0038	0.72	2.4349	0.0226	0.1307	0.0022	0.0565	0.0024	0.16	78	33.1	144.9	0.228	2218	17.5	2161	16	2108	29.5	102	105
PB 23	19.1	5.7044	0.0981	0.3475	0.0032	0.9	2.878	0.0265	0.1191	0.0021	0.1083	0.002	0.09	113	87.3	236.7	0.369	1923	15.3	1932	14.9	1942	31.1	99	98
PB 23	3.1	5.9873	0.1515	0.3539	0.0043	0.56	2.8256	0.0347	0.1227	0.0033	0.2561	0.0135	0.21	31.5	44.2	56.2	0.787	1953	20.6	1974	22	1996	48.4	98	97
PB 23	71.1	6.3398	0.101	0.3635	0.0034	0.94	2.7511	0.0258	0.1265	0.0019	0.1154	0.0019	0.07	100	69.1	205.2	0.337	1999	16.1	2024	13.9	2050	26.1	98	97
PB 23	4.1	4.3799	0.0875	0.3062	0.0027	0.01	3.2655	0.029	0.1037	0.0019	0.1751	0.0066	0.03	109	122.1	245	0.498	1722	13.4	1709	16.3	1692	34.3	100	101
PB 23	14.1	5.4261	0.0908	0.3181	0.0028	0.59	3.1441	0.0279	0.1237	0.0022	0.0718	0.006	0.16	64.6	35.9	189.4	0.19	1780	13.8	1889	14.4	2011	29	94	88
PB 23	29.1	5.7055	0.1078	0.3281	0.0031	0.81	3.048	0.0288	0.1261	0.0024	0.255	0.0103	0.14	39.2	58.5	75.5	0.775	1829	15	1932	16.3	2045	33.8	94	89
PB 23	75.1	4.419	0.0698	0.3046	0.0029	0.95	3.2825	0.0311	0.1052	0.0016	0.0933	0.0024	0.11	115	71.7	289	0.248	1714	14.3	1716	13.1	1718	27.4	99	99
PB 23	20.1	4.4056	0.0745	0.3061	0.0027	0.72	3.2668	0.0287	0.1044	0.0017	0.1362	0.0038	0.06	174	196.7	398.7	0.493	1722	13.3	1713	13.9	1703	30.7	100	101
PB 23	18.1	3.1967	0.1437	0.253	0.0057	0.11	3.953	0.0883	0.0916	0.0051	0.1679	0.0157	0.33	14.4	18.7	40.3	0.463	1454	29.1	1456	34.6	1460	106.4	99	99
PB 23	78.1	7.798	0.1688	0.4024	0.0053	0.58	2.4848	0.033	0.1405	0.0032	0.2248	0.0062	0.19	28.3	26.2	44.9	0.584	2180	24.5	2208	19.6	2234	39.3	98	97
PB 23	25.1	9.1643	0.1411	0.4373	0.0037	0.01	2.2869	0.0194	0.152	0.0023	0.335	0.0015	0.04	152	209.5	208.6	1.004	2339	16.7	2355	13.9	2369	25.6	99	98
PB 23	69.1	9.5903	0.1612	0.4536	0.0045	0.77	2.2045	0.0221	0.1533	0.0024	0.1141	0.0041	0.1	56.1	29.3	86.1	0.34	2411	20.1	2396	15.1	2384	26.3	100	101
PB 23	28.1	11.5078	0.2121	0.4832	0.0048	0.96	2.0695	0.0205	0.1727	0.0032	0.2739	0.0343	0.07	65.8	80.9	80.7	1.002	2541	20.7	2565	16.8	2584	30.4	99	98
PB 23	21.1	12.7617	0.2178	0.5169	0.005	0.45	1.9345	0.0188	0.1791	0.0031	0.2897	0.0128	0.12	92.4	100.8	109.5	0.921	2686	21.3	2662	15.9	2644	28.4	100	101
PB 23	24.1	13.1887	0.2205	0.5248	0.0049	0.75	1.9053	0.0178	0.1823	0.003	0.2053	0.0063	1.12	16.8	15.6	21	0.745	2720	20.8	2693	15.7	2674	28.2	100	101
PB 23	63.1	0.2911	0.0062	0.0403	0.0004	0.53	24.833	0.25	0.0524	0.0011	0.4343	0.038	0.13	46.6	908	728.6	1.246	254.5	2.5	259.4	4.9	304.3	49.8	98	83
PB 23	81.1	0.2963	0.0156	0.0411	0.0007	0.19	24.3284	0.3972	0.0523	0.003	0.213	0.0253	0.33	18.9	192.6	308.6	0.624	259.7	4.2	263.5	12.3	297.8	129.1	98	87
PB 23	48.1	0.2035	0.0253	0.0278	0.0007	0.67	35.9774	0.8451	0.0531	0.0072	0.2036	0.0282	0.83	6	86.5	156.3	0.553	176.7	4.1	188.1	21.9	333.1	269.7	93	53
PB 23	37.1	0.194	0.0048	0.0282	0.0003	0.59	35.4276	0.3257	0.0499	0.0012	0.1672	0.0042	0.08	79.7	1006	2096	0.48	179.4	1.6	180.1	4.1	188.2	56.1	99	95
PB 23	8.1	0.2256	0.025	0.0274	0.0009	0.17	36.466	1.1961	0.0597	0.0078	0.2519	0.0271	0.9	6	101.8	149.5	0.681	174.4	5.6	206.6	21.4	591.8	289.4	84	29
PB 23	53.1	1.8647	0.1014	0.1595	0.0042	0.61	6.2713	0.1659	0.0848	0.0056	0.1781	0.0241	1.43	4.9	7.9	20.3	0.391	953.8	23.4	1069	36.1	1311	134.9	89	72
PB 24	22.1	0.2889	0.0103	0.0403	0.0009	0.27	24.8324	0.5806	0.0520	0.0030	0.2360	0.0102	0.48	23	312	406	0.77	255	6	258	8	287	133	98	88
PB 24	24.1	0.2919	0.0164	0.0409	0.0012	0.17	24.4783	0.7090	0.0518	0.0043	0.2517	0.0150	1.03	9	104	155	0.67	258	7	260	13	277	181	99	93
PB 24	25.1	0.3357	0.0264	0.0429	0.0015	0.12	23.3051	0.8159	0.0567	0.0063	0.3153	0.0191	0.48	6	81	99	0.82	271	9	294	20	482	242	92	56
PB 24	68.1	0.3133	0.0171	0.0432	0.0009	0.05	23.1376	0.4977	0.0526	0.0036	0.1797	0.0134	0.76	13	115	225	0.51	273	6	277	13	310	152	98	87
PB 24	70.1	0.7383	0.0410	0.0839	0.0021	0.49	11.9160	0.2984	0.0638	0.0046	0.3184	0.0186	0.62	10	67	86	0.78	520	13	561	24	735	156	92	70
PB 24	15.1	0.6879	0.0313	0.0849	0.0024	0.44	11.7752	0.3266	0.0587	0.0041	0.3916	0.0116	0.46	13	107	98	1.09	525	14	532	19	558	154	98	94
PB 24	66.1	0.7270	0.0325	0.0857	0.0017	0.01	11.6736	0.2362	0.0615	0.0034	0.1233	0.0137	0.44	14	41	131	0.31	530	10	555	19	659	121	95	80
PB 24	6.1	0.7021	0.0220	0.0859	0.0012	0.33	11.6429	0.1619	0.0593	0.0020	0.1456	0.0129	0.32	18	58	165	0.35	531	7	540	13	578	74	98	91

PB 24	54.1	0.6982	0.0256	0.0860	0.0012	0.01	11.6276	0.1632	0.0589	0.0025	0.2044	0.0067	0.19	29	137	253	0.54	532	7	538	15	563	93	98	94
PB 24	74.1	0.7184	0.0400	0.0863	0.0027	0.49	11.5925	0.3568	0.0604	0.0047	0.3304	0.0261	1.19	7	45	58	0.78	533	16	550	23	618	162	97	86
PB 24	43.1	0.6960	0.0322	0.0863	0.0013	0.01	11.5842	0.1801	0.0585	0.0031	0.2108	0.0152	0.96	13	57	105	0.54	534	8	536	19	548	114	99	97
PB 24	13.1	0.6928	0.0300	0.0878	0.0023	0.06	11.3896	0.3018	0.0572	0.0040	0.6821	0.0199	0.26	18	218	113	1.93	543	14	535	18	500	143	101	108
PB 24	26.1	0.7494	0.0233	0.0899	0.0021	0.99	11.1276	0.2575	0.0605	0.0031	0.0100	0.0096	0.19	23	15	218	0.07	555	12	568	13	621	109	97	89
PB 24	83.1	0.7985	0.0458	0.0905	0.0031	0.05	11.0515	0.3819	0.0640	0.0051	0.1871	0.0214	1.19	8	31	70	0.45	558	19	596	26	742	167	93	75
PB 24	9.1	0.6909	0.0365	0.0907	0.0019	0.01	11.0290	0.2299	0.0553	0.0035	0.1718	0.0204	0.23	7	27	60	0.45	560	11	533	22	423	132	104	132
PB 24	5.1	0.7674	0.0183	0.0911	0.0010	0.17	10.9746	0.1257	0.0611	0.0014	0.0868	0.0055	0.52	17	32	156	0.20	562	6	578	11	642	52	97	87
PB 24	63.1	0.7799	0.0592	0.0914	0.0029	0.04	10.9402	0.3526	0.0619	0.0061	0.2448	0.0199	0.78	8	42	68	0.62	564	17	585	31	670	194	96	84
PB 24	85.1	0.7496	0.0232	0.0914	0.0011	0.19	10.9409	0.1334	0.0595	0.0018	0.2320	0.0126	0.32	35	162	279	0.58	564	7	568	13	585	67	99	96
PB 24	37.1	0.7419	0.0319	0.0914	0.0014	0.30	10.9366	0.1619	0.0589	0.0030	0.1637	0.0122	0.57	12	39	95	0.41	564	8	564	19	562	107	100	100
PB 24	1.1	0.7747	0.0218	0.0915	0.0012	0.59	10.9283	0.1448	0.0614	0.0018	0.2504	0.0172	0.29	21	104	161	0.65	564	7	582	13	653	64	96	86
PB 24	16.1	0.7779	0.0369	0.0923	0.0027	0.47	10.8383	0.3115	0.0611	0.0045	0.4367	0.0225	0.32	13	113	87	1.31	569	16	584	21	644	164	97	88
PB 24	21.1	0.7712	0.0393	0.0932	0.0028	0.55	10.7270	0.3209	0.0600	0.0046	0.0049	0.0066	0.64	9	0	88	0.00	575	16	581	22	604	164	98	95
PB 24	41.1	0.8153	0.0533	0.0938	0.0021	0.34	10.6661	0.2436	0.0631	0.0051	0.2465	0.0231	0.68	7	31	51	0.61	578	13	605	31	711	178	95	81
PB 24	53.1	0.8226	0.0291	0.0985	0.0014	0.01	10.1560	0.1396	0.0606	0.0024	0.0954	0.0072	0.20	26	51	216	0.24	605	8	610	16	625	86	99	96
PB 24	47.1	0.8932	0.0554	0.0994	0.0022	0.33	10.0654	0.2197	0.0652	0.0049	0.5014	0.0178	0.93	8	51	44	1.17	611	13	648	30	781	164	94	78
PB 24	2.1	0.8530	0.0299	0.1007	0.0016	0.19	9.9316	0.1540	0.0614	0.0024	0.4996	0.0130	0.23	17	138	100	1.37	618	9	626	16	655	84	98	94
PB 24	82.1	0.8527	0.0247	0.1010	0.0015	0.01	9.9018	0.1513	0.0612	0.0022	0.0555	0.0082	0.32	21	24	182	0.13	620	9	626	14	648	80	99	95
PB 24	69.1	0.8747	0.0394	0.1019	0.0021	0.38	9.8147	0.1997	0.0623	0.0034	0.1407	0.0102	0.37	14	45	105	0.43	626	12	638	21	683	120	98	91
PB 24	11.1	0.8751	0.0252	0.1020	0.0014	0.27	9.7993	0.1322	0.0622	0.0019	0.2650	0.0072	0.24	20	104	139	0.74	626	8	638	14	681	66	98	92
PB 24	93.1	0.9140	0.1134	0.1033	0.0032	0.34	9.6764	0.2986	0.0641	0.0089	0.3005	0.0274	1.07	4	20	29	0.69	634	19	659	57	746	285	96	84
PB 24	59.1	0.9345	0.0609	0.1047	0.0025	0.26	9.5515	0.2289	0.0647	0.0051	0.1703	0.0217	1.63	8	24	60	0.40	642	15	670	32	766	166	95	83
PB 24	27.1	0.9031	0.0221	0.1053	0.0022	0.35	9.4945	0.1976	0.0622	0.0028	0.0441	0.0033	0.13	40	36	319	0.11	646	13	653	12	681	97	98	94
PB 24	65.1	0.8896	0.0201	0.1062	0.0012	0.74	9.4188	0.1024	0.0608	0.0015	0.0499	0.0037	0.12	68	91	562	0.16	651	7	646	11	631	55	100	103
PB 24	36.1	0.9306	0.0449	0.1090	0.0030	0.07	9.1715	0.2559	0.0619	0.0046	0.2170	0.0215	0.70	15	55	99	0.56	667	18	668	25	671	176	99	99
PB 24	92.1	0.9481	0.0912	0.1111	0.0028	0.36	8.9993	0.2256	0.0619	0.0070	0.1169	0.0273	0.72	5	10	41	0.24	679	16	677	51	670	234	100	101
PB 24	75.1	1.5688	0.0587	0.1512	0.0035	0.26	6.6124	0.1523	0.0752	0.0039	0.1812	0.0152	0.75	12	25	57	0.43	908	20	958	23	1075	103	94	84
PB 24	88.1	1.5416	0.0659	0.1562	0.0024	0.79	6.4011	0.0992	0.0716	0.0033	0.1808	0.0152	0.06	13	30	59	0.51	936	14	947	26	974	94	98	96
PB 24	51.1	1.6289	0.0789	0.1611	0.0032	0.27	6.2087	0.1247	0.0733	0.0043	0.1045	0.0165	0.46	12	15	58	0.26	963	18	981	31	1024	121	98	94
PB 24	7.1	1.5902	0.0360	0.1614	0.0018	0.01	6.1962	0.0701	0.0715	0.0016	0.1426	0.0033	0.28	33	63	157	0.40	965	10	966	14	971	46	99	99
PB 24	3.1	1.6244	0.0334	0.1629	0.0017	0.18	6.1387	0.0631	0.0723	0.0014	0.1275	0.0038	0.06	45	76	218	0.35	973	9	980	13	995	40	99	97
PB 24	20.1	1.6942	0.0397	0.1664	0.0034	0.16	6.0098	0.1240	0.0738	0.0031	0.2766	0.0026	0.16	60	209	251	0.83	992	19	1006	15	1037	86	98	95
PB 24	84.1	1.7907	0.0690	0.1667	0.0042	0.34	5.9977	0.1517	0.0779	0.0041	0.1539	0.0145	0.39	11	18	47	0.39	994	23	1042	25	1144	108	95	86
PB 24	35.1	1.7185	0.0772	0.1691	0.0047	0.53	5.9136	0.1660	0.0737	0.0054	0.1624	0.0132	0.77	11	20	49	0.41	1007	26	1016	28	1033	140	99	97
PB 24	91.1	1.7273	0.0490	0.1699	0.0021	0.43	5.8870	0.0726	0.0738	0.0021	0.1218	0.0061	0.13	34	50	155	0.32	1011	12	1019	18	1035	57	99	97
PB 24	31.1	1.7886	0.0766	0.1710	0.0048	0.20	5.8469	0.1628	0.0758	0.0052	0.1678	0.0112	0.54	11	23	48	0.49	1018	26	1041	28	1091	138	97	93
PB 24	33.1	2.2016	0.0666	0.1970	0.0047	0.01	5.0770	0.1201	0.0811	0.0043	0.2295	0.0090	0.17	24	61	88	0.70	1159	25	1182	21	1223	104	98	94
PB 24	55.1	2.2712	0.0866	0.2014	0.0034	0.09	4.9650	0.0839	0.0818	0.0036	0.1117	0.0085	0.25	19	24	74	0.32	1183	18	1203	27	1240	89	98	95
PB 24	39.1	2.2891	0.0500	0.2049	0.0019	0.55	4.8804	0.0463	0.0810	0.0019	0.0906	0.0031	0.10	43	39	160	0.25	1202	10	1209	15	1222	47	99	98
PB 24	73.1	4.3652	0.0925	0.2990	0.0035	0.19	3.3444	0.0394	0.1059	0.0026	0.1610	0.0040	0.13	46	51	113	0.45	1686	18	1706	17	1730	45	98	97
PB 24	76.1	4.4297	0.1563	0.3001	0.0083	0.16	3.3325	0.0920	0.1071	0.0053	0.2031	0.0215	0.83	10	12	23	0.52	1692	41	1718	30	1750	93	98	96
PB 24	19.1	4.4522	0.1144	0.3011	0.0069	0.01	3.3206	0.0757	0.1072	0.0049	0.1358	0.0078	1.01	28	30	69	0.43	1697	34	1722	21	1753	83	98	96
PB 24	44.1	4.4170	0.0822	0.3052	0.0026	0.87	3.2761	0.0278	0.1050	0.0021	0.1152	0.0017	0.18	67	54	163	0.33	1717	13	1716	15	1713	36	100	100
PB 24	29.1	4.5083	0.1248	0.3065	0.0073	0.04	3.2631	0.0777	0.1067	0.0054	0.2082	0.0066	0.25	21	27	48	0.57	1723	36	1733	23	1744	91	99	98
PB 24	48.1	4.7634	0.1314	0.3160	0.0043	0.75	3.1645	0.0429	0.1093	0.0034	0.2282	0.0072	0.23	20	27	42	0.66	1770	21	1779	23	1788	58	99	98
PB 24	61.1	5.5622	0.2722	0.3334	0.0117	0.31	2.9994	0.1057	0.1210	0.0080	0.2929	0.0225	1.02	9	15	18	0.85	1855	57	1910	43	1971	119	97	94
PB 24	67.1	5.6741	0.1275	0.3439	0.0045	0.68	2.9077	0.0382	0.1197	0.0031	0.2743	0.0061	2.93	47	84	91	0.92	1906	22	1927	19	1951	46	98	97
PB 24	34.1	5.9121	0.1409	0.3505	0.0079	0.01	2.8531	0.0646	0.1223	0.0055	0.2459	0.0123	0.11	31	41	59	0.70	1937	38	1963	21	1991	81	98	97
PB 24	78.1	6.4096	0.1716	0.3639	0.0072	0.30	2.7484	0.0540	0.1278	0.0044	0.2401	0.0137	0.32	21	28	39	0.71	2000	34	2034	23	2067	62	98	96
PB 24	50.1	6.2340	0.1590	0.3688	0.0044	0.29	2.7115	0.0327	0.1226	0.0034	0.4368	0.0304	0.06	83	148	140	1.06	2024	21	2009	22	1994	49	100	101
PB 24	57.1	6.6259	0.3328	0.3786	0.0108	0.46	2.6414	0.0755	0.1269	0.0079	0.4542	0.0250	0.61	10	23	14	1.59	2070	51	2063	44	2056	108	100	100
PB 24	80.1	11.8371	0.2266	0.4858	0.0051	0.74	2.0586	0.0215	0.1767	0.0038	0.1257	0.0030	0.09	74	41	111	0.37	2552	22	2592	18	2622	36	98	97
PB 24	86.1	12.7604	0.2758	0.5081	0.0063	0.37	1.9681	0.0245	0.1821	0.0038	0.1723	0.0043	0.22	33	23	44	0.51	2649	27	2662	20	2673	35	99	99
PB 24	49.1	12.4958	0.2966	0.5106	0.0057	0.01	1.9586	0.0217	0.1775	0.0045	0.1183	0.0025	0.06	98	60	139	0.43	2659	24	2642	22	2630	42	100	101
PB 24	90.1	0.9715	0.0354	0.1111	0.0015	0.61	8.9972	0.1218	0.0634	0.0024	0.0972	0.0042	0.18	21	37	154	0.24	679	9	689	18	722	83	98	94
PB 24	46.1	0.7660	0.0311	0.0926	0.0014	0.01	10.8022	0.1576	0.0600	0.0028	0.1449	0.0094	0.34	12	38	99	0.38	571	8	578	18	604	108	98	94
PB 24	38.1	0.7770	0.0336	0.0928	0.0014	0.22	10.7794	0.1654	0.0607	0.0030	0.1366	0.0129	1.20	12	34	94	0.37	572	8	584	19	630	107	97	90
PB 24	94.1	0.6643	0.0519	0.0812	0.0017	0.36	12.3085	0.2625	0.0593	0.0050	0.4653	0.0411	0.42	15	195	101	1.94	504	10	517	31	578	186	97	87
PB 24	14.1	0.6107	0.0547	0.0814	0.0032	0.21	12.2791	0.4816	0.0544	0.0069	0.2364	0.0310	1.11	5	30	44	0.68	505	19	484	33	387	261	104	130
PB 24	64.1	0.8805	0.1768	0.0995	0.0089	0.19	10.0510	0.8962	0.0642	0.0187	0.3432	0.1061	2.18	3	16	21	0.74	611	51	641	84	748	457	95	81

PB 24	62.1	1.0976	0.0829	0.1191	0.0042	0.01	8.3934	0.2972	0.0668	0.0067	0.1989	0.0223	1.04	7	23	44	0.51	726	24	752	41	832	217	96	87
PB 24	42.1	1.1405	0.0292	0.1267	0.0013	0.61	7.8949	0.0798	0.0653	0.0019	0.2287	0.0045	0.17	33	109	182	0.60	769	7	773	14	784	59	99	98
PB 24	89.1	0.6017	0.0299	0.0759	0.0012	0.47	13.1730	0.2081	0.0575	0.0030	0.1450	0.0092	0.52	12	43	123	0.35	472	7	478	19	510	118	98	92
PB 24	17.1	0.6598	0.0698	0.0795	0.0038	0.27	12.5777	0.6059	0.0602	0.0090	0.2338	0.0406	2.23	4	23	34	0.67	493	23	515	42	610	293	95	80
PB 24	12.1	1.8240	0.0383	0.1789	0.0019	0.86	5.5895	0.0602	0.0739	0.0015	0.0725	0.0038	0.12	44	38	200	0.19	1061	11	1054	14	1040	42	100	102
PB 24	4.1	1.7990	0.0495	0.1744	0.0024	0.31	5.7339	0.0786	0.0748	0.0022	0.0966	0.0061	0.32	18	23	81	0.28	1036	13	1045	18	1064	59	99	97
PB 24	8.1	1.9092	0.0377	0.1831	0.0018	0.21	5.4627	0.0549	0.0756	0.0014	0.0838	0.0028	0.12	52	57	230	0.25	1084	10	1084	13	1086	37	99	99
PB 24	95.1	2.0294	0.0779	0.1856	0.0028	0.07	5.3886	0.0818	0.0793	0.0032	0.2083	0.0211	0.63	17	50	64	0.78	1097	15	1125	26	1180	81	97	92
PB 24	58.1	1.3858	0.0616	0.1452	0.0026	0.33	6.8857	0.1227	0.0692	0.0036	0.1084	0.0106	0.40	15	24	84	0.29	874	15	883	26	905	106	99	96
PB 24	87.1	1.1786	0.0491	0.1339	0.0019	0.01	7.4684	0.1074	0.0638	0.0028	0.1933	0.0087	0.18	19	60	110	0.55	810	11	791	23	736	92	102	110
PB 24	30.1	3.6121	0.1433	0.2704	0.0079	0.01	3.6981	0.1081	0.0969	0.0065	0.1222	0.0091	0.37	8	7	24	0.31	1543	40	1552	32	1565	126	99	98
PB 24	71.1	3.6816	0.0774	0.2725	0.0032	0.94	3.6692	0.0426	0.0980	0.0023	0.4080	0.0113	5.26	69	165	178	0.93	1554	16	1567	17	1586	46	99	97
PB 24	60.1	6.5503	0.1610	0.3741	0.0043	0.14	2.6729	0.0309	0.1270	0.0034	0.1109	0.0024	0.06	71	44	144	0.31	2049	20	2053	22	2057	47	99	99
PB 24	23.1	5.5176	0.1169	0.3355	0.0068	0.11	2.9807	0.0601	0.1193	0.0047	0.2104	0.0029	0.03	84	114	178	0.64	1865	33	1903	18	1946	71	97	95
PB 24	96.1	6.3526	0.1243	0.3727	0.0039	0.01	2.6830	0.0281	0.1236	0.0022	0.0178	0.0028	0.41	43	5	93	0.06	2042	18	2026	17	2009	31	100	101
PB 24	72.1	6.6084	0.1503	0.3720	0.0052	0.82	2.6884	0.0372	0.1288	0.0034	0.3009	0.0067	0.14	40	65	70	0.92	2039	24	2061	20	2082	47	98	97
PB 24	32.1	2.8262	0.2185	0.2308	0.0101	0.01	4.3337	0.1890	0.0888	0.0101	0.1908	0.0274	0.82	6	9	18	0.50	1338	53	1363	56	1401	213	98	95
PB 24	81.1	11.2934	0.2686	0.4568	0.0072	0.97	2.1893	0.0347	0.1793	0.0050	0.1603	0.0130	0.15	32	19	42	0.44	2425	32	2548	21	2647	46	95	91
PB 24	40.1	13.5100	0.2411	0.5363	0.0045	0.79	1.8645	0.0157	0.1827	0.0033	0.0544	0.0183	0.42	15	2	22	0.09	2768	19	2716	17	2677	29	101	103
PB 24	45.1	0.3574	0.0438	0.0482	0.0017	0.31	20.7480	0.7178	0.0538	0.0080	0.1501	0.0250	1.26	4	24	55	0.43	303	10	310	32	362	304	97	83
PB 24	18.1	0.4319	0.0270	0.0585	0.0019	0.16	17.0842	0.5416	0.0535	0.0050	0.4720	0.0269	0.38	11	157	107	1.46	367	11	365	19	351	201	100	104
PB 24	28.1	0.4896	0.0141	0.0639	0.0014	0.69	15.6414	0.3391	0.0555	0.0028	0.1885	0.0086	0.44	28	156	331	0.47	400	8	405	10	434	111	98	92
PB 24	79.1	10.1414	0.1932	0.4628	0.0045	0.02	2.1608	0.0210	0.1589	0.0033	0.1899	0.0053	0.06	99	93	152	0.61	2452	20	2448	17	2444	35	100	100
PB 24	77.1	22.6287	0.5223	0.6244	0.0117	0.95	1.6016	0.0299	0.2628	0.0072	0.1342	0.0177	0.46	35	32	34	0.95	3127	46	3211	22	3264	44	97	95
PB 24	52.1	0.5628	0.0306	0.0630	0.0013	0.01	15.8831	0.3334	0.0648	0.0042	0.2055	0.0175	0.52	12	77	143	0.54	394	8	453	20	769	148	86	51
PB 24	10.1	0.5916	0.1123	0.0874	0.0052	0.01	11.4458	0.6865	0.0491	0.0117	0.1767	0.0752	7.00	2	9	17	0.49	540	31	472	65	153	307	114	353
PB 24	56.1	1.0462	0.1237	0.0958	0.0049	0.17	10.4389	0.5329	0.0792	0.0111	0.1171	0.0611	1.88	3	9	28	0.32	590	29	727	65	1177	336	81	50
PB 31B	35.1	0.2969	0.0232	0.04	0.001	0.26	24.9884	0.6328	0.0538	0.0044	0.162	0.0177	0.47	9.7	67.2	180.7	0.372	252.9	6.3	264	18.1	362.8	195.8	95	69
PB 31B	38.1	0.3023	0.0172	0.0406	0.0007	0.46	24.6281	0.3953	0.054	0.0034	0.2222	0.0105	0.3	14.3	166.8	259.2	0.643	256.6	4	268.2	13.4	370.8	145	95	69
PB 31B	56.1	0.3092	0.0139	0.0431	0.0007	0.05	23.1934	0.3704	0.052	0.0027	0.1579	0.0134	0.53	11.3	96.6	203.2	0.475	272.1	4.3	273.6	10.8	286	116.5	99	95
PB 31B	19.1	0.3235	0.0161	0.0435	0.0007	0.34	22.9653	0.3445	0.0539	0.0031	0.1173	0.0409	0.4	9.1	79.2	152.7	0.518	274.8	4	284.6	12.2	365.9	127.8	96	75
PB 31B	33.1	0.6687	0.039	0.0826	0.0018	0.3	12.1018	0.2565	0.0587	0.0038	0.1562	0.0143	0.51	12.6	55.6	118.8	0.468	511.8	10.4	519.9	23.1	555.8	131.3	98	92
PB 31B	47.1	0.6564	0.0289	0.0831	0.0012	0.43	12.0382	0.1712	0.0573	0.0028	0.1919	0.021	0.55	14.3	41.9	139.3	0.301	514.4	7	512.4	17.8	503.5	105.9	100	102
PB 31B	71.1	0.6728	0.0206	0.0833	0.0009	0.92	12.0002	0.1261	0.0586	0.0019	0.3257	0.0198	0.49	18.8	82.2	139.6	0.589	516	5.2	522.4	12.5	550.6	73.2	98	93
PB 31B	54.1	0.6718	0.0255	0.0834	0.0013	0.38	11.9971	0.1799	0.0585	0.0026	0.1887	0.0294	0.51	12.6	79.8	108.8	0.733	516.1	7.4	521.8	15.5	546.8	95.5	98	94
PB 31B	2.1	0.6985	0.0388	0.0838	0.0013	0.48	11.9283	0.1865	0.0604	0.0038	0.2571	0.0357	0.32	16.5	105	143.1	0.734	519	7.8	537.9	23.2	619	131.7	96	83
PB 31B	74.1	0.677	0.0227	0.0847	0.0011	0.51	11.8034	0.1483	0.058	0.0021	0.278	0.006	0.17	28.4	179.3	236.5	0.758	524.2	6.3	525	13.6	528.2	78.2	99	99
PB 31B	15.1	0.6784	0.0223	0.0848	0.001	0.56	11.786	0.1349	0.058	0.0022	0.2305	0.0081	0.28	27.2	163.5	227	0.72	525	5.8	525.8	13.4	529.3	81.3	99	99
PB 31B	77.1	0.6917	0.0218	0.0853	0.001	0.91	11.7171	0.1403	0.0588	0.002	0.375	0.0065	3.19	26.2	160.7	174	0.924	527.9	6.1	533.8	13.1	559.1	74.1	98	94
PB 31B	78.1	0.6939	0.0175	0.0857	0.0009	0.52	11.6663	0.1161	0.0587	0.0015	0.0953	0.0042	0.28	44.3	107	426.1	0.251	530.2	5.1	535.2	10.4	556.6	56.7	99	95
PB 31B	9.1	0.6834	0.017	0.0858	0.0008	0.52	11.6566	0.1097	0.0578	0.0015	0.2121	0.011	0.1	48.7	212	428.3	0.495	530.6	4.8	528.8	10.2	521.3	56.6	100	101
PB 31B	11.1	0.6957	0.0255	0.0859	0.001	0.3	11.64	0.1368	0.0587	0.0024	0.1088	0.0076	0.41	26.2	65.9	243.7	0.27	531.3	6	536.2	15.4	557	86.6	99	95
PB 31B	48.1	0.701	0.0218	0.0861	0.001	0.23	11.6102	0.1379	0.059	0.0019	0.2458	0.0052	0.16	31.7	172.3	268.4	0.642	532.6	6.1	539.4	12.9	568.1	71.9	98	93
PB 31B	28.1	0.7208	0.0402	0.0863	0.0018	0.42	11.5941	0.2463	0.0606	0.0038	0.1719	0.0174	0.54	11.2	47.4	100.8	0.471	533.3	10.9	551.1	23.8	625.4	136.5	96	85
PB 31B	93.1	0.6862	0.0233	0.0864	0.0012	0.31	11.5703	0.157	0.0576	0.0023	0.2719	0.0084	0.26	23.6	175.2	195.7	0.895	534.4	7	530.5	13.9	514.1	86.3	100	103
PB 31B	4.1	0.7089	0.029	0.0867	0.0011	0.62	11.5311	0.1463	0.0593	0.0026	0.2337	0.0272	0.5	19.1	92.1	167.7	0.549	536.1	6.5	544.1	17	577.7	97.1	98	92
PB 31B	89.1	0.7368	0.0285	0.0871	0.0014	0.26	11.4851	0.1856	0.0614	0.0029	0.1495	0.0089	0.32	15.6	65.9	139.6	0.472	538.2	8.4	560.5	17	652.3	104.1	96	82
PB 31B	60.1	0.6889	0.0216	0.0871	0.0011	0.32	11.4773	0.1459	0.0573	0.002	0.2214	0.0214	0.41	34.7	173.6	301.9	0.575	538.5	6.6	532.1	12.7	504.9	73.1	101	106
PB 31B	67.1	0.7156	0.0267	0.0872	0.001	0.7	11.4716	0.1374	0.0595	0.0025	0.0602	0.0143	0.3	15.8	38.1	153.6	0.248	538.8	6.2	548.1	15.6	586.8	90.3	98	91
PB 31B	49.1	0.7067	0.0265	0.0874	0.0013	0.01	11.4472	0.1699	0.0587	0.0026	0.3032	0.0124	0.28	19.1	136.7	151.9	0.899	539.9	7.7	542.8	15.7	554.8	92.8	99	97
PB 31B	95.1	0.7099	0.0156	0.0874	0.0008	0.01	11.4462	0.1046	0.0589	0.0014	0.0141	0.0024	0.21	45.9	38.9	456.3	0.085	539.9	4.7	544.7	9.3	564.6	52.9	99	95
PB 31B	27.1	0.6978	0.0185	0.0874	0.0012	0.89	11.4406	0.1543	0.0579	0.0015	0.2725	0.0183	1.43	49.1	262.4	400.2	0.656	540.2	7	537.5	11	526.1	55.3	100	102
PB 31B	87.1	0.7161	0.0238	0.0874	0.0012	0.1	11.4371	0.1557	0.0594	0.0023	0.3568	0.0102	0.19	25.7	207.7	198.7	1.045	540.3	7.1	548.4	14.1	581.8	85.4	98	92
PB 31B	44.1	0.7093	0.0216	0.0876	0.001	0.3	11.4096	0.1345	0.0587	0.0019	0.2702	0.0075	0.25	38	266.4	309.9	0.86	541.6	6.1	544.3	12.8	555.7	70.3	99	97
PB 31B	62.1	0.7327	0.0431	0.0878	0.0015	0.1	11.3937	0.1966	0.0605	0.0043	0.1829	0.0164	0.57	9.4	40.7	82.5	0.493	542.3	9	558.1	25.6	623.1	151.6	97	87
PB 31B	82.1	0.706	0.0227	0.0879	0.0011	0.19	11.381	0.1384	0.0583	0.002	0.2659	0.0049	0.19	32.5	202.9	258	0.786	542.9	6.3	542.3	13.6	540	75.8	100	100
PB 31B	18.1	0.7309	0.0282	0.0882	0.0012	0.48	11.3322	0.148	0.0601	0.0026	0.1562	0.009	0.24	19.2	62.9	169	0.372	545.1	6.8	557.1	16.3	606.3	95.9	97	89
PB 31B	65.1	0.7247	0.0283	0.0883	0.0011	0.35	11.3192	0.1421	0.0595	0.0026	0.1702	0.0187	0.41	13.2	71.2	115.5	0.616	545.7	6.6	553.4	16.5	585.1	95.7	98	93
PB 31B	41.1	0.7395	0.0462	0.0886	0.0016	0.4	11.2856	0.2073	0.0605	0.0042	0.262	0.0229	0.48	9.9	69	78.7	0.876	547.3	9.6	562.1	26.9	622.7	151.6	97	87
PB 31B	63.1	0.7101	0.0199	0.0887	0.0009	0.62	11.2729	0.1107	0.0581	0.0018	0.2356	0.0048	0.12	37.2	221.6	312.4	0.709	547.9	5.2	544.8	11.7	531.8	65.1	100	103
PB 31B	17.1	0.7408	0.0338	0.0889	0.0013	0.58	11.2544	0.1678	0.0605	0.0032	0.0906	0.0247	0.27	17.9	52	158.3	0.328	548.8	7.8	562.9	19.3	620.3	108.2	97	88

PB 31B	32.1	0.7178	0.0186	0.0889	0.0012	0.81	11.2539	0.1492	0.0586	0.0015	0.1296	0.0061	0.68	40.2	174.4	355.6	0.491	548.8	7	549.4	11	551.9	54.4	99	99
PB 31B	37.1	0.741	0.033	0.089	0.0013	0.01	11.2315	0.1653	0.0604	0.003	0.1749	0.0167	0.33	14.7	54.8	134	0.409	549.8	7.8	563	19.4	616.5	109.6	97	89
PB 31B	42.1	0.741	0.0281	0.0892	0.0012	0.16	11.2162	0.1484	0.0603	0.0025	0.2499	0.024	0.43	22.2	148.3	176.5	0.84	550.5	7	563	16.4	613.4	91.7	97	89
PB 31B	86.1	0.7676	0.0346	0.0911	0.0017	0.18	10.972	0.203	0.0611	0.0035	0.1107	0.008	0.42	11.9	47	107.2	0.438	562.3	10	578.4	19.8	642.2	119.6	97	87
PB 31B	68.1	0.7735	0.0427	0.092	0.0015	0.5	10.8701	0.1755	0.061	0.0039	0.1921	0.013	0.49	10.6	47.7	89.9	0.531	567.3	8.8	581.8	24.3	638.6	136.4	97	88
PB 31B	58.1	0.7493	0.0163	0.0909	0.0009	0.83	10.9997	0.1135	0.0598	0.0014	0.0826	0.0056	1.05	51.1	106.7	467	0.228	560.9	5.5	567.8	9.5	595.5	49.8	98	94
PB 31B	52.1	0.735	0.0137	0.0917	0.0008	0.96	10.9073	0.0982	0.0581	0.0011	0.182	0.0054	0.46	122	604.1	1022	0.591	565.5	4.9	559.5	8.1	535.1	42.1	101	105
PB 31B	13.1	0.7461	0.0194	0.0917	0.0009	0.5	10.9018	0.1073	0.059	0.0017	0.0662	0.0031	0.08	40.8	65.9	368.9	0.179	565.8	5.3	566	11.3	566.8	63.8	99	99
PB 31B	14.1	0.7678	0.0282	0.0919	0.0012	0.22	10.8839	0.1386	0.0606	0.0025	0.1779	0.0149	0.64	25.5	96.9	219.5	0.441	566.6	6.9	578.5	16.1	625.3	88.8	97	90
PB 31B	53.1	0.75	0.0237	0.0922	0.0012	0.46	10.8465	0.141	0.059	0.0021	0.1311	0.0072	0.18	25.7	74	219.8	0.337	568.5	7.1	568.2	13.5	567	73.3	100	100
PB 31B	7.1	0.8214	0.0633	0.0927	0.0019	0.44	10.7922	0.2233	0.0643	0.0055	0.1925	0.0295	0.63	7.7	28.2	64.3	0.439	571.2	11.3	608.8	34.3	751.2	183.1	93	76
PB 31B	57.1	0.7315	0.0529	0.0896	0.0023	0.19	11.1611	0.2863	0.0592	0.0052	0.3799	0.0271	0.81	6	45.2	46.7	0.97	553.2	13.6	557.4	30.9	574.9	186.4	99	96
PB 31B	3.1	0.7848	0.0293	0.0929	0.0011	0.11	10.77	0.1324	0.0613	0.0025	0.1572	0.0056	0.23	21.5	69.7	179.4	0.389	572.4	6.7	588.2	16.9	649.8	89.3	97	88
PB 31B	10.1	0.8037	0.0313	0.093	0.0012	0.04	10.7532	0.1359	0.0627	0.0027	0.1501	0.0071	0.39	19	69.2	157.5	0.44	573.2	6.9	598.9	18	697.3	96.2	95	82
PB 31B	59.1	0.7708	0.0199	0.0936	0.0011	0.07	10.6888	0.1235	0.0598	0.0017	0.1425	0.0064	0.14	24.3	80.4	206.5	0.39	576.5	6.4	580.2	11.5	594.8	62.6	99	96
PB 31B	45.1	0.77	0.031	0.0937	0.0013	0.76	10.6695	0.1456	0.0596	0.0026	0.2349	0.0138	0.45	24.9	127.4	193.7	0.658	577.5	7.5	579.8	17.6	588.6	94	99	98
PB 31B	48.1	0.7728	0.0187	0.094	0.001	0.53	10.6332	0.1123	0.0596	0.0015	0.1017	0.0026	0.26	47	110.3	406.7	0.271	579.4	5.8	581.4	10.7	589.1	55.4	99	98
PB 31B	50.1	0.7924	0.0557	0.0941	0.0024	0.24	10.6226	0.2734	0.061	0.0052	0.2022	0.0319	0.35	13.9	46.7	117.4	0.398	580	14.2	592.5	31	640.9	176.1	97	90
PB 31B	21.1	0.7963	0.0264	0.0954	0.0011	0.99	10.4862	0.1227	0.0606	0.0023	0.0717	0.0051	0.08	57.4	94.2	459.6	0.205	587.2	6.6	594.8	14.6	623.8	78.6	98	94
PB 31B	12.1	0.8406	0.0586	0.0954	0.0018	0.02	10.4822	0.2	0.0639	0.0052	0.2009	0.013	2.28	8.7	47.7	67.2	0.71	587.4	10.8	619.5	33.4	738.4	179.5	94	79
PB 31B	90.1	0.7924	0.0512	0.0963	0.0024	0.01	10.3799	0.2618	0.0597	0.0049	0.0196	0.0138	1.57	6.9	13.5	63.8	0.212	592.9	14.3	592.5	27.3	591.1	163.1	100	100
PB 31B	40.1	0.837	0.0608	0.0965	0.002	0.35	10.3644	0.2166	0.0629	0.0052	0.2339	0.0372	0.53	8.4	41.3	63.9	0.646	593.8	11.8	617.5	33.8	705.5	176.4	96	84
PB 31B	72.1	0.8024	0.0339	0.0973	0.0013	0.41	10.2749	0.1369	0.0598	0.0028	0.0143	0.0068	0.21	14.6	5.1	127.7	0.04	598.7	7.6	598.2	19.5	596.2	107.5	100	100
PB 31B	1.1	0.8336	0.0516	0.0983	0.0017	0.25	10.1706	0.1716	0.0615	0.0043	0.4003	0.0186	0.4	12.5	85.7	81.9	1.046	604.6	9.7	615.6	27.7	656.3	137.8	98	92
PB 31B	36.1	0.84	0.0313	0.0994	0.0016	0.47	10.0647	0.1664	0.0613	0.0024	0.1545	0.0065	0.22	21.6	79.4	175	0.454	610.6	9.6	619.2	17.3	650.4	83.6	98	93
PB 31B	34.1	0.8359	0.0281	0.1006	0.0016	0.88	9.936	0.1541	0.0602	0.0021	0.2123	0.0176	0.05	31.7	165.6	245.2	0.675	618.2	9.1	616.9	15.6	612	73.8	100	101
PB 31B	16.1	0.8647	0.0203	0.103	0.001	0.86	9.7075	0.0902	0.0609	0.0016	0.3042	0.0087	1.44	76.7	454.8	525.3	0.866	632	5.6	632.7	11	634.9	55.4	99	99
PB 31B	5.1	0.8739	0.0264	0.103	0.0011	0.01	9.7064	0.104	0.0615	0.002	0.2847	0.007	0.13	42.7	224.6	287.6	0.781	632.1	6.5	637.7	14.4	657.4	69.2	99	96
PB 31B	83.1	0.9007	0.0336	0.1039	0.0015	0.2	9.6256	0.1371	0.0629	0.0026	0.1246	0.009	0.14	28.8	90	211.5	0.425	637.2	8.6	652.1	18	704.2	90	97	90
PB 31B	94.1	0.8797	0.0217	0.1042	0.0011	0.54	9.5996	0.099	0.0612	0.0017	0.1597	0.0039	0.18	40.5	153.7	296.2	0.519	638.8	6.3	640.8	11.7	648	59.3	99	98
PB 31B	79.1	0.9186	0.053	0.1047	0.0022	0.06	9.5504	0.2032	0.0636	0.0044	0.2233	0.0155	0.49	10	45.3	68	0.666	641.9	13	661.6	28.3	729.3	147.7	97	88
PB 31B	61.1	0.9014	0.0336	0.105	0.0013	0.34	9.5219	0.1174	0.0623	0.0025	0.3981	0.0106	0.23	21.3	139.9	129.2	1.082	643.8	7.5	652.5	17.8	682.8	88.9	98	94
PB 31B	26.1	0.9328	0.0407	0.1054	0.002	0.01	9.4908	0.1794	0.0642	0.003	0.4015	0.0283	0.41	21	131.1	129.1	1.016	645.8	11.6	669.1	21.5	748.5	102	96	86
PB 31B	80.1	0.8456	0.0244	0.1059	0.0012	0.78	9.4402	0.1037	0.0579	0.0019	0.1402	0.0049	1.06	29.6	196.1	214.3	0.915	649.1	6.8	622.3	13.6	525.9	68.4	104	123
PB 31B	76.1	0.9042	0.02	0.1083	0.001	0.15	9.2325	0.0847	0.0605	0.0013	0.1156	0.019	0.07	70.3	216.1	513.7	0.421	662.9	5.8	654	10.6	623.1	47	101	106
PB 31B	81.1	1.7837	0.0762	0.1724	0.0031	0.9	5.7999	0.1032	0.075	0.0037	0.1661	0.0161	0.36	17.4	35.8	90.5	0.395	1025	16.9	1040	27.6	1069	99.1	98	95
PB 31B	20.1	1.8448	0.0818	0.1763	0.003	0.28	5.6724	0.096	0.0759	0.004	0.1431	0.0093	0.32	13.1	22	57.1	0.386	1047	16.4	1062	29.6	1092	108.2	98	95
PB 31B	6.1	1.962	0.0852	0.1844	0.0028	0.37	5.424	0.0822	0.0772	0.0037	0.0953	0.0103	0.34	15.3	16.8	67.6	0.249	1091	15.2	1103	29.6	1126	98.7	98	96
PB 31B	70.1	1.8809	0.0798	0.1846	0.0027	0.1	5.4166	0.0801	0.0739	0.0036	0.4506	0.0112	0.27	15.5	64.3	53.6	1.2	1092	14.9	1074	27.6	1039	95.1	101	105
PB 31B	29.1	1.9669	0.0466	0.1884	0.0025	0.51	5.307	0.0708	0.0757	0.0017	0.1281	0.0038	0.03	60.4	95.5	251	0.38	1113	13.6	1104	15.8	1087	43.7	100	102
PB 31B	55.1	0.97	0.0353	0.1104	0.0017	0.42	9.058	0.1373	0.0637	0.0027	0.4517	0.0132	0.28	18.3	118.4	97.4	1.216	675.1	9.7	688.5	18	732.6	86.5	98	92
PB 31B	81.1	0.9521	0.0787	0.1022	0.0038	0.52	9.7895	0.362	0.0676	0.0071	0.1433	0.027	0.95	5.3	32.5	40.6	0.801	627	22	679.2	40.8	856.3	226	92	73
PB 31B	88.1	0.9417	0.0822	0.1043	0.0039	0.56	9.5836	0.3584	0.0655	0.0071	0.1581	0.0272	0.89	5.9	26.6	42.8	0.621	639.8	22.7	673.8	40	789	224.4	94	81
PB 31B	66.1	0.8368	0.0212	0.0986	0.0009	0.01	10.1467	0.0959	0.0616	0.0017	0.019	0.0051	1.94	25.7	13.5	225.3	0.06	605.9	5.5	617.4	11.7	659.5	59.1	98	91
PB 31B	69.1	0.9782	0.1314	0.1101	0.004	0.07	9.0822	0.3294	0.0644	0.0106	0.4389	0.0536	1.45	3.3	20.3	20	1.016	673.4	23.1	692.7	68.3	756	327.7	97	89
PB 31B	30.1	0.7957	0.0767	0.0915	0.003	0.51	10.9285	0.3627	0.0631	0.007	0.0475	0.0213	0.69	6.8	5.1	60.2	0.085	564.4	17.9	594.4	43.6	710.4	233.5	94	79
PB 31B	43.1	0.6223	0.0335	0.0779	0.0013	0.01	12.841	0.2069	0.058	0.0034	0.1347	0.0096	0.54	12.6	47	130.2	0.361	483.4	7.5	491.3	20.9	528.2	130.8	98	91
PB 31B	23.1	0.616	0.0311	0.0745	0.0012	0.07	13.4182	0.2178	0.06	0.0035	0.2392	0.0096	0.4	14.5	86.9	139.4	0.624	463.4	7.3	487.4	19.7	601.8	130.8	95	76
PB 31B	51.1	0.6095	0.0168	0.0764	0.0009	0.64	13.0922	0.1547	0.0579	0.0018	0.1663	0.0056	0.23	21.4	100.6	223.4	0.45	474.5	5.4	483.2	10.6	525	68.4	98	90
PB 31B	39.1	0.9801	0.0209	0.1135	0.0011	0.79	8.81	0.0882	0.0626	0.0014	0.0806	0.0024	0.17	63.2	116.5	469.8	0.248	693.1	6.6	693.6	10.7	695.4	47	99	99
PB 31B	31.1	1.126	0.0418	0.1237	0.0021	0.24	8.0841	0.1389	0.066	0.0026	0.0945	0.0107	0.65	17.6	30.7	116.7	0.264	751.8	12.2	765.8	20.5	807	86.9	98	93
PB 31B	64.1	1.4391	0.0427	0.1498	0.0017	0.79	6.6737	0.0742	0.0697	0.0023	0.2165	0.0115	0.3	21.2	63.5	110.4	0.575	900.1	9.3	905.3	17.7	918.2	68.4	99	98
PB 31B	85.1	2.1747	0.0639	0.1978	0.0028	0.11	5.0545	0.0721	0.0797	0.0028	0.2057	0.0055	0.34	23.2	54.5	84.6	0.644	1164	15.2	1173	20.4	1190	70.3	99	97
PB 31B	25.1	2.1077	0.0581	0.1977	0.0029	0.8	5.0584	0.0749	0.0773	0.0021	0.1336	0.0042	0.12	38	60.4	151.4	0.399	1163	15.7	1151	18.9	1130	53.3	101	102
PB 31B	8.1	2.2546	0.0433	0.2073	0.0018	0.01	4.8248	0.0416	0.0789	0.0015	0.1384	0.0051	0.45	80.7	107.1	303.7	0.353	1214	9.6	1198	13.6	1169	38.7	101	103
PB 31B	91.2	0.1756	0.0076	0.0249	0.0004	0.64	40.2194	0.6405	0.0512	0.0027	0.189	0.0088	0.38	15.6	231	475.7	0.486	158.3	2.5	164.3	6.6	251.4	121.5	96	62
PB 31B	24.1	0.4962	0.0141	0.0643	0.0007	0.28	15.553	0.1603	0.056	0.0018	0.0832	0.0041	0.13	35.7	107.6	463.4	0.232	401.7	4	409.1	9.6	451.2	71.2	98	89
PB 31B	75.1	3.0789	0.0817	0.238	0.0029	0.99	4.2017	0.0507	0.0938	0.0025	0.2265	0.0362	0.22	29.9	47.4	102.6	0.462	1376	14.8	1428	19	1505	48.5	96	91
PB 31B	84.1	3.6241	0.0852	0.2595	0.0029	0.9	3.8542	0.0435	0.1013	0.0025	0.1069	0.0038	0.16	37.8	38	107.8	0.353	1487	14.9	1555	18.7	1648	45.7	95	90
PB 31B	22.1	6.9927	0.125	0.3935	0.0035	0.81	2.5412	0.0226	0.1289	0.0025	0.0665	0.0039	0.16	70.2	28.6	149.7	0.191	2139	16.2	2111	16	2083	34.5	101	102
PB 31B	91.1	0.1884	0.0266	0.0238	0.0013	0.01	41.9296	2.2341	0.0573	0.0109	0.0043	0.0093	1.19	3.9	56.4	138.4	0.407	151.9	8	175.3	22.4	502.9	382.1	86	30

PB 31B	73.1	0.564	0.0121	0.0711	0.0006	0.92	14.0609	0.1243	0.0575	0.0012	0.036	0.0029	16.35	111	87.1	1418	0.061	442.9	3.8	454.2	7.9	511.6	47.8	97	86
PB -10	28.1	0.3127	0.0185	0.0414	0.0006	0.52	24.1349	0.3227	0.0547	0.0036	0.2117	0.0164	0.52	8	82	147	0.56	262	3	276	15	401	143	94	65
PB -10	26.1	0.3027	0.0071	0.0422	0.0003	0.59	23.7121	0.1923	0.0521	0.0013	0.2968	0.0058	0.12	43	628	756	0.83	266	2	269	6	288	58	99	92
PB -10	9.1	0.3134	0.0075	0.0425	0.0004	0.42	23.5546	0.2492	0.0535	0.0015	0.2951	0.0353	0.32	14	160	246	0.65	268	3	277	6	352	62	96	76
PB -10	84.1	0.3135	0.0193	0.0425	0.0008	0.61	23.5480	0.4275	0.0535	0.0036	0.2285	0.0349	0.22	22	319	357	0.89	268	5	277	15	352	152	96	76
PB -10	10.1	0.3065	0.0093	0.0429	0.0005	0.53	23.3358	0.2943	0.0519	0.0019	0.2071	0.0128	4.48	13	134	238	0.56	271	3	271	7	280	85	99	96
PB -10	6.1	0.6794	0.0201	0.0778	0.0011	0.19	12.8471	0.1823	0.0633	0.0023	0.2125	0.0137	0.16	10	51	93	0.55	483	7	526	12	719	84	91	67
PB -10	83.1	0.6369	0.0651	0.0789	0.0023	0.07	12.6791	0.3642	0.0586	0.0072	0.2239	0.0224	0.93	5	34	50	0.68	489	14	500	41	551	263	97	88
PB -10	13.1	0.6218	0.0205	0.0795	0.0011	0.58	12.5733	0.1703	0.0567	0.0022	0.1178	0.0084	0.72	14	50	143	0.35	493	6	491	13	480	83	100	102
PB -10	76.1	0.6693	0.0235	0.0844	0.0010	0.20	11.8502	0.1473	0.0575	0.0023	0.1454	0.0132	0.55	22	108	207	0.52	522	6	520	14	512	85	100	102
PB -10	89.1	0.7062	0.0280	0.0846	0.0012	0.27	11.8175	0.1610	0.0605	0.0025	0.0610	0.0074	0.41	14	25	133	0.19	524	7	543	17	623	93	96	84
PB -10	46.1	0.7126	0.0444	0.0850	0.0012	0.41	11.7622	0.1706	0.0608	0.0043	0.1850	0.0203	1.72	10	48	89	0.54	526	7	546	27	632	157	96	83
PB -10	92.1	0.7356	0.0323	0.0856	0.0013	0.36	11.6800	0.1724	0.0623	0.0030	0.1415	0.0126	0.59	21	63	183	0.34	530	8	560	19	685	103	94	77
PB -10	14.1	0.7031	0.0280	0.0860	0.0014	0.49	11.6306	0.1891	0.0593	0.0029	0.1412	0.0102	0.35	14	48	126	0.39	532	8	541	16	578	97	98	91
PB -10	64.1	0.6513	0.0421	0.0864	0.0016	0.30	11.5782	0.2140	0.0547	0.0041	0.1935	0.0150	0.95	13	58	117	0.49	534	10	509	25	400	155	104	133
PB -10	81.1	0.7105	0.0178	0.0880	0.0009	0.49	11.3673	0.1156	0.0586	0.0016	0.1577	0.0033	0.31	53	239	463	0.52	544	5	545	11	552	58	99	98
PB -10	78.1	0.7273	0.0394	0.0886	0.0015	0.21	11.2886	0.1970	0.0595	0.0038	0.0711	0.0115	0.47	12	23	105	0.22	547	9	555	24	587	138	98	93
PB -10	29.1	0.7139	0.0145	0.0888	0.0007	0.86	11.2596	0.0890	0.0583	0.0013	0.0389	0.0033	0.30	46	46	465	0.10	549	4	547	9	541	47	100	101
PB -10	34.1	0.7108	0.0160	0.0891	0.0007	0.09	11.2279	0.0922	0.0579	0.0014	0.0261	0.0034	0.09	32	24	318	0.08	550	4	545	10	525	53	100	104
PB -10	48.1	0.7998	0.0494	0.0892	0.0013	0.34	11.2064	0.1694	0.0650	0.0046	0.2636	0.0144	0.41	9	53	73	0.72	551	8	597	28	775	157	92	71
PB -10	5.1	0.7533	0.0152	0.0898	0.0009	0.36	11.1300	0.1070	0.0608	0.0014	0.2965	0.0043	0.15	27	174	208	0.84	555	5	570	9	632	49	97	87
PB -10	79.1	0.7448	0.0353	0.0926	0.0014	0.51	10.7951	0.1682	0.0583	0.0032	0.1565	0.0130	0.70	16	58	135	0.43	571	9	565	21	542	116	101	105
PB -10	31.1	0.6738	0.0652	0.0931	0.0017	0.39	10.7439	0.1977	0.0525	0.0056	0.3649	0.0296	0.18	8	60	54	1.11	574	10	523	37	308	189	109	186
PB -10	58.1	0.7819	0.0403	0.0936	0.0014	0.21	10.6789	0.1632	0.0606	0.0036	0.0461	0.0172	0.32	11	19	98	0.19	577	8	587	23	624	133	98	92
PB -10	57.1	0.7603	0.0505	0.0941	0.0017	0.32	10.6246	0.1933	0.0586	0.0046	0.4743	0.0154	0.54	12	115	79	1.45	580	10	574	29	552	163	100	105
PB -10	35.1	0.8478	0.0386	0.0984	0.0012	0.41	10.1628	0.1255	0.0625	0.0031	0.0648	0.0106	0.82	9	15	79	0.19	605	7	623	21	691	112	97	87
PB -10	7.1	0.8012	0.0261	0.0994	0.0014	0.05	10.0593	0.1457	0.0585	0.0023	0.1477	0.0191	0.04	13	47	100	0.47	611	8	598	14	547	79	102	111
PB -10	61.1	0.8512	0.0314	0.1002	0.0013	0.52	9.9752	0.1270	0.0616	0.0026	0.5891	0.0202	0.13	31	304	174	1.74	616	8	625	17	660	92	98	93
PB -10	66.1	0.8348	0.0278	0.1005	0.0012	0.37	9.9549	0.1153	0.0603	0.0023	0.0906	0.0045	0.48	22	44	172	0.26	617	7	616	15	613	82	100	100
PB -10	91.1	0.8586	0.0247	0.1016	0.0011	0.89	9.8470	0.1062	0.0613	0.0018	0.0242	0.0052	0.18	25	23	211	0.11	624	6	629	14	651	63	99	95
PB -10	17.1	0.8484	0.0331	0.1018	0.0017	0.63	9.8185	0.1616	0.0604	0.0029	0.1541	0.0070	0.14	13	46	99	0.47	625	10	624	18	619	99	100	101
PB -10	77.1	0.8622	0.0361	0.1023	0.0015	0.30	9.7783	0.1419	0.0611	0.0029	0.1473	0.0080	0.86	17	59	131	0.45	628	9	631	20	644	102	99	97
PB -10	55.1	0.8739	0.0382	0.1023	0.0014	0.81	9.7715	0.1350	0.0619	0.0030	0.2737	0.0210	0.28	24	111	158	0.70	628	8	638	21	672	108	98	93
PB -10	86.1	0.8807	0.0298	0.1024	0.0012	0.31	9.7655	0.1192	0.0624	0.0022	0.2229	0.0066	0.27	21	100	149	0.67	629	7	641	16	687	75	97	91
PB -10	67.1	0.8677	0.0226	0.1027	0.0010	0.28	9.7343	0.0951	0.0613	0.0018	0.2373	0.0125	0.14	39	192	288	0.67	630	6	634	12	649	62	99	97
PB -10	65.1	0.8930	0.0401	0.1042	0.0015	0.63	9.5938	0.1408	0.0621	0.0032	0.1218	0.0122	0.58	16	44	119	0.37	639	9	648	21	679	106	98	94
PB -10	72.1	0.8872	0.0369	0.1044	0.0014	0.33	9.5753	0.1317	0.0616	0.0031	0.0916	0.0085	0.40	16	29	122	0.24	640	8	645	20	661	103	99	96
PB -10	71.1	0.8891	0.0206	0.1051	0.0010	0.79	9.5121	0.0863	0.0613	0.0016	0.0641	0.0035	0.11	46	65	375	0.17	644	6	646	11	651	55	99	98
PB -10	40.1	0.9551	0.1072	0.1170	0.0027	0.74	8.5503	0.1965	0.0592	0.0074	0.0886	0.0270	5.20	4	7	30	0.25	713	16	681	57	576	259	104	123
PB -10	42.1	1.0242	0.0283	0.1177	0.0011	0.29	8.4980	0.0760	0.0631	0.0019	0.0954	0.0039	0.73	30	54	208	0.26	717	6	716	14	713	62	100	100
PB -10	30.1	1.0846	0.0429	0.1195	0.0014	0.33	8.3662	0.0980	0.0658	0.0029	0.1243	0.0156	0.18	11	24	75	0.32	728	8	746	21	800	94	97	90
PB -10	38.1	1.6238	0.0341	0.1617	0.0014	0.93	6.1828	0.0517	0.0728	0.0015	0.1001	0.0025	2.37	80	113	401	0.28	966	7	980	13	1009	42	98	95
PB -10	51.1	1.6600	0.0458	0.1627	0.0017	0.87	6.1471	0.0653	0.0740	0.0023	0.0902	0.0071	0.43	29	37	144	0.26	972	10	993	17	1042	62	97	93
PB -10	44.1	1.6292	0.0422	0.1629	0.0015	0.42	6.1375	0.0557	0.0725	0.0020	0.3079	0.0064	0.32	40	170	170	1.00	973	8	982	16	1001	56	99	97
PB -10	69.1	1.6565	0.0366	0.1647	0.0015	0.52	6.0704	0.0562	0.0729	0.0018	0.0392	0.0048	0.13	39	21	200	0.11	983	8	992	14	1012	51	99	97
PB -10	96.1	1.7299	0.0630	0.1653	0.0023	0.73	6.0499	0.0852	0.0759	0.0029	0.1910	0.0103	0.39	16	38	72	0.53	986	13	1020	23	1093	78	96	90
PB -10	27.1	1.6830	0.0344	0.1668	0.0014	0.25	5.9944	0.0502	0.0732	0.0016	0.2076	0.0040	0.22	40	106	181	0.59	995	8	1002	13	1019	44	99	97
PB -10	25.1	1.7171	0.0413	0.1687	0.0015	0.09	5.9270	0.0540	0.0738	0.0019	0.2170	0.0208	0.16	29	87	127	0.69	1005	9	1015	15	1036	51	99	96
PB -10	32.1	1.7784	0.0382	0.1742	0.0015	0.59	5.7402	0.0494	0.0740	0.0017	0.1608	0.0054	2.53	35	74	155	0.48	1035	8	1038	14	1043	46	99	99
PB -10	45.1	1.8542	0.0843	0.1769	0.0024	0.49	5.6517	0.0772	0.0760	0.0038	0.2493	0.0188	0.23	13	39	52	0.75	1050	13	1065	31	1095	103	98	95
PB -10	41.1	1.8364	0.1136	0.1774	0.0030	0.01	5.6371	0.0954	0.0751	0.0052	0.1603	0.0203	0.94	7	11	30	0.38	1053	17	1059	41	1071	137	99	98
PB -10	16.1	1.8565	0.0480	0.1782	0.0023	0.01	5.6131	0.0733	0.0756	0.0024	0.0764	0.0072	0.30	18	19	83	0.22	1057	13	1066	17	1084	62	99	97
PB -10	49.1	2.2012	0.0973	0.1960	0.0032	0.19	5.1010	0.0829	0.0814	0.0042	0.0877	0.0075	1.19	10	10	42	0.24	1154	17	1181	31	1232	103	97	93
PB -10	19.1	2.1412	0.0439	0.1962	0.0021	0.62	5.0970	0.0542	0.0792	0.0019	0.1269	0.0055	0.14	31	52	120	0.43	1155	11	1162	14	1176	47	99	98
PB -10	50.1	2.2098	0.0563	0.1996	0.0021	0.01	5.0106	0.0517	0.0803	0.0023	0.0938	0.0065	1.23	31	41	124	0.33	1173	11	1184	18	1205	55	99	97
PB -10	43.1	4.2506	0.1317	0.2892	0.0036	0.87	3.4573	0.0427	0.1066	0.0037	0.3475	0.0113	0.20	18	42	44	0.96	1638	18	1684	27	1742	66	97	94
PB -10	12.1	4.3075	0.0659	0.2941	0.0026	0.54	3.4002	0.0297	0.1062	0.0018	0.1795	0.0037	0.10	34	48	88	0.55	1662	13	1695	13	1736	32	98	95
PB -10	80.1	4.4389	0.0911	0.3024	0.0030	0.01	3.3069	0.0331	0.1065	0.0023	0.2036	0.0305	0.22	61	90	144	0.63	1703	15	1720	17	1740	40	99	97
PB -10	37.1	6.2902	0.1493	0.3494	0.0036	0.80	2.8624	0.0299	0.1306	0.0033	0.2506	0.0107	0.32	27	43	56	0.77	1932	17	2017	21	2106	44	95	91
PB -10	63.1	6.0349	0.1312	0.3529	0.0039	0.67	2.8338	0.0312	0.1240	0.0031	0.3741	0.0434	0.30	22	36	41	0.89	1948	18	1981	19	2015	45	98	96
PB -10	15.1	6.0107	0.0830	0.3553	0.0028	0.24	2.8143	0.0219	0.1227	0.0018	0.0795	0.0013	0.05	87	49	189	0.26	1960	13	1977	12	1996	25	99	98

PB -10	1.1	0.8602	0.0314	0.0942	0.0017	0.08	10.6176	0.1908	0.0662	0.0030	0.1252	0.0141	0.39	8	22	69	0.32	580	10	630	18	814	98	92	71
PB -10	85.1	0.8447	0.0767	0.0969	0.0026	0.48	10.3166	0.2757	0.0632	0.0066	0.1579	0.0255	0.66	5	15	37	0.39	596	15	622	42	715	233	95	83
PB -10	73.1	0.8951	0.0942	0.1010	0.0032	0.53	9.9015	0.3147	0.0643	0.0082	0.3308	0.0315	0.79	5	30	36	0.86	620	19	649	52	751	280	95	82
PB -10	70.1	0.8943	0.0701	0.1022	0.0024	0.04	9.7867	0.2346	0.0635	0.0060	0.1630	0.0209	0.47	7	19	50	0.38	627	14	649	38	724	201	96	86
PB -10	54.1	0.7044	0.0929	0.0892	0.0028	0.34	11.2109	0.3550	0.0573	0.0087	0.1939	0.0244	2.21	4	20	37	0.55	551	17	541	52	502	300	101	109
PB -10	33.1	1.1476	0.0354	0.1244	0.0013	0.89	8.0395	0.0830	0.0669	0.0021	0.1912	0.0096	1.51	15	46	82	0.56	756	7	776	16	835	66	97	90
PB -10	59.1	1.1458	0.0427	0.1286	0.0016	0.07	7.7761	0.0968	0.0646	0.0027	0.0840	0.0063	0.53	19	31	122	0.25	780	9	775	20	762	88	100	102
PB -10	87.1	1.2932	0.0560	0.1383	0.0021	0.04	7.2284	0.1096	0.0678	0.0032	0.1739	0.0137	0.58	12	33	67	0.50	835	12	843	24	862	93	99	96
PB -10	74.1	0.3051	0.0294	0.0405	0.0011	0.46	24.6894	0.6420	0.0546	0.0061	0.3297	0.0227	0.55	12	212	209	1.02	256	7	270	23	398	223	94	64
PB -10	11.1	0.2938	0.0081	0.0398	0.0005	0.35	25.1481	0.2986	0.0536	0.0018	0.2375	0.0081	0.20	16	223	312	0.71	251	3	262	6	354	76	96	71
PB -10	36.1	0.2945	0.0153	0.0433	0.0005	0.30	23.1196	0.2669	0.0494	0.0028	0.2632	0.0121	0.53	13	179	221	0.81	273	3	262	12	166	117	104	164
PB -10	47.1	0.3459	0.0196	0.0438	0.0006	0.42	22.8366	0.3020	0.0573	0.0037	0.1368	0.0149	0.94	9	65	170	0.39	276	4	302	15	503	146	91	54
PB -10	2.1	0.3311	0.0066	0.0439	0.0004	0.70	22.7862	0.2093	0.0547	0.0012	0.0137	0.0070	0.03	28	16	542	0.03	277	3	290	5	401	50	95	69
PB -10	98.1	0.3049	0.0117	0.0392	0.0005	0.50	25.5228	0.2989	0.0564	0.0024	0.3127	0.0193	0.74	7	110	119	0.93	248	3	270	9	469	89	91	52
PB -10	95.1	0.3227	0.0130	0.0458	0.0006	0.83	21.8196	0.2715	0.0511	0.0023	0.1187	0.0057	2.47	24	136	431	0.32	289	4	284	10	244	103	101	118
PB -10	68.1	2.2784	0.0449	0.2052	0.0018	0.86	4.8727	0.0419	0.0805	0.0017	0.1589	0.0096	0.21	58	93	217	0.43	1203	9	1206	14	1210	42	99	99
PB -10	22.1	1.9751	0.0388	0.1833	0.0019	0.84	5.4569	0.0560	0.0782	0.0018	0.1772	0.0094	0.45	25	56	103	0.55	1085	10	1107	13	1151	45	97	94
PB -10	52.1	2.0094	0.0685	0.1870	0.0024	0.25	5.3486	0.0688	0.0779	0.0030	0.2680	0.0096	0.10	23	69	85	0.81	1105	13	1119	24	1146	79	98	96
PB -10	90.1	1.5924	0.0675	0.1568	0.0025	0.01	6.3792	0.1002	0.0737	0.0034	0.1596	0.0151	1.89	13	29	62	0.47	939	14	967	27	1033	95	97	90
PB -10	75.1	1.5863	0.0588	0.1575	0.0023	0.01	6.3500	0.0916	0.0731	0.0031	0.2669	0.0081	0.91	18	67	80	0.84	943	13	965	23	1016	88	97	92
PB -10	53.1	6.3891	0.1170	0.3645	0.0031	0.82	2.7434	0.0235	0.1271	0.0024	0.1850	0.0114	0.73	100	113	191	0.59	2004	15	2031	16	2059	33	98	97
PB -10	97.1	5.7584	0.0726	0.3400	0.0023	0.01	2.9409	0.0202	0.1228	0.0013	0.0307	0.0017	0.05	92	24	218	0.11	1887	11	1940	11	1998	19	97	94
PB -10	3.1	6.4162	0.1210	0.3616	0.0043	0.35	2.7658	0.0332	0.1287	0.0027	0.2139	0.0102	0.15	21	27	39	0.68	1990	21	2035	16	2080	37	97	95
PB -10	88.1	5.7329	0.1626	0.3399	0.0047	0.59	2.9419	0.0409	0.1223	0.0036	0.5287	0.0334	0.31	27	78	44	1.77	1886	23	1936	25	1990	52	97	94
PB -10	39.1	5.8426	0.1197	0.3424	0.0031	1.00	2.9202	0.0264	0.1237	0.0027	0.1767	0.0093	0.05	49	51	96	0.53	1898	15	1953	18	2011	38	97	94
PB -10	23.1	5.2937	0.0958	0.3362	0.0037	0.08	2.9743	0.0325	0.1142	0.0024	0.2936	0.0079	0.42	32	74	66	1.12	1868	18	1868	15	1867	38	100	100
PB -10	8.1	5.4387	0.0861	0.3585	0.0028	0.69	2.7898	0.0218	0.1100	0.0017	0.1766	0.0113	0.91	8	11	18	0.59	1975	13	1891	12	1800	27	104	109
PB -10	56.1	5.2769	0.0997	0.3184	0.0028	0.60	3.1403	0.0280	0.1202	0.0025	0.1438	0.0028	0.07	61	65	139	0.46	1782	14	1865	16	1959	36	95	90
PB -10	21.1	4.8402	0.1001	0.3200	0.0040	0.36	3.1250	0.0389	0.1097	0.0027	0.2376	0.0047	1.17	22	41	51	0.81	1790	20	1792	17	1794	44	99	99
PB -10	18.1	2.8365	0.0461	0.2370	0.0021	0.58	4.2194	0.0368	0.0868	0.0016	0.1644	0.0048	0.14	53	76	171	0.45	1371	11	1365	12	1356	35	100	101
PB -10	62.1	0.4318	0.0171	0.0586	0.0007	0.70	17.0552	0.2127	0.0534	0.0024	0.1927	0.0080	0.23	25	170	322	0.53	367	5	364	12	346	102	100	106
PB -10	24.1	0.4750	0.0249	0.0614	0.0012	0.07	16.2893	0.3288	0.0561	0.0037	0.5069	0.0192	0.23	11	160	113	1.42	384	8	395	17	457	143	97	84
PB -10	20.1	0.5201	0.0317	0.0649	0.0016	0.04	15.3978	0.3742	0.0581	0.0045	0.1894	0.0181	1.06	7	46	78	0.60	406	10	425	22	533	162	95	76
PB -10	82.1	0.3710	0.0191	0.0499	0.0008	0.01	20.0339	0.3154	0.0539	0.0031	0.2230	0.0101	0.29	14	148	209	0.71	314	5	320	14	367	126	97	85
PB -10	94.1	2.9613	0.2758	0.2316	0.0088	0.01	4.3182	0.1639	0.0927	0.0104	0.2572	0.0411	2.35	3	8	10	0.78	1343	46	1398	75	1483	235	96	90
PB -10	93.1	10.9703	0.2361	0.4736	0.0052	0.83	2.1115	0.0232	0.1680	0.0035	0.4016	0.0043	0.04	48	79	61	1.30	2499	23	2521	20	2538	34	99	98
PB -10	60.1	12.1974	0.2096	0.4902	0.0042	0.01	2.0401	0.0176	0.1805	0.0032	0.1450	0.0173	0.46	12	5	18	0.30	2572	18	2620	16	2657	30	98	96
PB -10	4.1	0.3745	0.0151	0.0447	0.0008	0.29	22.3800	0.4019	0.0608	0.0031	0.1777	0.0151	0.50	8	60	128	0.47	282	5	323	11	632	112	87	44
PB 22	49.1	0.2750	0.0273	0.0403	0.0010	0.35	24.8321	0.6178	0.0495	0.0057	0.2777	0.0380	2.03	6	109	112	0.97	255	6	247	22	173	186	103	147
PB 22	89.1	0.2890	0.0081	0.0404	0.0006	0.01	24.7695	0.3496	0.0519	0.0015	0.1509	0.0057	0.80	21	176	409	0.43	255	4	258	6	282	69	98	90
PB 22	60.1	0.3004	0.0121	0.0405	0.0005	0.31	24.7077	0.3257	0.0538	0.0024	0.1393	0.0078	0.24	19	148	358	0.41	256	3	267	10	364	107	95	70
PB 22	24.1	0.3163	0.0328	0.0410	0.0008	0.27	24.3966	0.4908	0.0560	0.0067	0.2747	0.0260	0.83	5	58	80	0.73	259	5	279	25	451	248	92	57
PB 22	65.1	0.2914	0.0101	0.0413	0.0005	0.01	24.1974	0.2668	0.0511	0.0019	0.0498	0.0082	0.27	20	48	405	0.12	261	3	260	8	247	86	100	105
PB 22	55.1	0.2821	0.0316	0.0422	0.0011	0.11	23.6900	0.6231	0.0485	0.0064	0.2212	0.0251	2.34	5	55	84	0.66	267	7	252	25	122	229	105	218
PB 22	33.1	0.3061	0.0135	0.0425	0.0006	0.50	23.5033	0.3306	0.0522	0.0027	0.2119	0.0139	0.61	14	139	246	0.57	269	4	271	10	294	115	99	91
PB 22	9.1	0.3179	0.0118	0.0428	0.0005	0.33	23.3784	0.2824	0.0539	0.0021	0.2006	0.0113	0.25	19	183	328	0.56	270	3	280	9	367	88	96	73
PB 22	34.1	0.2936	0.0217	0.0431	0.0009	0.01	23.1787	0.4733	0.0493	0.0044	0.2400	0.0210	5.15	8	97	136	0.71	272	6	261	17	165	183	104	165
PB 22	5.1	0.3596	0.0353	0.0445	0.0011	0.01	22.4472	0.5372	0.0585	0.0065	0.3811	0.0342	2.09	6	89	84	1.05	281	7	312	26	550	248	90	51
PB 22	50.1	0.6148	0.0225	0.0773	0.0010	0.67	12.9419	0.1624	0.0577	0.0023	0.2217	0.0128	0.47	23	135	216	0.63	480	6	487	14	519	89	98	92
PB 22	36.1	0.6209	0.0127	0.0783	0.0007	0.17	12.7708	0.1102	0.0575	0.0013	0.0420	0.0022	0.13	47	61	507	0.12	486	4	490	8	511	50	99	95
PB 22	28.1	0.6797	0.0425	0.0798	0.0017	0.01	12.5285	0.2656	0.0618	0.0049	0.1893	0.0173	0.39	8	42	74	0.56	495	10	527	26	666	174	94	74
PB 22	44.1	0.6613	0.0295	0.0801	0.0013	0.01	12.4894	0.2008	0.0599	0.0030	0.5360	0.0142	0.33	18	148	128	1.16	497	8	515	18	600	115	96	82
PB 22	29.1	0.6519	0.0312	0.0823	0.0013	0.01	12.1511	0.1951	0.0575	0.0033	0.1531	0.0121	0.48	10	45	96	0.47	510	8	510	19	509	123	100	100
PB 22	76.1	0.6556	0.0274	0.0825	0.0012	0.08	12.1149	0.1761	0.0576	0.0028	0.0653	0.0112	0.76	10	15	103	0.14	511	7	512	17	515	104	99	99
PB 22	43.1	0.6736	0.0207	0.0830	0.0010	0.50	12.0484	0.1418	0.0589	0.0020	0.0780	0.0059	0.71	26	52	244	0.21	514	6	523	13	562	73	98	91
PB 22	47.1	0.6605	0.0418	0.0832	0.0017	0.12	12.0174	0.2497	0.0576	0.0042	0.2770	0.0149	0.59	10	67	86	0.78	515	10	515	26	514	157	100	100
PB 22	20.1	0.6834	0.0586	0.0835	0.0015	0.49	11.9703	0.2139	0.0593	0.0057	0.0753	0.0205	1.02	5	9	49	0.19	517	9	529	35	579	193	97	89
PB 22	39.1	0.6954	0.0407	0.0838	0.0017	0.11	11.9285	0.2409	0.0602	0.0041	0.1536	0.0153	0.53	9	35	78	0.44	519	10	536	25	609	154	96	85
PB 22	57.1	0.6879	0.0358	0.0841	0.0014	0.18	11.8901	0.1953	0.0593	0.0035	0.1738	0.0120	0.74	13	57	120	0.48	521	8	532	21	579	124	97	89
PB 22	78.1	0.7217	0.0398	0.0851	0.0016	0.01	11.7468	0.2196	0.0615	0.0040	0.1538	0.0100	1.00	9	35	84	0.41	527	10	552	23	656	142	95	80
PB 22	77.1	0.7069	0.0479	0.0853	0.0019	0.70	11.7289	0.2574	0.0601	0.0048	0.2384	0.0258	0.37	8	46	69	0.67	527	11	543	29	608	180	97	86

PB 22	18.1	0.6993	0.0319	0.0853	0.0010	0.60	11.7214	0.1306	0.0594	0.0030	0.1217	0.0094	0.51	11	32	101	0.31	528	6	538	19	583	109	98	90
PB 22	61.1	0.7012	0.0450	0.0854	0.0016	0.16	11.7133	0.2153	0.0596	0.0043	0.1238	0.0093	1.84	9	37	88	0.42	528	9	540	28	588	166	97	89
PB 22	41.1	0.6966	0.0354	0.0856	0.0015	0.67	11.6880	0.2071	0.0591	0.0035	0.1524	0.0113	0.46	11	43	93	0.46	529	9	537	21	569	127	98	93
PB 22	7.1	0.7050	0.0231	0.0860	0.0010	0.67	11.6261	0.1371	0.0594	0.0020	0.1107	0.0100	0.18	21	71	196	0.36	532	6	542	14	583	72	98	91
PB 22	86.1	0.7174	0.0292	0.0861	0.0018	0.11	11.6088	0.2367	0.0604	0.0029	0.2644	0.0142	0.32	12	78	95	0.82	533	10	549	17	618	106	97	86
PB 22	82.1	0.7010	0.0202	0.0870	0.0010	0.20	11.4938	0.1315	0.0584	0.0019	0.0754	0.0044	0.23	25	52	239	0.22	538	6	539	12	546	71	99	98
PB 22	83.1	0.7007	0.0130	0.0870	0.0008	0.10	11.4901	0.1007	0.0584	0.0011	0.0342	0.0015	0.06	79	80	776	0.10	538	5	539	8	545	41	99	98
PB 22	46.1	0.7562	0.0545	0.0871	0.0022	0.13	11.4855	0.2838	0.0630	0.0052	0.3971	0.0227	0.98	8	71	59	1.22	538	13	572	31	708	193	94	76
PB 22	84.1	0.7243	0.0202	0.0883	0.0010	0.20	11.3211	0.1276	0.0595	0.0018	0.3471	0.0048	0.15	32	253	245	1.03	546	6	553	12	584	66	98	93
PB 22	95.1	0.7341	0.0208	0.0899	0.0013	0.04	11.1281	0.1644	0.0592	0.0018	0.2638	0.0112	0.32	22	136	174	0.78	555	8	559	12	576	68	99	96
PB 22	88.1	0.7382	0.0145	0.0909	0.0010	0.62	10.9974	0.1224	0.0589	0.0011	0.0768	0.0025	0.17	53	108	493	0.22	561	6	561	9	563	40	99	99
PB 22	16.1	0.8503	0.0444	0.0949	0.0012	0.19	10.5348	0.1364	0.0650	0.0038	0.1119	0.0104	0.52	7	16	58	0.28	585	7	625	25	773	126	93	75
PB 22	62.1	0.7704	0.0591	0.0952	0.0019	0.06	10.5097	0.2152	0.0587	0.0051	0.4529	0.0206	0.40	9	73	59	1.22	586	12	580	33	557	179	101	105
PB 22	12.1	0.8056	0.0222	0.0965	0.0010	0.32	10.3665	0.1117	0.0606	0.0016	0.0995	0.0048	0.15	28	74	238	0.31	594	6	600	12	624	58	98	95
PB 22	90.1	0.8032	0.0271	0.0966	0.0017	0.88	10.3511	0.1783	0.0603	0.0023	0.1213	0.0099	0.35	15	38	109	0.35	595	10	599	15	614	83	99	96
PB 22	26.1	0.8423	0.0320	0.0975	0.0014	0.01	10.2519	0.1428	0.0626	0.0028	0.2931	0.0078	0.37	17	108	121	0.90	600	8	620	18	696	96	96	86
PB 22	14.1	0.8483	0.0429	0.0979	0.0012	0.41	10.2174	0.1268	0.0629	0.0036	0.1654	0.0164	0.96	11	37	80	0.46	602	7	624	24	704	118	96	85
PB 22	45.1	0.8297	0.0285	0.0981	0.0013	0.61	10.1903	0.1328	0.0613	0.0023	0.0856	0.0056	0.23	21	41	171	0.24	604	8	614	16	651	82	98	92
PB 22	92.1	0.8228	0.0193	0.0986	0.0013	0.53	10.1431	0.1288	0.0605	0.0014	0.1635	0.0040	0.14	31	114	239	0.48	606	7	610	11	623	50	99	97
PB 22	3.1	0.8301	0.0189	0.0992	0.0010	0.08	10.0831	0.0997	0.0607	0.0013	0.0919	0.0023	0.07	51	114	408	0.28	610	6	614	11	629	46	99	96
PB 22	35.1	0.8454	0.0630	0.0995	0.0024	0.32	10.0542	0.2452	0.0616	0.0054	0.6530	0.0336	0.39	11	111	55	2.01	611	14	622	34	662	186	98	92
PB 22	48.1	0.8156	0.0415	0.1002	0.0017	0.01	9.9759	0.1729	0.0590	0.0035	0.1439	0.0108	1.13	12	35	93	0.38	616	10	606	23	568	125	101	108
PB 22	1.1	0.9030	0.0587	0.1007	0.0019	0.01	9.9289	0.1895	0.0650	0.0047	0.2209	0.0183	0.49	8	35	53	0.65	619	11	653	32	775	144	94	79
PB 22	80.1	0.8518	0.0194	0.1007	0.0010	0.40	9.9272	0.0997	0.0613	0.0015	0.2103	0.0064	0.11	46	197	333	0.59	619	6	626	11	651	52	98	95
PB 22	56.1	0.8608	0.0231	0.1012	0.0010	0.20	9.8846	0.1020	0.0617	0.0018	0.1031	0.0033	0.21	31	68	242	0.28	621	6	631	13	664	62	98	93
PB 22	37.1	0.8576	0.0652	0.1012	0.0026	0.01	9.8782	0.2519	0.0614	0.0057	0.1109	0.0147	0.72	6	14	48	0.30	622	15	629	36	655	196	98	94
PB 22	63.1	0.8918	0.0555	0.1015	0.0019	0.35	9.8508	0.1799	0.0637	0.0044	0.1903	0.0189	0.48	9	31	64	0.48	623	11	647	30	732	149	96	85
PB 22	38.1	0.8356	0.1002	0.1022	0.0038	0.04	9.7814	0.3674	0.0593	0.0088	0.4103	0.0325	1.69	5	37	30	1.22	628	22	617	55	577	307	101	108
PB 22	58.1	0.9156	0.0290	0.1034	0.0012	0.32	9.6710	0.1160	0.0642	0.0022	0.0641	0.0061	0.23	20	29	162	0.18	634	7	660	16	749	75	96	84
PB 22	32.1	0.9085	0.0521	0.1035	0.0021	0.01	9.6625	0.1951	0.0637	0.0045	0.3262	0.0584	0.58	6	29	45	0.66	635	12	656	28	731	158	96	86
PB 22	51.1	1.7237	0.0654	0.1687	0.0024	0.59	5.9261	0.0856	0.0741	0.0032	0.1042	0.0068	0.31	13	17	60	0.27	1005	14	1017	24	1044	88	98	96
PB 22	17.1	1.7419	0.0489	0.1694	0.0015	0.01	5.9034	0.0531	0.0746	0.0022	0.3100	0.1186	0.32	24	76	89	0.86	1009	8	1024	18	1057	60	98	95
PB 22	85.1	1.7714	0.0409	0.1721	0.0023	0.53	5.8117	0.0780	0.0747	0.0018	0.1331	0.0052	0.21	26	44	114	0.39	1024	13	1035	15	1060	48	98	96
PB 22	42.1	1.7842	0.0504	0.1731	0.0021	0.01	5.7769	0.0709	0.0748	0.0023	0.1446	0.0054	0.59	27	54	117	0.46	1029	12	1040	19	1062	64	98	96
PB 22	21.1	0.9246	0.0244	0.1077	0.0009	0.35	9.2823	0.0752	0.0622	0.0017	0.0799	0.0044	0.14	27	50	203	0.25	660	5	665	13	682	60	99	96
PB 22	53.1	0.7470	0.0293	0.0921	0.0012	0.58	10.8577	0.1448	0.0588	0.0026	0.1533	0.0088	0.59	18	62	154	0.40	568	7	567	17	561	94	100	101
PB 22	15.1	0.9024	0.0245	0.1068	0.0009	0.59	9.3606	0.0771	0.0613	0.0017	0.0706	0.0043	0.18	24	39	187	0.21	654	5	653	13	649	63	100	100
PB 22	4.1	0.8068	0.0457	0.0932	0.0016	0.08	10.7249	0.1799	0.0628	0.0039	0.3666	0.0168	1.00	11	78	74	1.05	575	9	601	25	700	126	95	82
PB 22	31.1	0.8993	0.0186	0.1056	0.0009	0.59	9.4717	0.0839	0.0618	0.0014	0.3518	0.0028	0.06	57	382	355	1.08	647	5	651	10	666	48	99	97
PB 22	22.1	0.8900	0.0543	0.1053	0.0015	0.44	9.4938	0.1350	0.0613	0.0042	0.1009	0.0106	1.05	8	17	56	0.30	646	9	646	29	649	144	99	99
PB 22	72.1	0.9058	0.0490	0.1044	0.0017	0.28	9.5772	0.1561	0.0629	0.0038	0.3208	0.0157	0.30	12	66	77	0.86	640	10	655	26	705	125	97	90
PB 22	91.1	0.7805	0.0167	0.0935	0.0011	0.38	10.7005	0.1304	0.0606	0.0013	0.2671	0.0118	0.31	39	241	294	0.82	576	7	586	10	624	48	98	92
PB 22	70.1	0.7775	0.0389	0.0941	0.0014	0.01	10.6296	0.1608	0.0599	0.0033	0.5531	0.0149	0.09	17	174	106	1.64	580	8	584	22	601	125	99	96
PB 22	93.1	0.7752	0.0148	0.0944	0.0010	0.52	10.5900	0.1143	0.0595	0.0011	0.0654	0.0019	0.24	60	106	540	0.20	582	6	583	8	587	38	99	99
PB 22	11.1	0.8719	0.0305	0.1035	0.0013	0.44	9.6654	0.1181	0.0611	0.0022	0.1473	0.0055	0.50	19	70	142	0.49	635	7	637	16	644	76	99	98
PB 22	81.1	0.7413	0.0212	0.0910	0.0010	0.43	10.9857	0.1248	0.0591	0.0019	0.1758	0.0097	0.23	26	126	218	0.58	562	6	563	12	570	68	99	98
PB 22	87.1	0.8408	0.0435	0.0912	0.0025	0.25	10.9674	0.3018	0.0669	0.0044	0.1851	0.0208	1.56	6	28	51	0.55	563	15	620	25	834	152	90	67
PB 22	54.1	0.5887	0.0353	0.0742	0.0013	0.10	13.4820	0.2415	0.0576	0.0040	0.2002	0.0235	0.74	10	43	99	0.44	461	8	470	22	513	138	98	89
PB 22	75.1	0.6008	0.0417	0.0748	0.0016	0.04	13.3750	0.2946	0.0583	0.0047	0.1510	0.0249	0.53	15	93	151	0.62	465	10	478	27	540	180	97	86
PB 22	64.1	1.1232	0.1421	0.1243	0.0043	0.01	8.0431	0.2765	0.0655	0.0094	0.1610	0.0407	1.92	4	8	21	0.39	755	25	765	67	791	283	98	95
PB 22	13.1	1.1642	0.0293	0.1269	0.0010	0.39	7.8822	0.0635	0.0666	0.0018	0.3361	0.0151	0.15	30	163	157	1.04	770	6	784	14	824	56	98	93
PB 22	94.1	4.1384	0.1001	0.2854	0.0046	0.34	3.5038	0.0562	0.1052	0.0027	0.2270	0.0110	0.25	20	35	49	0.72	1619	23	1662	19	1717	47	97	94
PB 22	69.1	5.1792	0.1455	0.3272	0.0043	0.42	3.0561	0.0401	0.1148	0.0035	0.2249	0.0057	0.22	21	32	45	0.70	1825	21	1849	24	1877	55	98	97
PB 22	52.1	5.1618	0.1648	0.3309	0.0051	0.20	3.0218	0.0468	0.1131	0.0042	0.6903	0.0407	0.82	12	32	19	1.70	1843	25	1846	27	1850	66	99	99
PB 22	10.1	5.7845	0.1149	0.3463	0.0036	0.50	2.8878	0.0301	0.1212	0.0023	0.2105	0.0068	0.10	50	67	100	0.67	1917	17	1944	17	1973	33	98	97
PB 22	19.1	6.2719	0.0959	0.3642	0.0024	0.19	2.7460	0.0181	0.1249	0.0019	0.0405	0.0018	0.07	72	19	156	0.12	2002	11	2015	13	2028	27	99	98
PB 22	40.1	6.1504	0.1379	0.3675	0.0042	0.35	2.7211	0.0314	0.1214	0.0030	0.3596	0.0056	0.28	43	82	74	1.10	2018	20	1997	19	1977	43	101	102
PB 22	66.1	4.6521	0.0927	0.3102	0.0030	0.98	3.2239	0.0309	0.1088	0.0020	0.1567	0.0024	0.28	59	75	155	0.49	1742	15	1759	16	1779	35	99	97
PB 22	79.1	0.3598	0.0202	0.0468	0.0008	0.01	21.3634	0.3852	0.0557	0.0037	0.2368	0.0162	0.73	10	105	155	0.68	295	5	312	16	442	151	94	66
PB 22	59.1	0.3404	0.0146	0.0464	0.0006	0.01	21.5613	0.2880	0.0532	0.0025	0.1011	0.0497	0.57	13	57	229	0.25	292	4	298	11	339	107	98	86
PB 22	2.1	0.3357	0.0145	0.0451	0.0006	0.09	22.1772	0.2987	0.0540	0.0024	0.1965	0.0078	0.22	17	166	269	0.62	284	4	294	11	371	102	96	76

PB 22	96.1	3.6543	0.0647	0.2745	0.0030	0.01	3.6433	0.0395	0.0966	0.0016	0.1297	0.0024	0.14	65	75	181	0.42	1564	15	1561	14	1559	30	100	100
PB 22	23.1	1.3943	0.1010	0.1418	0.0026	0.22	7.0502	0.1278	0.0713	0.0059	0.1574	0.0194	0.35	8	18	41	0.43	855	15	887	44	966	169	96	88
PB 22	30.1	1.6225	0.0924	0.1566	0.0035	0.84	6.3840	0.1431	0.0751	0.0055	0.1506	0.0163	0.43	10	20	55	0.37	938	20	979	36	1072	151	95	87
PB 22	67.1	0.4626	0.0543	0.0618	0.0017	0.01	16.1780	0.4386	0.0543	0.0073	0.1647	0.0314	0.00	4	22	51	0.43	387	10	386	37	383	277	100	101
PB 22	68.1	6.9475	0.1339	0.3776	0.0036	0.82	2.6486	0.0255	0.1335	0.0026	0.1081	0.0026	0.06	56	31	108	0.29	2065	17	2105	17	2144	34	98	96
PB 22	74.1	7.5097	0.1634	0.3780	0.0048	0.86	2.6456	0.0335	0.1441	0.0035	0.2116	0.0273	0.16	27	29	52	0.55	2067	22	2174	19	2277	41	95	90
PB 22	6.1	10.2552	0.1782	0.4476	0.0043	0.89	2.2341	0.0216	0.1662	0.0026	0.1251	0.0028	0.05	72	49	112	0.44	2385	19	2458	16	2519	26	97	94
PB 22	25.1	11.2091	0.1831	0.4743	0.0045	0.93	2.1085	0.0201	0.1714	0.0031	0.1336	0.0070	0.08	64	48	93	0.52	2502	20	2541	15	2572	30	98	97
PB 22	73.1	12.4798	0.2012	0.4912	0.0046	0.10	2.0359	0.0189	0.1843	0.0031	0.1605	0.0078	0.10	80	62	116	0.53	2576	20	2641	15	2692	27	97	95
PB 22	27.1	14.9753	0.2134	0.5327	0.0042	0.11	1.8771	0.0149	0.2039	0.0030	0.1214	0.0026	0.12	55	32	72	0.45	2753	18	2814	14	2858	24	97	96
PB 22	71.1	23.2223	0.4711	0.6301	0.0066	0.58	1.5870	0.0167	0.2673	0.0052	0.1465	0.0129	1.46	12	7	13	0.55	3150	26	3236	18	3290	29	97	95
PB 22	8.1	0.9511	0.3345	0.1072	0.0086	0.35	9.3261	0.7448	0.0643	0.0266	0.4969	0.0846	2.82	2	13	8	1.53	657	50	679	153	752	614	96	87
PB -2A	85.1	0.2894	0.0188	0.0406	0.0009	0.19	24.6504	0.5210	0.0517	0.0040	0.3934	0.0467	0.40	19	341	286	1.19	0.256	0.005	0.258	0.014	0.274	0.167	99	93
PB -2A	62.2	0.2921	0.0119	0.0413	0.0006	0.05	24.2039	0.3400	0.0513	0.0022	0.3986	0.0340	0.18	45	909	643	1.41	0.261	0.004	0.260	0.009	0.253	0.094	100	103
PB -2A	93.1	0.3051	0.0113	0.0426	0.0006	0.19	23.4481	0.3420	0.0519	0.0023	0.0128	0.0086	0.51	19	24	396	0.06	0.269	0.004	0.270	0.009	0.281	0.099	99	95
PB -2A	76.1	0.3094	0.0143	0.0429	0.0007	0.25	23.3224	0.3939	0.0523	0.0027	0.2353	0.0202	1.17	15	125	258	0.48	0.271	0.004	0.274	0.011	0.300	0.120	98	90
PB -2A	79.1	0.3070	0.0118	0.0432	0.0006	0.43	23.1475	0.3415	0.0515	0.0022	0.2661	0.0114	0.17	30	392	493	0.80	0.273	0.004	0.272	0.009	0.265	0.095	100	102
PB -2A	12.1	0.5955	0.0245	0.0758	0.0010	0.26	13.1870	0.1805	0.0570	0.0027	0.1450	0.0257	0.45	20	113	198	0.57	0.471	0.006	0.474	0.015	0.490	0.102	99	96
PB -2A	70.1	0.5793	0.0266	0.0759	0.0012	0.36	13.1759	0.2042	0.0554	0.0027	0.1884	0.0069	0.33	21	112	206	0.54	0.472	0.007	0.464	0.017	0.427	0.108	101	110
PB -2A	80.1	0.5986	0.0204	0.0762	0.0011	0.56	13.1179	0.1895	0.0570	0.0021	0.1497	0.0077	0.44	21	72	215	0.33	0.474	0.007	0.476	0.013	0.490	0.080	99	96
PB -2A	2.1	0.6830	0.0361	0.0853	0.0015	0.46	11.7184	0.1998	0.0580	0.0037	0.2768	0.0260	0.75	14	85	120	0.71	0.528	0.009	0.529	0.022	0.532	0.140	99	99
PB -2A	20.1	0.6712	0.0209	0.0853	0.0008	0.66	11.7205	0.1053	0.0571	0.0020	0.1647	0.0074	0.52	25	123	229	0.54	0.528	0.005	0.521	0.013	0.494	0.075	101	106
PB -2A	31.1	0.6893	0.0356	0.0859	0.0011	0.34	11.6364	0.1500	0.0582	0.0032	0.1020	0.0116	0.38	16	44	134	0.33	0.531	0.007	0.532	0.022	0.536	0.127	99	99
PB -2A	26.1	0.6851	0.0306	0.0870	0.0010	0.52	11.4885	0.1284	0.0571	0.0027	0.2640	0.0145	0.27	27	144	199	0.72	0.538	0.006	0.530	0.018	0.495	0.098	101	108
PB -2A	81.1	0.6844	0.0246	0.0871	0.0013	0.63	11.4817	0.1703	0.0570	0.0022	0.1051	0.0063	1.29	26	81	258	0.32	0.538	0.008	0.529	0.015	0.491	0.087	101	109
PB -2A	72.1	0.7114	0.0458	0.0874	0.0020	0.36	11.4394	0.2589	0.0590	0.0045	0.2436	0.0144	0.56	12	69	99	0.69	0.540	0.012	0.546	0.028	0.568	0.165	99	95
PB -2A	83.1	0.6911	0.0230	0.0874	0.0012	0.28	11.4404	0.1625	0.0573	0.0021	0.1811	0.0064	0.33	42	176	367	0.48	0.540	0.007	0.533	0.014	0.505	0.079	101	107
PB -2A	73.1	0.7114	0.0250	0.0881	0.0013	0.68	11.3527	0.1660	0.0586	0.0023	0.1166	0.0470	0.35	27	48	251	0.19	0.544	0.008	0.546	0.015	0.551	0.083	99	98
PB -2A	14.1	0.7046	0.0229	0.0881	0.0008	0.65	11.3456	0.1047	0.0580	0.0021	0.2014	0.0178	0.25	18	86	158	0.55	0.545	0.005	0.542	0.014	0.529	0.079	100	102
PB -2A	61.1	0.7174	0.0400	0.0882	0.0016	0.37	11.3436	0.2043	0.0590	0.0035	0.4348	0.0389	0.92	16	134	117	1.15	0.545	0.009	0.549	0.024	0.568	0.132	99	95
PB -2A	87.1	0.7045	0.0267	0.0886	0.0014	0.01	11.2841	0.1791	0.0577	0.0026	0.3159	0.0101	0.70	27	166	202	0.82	0.547	0.008	0.541	0.016	0.517	0.103	101	105
PB -2A	50.1	0.6988	0.0252	0.0885	0.0008	0.62	11.3012	0.1035	0.0573	0.0022	0.2563	0.0045	0.29	44	263	350	0.75	0.547	0.005	0.538	0.015	0.502	0.084	101	108
PB -2A	90.1	0.7095	0.0139	0.0887	0.0010	0.81	11.2750	0.1229	0.0580	0.0013	0.1458	0.0032	0.36	77	282	680	0.42	0.548	0.006	0.544	0.008	0.530	0.050	100	103
PB -2A	33.1	0.7199	0.0226	0.0898	0.0008	0.15	11.1412	0.1005	0.0582	0.0018	0.1431	0.0041	0.19	39	160	319	0.50	0.554	0.005	0.551	0.013	0.536	0.069	100	103
PB -2A	37.1	0.7187	0.0222	0.0898	0.0007	0.36	11.1396	0.0869	0.0581	0.0018	0.1427	0.0044	0.09	40	155	323	0.48	0.554	0.004	0.550	0.013	0.532	0.066	100	104
PB -2A	10.1	0.7566	0.0237	0.0912	0.0011	0.01	10.9599	0.1283	0.0601	0.0021	0.0781	0.0053	0.41	22	49	204	0.24	0.563	0.006	0.572	0.014	0.609	0.079	98	92
PB -2A	13.1	0.7324	0.0146	0.0913	0.0007	0.49	10.9585	0.0789	0.0582	0.0013	0.1990	0.0133	0.00	48	226	410	0.55	0.563	0.004	0.558	0.009	0.538	0.048	100	104
PB -2A	88.1	0.7404	0.0203	0.0913	0.0012	0.98	10.9571	0.1414	0.0588	0.0019	0.1029	0.0375	0.08	38	83	331	0.25	0.563	0.007	0.563	0.012	0.561	0.068	100	100
PB -2A	16.1	0.7454	0.0198	0.0918	0.0008	0.52	10.8976	0.0906	0.0589	0.0017	0.0782	0.0050	0.63	28	69	257	0.27	0.566	0.005	0.566	0.011	0.564	0.064	100	100
PB -2A	64.1	0.7396	0.0185	0.0917	0.0011	0.73	10.8999	0.1265	0.0585	0.0014	0.0599	0.0067	0.00	77	107	706	0.15	0.566	0.006	0.562	0.011	0.547	0.051	100	103
PB -2A	65.1	0.7547	0.0246	0.0926	0.0012	0.47	10.7934	0.1434	0.0591	0.0019	0.0999	0.0229	0.89	42	72	367	0.20	0.571	0.007	0.571	0.014	0.570	0.074	100	100
PB -2A	40.1	0.7556	0.0283	0.0931	0.0008	0.47	10.7394	0.0935	0.0588	0.0022	0.1415	0.0074	0.18	30	109	235	0.47	0.574	0.005	0.571	0.016	0.562	0.084	100	102
PB -2A	17.1	0.7715	0.0203	0.0944	0.0008	0.22	10.5986	0.0888	0.0593	0.0017	0.1346	0.0088	0.39	32	103	275	0.38	0.581	0.005	0.581	0.012	0.578	0.065	100	100
PB -2A	9.1	0.7757	0.0168	0.0951	0.0008	0.62	10.5109	0.0932	0.0591	0.0014	0.0329	0.0118	0.11	50	27	457	0.06	0.586	0.005	0.583	0.010	0.572	0.053	100	102
PB -2A	4.1	0.7892	0.0320	0.0954	0.0013	0.36	10.4817	0.1479	0.0600	0.0028	0.2585	0.0196	0.39	15	85	119	0.72	0.587	0.008	0.591	0.018	0.603	0.103	99	97
PB -2A	82.1	0.7903	0.0255	0.0960	0.0014	0.83	10.4183	0.1475	0.0597	0.0020	0.1534	0.0042	0.24	32	111	256	0.43	0.591	0.008	0.591	0.014	0.593	0.071	99	99
PB -2A	1.1	0.7932	0.0340	0.0965	0.0014	0.23	10.3639	0.1525	0.0596	0.0030	0.0701	0.0117	0.00	21	36	181	0.20	0.594	0.008	0.593	0.020	0.590	0.118	100	100
PB -2A	46.1	0.8009	0.0345	0.0974	0.0009	0.09	10.2648	0.0960	0.0596	0.0027	0.1826	0.0280	1.02	18	75	132	0.57	0.599	0.005	0.597	0.019	0.590	0.096	100	101
PB -2A	53.1	0.7882	0.0580	0.0976	0.0014	0.45	10.2500	0.1429	0.0586	0.0047	0.1039	0.0115	1.08	13	30	104	0.29	0.600	0.008	0.590	0.032	0.552	0.162	101	108
PB -2A	66.1	0.8114	0.0683	0.0975	0.0024	0.29	10.2591	0.2480	0.0604	0.0057	0.1018	0.0151	0.41	8	22	67	0.33	0.600	0.014	0.603	0.038	0.617	0.207	99	97
PB -2A	49.1	0.8023	0.0269	0.0981	0.0009	0.73	10.1969	0.0893	0.0593	0.0021	0.1012	0.0034	0.61	49	136	420	0.32	0.603	0.005	0.598	0.015	0.580	0.076	100	104
PB -2A	59.1	0.8073	0.0698	0.0980	0.0015	0.01	10.2016	0.1612	0.0597	0.0056	0.2529	0.0195	0.60	11	59	80	0.74	0.603	0.009	0.601	0.039	0.594	0.214	100	101
PB -2A	22.1	0.8063	0.0308	0.0982	0.0010	0.38	10.1851	0.1050	0.0596	0.0025	0.1559	0.0090	0.64	14	55	108	0.51	0.604	0.006	0.600	0.017	0.588	0.089	100	102
PB -2A	91.1	0.8257	0.0222	0.0991	0.0013	0.65	10.0914	0.1312	0.0604	0.0020	0.1472	0.0059	0.20	43	147	336	0.44	0.609	0.008	0.611	0.012	0.619	0.072	99	98
PB -2A	84.1	0.8737	0.0315	0.1029	0.0016	0.56	9.7169	0.1523	0.0616	0.0027	0.0685	0.0121	0.36	22	29	176	0.17	0.631	0.009	0.638	0.017	0.659	0.093	99	95
PB -2A	24.1	0.9040	0.0639	0.1045	0.0017	0.62	9.5664	0.1553	0.0627	0.0051	0.4804	0.0211	0.57	9	79	54	1.45	0.641	0.010	0.654	0.034	0.699	0.166	98	91
PB -2A	29.1	0.8762	0.0365	0.1046	0.0012	0.72	9.5626	0.1059	0.0608	0.0027	0.1812	0.0171	1.22	48	204	342	0.60	0.641	0.007	0.639	0.020	0.631	0.093	100	101
PB -2A	3.1	0.9074	0.0460	0.1048	0.0018	0.01	9.5417	0.1651	0.0628	0.0037	0.1669	0.0135	0.40	11	30	80	0.37	0.642	0.011	0.656	0.024	0.701	0.128	97	91
PB -2A	55.1	0.8627	0.0296	0.1052	0.0009	0.74	9.5033	0.0852	0.0595	0.0021	0.0326	0.0046	0.39	38	33	312	0.10	0.645	0.005	0.632	0.016	0.584	0.078	102	110
PB -2A	23.1	0.8982	0.0434	0.1068	0.0013	0.32	9.3664	0.1159	0.0610	0.0032	0.3681	0.0312	0.71	15	99	94	1.05	0.654	0.008	0.651	0.023	0.640	0.117	100	102
PB -2A	42.1	0.9227	0.0720	0.1073	0.0016	0.12	9.3237	0.1373	0.0624	0.0052	0.3518	0.0192	0.73	11	70	63	1.10	0.657	0.009	0.664	0.039	0.688	0.182	98	95

PB -2A	45.1	0.9216	0.0683	0.1092	0.0015	0.42	9.1596	0.1266	0.0612	0.0048	0.1555	0.0106	1.26	12	38	79	0.48	0.668	0.009	0.663	0.036	0.647	0.168	100	103
PB -2A	51.1	1.8371	0.0585	0.1784	0.0016	0.35	5.6058	0.0511	0.0747	0.0025	0.1070	0.0037	1.65	39	56	167	0.34	1.058	0.009	1.059	0.021	1.060	0.067	99	99
PB -2A	39.1	1.9144	0.0822	0.1814	0.0020	0.25	5.5140	0.0595	0.0766	0.0035	0.1262	0.0086	0.20	18	31	72	0.43	1.074	0.011	1.086	0.030	1.110	0.095	98	96
PB -2A	15.1	1.9665	0.0307	0.1844	0.0012	0.91	5.4241	0.0364	0.0774	0.0013	0.1857	0.0088	0.11	85	205	362	0.57	1.091	0.007	1.104	0.011	1.130	0.034	98	96
PB -2A	43.1	1.9638	0.0438	0.1854	0.0013	0.97	5.3924	0.0377	0.0768	0.0016	0.1820	0.0056	1.58	120	295	429	0.69	1.097	0.007	1.103	0.014	1.116	0.041	99	98
PB -2A	30.1	1.9907	0.0539	0.1876	0.0017	0.24	5.3294	0.0480	0.0769	0.0021	0.1079	0.0048	0.04	41	56	159	0.35	1.109	0.009	1.112	0.019	1.120	0.056	99	98
PB -2A	21.1	6.9024	0.1011	0.3847	0.0027	0.77	2.5996	0.0181	0.1301	0.0021	0.0257	0.0055	0.20	106	13	235	0.06	2.098	0.012	2.099	0.013	2.100	0.028	99	99
PB -2A	94.1	6.9334	0.1089	0.3874	0.0044	0.43	2.5816	0.0296	0.1298	0.0025	0.2266	0.0042	0.08	75	87	133	0.65	2.111	0.021	2.103	0.014	2.096	0.033	100	100
PB -2A	86.1	7.1047	0.1277	0.3933	0.0051	0.34	2.5427	0.0328	0.1310	0.0029	0.1513	0.0134	0.20	51	37	96	0.38	2.138	0.023	2.125	0.016	2.112	0.038	100	101
PB -2A	28.1	0.3370	0.0193	0.0463	0.0006	0.04	21.5815	0.2802	0.0527	0.0032	0.1300	0.0099	0.50	15	100	236	0.42	0.292	0.004	0.295	0.015	0.318	0.137	99	91
PB -2A	67.1	4.7254	0.1084	0.3185	0.0039	0.39	3.1397	0.0386	0.1076	0.0023	0.1989	0.0123	0.10	51	65	114	0.57	1.782	0.019	1.772	0.019	1.759	0.039	100	101
PB -2A	8.1	5.3803	0.0940	0.3415	0.0030	0.01	2.9281	0.0258	0.1143	0.0022	0.2622	0.0078	0.07	67	126	134	0.94	1.894	0.015	1.882	0.015	1.868	0.034	100	101
PB -2A	78.1	0.4885	0.0154	0.0640	0.0009	0.92	15.6290	0.2118	0.0554	0.0019	0.3242	0.0100	0.64	41	424	500	0.85	0.400	0.005	0.404	0.010	0.427	0.075	98	93
PB -2A	18.1	0.6245	0.0209	0.0794	0.0007	0.48	12.5919	0.1173	0.0570	0.0021	0.1249	0.0076	0.17	17	67	167	0.40	0.493	0.004	0.493	0.013	0.493	0.080	99	99
PB -2A	48.1	0.6313	0.0200	0.0803	0.0006	0.37	12.4573	0.0977	0.0570	0.0018	0.2299	0.0209	0.18	40	243	349	0.70	0.498	0.004	0.497	0.012	0.493	0.071	100	100
PB -2A	95.1	1.3671	0.0202	0.1445	0.0014	0.91	6.9202	0.0659	0.0686	0.0012	0.0635	0.0115	3.93	132	121	957	0.13	0.870	0.008	0.875	0.009	0.887	0.035	99	98
PB -2A	57.1	2.5905	0.1446	0.2292	0.0032	0.24	4.3639	0.0610	0.0820	0.0050	0.2732	0.0117	0.74	18	48	53	0.91	1.330	0.017	1.298	0.041	1.245	0.120	102	106
PB -2A	52.1	0.6437	0.0166	0.0821	0.0006	0.56	12.1741	0.0942	0.0568	0.0015	0.2939	0.0032	0.07	154	1123	1267	0.89	0.509	0.004	0.505	0.010	0.485	0.058	100	104
PB -2A	34.1	0.9575	0.0349	0.1121	0.0011	0.65	8.9221	0.0910	0.0620	0.0024	0.2730	0.0090	0.12	31	182	176	1.04	0.685	0.007	0.682	0.018	0.673	0.082	100	101
PB -2A	38.1	1.1156	0.0531	0.1263	0.0013	0.66	7.9156	0.0831	0.0640	0.0031	0.1706	0.0281	0.63	17	49	91	0.54	0.767	0.008	0.761	0.025	0.743	0.101	100	103
PB -2A	25.1	1.1568	0.0503	0.1297	0.0015	0.37	7.7072	0.0905	0.0647	0.0030	0.0494	0.0072	0.28	17	18	104	0.17	0.786	0.009	0.780	0.024	0.763	0.097	100	103
PB -2A	35.1	1.2344	0.0549	0.1356	0.0016	0.70	7.3733	0.0896	0.0660	0.0032	0.1707	0.0077	0.21	18	56	97	0.58	0.820	0.009	0.816	0.025	0.807	0.102	100	101
PB -2A	77.1	1.6784	0.0374	0.1681	0.0020	0.05	5.9489	0.0721	0.0724	0.0016	0.1651	0.0053	0.07	57	123	254	0.49	1.002	0.011	1.000	0.014	0.998	0.046	100	100
PB -2A	58.1	2.0736	0.0465	0.1965	0.0015	0.61	5.0889	0.0381	0.0765	0.0017	0.0938	0.0028	0.08	116	123	472	0.26	1.157	0.008	1.140	0.015	1.109	0.046	101	104
PB -2A	56.1	1.7469	0.0417	0.1730	0.0013	0.67	5.7793	0.0446	0.0732	0.0018	0.0543	0.0020	0.07	98	74	453	0.16	1.029	0.007	1.026	0.015	1.020	0.049	100	100
PB -2A	19.1	1.8355	0.0375	0.1775	0.0014	0.70	5.6332	0.0437	0.0750	0.0017	0.3718	0.1604	0.18	98	143	454	0.32	1.053	0.008	1.058	0.013	1.068	0.046	99	98
PB -2A	41.1	0.3065	0.0550	0.0405	0.0010	0.31	24.6628	0.6372	0.0548	0.0107	0.3365	0.0346	0.62	5	86	76	1.14	0.256	0.006	0.271	0.044	0.405	0.335	94	63
PB -2A	62.1	0.2987	0.0198	0.0412	0.0008	0.37	24.3004	0.4598	0.0526	0.0039	0.1998	0.0145	0.38	14	142	244	0.58	0.260	0.005	0.265	0.016	0.313	0.164	97	82
PB -2A	7.1	0.3026	0.0200	0.0415	0.0008	0.33	24.1076	0.4646	0.0529	0.0041	0.2272	0.0137	1.31	10	134	189	0.71	0.262	0.005	0.268	0.016	0.325	0.171	97	80
PB -2A	11.1	0.2931	0.0957	0.0417	0.0032	0.20	23.9544	1.8568	0.0509	0.0206	0.6439	0.0762	2.68	2	66	32	2.04	0.264	0.020	0.261	0.071	0.237	0.525	101	111
PB -2A	32.1	0.3255	0.0231	0.0443	0.0007	0.29	22.5607	0.3473	0.0533	0.0042	0.1882	0.0174	0.26	13	127	207	0.61	0.280	0.004	0.286	0.018	0.340	0.180	97	82
PB -2A	44.1	0.3293	0.0429	0.0468	0.0009	0.52	21.3886	0.4039	0.0511	0.0072	0.2529	0.0423	0.30	8	107	106	1.01	0.295	0.005	0.289	0.034	0.244	0.237	101	120
PB -2A	71.1	0.3659	0.0334	0.0488	0.0012	0.38	20.4942	0.4879	0.0544	0.0056	0.1571	0.0146	1.01	9	61	139	0.44	0.307	0.007	0.317	0.025	0.387	0.211	97	79
PB -2A	92.1	0.6427	0.0219	0.0795	0.0012	0.03	12.5763	0.1864	0.0586	0.0024	0.1093	0.0080	0.59	26	69	258	0.27	0.493	0.007	0.504	0.014	0.553	0.091	97	89
PB -2A	89.1	0.6837	0.0700	0.0818	0.0028	0.19	12.2322	0.4155	0.0607	0.0080	0.3765	0.0418	1.06	6	45	51	0.89	0.507	0.017	0.529	0.042	0.627	0.279	95	80
PB -2A	6.1	0.5666	0.0412	0.0819	0.0016	0.01	12.2080	0.2457	0.0502	0.0043	0.2541	0.0291	0.25	13	94	118	0.80	0.508	0.010	0.456	0.026	0.203	0.183	111	250
PB -2A	69.1	0.7657	0.0835	0.0855	0.0027	0.34	11.6916	0.3657	0.0649	0.0083	0.4635	0.0348	0.64	7	65	49	1.33	0.529	0.016	0.577	0.051	0.772	0.302	91	68
PB -2A	68.1	0.7322	0.0353	0.0871	0.0015	0.01	11.4751	0.1932	0.0609	0.0031	0.3201	0.0112	0.29	21	141	157	0.90	0.539	0.009	0.558	0.021	0.637	0.113	96	84
PB -2A	36.1	0.6800	0.0450	0.0876	0.0013	0.57	11.4133	0.1717	0.0563	0.0041	0.1570	0.0101	0.88	12	54	98	0.55	0.541	0.008	0.527	0.027	0.464	0.155	102	116
PB -2A	60.1	0.7739	0.0946	0.0920	0.0019	0.01	10.8754	0.2271	0.0610	0.0084	0.0476	0.0256	0.92	7	8	59	0.13	0.567	0.011	0.582	0.054	0.641	0.295	97	88
PB -2A	75.1	0.8484	0.0443	0.0984	0.0020	0.33	10.1585	0.2036	0.0625	0.0037	0.2194	0.0400	0.18	11	52	78	0.66	0.605	0.012	0.624	0.024	0.692	0.127	97	87
PB -2A	74.1	1.0050	0.1429	0.1067	0.0052	0.25	9.3729	0.4534	0.0683	0.0124	0.5200	0.0544	3.68	5	41	29	1.45	0.653	0.030	0.706	0.075	0.878	0.368	92	74
PB -2A	27.1	0.9366	0.1055	0.1068	0.0027	0.30	9.3622	0.2382	0.0636	0.0078	0.3442	0.0240	0.98	7	41	40	1.01	0.654	0.016	0.671	0.053	0.728	0.264	97	89
PB -2A	5.1	1.0064	0.1003	0.1071	0.0036	0.18	9.3410	0.3117	0.0682	0.0084	0.4971	0.0600	2.42	4	37	23	1.64	0.656	0.021	0.707	0.052	0.874	0.262	92	75
PB -2A	54.1	0.8801	0.0708	0.1073	0.0016	0.12	9.3191	0.1407	0.0595	0.0052	0.3777	0.0412	0.27	17	100	98	1.02	0.657	0.009	0.641	0.037	0.585	0.178	102	112
PB -2A	47.1	0.9433	0.0475	0.1145	0.0012	0.57	8.7330	0.0914	0.0597	0.0031	0.3213	0.0149	0.15	22	144	122	1.19	0.699	0.007	0.675	0.024	0.594	0.108	103	117
PB -2A	63.1	1.5961	0.0593	0.1715	0.0025	0.97	5.8311	0.0859	0.0675	0.0027	0.2301	0.0071	4.37	25	110	101	1.08	1.020	0.014	0.969	0.024	0.853	0.082	105	119
PB -2C	82.1	0.6450	0.0286	0.0816	0.0010	0.49	12.2501	0.1455	0.0573	0.0026	0.1242	0.0401	0.50	19	73	182	0.40	0.506	0.006	0.505	0.018	0.503	0.100	100	100
PB -2C	83.1	0.6521	0.0294	0.0818	0.0010	0.27	12.2314	0.1487	0.0578	0.0027	0.3897	0.0113	0.12	24	249	189	1.32	0.507	0.006	0.510	0.018	0.524	0.106	99	96
PB -2C	76.1	0.6446	0.0151	0.0821	0.0007	0.38	12.1825	0.1065	0.0570	0.0012	0.1542	0.0025	0.10	65	293	608	0.48	0.509	0.004	0.505	0.009	0.490	0.047	100	103
PB -2C	29.1	0.6511	0.0196	0.0827	0.0008	0.40	12.0852	0.1156	0.0571	0.0018	0.0845	0.0041	0.17	35	92	349	0.27	0.512	0.005	0.509	0.012	0.494	0.068	100	103
PB -2C	73.1	0.6544	0.0201	0.0826	0.0008	0.01	12.1093	0.1200	0.0575	0.0017	0.1493	0.0032	0.17	33	149	315	0.47	0.512	0.005	0.511	0.012	0.510	0.068	100	100
PB -2C	32.1	0.6624	0.0264	0.0832	0.0010	0.46	12.0234	0.1488	0.0578	0.0024	0.2529	0.0625	2.57	11	53	105	0.51	0.515	0.006	0.516	0.016	0.521	0.092	99	98
PB -2C	3.1	0.7191	0.0252	0.0885	0.0011	0.62	11.3050	0.1392	0.0590	0.0024	0.0919	0.0056	1.01	26	72	253	0.28	0.546	0.006	0.550	0.015	0.566	0.088	99	96
PB -2C	62.1	0.7338	0.0346	0.0893	0.0013	0.01	11.2006	0.1604	0.0596	0.0031	0.1467	0.0069	0.44	17	73	153	0.48	0.551	0.008	0.559	0.020	0.589	0.113	98	93
PB -2C	18.1	0.7316	0.0235	0.0894	0.0010	0.93	11.1830	0.1190	0.0593	0.0020	0.0178	0.0055	0.28	28	17	275	0.06	0.552	0.006	0.558	0.014	0.580	0.075	99	95
PB -2C	55.1	0.7103	0.0352	0.0894	0.0014	0.69	11.1846	0.1746	0.0576	0.0032	0.2410	0.0094	1.16	15	111	126	0.88	0.552	0.008	0.545	0.021	0.515	0.121	101	107
PB -2C	79.1	0.7334	0.0195	0.0907	0.0009	0.30	11.0209	0.1036	0.0586	0.0015	0.0597	0.0051	0.17	58	116	534	0.22	0.560	0.005	0.559	0.011	0.553	0.057	100	101
PB -2C	30.1	0.7404	0.0297	0.0915	0.0011	0.40	10.9315	0.1367	0.0587	0.0025	0.1963	0.0060	0.13	21	111	176	0.63	0.564	0.007	0.563	0.018	0.556	0.098	100	101
PB -2C	77.1	0.7306	0.0178	0.0915	0.0008	0.72	10.9251	0.0966	0.0579	0.0013	0.0839	0.0090	0.25	58	117	509	0.23	0.565	0.005	0.557	0.010	0.526	0.049	101	107
PB -2C	58.1	0.7569	0.0304	0.0933	0.0013	0.15	10.7149	0.1448	0.0588	0.0026	0.1202	0.0076	0.37	19	62	159	0.39	0.575	0.007	0.572	0.018	0.561	0.093	100	102

PB -2C	88.1	0.7704	0.0351	0.0933	0.0014	0.28	10.7180	0.1558	0.0599	0.0031	0.1826	0.0110	0.60	15	62	120	0.52	0.575	0.008	0.580	0.020	0.600	0.113	99	95
PB -2C	94.1	0.7697	0.0164	0.0934	0.0008	0.37	10.7099	0.0871	0.0598	0.0013	0.1903	0.0084	0.15	54	246	431	0.57	0.575	0.004	0.580	0.009	0.596	0.049	99	96
PB -2C	24.1	0.7772	0.0352	0.0935	0.0013	0.36	10.6996	0.1508	0.0603	0.0030	0.1898	0.0067	0.27	21	105	166	0.63	0.576	0.008	0.584	0.020	0.615	0.107	98	93
PB -2C	37.1	0.7867	0.0321	0.0941	0.0015	0.46	10.6280	0.1738	0.0606	0.0028	0.1751	0.0137	1.55	15	65	126	0.52	0.580	0.009	0.589	0.018	0.627	0.098	98	92
PB -2C	4.1	0.7811	0.0242	0.0946	0.0011	0.37	10.5756	0.1212	0.0599	0.0021	0.1230	0.0078	0.21	27	84	233	0.36	0.582	0.006	0.586	0.014	0.600	0.079	99	97
PB -2C	60.1	0.7742	0.0191	0.0948	0.0009	0.10	10.5509	0.1018	0.0592	0.0014	0.0508	0.0028	0.17	48	78	438	0.18	0.584	0.005	0.582	0.011	0.576	0.053	100	101
PB -2C	11.1	0.7794	0.0244	0.0955	0.0011	0.51	10.4726	0.1195	0.0592	0.0021	0.1503	0.0257	0.92	22	89	177	0.51	0.588	0.006	0.585	0.014	0.574	0.075	100	102
PB -2C	1.1	0.7958	0.0355	0.0962	0.0014	0.62	10.3948	0.1537	0.0600	0.0032	0.1564	0.0091	0.67	17	74	146	0.50	0.592	0.008	0.594	0.020	0.604	0.116	99	98
PB -2C	56.1	0.8052	0.0665	0.0966	0.0024	0.43	10.3554	0.2567	0.0605	0.0058	0.2972	0.0173	0.25	8	63	56	1.14	0.594	0.014	0.600	0.038	0.620	0.219	99	95
PB -2C	39.1	0.7945	0.0306	0.0970	0.0015	0.01	10.3129	0.1593	0.0594	0.0025	0.1369	0.0081	0.20	14	49	115	0.42	0.597	0.009	0.594	0.017	0.583	0.094	100	102
PB -2C	31.1	0.7976	0.0308	0.0975	0.0012	0.65	10.2605	0.1228	0.0594	0.0025	0.1313	0.0064	0.29	27	97	217	0.45	0.600	0.007	0.595	0.017	0.580	0.089	100	103
PB -2C	61.1	0.8087	0.0246	0.0980	0.0011	0.11	10.2077	0.1112	0.0599	0.0019	0.0813	0.0044	0.13	33	76	279	0.27	0.602	0.006	0.602	0.014	0.599	0.070	100	100
PB -2C	43.1	0.8164	0.0317	0.0980	0.0016	0.39	10.2014	0.1627	0.0604	0.0027	0.0233	0.0103	0.54	12	13	114	0.11	0.603	0.009	0.606	0.018	0.618	0.099	99	97
PB -2C	2.1	0.8360	0.0379	0.1005	0.0015	0.12	9.9508	0.1507	0.0603	0.0032	0.1655	0.0109	0.74	15	56	119	0.47	0.617	0.009	0.617	0.021	0.616	0.118	100	100
PB -2C	85.1	0.8378	0.0463	0.1004	0.0018	0.01	9.9611	0.1750	0.0605	0.0039	0.0980	0.0115	0.51	11	25	86	0.29	0.617	0.010	0.618	0.026	0.622	0.139	99	99
PB -2C	57.1	0.8554	0.0193	0.1024	0.0009	0.28	9.7630	0.0893	0.0606	0.0013	0.0970	0.0084	0.25	59	138	478	0.29	0.629	0.005	0.628	0.010	0.624	0.047	100	100
PB -2C	86.1	0.8749	0.0193	0.1039	0.0009	0.10	9.6209	0.0801	0.0611	0.0014	0.1068	0.0065	0.10	47	106	361	0.29	0.637	0.005	0.638	0.010	0.641	0.050	99	99
PB -2C	63.1	0.8825	0.0197	0.1052	0.0010	0.91	9.5087	0.0879	0.0609	0.0013	0.1573	0.0029	0.33	72	243	484	0.50	0.645	0.006	0.642	0.011	0.634	0.047	100	101
PB -2C	17.1	0.8974	0.0355	0.1054	0.0014	0.87	9.4885	0.1217	0.0618	0.0027	0.1179	0.0231	0.22	25	98	197	0.50	0.646	0.008	0.650	0.019	0.666	0.094	99	97
PB -2C	84.1	0.9091	0.0537	0.1055	0.0020	0.03	9.4781	0.1780	0.0625	0.0044	0.4142	0.0141	1.40	12	87	68	1.27	0.647	0.012	0.657	0.028	0.691	0.151	98	93
PB -2C	90.1	0.8880	0.0228	0.1067	0.0010	0.01	9.3755	0.0863	0.0604	0.0017	0.2943	0.0083	0.12	46	264	301	0.88	0.653	0.006	0.645	0.012	0.617	0.058	101	105
PB -2C	54.1	0.9015	0.0264	0.1072	0.0012	0.73	9.3305	0.1018	0.0610	0.0018	0.2808	0.0052	0.37	35	212	235	0.90	0.656	0.007	0.653	0.014	0.639	0.064	100	102
PB -2C	48.1	0.8910	0.0348	0.1077	0.0017	0.01	9.2838	0.1464	0.0600	0.0026	0.2471	0.0101	0.21	15	85	102	0.83	0.659	0.010	0.647	0.019	0.603	0.094	101	109
PB -2C	16.1	0.9158	0.0500	0.1082	0.0018	0.17	9.2444	0.1537	0.0614	0.0038	0.3155	0.0119	0.34	16	103	99	1.04	0.662	0.010	0.660	0.026	0.653	0.129	100	101
PB -2C	53.1	0.9231	0.0184	0.1093	0.0009	0.24	9.1490	0.0777	0.0613	0.0011	0.2532	0.0035	0.06	114	700	772	0.91	0.669	0.005	0.664	0.010	0.648	0.039	100	103
PB -2C	59.1	0.9285	0.0196	0.1097	0.0010	0.17	9.1123	0.0806	0.0614	0.0012	0.0813	0.0020	0.09	82	180	627	0.29	0.671	0.006	0.667	0.010	0.652	0.043	100	102
PB -2C	46.1	0.9256	0.0245	0.1102	0.0012	0.74	9.0754	0.0998	0.0609	0.0017	0.2758	0.0226	0.28	35	200	233	0.86	0.674	0.007	0.665	0.013	0.637	0.058	101	105
PB -2C	33.1	0.9437	0.0450	0.1109	0.0016	0.37	9.0175	0.1327	0.0617	0.0033	0.3207	0.0111	0.52	18	132	111	1.19	0.678	0.009	0.675	0.023	0.664	0.111	100	102
PB -2C	65.1	1.8021	0.0368	0.1756	0.0016	0.93	5.6949	0.0516	0.0744	0.0015	0.2203	0.0022	0.05	78	261	345	0.76	1.043	0.009	1.046	0.014	1.053	0.042	99	99
PB -2C	66.1	1.8310	0.0537	0.1791	0.0020	0.13	5.5828	0.0631	0.0741	0.0023	0.1869	0.0037	0.15	30	79	126	0.62	1.062	0.011	1.057	0.019	1.045	0.064	100	101
PB -2C	9.1	1.8702	0.0578	0.1801	0.0023	0.78	5.5528	0.0697	0.0753	0.0027	0.1252	0.0051	0.19	29	47	125	0.38	1.067	0.012	1.071	0.020	1.077	0.072	99	99
PB -2C	81.1	1.8703	0.0374	0.1830	0.0016	0.41	5.4654	0.0465	0.0741	0.0013	0.1251	0.0019	0.12	88	107	379	0.28	1.083	0.008	1.071	0.013	1.045	0.037	101	103
PB -2C	25.1	1.9244	0.0489	0.1840	0.0017	0.20	5.4359	0.0505	0.0759	0.0020	0.2330	0.0051	0.16	52	173	202	0.86	1.089	0.009	1.090	0.017	1.092	0.053	99	99
PB -2C	22.1	1.9020	0.0601	0.1856	0.0021	0.28	5.3872	0.0623	0.0743	0.0026	0.1261	0.0068	0.64	31	58	128	0.45	1.098	0.012	1.082	0.021	1.050	0.069	101	104
PB -2C	36.1	2.3520	0.0555	0.2126	0.0018	0.72	4.7032	0.0403	0.0802	0.0018	0.1141	0.0189	0.10	50	53	182	0.29	1.243	0.010	1.228	0.016	1.203	0.044	101	103
PB -2C	70.1	2.4122	0.0605	0.2160	0.0023	0.30	4.6299	0.0486	0.0810	0.0021	0.1471	0.0047	0.14	39	64	141	0.46	1.261	0.012	1.246	0.018	1.221	0.050	101	103
PB -2C	23.1	2.4268	0.0619	0.2166	0.0021	0.47	4.6169	0.0457	0.0813	0.0022	0.1616	0.0083	0.10	57	110	196	0.56	1.264	0.011	1.251	0.018	1.228	0.052	101	102
PB -2C	19.1	0.8979	0.0882	0.1039	0.0029	0.01	9.6246	0.2669	0.0627	0.0075	0.0953	0.0219	1.26	6	15	49	0.31	0.637	0.017	0.651	0.044	0.697	0.227	97	91
PB -2C	78.1	0.9613	0.0559	0.1146	0.0017	0.07	8.7240	0.1276	0.0608	0.0038	0.3048	0.0456	0.37	12	58	77	0.75	0.700	0.010	0.684	0.030	0.633	0.133	102	110
PB -2C	64.1	1.0263	0.0353	0.1189	0.0014	0.15	8.4107	0.1001	0.0626	0.0023	0.0497	0.0053	0.29	28	30	199	0.15	0.724	0.008	0.717	0.018	0.695	0.078	100	104
PB -2C	52.1	1.0685	0.0251	0.1241	0.0012	0.92	8.0592	0.0764	0.0625	0.0014	0.1059	0.0078	0.20	72	160	498	0.32	0.754	0.007	0.738	0.012	0.690	0.050	102	109
PB -2C	92.1	0.7944	0.0180	0.0973	0.0008	0.55	10.2775	0.0857	0.0592	0.0014	0.1094	0.0030	0.06	55	173	438	0.40	0.599	0.005	0.594	0.010	0.575	0.052	100	104
PB -2C	35.1	0.6791	0.0371	0.0850	0.0014	0.01	11.7642	0.1907	0.0579	0.0035	0.2615	0.0204	0.21	19	140	158	0.88	0.526	0.008	0.526	0.023	0.528	0.130	99	99
PB -2C	91.1	0.6824	0.0314	0.0855	0.0012	0.50	11.6932	0.1675	0.0579	0.0030	0.2416	0.0154	0.36	14	78	115	0.68	0.529	0.007	0.528	0.019	0.525	0.113	100	100
PB -2C	75.2	2.2145	0.0437	0.2067	0.0017	0.88	4.8375	0.0403	0.0777	0.0014	0.1040	0.0017	0.27	73	142	280	0.51	1.211	0.009	1.186	0.014	1.139	0.036	102	106
PB -2C	6.1	10.8682	0.2217	0.4447	0.0052	0.97	2.2485	0.0265	0.1772	0.0044	0.1720	0.0120	0.30	41	50	59	0.84	2.372	0.024	2.512	0.019	2.627	0.042	94	90
PB -2C	80.1	10.9482	0.1917	0.4591	0.0039	0.45	2.1781	0.0184	0.1730	0.0027	0.2531	0.0027	0.04	105	141	152	0.93	2.436	0.017	2.519	0.016	2.586	0.025	96	94
PB -2C	10.1	12.1751	0.2359	0.4757	0.0054	0.99	2.1019	0.0237	0.1856	0.0042	0.1505	0.0036	0.16	48	35	65	0.55	2.509	0.023	2.618	0.019	2.704	0.039	95	92
PB -2C	74.1	12.2344	0.2193	0.4883	0.0042	0.21	2.0481	0.0175	0.1817	0.0028	0.1430	0.0048	0.14	39	26	55	0.47	2.563	0.018	2.623	0.016	2.669	0.025	97	96
PB -2C	5.1	0.6037	0.0358	0.0784	0.0014	0.19	12.7487	0.2275	0.0558	0.0038	0.3259	0.0432	2.38	2	7	23	0.32	0.487	0.008	0.480	0.022	0.445	0.145	101	109
PB -2C	69.1	1.1794	0.0384	0.1300	0.0015	0.17	7.6920	0.0901	0.0658	0.0023	0.2650	0.0104	0.29	25	98	141	0.70	0.788	0.009	0.791	0.018	0.800	0.076	99	98
PB -2C	95.1	1.4280	0.0531	0.1480	0.0020	0.99	6.7559	0.0909	0.0700	0.0037	0.1789	0.1480	1.42	9	35	56	0.63	0.890	0.011	0.901	0.022	0.928	0.125	98	95
PB -2C	13.1	4.1121	0.0968	0.2917	0.0029	0.84	3.4286	0.0343	0.1023	0.0025	0.1446	0.0537	0.10	43	34	113	0.30	1.650	0.015	1.657	0.019	1.665	0.046	99	99
PB -2C	87.1	4.6354	0.0734	0.3126	0.0022	0.53	3.1992	0.0228	0.1076	0.0017	0.2361	0.0077	0.06	103	157	231	0.68	1.753	0.011	1.756	0.013	1.758	0.029	99	99
PB -2C	38.1	4.9014	0.1030	0.3244	0.0032	0.91	3.0824	0.0304	0.1096	0.0022	0.1227	0.0034	0.04	62	65	143	0.46	1.811	0.016	1.802	0.018	1.792	0.036	100	101
PB -2C	40.1	5.5224	0.1101	0.3478	0.0032	0.01	2.8754	0.0266	0.1152	0.0021	0.1790	0.0019	0.06	84	119	180	0.66	1.924	0.015	1.904	0.017	1.882	0.034	101	102
PB -2C	71.1	0.2878	0.0614	0.0407	0.0017	0.34	24.5866	1.0572	0.0513	0.0130	0.3017	0.0447	1.54	6	120	102	1.18	0.257	0.011	0.257	0.048	0.255	0.294	100	100
PB -2C	72.1	0.2900	0.0189	0.0411	0.0007	0.27	24.3183	0.4001	0.0512	0.0036	0.5065	0.0381	2.68	4	88	64	1.38	0.260	0.004	0.259	0.014	0.248	0.152	100	104
PB -2C	12.1	0.3037	0.0133	0.0428	0.0006	0.11	23.3898	0.3185	0.0515	0.0026	0.1853	0.0080	0.79	21	220	368	0.60	0.270	0.004	0.269	0.010	0.264	0.116	100	102
PB -2C	34.1	0.3259	0.0115	0.0450	0.0005	0.62	22.2387	0.2330	0.0526	0.0020	0.1235	0.0050	0.17	29	216	511	0.42	0.284	0.003	0.286	0.009	0.310	0.085	99	91
PB -2C	26.1	0.3922	0.0166	0.0530	0.0006	0.51	18.8823	0.2315	0.0537	0.0025	0.1644	0.0065	0.17	20	149	292	0.51	0.333	0.004	0.336	0.012	0.359	0.109	99	92

PB -2C	49.1	0.4027	0.0157	0.0545	0.0007	0.32	18.3560	0.2329	0.0536	0.0022	0.1876	0.0087	0.25	22	204	308	0.66	0.342	0.004	0.344	0.011	0.355	0.094	99	96
PB -2C	67.1	0.4839	0.0330	0.0645	0.0011	0.05	15.5009	0.2703	0.0544	0.0042	0.3873	0.0199	0.46	11	125	112	1.12	0.403	0.007	0.401	0.022	0.388	0.171	100	104
PB -2C	7.1	6.1561	0.1079	0.3529	0.0032	0.44	2.8338	0.0255	0.1265	0.0025	0.0763	0.0025	0.07	81	45	178	0.25	1.948	0.015	1.998	0.015	2.050	0.035	97	95
PB -2C	75.1	8.9368	0.2269	0.4168	0.0049	0.83	2.3995	0.0281	0.1555	0.0038	0.0980	0.0210	0.00	2	3	-5	-0.51	2.246	0.022	2.332	0.022	2.408	0.041	96	93
PB -2C	41.1	20.3712	0.4533	0.5739	0.0075	0.92	1.7424	0.0227	0.2574	0.0056	0.1732	0.0269	0.19	50	33	63	0.53	2.924	0.031	3.109	0.021	3.231	0.034	94	90
PB -2C	93.1	0.2971	0.0119	0.0413	0.0005	0.31	24.2050	0.2904	0.0522	0.0024	0.2412	0.0152	0.23	29	379	498	0.76	0.261	0.003	0.264	0.009	0.292	0.102	98	89
PB -2C	50.1	0.2933	0.0143	0.0420	0.0006	0.26	23.8106	0.3418	0.0507	0.0027	0.2704	0.0074	0.36	18	261	301	0.87	0.265	0.004	0.261	0.011	0.225	0.121	101	117
PB -2C	47.1	0.2929	0.0137	0.0421	0.0007	0.50	23.7764	0.3888	0.0505	0.0026	0.3635	0.0223	1.62	13	222	218	1.02	0.266	0.004	0.261	0.011	0.219	0.116	101	121
PB -2C	89.1	0.3070	0.0203	0.0421	0.0008	0.49	23.7267	0.4337	0.0528	0.0041	0.1257	0.0145	0.63	10	74	190	0.39	0.266	0.005	0.272	0.016	0.321	0.176	97	82
PB -2C	20.1	0.4014	0.0802	0.0434	0.0025	0.41	23.0604	1.3446	0.0671	0.0162	0.9529	0.0629	2.26	4	108	38	2.82	0.274	0.016	0.343	0.057	0.842	0.518	79	32
PB -2C	68.1	0.5711	0.0623	0.0693	0.0019	0.57	14.4298	0.3959	0.0598	0.0076	0.1094	0.0267	0.92	5	21	56	0.38	0.432	0.012	0.459	0.043	0.595	0.278	94	72
PB -2C	51.1	0.5167	0.0483	0.0695	0.0017	0.57	14.3970	0.3579	0.0540	0.0058	0.3827	0.0275	0.56	8	97	69	1.41	0.433	0.010	0.423	0.031	0.369	0.234	102	117
PB -2C	15.1	0.6242	0.0863	0.0776	0.0028	0.54	12.8887	0.4724	0.0583	0.0095	0.2978	0.0312	0.66	8	80	68	1.17	0.482	0.017	0.492	0.054	0.543	0.339	97	88
PB -2C	27.1	0.6710	0.0266	0.0824	0.0010	0.04	12.1355	0.1504	0.0591	0.0025	0.2393	0.0071	0.30	23	150	205	0.73	0.510	0.006	0.521	0.016	0.569	0.095	97	89
PB -2C	8.1	0.7518	0.0680	0.0872	0.0023	0.36	11.4676	0.3013	0.0625	0.0068	0.6577	0.0223	1.17	9	120	60	2.00	0.539	0.014	0.569	0.039	0.692	0.241	94	77
PB -2C	42.1	0.7879	0.0383	0.0922	0.0019	0.01	10.8407	0.2186	0.0619	0.0035	0.6684	0.0181	0.55	14	179	81	2.20	0.569	0.011	0.590	0.022	0.672	0.127	96	84
PB -2C	21.1	0.7811	0.0373	0.0925	0.0014	0.01	10.8103	0.1611	0.0612	0.0033	0.1033	0.0073	0.30	17	55	150	0.36	0.570	0.008	0.586	0.021	0.648	0.120	97	88
PB -2C	45.1	0.7830	0.0450	0.0995	0.0022	0.29	10.0476	0.2171	0.0571	0.0039	0.1966	0.0761	0.79	10	87	69	1.26	0.612	0.013	0.587	0.025	0.494	0.147	104	123
PB -2C	14.1	0.9591	0.0992	0.1085	0.0033	0.23	9.2136	0.2800	0.0641	0.0079	0.4003	0.0245	0.61	8	62	46	1.34	0.664	0.019	0.683	0.052	0.745	0.274	97	89
PB -2C	44.1	0.9063	0.0428	0.1097	0.0021	0.16	9.1176	0.1745	0.0599	0.0033	0.3765	0.0204	0.31	14	97	72	1.36	0.671	0.012	0.655	0.023	0.601	0.120	102	111
PB -2C	28.1	17.1616	0.3215	0.5721	0.0043	0.40	1.7479	0.0132	0.2176	0.0036	0.1080	0.0046	-1.54	-3	-3	-4	0.62	2.916	0.018	2.944	0.018	2.963	0.027	99	98
PB -18	25.1	0.6915	0.0232	0.0860	0.0008	0.50	11.6259	0.1146	0.0583	0.0022	0.1637	0.0201	0.28	16	52	149	0.35	0.532	0.005	0.534	0.014	0.541	0.081	99	98
PB -18	24.1	0.6952	0.0270	0.0862	0.0010	0.42	11.5987	0.1370	0.0585	0.0026	0.1640	0.0213	1.14	15	51	127	0.40	0.533	0.006	0.536	0.016	0.548	0.096	99	97
PB -18	6.1	0.7091	0.0373	0.0863	0.0013	0.24	11.5901	0.1737	0.0596	0.0037	0.3430	0.0220	0.74	13	92	107	0.87	0.534	0.008	0.544	0.022	0.589	0.136	98	90
PB -18	16.1	0.7093	0.0205	0.0872	0.0007	0.64	11.4659	0.0965	0.0590	0.0018	0.1030	0.0488	0.15	29	25	280	0.09	0.539	0.004	0.544	0.012	0.567	0.067	99	95
PB -18	5.1	0.7054	0.0162	0.0876	0.0006	0.78	11.4157	0.0744	0.0584	0.0014	0.0263	0.0024	0.06	73	46	723	0.06	0.541	0.003	0.542	0.010	0.545	0.051	99	99
PB -18	64.1	0.6970	0.0353	0.0875	0.0013	0.41	11.4337	0.1749	0.0578	0.0033	0.2040	0.0123	0.38	18	99	161	0.61	0.541	0.008	0.537	0.021	0.522	0.128	100	103
PB -18	40.1	0.6906	0.0291	0.0876	0.0013	0.44	11.4107	0.1714	0.0572	0.0027	0.1013	0.0067	0.60	14	37	127	0.29	0.542	0.008	0.533	0.017	0.497	0.103	101	108
PB -18	81.1	0.6947	0.0399	0.0881	0.0013	0.19	11.3535	0.1620	0.0572	0.0036	0.2999	0.0182	0.64	24	195	204	0.96	0.544	0.007	0.536	0.024	0.500	0.144	101	108
PB -18	88.1	0.7231	0.0335	0.0905	0.0013	0.44	11.0542	0.1629	0.0580	0.0030	0.1578	0.0570	1.25	28	81	261	0.31	0.558	0.008	0.552	0.020	0.529	0.112	101	105
PB -18	37.1	0.7375	0.0192	0.0906	0.0010	0.34	11.0331	0.1212	0.0590	0.0017	0.0693	0.0038	0.11	27	50	243	0.21	0.559	0.006	0.561	0.011	0.568	0.061	99	98
PB -18	58.1	0.7352	0.0201	0.0915	0.0010	0.93	10.9272	0.1196	0.0583	0.0017	0.1145	0.0032	0.22	53	124	428	0.29	0.564	0.006	0.560	0.012	0.540	0.063	100	104
PB -18	43.1	0.7604	0.0211	0.0919	0.0011	0.32	10.8812	0.1256	0.0600	0.0018	0.0806	0.0047	0.23	23	43	202	0.21	0.567	0.006	0.574	0.012	0.604	0.066	98	93
PB -18	28.1	0.7477	0.0212	0.0921	0.0011	0.50	10.8571	0.1261	0.0589	0.0018	0.1745	0.0068	0.36	27	103	221	0.47	0.568	0.006	0.567	0.012	0.562	0.063	100	100
PB -18	91.1	0.7764	0.0547	0.0934	0.0019	0.38	10.7057	0.2173	0.0603	0.0049	0.3265	0.0130	0.62	18	104	130	0.80	0.576	0.011	0.583	0.031	0.614	0.177	98	93
PB -18	46.1	0.7750	0.0236	0.0936	0.0011	0.38	10.6784	0.1302	0.0600	0.0020	0.0573	0.0043	0.26	22	34	198	0.17	0.577	0.007	0.583	0.013	0.604	0.072	99	95
PB -18	38.1	0.7746	0.0185	0.0943	0.0010	0.75	10.5989	0.1110	0.0595	0.0015	0.1148	0.0143	0.07	36	86	305	0.28	0.581	0.006	0.582	0.011	0.587	0.057	99	98
PB -18	57.1	0.7745	0.0310	0.0947	0.0013	0.73	10.5553	0.1480	0.0593	0.0027	0.1205	0.0085	0.37	23	60	178	0.33	0.584	0.008	0.582	0.018	0.578	0.096	100	100
PB -18	26.1	0.7885	0.0243	0.0950	0.0012	0.64	10.5270	0.1307	0.0602	0.0020	0.1340	0.0057	0.15	22	63	173	0.37	0.585	0.007	0.590	0.014	0.611	0.070	99	95
PB -18	1.1	0.7939	0.0306	0.0965	0.0011	0.66	10.3662	0.1168	0.0597	0.0026	0.1835	0.0098	0.52	19	82	153	0.54	0.594	0.006	0.593	0.018	0.592	0.096	100	100
PB-18	77.1	0.7759	0.0622	0.0965	0.0017	0.17	10.3667	0.1867	0.0583	0.0051	0.1131	0.0140	0.88	10	27	88	0.31	0.594	0.010	0.583	0.035	0.542	0.182	101	109
PB -18	54.1	0.7937	0.0380	0.0978	0.0015	0.91	10.2262	0.1594	0.0589	0.0032	0.0824	0.0141	0.38	22	40	184	0.22	0.601	0.009	0.593	0.021	0.562	0.112	101	106
PB -18	7.1	0.8207	0.0355	0.0985	0.0012	0.39	10.1571	0.1279	0.0605	0.0030	0.2638	0.0087	1.54	19	112	131	0.86	0.605	0.007	0.608	0.020	0.620	0.106	99	97
PB -18	93.1	0.8398	0.0411	0.0991	0.0016	0.42	10.0878	0.1606	0.0614	0.0034	0.1064	0.0096	0.64	22	47	176	0.27	0.609	0.009	0.619	0.023	0.655	0.119	98	93
PB -18	61.1	0.8370	0.0521	0.1001	0.0018	0.53	9.9891	0.1846	0.0606	0.0043	0.1575	0.0141	0.92	13	42	103	0.41	0.615	0.011	0.618	0.028	0.627	0.147	99	98
PB-18	41.1	0.8452	0.0479	0.1020	0.0020	0.15	9.8085	0.1892	0.0601	0.0039	0.3071	0.0189	0.85	11	60	71	0.85	0.626	0.012	0.622	0.026	0.608	0.137	100	102
PB -18	73.1	0.8615	0.0352	0.1037	0.0013	0.21	9.6398	0.1180	0.0602	0.0027	0.0546	0.0072	0.14	23	29	195	0.15	0.636	0.007	0.631	0.019	0.612	0.096	100	103
PB -18	94.1	1.1292	0.0438	0.1275	0.0018	0.50	7.8446	0.1080	0.0642	0.0028	0.2108	0.0053	0.25	37	108	216	0.50	0.773	0.010	0.767	0.021	0.750	0.090	100	103
PB -18	20.1	1.2021	0.0363	0.1303	0.0012	0.81	7.6739	0.0696	0.0669	0.0022	0.1401	0.0098	0.24	15	37	89	0.42	0.790	0.007	0.802	0.016	0.835	0.066	98	94
PB-18	65.1	1.1915	0.0301	0.1327	0.0013	0.31	7.5335	0.0746	0.0651	0.0018	0.0624	0.0051	0.11	54	61	350	0.17	0.803	0.007	0.797	0.014	0.778	0.057	100	103
PB -18	39.1	1.6550	0.0428	0.1626	0.0019	0.58	6.1502	0.0726	0.0738	0.0020	0.1252	0.0054	0.06	30	50	144	0.34	0.971	0.011	0.991	0.016	1.037	0.055	97	93
PB -18	22.1	1.6974	0.0477	0.1644	0.0015	0.55	6.0809	0.0546	0.0749	0.0023	0.1422	0.0079	0.21	20	38	91	0.42	0.981	0.008	1.008	0.018	1.065	0.062	97	92
PB -18	75.1	1.6055	0.0504	0.1651	0.0018	0.87	6.0558	0.0655	0.0705	0.0026	0.0322	0.0056	1.83	30	26	162	0.16	0.985	0.010	0.972	0.021	0.943	0.078	101	104
PB -18	18.1	1.6526	0.0487	0.1661	0.0016	0.01	6.0220	0.0563	0.0722	0.0023	0.1788	0.0074	0.22	17	41	75	0.54	0.990	0.009	0.991	0.019	0.991	0.064	99	99
PB -18	68.1	1.7127	0.0871	0.1675	0.0030	0.01	5.9701	0.1060	0.0742	0.0044	0.1330	0.0113	0.55	14	22	66	0.34	0.998	0.016	1.013	0.032	1.046	0.119	98	95
PB -18	79.1	1.7517	0.0508	0.1725	0.0019	0.63	5.7957	0.0625	0.0736	0.0023	0.2231	0.0074	0.97	43	128	195	0.65	1.026	0.010	1.028	0.019	1.031	0.063	99	99
PB -18	67.1	1.7965	0.0806	0.1737	0.0028	0.01	5.7574	0.0932	0.0750	0.0039	0.3146	0.0122	0.58	19	67	79	0.84	1.032	0.015	1.044	0.029	1.069	0.106	98	96
PB -18	9.1	1.7964	0.0906	0.1742	0.0030	0.10	5.7417	0.1003	0.0748	0.0044	0.2816	0.0105	1.40	10	32	40	0.80	1.035	0.017	1.044	0.033	1.063	0.120	99	97
PB -18	78.1	5.3221	0.0986	0.3405	0.0032	0.33	2.9365	0.0276	0.1133	0.0023	0.2599	0.0438	0.10	50	66	113	0.59	1.889	0.015	1.872	0.016	1.854	0.037	100	101
PB -18	12.1	5.4354	0.1501	0.3408	0.0051	0.34	2.9342	0.0437	0.1157	0.0038	0.1919	0.0109	0.49	22	28	46	0.61	1.891	0.024	1.890	0.024	1.890	0.058	100	100
PB -18	21.1	5.6959	0.1166	0.3423	0.0020	0.67	2.9218	0.0171	0.1207	0.0024	0.1265	0.0137	0.06	83	48	196	0.24	1.898	0.010	1.931	0.018	1.967	0.036	98	96

PB -18	60.1	5.7454	0.2227	0.3572	0.0066	0.72	2.7995	0.0515	0.1167	0.0055	0.2646	0.0246	0.69	18	22	34	0.63	1.969	0.031	1.938	0.034	1.906	0.085	101	103
PB -18	3.1	3.1082	0.1064	0.2467	0.0032	0.01	4.0527	0.0526	0.0914	0.0036	0.1875	0.0100	0.28	16	26	49	0.54	1.422	0.017	1.435	0.027	1.454	0.077	99	97
PB -18	70.1	3.7327	0.1348	0.2765	0.0043	0.29	3.6163	0.0563	0.0979	0.0041	0.1841	0.0109	0.42	19	24	51	0.47	1.574	0.022	1.578	0.029	1.585	0.078	99	99
PB -18	2.1	3.8208	0.0965	0.2906	0.0026	0.28	3.4407	0.0308	0.0953	0.0026	0.1489	0.0070	0.19	38	46	100	0.45	1.645	0.013	1.597	0.021	1.535	0.052	102	107
PB -18	8.1	4.5002	0.1444	0.3096	0.0040	0.44	3.2300	0.0422	0.1054	0.0039	0.2837	0.0265	0.85	21	35	47	0.74	1.739	0.020	1.731	0.027	1.722	0.068	100	100
PB -18	76.1	4.5626	0.0821	0.3098	0.0028	0.01	3.2278	0.0296	0.1068	0.0020	0.1553	0.0034	0.23	85	92	219	0.42	1.740	0.014	1.742	0.015	1.746	0.034	99	99
PB -18	62.1	6.6605	0.2003	0.3805	0.0056	0.46	2.6279	0.0389	0.1269	0.0045	0.3389	0.0093	0.32	24	41	41	1.01	2.079	0.026	2.067	0.026	2.056	0.062	100	101
PB -18	50.1	7.0799	0.1292	0.3901	0.0038	0.55	2.5633	0.0249	0.1316	0.0024	0.1332	0.0042	0.05	89	65	167	0.39	2.123	0.018	2.122	0.016	2.120	0.032	100	100
PB -18	72.1	1.8146	0.0455	0.1785	0.0018	0.01	5.6015	0.0567	0.0737	0.0019	0.1805	0.0042	0.34	56	117	249	0.47	1.059	0.010	1.051	0.016	1.034	0.053	100	102
PB -18	33.1	1.6563	0.0537	0.1613	0.0022	0.76	6.1990	0.0859	0.0745	0.0026	0.0719	0.0055	0.27	16	18	82	0.22	0.964	0.012	0.992	0.020	1.054	0.068	97	91
PB-18	53.1	1.6679	0.1341	0.1716	0.0046	0.55	5.8285	0.1559	0.0705	0.0067	0.1242	0.0398	0.62	12	26	53	0.49	1.021	0.025	0.996	0.051	0.943	0.207	102	108
PB -18	74.1	1.5502	0.0716	0.1559	0.0022	0.84	6.4163	0.0894	0.0721	0.0034	0.1167	0.0130	0.55	25	37	162	0.23	0.934	0.012	0.951	0.027	0.990	0.093	98	94
PB -18	52.1	1.9068	0.0510	0.1844	0.0021	0.17	5.4236	0.0627	0.0750	0.0022	0.1282	0.0034	0.17	36	59	153	0.39	1.091	0.012	1.083	0.018	1.069	0.059	100	102
PB -18	71.1	1.9000	0.0435	0.1849	0.0018	0.71	5.4089	0.0518	0.0745	0.0018	0.0475	0.0293	0.36	42	61	187	0.33	1.094	0.010	1.081	0.015	1.056	0.049	101	103
PB -18	17.1	2.2061	0.0743	0.1939	0.0024	0.32	5.1563	0.0638	0.0825	0.0031	0.1694	0.0128	0.59	10	16	37	0.44	1.143	0.013	1.183	0.024	1.257	0.077	96	90
PB -18	90.1	0.9712	0.0321	0.1102	0.0014	0.59	9.0752	0.1127	0.0639	0.0022	0.0549	0.0056	0.18	40	40	294	0.14	0.674	0.008	0.689	0.016	0.739	0.073	97	91
PB -18	51.1	0.9676	0.0415	0.1114	0.0017	0.90	8.9764	0.1343	0.0630	0.0031	0.0865	0.0190	0.90	19	25	148	0.17	0.681	0.010	0.687	0.022	0.708	0.105	99	96
PB -18	82.1	1.0270	0.0612	0.1178	0.0018	0.88	8.4892	0.1316	0.0632	0.0042	0.2364	0.0132	2.44	15	101	91	1.11	0.718	0.011	0.717	0.031	0.716	0.143	100	100
PB-18	88.2	0.7597	0.0858	0.0947	0.0028	0.35	10.5599	0.3070	0.0582	0.0075	0.2712	0.0243	3.20	9	70	71	0.99	0.583	0.016	0.574	0.048	0.537	0.270	101	108
PB -18	66.1	0.7324	0.1220	0.0886	0.0039	0.11	11.2839	0.4938	0.0599	0.0118	0.0571	0.0355	1.87	5	9	44	0.20	0.547	0.023	0.558	0.077	0.601	0.361	98	91
PB -18	59.1	0.7256	0.1282	0.0903	0.0041	0.16	11.0789	0.4997	0.0583	0.0128	0.1572	0.0593	1.66	5	19	48	0.39	0.557	0.024	0.554	0.073	0.541	0.379	100	102
PB -18	23.1	0.6328	0.0223	0.0796	0.0008	0.40	12.5666	0.1317	0.0577	0.0022	0.1290	0.0124	0.27	12	43	117	0.36	0.494	0.005	0.498	0.014	0.517	0.088	99	95
PB -18	4.1	0.6746	0.0287	0.0838	0.0010	0.01	11.9310	0.1454	0.0584	0.0028	0.1469	0.0110	0.97	15	50	143	0.35	0.519	0.006	0.524	0.017	0.544	0.106	99	95
PB -18	14.1	0.3057	0.0106	0.0425	0.0004	0.58	23.5121	0.2257	0.0521	0.0020	0.1752	0.0301	0.23	17	196	278	0.71	0.269	0.003	0.271	0.008	0.291	0.086	99	92
PB -18	86.1	0.5579	0.0206	0.0717	0.0009	0.13	13.9556	0.1764	0.0565	0.0023	0.4088	0.0089	0.20	45	422	419	1.01	0.446	0.005	0.450	0.013	0.471	0.090	99	94
PB -18	35.1	0.6405	0.0415	0.0795	0.0016	0.11	12.5817	0.2599	0.0584	0.0045	0.1412	0.0178	0.49	8	32	75	0.43	0.493	0.010	0.503	0.026	0.547	0.167	98	90
PB -18	80.1	12.7728	0.2183	0.5123	0.0050	0.89	1.9520	0.0189	0.1808	0.0031	0.1340	0.0095	0.04	77	41	119	0.34	2.666	0.021	2.663	0.015	2.660	0.028	100	100
PB -18	92.1	0.2947	0.0188	0.0401	0.0007	0.50	24.9522	0.4448	0.0533	0.0038	0.2989	0.0205	0.29	24	309	407	0.76	0.253	0.004	0.262	0.015	0.343	0.159	96	73
PB -18	85.1	0.3486	0.0535	0.0417	0.0016	0.56	23.9929	0.9415	0.0607	0.0109	0.1223	0.0311	1.86	5	35	106	0.33	0.263	0.010	0.304	0.040	0.627	0.338	86	41
PB -18	84.1	0.3008	0.0907	0.0419	0.0026	0.24	23.8913	1.4742	0.0521	0.0183	0.1643	0.0676	8.58	4	31	66	0.48	0.264	0.016	0.267	0.069	0.291	0.405	98	90
PB -18	47.1	0.3082	0.0147	0.0439	0.0007	0.55	22.7715	0.3480	0.0509	0.0028	0.2045	0.0086	0.34	13	129	225	0.58	0.277	0.004	0.273	0.011	0.236	0.127	101	117
PB -18	29.1	0.3308	0.0111	0.0450	0.0006	0.01	22.2053	0.2779	0.0533	0.0019	0.1690	0.0063	0.43	23	164	374	0.44	0.284	0.003	0.290	0.008	0.340	0.083	97	83
PB -18	44.1	0.3369	0.0237	0.0459	0.0010	0.57	21.7707	0.4639	0.0532	0.0045	0.2576	0.0291	0.61	9	94	135	0.70	0.290	0.006	0.295	0.018	0.337	0.179	98	85
PB -18	83.1	0.3658	0.0882	0.0463	0.0020	0.01	21.5855	0.9169	0.0573	0.0153	0.1781	0.0671	1.43	3	28	55	0.50	0.292	0.012	0.317	0.066	0.502	0.431	92	58
PB -18	29.2	0.3542	0.0123	0.0481	0.0006	0.53	20.7693	0.2658	0.0534	0.0020	0.2280	0.0174	0.50	19	159	288	0.55	0.303	0.004	0.308	0.009	0.344	0.086	98	88
PB -18	48.1	0.5829	0.0368	0.0725	0.0014	0.55	13.7842	0.2654	0.0583	0.0043	0.1386	0.0132	1.37	13	58	133	0.44	0.451	0.008	0.466	0.024	0.540	0.164	96	83
PB -18	45.1	0.5587	0.0308	0.0738	0.0013	0.66	13.5413	0.2387	0.0549	0.0034	0.0957	0.0130	0.28	13	48	130	0.37	0.459	0.008	0.451	0.019	0.407	0.130	101	112
PB -18	56.1	0.5467	0.0344	0.0744	0.0014	0.73	13.4472	0.2456	0.0533	0.0038	0.1136	0.0123	0.60	15	45	148	0.30	0.462	0.008	0.443	0.023	0.342	0.152	104	135
PB -18	31.1	0.6899	0.0421	0.0815	0.0017	0.01	12.2771	0.2520	0.0614	0.0043	0.2022	0.0272	0.91	6	21	54	0.38	0.505	0.010	0.533	0.025	0.654	0.157	94	77
PB -18	15.1	0.7208	0.0357	0.0854	0.0013	0.12	11.7098	0.1842	0.0612	0.0035	0.1175	0.0136	0.65	6	19	54	0.35	0.528	0.008	0.551	0.021	0.647	0.127	95	81
PB -18	69.1	0.7256	0.0457	0.0877	0.0016	0.75	11.3979	0.2122	0.0600	0.0043	0.1535	0.0117	1.22	14	53	125	0.42	0.542	0.010	0.554	0.027	0.603	0.159	97	89
PB -18	42.1	0.7624	0.0460	0.0895	0.0018	0.16	11.1721	0.2303	0.0618	0.0044	0.3940	0.0170	0.47	10	77	69	1.11	0.553	0.011	0.575	0.027	0.666	0.152	96	82
PB -18	63.1	0.7805	0.1010	0.0915	0.0032	0.34	10.9259	0.3862	0.0619	0.0097	0.2461	0.0345	1.78	6	31	45	0.68	0.565	0.019	0.586	0.060	0.669	0.306	96	84
PB -18	36.1	0.8073	0.0416	0.0937	0.0017	0.46	10.6675	0.1924	0.0625	0.0036	0.1189	0.0103	1.14	9	25	77	0.33	0.578	0.010	0.601	0.023	0.690	0.127	96	83
PB -18	87.1	0.7462	0.0513	0.0940	0.0018	0.40	10.6396	0.2083	0.0576	0.0046	0.0781	0.0139	0.31	18	28	146	0.19	0.579	0.011	0.566	0.030	0.514	0.176	102	112
PB -18	49.1	0.8756	0.0583	0.1002	0.0022	0.05	9.9819	0.2152	0.0634	0.0049	0.2235	0.0150	0.41	10	44	72	0.61	0.615	0.013	0.639	0.033	0.721	0.179	96	85
PB -18	27.1	0.9042	0.0492	0.1031	0.0020	0.40	9.6994	0.1837	0.0636	0.0040	0.1776	0.0120	0.16	9	28	61	0.46	0.633	0.011	0.654	0.027	0.729	0.132	96	86
PB -18	34.1	1.8481	0.2648	0.1614	0.0089	0.01	6.1949	0.3410	0.0830	0.0144	0.1883	0.0637	1.99	2	5	10	0.55	0.965	0.049	1.063	0.103	1.270	0.350	90	75
PB -18	32.1	1.8213	0.0808	0.1706	0.0031	0.22	5.8618	0.1062	0.0774	0.0040	0.1516	0.0124	1.80	10	20	43	0.46	1.015	0.017	1.053	0.029	1.132	0.100	96	89
PB -18	55.1	1.8493	0.0654	0.1860	0.0026	0.65	5.3755	0.0740	0.0721	0.0029	0.1884	0.0093	0.55	31	60	121	0.50	1.100	0.014	1.063	0.023	0.989	0.078	103	111
PB -18	89.1	2.4238	0.1404	0.2036	0.0045	0.82	4.9112	0.1087	0.0863	0.0060	0.2661	0.0257	0.36	34	74	131	0.57	1.195	0.024	1.250	0.043	1.346	0.136	95	88
PB -11	63.1	0.6932	0.0318	0.0875	0.0013	0.39	11.4338	0.1761	0.0575	0.0027	0.1142	0.0111	0.36	18	44	168	0.26	0.540	0.008	0.535	0.019	0.510	0.101	101	105
PB -11	2.1	0.7155	0.0306	0.0881	0.0010	0.02	11.3513	0.1284	0.0589	0.0027	0.1301	0.0073	0.07	20	60	174	0.35	0.544	0.006	0.548	0.018	0.564	0.103	99	96
PB -11	44.1	0.7045	0.0163	0.0882	0.0008	0.76	11.3340	0.1050	0.0579	0.0014	0.0922	0.0030	0.20	45	105	406	0.26	0.545	0.005	0.541	0.010	0.526	0.053	100	103
PB -11	47	0.7447	0.0407	0.0914	0.0015	0.26	10.9439	0.1793	0.0591	0.0033	0.0903	0.0107	0.90	14	31	121	0.25	0.564	0.009	0.565	0.024	0.571	0.125	99	98
PB -11	2.2	0.7458	0.0399	0.0922	0.0012	0.41	10.8460	0.1439	0.0587	0.0034	0.1374	0.0096	0.37	13	45	112	0.40	0.569	0.007	0.566	0.023	0.555	0.125	100	102
PB -11	21.1	0.7698	0.0300	0.0925	0.0010	0.26	10.8120	0.1162	0.0604	0.0026	0.1213	0.0096	0.41	13	39	109	0.36	0.570	0.006	0.580	0.017	0.617	0.095	98	92
PB -11	60.1	0.7716	0.0229	0.0926	0.0013	0.54	10.7988	0.1468	0.0604	0.0016	0.0696	0.0046	0.31	36	61	314	0.20	0.571	0.007	0.581	0.013	0.619	0.061	98	92
PB -11	40	0.7535	0.0382	0.0935	0.0013	0.51	10.6956	0.1465	0.0584	0.0032	0.3737	0.0291	0.23	16	116	104	1.11	0.576	0.008	0.570	0.022	0.547	0.118	101	105
PB -11	37.1	0.7633	0.0498	0.0937	0.0015	0.16	10.6704	0.1734	0.0591	0.0043	0.2829	0.0191	0.45	10	52	68	0.76	0.577	0.009	0.576	0.030	0.570	0.157	100	101
PB -11	69.1	0.7909	0.0191	0.0975	0.0009	0.63	10.2606	0.0896	0.0589	0.0015	0.0093	0.0027	0.14	51	14	459	0.03	0.600	0.005	0.592	0.011	0.562	0.056	101	106

PB -11	90	0.8070	0.0231	0.0990	0.0009	0.69	10.0977	0.0967	0.0591	0.0017	0.0079	0.0026	0.54	52	11	451	0.03	0.609	0.006	0.601	0.013	0.571	0.064	101	106
PB -11	23.1	0.8310	0.0287	0.0992	0.0010	0.60	10.0793	0.1048	0.0607	0.0023	0.2892	0.0083	0.62	20	118	129	0.92	0.610	0.006	0.614	0.016	0.630	0.086	99	96
PB -11	61.1	0.8238	0.0222	0.0995	0.0013	0.82	10.0471	0.1311	0.0600	0.0014	0.0788	0.0028	0.12	41	73	344	0.21	0.612	0.008	0.610	0.012	0.605	0.051	100	101
PB -11	29.1	0.8335	0.0164	0.1008	0.0008	0.59	9.9216	0.0766	0.0600	0.0013	0.2985	0.0076	0.09	46	225	308	0.73	0.619	0.005	0.616	0.009	0.603	0.046	100	102
PB -11	68.1	0.8303	0.0486	0.1008	0.0018	0.15	9.9170	0.1778	0.0597	0.0036	0.6692	0.0376	0.27	19	174	108	1.62	0.619	0.011	0.614	0.027	0.593	0.133	100	104
PB -11	66.1	0.8494	0.0225	0.1018	0.0013	0.73	9.8275	0.1248	0.0605	0.0015	0.1063	0.0027	0.21	49	119	387	0.31	0.625	0.008	0.624	0.012	0.623	0.053	100	100
PB -11	76.1	0.8664	0.0298	0.1025	0.0011	0.47	9.7607	0.1091	0.0613	0.0024	0.0264	0.0060	0.40	25	15	208	0.07	0.629	0.007	0.634	0.016	0.651	0.084	99	96
PB -11	8.1	0.8570	0.0279	0.1028	0.0010	0.87	9.7290	0.0921	0.0605	0.0021	0.2103	0.0077	0.26	35	143	238	0.60	0.631	0.006	0.628	0.015	0.620	0.075	100	101
PB -11	27.1	0.8726	0.0261	0.1028	0.0010	0.20	9.7287	0.0939	0.0616	0.0020	0.0682	0.0082	0.18	21	31	158	0.20	0.631	0.006	0.637	0.015	0.659	0.074	99	95
PB -11	43.1	0.8419	0.0312	0.1031	0.0012	0.39	9.7028	0.1124	0.0592	0.0024	0.1823	0.0095	0.36	18	69	130	0.53	0.632	0.007	0.620	0.017	0.576	0.085	101	109
PB -11	78.1	0.8686	0.0274	0.1030	0.0011	0.59	9.7114	0.1009	0.0612	0.0022	0.1280	0.0092	0.30	30	72	226	0.32	0.632	0.006	0.635	0.015	0.646	0.074	99	97
PB -11	13.1	0.8769	0.0338	0.1039	0.0011	0.01	9.6215	0.1036	0.0612	0.0026	0.1926	0.0143	0.63	18	73	125	0.59	0.637	0.007	0.639	0.018	0.646	0.088	99	98
PB -11	55	0.9128	0.0497	0.1060	0.0018	0.21	9.4374	0.1575	0.0625	0.0037	0.0758	0.0104	1.46	11	20	84	0.24	0.649	0.010	0.659	0.028	0.691	0.127	98	94
PB -11	53	0.9050	0.0237	0.1065	0.0013	0.66	9.3896	0.1164	0.0616	0.0015	0.0969	0.0034	0.21	44	100	324	0.31	0.652	0.008	0.654	0.013	0.661	0.052	99	98
PB -11	51	0.8915	0.0297	0.1071	0.0014	0.77	9.3404	0.1249	0.0604	0.0020	0.1373	0.0121	0.27	28	68	204	0.33	0.656	0.008	0.647	0.016	0.618	0.070	101	106
PB -11	11.1	0.9544	0.0262	0.1104	0.0010	0.93	9.0558	0.0794	0.0627	0.0018	0.0197	0.0166	0.39	26	21	170	0.12	0.675	0.006	0.680	0.014	0.697	0.062	99	96
PB -11	45	0.9348	0.0299	0.1109	0.0015	0.66	9.0172	0.1199	0.0611	0.0019	0.0124	0.0046	0.57	36	13	283	0.05	0.678	0.009	0.670	0.016	0.644	0.065	101	105
PB -11	12.1	0.9568	0.0339	0.1124	0.0011	0.26	8.9001	0.0902	0.0618	0.0024	0.1428	0.0074	1.15	15	61	109	0.56	0.686	0.007	0.682	0.018	0.666	0.081	100	103
PB -11	38.1	1.6642	0.0338	0.1663	0.0015	0.38	6.0149	0.0548	0.0726	0.0015	0.0468	0.0036	0.08	55	32	271	0.12	0.991	0.008	0.995	0.013	1.003	0.042	99	98
PB -11	86	1.7408	0.0995	0.1699	0.0031	0.49	5.8874	0.1066	0.0743	0.0047	0.2997	0.0111	1.12	14	43	51	0.83	1.011	0.017	1.024	0.037	1.050	0.130	98	96
PB -11	73.1	1.7491	0.0429	0.1739	0.0016	0.01	5.7500	0.0536	0.0729	0.0020	0.2056	0.0043	0.24	51	117	213	0.55	1.034	0.009	1.027	0.016	1.012	0.054	100	102
PB -11	6.1	1.7777	0.0636	0.1742	0.0019	0.37	5.7410	0.0629	0.0740	0.0028	0.0994	0.0056	0.28	23	30	105	0.28	1.035	0.010	1.037	0.023	1.042	0.076	99	99
PB -11	89	1.8328	0.1035	0.1749	0.0032	0.12	5.7166	0.1036	0.0760	0.0049	0.4614	0.0155	0.74	14	70	48	1.47	1.039	0.017	1.057	0.038	1.095	0.131	98	94
PB -11	57.1	1.7923	0.0656	0.1772	0.0027	0.32	5.6425	0.0864	0.0733	0.0026	0.0909	0.0063	0.47	21	23	95	0.24	1.052	0.015	1.043	0.024	1.024	0.070	100	102
PB -11	85	1.7871	0.0507	0.1781	0.0018	0.99	5.6143	0.0562	0.0728	0.0022	0.2797	0.0129	0.99	46	171	176	0.97	1.057	0.010	1.041	0.019	1.008	0.062	101	104
PB -11	54	1.8443	0.1419	0.1800	0.0040	0.73	5.5563	0.1220	0.0743	0.0063	0.9731	0.2994	0.62	14	73	47	1.56	1.067	0.022	1.061	0.052	1.050	0.174	100	101
PB -11	52	2.3068	0.0587	0.2061	0.0027	0.62	4.8510	0.0627	0.0812	0.0020	0.0851	0.0054	0.56	35	38	132	0.28	1.208	0.014	1.214	0.018	1.225	0.048	99	98
PB -11	1.1	2.3605	0.0580	0.2115	0.0018	0.47	4.7272	0.0403	0.0809	0.0020	0.1269	0.0027	0.07	65	81	232	0.35	1.237	0.010	1.231	0.018	1.220	0.049	100	101
PB -11	20.1	2.4793	0.0789	0.2186	0.0023	0.34	4.5751	0.0489	0.0823	0.0028	0.2238	0.0109	1.05	10	23	33	0.69	1.274	0.012	1.266	0.023	1.252	0.065	100	101
PB -11	92	3.0262	0.1430	0.2401	0.0042	0.16	4.1642	0.0729	0.0914	0.0049	0.1770	0.0127	0.66	13	20	39	0.52	1.387	0.022	1.414	0.036	1.455	0.100	98	95
PB -11	32.1	2.9006	0.1295	0.2407	0.0036	0.40	4.1551	0.0617	0.0874	0.0044	0.2094	0.0162	2.57	8	14	24	0.59	1.390	0.019	1.382	0.033	1.370	0.095	100	101
PB -11	88	2.9825	0.0630	0.2451	0.0021	0.49	4.0795	0.0348	0.0882	0.0018	0.1225	0.0036	0.15	85	95	260	0.36	1.413	0.011	1.403	0.016	1.388	0.039	100	101
PB -11	83	5.2399	0.1041	0.3257	0.0027	0.57	3.0704	0.0257	0.1167	0.0021	0.0593	0.0038	0.10	90	32	202	0.16	1.817	0.013	1.859	0.016	1.906	0.032	97	95
PB -11	36.1	5.3000	0.0866	0.3295	0.0028	0.99	3.0347	0.0262	0.1167	0.0020	0.1701	0.0143	0.08	51	81	140	0.58	1.836	0.014	1.869	0.014	1.906	0.031	98	96
PB -11	67.1	5.2463	0.1392	0.3325	0.0049	0.92	3.0078	0.0442	0.1144	0.0029	0.2558	0.0169	0.89	28	45	66	0.68	1.850	0.024	1.860	0.024	1.871	0.046	99	98
PB -11	10.1	6.2925	0.1519	0.3670	0.0033	0.64	2.7246	0.0248	0.1243	0.0031	0.3599	0.0073	0.17	57	105	96	1.09	2.015	0.016	2.017	0.021	2.019	0.044	99	99
PB -11	18.1	6.5178	0.1446	0.3681	0.0036	0.51	2.7167	0.0262	0.1284	0.0029	0.2229	0.0176	0.48	31	46	54	0.86	2.020	0.017	2.048	0.019	2.077	0.041	98	97
PB -11	80.1	6.1950	0.1299	0.3696	0.0036	0.09	2.7058	0.0261	0.1216	0.0028	0.3942	0.0425	0.11	66	127	114	1.11	2.027	0.017	2.004	0.018	1.979	0.041	101	102
PB -11	87	6.5373	0.1395	0.3716	0.0035	0.87	2.6910	0.0250	0.1276	0.0027	0.1399	0.0257	0.02	85	70	156	0.45	2.037	0.016	2.051	0.019	2.065	0.036	99	98
PB -11	19.1	6.6046	0.1308	0.3731	0.0032	0.58	2.6803	0.0228	0.1284	0.0027	0.2281	0.0100	0.47	41	47	74	0.64	2.044	0.015	2.060	0.017	2.076	0.037	99	98
PB -11	15.1	6.6653	0.1160	0.3768	0.0028	0.70	2.6539	0.0196	0.1283	0.0023	0.1387	0.0033	0.07	67	54	130	0.42	2.061	0.013	2.068	0.015	2.075	0.032	99	99
PB -11	14.1	6.6585	0.1572	0.3782	0.0039	0.80	2.6443	0.0270	0.1277	0.0033	0.2605	0.0069	0.24	23	31	40	0.78	2.068	0.018	2.067	0.021	2.067	0.045	100	100
PB -11	9.1	12.1844	0.2676	0.5007	0.0041	0.28	1.9970	0.0163	0.1765	0.0037	0.3317	0.0251	0.32	16	21	19	1.14	2.617	0.018	2.619	0.020	2.620	0.034	99	99
PB -11	49	12.7978	0.2320	0.5135	0.0063	0.69	1.9475	0.0240	0.1808	0.0029	0.3247	0.0050	0.08	58	68	70	0.97	2.671	0.027	2.665	0.017	2.660	0.026	100	100
PB -11	4.1	13.2578	0.2941	0.5201	0.0046	0.01	1.9226	0.0171	0.1849	0.0041	0.1776	0.0097	0.07	55	42	70	0.60	2.700	0.020	2.698	0.021	2.697	0.036	100	100
PB -11	4.2	13.7492	0.2888	0.5329	0.0045	0.88	1.8764	0.0157	0.1871	0.0040	0.1314	0.0029	0.10	76	59	99	0.59	2.754	0.019	2.733	0.020	2.717	0.035	100	101
PB -11	79.1	7.4242	0.1852	0.3904	0.0047	0.15	2.5613	0.0311	0.1379	0.0039	0.1066	0.0045	0.53	26	16	51	0.31	2.125	0.022	2.164	0.022	2.201	0.049	98	96
PB -11	56	7.1233	0.1229	0.3729	0.0043	0.76	2.6820	0.0313	0.1386	0.0020	0.1143	0.0048	0.26	73	62	141	0.44	2.043	0.020	2.127	0.015	2.209	0.025	96	92
PB -11	84	5.5483	0.1080	0.3470	0.0028	0.01	2.8821	0.0235	0.1160	0.0021	0.0295	0.0009	0.20	56	13	126	0.10	1.920	0.014	1.908	0.016	1.895	0.033	100	101
PB -11	71.1	6.4586	0.1434	0.3604	0.0038	0.65	2.7750	0.0290	0.1300	0.0032	0.3704	0.0093	0.10	41	74	69	1.07	1.984	0.018	2.040	0.019	2.098	0.043	97	94
PB -11	46	3.4848	0.0880	0.2640	0.0036	0.76	3.7874	0.0511	0.0957	0.0022	0.1058	0.0061	0.22	33	28	96	0.30	1.510	0.018	1.524	0.020	1.542	0.044	99	97
PB -11	20.2	2.5784	0.0542	0.2210	0.0017	0.37	4.5244	0.0357	0.0846	0.0019	0.2023	0.0041	0.37	45	102	146	0.70	1.287	0.009	1.295	0.015	1.307	0.044	99	98
PB -11	35.1	1.6411	0.0304	0.1649	0.0014	0.67	6.0657	0.0530	0.0722	0.0013	0.0654	0.0018	0.08	66	49	309	0.16	0.984	0.008	0.986	0.012	0.991	0.037	99	99
PB -11	81.1	1.5780	0.1106	0.1566	0.0033	0.65	6.3864	0.1346	0.0731	0.0060	0.0956	0.0111	0.52	9	12	44	0.28	0.938	0.019	0.962	0.044	1.016	0.165	97	92
PB -11	17.1	1.5681	0.0660	0.1622	0.0020	0.01	6.1650	0.0769	0.0701	0.0033	0.2481	0.0242	0.64	14	50	57	0.88	0.969	0.011	0.958	0.026	0.932	0.095	101	104
PB -11	3.1	1.9649	0.0680	0.1857	0.0020	0.46	5.3838	0.0577	0.0767	0.0028	0.1867	0.0055	0.28	27	51	102	0.50	1.098	0.011	1.104	0.023	1.114	0.073	99	98
PB -11	42.1	2.0568	0.1163	0.1899	0.0033	0.20	5.2657	0.0917	0.0785	0.0048	0.1990	0.0176	1.48	7	16	28	0.56	1.121	0.018	1.135	0.038	1.161	0.122	98	96
PB -11	70.1	2.2358	0.0653	0.2031	0.0023	0.87	4.9233	0.0548	0.0798	0.0026	0.1299	0.0144	0.09	32	45	120	0.38	1.192	0.012	1.192	0.021	1.193	0.065	99	99
PB -11	30.1	1.1291	0.0239	0.1276	0.0010	0.41	7.8374	0.0638	0.0642	0.0015	0.3817	0.0062	0.32	48	242	234	1.03	0.774	0.006	0.767	0.011	0.748	0.048	100	103
PB -11	39.1	0.7666	0.0323	0.0950	0.0012	0.67	10.5268	0.1297	0.0585	0.0026	0.2874	0.0073	0.79	15	89	105	0.85	0.585	0.007	0.578	0.019	0.550	0.099	101	106
PB -11	40.1	0.7724	0.0222	0.0951	0.0010	0.01	10.5138	0.1069	0.0589	0.0018	0.4399	0.0083	0.63	38	267	241	1.11	0.586	0.006	0.581	0.013	0.563	0.065	100	103

PB -11	59.1	0.7086	0.0385	0.0871	0.0015	0.48	11.4814	0.1942	0.0590	0.0032	0.2570	0.0094	0.44	16	88	128	0.68	0.538	0.009	0.544	0.023	0.567	0.117	98	94
PB -11	33.1	0.7824	0.0322	0.0944	0.0011	0.99	10.5941	0.1206	0.0601	0.0024	0.1284	0.0095	0.20	16	45	94	0.48	0.581	0.006	0.587	0.017	0.608	0.089	99	95
PB -11	74.1	0.6699	0.0491	0.0835	0.0015	0.43	11.9794	0.2223	0.0582	0.0051	0.3839	0.0504	0.89	8	65	56	1.17	0.517	0.009	0.521	0.029	0.537	0.168	99	96
PB -11	48	0.6721	0.0494	0.0847	0.0016	0.42	11.8117	0.2209	0.0576	0.0045	0.1470	0.0170	1.25	9	40	88	0.45	0.524	0.009	0.522	0.029	0.514	0.160	100	101
PB -11	25.1	0.2955	0.0138	0.0420	0.0005	0.39	23.8379	0.2764	0.0511	0.0026	0.0963	0.0115	0.21	17	94	310	0.31	0.265	0.003	0.263	0.011	0.245	0.123	100	108
PB -11	24.1	0.4348	0.0146	0.0585	0.0006	0.01	17.1021	0.1652	0.0539	0.0020	0.1848	0.0074	0.41	20	140	252	0.55	0.366	0.003	0.367	0.010	0.368	0.084	99	99
PB -11	28.1	0.5618	0.0271	0.0737	0.0009	0.55	13.5776	0.1644	0.0553	0.0029	0.2567	0.0109	0.44	12	73	108	0.67	0.458	0.005	0.453	0.018	0.425	0.117	101	107
PB -11	5.1	0.5817	0.0169	0.0745	0.0007	0.21	13.4282	0.1176	0.0567	0.0017	0.0132	0.0025	0.03	41	19	464	0.04	0.463	0.004	0.466	0.011	0.478	0.067	99	96
PB -11	7.1	0.6066	0.0401	0.0767	0.0012	0.01	13.0296	0.2011	0.0573	0.0040	0.1176	0.0138	0.32	11	35	109	0.33	0.477	0.007	0.481	0.026	0.504	0.170	99	94
PB -11	64.1	0.6289	0.0206	0.0799	0.0011	0.76	12.5130	0.1686	0.0571	0.0018	0.2394	0.0061	0.32	36	200	321	0.62	0.496	0.006	0.495	0.013	0.494	0.068	100	100
PB -11	16.1	0.6401	0.0212	0.0802	0.0007	0.72	12.4708	0.1165	0.0579	0.0021	0.1136	0.0090	0.50	20	65	199	0.32	0.497	0.004	0.502	0.013	0.526	0.079	98	94
PB -11	72.1	10.2943	0.2008	0.4654	0.0045	0.42	2.1488	0.0209	0.1604	0.0034	0.2964	0.0074	0.07	54	67	74	0.92	2.463	0.020	2.462	0.018	2.460	0.036	100	100
PB -11	31.1	0.2717	0.0508	0.0416	0.0012	0.08	24.0241	0.7075	0.0473	0.0093	0.2775	0.0556	2.97	3	33	47	0.70	0.263	0.008	0.244	0.039	0.066	0.226	107	397
PB -11	77.1	0.3238	0.0175	0.0464	0.0006	0.14	21.5662	0.2992	0.0507	0.0031	0.1460	0.0112	0.37	16	128	283	0.45	0.292	0.004	0.285	0.013	0.225	0.142	102	129
PB -11	62.1	0.5863	0.0630	0.0812	0.0019	0.28	12.3133	0.2930	0.0524	0.0060	0.1508	0.0247	1.95	7	26	62	0.42	0.503	0.012	0.468	0.040	0.301	0.227	107	167
PB -11	91	0.7173	0.0359	0.0863	0.0012	0.42	11.5822	0.1658	0.0603	0.0033	0.1539	0.0070	0.51	16	58	137	0.43	0.534	0.007	0.549	0.021	0.613	0.120	97	87
PB -11	58.1	0.7364	0.0436	0.0881	0.0016	0.52	11.3467	0.2070	0.0606	0.0036	0.3238	0.0125	0.43	14	94	107	0.88	0.544	0.010	0.560	0.026	0.625	0.133	97	87
PB -11	75.1	0.8956	0.0674	0.1018	0.0021	0.32	9.8269	0.2068	0.0638	0.0057	0.2971	0.0228	1.66	9	45	59	0.77	0.625	0.013	0.649	0.038	0.736	0.198	96	84
PB -11	26.1	0.8340	0.0254	0.1027	0.0010	0.56	9.7352	0.0927	0.0589	0.0020	0.2800	0.0082	0.37	22	117	148	0.79	0.630	0.006	0.616	0.014	0.563	0.073	102	111
PB -11	50	0.8392	0.0394	0.1036	0.0016	0.28	9.6535	0.1465	0.0588	0.0028	0.1682	0.0110	0.40	21	77	153	0.51	0.635	0.009	0.619	0.022	0.558	0.105	102	113
PB -11	22.1	0.9601	0.0212	0.1157	0.0009	0.80	8.6413	0.0699	0.0602	0.0015	0.2832	0.0258	0.06	45	208	289	0.72	0.706	0.005	0.683	0.011	0.610	0.051	103	115
PB -11	34.1	0.9719	0.0359	0.1174	0.0013	0.91	8.5154	0.0934	0.0600	0.0026	0.2996	0.0140	0.14	17	98	101	0.97	0.716	0.007	0.689	0.019	0.605	0.092	103	118
PB -11	65.1	1.2397	0.0298	0.1311	0.0016	0.98	7.6292	0.0919	0.0686	0.0016	0.0494	0.0021	3.48	59	74	372	0.20	0.794	0.009	0.819	0.014	0.887	0.047	96	89
PB -11	41.1	1.3909	0.3058	0.1443	0.0070	0.17	6.9276	0.3367	0.0699	0.0177	0.1294	0.0594	7.62	2	3	10	0.33	0.869	0.039	0.885	0.132	0.925	0.517	98	93
PB -11	82.1	3.9140	0.0854	0.2687	0.0024	0.84	3.7219	0.0338	0.1057	0.0022	0.2665	0.0164	1.53	105	188	235	0.80	1.534	0.012	1.617	0.017	1.726	0.038	94	88
PB -12	4.1	0.6641	0.0597	0.0834	0.0021	0.15	11.9953	0.3030	0.0578	0.0062	0.1679	0.0333	3.17	5	21	41	0.52	0.516	0.013	0.517	0.037	0.521	0.216	99	99
PB -12	56.1	0.6648	0.0399	0.0836	0.0011	0.26	11.9656	0.1565	0.0577	0.0037	0.2755	0.0132	0.33	13	79	101	0.78	0.517	0.007	0.518	0.024	0.518	0.142	99	99
PB -12	78.1	0.6662	0.0400	0.0835	0.0013	0.01	11.9730	0.1932	0.0578	0.0039	0.5198	0.0451	0.47	18	155	124	1.25	0.517	0.008	0.518	0.023	0.524	0.138	99	98
PB -12	81.1	0.6814	0.0300	0.0840	0.0011	0.01	11.9117	0.1588	0.0589	0.0029	0.1040	0.0189	1.12	16	28	146	0.19	0.520	0.007	0.528	0.018	0.562	0.105	98	92
PB -12	34.1	0.6722	0.0165	0.0850	0.0007	0.89	11.7646	0.1028	0.0574	0.0014	0.1064	0.0072	0.36	52	145	482	0.30	0.526	0.004	0.522	0.010	0.505	0.052	100	104
PB -12	74.1	0.6875	0.0270	0.0850	0.0010	0.25	11.7621	0.1451	0.0587	0.0026	0.2315	0.0101	0.54	16	78	133	0.59	0.526	0.006	0.531	0.016	0.554	0.094	99	94
PB -12	68.1	0.7565	0.0233	0.0933	0.0008	0.23	10.7167	0.0896	0.0588	0.0020	0.0678	0.0067	0.18	21	35	181	0.19	0.575	0.005	0.572	0.013	0.560	0.071	100	102
PB -12	66.1	0.7587	0.0530	0.0943	0.0014	0.01	10.6070	0.1536	0.0584	0.0045	0.2270	0.0247	0.81	8	33	66	0.50	0.581	0.008	0.573	0.030	0.543	0.162	101	106
PB -12	47.1	0.7845	0.0280	0.0945	0.0009	0.01	10.5785	0.1040	0.0602	0.0022	0.1768	0.0065	0.36	27	98	200	0.49	0.582	0.005	0.588	0.016	0.610	0.081	99	95
PB -12	71.1	0.7723	0.0193	0.0947	0.0009	0.87	10.5591	0.1038	0.0591	0.0015	0.1964	0.0043	0.18	34	187	250	0.75	0.583	0.005	0.581	0.011	0.573	0.055	100	101
PB -12	24.1	0.7773	0.0432	0.0959	0.0014	0.86	10.4240	0.1500	0.0588	0.0035	0.1281	0.0149	2.02	10	53	75	0.71	0.591	0.008	0.584	0.024	0.558	0.129	101	105
PB -12	42.1	0.8526	0.0583	0.1007	0.0012	0.36	9.9309	0.1175	0.0614	0.0044	0.1395	0.0420	0.80	7	39	48	0.81	0.618	0.007	0.626	0.032	0.654	0.154	98	94
PB -12	46.1	0.8352	0.0350	0.1008	0.0008	0.33	9.9167	0.0816	0.0601	0.0027	0.1460	0.0090	0.08	22	70	160	0.44	0.619	0.005	0.616	0.020	0.606	0.099	100	102
PB -12	41.1	0.8504	0.0226	0.1022	0.0006	0.57	9.7871	0.0618	0.0604	0.0016	0.0025	0.0020	0.13	45	2	360	0.01	0.627	0.004	0.625	0.012	0.617	0.058	100	101
PB -12	26.1	0.8699	0.0351	0.1023	0.0012	0.70	9.7721	0.1154	0.0617	0.0024	0.0779	0.0296	0.69	16	12	125	0.10	0.628	0.007	0.636	0.019	0.662	0.081	98	94
PB -12	76.1	0.8914	0.0321	0.1037	0.0013	0.49	9.6391	0.1180	0.0623	0.0025	0.1399	0.0081	0.36	17	41	120	0.34	0.636	0.007	0.647	0.018	0.685	0.089	98	92
PB -12	18.1	1.3732	0.0352	0.1413	0.0012	0.75	7.0759	0.0604	0.0705	0.0018	0.1362	0.0070	0.08	40	72	197	0.37	0.852	0.007	0.878	0.015	0.942	0.051	97	90
PB -12	52.2	1.3674	0.0391	0.1434	0.0013	0.20	6.9746	0.0624	0.0692	0.0021	0.0984	0.0052	0.37	30	61	160	0.38	0.864	0.007	0.875	0.017	0.904	0.062	98	95
PB -12	19.1	1.3672	0.0411	0.1442	0.0014	0.98	6.9349	0.0679	0.0688	0.0021	0.0561	0.0097	0.74	19	25	82	0.31	0.868	0.008	0.875	0.017	0.892	0.062	99	97
PB -12	23.1	1.4183	0.0336	0.1456	0.0012	0.90	6.8674	0.0561	0.0706	0.0017	0.1182	0.0035	0.01	48	87	228	0.38	0.876	0.007	0.897	0.015	0.947	0.051	97	92
PB -12	61.1	1.4285	0.0285	0.1461	0.0010	0.81	6.8444	0.0474	0.0709	0.0015	0.0613	0.0087	0.64	36	29	205	0.14	0.879	0.006	0.901	0.012	0.955	0.043	97	92
PB -12	72.1	1.6460	0.0400	0.1620	0.0017	0.80	6.1715	0.0630	0.0737	0.0019	0.2298	0.0049	0.08	33	85	135	0.64	0.968	0.009	0.988	0.015	1.033	0.052	97	93
PB -12	31.1	1.6192	0.0383	0.1646	0.0015	0.01	6.0764	0.0553	0.0714	0.0016	0.1443	0.0133	0.20	48	101	210	0.48	0.982	0.008	0.978	0.015	0.968	0.046	100	101
PB -12	7.1	1.7033	0.0323	0.1652	0.0015	0.98	6.0538	0.0546	0.0748	0.0014	0.1064	0.0042	0.05	95	134	412	0.33	0.986	0.008	1.010	0.012	1.063	0.038	97	92
PB -12	94.1	1.7997	0.0511	0.1753	0.0016	0.94	5.7038	0.0505	0.0745	0.0022	0.0995	0.0018	0.23	67	84	300	0.28	1.041	0.009	1.045	0.019	1.054	0.059	99	98
PB -12	14.1	1.8020	0.0343	0.1757	0.0012	0.05	5.6917	0.0400	0.0744	0.0013	0.1260	0.0018	0.07	98	178	382	0.47	1.043	0.007	1.046	0.012	1.052	0.035	99	99
PB -12	59.1	1.8176	0.0618	0.1761	0.0017	0.64	5.6772	0.0564	0.0748	0.0029	0.1001	0.0119	0.37	13	19	56	0.34	1.046	0.010	1.052	0.023	1.064	0.076	99	98
PB -12	53.1	1.7791	0.0431	0.1772	0.0014	0.01	5.6449	0.0455	0.0728	0.0018	0.1236	0.0022	0.10	84	133	361	0.37	1.051	0.008	1.038	0.016	1.009	0.049	101	104
PB -12	65.1	1.9016	0.0314	0.1771	0.0011	0.86	5.6451	0.0364	0.0779	0.0013	0.1251	0.0018	0.05	72	108	295	0.36	1.051	0.006	1.082	0.011	1.143	0.033	97	91
PB -12	8.1	1.8010	0.0365	0.1782	0.0017	0.57	5.6104	0.0529	0.0733	0.0015	0.0964	0.0080	0.12	83	91	339	0.27	1.057	0.009	1.046	0.013	1.022	0.041	101	103
PB -12	38.1	4.1648	0.1122	0.3013	0.0023	0.76	3.3185	0.0252	0.1002	0.0026	0.2858	0.0255	0.15	26	52	59	0.88	1.698	0.011	1.667	0.022	1.629	0.049	101	104
PB -12	51.1	4.4720	0.1119	0.3022	0.0027	0.89	3.3086	0.0295	0.1073	0.0027	0.2174	0.0080	0.21	38	52	83	0.63	1.702	0.013	1.726	0.021	1.754	0.046	98	97
PB -12	17.1	4.4314	0.0911	0.3047	0.0025	0.83	3.2822	0.0272	0.1055	0.0021	0.1599	0.0048	0.20	54	71	113	0.63	1.714	0.012	1.718	0.017	1.723	0.036	99	99
PB -12	57.1	4.5127	0.1446	0.3091	0.0034	0.83	3.2349	0.0354	0.1059	0.0035	0.3552	0.0099	0.24	25	50	48	1.04	1.736	0.017	1.733	0.026	1.730	0.060	100	100
PB -12	91.1	4.6775	0.1358	0.3151	0.0031	0.55	3.1735	0.0310	0.1077	0.0032	0.2196	0.0054	0.21	50	74	111	0.67	1.766	0.015	1.763	0.025	1.760	0.056	100	100
PB -12	54.1	5.6765	0.1456	0.3492	0.0032	0.43	2.8637	0.0260	0.1179	0.0032	0.2202	0.0044	0.33	46	63	90	0.70	1.931	0.015	1.928	0.022	1.925	0.046	100	100

PB -12	5.1	5.9395	0.1278	0.3509	0.0040	0.68	2.8499	0.0321	0.1228	0.0027	0.1980	0.0111	0.04	61	76	110	0.69	1.939	0.019	1.967	0.019	1.997	0.040	98	97
PB -12	49.1	5.9261	0.1408	0.3567	0.0031	0.04	2.8032	0.0243	0.1205	0.0029	0.2519	0.0040	0.27	61	85	111	0.77	1.967	0.015	1.965	0.021	1.963	0.043	100	100
PB -12	29.1	6.0099	0.1615	0.3603	0.0042	0.25	2.7755	0.0327	0.1210	0.0032	0.3783	0.0158	0.53	39	85	63	1.36	1.984	0.020	1.977	0.023	1.971	0.046	100	100
PB -12	30.1	6.0953	0.1116	0.3657	0.0032	0.59	2.7347	0.0236	0.1209	0.0020	0.1549	0.0055	0.00	80	82	151	0.54	2.009	0.015	1.990	0.016	1.969	0.029	100	102
PB -12	89.1	6.5718	0.1803	0.3737	0.0035	0.83	2.6759	0.0254	0.1275	0.0035	0.1552	0.0038	0.04	63	61	118	0.52	2.047	0.017	2.056	0.024	2.064	0.048	99	99
PB -12	12.1	6.6911	0.1210	0.3759	0.0036	0.35	2.6604	0.0252	0.1291	0.0023	0.1444	0.0022	0.11	85	71	151	0.47	2.057	0.017	2.071	0.016	2.086	0.031	99	98
PB -12	55.1	6.6108	0.1595	0.3765	0.0033	0.13	2.6562	0.0234	0.1274	0.0031	0.3554	0.0050	0.26	59	105	95	1.11	2.060	0.016	2.061	0.021	2.062	0.043	99	99
PB -12	11.1	6.8385	0.1341	0.3842	0.0040	0.62	2.6025	0.0268	0.1291	0.0025	0.0614	0.0286	0.15	64	10	120	0.08	2.096	0.018	2.091	0.017	2.085	0.035	100	100
PB -12	73.1	0.3118	0.0074	0.0439	0.0004	0.59	22.7581	0.2058	0.0515	0.0013	0.1289	0.0148	0.33	51	383	851	0.45	0.277	0.002	0.276	0.006	0.262	0.056	100	105
PB -12	84.1	0.3261	0.0107	0.0452	0.0006	0.25	22.1404	0.3068	0.0524	0.0021	0.2193	0.0159	0.76	9	77	140	0.55	0.285	0.004	0.287	0.008	0.301	0.090	99	94
PB -12	25.1	0.3631	0.0107	0.0502	0.0005	0.77	19.9308	0.1847	0.0525	0.0016	0.2047	0.0264	2.43	26	192	391	0.49	0.316	0.003	0.315	0.008	0.307	0.066	100	102
PB -12	92.1	0.5898	0.0357	0.0751	0.0010	0.56	13.3236	0.1753	0.0570	0.0038	0.1824	0.0156	0.22	18	100	175	0.57	0.467	0.006	0.471	0.023	0.491	0.147	99	94
PB -12	6.1	0.6309	0.0185	0.0795	0.0009	0.93	12.5755	0.1400	0.0575	0.0019	0.0962	0.0650	0.24	23	5	241	0.02	0.493	0.005	0.497	0.012	0.512	0.071	99	96
PB -12	39.1	0.6399	0.0465	0.0806	0.0009	0.46	12.4012	0.1457	0.0576	0.0045	0.1777	0.0091	0.53	11	54	96	0.56	0.500	0.006	0.502	0.029	0.513	0.175	99	97
PB -12	45.1	0.6449	0.0251	0.0809	0.0006	0.78	12.3569	0.0944	0.0578	0.0023	0.2064	0.0085	0.32	25	141	227	0.62	0.502	0.004	0.505	0.015	0.522	0.087	99	96
PB -12	87.1	12.3264	0.3128	0.4942	0.0044	0.01	2.0235	0.0181	0.1809	0.0044	0.1597	0.0035	0.15	31	21	43	0.49	2.589	0.019	2.630	0.023	2.661	0.040	98	97
PB -12	63.1	12.9754	0.1826	0.5147	0.0033	0.09	1.9430	0.0126	0.1828	0.0026	0.1454	0.0032	0.22	20	11	27	0.41	2.677	0.014	2.678	0.013	2.679	0.024	99	99
PB -12	37.1	13.1504	0.2549	0.5217	0.0033	0.01	1.9170	0.0123	0.1828	0.0033	0.1252	0.0025	0.13	71	39	92	0.42	2.706	0.014	2.691	0.018	2.679	0.030	100	101
PB -12	79.1	0.7112	0.0217	0.0870	0.0009	0.72	11.4955	0.1240	0.0593	0.0020	0.5093	0.0183	0.52	29	277	185	1.50	0.538	0.006	0.545	0.013	0.578	0.071	98	93
PB -12	64.1	0.7560	0.0349	0.0907	0.0010	0.33	11.0307	0.1202	0.0605	0.0032	0.2071	0.0139	0.90	11	53	89	0.60	0.559	0.006	0.572	0.021	0.621	0.116	97	90
PB -12	22.1	0.8955	0.1293	0.1060	0.0037	0.01	9.4356	0.3261	0.0613	0.0104	1.1180	0.0699	1.92	4	53	15	3.50	0.649	0.021	0.649	0.070	0.649	0.348	100	100
PB -12	36.1	0.9108	0.0382	0.1067	0.0013	0.04	9.3682	0.1104	0.0619	0.0027	0.1282	0.0073	0.00	16	45	114	0.39	0.654	0.007	0.658	0.021	0.670	0.100	99	97
PB -12	58.1	0.9232	0.0224	0.1085	0.0008	0.01	9.2199	0.0690	0.0617	0.0016	0.0264	0.0069	0.13	29	13	223	0.06	0.664	0.005	0.664	0.012	0.665	0.056	99	99
PB -12	77.1	0.7917	0.0220	0.0960	0.0010	0.52	10.4117	0.1075	0.0598	0.0018	0.0753	0.0066	0.27	25	36	206	0.18	0.591	0.006	0.592	0.012	0.596	0.066	99	99
PB -12	85.1	0.8355	0.0712	0.0981	0.0017	0.25	10.1911	0.1808	0.0618	0.0058	0.1173	0.0211	0.95	8	20	62	0.32	0.603	0.010	0.617	0.040	0.666	0.203	97	90
PB -12	48.1	0.8232	0.0349	0.0980	0.0011	0.01	10.2039	0.1116	0.0609	0.0027	0.2448	0.0092	1.18	17	86	113	0.76	0.603	0.006	0.610	0.019	0.636	0.098	98	94
PB -12	20.1	1.1538	0.0364	0.1262	0.0013	0.01	7.9209	0.0790	0.0663	0.0022	0.0631	0.0046	0.31	23	24	129	0.18	0.766	0.007	0.779	0.017	0.815	0.069	98	94
PB -12	43.1	1.2007	0.0326	0.1333	0.0009	0.84	7.5012	0.0490	0.0653	0.0018	0.2897	0.0202	0.31	41	146	208	0.70	0.807	0.005	0.801	0.015	0.785	0.057	100	102
PB -12	52.1	1.4208	0.0609	0.1502	0.0017	0.43	6.6566	0.0757	0.0686	0.0031	0.1799	0.0122	0.31	15	38	72	0.54	0.902	0.010	0.898	0.026	0.887	0.092	100	101
PB -12	27.1	2.1143	0.0503	0.1953	0.0018	0.38	5.1195	0.0484	0.0785	0.0018	0.0925	0.0074	0.69	37	34	137	0.25	1.150	0.010	1.153	0.016	1.160	0.045	99	99
PB -12	93.1	2.1352	0.1201	0.1966	0.0029	0.77	5.0871	0.0738	0.0788	0.0048	0.1384	0.0122	1.06	14	23	53	0.43	1.157	0.015	1.160	0.037	1.167	0.113	99	99
PB -12	88.1	1.9078	0.0612	0.1831	0.0018	0.87	5.4605	0.0527	0.0756	0.0025	0.1481	0.0047	0.10	52	87	211	0.41	1.084	0.010	1.084	0.021	1.083	0.065	100	100
PB -12	21.1	2.3456	0.0721	0.2136	0.0023	0.36	4.6815	0.0503	0.0796	0.0025	0.1320	0.0146	1.01	32	43	110	0.39	1.248	0.012	1.226	0.022	1.188	0.064	101	105
PB -12	40.1	2.6145	0.1128	0.2226	0.0023	0.39	4.4924	0.0456	0.0852	0.0038	0.2081	0.0123	0.88	17	35	52	0.67	1.296	0.012	1.305	0.031	1.320	0.084	99	98
PB -12	40.2	2.7139	0.0885	0.2258	0.0019	0.78	4.4296	0.0367	0.0872	0.0029	0.0923	0.0065	0.20	19	19	64	0.29	1.312	0.010	1.332	0.024	1.365	0.064	98	96
PB -12	69.1	2.9010	0.1427	0.2394	0.0035	0.26	4.1767	0.0604	0.0879	0.0050	0.1454	0.0152	0.23	7	9	23	0.39	1.384	0.018	1.382	0.038	1.380	0.113	100	100
PB -12	15.1	3.1343	0.0722	0.2457	0.0021	0.19	4.0705	0.0355	0.0925	0.0021	0.1453	0.0035	0.54	37	68	101	0.68	1.416	0.011	1.441	0.018	1.478	0.042	98	95
PB -12	28.1	3.0885	0.1025	0.2514	0.0031	0.24	3.9781	0.0486	0.0891	0.0030	0.2278	0.0436	1.12	13	28	36	0.77	1.446	0.016	1.430	0.025	1.407	0.064	101	102
PB -12	50.1	3.2024	0.0759	0.2570	0.0021	0.22	3.8913	0.0322	0.0904	0.0022	0.1148	0.0089	2.23	77	65	229	0.29	1.474	0.011	1.458	0.018	1.434	0.045	101	102
PB -12	38.2	3.9074	0.0790	0.2824	0.0017	0.91	3.5416	0.0211	0.1004	0.0020	0.0756	0.0018	0.11	76	73	197	0.37	1.603	0.009	1.615	0.016	1.631	0.036	99	98
PB -12	62.1	4.0744	0.0579	0.2854	0.0017	0.59	3.5044	0.0213	0.1036	0.0015	0.1732	0.0037	0.16	110	141	264	0.54	1.618	0.009	1.649	0.011	1.689	0.026	98	95
PB -12	33.1	4.1923	0.0771	0.2867	0.0024	0.21	3.4874	0.0295	0.1060	0.0018	0.1849	0.0054	0.35	67	128	158	0.81	1.625	0.012	1.673	0.015	1.732	0.031	97	93
PB -12	67.1	5.1927	0.0950	0.3309	0.0025	0.82	3.0219	0.0226	0.1138	0.0022	0.1544	0.0042	0.03	39	38	85	0.45	1.843	0.012	1.851	0.015	1.861	0.035	99	99
PB -12	86.1	6.8410	0.2084	0.3672	0.0040	0.73	2.7235	0.0294	0.1351	0.0043	0.2160	0.0048	0.17	36	44	65	0.67	2.016	0.019	2.091	0.027	2.166	0.056	96	93
PB -12	90.1	7.4118	0.2347	0.3895	0.0044	0.41	2.5676	0.0290	0.1380	0.0046	0.1611	0.0069	0.23	25	22	45	0.49	2.120	0.020	2.162	0.029	2.203	0.058	98	96
PB -12	80.1	0.1913	0.0239	0.0243	0.0007	0.37	41.1641	1.1726	0.0571	0.0078	0.3926	0.0446	0.00	7	178	178	1.00	0.155	0.004	0.178	0.021	0.495	0.187	87	31
PB -12	1.1	0.2784	0.0140	0.0385	0.0006	0.25	25.9718	0.4018	0.0524	0.0029	0.7288	0.0188	0.20	20	505	247	2.05	0.244	0.004	0.249	0.011	0.305	0.135	97	79
PB -12	75.1	0.3001	0.0440	0.0391	0.0012	0.19	25.5965	0.8053	0.0557	0.0093	0.2778	0.0358	2.42	4	43	67	0.64	0.247	0.008	0.266	0.035	0.441	0.341	92	56
PB -12	82.1	0.2926	0.0147	0.0430	0.0008	0.53	23.2551	0.4455	0.0494	0.0030	0.2136	0.0214	1.70	7	71	123	0.58	0.271	0.005	0.261	0.012	0.165	0.122	104	164
PB -12	82.2	0.3002	0.0100	0.0431	0.0006	0.22	23.1756	0.3178	0.0505	0.0020	0.2389	0.0119	1.20	13	149	210	0.71	0.272	0.004	0.267	0.008	0.216	0.088	102	125
PB -12	92.2	0.5678	0.0378	0.0748	0.0010	0.09	13.3652	0.1838	0.0550	0.0040	0.2317	0.0284	0.97	16	103	151	0.69	0.465	0.006	0.457	0.024	0.414	0.159	101	112
PB -12	83.1	0.6760	0.0151	0.0829	0.0009	0.49	12.0555	0.1318	0.0591	0.0015	0.2211	0.0090	0.15	22	105	181	0.58	0.514	0.005	0.524	0.009	0.571	0.057	97	89
PB -12	10.1	0.7040	0.0185	0.0849	0.0009	0.73	11.7791	0.1271	0.0601	0.0016	0.0049	0.0068	0.09	49	2	469	0.01	0.525	0.005	0.541	0.011	0.609	0.059	97	86
PB -12	44.1	0.6667	0.0669	0.0864	0.0013	0.01	11.5803	0.1725	0.0560	0.0060	0.2087	0.0336	0.92	8	39	64	0.61	0.534	0.008	0.519	0.041	0.452	0.224	102	118
PB -12	32.1	0.7752	0.0757	0.0902	0.0019	0.66	11.0819	0.2332	0.0623	0.0066	0.1899	0.0287	1.51	6	29	50	0.58	0.557	0.011	0.583	0.044	0.685	0.245	95	81
PB -12	70.1	0.8461	0.1001	0.0962	0.0028	0.48	10.3993	0.3073	0.0638	0.0087	0.1075	0.0393	3.24	4	8	30	0.25	0.592	0.017	0.623	0.053	0.736	0.288	95	80
PB -12	9.1	0.9076	0.0431	0.1022	0.0017	0.16	9.7834	0.1616	0.0644	0.0035	0.2341	0.0166	0.75	14	62	92	0.67	0.627	0.010	0.656	0.023	0.755	0.116	95	83
PB -12	35.1	0.8615	0.0195	0.1053	0.0009	0.68	9.4962	0.0808	0.0593	0.0013	0.0497	0.0101	0.24	51	76	396	0.19	0.645	0.005	0.631	0.011	0.579	0.048	102	111
PB -12	16.1	0.8746	0.1108	0.1088	0.0032	0.15	9.1918	0.2692	0.0583	0.0081	0.3230	0.0423	0.97	5	30	29	1.01	0.666	0.019	0.638	0.056	0.541	0.287	104	122
PB -12	13.1	1.0194	0.0462	0.1120	0.0015	0.77	8.9256	0.1189	0.0660	0.0032	0.2628	0.0230	0.95	13	63	71	0.89	0.685	0.009	0.714	0.023	0.806	0.104	95	84
PB -12	3.1	1.4873	0.0324	0.1426	0.0014	0.91	7.0119	0.0702	0.0756	0.0017	0.0497	0.0026	3.10	52	44	280	0.16	0.859	0.008	0.925	0.013	1.085	0.044	92	79

PB -12	60.1	1.6506	0.1668	0.1499	0.0037	0.64	6.6696	0.1640	0.0798	0.0094	0.5736	0.0363	1.42	4	29	18	1.56	0.901	0.021	0.990	0.065	1.193	0.253	90	75
PB -12	2.1	1.6282	0.0679	0.1625	0.0026	0.70	6.1529	0.0990	0.0727	0.0034	0.1472	0.0156	8.74	17	27	61	0.43	0.971	0.014	0.981	0.026	1.004	0.091	98	96
PB -12	5.2	4.0790	0.1232	0.2596	0.0026	1.00	3.8523	0.0391	0.1140	0.0033	0.1699	0.0621	1.27	43	73	113	0.65	1.488	0.013	1.650	0.023	1.864	0.052	90	79
PB-32	34.1	0.6793	0.0191	0.0846	0.0008	0.97	11.8196	0.1094	0.0582	0.0016	0.0247	0.0037	0.1	133	2.8	1392	0.002	523.6	4.6	526.4	11.5	538.6	61.3	99	97
PB-32	47.1	0.6632	0.0394	0.0846	0.0015	0.41	11.8172	0.2052	0.0568	0.0039	0.2608	0.0121	1	30.9	-	274.8	-	523.7	8.7	516.5	23.3	485.2	138.8	101	107
PB-32	93.1	0.6862	0.0374	0.0855	0.0014	0.13	11.6972	0.1875	0.0582	0.0036	0.0972	0.0099	2.07	27.7	30	285.4	0.105	528.8	8.1	530.5	22.3	537.8	133.6	99	98
PB-32	6.1	0.6894	0.024	0.0862	0.0011	0.28	11.6012	0.1428	0.058	0.0022	0.3655	0.0078	0.55	51.3	344.5	416.7	0.827	533	6.3	532.4	14.4	530	83.4	100	100
PB-32	72.1	0.7119	0.0293	0.087	0.0008	0.01	11.492	0.112	0.0593	0.0026	0.2024	0.0071	0.27	47.5	-	421.1	-	537.9	5	545.9	17.2	579.3	92.6	98	92
PB-32	87.1	0.7008	0.0247	0.088	0.0011	0.71	11.3683	0.1365	0.0578	0.0022	0.5626	0.0298	0.16	107	645.4	728.9	0.885	543.5	6.3	539.3	14.8	521.6	84.2	100	104
PB-32	79.1	0.6964	0.0232	0.088	0.0009	0.35	11.3664	0.1176	0.0574	0.0021	0.1498	0.0068	0.58	45.7	-	420.2	-	543.6	5.4	536.6	13.7	507.2	77.5	101	107
PB-32	26.1	0.7185	0.0316	0.0885	0.0012	0.28	11.3005	0.1512	0.0589	0.0028	0.4271	0.0081	0.25	51.4	207.3	389.3	0.532	546.6	7	549.8	18.8	563	106.4	99	97
PB-32	17.1	0.7168	0.0466	0.0888	0.0013	0.25	11.2654	0.1611	0.0586	0.004	0.0385	0.0117	1.1	21.4	149.7	222.4	0.673	548.2	7.5	548.8	27.8	551	156	99	99
PB-32	29.1	0.7234	0.0243	0.089	0.0009	0.01	11.2317	0.1194	0.0589	0.0021	0.0855	0.0038	0.15	65.7	61.2	640.8	0.096	549.8	5.6	552.7	14.3	564.5	78.1	99	97
PB-32	59.1	0.7116	0.0283	0.0896	0.0008	0.58	11.1644	0.1055	0.0576	0.0024	0.0672	0.0078	0.44	47	-	450.6	-	553	5	545.7	16.6	515.4	88.2	101	107
PB-32	22.1	0.7349	0.0586	0.0911	0.0015	0.33	10.975	0.1827	0.0585	0.005	0.0592	0.0097	0.42	16.5	57.3	159.9	0.358	562.1	9	559.4	34.4	548.4	192.2	100	102
PB-32	27.1	0.7582	0.0234	0.0928	0.0009	0.45	10.7739	0.1066	0.0592	0.0019	0.0763	0.0047	0.11	99.2	127.9	935.7	0.137	572.2	5.4	572.9	13.3	576	67.4	99	99
PB-32	15.1	0.7764	0.034	0.094	0.001	0.37	10.6409	0.1156	0.0599	0.0028	0.2062	0.0114	0.49	52.1	76.3	439.6	0.174	579	6	583.4	19.4	600.5	100.1	99	96
PB-32	57.1	0.7926	0.0414	0.0944	0.0015	0.73	10.5914	0.1655	0.0609	0.0036	0.2508	0.0126	0.5	30.9	91.3	250.9	0.364	581.6	8.7	592.6	23.4	635.1	126.5	98	91
PB-32	70.1	0.7867	0.0224	0.0945	0.0008	0.01	10.5777	0.0856	0.0603	0.0018	0.0365	0.0025	0.11	96.6	-	915.1	-	582.3	4.5	589.3	12.7	616.1	62.5	98	94
PB-32	25.1	0.7653	0.0345	0.0947	0.0012	0.29	10.556	0.139	0.0586	0.0029	0.0629	0.0063	1.13	40.1	15.7	379.5	0.041	583.5	7.3	577.1	19.4	551.9	102	101	105
PB-32	20.1	0.761	0.0706	0.0949	0.0017	0.56	10.542	0.1893	0.0582	0.0059	0.3605	0.062	1.14	23.3	-	162.8	-	584.2	10	574.6	38.4	536.7	200.6	101	108
PB-32	19.1	0.7813	0.0345	0.0953	0.001	0.61	10.4879	0.1148	0.0594	0.0027	0.2968	0.0354	0.58	49.2	156.9	396.4	0.396	587.1	6.1	586.2	19.6	582.9	99.5	100	100
PB-32	88.1	0.7862	0.023	0.0961	0.0011	0.51	10.4084	0.1138	0.0593	0.0019	0.1191	0.0036	0.23	92	59.3	807.7	0.073	591.4	6.2	589	13.3	579.8	70.4	100	101
PB-32	73.1	0.8107	0.0257	0.0965	0.001	0.29	10.3599	0.1071	0.0609	0.0021	0.0569	0.0068	0.24	44.4	-	395.4	-	594	5.9	602.8	14.5	636.2	73.3	98	93
PB-32	60.1	0.8041	0.026	0.0973	0.0011	0.65	10.2785	0.1138	0.0599	0.0021	0.0715	0.0041	0.44	75.9	110.7	689.2	0.161	598.5	6.3	599.1	14.7	601.5	76.8	99	99
PB-32	38.1	0.8232	0.0357	0.0981	0.0014	0.76	10.1972	0.1473	0.0609	0.003	0.1519	0.0097	1.55	35.5	-	306.5	-	603.1	8.3	609.8	19.9	635.1	106.3	98	94
PB-32	36.1	0.8246	0.0292	0.0985	0.0011	0.1	10.1512	0.1152	0.0607	0.0023	0.1988	0.0042	0.24	64.4	47.3	514.6	0.092	605.7	6.6	610.6	16.5	629.1	84.8	99	96
PB-32	41.1	0.8368	0.0366	0.0991	0.0014	0.01	10.0942	0.1476	0.0613	0.003	0.0851	0.0071	1.04	33.8	-	303.5	-	608.9	8.5	617.4	20.4	648.4	108.2	98	93
PB-32	82.1	0.8278	0.0423	0.1005	0.0014	0.64	9.947	0.1429	0.0597	0.0034	0.121	0.0253	0.6	50.5	-	413	-	617.5	8.5	612.4	23.3	593.4	116.6	100	104
PB-32	35.1	0.8916	0.0349	0.106	0.0013	0.01	9.4371	0.1136	0.061	0.0026	0.0807	0.0055	0.65	49.1	60.8	409.6	0.148	649.3	7.4	647.2	18.6	640.1	88.8	100	101
PB-32	68.1	0.9168	0.042	0.1063	0.0011	0.23	9.4075	0.1011	0.0625	0.003	0.047	0.0082	0.82	30.9	-	261.4	-	651.2	6.6	660.6	22.7	693	108.3	98	93
PB-32	86.1	0.923	0.0375	0.1078	0.0014	0.39	9.2806	0.1247	0.0621	0.0028	0.0685	0.0095	0.31	44.2	-	361.8	-	659.7	8.4	664	19.5	678.6	91.9	99	97
PB-32	61.1	0.9434	0.0417	0.1086	0.0011	0.01	9.2064	0.0964	0.063	0.0029	0.1543	0.0073	0.44	36	-	264.8	-	664.7	6.6	674.7	22.3	708.1	101.6	98	93
PB-32	12.1	1.7506	0.0438	0.1685	0.0019	0.8	5.9331	0.0655	0.0753	0.002	0.0826	0.0078	0.36	53.6	125	266.9	0.468	1004	10.2	1027	16	1077	53.2	97	93
PB-32	91.1	1.6938	0.0509	0.1695	0.002	0.5	5.9009	0.0683	0.0725	0.0023	0.1422	0.0055	0.55	74.7	27.3	360.4	0.076	1009	10.8	1006	19	999.7	64.5	100	100
PB-32	77.1	1.7235	0.0566	0.1711	0.0019	0.58	5.8446	0.0661	0.0731	0.0026	0.115	0.0198	0.31	39.6	87.3	179.6	0.486	1018	10.7	1017	20.9	1016	70.2	100	100
PB-32	30.1	1.7311	0.0596	0.1712	0.002	0.36	5.8425	0.0682	0.0734	0.0027	0.1207	0.0043	0.63	62.3	17.2	306.8	0.056	1019	11	1020	21.9	1024	72.7	99	99
PB-32	64.1	1.7868	0.0602	0.1713	0.0016	0.01	5.837	0.0547	0.0756	0.0027	0.1135	0.0061	0.69	57.5	-	279.6	-	1019	8.8	1041	21.9	1086	70.5	97	93
PB-32	37.1	1.7805	0.0442	0.1719	0.0017	0.87	5.8189	0.0582	0.0751	0.0019	0.1093	0.0022	0.24	161	-	752.8	-	1022	9.4	1038	15.8	1072	50.6	98	95
PB-32	83.1	1.7911	0.0799	0.1722	0.0025	0.57	5.8071	0.0858	0.0754	0.0038	0.1066	0.0138	0.12	26.5	46	125.8	0.366	1024	14	1042	29.2	1080	101.8	98	94
PB-32	54.1	1.8056	0.0602	0.1748	0.0021	0.36	5.7206	0.07	0.0749	0.0027	0.0587	0.0062	0.19	68.6	76.7	349.4	0.22	1039	11.8	1048	22.1	1066	75	99	97
PB-32	80.1	1.8563	0.0565	0.1759	0.0019	0.41	5.6843	0.0629	0.0765	0.0025	0.1926	0.008	0.83	49.1	-	215.2	-	1045	10.6	1066	20.2	1109	65.9	98	94
PB-32	52.1	4.2451	0.1124	0.2926	0.0033	0.4	3.4181	0.038	0.1052	0.0029	0.2181	0.0038	0.98	110	83.3	283.2	0.294	1654	16.2	1683	21.7	1719	51.4	98	96
PB-32	48.1	4.3413	0.0918	0.2959	0.0027	0.01	3.3792	0.0309	0.1064	0.0022	0.1754	0.0055	0.09	311	-	823.3	-	1671	13.4	1701	17.3	1739	38.4	98	96
PB-32	7.1	4.3426	0.1223	0.3028	0.004	0.76	3.3028	0.0434	0.104	0.0032	0.1873	0.0076	2.31	43.7	115.4	107.1	1.077	1705	19.7	1702	23.2	1697	57.9	100	100
PB-32	33.1	4.4558	0.1613	0.303	0.0044	0.48	3.3008	0.0484	0.1067	0.0044	0.1346	0.0095	0.25	36.1	37.5	97.2	0.386	1706	22	1723	29.9	1743	73.5	99	97
PB-32	90.1	4.3888	0.1452	0.3042	0.0043	0.34	3.2874	0.0464	0.1046	0.0039	0.18	0.0093	0.34	43.2	26.7	111.7	0.239	1712	21.2	1710	26.9	1708	66.5	100	100
PB-32	81.1	4.4727	0.1053	0.305	0.0029	0.01	3.2784	0.031	0.1063	0.0026	0.2919	0.0061	0.16	109	-	248.5	-	1716	14.2	1726	19.5	1738	44.9	99	98
PB-32	23.1	5.7977	0.1836	0.3449	0.0038	0.45	2.8995	0.0321	0.1219	0.004	0.2994	0.007	0.4	47.6	-	97.7	-	1910	18.3	1946	27.3	1985	58.2	98	96
PB-32	94.1	5.7278	0.1325	0.3466	0.0037	0.86	2.8854	0.0307	0.1199	0.0029	0.2018	0.006	0.26	146	166.7	319.1	0.522	1918	17.7	1936	19.9	1954	43.2	99	98
PB-32	18.1	5.7145	0.172	0.3485	0.0036	0.25	2.8696	0.03	0.1189	0.0037	1.5158	0.0104	0.11	114	327.3	123.1	2.658	1927	17.5	1934	26.1	1940	55.2	99	99
PB-32	3.1	5.8593	0.1171	0.3539	0.0036	0.34	2.8255	0.029	0.1201	0.0025	0.4092	0.0049	0.08	141	305.2	256	1.192	1953	17.3	1955	17.3	1957	37.7	99	99
PB-32	49.1	0.6178	0.0334	0.0791	0.0012	0.42	12.6498	0.1956	0.0567	0.0034	0.2198	0.0085	0.96	34.3	205	337.9	0.607	490.5	7.3	488.5	21	479.1	136.7	100	102
PB-32	84.1	0.6183	0.0334	0.0791	0.0012	0.17	12.6401	0.1848	0.0567	0.0035	0.2215	0.0115	0.68	21.1	-	200.8	-	490.8	6.9	488.8	21	479.3	130.8	100	102
PB-32	43.1	0.6387	0.018	0.0805	0.0008	0.26	12.423	0.129	0.0575	0.0017	0.1036	0.0025	0.18	111	-	1192	-	499.1	5	501.5	11.1	512.6	64.1	99	97
PB-32	42.1	0.6593	0.0209	0.0824	0.0009	0.32	12.132	0.138	0.058	0.002	0.0097	0.0033	0.5	70.4	-	810.9	-	510.6	5.6	514.2	12.9	530.3	76.2	99	96
PB-32	71.1	0.8544	0.0221	0.1024	0.0008	0.01	9.7635	0.0757	0.0605	0.0016	0.0929	0.0027	0.24	144	-	1206	-	628.6	4.6	627.1	12.1	621.7	56	100	101
PB-32	62.1	0.9721	0.0331	0.114	0.001	0.83	8.7725	0.0785	0.0619	0.0022	0.1214	0.0064	0.5	67.2	-	523.3	-	695.9	5.9	689.6	17.2	669	77.3	100	104
PB-32	67.1	1.9047	0.0717	0.1791	0.0018	0.3	5.5843	0.0561	0.0771	0.0031	0.0684	0.0209	0.36	34.8	-	163.4	-	1062	9.8	1083	25.1	1125	79.9	98	94
PB-32	65.1	1.8315	0.0458	0.1795	0.0014	0.43	5.5726	0.0436	0.074	0.0019	0.1211	0.0039	0.25	147	-	684	-	1064	7.7	1057	16.5	1042	51.6	100	102
PB-32	13.1	1.9572	0.0625	0.1851	0.0018	0.62	5.4016	0.0514	0.0767	0.0025	0.1383	0.0066	0.18	72.3	26.4	303.8	0.087	1095	9.6	1101	21.6	1113	65.6	99	98

PB-32	28.1	1.7921	0.2277	0.1785	0.0073	0.01	5.6019	0.2299	0.0728	0.0111	0.468	0.0361	1.35	9	31.1	33	0.942	1059	39.7	1043	82.5	1009	312.7	101	104
PB-32	16.1	1.8743	0.2457	0.1775	0.0056	0.01	5.6334	0.1765	0.0766	0.0112	0.4709	0.0362	1.4	8.4	44	31	1.42	1053	30.3	1072	90.1	1110	318.9	98	94
PB-32	92.1	1.7668	0.0945	0.1735	0.0031	0.43	5.7621	0.1027	0.0738	0.0046	0.1207	0.0177	1.44	26.5	39.8	130	0.306	1032	17	1033	33.2	1037	114.5	99	99
PB-32	66.1	1.6053	0.072	0.1604	0.0018	0.77	6.2329	0.0691	0.0726	0.0035	0.1925	0.0106	1.3	38.3	-	191.3	-	959.2	9.9	972.3	28.2	1002	99.9	98	95
PB-32	63.1	1.5951	0.0446	0.1607	0.0013	0.01	6.2214	0.0518	0.072	0.0021	0.1916	0.0038	0.3	99.3	-	480.5	-	960.9	7.4	968.3	17.5	985.2	58.1	99	97
PB-32	96.1	1.6065	0.0364	0.1631	0.0016	0.69	6.1324	0.059	0.0714	0.0017	0.1766	0.0022	0.2	216	346	1060	0.326	973.8	8.7	972.7	14.1	970.3	47.1	100	100
PB-32	50.1	1.6196	0.0565	0.1641	0.002	0.59	6.0948	0.0754	0.0716	0.0027	0.2635	0.0084	0.17	68.2	308	307.9	1	979.4	11.3	977.8	22	974.3	77.8	100	100
PB-32	1.1	1.3811	0.0504	0.1462	0.002	0.06	6.8404	0.093	0.0685	0.0028	0.1857	0.0097	0.13	34.2	59.1	182.3	0.324	879.6	11.2	880.9	21.6	884.3	86.3	99	99
PB-32	32.1	1.3835	0.1189	0.1498	0.0039	0.41	6.6762	0.1757	0.067	0.007	0.2083	0.0245	1.21	14.7	3	79.6	0.037	899.8	22.1	881.9	52.4	837.4	222.5	102	107
PB-32	14.1	5.1798	0.1268	0.3147	0.0027	0.97	3.1779	0.0274	0.1194	0.003	0.1992	0.0067	0.09	101	29.5	251.2	0.118	1764	13.4	1849	21.7	1947	45.7	95	90
PB-32	21.1	7.0347	0.1589	0.3696	0.003	0.9	2.7057	0.0217	0.138	0.003	0.0914	0.0028	0.1	193	109.1	432.8	0.252	2028	14	2116	20	2203	38	95	92
PB-32	45.1	6.6917	0.1544	0.3761	0.0039	0.29	2.659	0.0278	0.129	0.0031	0.3233	0.0034	0.19	139	-	257.1	-	2058	18.4	2072	20.3	2085	41.9	99	98
PB-32	51.1	7.0986	0.2226	0.3849	0.0054	0.1	2.5979	0.0366	0.1337	0.0047	0.1037	0.0064	0.63	47.3	208	99.5	2.09	2099	25.3	2124	27.9	2148	60.5	98	97
PB-32	85.1	6.6396	0.1464	0.3891	0.004	0.95	2.5699	0.0264	0.1238	0.0029	0.1475	0.0084	0.27	123	83.5	259.3	0.322	2119	18.6	2065	19.7	2011	41.4	102	105
PB-32	59.1	7.6646	0.1813	0.3915	0.004	0.99	2.5541	0.0263	0.142	0.0035	0.1074	0.0067	0.06	160	-	324.2	-	2130	18.6	2193	21	2252	42.3	97	94
PB-32	75.1	1.1503	0.039	0.1272	0.0014	0.14	7.8605	0.0876	0.0656	0.0024	0.1755	0.0077	0.98	46	-	281.3	-	772	8.1	777.4	18.6	792.9	78.2	99	97
PB-32	11.1	1.1658	0.0317	0.1283	0.0014	0.6	7.7938	0.0871	0.0659	0.002	0.1856	0.0042	0.12	66.8	27.8	404.7	0.069	778.2	8.2	784.7	15	803.1	62.6	99	96
PB-32	56.1	1.2685	0.0461	0.1365	0.0017	0.38	7.3234	0.0929	0.0674	0.0027	0.2967	0.0092	0.51	64.3	359	353.1	1.017	825.1	9.8	831.7	20.8	849.5	83.1	99	97
PB-32	55.1	9.3775	0.2469	0.4519	0.0054	0.02	2.213	0.0265	0.1505	0.0043	0.2007	0.0065	0.79	16.9	-	28.7	-	2404	24	2376	24.2	2352	48.8	101	102
PB-32	40.1	10.0537	0.2222	0.4532	0.0047	0.84	2.2066	0.0229	0.1609	0.0037	0.3856	0.0047	0.24	158	-	231.1	-	2409	20.8	2440	20.5	2465	38.7	98	97
PB-32	89.1	12.7584	0.3908	0.4964	0.0081	0.81	2.0144	0.0328	0.1864	0.0062	0.0795	0.0105	0.31	34.3	28.7	52.2	0.55	2599	34.8	2662	27.4	2711	53.4	97	95
PB-32	74.1	15.993	0.3923	0.5573	0.0068	0.23	1.7943	0.0219	0.2081	0.0054	0.2027	0.0094	0.37	46	-	56.3	-	2856	28.2	2876	23.8	2891	42.7	99	98
PB-32	39.1	0.288	0.0131	0.0401	0.0006	0.15	24.9174	0.3471	0.0521	0.0026	0.2305	0.0056	1.31	46.7	-	916.4	-	253.7	3.5	257	10.3	287.6	115.5	98	88
PB-32	31.1	0.2859	0.0239	0.0411	0.0008	0.37	24.3247	0.501	0.0504	0.0048	0.1882	0.0151	1.11	19.9	105	390.7	0.269	259.7	5.2	255.3	18.8	214.9	190	101	120
PB-32	8.1	0.7112	0.0773	0.0782	0.0024	0.01	12.7832	0.3897	0.0659	0.0081	0.429	0.1126	0.75	10.3	14.1	93.8	0.151	485.5	14.2	545.5	46.9	804.4	297.7	89	60
PB-32	10.1	0.6768	0.0738	0.0786	0.0023	0.36	12.7164	0.3691	0.0624	0.008	0.2667	0.0366	2.66	8	215.3	81.8	2.633	488	13.6	524.8	45.3	688.5	301.5	92	70
PB-32	2.1	0.6722	0.0672	0.0799	0.0021	0.15	12.5164	0.3343	0.061	0.0069	0.2086	0.0337	0.82	10.1	88.3	99.2	0.89	495.5	12.7	522.1	39.9	640	235.1	94	77
PB-32	9.1	0.7208	0.0844	0.0864	0.0026	0.51	11.5744	0.346	0.0605	0.008	0.3467	0.0363	0	9.3	142.2	76.4	1.86	534.2	15.3	551.2	49	621.9	251.8	96	85
PB-32	78.1	0.7263	0.0239	0.0875	0.0009	0.01	11.4222	0.1225	0.0602	0.0021	0.2599	0.0063	0.54	51.1	-	428.7	-	541	5.6	554.4	14.2	609.6	79.2	97	88
PB-32	58.1	0.7524	0.0384	0.0896	0.0014	0.57	11.1545	0.1721	0.0609	0.0035	0.1151	0.0127	0.27	33.1	260.9	294.4	0.886	553.5	8.2	569.6	23.1	634.7	130.3	97	87
PB-32	95.1	0.7802	0.0737	0.0915	0.0023	0.57	10.9269	0.2796	0.0618	0.0068	0.2117	0.0303	1.04	14.1	57.2	120.4	0.475	564.5	13.8	585.6	41.8	668.1	235.9	96	84
PB-32	53.1	0.7258	0.0492	0.0917	0.0017	0.03	10.9062	0.1999	0.0574	0.0043	0.0645	0.0106	1.69	19.6	283.4	189.8	1.493	565.5	9.9	554.1	28.5	507.2	163.8	102	111
PB-32	44.1	0.8004	0.0745	0.092	0.0026	0.65	10.875	0.308	0.0631	0.0063	0.2058	0.0229	0.68	43.4	-	323.9	-	567.1	15.3	597.1	43.1	712.7	223.7	94	79
PB-32	24.1	0.8116	0.0733	0.0938	0.0018	0.18	10.6635	0.2005	0.0628	0.0061	0.1003	0.0238	0.68	17.3	30.4	159.7	0.19	577.8	10.4	603.3	39.6	700.4	202.9	95	82
PB-32	4.1	0.84	0.043	0.0979	0.0016	0.65	10.2101	0.1657	0.0622	0.0037	0.167	0.0126	1.68	19.8	220	175.2	1.255	602.3	9.3	619.1	24	681	131.9	97	88
PB-32	46.1	0.8781	0.052	0.1004	0.0019	0.01	9.9626	0.1871	0.0634	0.0043	0.181	0.0136	1.48	23.2	-	185.7	0.072	616.6	11	640	27.8	723.3	145.6	96	85
PB-32	5.1	1.0529	0.0802	0.1154	0.0026	0.29	8.6644	0.1972	0.0662	0.0057	0.1108	0.0311	0.71	13.8	93	99.5	0.935	704.1	15.2	730.3	41	811.7	192.7	96	86
PB-32	76.1	1.2947	0.1031	0.1332	0.0032	0.01	7.5052	0.1783	0.0705	0.0063	0.1025	0.0273	2.39	8.5	13.3	51.9	0.256	806.3	17.9	843.4	47.4	942.1	196.4	95	85
PB-33	50.1	0.6617	0.0250	0.0834	0.0008	0.33	11.9956	0.1110	0.0576	0.0023	0.2566	0.0060	0.74	58	4	557	0.01	516	5	516	15	513	89	100	100
PB-33	68.1	0.6780	0.0319	0.0855	0.0009	0.58	11.7008	0.1220	0.0575	0.0028	0.1485	0.0097	3.03	47	17	468	0.04	529	5	526	19	512	106	100	103
PB-33	26.1	0.7062	0.0450	0.0865	0.0013	0.23	11.5643	0.1790	0.0592	0.0043	0.1268	0.0105	0.62	27	20	264	0.07	535	8	543	27	576	163	98	92
PB-33	91.1	0.7006	0.0226	0.0866	0.0011	0.01	11.5515	0.1426	0.0587	0.0020	0.0760	0.0083	0.74	58	154	615	0.25	535	6	539	14	556	78	99	96
PB-33	87.1	0.6848	0.0243	0.0866	0.0012	0.52	11.5506	0.1544	0.0574	0.0022	0.1308	0.0074	0.48	42	79	407	0.20	535	7	530	15	506	86	101	105
PB-33	79.1	0.7009	0.0204	0.0880	0.0008	0.32	11.3638	0.0989	0.0578	0.0017	0.0441	0.0046	0.34	107	21	1159	0.02	544	5	539	12	521	64	100	104
PB-33	17.1	0.7042	0.0336	0.0880	0.0010	0.39	11.3601	0.1328	0.0580	0.0029	0.2069	0.0193	0.69	35	17	328	0.05	544	6	541	20	531	112	100	102
PB-33	4.1	0.7095	0.0226	0.0887	0.0010	0.14	11.2757	0.1332	0.0580	0.0021	0.1694	0.0069	0.68	35	10	331	0.03	548	6	545	13	531	80	100	103
PB-33	29.1	0.7066	0.0470	0.0891	0.0014	0.40	11.2235	0.1763	0.0575	0.0043	0.1246	0.0192	0.75	27	10	268	0.04	550	8	543	27	512	160	101	107
PB-33	14.1	0.7075	0.0269	0.0893	0.0009	0.37	11.2018	0.1092	0.0575	0.0023	0.1526	0.0085	1.31	44	10	426	0.02	551	5	543	16	510	84	101	108
PB-33	64.1	0.7151	0.0292	0.0893	0.0009	0.76	11.2012	0.1070	0.0581	0.0025	0.0751	0.0073	0.97	62	3	632	0.01	551	5	548	17	533	92	100	103
PB-33	80.1	0.7205	0.0475	0.0892	0.0013	0.45	11.2107	0.1594	0.0586	0.0041	0.0999	0.0150	4.29	26	-	259	-	551	8	551	27	552	152	99	99
PB-33	62.1	0.7432	0.0368	0.0920	0.0010	0.30	10.8691	0.1197	0.0586	0.0031	0.0416	0.0073	0.80	44	-9	439	-0.02	567	6	564	22	552	116	100	102
PB-33	21.1	0.7431	0.0274	0.0923	0.0009	0.01	10.8340	0.1034	0.0584	0.0023	0.0975	0.0066	0.30	47	6	449	0.01	569	5	564	16	544	82	100	104
PB-33	31.1	0.7449	0.0210	0.0925	0.0008	0.49	10.8146	0.0929	0.0584	0.0018	0.0829	0.0040	0.12	89	4	853	0.01	570	5	565	12	546	68	100	104
PB-33	19.1	0.7488	0.0189	0.0931	0.0007	0.73	10.7385	0.0816	0.0583	0.0015	0.1000	0.0137	0.17	112	37	1108	0.03	574	4	568	11	542	55	101	105
PB-33	11.1	0.7620	0.0182	0.0943	0.0009	0.50	10.6053	0.0986	0.0586	0.0015	0.3819	0.0037	0.27	69	52	519	0.10	581	5	575	10	553	55	100	105
PB-33	37.1	0.7828	0.0323	0.0945	0.0011	0.23	10.5860	0.1213	0.0601	0.0026	0.0873	0.0066	0.75	46	6	440	0.01	582	6	587	18	607	97	99	95
PB-33	65.1	0.7661	0.0247	0.0947	0.0008	0.22	10.5632	0.0875	0.0587	0.0019	0.1766	0.0043	0.20	104	33	893	0.04	583	5	578	14	556	70	100	104
PB-33	1.1	0.7695	0.0244	0.0952	0.0011	0.39	10.4997	0.1231	0.0586	0.0021	0.0670	0.0057	0.54	28	28	265	0.11	587	7	580	14	552	79	101	106
PB-33	70.1	0.7703	0.0243	0.0956	0.0008	0.01	10.4568	0.0851	0.0584	0.0019	0.1455	0.0050	0.44	101	89	902	0.10	589	5	580	14	546	69	101	107
PB-33	60.1	0.7925	0.0243	0.0958	0.0008	0.24	10.4369	0.0859	0.0600	0.0019	0.0383	0.0051	0.22	68	19	668	0.03	590	5	593	14	603	70	99	97
PB-33	42.1	0.7690	0.0242	0.0960	0.0009	0.01	10.4128	0.0986	0.0581	0.0019	0.1230	0.0067	0.08	96	23	868	0.03	591	5	579	14	533	72	102	110

PB-33	36.1	0.7967	0.0472	0.0965	0.0014	0.18	10.3652	0.1529	0.0599	0.0040	0.0662	0.0109	1.35	27	23	250	0.09	594	8	595	27	600	146	99	99
PB-33	18.1	0.7855	0.0281	0.0976	0.0009	0.50	10.2453	0.0971	0.0584	0.0022	0.1489	0.0070	0.17	49	33	429	0.08	600	5	589	16	544	81	101	110
PB-33	96.1	0.9092	0.0344	0.1049	0.0015	0.41	9.5373	0.1386	0.0629	0.0026	0.4420	0.0133	1.24	44	190	290	0.66	643	9	657	18	705	88	97	91
PB-33	74.1	0.8821	0.0308	0.1054	0.0010	0.09	9.4880	0.0921	0.0607	0.0022	0.0501	0.0048	0.49	64	22	572	0.04	646	6	642	17	629	80	100	102
PB-33	30.1	0.8941	0.0297	0.1057	0.0010	0.17	9.4589	0.0921	0.0613	0.0023	0.1733	0.0051	0.07	75	44	576	0.08	648	6	649	16	651	81	99	99
PB-33	46.1	0.8897	0.0231	0.1058	0.0009	0.01	9.4499	0.0820	0.0610	0.0016	0.0795	0.0037	0.29	117	3	997	0.00	648	5	646	12	639	59	100	101
PB-33	88.1	0.9060	0.0331	0.1064	0.0015	0.20	9.4001	0.1300	0.0618	0.0025	0.1312	0.0088	0.45	35	56	280	0.20	652	9	655	17	666	86	99	97
PB-33	90.1	0.8894	0.0225	0.1067	0.0010	0.72	9.3740	0.0900	0.0605	0.0015	0.6852	0.0231	0.58	176	563	942	0.60	653	6	646	12	620	53	101	105
PB-33	20.1	0.8892	0.0562	0.1072	0.0016	0.32	9.3262	0.1400	0.0601	0.0041	0.1109	0.0151	0.53	22	4	173	0.02	657	9	646	30	609	150	101	107
PB-33	22.1	0.9126	0.0371	0.1081	0.0012	0.01	9.2470	0.0984	0.0612	0.0026	0.1742	0.0107	5.12	36	28	272	0.10	662	7	659	20	647	95	100	102
PB-33	67.1	0.9266	0.0526	0.1085	0.0013	0.09	9.2134	0.1141	0.0619	0.0037	0.4448	0.0110	0.32	45	68	276	0.25	664	8	666	28	671	135	99	98
PB-33	75.1	0.9409	0.0389	0.1089	0.0012	0.48	9.1789	0.0997	0.0626	0.0027	0.1294	0.0081	0.29	50	40	401	0.10	667	7	673	21	696	96	98	95
PB-33	83.1	0.9458	0.0294	0.1112	0.0010	0.45	8.9915	0.0821	0.0617	0.0020	0.1395	0.0063	0.00	91	89	705	0.13	680	6	676	15	663	69	100	102
PB-33	5.1	0.9458	0.0435	0.1114	0.0018	0.10	8.9778	0.1470	0.0616	0.0033	0.1698	0.0124	0.74	18	7	137	0.05	681	11	676	22	660	114	100	103
PB-33	44.1	0.9400	0.0459	0.1115	0.0014	0.02	8.9655	0.1149	0.0611	0.0033	0.0844	0.0092	0.26	39	32	319	0.10	682	8	673	24	644	116	101	105
PB-33	55.1	1.1928	0.0574	0.1294	0.0015	0.01	7.7298	0.0914	0.0669	0.0035	0.1965	0.0142	0.74	35	14	223	0.06	784	9	797	27	834	112	98	94
PB-33	63.1	1.1546	0.0366	0.1318	0.0011	0.08	7.5875	0.0641	0.0635	0.0020	0.0663	0.0038	0.08	83	48	570	0.09	798	6	779	17	726	68	102	109
PB-33	72.1	1.2287	0.0520	0.1337	0.0014	0.58	7.4817	0.0775	0.0667	0.0030	0.1900	0.0057	0.47	50	49	313	0.16	809	8	814	23	828	91	99	97
PB-33	95.1	1.2712	0.0374	0.1368	0.0016	0.01	7.3087	0.0863	0.0674	0.0021	0.1211	0.0078	4.28	57	63	346	0.18	827	9	833	17	850	64	99	97
PB-33	78.1	1.8111	0.0469	0.1781	0.0015	0.73	5.6134	0.0487	0.0737	0.0019	0.1110	0.0035	0.12	114	271	579	0.47	1057	8	1050	17	1034	53	100	102
PB-33	56.1	1.7341	0.0342	0.1735	0.0012	0.82	5.7638	0.0383	0.0725	0.0014	0.0545	0.0027	0.05	171	29	931	0.03	1031	6	1021	13	1000	40	100	103
PB-33	23.1	1.8115	0.0587	0.1762	0.0018	0.17	5.6755	0.0569	0.0746	0.0025	0.2845	0.0080	0.66	54	58	229	0.25	1046	10	1050	21	1057	69	99	98
PB-33	58.1	4.4136	0.0803	0.3087	0.0021	0.44	3.2392	0.0219	0.1037	0.0018	0.0906	0.0042	0.52	219	22	607	0.04	1734	10	1715	15	1691	32	101	102
PB-33	49.1	4.6455	0.1021	0.3144	0.0025	0.52	3.1806	0.0254	0.1072	0.0024	0.2844	0.0048	0.18	133	17	320	0.05	1762	12	1758	18	1752	41	100	100
PB-33	39.1	4.4261	0.0919	0.3091	0.0026	0.74	3.2347	0.0274	0.1038	0.0022	0.1276	0.0024	0.05	150	2	410	0.01	1737	13	1717	17	1694	40	101	102
PB-33	3.1	4.5184	0.0868	0.3101	0.0030	0.92	3.2245	0.0313	0.1057	0.0023	0.1994	0.0094	0.58	59	1	145	0.00	1741	15	1734	16	1726	39	100	100
PB-33	9.1	4.5590	0.0771	0.3164	0.0026	0.01	3.1601	0.0259	0.1045	0.0019	0.1631	0.0033	0.08	95	5	246	0.02	1772	13	1742	14	1705	32	101	103
PB-33	53.1	1.0291	0.0480	0.1197	0.0013	0.45	8.3524	0.0909	0.0623	0.0031	0.0622	0.0075	2.53	36	-	281	-	729	8	719	23	686	103	101	106
PB-33	32.1	0.7328	0.0244	0.0914	0.0009	0.77	10.9415	0.1046	0.0581	0.0021	0.2271	0.0071	0.65	70	3	612	0.00	564	5	558	14	535	82	101	105
PB-33	38.1	0.6668	0.0278	0.0831	0.0009	0.46	12.0369	0.1353	0.0582	0.0026	0.0643	0.0061	0.33	53	14	597	0.02	515	6	519	17	538	98	99	95
PB-33	12.1	0.6631	0.0161	0.0833	0.0008	0.78	12.0043	0.1132	0.0577	0.0015	0.0887	0.0062	3.78	47	2	468	0.00	516	5	517	10	520	58	99	99
PB-33	25.1	0.8145	0.0220	0.0983	0.0008	0.01	10.1713	0.0864	0.0601	0.0017	0.0834	0.0053	0.64	104	35	913	0.04	605	5	605	12	607	64	99	99
PB-33	92.1	0.8068	0.0256	0.0996	0.0012	0.03	10.0438	0.1199	0.0588	0.0019	0.1646	0.0125	0.31	69	137	579	0.24	612	7	601	14	559	73	101	109
PB-33	76.1	0.8484	0.0350	0.1028	0.0011	0.40	9.7316	0.1034	0.0599	0.0026	0.1142	0.0066	0.87	54	147	474	0.31	631	6	624	19	599	93	101	105
PB-33	45.1	0.8595	0.0338	0.1031	0.0011	0.56	9.7006	0.1076	0.0605	0.0026	0.0245	0.0054	0.35	53	19	495	0.04	633	7	630	19	621	95	100	101
PB-33	16.1	0.8600	0.0251	0.1036	0.0009	0.79	9.6540	0.0813	0.0602	0.0018	0.1505	0.0049	0.42	68	19	554	0.04	635	5	630	14	611	65	100	103
PB-33	59.1	0.9531	0.0266	0.1122	0.0009	0.48	8.9137	0.0701	0.0616	0.0018	0.0900	0.0052	0.46	90	15	727	0.02	685	5	680	14	661	60	100	103
PB-33	10.1	0.9712	0.0683	0.1134	0.0028	0.71	8.8162	0.2180	0.0621	0.0054	0.2415	0.0185	1.64	10	5	74	0.07	693	16	689	35	678	187	100	102
PB-33	24.1	0.9953	0.0568	0.1144	0.0016	0.37	8.7413	0.1224	0.0631	0.0040	0.1010	0.0108	1.61	22	31	175	0.18	698	9	701	29	712	132	99	98
PB-33	48.1	1.0153	0.0455	0.1186	0.0014	0.15	8.4295	0.1010	0.0621	0.0031	0.1378	0.0072	1.30	49	36	361	0.10	723	8	712	22	677	100	101	106
PB-33	40.1	1.0694	0.0355	0.1205	0.0012	0.31	8.2996	0.0853	0.0644	0.0023	0.1402	0.0048	0.18	75	25	541	0.05	733	7	739	18	754	78	99	97
PB-33	2.1	0.9566	0.0187	0.1127	0.0009	0.69	8.8723	0.0720	0.0616	0.0013	0.0610	0.0025	0.60	88	22	718	0.03	689	5	682	10	659	44	101	104
PB-33	93.1	1.0992	0.0316	0.1240	0.0014	0.60	8.0634	0.0895	0.0643	0.0019	0.0757	0.0063	1.18	67	5	464	0.01	754	8	753	15	751	61	100	100
PB-33	89.1	1.4183	0.0563	0.1480	0.0024	0.37	6.7565	0.1095	0.0695	0.0031	0.1803	0.0130	0.39	33	47	186	0.26	890	14	897	24	914	94	99	97
PB-33	51.1	1.4405	0.0278	0.1520	0.0010	0.98	6.5786	0.0418	0.0687	0.0013	0.0649	0.0030	1.55	223	13	1385	0.01	912	5	906	12	891	38	100	102
PB-33	54.1	1.6687	0.0564	0.1666	0.0016	0.04	6.0019	0.0577	0.0726	0.0026	0.1211	0.0064	0.14	53	19	279	0.07	993	9	997	22	1004	77	99	98
PB-33	15.1	1.5708	0.0389	0.1592	0.0013	0.62	6.2821	0.0506	0.0716	0.0018	0.2656	0.0046	4.35	86	26	399	0.06	952	7	959	16	974	53	99	97
PB-33	81.1	4.3209	0.1487	0.2976	0.0035	0.01	3.3605	0.0393	0.1053	0.0039	0.1607	0.0077	0.28	47	41	130	0.32	1679	17	1697	28	1720	67	98	97
PB-33	69.1	4.9076	0.1663	0.3209	0.0035	0.31	3.1158	0.0338	0.1109	0.0039	0.1148	0.0084	0.70	51	26	132	0.20	1794	17	1804	28	1814	61	99	98
PB-33	34.1	4.7303	0.0815	0.3245	0.0023	0.01	3.0815	0.0216	0.1057	0.0019	0.2048	0.0185	0.09	246	27	574	0.05	1812	11	1773	14	1727	33	102	104
PB-33	71.1	5.5222	0.1366	0.3400	0.0029	0.86	2.9408	0.0248	0.1178	0.0029	0.2150	0.0053	0.16	95	-	215	-	1887	14	1904	21	1923	44	99	98
PB-33	6.1	5.7583	0.0941	0.3507	0.0029	0.25	2.8510	0.0238	0.1191	0.0020	0.0988	0.0030	0.13	87	4	206	0.02	1938	14	1940	14	1942	31	99	99
PB-33	82.1	6.1697	0.1463	0.3743	0.0034	0.25	2.6719	0.0245	0.1196	0.0029	0.4930	0.0191	0.79	83	194	151	1.28	2049	16	2000	21	1950	44	102	105
PB-33	41.1	6.2346	0.1342	0.3746	0.0034	0.82	2.6695	0.0243	0.1207	0.0027	0.2204	0.0047	0.50	128	33	266	0.12	2051	16	2009	19	1967	40	102	104
PB-33	94.1	6.5609	0.1502	0.3790	0.0041	0.29	2.6389	0.0285	0.1256	0.0028	0.3214	0.0106	0.09	91	5	168	0.03	2071	19	2054	20	2037	40	100	101
PB-33	57.1	6.7814	0.1297	0.3855	0.0028	0.09	2.5940	0.0190	0.1276	0.0025	0.1664	0.0048	0.14	146	8	304	0.03	2102	13	2083	17	2065	34	100	101
PB-33	77.1	7.1191	0.2557	0.3926	0.0053	0.01	2.5468	0.0343	0.1315	0.0050	0.1172	0.0117	0.45	33	30	70	0.43	2135	24	2126	31	2118	66	100	100
PB-33	27.1	7.7915	0.1829	0.4087	0.0044	0.55	2.4470	0.0264	0.1383	0.0035	0.3126	0.0068	0.18	80	6	133	0.04	2209	20	2207	21	2206	45	100	100
PB-33	84.1	7.5533	0.1919	0.4116	0.0041	0.39	2.4296	0.0242	0.1331	0.0034	0.2527	0.0067	0.08	81	11	149	0.07	2222	19	2179	23	2139	46	101	103
PB-33	52.1	9.1241	0.1622	0.4202	0.0030	0.08	2.3798	0.0169	0.1575	0.0027	0.1399	0.0316	0.25	129	9	223	0.04	2261	14	2351	16	2429	29	96	93
PB-33	73.1	9.1469	0.1897	0.4330	0.0037	0.49	2.3094	0.0195	0.1532	0.0031	0.6240	0.0055	0.12	218	159	303	0.52	2319	17	2353	19	2382	35	98	97

PB-33	7.1	9.5010	0.1804	0.4558	0.0049	0.51	2.1937	0.0238	0.1512	0.0032	0.3656	0.0073	0.15	42	8	62	0.14	2421	22	2388	17	2359	35	101	102
PB-33	86.1	11.5002	0.2422	0.4908	0.0048	0.49	2.0375	0.0198	0.1699	0.0034	0.1028	0.0061	5.09	78	30	138	0.22	2574	21	2565	19	2557	33	100	100
PB-33	61.1	12.1160	0.2544	0.5007	0.0040	0.42	1.9971	0.0158	0.1755	0.0035	0.1978	0.0024	0.20	154	41	234	0.18	2617	17	2613	20	2611	33	100	100
PB-33	28.1	12.7832	0.2537	0.5173	0.0051	0.49	1.9332	0.0189	0.1792	0.0038	0.2482	0.0061	0.15	103	13	142	0.09	2688	22	2664	19	2646	35	100	101
PB-33	35.1	12.9830	0.3342	0.5321	0.0072	0.29	1.8794	0.0255	0.1770	0.0050	0.1572	0.0064	0.27	45	4	64	0.07	2750	30	2678	25	2625	48	102	104
PB-33	66.1	0.2894	0.0157	0.0423	0.0004	0.47	23.6589	0.2504	0.0496	0.0028	0.2248	0.0082	0.34	55	58	1045	0.06	267	3	258	12	179	121	103	149
PB-33	8.1	0.6895	0.0354	0.0883	0.0015	0.59	11.3226	0.1978	0.0566	0.0034	0.6625	0.0632	0.12	19	77	127	0.61	546	9	533	21	477	133	102	114
PB-33	47.1	0.7393	0.0155	0.0939	0.0007	0.01	10.6454	0.0818	0.0571	0.0012	0.1950	0.1118	2.74	211	17	1967	0.01	579	4	562	9	495	46	102	117
PB-33	13.1	0.8111	0.0377	0.1005	0.0012	0.63	9.9477	0.1139	0.0585	0.0029	0.1192	0.0087	0.66	34	-2	289	-0.01	618	7	603	21	549	107	102	112
PB-33	85.1	0.8429	0.0291	0.1035	0.0013	0.01	9.6606	0.1247	0.0591	0.0022	0.1113	0.0100	1.77	44	-2	375	-0.01	635	8	621	16	569	81	102	111
PB-33	33.1	1.2125	0.0387	0.1375	0.0013	0.25	7.2704	0.0704	0.0639	0.0023	0.1629	0.0055	0.54	73	7	445	0.02	831	8	806	18	739	74	103	112
PB-33	43.1	0.7949	0.1189	0.0963	0.0030	0.47	10.3842	0.3197	0.0599	0.0105	0.1707	0.0328	4.95	10	5	87	0.06	593	18	594	70	599	372	99	98
PB-34	73.1	0.6521	0.031	0.0824	0.0011	0.21	12.1352	0.1653	0.0574	0.0028	0.0676	0.0103	0.59	35	12.8	368.4	0.035	510.5	6.7	509.8	18.9	506.7	107	100	100
PB-34	80.1	0.6612	0.0397	0.0839	0.0013	0.21	11.9213	0.1864	0.0572	0.0037	0.2408	0.0307	0.72	29	51.1	272.6	0.188	519.3	7.8	515.4	24	498.1	134.5	100	104
PB-34	18.1	0.678	0.0414	0.0864	0.0012	0.09	11.5791	0.166	0.0569	0.0037	0.137	0.014	0.73	24.6	3.1	230.1	0.014	534	7.3	525.6	25.3	489.3	147.7	101	109
PB-34	84.1	0.7015	0.068	0.0868	0.002	0.14	11.5229	0.2608	0.0586	0.0063	0.3986	0.0323	0.88	13.7	-	102.9	-	536.5	11.7	539.7	39.8	553.3	226.5	99	96
PB-34	79.1	0.6876	0.0287	0.0868	0.0011	0.4	11.5172	0.145	0.0574	0.0025	0.1746	0.0047	0.22	42.8	68	387	0.176	536.7	6.5	531.4	17.3	508.4	93.6	101	105
PB-34	17.1	0.6997	0.0205	0.087	0.0008	0.77	11.488	0.1106	0.0583	0.0017	0.0197	0.0032	0.25	101	2.5	1068	0.002	538	5	538.6	12.2	540.8	62.7	99	99
PB-34	81.1	0.7052	0.0393	0.0872	0.0013	0.73	11.4686	0.1732	0.0587	0.0034	0.0394	0.0109	0.43	24.9	5.4	239.9	0.023	538.9	7.8	541.9	23.1	554.4	124.8	99	97
PB-34	42.1	0.7274	0.0297	0.0895	0.0011	0.16	11.1763	0.1436	0.059	0.0026	0.1624	0.0081	0.32	50.7	154.4	446	0.346	552.4	6.8	555	17.5	565.7	100.5	99	97
PB-34	74.1	0.7321	0.0419	0.0896	0.0014	0.33	11.1653	0.1763	0.0593	0.0036	0.153	0.0092	0.51	21.3	22.7	186.7	0.122	553	8.4	557.8	25.2	577.5	139.1	99	95
PB-34	76.1	0.7384	0.0428	0.0902	0.0015	0.22	11.081	0.1782	0.0593	0.0036	0.2479	0.0095	0.37	24.7	3	205.1	0.015	557	8.6	561.5	25.6	579.7	140.8	99	96
PB-34	7.1	0.7308	0.038	0.0906	0.0012	0.5	11.0328	0.1427	0.0585	0.0032	0.0084	0.0078	0.49	32.1	27.7	327.2	0.085	559.3	6.9	557.1	22.7	547.8	121.9	100	102
PB-34	94.1	0.7522	0.0351	0.0916	0.0011	0.62	10.9148	0.1275	0.0595	0.0029	0.2127	0.013	0.64	46.5	88.6	388.6	0.228	565.1	6.3	569.5	20.1	587	103.8	99	96
PB-34	48.1	0.7428	0.0267	0.0917	0.001	0.15	10.9021	0.1244	0.0587	0.0023	0.0056	0.0063	0.38	56.4	38	568	0.067	565.7	6.2	564.1	15.4	557.3	83.3	100	101
PB-34	20.1	0.7644	0.0247	0.0924	0.0009	0.05	10.8252	0.1097	0.06	0.0019	0.0817	0.0032	0.56	74.3	9.6	683	0.014	569.6	5.5	576.5	14.2	604	71	98	94
PB-34	50.1	0.7459	0.0761	0.0935	0.0027	0.67	10.6915	0.303	0.0578	0.007	0.1174	0.0228	0.65	17.6	14.1	153.2	0.092	576.4	15.6	565.8	44.4	523.7	240.9	101	110
PB-34	58.1	0.7868	0.063	0.0936	0.0023	0.01	10.6822	0.26	0.061	0.0056	0.2349	0.0237	0	19	22.4	154.8	0.145	576.9	13.3	589.3	36.4	637.7	213.5	97	90
PB-34	91.1	0.769	0.033	0.0936	0.001	0.39	10.6781	0.1185	0.0596	0.0027	0.1476	0.0077	0.58	36.6	6.8	316.7	0.021	577.1	6.1	579.2	19	587.5	96.8	99	98
PB-34	24.1	0.783	0.0403	0.0939	0.0012	0.4	10.6511	0.1393	0.0605	0.0033	0.03	0.01	0.5	28.1	11.3	263.3	0.043	578.5	7.3	587.2	23.2	620.9	119.4	98	93
PB-34	72.1	0.7741	0.0398	0.0942	0.0013	0.27	10.6102	0.1475	0.0596	0.0033	0.1737	0.0115	0.34	25.5	-	211.7	-	580.6	7.7	582.1	22.9	588	120.2	99	98
PB-34	26.1	0.7742	0.0305	0.0945	0.0012	0.65	10.5854	0.1301	0.0594	0.0025	0.044	0.0069	0.65	44.8	0.6	389.3	0.002	581.9	6.9	582.2	17.5	583.2	91.6	99	99
PB-34	30.1	0.7961	0.0312	0.0967	0.0012	0.79	10.3367	0.1272	0.0597	0.0025	0.0545	0.0145	0.16	45.4	-	378.9	-	595.3	7	594.6	17.3	592.1	92.5	100	100
PB-34	82.1	0.8044	0.0274	0.0979	0.0011	0.5	10.2145	0.1172	0.0596	0.002	0.0873	0.0097	0.28	75.1	42.6	667.4	0.064	602.1	6.6	599.3	15.4	588.8	74	100	102
PB-34	23.1	0.8161	0.0412	0.098	0.0013	0.52	10.2085	0.1335	0.0604	0.0032	0.179	0.0076	0.64	38.2	22.7	302.6	0.075	602.4	7.5	605.9	23	618.9	112.5	99	97
PB-34	40.1	0.7949	0.0517	0.0986	0.0018	0.08	10.1396	0.1873	0.0585	0.0044	0.1698	0.0235	0.91	32.5	38	250.4	0.152	606.3	10.7	594	29.9	547	172.1	102	110
PB-34	87.1	0.8185	0.0215	0.0987	0.0008	0.69	10.1312	0.0856	0.0601	0.0016	0.0217	0.0024	0.06	109	15.2	993.3	0.015	606.8	4.9	607.2	12	608.7	56.5	99	99
PB-34	67.1	0.8386	0.0365	0.0992	0.0012	0.01	10.0852	0.1267	0.0613	0.0028	0.0046	0.006	1.42	24.4	-	223.6	-	609.5	7.3	618.4	20	651.2	96.8	98	93
PB-34	93.1	0.8323	0.0282	0.0995	0.001	0.99	10.0473	0.099	0.0606	0.002	0.0904	0.0955	0.04	87.2	27.8	821.7	0.034	611.7	5.7	614.9	15	626.8	67.7	99	97
PB-34	5.1	0.8202	0.0402	0.0998	0.0012	0.92	10.0247	0.1218	0.0596	0.0033	0.0356	0.0133	1.06	24.9	30.2	222	0.136	613	7.2	608.1	23	590.2	114.1	100	103
PB-34	45.1	0.8425	0.0345	0.1015	0.0013	0.59	9.8529	0.127	0.0602	0.0027	0.0862	0.0065	0.78	48.8	86.6	405.8	0.213	623.2	7.7	620.5	19	611	98.4	100	101
PB-34	9.1	0.877	0.0392	0.1027	0.0013	0.17	9.7402	0.1186	0.062	0.0029	0.1145	0.0059	1.02	39.4	33.6	317.6	0.106	630	7.3	639.3	21.8	672.4	108	98	93
PB-34	41.1	0.8893	0.0315	0.1036	0.0012	0.63	9.6557	0.1132	0.0623	0.0025	0.0878	0.0056	0.21	61	-	500	-	635.3	7.1	646	16.9	683.7	82.5	98	92
PB-34	69.1	0.9147	0.0408	0.105	0.0014	0.02	9.5204	0.1251	0.0632	0.0029	0.0824	0.0118	0.34	24.1	-	193.5	-	643.9	8	659.5	21.6	713.6	101.9	97	90
PB-34	88.1	1.4386	0.093	0.1482	0.0024	0.01	6.7459	0.1074	0.0704	0.005	0.1704	0.0188	1	17.8	19.3	93.2	0.207	891.1	13.3	905.1	38.8	939.5	145.9	98	94
PB-34	39.1	1.4616	0.1128	0.1514	0.0038	0.53	6.6032	0.1645	0.07	0.0065	0.1078	0.0221	1.18	14.9	-	81.7	-	909	21.2	914.7	48.6	928.3	203.4	99	97
PB-34	50.1	1.5416	0.0416	0.1531	0.0015	0.99	6.5337	0.0656	0.0731	0.0022	0.1285	0.0055	0.26	76	40.9	388.9	0.105	918.1	8.7	947.1	17.1	1015	62.4	96	90
PB-34	68.1	1.4296	0.1161	0.1537	0.0033	0.27	6.506	0.139	0.0675	0.0062	0.6877	0.0258	0.14	15.3	-	54.1	-	921.7	18.4	901.4	50.2	852	197.1	102	108
PB-34	96.1	1.8304	0.0659	0.177	0.0019	0.69	5.6496	0.0609	0.075	0.0028	0.1213	0.0072	0.23	40.3	6	176.9	0.034	1051	10.5	1056	23.7	1069	75.5	99	98
PB-34	54.1	1.8789	0.0643	0.1786	0.0023	0.79	5.5976	0.0707	0.0763	0.0028	0.1333	0.0061	0.64	48.3	66	213.2	0.309	1060	12.3	1074	22.6	1102	74.1	98	96
PB-34	83.1	1.778	0.089	0.1787	0.0028	0.27	5.5953	0.0878	0.0722	0.0038	0.1553	0.0131	0.78	27	29.3	121.8	0.241	1060	15.3	1037	32.5	990.2	105.7	102	107
PB-34	29.1	1.8223	0.0661	0.1806	0.0023	0.78	5.5359	0.0705	0.0732	0.0029	0.2302	0.0086	0.45	74	32.3	311.9	0.104	1071	12.6	1054	23.9	1019	79.6	101	105
PB-34	52.1	4.4845	0.1143	0.3049	0.0033	0.74	3.2798	0.0355	0.1067	0.0028	0.1941	0.004	0.18	94.2	1.7	231.9	0.007	1716	16.3	1728	21.2	1743	48.9	99	98
PB-34	78.1	4.4247	0.2073	0.3053	0.0055	0.72	3.2752	0.0593	0.1051	0.0056	0.2112	0.0287	0.41	29.7	-	73.8	-	1718	27.6	1717	40	1716	96.6	100	100
PB-34	13.1	4.5407	0.1408	0.3106	0.0036	0.51	3.2193	0.0372	0.106	0.0033	0.1872	0.0123	0.18	64.5	7.5	156.9	0.048	1744	17.7	1739	25.6	1732	56.4	100	100
PB-34	27.1	4.5842	0.1437	0.3117	0.004	0.96	3.2081	0.0413	0.1067	0.0035	0.1763	0.0085	1.16	75.1	13.2	201.7	0.066	1749	19.8	1746	26	1743	59.9	100	100
PB-34	53.1	5.7145	0.1195	0.3405	0.003	0.28	2.9371	0.0256	0.1217	0.0025	0.0374	0.0099	5.97	2.4	-	0.3	-	1889	14.3	1934	18.3	1982	37.3	97	95
PB-34	60.1	5.9185	0.1214	0.3416	0.003	0.95	2.9272	0.0254	0.1257	0.0025	0.253	0.0205	0.24	190	32.2	397.7	0.081	1895	14.2	1964	17.7	2038	35.7	96	92
PB-34	3.1	5.7638	0.1651	0.3463	0.0038	0.01	2.8875	0.0318	0.1207	0.0034	0.1711	0.012	0.25	53.2	46.1	116.4	0.396	1917	18.3	1941	24.8	1967	50.2	98	97
PB-34	57.1	5.8506	0.1672	0.3489	0.0045	0.84	2.8664	0.0372	0.1216	0.0036	0.2399	0.0072	0.55	76.4	68.1	152.5	0.446	1929	21.6	1954	24.4	1980	53.3	98	97
PB-34	66.1	1.3207	0.0373	0.1411	0.0014	0.78	7.0859	0.0714	0.0679	0.0019	0.026	0.0056	0.1	64.5	-	397.3	-	851	8	854.8	16.3	864.8	56.7	99	98

PB-34	92.1	1.3325	0.0433	0.1429	0.0014	0.6	6.9991	0.0681	0.0676	0.0023	0.1904	0.0071	0.47	57.4	6.4	313.9	0.02	860.9	7.8	860	18.7	857.6	69	100	100
PB-34	37.1	0.9291	0.0491	0.1094	0.0018	0.04	9.1385	0.1477	0.0616	0.0036	0.1317	0.011	0.37	31.8	91.2	231.6	0.394	669.4	10.3	667.2	25.7	659.5	127.2	100	101
PB-34	22.1	0.9672	0.0294	0.112	0.0011	0.41	8.9315	0.0882	0.0627	0.0019	0.0095	0.0038	0.31	76.2	3.6	608.8	0.006	684.1	6.4	687	15.3	696.5	65.8	99	98
PB-34	62.1	0.9666	0.0543	0.1126	0.0017	0.87	8.8822	0.137	0.0623	0.0036	0.1576	0.0127	0.26	24	-	159	-	687.7	10.1	686.7	28.3	683.3	130.3	100	100
PB-34	47.1	1.6854	0.094	0.1688	0.0032	0.01	5.9253	0.1119	0.0724	0.0047	0.3069	0.0145	0.36	28	76.8	120.4	0.638	1005	17.6	1003	35.4	998.1	131.2	100	100
PB-34	44.1	1.7489	0.0625	0.169	0.0022	0.54	5.9188	0.0773	0.0751	0.0031	0.282	0.0174	0.21	51.8	133.9	218.4	0.613	1006	12.2	1027	23.9	1071	84	98	94
PB-34	34.1	1.707	0.0903	0.1701	0.003	0.15	5.8796	0.1034	0.0728	0.0043	0.09	0.0131	1.38	23.7	15.3	114.5	0.134	1013	16.5	1011	33.9	1008	121.4	100	100
PB-34	95.1	1.5639	0.0396	0.1622	0.0014	0.9	6.1657	0.0523	0.0699	0.0018	0.088	0.0044	0.11	139	26.1	729.8	0.036	968.9	7.6	956	15.7	926.4	51.7	101	104
PB-34	10.1	1.5431	0.0484	0.1627	0.0017	0.9	6.1473	0.0639	0.0688	0.0022	0.0788	0.0034	0.37	137	9.2	675	0.014	971.6	9.4	947.7	19.4	892.6	65	102	108
PB-34	59.1	6.1043	0.1538	0.3543	0.004	0.9	2.8226	0.032	0.125	0.0033	0.267	0.0043	0.15	95.7	37.5	183.9	0.204	1955	19.1	1991	22	2028	46.9	98	96
PB-34	86.1	6.0079	0.1302	0.3554	0.003	0.72	2.8136	0.0236	0.1226	0.0026	0.0421	0.0037	1.04	185	-	425.7	-	1960	14.2	1977	18.9	1994	37.6	99	98
PB-34	65.1	6.6232	0.1459	0.3602	0.0036	0.98	2.7759	0.0274	0.1333	0.0028	0.1371	0.0041	0.03	83.5	139	169.4	0.821	1983	16.8	2062	19.4	2142	35.8	96	92
PB-34	85.1	6.4787	0.1475	0.3612	0.0032	0.61	2.7689	0.0245	0.1301	0.0029	0.0893	0.0047	0.4	90	53.4	199.8	0.267	1988	15.1	2043	20	2099	39.4	97	94
PB-34	56.1	6.325	0.1887	0.3629	0.0051	0.44	2.7554	0.0388	0.1264	0.0041	0.221	0.0089	1.38	51.1	5.5	102.7	0.054	1996	24.1	2022	26.3	2049	58	98	97
PB-34	1.1	6.3112	0.1534	0.364	0.0036	0.01	2.7473	0.0269	0.1258	0.0029	0.1753	0.007	0.2	57.3	23.2	118	0.196	2001	16.9	2020	21.3	2039	40.6	99	98
PB-34	6.1	6.5694	0.1979	0.3763	0.0044	0.23	2.6573	0.0308	0.1266	0.0038	0.4488	0.0163	0.57	72.5	14.3	120.7	0.119	2059	20.5	2055	26.4	2051	52.5	100	100
PB-34	90.1	3.8265	0.1555	0.2856	0.0037	0.77	3.5018	0.0458	0.0972	0.0044	0.2167	0.0126	0.67	24.1	26.2	63.6	0.413	1619	18.8	1598	33	1571	84.4	101	103
PB-34	75.1	5.5333	0.1998	0.3393	0.0053	0.27	2.9468	0.0456	0.1183	0.0045	0.1985	0.0473	0.17	47.2	29.5	79	0.373	1884	25.3	1906	31.7	1930	68.4	98	97
PB-34	64.1	6.7634	0.145	0.3842	0.0036	0.98	2.603	0.0247	0.1277	0.0026	0.1193	0.0139	1.94	56.9	-	114.1	-	2096	17.2	2081	19.7	2066	36.3	100	101
PB-34	63.1	7.0678	0.1557	0.389	0.0038	0.83	2.5709	0.0252	0.1318	0.0027	0.1306	0.0044	0.18	88.7	-	178.1	-	2118	17.7	2120	19.5	2122	35.5	99	99
PB-34	25.1	7.1314	0.2099	0.4019	0.0053	0.86	2.488	0.0327	0.1287	0.0042	0.3686	0.0081	0.89	55.1	14.7	88.4	0.166	2178	24.5	2128	27.1	2080	57.3	102	104
PB-34	36.1	3.6943	0.1397	0.2659	0.0041	0.7	3.7615	0.0573	0.1008	0.0041	0.1362	0.0138	0.62	39.3	-	106.1	-	1520	20.6	1570	29.7	1639	75.4	96	92
PB-34	61.1	3.8731	0.1247	0.2723	0.0035	0.95	3.6722	0.0472	0.1032	0.0032	0.1527	0.0102	1.55	34.1	-	85.5	-	1553	17.4	1608	24.8	1682	57	96	92
PB-34	28.1	4.1235	0.1737	0.2927	0.0049	0.76	3.4162	0.0576	0.1022	0.0044	0.3692	0.0192	0.13	61.8	47.5	130.6	0.364	1655	24.1	1659	30.7	1664	75.9	99	99
PB-34	71.1	1.0035	0.0495	0.1177	0.0016	0.54	8.4975	0.1172	0.0618	0.0032	0.2887	0.0234	0.22	35.4	-	218.1	-	717.2	9.3	705.6	24.6	668.8	106.7	101	107
PB-34	43.1	1.1703	0.0433	0.1278	0.0016	0.01	7.8268	0.0996	0.0664	0.0027	0.2424	0.008	0.56	49.5	-	295.9	-	775.1	9.3	786.8	20.5	820.1	89.3	98	94
PB-34	49.1	1.1566	0.0357	0.1304	0.0014	0.49	7.6659	0.0821	0.0643	0.0021	0.0106	0.0036	0.63	84.3	19.9	586.6	0.034	790.4	8	780.4	16.8	751.7	68.6	101	105
PB-34	8.1	0.6201	0.1278	0.078	0.0026	0.28	12.823	0.4286	0.0577	0.012	0.3279	0.0397	5.05	6.4	9.9	57.4	0.173	484.1	15.6	489.9	82.9	517.3	382.2	98	93
PB-34	89.1	10.2391	0.2703	0.453	0.005	0.25	2.2076	0.0242	0.1639	0.0044	0.067	0.0093	2.39	4	13	8.4	1.548	2409	21.9	2457	24.1	2497	45.9	98	96
PB-34	51.1	10.3407	0.2473	0.4576	0.0053	0.75	2.1855	0.0254	0.1639	0.004	0.1381	0.0104	0.17	88.2	6.5	144	0.045	2429	23.6	2466	22.5	2496	41.8	98	97
PB-34	2.1	11.3349	0.3247	0.4716	0.0057	0.93	2.1206	0.0254	0.1743	0.005	0.1613	0.0074	0.47	67.9	26.7	95	0.281	2491	24.7	2551	26.9	2600	47.4	97	95
PB-34	21.1	10.2345	0.2455	0.4763	0.0049	0.06	2.0994	0.0215	0.1558	0.0036	0.1642	0.0135	0.34	29.4	8.7	46	0.188	2511	21.3	2456	22.2	2411	39.4	102	104
PB-34	33.1	13.1435	0.3374	0.5199	0.0063	0.26	1.9234	0.0234	0.1833	0.0048	0.1442	0.0074	0.33	95.7	15.1	133.4	0.113	2699	26.8	2690	24	2683	42.8	100	100
PB-34	31.1	12.8908	0.2964	0.5227	0.0051	0.53	1.9133	0.0186	0.1789	0.0039	0.1313	0.0081	1.1	10.1	-	14.3	-	2710	21.5	2672	21.3	2643	36	101	102
PB-34	12.1	0.2872	0.0348	0.0415	0.0008	0.67	24.0753	0.4785	0.0502	0.0065	0.2954	0.0251	0.71	14.1	21	239.6	0.088	262.3	5.1	256.4	27.1	202.1	246.5	102	129
PB-34	35.1	0.5096	0.0229	0.0626	0.0009	0.98	15.9871	0.2206	0.0591	0.0027	0.0697	0.0091	2.93	74	32	682.9	0.047	391.1	5.2	418.2	15.5	570.5	100.3	93	68
PB-34	55.1	0.6625	0.0849	0.0779	0.0028	0.49	12.8358	0.4692	0.0617	0.0094	0.1712	0.0312	3.31	10.1	29.3	106.3	0.276	483.6	17.1	516.2	52	662.9	332.9	93	72
PB-34	11.1	0.66	0.0597	0.0796	0.0015	0.22	12.5567	0.2352	0.0601	0.0058	0.3141	0.0323	2.48	13.2	10.9	122.1	0.089	494	8.9	514.6	38.4	607.4	232	95	81
PB-34	16.1	0.6636	0.0411	0.0824	0.0012	0.28	12.1405	0.1808	0.0584	0.0038	0.0449	0.0172	6.89	23.1	-	236.2	-	510.2	7.3	516.8	25.6	546	155	98	93
PB-34	4.1	0.6853	0.0609	0.0826	0.0015	0.23	12.1134	0.2182	0.0602	0.0058	0.1559	0.025	3.8	14.8	15.6	150.8	0.104	511.3	8.9	530	36.8	611.1	211.9	96	83
PB-34	14.1	0.6296	0.0563	0.083	0.0015	0.28	12.0504	0.2234	0.055	0.0053	0.1379	0.0184	1.26	13	17.9	124.1	0.144	513.9	9.2	495.8	35.9	413.2	216.4	103	124
PB-34	46.1	0.6862	0.0781	0.0897	0.0026	0.12	11.1497	0.3204	0.0555	0.0074	0.097	0.0262	0.61	13.4	-	118.4	-	553.7	15.2	530.5	46	432	275.4	104	128
PB-34	15.1	0.716	0.0451	0.0914	0.0013	0.66	10.9458	0.1598	0.0568	0.0037	0.0703	0.0142	1.56	19.9	-	179.8	-	563.6	7.9	548.3	26.2	485.3	140.3	102	116
PB-34	70.1	0.7973	0.0359	0.0938	0.0012	0.48	10.6631	0.1378	0.0617	0.0029	0.0322	0.0097	0.66	22.6	94.1	210.4	0.447	577.9	7.1	595.3	20.4	662.4	102.8	97	87
PB-34	32.1	0.8492	0.0538	0.0976	0.0018	0.19	10.2471	0.1913	0.0631	0.0046	0.1186	0.0197	1.56	22.2	-	176.6	-	600.3	10.7	624.2	29.9	711.9	161.1	96	84
PB-34	77.1	0.9403	0.0739	0.107	0.0022	0.17	9.3441	0.1885	0.0637	0.0056	0.2121	0.0179	1.38	14.8	38	106	0.359	655.4	12.6	673.1	38.5	732.6	184.1	97	89
PB-34	19.1	1.5309	0.0904	0.1512	0.0024	0.18	6.6156	0.1057	0.0735	0.0048	0.1472	0.0151	0.29	22.8	17.6	121.4	0.145	907.4	13.5	942.9	36.6	1027	132.5	96	88
PB-35	84.1	0.7462	0.0504	0.0934	0.0012	0.01	10.7080	0.1372	0.0579	0.0041	0.2360	0.0194	0.73	18	-	134	-	576	7	566	29	528	148	101	109
PB-35	45.1	0.7724	0.0300	0.0940	0.0017	0.88	10.6407	0.1937	0.0596	0.0023	0.0656	0.0661	0.78	36	1	355	0.00	579	10	581	17	589	89	99	98
PB-35	29.1	0.7666	0.0327	0.0946	0.0014	0.55	10.5744	0.1568	0.0588	0.0028	0.0551	0.0138	0.00	37	18	363	0.05	583	8	578	19	559	107	100	104
PB-35	6.1	0.7882	0.0202	0.0966	0.0011	0.93	10.3553	0.1173	0.0592	0.0016	0.0782	0.0154	0.25	67	35	593	0.06	594	7	590	11	574	59	100	103
PB-35	25.1	0.8192	0.0575	0.0974	0.0022	0.27	10.2641	0.2358	0.0610	0.0051	0.2904	0.0182	0.54	14	36	105	0.35	599	13	608	33	639	180	98	93
PB-35	4.1	0.7880	0.0339	0.0975	0.0016	0.94	10.2540	0.1661	0.0586	0.0026	0.1586	0.0297	2.29	20	32	169	0.19	600	9	590	18	552	99	101	108
PB-35	70.1	0.8136	0.0805	0.0979	0.0017	0.06	10.2142	0.1749	0.0603	0.0067	0.1921	0.0182	4.07	8	25	63	0.40	602	10	605	46	613	240	99	98
PB-35	11.1	0.8140	0.0416	0.0982	0.0018	0.23	10.1864	0.1846	0.0601	0.0036	0.1861	0.0188	0.61	26	81	219	0.37	604	10	605	23	609	127	99	99
PB-35	30.1	0.8135	0.0186	0.0992	0.0009	0.43	10.0828	0.0884	0.0595	0.0015	0.0173	0.0033	0.21	100	7	938	0.01	610	5	604	10	585	52	100	104
PB-35	60.1	0.8433	0.0408	0.1007	0.0017	0.29	9.9267	0.1721	0.0607	0.0034	0.1165	0.0096	0.43	19	35	160	0.22	619	10	621	22	629	115	99	98
PB-35	49.1	0.8506	0.0255	0.1010	0.0013	0.84	9.9056	0.1239	0.0611	0.0020	0.0071	0.0060	0.66	41	-	374	-	620	7	625	14	643	70	99	96
PB-35	1.1	0.8256	0.0443	0.1011	0.0019	0.64	9.8936	0.1825	0.0592	0.0036	0.0254	0.0101	0.61	20	-	178	-	621	11	611	24	576	136	101	107
PB-35	9.1	0.8556	0.0531	0.1021	0.0022	0.50	9.7897	0.2099	0.0608	0.0043	0.2039	0.0166	0.21	21	78	151	0.51	627	13	628	30	630	158	99	99
PB-35	78.1	0.8885	0.0333	0.1036	0.0010	0.65	9.6567	0.0909	0.0622	0.0024	0.2221	0.0194	1.33	15	6	119	0.05	635	6	646	18	682	83	98	93

PB-35	16.1	0.8850	0.0353	0.1051	0.0016	0.78	9.5116	0.1472	0.0611	0.0027	0.2843	0.0844	0.73	32	18	243	0.07	644	10	644	19	641	102	100	100
PB-35	62.1	0.9296	0.0661	0.1071	0.0014	0.71	9.3410	0.1251	0.0630	0.0049	0.2870	0.0104	1.06	9	-	67	-	656	8	667	35	708	164	98	92
PB-35	50.1	0.8920	0.0298	0.1071	0.0014	0.68	9.3389	0.1255	0.0604	0.0022	0.1673	0.0195	0.83	39	110	312	0.35	656	8	647	16	619	80	101	106
PB-35	74.1	0.9232	0.0365	0.1079	0.0010	0.36	9.2671	0.0885	0.0621	0.0025	0.1140	0.0062	0.45	26	-	197	-	661	6	664	19	676	86	99	97
PB-35	17.1	0.9399	0.0891	0.1085	0.0035	0.27	9.2180	0.2948	0.0628	0.0069	0.0650	0.0268	1.59	15	9	111	0.08	664	20	673	46	703	224	98	94
PB-35	46.1	0.9033	0.0574	0.1092	0.0026	0.40	9.1562	0.2191	0.0600	0.0040	0.1179	0.0156	0.75	13	28	104	0.26	668	15	654	30	603	144	102	110
PB-35	32.1	0.9153	0.0268	0.1102	0.0012	0.55	9.0766	0.0961	0.0603	0.0020	0.0773	0.0037	0.66	50	23	380	0.06	674	7	660	14	613	69	102	109
PB-35	31.1	0.9508	0.0534	0.1102	0.0021	0.63	9.0737	0.1725	0.0626	0.0042	0.1474	0.0391	0.73	18	1	150	0.00	674	12	679	28	694	148	99	97
PB-35	76.1	0.9428	0.0309	0.1113	0.0010	0.63	8.9815	0.0774	0.0614	0.0021	0.1590	0.0072	0.49	35	29	256	0.11	681	6	674	16	654	72	100	104
PB-35	19.1	1.6091	0.0892	0.1679	0.0036	0.56	5.9573	0.1293	0.0695	0.0046	0.1788	0.0193	1.68	19	-	90	-	1000	20	974	34	914	132	102	109
PB-35	67.1	1.8005	0.1284	0.1724	0.0028	0.60	5.7998	0.0944	0.0757	0.0055	0.1722	0.0289	0.15	17	19	93	0.20	1025	15	1046	47	1088	157	98	94
PB-35	36.1	1.8091	0.1175	0.1749	0.0043	0.51	5.7161	0.1411	0.0750	0.0058	0.2135	0.0150	0.67	12	13	52	0.24	1039	24	1049	41	1069	150	99	97
PB-35	51.1	1.8466	0.0368	0.1794	0.0018	0.99	5.5735	0.0556	0.0746	0.0015	0.0859	0.0058	0.73	106	-	577	-	1064	10	1062	13	1059	39	100	100
PB-35	26.1	1.8638	0.1065	0.1796	0.0040	0.68	5.5672	0.1254	0.0753	0.0052	0.4444	0.0177	0.22	15	-	54	-	1065	22	1068	39	1075	142	99	99
PB-35	10.1	0.7416	0.0252	0.0930	0.0013	0.31	10.7487	0.1453	0.0578	0.0022	0.0928	0.0057	0.21	42	21	390	0.05	574	7	563	15	523	85	101	109
PB-35	34.1	0.9899	0.0293	0.1118	0.0012	0.99	8.9483	0.0988	0.0642	0.0022	0.0312	0.0166	0.22	30	8	304	0.03	683	7	699	15	750	73	97	91
PB-35	66.1	0.9533	0.0195	0.1128	0.0007	0.86	8.8663	0.0516	0.0613	0.0012	0.0500	0.0024	0.06	106	52	866	0.06	689	4	680	10	650	44	101	106
PB-35	5.1	0.6934	0.0213	0.0871	0.0011	0.56	11.4766	0.1440	0.0577	0.0019	0.2772	0.0038	0.56	61	143	515	0.28	539	7	535	13	519	74	100	103
PB-35	7.1	0.7185	0.0438	0.0872	0.0018	0.08	11.4709	0.2385	0.0598	0.0042	0.2280	0.0199	0.37	16	148	139	1.07	539	11	550	26	596	161	98	90
PB-35	37.1	0.7297	0.0377	0.0904	0.0019	0.53	11.0669	0.2305	0.0586	0.0031	0.1259	0.0193	0.27	25	12	233	0.05	558	11	556	22	551	118	100	101
PB-35	79.1	0.6246	0.0325	0.0808	0.0009	0.85	12.3728	0.1364	0.0561	0.0029	0.2969	0.1060	1.32	24	185	199	0.93	501	5	493	20	455	116	101	110
PB-35	21.1	0.6626	0.0396	0.0819	0.0017	0.23	12.2170	0.2518	0.0587	0.0040	0.3432	0.0179	0.66	23	15	194	0.08	507	10	516	24	556	150	98	91
PB-35	39.1	0.6624	0.0223	0.0823	0.0014	0.69	12.1467	0.2054	0.0584	0.0019	0.1112	0.0079	0.22	37	34	384	0.09	510	8	516	14	543	71	98	93
PB-35	44.1	0.6758	0.0414	0.0848	0.0019	0.20	11.7955	0.2653	0.0578	0.0038	0.2960	0.0153	0.79	16	33	142	0.23	525	11	524	25	523	141	100	100
PB-35	63.1	0.6637	0.0255	0.0850	0.0007	0.25	11.7707	0.0972	0.0567	0.0023	0.8389	0.0213	0.08	48	187	292	0.64	526	4	517	16	478	90	101	109
PB-35	68.1	1.0027	0.0505	0.1183	0.0012	0.79	8.4517	0.0869	0.0615	0.0032	0.2935	0.0149	0.86	24	37	123	0.30	721	7	705	24	655	108	102	109
PB-35	58.1	1.0876	0.1429	0.1239	0.0054	0.01	8.0739	0.3524	0.0637	0.0099	0.2283	0.0465	0.41	6	70	34	2.07	753	31	747	68	731	339	100	102
PB-35	65.1	1.1259	0.0511	0.1271	0.0013	0.39	7.8702	0.0780	0.0643	0.0030	0.1371	0.0083	0.25	22	8	141	0.06	771	7	766	25	750	103	100	102
PB-35	22.1	1.5917	0.0650	0.1619	0.0028	0.27	6.1764	0.1067	0.0713	0.0033	0.1917	0.0206	0.26	26	6	122	0.05	967	16	967	25	966	96	100	100
PB-35	15.1	1.6242	0.1030	0.1649	0.0042	0.78	6.0637	0.1531	0.0714	0.0054	0.3289	0.0165	1.96	14	34	58	0.59	984	23	980	40	970	158	100	101
PB-35	64.1	1.6932	0.0585	0.1678	0.0015	0.40	5.9612	0.0516	0.0732	0.0026	0.1412	0.0070	0.69	23	3	110	0.03	1000	8	1006	22	1020	74	99	98
PB-35	14.1	1.8317	0.0771	0.1824	0.0032	0.39	5.4829	0.0958	0.0728	0.0035	0.0784	0.0078	0.75	33	9	154	0.06	1080	17	1057	27	1009	91	102	106
PB-35	2.1	1.9541	0.0517	0.1876	0.0024	0.45	5.3315	0.0669	0.0756	0.0022	0.2154	0.0044	0.23	56	-	231	-	1108	13	1100	18	1083	61	100	102
PB-35	59.1	1.9355	0.0415	0.1878	0.0019	0.73	5.3255	0.0552	0.0748	0.0017	0.0882	0.0045	0.15	83	53	374	0.14	1109	11	1094	14	1062	45	101	104
PB-35	54.1	2.0658	0.0513	0.1942	0.0023	0.68	5.1502	0.0605	0.0772	0.0021	0.1770	0.0039	0.10	49	16	204	0.08	1144	12	1138	17	1125	54	100	101
PB-35	52.1	3.9850	0.0865	0.2838	0.0033	0.92	3.5241	0.0406	0.1019	0.0024	0.2084	0.0037	0.15	60	35	164	0.21	1610	16	1631	18	1658	44	98	97
PB-35	80.1	4.0047	0.0717	0.2877	0.0020	0.50	3.4754	0.0240	0.1009	0.0017	0.1396	0.0120	0.85	44	55	124	0.44	1630	10	1635	14	1642	30	99	99
PB-35	48.1	4.1795	0.0903	0.2920	0.0045	0.79	3.4251	0.0522	0.1038	0.0020	0.1746	0.0104	0.38	60	32	165	0.20	1651	22	1670	18	1694	35	98	97
PB-35	82.1	4.9267	0.1600	0.3056	0.0036	0.96	3.2724	0.0380	0.1169	0.0038	0.3321	0.0167	0.42	38	4	78	0.06	1719	18	1807	27	1910	58	95	90
PB-35	38.1	4.3808	0.1089	0.3094	0.0052	0.37	3.2317	0.0539	0.1027	0.0023	0.1953	0.0059	0.05	47	46	116	0.40	1738	25	1709	20	1673	42	101	103
PB-35	24.1	4.7774	0.1421	0.3227	0.0051	0.63	3.0987	0.0494	0.1074	0.0036	0.2604	0.0086	0.42	40	10	91	0.11	1803	25	1781	25	1755	62	101	102
PB-35	77.1	5.6974	0.0967	0.3369	0.0023	0.06	2.9681	0.0206	0.1226	0.0019	0.1968	0.0058	0.24	36	-	80	-	1872	11	1931	14	1995	28	96	93
PB-35	43.1	5.3655	0.1449	0.3414	0.0062	0.82	2.9289	0.0531	0.1140	0.0029	0.3144	0.0133	0.15	39	19	80	0.23	1894	30	1879	23	1864	46	100	101
PB-35	83.1	6.0226	0.2407	0.3428	0.0051	0.73	2.9172	0.0433	0.1274	0.0051	0.1612	0.0092	0.58	14	-	31	-	1900	25	1979	35	2063	73	96	92
PB-35	3.1	5.9834	0.1113	0.3472	0.0037	0.90	2.8798	0.0308	0.1250	0.0024	0.0585	0.0087	0.32	132	7	315	0.02	1921	18	1973	16	2028	34	97	94
PB-35	69.1	5.8722	0.1061	0.3578	0.0021	0.48	2.7952	0.0163	0.1190	0.0021	0.1315	0.0057	0.07	125	-	282	-	1972	10	1957	16	1942	31	100	101
PB-35	18.1	6.0481	0.2196	0.3583	0.0075	0.01	2.7913	0.0581	0.1224	0.0052	0.3846	0.0323	0.18	39	9	72	0.13	1974	35	1983	31	1992	75	99	99
PB-35	53.1	6.0539	0.1090	0.3652	0.0036	0.01	2.7383	0.0271	0.1202	0.0022	0.3051	0.0075	0.50	112	123	216	0.57	2007	17	1984	16	1960	33	101	102
PB-35	42.1	6.6482	0.1304	0.3825	0.0057	0.65	2.6145	0.0389	0.1261	0.0020	0.1842	0.0184	0.10	69	47	140	0.34	2088	27	2066	17	2044	28	101	102
PB-35	40.1	6.7871	0.1550	0.3900	0.0063	0.93	2.5638	0.0417	0.1262	0.0026	0.2570	0.0073	0.21	68	9	128	0.07	2123	30	2084	20	2046	36	101	103
PB-35	33.1	7.2789	0.2155	0.3979	0.0065	0.17	2.5130	0.0408	0.1327	0.0046	0.2646	0.0161	0.33	24	-	43	-	2160	30	2146	26	2134	61	100	101
PB-35	56.1	10.0964	0.1765	0.4425	0.0044	0.61	2.2599	0.0225	0.1655	0.0029	0.0805	0.0033	0.08	74	47	132	0.36	2362	20	2444	16	2513	29	96	94
PB-35	12.1	10.9884	0.2007	0.4626	0.0049	0.47	2.1618	0.0231	0.1723	0.0031	0.0467	0.0104	0.22	20	12	30	0.41	2451	22	2522	16	2580	30	97	94
PB-35	75.1	10.4977	0.1890	0.4779	0.0037	0.67	2.0927	0.0163	0.1593	0.0027	0.0549	0.0047	0.09	76	76	132	0.57	2518	16	2480	17	2449	29	101	102
PB-35	81.1	13.4454	0.2995	0.5089	0.0053	0.81	1.9652	0.0203	0.1916	0.0041	0.0893	0.0119	0.23	41	58	64	0.90	2652	23	2712	21	2756	35	97	96
PB-35	47.1	14.3314	0.2986	0.5378	0.0086	0.32	1.8596	0.0299	0.1933	0.0034	0.2399	0.0271	0.06	112	33	147	0.22	2774	36	2772	19	2770	28	100	100
PB-35	41.1	0.2937	0.0134	0.0401	0.0008	0.92	24.9494	0.4776	0.0532	0.0024	0.0693	0.0127	4.61	23	38	457	0.08	253	5	262	11	335	104	96	75
PB-35	28.1	0.3308	0.0290	0.0485	0.0012	0.53	20.6016	0.4895	0.0494	0.0050	0.3147	0.0210	0.00	16	82	227	0.36	306	7	290	22	168	196	105	181
PB-35	8.1	0.4448	0.0193	0.0606	0.0009	0.48	16.4957	0.2507	0.0532	0.0026	0.2842	0.0098	0.30	36	162	433	0.38	379	6	374	14	338	110	101	112
PB-35	27.1	0.6994	0.0430	0.0850	0.0017	0.59	11.7647	0.2352	0.0597	0.0044	0.5044	0.0417	0.51	20	77	150	0.51	526	10	538	26	592	157	97	88
PB-35	13.1	0.6699	0.0331	0.0862	0.0015	0.28	11.6008	0.2016	0.0564	0.0032	0.1336	0.0071	0.42	21	-	203	-	533	9	521	20	467	122	102	114

PB-35	23.1	0.7172	0.1044	0.0992	0.0040	0.26	10.0827	0.4036	0.0524	0.0092	0.2567	0.0480	2.17	8	12	62	0.19	610	23	549	56	305	291	111	199
PB-35	57.1	0.7738	0.0600	0.0997	0.0024	0.35	10.0340	0.2399	0.0563	0.0053	0.0971	0.0307	1.27	10	53	92	0.58	612	14	582	33	465	185	105	131
PB-35	71.1	0.8417	0.0501	0.0999	0.0011	0.66	10.0131	0.1146	0.0611	0.0039	0.5694	0.0517	17.00	20	6	135	0.04	614	7	620	28	644	146	98	95
PB-35	72.1	0.8186	0.3177	0.1029	0.0059	0.67	9.7167	0.5526	0.0577	0.0237	0.1888	0.0996	5.92	2	58	14	4.10	632	34	607	171	518	603	103	121
PB-35	55.1	0.9581	0.0944	0.1062	0.0036	0.87	9.4195	0.3168	0.0655	0.0073	0.1050	0.0430	0.57	9	47	78	0.60	650	21	682	45	789	208	95	82
PB-35	35.1	1.0031	0.0822	0.1070	0.0031	0.40	9.3492	0.2727	0.0680	0.0068	0.1615	0.0255	1.50	9	24	71	0.34	655	18	705	44	869	227	92	75
PB-35	20.1	1.2926	0.0298	0.1411	0.0015	0.79	7.0877	0.0757	0.0664	0.0016	0.0841	0.0180	24.38	104	24	626	0.04	851	9	842	13	820	50	100	103
PB-35	73.1	3.4625	0.0793	0.2448	0.0021	0.99	4.0842	0.0357	0.1026	0.0020	0.1520	0.0082	0.02	77	-	193	-	1412	11	1519	16	1671	35	92	84
PB-35	61.1	4.9833	0.1331	0.2982	0.0026	0.93	3.3536	0.0292	0.1212	0.0034	0.2184	0.0056	0.28	35	29	84	0.34	1682	13	1817	23	1974	50	92	85
PB-36	55	0.7994	0.0190	0.0973	0.0010	0.66	10.2810	0.1048	0.0596	0.0014	0.0323	0.0043	0.11	64	70	584	0.12	598	6	597	11	589	52	100	101
PB-36	19.1	0.7990	0.0337	0.0979	0.0015	0.19	10.2122	0.1555	0.0592	0.0026	0.3989	0.0116	0.31	32	57	220	0.257	602	9	596	19	574	94	100	104
PB-36	33.1	0.7984	0.0336	0.0981	0.0017	0.41	10.1910	0.1735	0.0590	0.0028	0.1221	0.0088	1.05	17	16	148	0.11	603	10	596	19	568	102	101	106
PB-36	47.1	0.8084	0.0353	0.0987	0.0014	0.39	10.1310	0.1394	0.0594	0.0028	0.1357	0.0107	0.40	29	45	234	0.19	607	8	602	20	582	99	100	104
PB-36	18.1	0.8403	0.0328	0.0993	0.0015	0.42	10.0750	0.1522	0.0614	0.0025	0.3834	0.0129	0.77	25	12	178	0.066	610	9	619	18	653	91	98	93
PB-36	12.1	0.8314	0.0241	0.0994	0.0007	0.40	10.0634	0.0735	0.0607	0.0018	0.1807	0.0105	0.11	46	136	373	0.365	611	4	614	13	628	65	99	97
PB-36	71.1	0.8069	0.0376	0.0997	0.0020	0.43	10.0256	0.2034	0.0587	0.0032	0.2816	0.0074	0.47	27	30	201	0.15	613	12	601	21	555	117	102	110
PB-36	16.1	0.8436	0.0232	0.1004	0.0013	0.63	9.9645	0.1336	0.0610	0.0017	0.0871	0.0043	0.86	59	39	511	0.076	617	8	621	13	638	61	99	96
PB-36	62.1	0.8254	0.0480	0.1004	0.0024	0.46	9.9627	0.2351	0.0596	0.0041	0.1441	0.0139	1.90	19	45	154	0.29	617	14	611	27	591	153	100	104
PB-36	37.1	0.8359	0.0684	0.1005	0.0023	0.42	9.9517	0.2307	0.0603	0.0055	0.2328	0.0206	1.50	11	35	89	0.40	617	14	617	38	615	198	100	100
PB-36	14.1	0.8365	0.0330	0.1009	0.0015	0.42	9.9090	0.1485	0.0601	0.0024	0.1039	0.0076	1.00	27	20	225	0.09	620	9	617	18	608	85	100	101
PB-36	26.1	0.8367	0.0250	0.1009	0.0015	0.83	9.9076	0.1467	0.0601	0.0020	0.2036	0.0079	1.10	34	53	260	0.204	620	9	617	14	608	73	100	101
PB-36	34.1	0.8323	0.0295	0.1012	0.0016	0.42	9.8841	0.1565	0.0597	0.0023	0.0496	0.0087	0.38	21	15	189	0.08	621	9	615	16	592	84	101	105
PB-36	67.1	0.8569	0.0227	0.1022	0.0015	0.89	9.7809	0.1457	0.0608	0.0018	0.1723	0.0071	0.81	54	91	420	0.22	628	9	628	13	632	67	99	99
PB-36	24.1	0.8437	0.0203	0.1023	0.0013	0.01	9.7759	0.1262	0.0598	0.0014	0.3251	0.0238	0.24	86	108	579	0.186	628	8	621	11	597	52	101	105
PB-36	68.1	0.8410	0.0478	0.1027	0.0024	0.16	9.7376	0.2276	0.0594	0.0041	0.2140	0.0302	1.30	16	57	128	0.45	630	14	620	27	582	152	101	108
PB-36	58	0.8887	0.0367	0.1030	0.0014	0.53	9.7114	0.1307	0.0626	0.0028	0.2381	0.0697	0.28	20	67	145	0.46	632	8	646	20	694	100	97	90
PB-36	38.1	0.8761	0.0232	0.1033	0.0010	0.39	9.6783	0.0975	0.0615	0.0016	0.0701	0.0057	0.17	49	54	411	0.13	634	6	639	13	657	57	99	96
PB-36	8.1	0.8744	0.0250	0.1034	0.0008	0.66	9.6753	0.0714	0.0614	0.0018	0.1787	0.0299	2.59	50	71	386	0.184	634	5	638	14	652	64	99	97
PB-36	50	0.8753	0.0266	0.1037	0.0012	0.75	9.6431	0.1107	0.0612	0.0020	0.4579	0.0462	0.23	36	138	233	0.59	636	7	639	15	647	69	99	98
PB-36	61.1	0.8587	0.0254	0.1039	0.0016	0.82	9.6212	0.1518	0.0599	0.0020	0.1840	0.1947	0.28	39	-	392	-	637	10	629	14	601	71	101	106
PB-36	54	0.8517	0.0364	0.1042	0.0014	0.87	9.5927	0.1333	0.0593	0.0026	0.0958	0.0141	2.41	30	183	264	0.69	639	8	626	19	577	92	102	110
PB-36	51	0.8917	0.0345	0.1049	0.0013	0.01	9.5308	0.1224	0.0616	0.0026	0.1894	0.0081	0.19	31	77	225	0.34	643	8	647	19	662	91	99	97
PB-36	28.1	0.8614	0.0238	0.1051	0.0015	0.84	9.5170	0.1388	0.0595	0.0017	0.1052	0.0606	0.28	49	28	360	0.08	644	9	631	13	584	59	102	110
PB-36	17.1	2.3179	0.0443	0.2045	0.0025	0.99	4.8896	0.0605	0.0822	0.0016	0.2406	0.0083	1.06	122	88	468	0.188	1200	14	1218	14	1250	37	98	95
PB-36	48.1	2.3826	0.0750	0.2092	0.0026	0.01	4.7803	0.0604	0.0826	0.0027	0.1143	0.0074	0.33	30	22	117	0.19	1225	14	1237	23	1260	66	98	97
PB-36	25.1	2.4282	0.0844	0.2122	0.0033	0.99	4.7116	0.0728	0.0830	0.0035	0.1987	0.0483	1.11	13	27	50	0.534	1241	20	1251	26	1269	81	99	97
PB-36	29.1	2.3830	0.0468	0.2135	0.0028	1.00	4.6847	0.0624	0.0810	0.0016	0.1569	0.0828	0.07	71	28	232	0.12	1247	15	1238	14	1221	40	100	102
PB-36	11.1	2.3899	0.0540	0.2143	0.0015	0.35	4.6654	0.0319	0.0809	0.0018	0.0906	0.0035	0.08	62	18	258	0.071	1252	8	1240	16	1218	44	100	102
PB-36	69.1	7.0455	0.1647	0.3802	0.0068	0.97	2.6304	0.0468	0.1344	0.0038	0.2347	0.0266	1.33	46	9	84	0.11	2077	32	2117	21	2156	49	98	96
PB-36	30.1	7.3277	0.1452	0.3898	0.0057	0.89	2.5654	0.0378	0.1363	0.0029	0.2187	0.0239	0.00	49	-	94	-	2122	27	2152	18	2181	37	98	97
PB-36	21.1	7.6239	0.3265	0.4032	0.0083	0.65	2.4802	0.0513	0.1371	0.0064	0.1774	0.0263	0.00	12	7	22	0.293	2184	38	2188	39	2191	83	99	99
PB-36	60	2.5717	0.0506	0.2254	0.0022	0.89	4.4365	0.0441	0.0827	0.0016	0.0949	0.0439	0.29	50	11	174	0.07	1310	12	1293	14	1263	39	101	103
PB-36	49	7.9050	0.1180	0.4250	0.0040	0.02	2.3531	0.0220	0.1349	0.0019	0.2580	0.0131	0.30	104	67	169	0.40	2283	18	2220	13	2163	24	102	105
PB-36	52	6.8128	0.1092	0.3860	0.0038	0.94	2.5906	0.0252	0.1280	0.0020	0.1243	0.0085	0.08	78	-	157	-	2104	18	2087	14	2071	28	100	101
PB-36	72.1	0.5953	0.0243	0.0759	0.0014	0.01	13.1816	0.2445	0.0569	0.0027	0.1438	0.0088	0.68	37	37	390	0.09	471	8	474	16	488	106	99	96
PB-36	43.1	0.6625	0.0472	0.0832	0.0017	0.45	12.0146	0.2393	0.0577	0.0046	0.1915	0.0192	0.81	13	14	121	0.12	515	10	516	29	519	180	99	99
PB-36	44	1.1406	0.0368	0.1261	0.0015	0.95	7.9307	0.0932	0.0656	0.0021	0.2476	0.0225	3.65	44	135	265	0.51	766	8	773	17	794	68	99	96
PB-36	66.1	1.2335	0.0448	0.1351	0.0025	0.68	7.4010	0.1372	0.0662	0.0028	0.1312	0.0120	0.57	33	35	197	0.18	817	14	816	21	813	90	100	100
PB-36	20.1	1.2570	0.0270	0.1408	0.0018	0.98	7.1043	0.0895	0.0648	0.0014	0.1099	0.0154	0.70	90	49	590	0.084	849	10	827	12	767	46	102	110
PB-36	53	1.3090	0.0351	0.1414	0.0016	0.96	7.0732	0.0805	0.0672	0.0018	0.1611	0.0081	0.21	51	71	284	0.25	853	9	850	15	842	55	100	101
PB-36	36.1	1.7369	0.0321	0.1720	0.0023	0.88	5.8148	0.0761	0.0732	0.0014	0.0220	0.0019	0.11	73	-	386	0.00	1023	12	1022	12	1021	40	100	100
PB-36	39.1	2.0279	0.0957	0.1852	0.0032	0.45	5.3997	0.0941	0.0794	0.0042	0.2397	0.0335	1.45	14	5	58	0.09	1095	18	1125	33	1183	110	97	92
PB-36	59	4.7398	0.1565	0.3190	0.0048	0.42	3.1344	0.0472	0.1078	0.0040	0.1519	0.0080	0.41	17	35	41	0.85	1785	23	1774	28	1762	67	100	101
PB-36	41.1	5.6962	0.1122	0.3311	0.0031	0.53	3.0203	0.0281	0.1248	0.0022	0.0565	0.0024	0.18	136	33	335	0.10	1844	15	1931	17	2026	31	95	91
PB-36	57	6.0153	0.1515	0.3628	0.0047	0.78	2.7562	0.0358	0.1202	0.0033	0.3067	0.0107	0.31	34	42	66	0.64	1996	22	1978	22	1960	49	100	101
PB-36	64.1	6.3037	0.1741	0.3821	0.0074	0.30	2.6169	0.0507	0.1196	0.0039	0.2526	0.0187	0.45	38	13	75	0.18	2086	34	2019	24	1951	57	103	106
PB-36	31.1	10.1601	0.2187	0.4464	0.0072	0.95	2.2401	0.0360	0.1651	0.0040	0.0876	0.0142	0.44	17	-	28	-	2379	32	2450	20	2508	41	97	94
PB-36	9.1	0.8958	0.0282	0.1056	0.0008	0.78	9.4714	0.0745	0.0615	0.0020	0.2016	0.0135	1.35	43	70	338	0.206	647	5	650	16	658	76	99	98
PB-36	1.1	0.9348	0.0402	0.1074	0.0011	0.69	9.3074	0.0914	0.0631	0.0028	0.2150	0.0736	0.76	17	12	121	0.102	658	6	670	21	712	96	98	92
PB-36	35.1	0.9099	0.0365	0.1076	0.0018	0.84	9.2939	0.1579	0.0613	0.0027	0.0875	0.0258	1.57	17	27	144	0.19	659	11	657	19	651	96	100	101
PB-36	46.1	0.8972	0.0290	0.1076	0.0012	0.82	9.2900	0.1044	0.0604	0.0020	0.2162	0.0060	1.16	40	4	299	0.01	659	7	650	15	620	72	101	106

PB-36	65.1	0.9275	0.0408	0.1105	0.0022	0.45	9.0478	0.1798	0.0609	0.0031	0.1850	0.0088	0.97	26	73	191	0.38	676	13	666	22	634	111	101	106
PB-36	2.1	0.7544	0.0757	0.0929	0.0017	0.01	10.7700	0.1937	0.0589	0.0064	0.6359	0.0363	0.20	12	37	79	0.472	572	10	571	45	564	228	100	101
PB-36	32.1	0.7713	0.0523	0.0929	0.0021	0.48	10.7617	0.2375	0.0602	0.0045	0.1755	0.0185	0.79	10	21	86	0.24	573	12	581	30	611	167	98	93
PB-36	45.1	0.7943	0.0474	0.0948	0.0017	0.01	10.5450	0.1905	0.0608	0.0040	0.1317	0.0153	0.89	14	49	118	0.41	584	10	594	27	630	151	98	92
PB-36	91.1	0.7934	0.0391	0.0962	0.0010	0.22	10.3908	0.1076	0.0598	0.0031	0.2480	0.0139	0.81	23	40	186	0.215	592	6	593	22	596	110	99	99
PB-36	3.1	0.8064	0.0167	0.0963	0.0006	1.00	10.3796	0.0596	0.0607	0.0014	0.0542	0.0042	2.26	101	57	915	0.063	593	3	600	10	629	49	98	94
PB-36	40.1	0.7773	0.0514	0.0964	0.0018	0.01	10.3776	0.1939	0.0585	0.0045	0.1805	0.0208	1.90	14	8	117	0.07	593	11	584	29	549	154	101	108
PB-36	4.1	0.0877	0.0111	0.0135	0.0002	0.11	74.2843	1.2980	0.0473	0.0065	0.4733	0.0362	0.81	12	204	583	0.35	86	2	85	10	63	183	100	137
PB-36	70.1	0.4604	0.0849	0.0656	0.0034	0.40	15.2439	0.7888	0.0509	0.0093	0.2083	0.1296	18.27	19	141	211	0.67	410	20	385	57	237	283	106	173
PB-36	27.1	0.6674	0.0210	0.0799	0.0013	0.98	12.5234	0.2082	0.0606	0.0018	0.1728	0.0081	4.52	41	49	325	0.15	495	8	519	12	626	62	95	79
PB-36	22.1	0.6494	0.0698	0.0844	0.0019	0.71	11.8478	0.2691	0.0558	0.0063	0.1718	0.0363	1.55	8	17	76	0.219	522	11	508	43	445	245	102	117
PB-36	10.1	0.8077	0.0580	0.0954	0.0013	0.38	10.4798	0.1421	0.0614	0.0047	0.1714	0.0171	1.02	11	17	101	0.172	588	8	601	32	653	173	97	89
PB-36	6.1	0.8328	0.0606	0.0955	0.0014	0.34	10.4747	0.1500	0.0633	0.0048	0.3946	0.1039	0.46	15	34	106	0.319	588	8	615	33	717	165	95	81
PB-36	23.1	0.7902	0.0954	0.1026	0.0025	0.01	9.7503	0.2367	0.0559	0.0074	0.2665	0.0303	2.75	7	18	54	0.342	629	15	591	51	448	243	106	140
PB-36	5.1	0.8992	0.0320	0.1029	0.0009	0.90	9.7165	0.0821	0.0634	0.0024	0.2369	0.0081	5.05	42	64	317	0.201	632	5	651	18	721	88	96	87
PB-36	13.1	1.0336	0.0553	0.1090	0.0018	0.68	9.1741	0.1541	0.0688	0.0041	0.1333	0.1021	6.05	42	38	286	0.134	667	11	721	30	892	142	92	74
PB-36	63.1	2.1111	0.0605	0.1724	0.0031	0.99	5.8004	0.1034	0.0888	0.0025	0.0086	0.0115	4.03	76	25	303	0.08	1025	17	1152	18	1400	53	88	73
PB-36	42.1	1.9492	0.0590	0.1936	0.0022	0.88	5.1664	0.0599	0.0730	0.0023	0.0741	0.0149	0.35	27	20	129	0.15	1141	12	1098	20	1015	64	103	112
PB-36	15.1	4.9706	0.0895	0.2940	0.0037	1.00	3.4011	0.0423	0.1226	0.0022	0.1095	0.0037	0.55	80	20	189	0.104	1662	18	1814	16	1995	33	91	83
PB-36	56	5.9098	0.1445	0.3288	0.0043	0.94	3.0413	0.0398	0.1304	0.0034	0.1409	0.0097	0.49	27	32	57	0.56	1833	21	1963	21	2103	47	93	87
PB-37	77.1	0.3175	0.0223	0.0412	0.0005	0.45	24.2771	0.3026	0.0559	0.0040	0.1810	0.0149	1.46	10	97	204	0.47	0.260	0.003	0.280	0.017	0.448	0.152	92	
PB-37	94.1	0.2808	0.0127	0.0420	0.0004	0.29	23.8337	0.2199	0.0485	0.0022	0.2453	0.0107	2.34	19	205	340	0.60	0.265	0.002	0.251	0.010	0.125	0.099	105	
PB-37	61.1	0.6341	0.0229	0.0808	0.0008	0.75	12.3801	0.1207	0.0569	0.0020	0.0054	0.0045	0.10	53	12	605	0.02	0.501	0.005	0.499	0.014	0.489	0.076	100	
PB-37	49.1	0.6525	0.0522	0.0821	0.0011	0.47	12.1841	0.1690	0.0577	0.0046	0.1361	0.0190	1.78	11	40	111	0.36	0.508	0.007	0.510	0.031	0.517	0.155	99	
PB-37	62.1	0.6570	0.0252	0.0821	0.0008	0.79	12.1846	0.1244	0.0581	0.0022	0.1296	0.0108	1.74	21	70	223	0.32	0.508	0.005	0.513	0.016	0.532	0.084	99	
PB-37	71.1	0.6680	0.0366	0.0825	0.0011	0.31	12.1166	0.1620	0.0587	0.0031	0.1455	0.0085	1.36	20	95	199	0.48	0.511	0.007	0.519	0.022	0.556	0.111	98	
PB-37	95.1	0.6539	0.0208	0.0829	0.0007	0.5	12.0623	0.1069	0.0572	0.0019	0.0352	0.0027	1.22	73	74	827	0.09	0.513	0.004	0.511	0.013	0.500	0.073	100	
PB-37	35.1	0.6802	0.0329	0.0835	0.0009	0.65	11.9746	0.1303	0.0591	0.0028	0.1099	0.0248	0.52	14	48	121	0.39	0.517	0.005	0.527	0.020	0.570	0.104	98	
PB-37	56.1	0.6605	0.0349	0.0840	0.0010	0.26	11.9097	0.1417	0.0571	0.0029	0.2004	0.0066	0.00	36	196	358	0.55	0.520	0.006	0.515	0.021	0.494	0.113	100	
PB-37	96.1	0.6750	0.0234	0.0847	0.0008	0.4	11.8039	0.1070	0.0578	0.0020	0.0634	0.0045	1.14	36	66	391	0.17	0.524	0.005	0.524	0.014	0.522	0.078	100	
PB-37	81.1	0.6737	0.0205	0.0853	0.0009	0.28	11.7249	0.1218	0.0573	0.0017	0.0255	0.0053	0.00	50	28	547	0.05	0.528	0.005	0.523	0.012	0.503	0.064	100	
PB-37	79.1	0.7099	0.0325	0.0856	0.0009	0.28	11.6843	0.1259	0.0602	0.0027	0.1668	0.0073	0.00	28	114	272	0.42	0.529	0.005	0.545	0.019	0.609	0.099	97	
PB-37	67.1	0.6979	0.0309	0.0856	0.0012	0.62	11.6759	0.1621	0.0591	0.0025	0.0339	0.0092	3.91	32	45	313	0.15	0.530	0.007	0.538	0.019	0.571	0.094	98	
PB-37	1.1	0.7013	0.0216	0.0860	0.0006	0.32	11.6221	0.0867	0.0591	0.0019	0.3088	0.0053	0.77	50	351	420	0.84	0.532	0.004	0.540	0.013	0.571	0.070	98	
PB-37	88.1	0.6945	0.0245	0.0864	0.0008	0.19	11.5730	0.1089	0.0583	0.0020	0.0416	0.0037	0.30	38	45	411	0.11	0.534	0.005	0.535	0.015	0.541	0.075	99	
PB-37	17.1	0.6969	0.0256	0.0876	0.0009	0.62	11.4141	0.1125	0.0577	0.0021	0.2279	0.0068	0.00	32	142	280	0.51	0.541	0.005	0.537	0.015	0.518	0.080	100	
PB-37	48.1	0.7485	0.0245	0.0928	0.0008	0.77	10.7756	0.0969	0.0585	0.0021	0.0054	0.0058	0.89	47	8	477	0.02	0.572	0.005	0.567	0.015	0.548	0.075	100	
PB-37	9.1	0.7156	0.0508	0.0935	0.0011	0.45	10.6938	0.1302	0.0555	0.0038	0.0677	0.0156	5.08	14	23	139	0.17	0.576	0.007	0.548	0.031	0.433	0.133	105	
PB-37	26.1	0.7644	0.0229	0.0935	0.0010	0.42	10.6952	0.1159	0.0593	0.0017	0.0382	0.0065	1.50	43	38	405	0.09	0.576	0.006	0.577	0.013	0.578	0.063	99	
PB-37	86.1	0.7581	0.0317	0.0937	0.0008	0.33	10.6715	0.0949	0.0587	0.0024	0.1135	0.0106	2.88	31	76	276	0.28	0.577	0.005	0.573	0.018	0.555	0.088	100	
PB-37	11.1	0.7730	0.0280	0.0941	0.0010	0.35	10.6242	0.1168	0.0596	0.0020	0.0444	0.0091	0.54	36	33	361	0.09	0.580	0.006	0.581	0.016	0.588	0.072	99	
PB-37	57.1	0.7726	0.0270	0.0946	0.0011	0.82	10.5687	0.1245	0.0592	0.0019	0.0744	0.0101	0.68	69	121	710	0.17	0.583	0.007	0.581	0.015	0.575	0.069	100	
PB-37	84.1	0.7851	0.0274	0.0954	0.0010	0.5	10.4774	0.1060	0.0597	0.0020	0.1229	0.0063	0.33	40	102	357	0.28	0.588	0.006	0.588	0.016	0.591	0.072	99	
PB-37	15.1	0.7723	0.0293	0.0956	0.0010	0.44	10.4568	0.1064	0.0586	0.0023	0.1450	0.0094	2.92	34	120	277	0.43	0.589	0.006	0.581	0.017	0.551	0.085	101	
PB-37	73.1	0.7719	0.0271	0.0957	0.0011	0.25	10.4460	0.1191	0.0585	0.0020	0.1888	0.0073	0.55	27	121	240	0.51	0.589	0.006	0.581	0.016	0.548	0.076	101	
PB-37	75.1	0.8030	0.0323	0.0967	0.0010	0.41	10.3396	0.1062	0.0602	0.0023	0.0971	0.0058	0.00	29	67	266	0.25	0.595	0.006	0.599	0.018	0.611	0.086	99	
PB-37	45.1	0.8278	0.0429	0.0975	0.0009	0.21	10.2542	0.0927	0.0616	0.0033	0.2162	0.0236	0.00	18	91	141	0.64	0.600	0.005	0.612	0.024	0.659	0.112	97	
PB-37	3.1	0.8156	0.0262	0.0980	0.0008	0.66	10.2047	0.0843	0.0604	0.0020	0.0577	0.0036	0.28	52	68	478	0.14	0.603	0.005	0.606	0.015	0.617	0.071	99	
PB-37	41.1	0.7712	0.0268	0.0980	0.0009	0.81	10.2050	0.0916	0.0571	0.0020	0.0084	0.0128	1.99	40	3	358	0.01	0.603	0.005	0.580	0.016	0.494	0.077	103	
PB-37	27.1	0.8253	0.0302	0.0989	0.0011	0.02	10.1093	0.1126	0.0605	0.0021	0.2929	0.0068	0.05	28	165	215	0.77	0.608	0.006	0.611	0.017	0.622	0.074	99	
PB-37	78.1	0.8404	0.0240	0.1009	0.0010	0.51	9.9083	0.1006	0.0604	0.0016	0.0094	0.0066	1.15	28	7	269	0.03	0.620	0.006	0.619	0.013	0.618	0.058	100	
PB-37	74.1	0.7999	0.0336	0.1019	0.0012	0.18	9.8183	0.1116	0.0570	0.0023	0.4067	0.0091	0.39	26	203	177	1.15	0.625	0.007	0.597	0.019	0.490	0.087	104	
PB-37	46.1	0.8449	0.0282	0.1020	0.0009	0.88	9.8040	0.0866	0.0601	0.0021	0.0486	0.0050	1.31	54	79	461	0.17	0.626	0.005	0.622	0.016	0.606	0.074	100	
PB-37	65.1	0.8472	0.0463	0.1023	0.0011	0.28	9.7715	0.1090	0.0600	0.0033	0.2527	0.0258	3.09	26	153	191	0.80	0.628	0.007	0.623	0.026	0.605	0.122	100	
PB-37	14.1	0.8760	0.0328	0.1034	0.0010	0.02	9.6686	0.0955	0.0614	0.0023	0.0789	0.0088	1.61	23	42	191	0.22	0.634	0.006	0.639	0.018	0.654	0.080	99	
PB-37	8.1	0.8878	0.0339	0.1036	0.0012	0.24	9.6482	0.1151	0.0621	0.0023	0.0815	0.0139	4.59	15	42	126	0.33	0.636	0.007	0.645	0.019	0.678	0.084	98	
PB-37	87.1	0.9013	0.0415	0.1036	0.0010	0.25	9.6480	0.0930	0.0631	0.0029	0.1723	0.0069	0.52	18	77	145	0.53	0.636	0.006	0.652	0.022	0.711	0.096	97	
PB-37	80.1	0.8556	0.0410	0.1043	0.0013	0.39	9.5912	0.1211	0.0595	0.0029	0.2957	0.0158	1.27	15	86	110	0.78	0.639	0.008	0.628	0.022	0.586	0.103	101	
PB-37	66.1	0.8964	0.0313	0.1052	0.0010	0.57	9.5051	0.0923	0.0618	0.0021	0.1834	0.0172	7.87	55	240	416	0.58	0.645	0.006	0.650	0.017	0.667	0.073	99	
PB-37	38.1	0.9251	0.0352	0.1059	0.0010	0.3	9.4457	0.0931	0.0634	0.0024	0.0829	0.0073	0.67	26	58	209	0.28	0.649	0.006	0.665	0.019	0.721	0.083	97	
PB-37	22.1	0.8910	0.0613	0.1071	0.0014	0.47	9.3399	0.1210	0.0604	0.0038	0.2356	0.0155	1.56	19	86	141	0.61	0.656	0.008	0.647	0.031	0.616	0.131	101	

PB-37	29.1	0.9048	0.0560	0.1078	0.0012	0.14	9.2775	0.1022	0.0609	0.0035	0.2619	0.0141	3.68	16	75	104	0.72	0.660	0.007	0.654	0.030	0.635	0.128	100	
PB-37	24.1	0.9298	0.0352	0.1084	0.0011	0.62	9.2229	0.0939	0.0622	0.0022	0.0570	0.0037	0.45	37	46	314	0.15	0.664	0.006	0.668	0.019	0.681	0.075	99	
PB-37	58.1	0.9363	0.0582	0.1085	0.0013	0.54	9.2142	0.1088	0.0626	0.0038	0.2784	0.0101	0.05	26	132	198	0.67	0.664	0.007	0.671	0.031	0.694	0.131	98	
PB-37	82.1	0.9335	0.0242	0.1088	0.0011	0.37	9.1906	0.0966	0.0622	0.0015	0.0125	0.0020	0.00	89	28	765	0.04	0.666	0.007	0.669	0.013	0.682	0.054	99	
PB-37	25.1	0.9166	0.0310	0.1092	0.0012	0.67	9.1537	0.0979	0.0609	0.0019	0.0387	0.0031	0.91	44	38	376	0.10	0.668	0.007	0.661	0.016	0.634	0.068	101	
PB-37	76.1	0.9576	0.0310	0.1112	0.0012	0.57	8.9918	0.0981	0.0625	0.0018	0.1101	0.0059	0.41	30	69	237	0.29	0.680	0.007	0.682	0.016	0.690	0.060	99	
PB-37	68.1	1.0263	0.0384	0.1164	0.0015	0.21	8.5879	0.1076	0.0639	0.0022	0.0185	0.0035	1.70	54	26	438	0.06	0.710	0.008	0.717	0.019	0.739	0.074	99	
PB-37	40.1	1.0122	0.0404	0.1182	0.0011	0.62	8.4630	0.0808	0.0621	0.0024	0.0655	0.0061	0.42	42	51	315	0.16	0.720	0.007	0.710	0.020	0.679	0.079	101	
PB-37	53.1	1.1005	0.0462	0.1269	0.0012	0.63	7.8826	0.0757	0.0629	0.0023	0.1362	0.0067	0.90	33	143	199	0.72	0.770	0.007	0.754	0.022	0.705	0.076	102	
PB-37	23.1	1.1896	0.0554	0.1308	0.0013	0.17	7.6447	0.0784	0.0660	0.0029	0.0770	0.0056	0.68	28	37	191	0.19	0.792	0.008	0.796	0.025	0.805	0.090	99	
PB-37	43.1	1.1618	0.0359	0.1315	0.0012	0.31	7.6050	0.0688	0.0641	0.0020	0.1356	0.0035	0.21	80	178	503	0.36	0.796	0.007	0.783	0.017	0.744	0.067	101	
PB-37	33.1	1.2328	0.0399	0.1333	0.0014	0.56	7.5005	0.0782	0.0671	0.0021	0.2898	0.0056	0.00	58	216	310	0.70	0.807	0.008	0.816	0.018	0.840	0.065	98	
PB-37	54.1	1.2116	0.0561	0.1346	0.0013	0.54	7.4270	0.0736	0.0653	0.0028	0.1265	0.0083	1.60	26	102	162	0.63	0.814	0.008	0.806	0.026	0.783	0.092	101	
PB-37	70.1	1.2948	0.0542	0.1401	0.0018	0.79	7.1390	0.0941	0.0670	0.0027	0.1265	0.0099	6.28	34	88	227	0.39	0.845	0.010	0.843	0.024	0.839	0.083	100	
PB-37	52.1	1.3070	0.0739	0.1457	0.0015	0.26	6.8643	0.0684	0.0651	0.0034	0.1547	0.0172	1.76	17	41	95	0.43	0.877	0.008	0.849	0.032	0.776	0.104	103	
PB-37	19.1	1.4066	0.0651	0.1482	0.0015	0.14	6.7476	0.0688	0.0688	0.0030	0.1826	0.0110	1.33	20	52	111	0.47	0.891	0.008	0.892	0.027	0.894	0.089	99	
PB-37	90.1	1.3796	0.0645	0.1488	0.0015	0.77	6.7199	0.0664	0.0672	0.0030	0.1289	0.0135	0.46	21	33	108	0.30	0.894	0.008	0.880	0.027	0.845	0.091	101	
PB-37	6.1	1.4295	0.0396	0.1495	0.0011	0.88	6.6884	0.0508	0.0693	0.0021	0.0072	0.0028	0.37	193	29	1193	0.02	0.898	0.006	0.901	0.017	0.909	0.059	99	
PB-37	5.1	1.4922	0.0687	0.1519	0.0013	0.36	6.5833	0.0542	0.0712	0.0034	0.3622	0.0089	0.50	29	113	138	0.82	0.912	0.007	0.927	0.028	0.964	0.099	98	
PB-37	16.1	1.4676	0.0587	0.1537	0.0015	0.21	6.5042	0.0638	0.0692	0.0027	0.0539	0.0071	0.40	23	18	133	0.13	0.922	0.008	0.917	0.024	0.906	0.082	100	
PB-37	13.1	1.5611	0.0602	0.1586	0.0017	0.21	6.3069	0.0678	0.0714	0.0027	0.1091	0.0076	0.37	23	34	122	0.28	0.949	0.009	0.955	0.024	0.969	0.080	99	
PB-37	55.1	1.5780	0.0584	0.1600	0.0020	0.63	6.2516	0.0771	0.0715	0.0024	0.1097	0.0072	0.70	55	130	294	0.44	0.957	0.011	0.962	0.023	0.973	0.069	99	
PB-37	51.1	1.5437	0.0681	0.1609	0.0015	0.99	6.2141	0.0582	0.0696	0.0027	0.1983	0.0216	1.11	30	88	147	0.60	0.962	0.008	0.948	0.027	0.916	0.074	101	
PB-37	21.1	1.5771	0.0557	0.1662	0.0017	0.87	6.0162	0.0613	0.0688	0.0022	0.1394	0.0045	0.24	74	148	424	0.35	0.991	0.009	0.961	0.021	0.893	0.065	103	
PB-37	59.1	1.6498	0.1088	0.1698	0.0025	0.03	5.8893	0.0856	0.0705	0.0044	0.2099	0.0156	2.44	11	35	55	0.64	1.011	0.014	0.989	0.040	0.942	0.121	102	
PB-37	64.1	1.8089	0.0916	0.1716	0.0018	0.52	5.8279	0.0608	0.0765	0.0038	0.1734	0.0074	0.16	31	72	143	0.50	1.021	0.010	1.049	0.033	1.107	0.098	97	
PB-37	39.1	1.7793	0.0675	0.1723	0.0016	0.35	5.8035	0.0543	0.0749	0.0028	0.2740	0.0063	0.04	40	117	167	0.70	1.025	0.009	1.038	0.025	1.066	0.074	98	
PB-37	92.1	1.7835	0.0512	0.1740	0.0015	0.42	5.7464	0.0511	0.0743	0.0022	0.1839	0.0025	0.19	105	242	483	0.50	1.034	0.009	1.039	0.019	1.050	0.060	99	
PB-37	93.1	1.7997	0.0748	0.1745	0.0016	0.39	5.7316	0.0538	0.0748	0.0032	0.1057	0.0073	1.35	22	31	113	0.28	1.037	0.009	1.045	0.028	1.063	0.087	99	
PB-37	12.1	1.7510	0.0822	0.1751	0.0021	0.78	5.7122	0.0670	0.0725	0.0032	0.1689	0.0148	0.65	26	62	119	0.53	1.040	0.011	1.028	0.030	1.001	0.089	101	
PB-37	42.1	1.8330	0.0706	0.1756	0.0016	0.66	5.6953	0.0533	0.0757	0.0028	0.1393	0.0044	1.34	54	86	230	0.37	1.043	0.009	1.057	0.025	1.087	0.073	98	
PB-37	91.1	1.8998	0.0529	0.1795	0.0016	0.96	5.5720	0.0508	0.0768	0.0022	0.2166	0.0220	1.89	161	384	754	0.51	1.064	0.009	1.081	0.018	1.115	0.056	98	
PB-37	72.1	1.8551	0.0754	0.1820	0.0023	0.03	5.4935	0.0680	0.0739	0.0028	0.2037	0.0074	0.76	36	99	152	0.65	1.078	0.012	1.065	0.027	1.039	0.075	101	
PB-37	44.1	1.9139	0.0602	0.1839	0.0017	0.59	5.4374	0.0493	0.0755	0.0024	0.0376	0.0043	0.76	50	28	241	0.12	1.088	0.009	1.086	0.021	1.081	0.065	100	
PB-37	60.1	1.9242	0.1097	0.1884	0.0028	0.66	5.3091	0.0780	0.0741	0.0039	0.0510	0.0203	5.17	11	20	42	0.47	1.112	0.015	1.090	0.036	1.044	0.104	102	
PB-37	31.1	3.1137	0.0938	0.2454	0.0026	0.56	4.0755	0.0436	0.0920	0.0026	0.1673	0.0067	0.59	36	43	111	0.39	1.415	0.014	1.436	0.023	1.468	0.056	98	
PB-37	85.1	4.4833	0.1212	0.3029	0.0028	0.53	3.3018	0.0303	0.1074	0.0028	0.1252	0.0017	0.16	116	101	322	0.31	1.705	0.014	1.728	0.023	1.755	0.048	98	
PB-37	7.1	4.5293	0.1418	0.3049	0.0033	0.48	3.2795	0.0352	0.1077	0.0030	0.1577	0.0091	1.09	29	36	78	0.47	1.716	0.016	1.736	0.026	1.761	0.051	98	
PB-37	18.1	4.4429	0.1414	0.3058	0.0032	0.68	3.2704	0.0339	0.1054	0.0034	0.2904	0.0132	0.65	37	61	86	0.71	1.720	0.016	1.720	0.026	1.721	0.058	99	
PB-37	4.1	4.5462	0.1237	0.3097	0.0024	0.77	3.2287	0.0249	0.1065	0.0030	0.1966	0.0045	0.00	87	114	216	0.53	1.739	0.012	1.739	0.022	1.740	0.051	99	
PB-37	89.1	4.6147	0.1276	0.3135	0.0028	0.29	3.1897	0.0284	0.1068	0.0028	0.1736	0.0031	0.10	118	153	299	0.51	1.758	0.014	1.752	0.023	1.745	0.049	100	
PB-37	34.1	5.4644	0.1570	0.3339	0.0041	0.86	2.9949	0.0365	0.1187	0.0033	0.3120	0.0302	0.00	31	33	60	0.54	1.857	0.020	1.895	0.024	1.937	0.049	98	
PB-37	37.1	5.4086	0.1822	0.3380	0.0034	0.45	2.9586	0.0295	0.1161	0.0037	0.3334	0.0130	0.00	39	73	78	0.94	1.877	0.016	1.886	0.029	1.896	0.059	99	
PB-37	50.1	5.7826	0.1884	0.3463	0.0034	0.87	2.8877	0.0283	0.1211	0.0034	0.2556	0.0373	0.24	89	203	193	1.05	1.917	0.016	1.944	0.028	1.973	0.050	98	
PB-37	28.1	6.0069	0.1686	0.3635	0.0044	0.44	2.7510	0.0334	0.1198	0.0031	0.2272	0.0132	0.07	31	47	62	0.76	1.999	0.021	1.977	0.025	1.954	0.046	101	
PB-37	20.1	6.3746	0.2206	0.3674	0.0039	0.89	2.7220	0.0291	0.1258	0.0038	0.1580	0.0071	0.25	32	29	70	0.41	2.017	0.018	2.029	0.029	2.041	0.053	99	
PB-37	47.1	6.5691	0.1883	0.3723	0.0036	0.69	2.6863	0.0256	0.1280	0.0038	0.1433	0.0030	0.47	98	95	201	0.47	2.040	0.017	2.055	0.025	2.070	0.052	99	
PB-37	69.1	6.6276	0.1966	0.3725	0.0046	0.48	2.6842	0.0334	0.1290	0.0035	0.1380	0.0061	0.54	147	147	300	0.49	2.041	0.022	2.063	0.026	2.085	0.047	98	
PB-37	2.1	6.8707	0.1782	0.3863	0.0030	0.01	2.5884	0.0201	0.1290	0.0034	0.2498	0.0047	0.00	0	0	0	8.37	2.106	0.014	2.095	0.023	2.084	0.047	100	
PB-37	32.1	7.3900	0.1891	0.4100	0.0042	0.25	2.4390	0.0251	0.1307	0.0031	0.1322	0.0041	0.35	104	68	204	0.33	2.215	0.019	2.160	0.023	2.108	0.042	102	
PB-37	36.1	11.2335	0.2883	0.4657	0.0051	0.9	2.1474	0.0234	0.1750	0.0041	0.1231	0.0026	1.26	156	95	264	0.36	2.465	0.022	2.543	0.023	2.606	0.039	96	
PB-37	63.1	11.2949	0.2964	0.4820	0.0049	0.67	2.0746	0.0209	0.1700	0.0043	0.1124	0.0039	0.94	70	39	103	0.38	2.536	0.021	2.548	0.024	2.557	0.042	99	
PB-37	83.1	12.3177	0.3413	0.5036	0.0058	0.9	1.9857	0.0230	0.1774	0.0046	0.3327	0.0066	0.58	43	59	62	0.95	2.629	0.025	2.629	0.027	2.629	0.044	100	
PB-37	30.1	31.7403	0.7139	0.7527	0.0083	0.14	1.3285	0.0146	0.3058	0.0062	0.0619	0.0030	0.47	69	28	81	0.35	3.617	0.030	3.542	0.022	3.500	0.031	102	
PB-37	10.1	0.7210	0.0616	0.1036	0.0014	0.66	9.6532	0.1330	0.0505	0.0044	0.2587	0.0307	10.41	13	118	90	1.32	0.635	0.008	0.551	0.037	0.217	0.146	115	
PB-38	52.1	0.6994	0.0226	0.0867	0.0009	0.57	11.5317	0.1236	0.0585	0.002	0.0882	0.0085	0.31	44	46.9	428.1	0.109	536	5.5	538	13	548	77.2	99	97
PB-38	75.1	0.7028	0.0199	0.0875	0.001	0.69	11.4263	0.1246	0.0582	0.0018	0.0609	0.0067	0.64	63.5	2.2	640.1	0.003	541	5.7	541	12	539	67.3	100	100
PB-38	68.1	0.7066	0.0236	0.0886	0.0008	0.29	11.2836	0.1007	0.0578	0.0021	0.0308	0.0088	0.37	35.3	2.4	357.9	0.007	547	4.7	543	14	523	79.7	100	104
PB-38	8.1	0.7106	0.059	0.0887	0.0019	0.61	11.2779	0.2386	0.0581	0.0059	0.2352	0.0264	0.36	15.6	36.4	131.9	0.276	548	11.1	545	36	535	210.2	100	102
PB-38	82.1	0.7203	0.0282	0.0901	0.0013	0.45	11.0975	0.1564	0.058	0.0026	0.0765	0.0091	0.47	31.8	52.6	304.4	0.173	556	7.5	551	16	529	94.2	100	105
PB-38	1.1	0.7237	0.0409	0.0902	0.0014	0.27	11.0851	0.1753	0.0582	0.0037	0.2968	0.1057	0.92	19.3	56.9	162.6	0.35	557	8.4	553	24	537	147.0	100	103

PB-38	34.1	0.7364	0.0318	0.0909	0.001	0.69	11.0041	0.124	0.0588	0.0027	0.6173	0.0134	0.43	50.3	198.7	320.5	0.62	561	6.0	560	19	559	100.8	100	100
PB-38	70.1	0.7536	0.0237	0.092	0.0008	0.01	10.8718	0.0935	0.0594	0.002	0.2352	0.0061	0.28	47.2	14.7	390.1	0.038	567	4.7	570	14	582	74.5	99	97
PB-38	92.1	0.7824	0.0303	0.0954	0.0013	0.4	10.486	0.1436	0.0595	0.0026	0.203	0.0068	0.43	47.8	12.1	377.8	0.032	587	7.7	587	17	586	95.7	100	100
PB-38	19.1	0.7748	0.0324	0.0955	0.0011	0.74	10.4712	0.1166	0.0588	0.0027	0.2836	0.0172	0.1	43.5	103	328.1	0.314	588	6.3	583	18	561	98.4	100	104
PB-38	66.1	0.7952	0.0278	0.096	0.0009	0.27	10.4187	0.0974	0.0601	0.0023	0.3436	0.0209	0.64	45.3	8	323.3	0.025	591	5.3	594	16	607	85.8	99	97
PB-38	53.1	0.7894	0.0232	0.0963	0.001	0.56	10.3808	0.1055	0.0594	0.0019	0.0783	0.0047	0.89	47.1	-	425.6	-	593	5.8	591	13	583	67.3	100	101
PB-38	63.1	0.7843	0.0332	0.0964	0.001	0.27	10.3765	0.1122	0.059	0.0028	0.1809	0.0119	0.33	31.8	2.2	261.1	0.008	593	6.1	588	19	568	107.6	100	104
PB-38	37.1	0.8103	0.0476	0.0969	0.0013	0.45	10.318	0.1373	0.0606	0.0039	0.2143	0.0151	1	22.6	115.5	179.2	0.644	596	7.6	603	27	626	135.2	98	95
PB-38	16.1	0.8553	0.0317	0.1025	0.0011	0.33	9.7546	0.1005	0.0605	0.0025	0.1654	0.0076	0.19	44.4	63.4	344.5	0.184	629	6.2	628	17	622	88.0	100	101
PB-38	4.1	0.8598	0.031	0.1032	0.0011	0.47	9.689	0.1076	0.0604	0.0024	0.0433	0.0072	0.19	40.3	22.1	331.9	0.066	633	6.7	630	17	619	84.8	100	102
PB-38	74.1	0.8572	0.0337	0.1041	0.0015	0.38	9.6105	0.1393	0.0597	0.0027	0.0384	0.0085	0.57	31.7	67.6	269.6	0.251	638	8.8	629	18	595	95.8	101	107
PB-38	47.1	0.9765	0.0422	0.1103	0.0012	0.01	9.0637	0.0998	0.0642	0.0029	0.0984	0.0099	1.15	21	533.9	159.2	3.354	675	7.1	692	22	748	99.1	97	90
PB-38	26.1	0.9562	0.0383	0.1115	0.0012	0.1	8.9671	0.0998	0.0622	0.0026	0.0345	0.0105	0.62	31.6	0.7	247.5	0.003	682	7.2	681	20	681	90.0	100	100
PB-38	30.1	0.9822	0.0479	0.1122	0.0014	0.01	8.9136	0.1147	0.0635	0.0034	0.1091	0.0075	0.52	19.2	11.1	142.3	0.078	685	8.4	695	25	725	114.2	98	94
PB-38	67.1	0.9663	0.0318	0.1134	0.001	0.09	8.8171	0.0789	0.0618	0.0022	0.3024	0.006	0.54	47.8	69.7	303.6	0.229	693	5.9	687	16	667	74.4	100	103
PB-38	84.1	1.4463	0.0527	0.1527	0.0022	0.01	6.5488	0.0961	0.0687	0.0029	0.2388	0.0092	1.15	41	19	203.7	0.093	916	12.5	908	22	890	87.5	100	102
PB-38	89.1	1.5379	0.0744	0.1535	0.0028	0.55	6.5145	0.1187	0.0727	0.0041	0.1002	0.0137	0.77	23.7	-	134.7	-	921	15.6	946	30	1005	116.0	97	91
PB-38	14.1	1.4705	0.0395	0.1542	0.0014	0.44	6.4869	0.0572	0.0692	0.0019	0.2474	0.0073	0.1	77.5	65	374.6	0.174	924	7.6	918	16	904	56.2	100	102
PB-38	73.1	1.6487	0.0556	0.1627	0.0023	0.93	6.1456	0.0868	0.0735	0.003	0.1896	0.0514	0.49	53.4	48.1	250.5	0.192	972	12.8	989	22	1027	80.7	98	94
PB-38	76.1	1.6479	0.0418	0.1641	0.0017	0.01	6.0928	0.0647	0.0728	0.002	0.1192	0.003	0.38	60.5	47.8	306.7	0.156	980	9.7	989	16	1009	56.7	99	97
PB-38	5.1	1.6275	0.1205	0.1642	0.0037	0.59	6.0898	0.1377	0.0719	0.0066	0.1866	0.0186	0.71	12.8	72.3	60	1.206	980	20.7	981	48	983	181.6	99	99
PB-38	51.1	1.6654	0.0653	0.1657	0.0023	0.01	6.0352	0.0855	0.0729	0.0032	0.2574	0.0274	2.85	22	22.5	98.4	0.228	988	13.0	995	25	1011	88.3	99	97
PB-38	15.1	1.688	0.0726	0.1685	0.0021	0.84	5.9358	0.0744	0.0727	0.0035	0.0623	0.009	0.29	25.4	9.5	121.4	0.079	1004	11.7	1004	28	1005	96.0	99	99
PB-38	46.1	1.9944	0.0519	0.1863	0.0015	0.09	5.3691	0.044	0.0777	0.002	0.1282	0.0064	0.74	72.8	25.6	316.3	0.081	1101	8.3	1114	18	1138	51.3	98	96
PB-38	9.1	1.8958	0.0564	0.1863	0.002	0.48	5.3688	0.0575	0.0738	0.0025	0.2006	0.0082	0.18	59.2	84.8	248.7	0.341	1101	10.8	1080	20	1037	68.0	101	106
PB-38	31.1	1.8984	0.0506	0.1877	0.0016	0.11	5.3277	0.0453	0.0734	0.002	0.1786	0.0076	0.18	121	156.2	506.7	0.308	1109	8.7	1081	18	1024	53.6	102	108
PB-38	43.1	4.3322	0.0977	0.297	0.0023	0.01	3.3674	0.0255	0.1058	0.0023	0.1236	0.0025	0.07	125	89.9	324.8	0.277	1676	11.2	1700	19	1728	39.2	98	96
PB-38	69.1	4.4352	0.093	0.3041	0.0022	0.78	3.2881	0.0236	0.1058	0.0023	0.1241	0.0031	0.2	114	25.1	293.2	0.086	1712	10.8	1719	17	1728	40.0	99	99
PB-38	3.1	4.4398	0.1551	0.3042	0.0044	0.68	3.2875	0.048	0.1059	0.0043	0.1886	0.0092	0.84	24	-	59.9	-	1712	21.9	1720	28	1729	73.8	99	99
PB-38	42.1	4.5472	0.1456	0.3046	0.0033	0.21	3.2825	0.0359	0.1083	0.0036	0.2845	0.0112	0.35	32	26.1	74	0.352	1714	16.5	1740	27	1770	61.4	98	96
PB-38	80.1	4.5333	0.1089	0.3072	0.0036	0.87	3.2557	0.0376	0.107	0.0029	0.1877	0.0214	0.22	77.3	-	186.8	-	1727	17.5	1737	20	1750	48.9	99	98
PB-38	93.1	5.7	0.1312	0.3457	0.0036	0.73	2.8931	0.0302	0.1196	0.003	0.1899	0.0059	0.26	154	61.4	351.9	0.174	1914	17.3	1931	19	1950	43.7	99	98
PB-38	27.1	5.7051	0.1508	0.3457	0.0033	0.81	2.8928	0.0279	0.1197	0.0032	0.2508	0.0065	0.21	64.8	67.3	130	0.518	1914	16.0	1932	23	1952	47.2	99	98
PB-38	81.1	5.8437	0.1776	0.3492	0.0056	0.65	2.8637	0.046	0.1214	0.0044	0.2609	0.0105	0.7	31	8.6	64.1	0.133	1931	26.8	1953	26	1977	64.2	98	97
PB-38	23.1	5.8102	0.1585	0.3509	0.0038	0.8	2.8502	0.0306	0.1201	0.0035	0.1983	0.0076	0.78	47	69.6	94	0.741	1939	18.0	1948	24	1958	52.6	99	99
PB-38	61.1	5.8073	0.1187	0.3553	0.0025	0.75	2.8148	0.02	0.1186	0.0025	0.1639	0.0038	0	138	25	297.2	0.084	1960	12.1	1948	18	1935	38.5	100	101
PB-38	88.1	6.6481	0.1561	0.3671	0.0041	0.57	2.7242	0.0303	0.1314	0.0034	0.071	0.0031	0.16	90.5	3.3	203.9	0.016	2016	19.2	2066	21	2116	44.9	97	95
PB-38	91.1	6.3746	0.1428	0.3695	0.0038	0.33	2.7062	0.028	0.1251	0.003	0.2167	0.0103	0.17	157	29.5	305.9	0.096	2027	18.0	2029	19	2030	42.3	99	99
PB-38	72.1	6.4969	0.1299	0.3731	0.0026	0.59	2.68	0.0187	0.1263	0.0026	0.132	0.0199	0.44	139	25.5	293.7	0.087	2044	12.2	2046	18	2047	36.4	99	99
PB-38	20.1	6.5881	0.1639	0.3783	0.0038	0.52	2.6436	0.0267	0.1263	0.0033	0.3979	0.0051	0.39	62.4	49.6	106.6	0.466	2068	17.9	2058	22	2047	47.1	100	101
PB-38	2.1	6.7979	0.1955	0.379	0.0051	0.43	2.6384	0.0358	0.1301	0.0044	0.4033	0.01	0.31	32.8	68.9	55	1.253	2072	24.1	2085	26	2099	60.1	99	98
PB-38	39.1	6.6532	0.1644	0.3791	0.0033	0.97	2.6375	0.023	0.1273	0.003	0.1594	0.0058	0.15	112	10.3	205.2	0.05	2072	15.4	2066	21	2061	41.3	100	100
PB-38	21.1	6.8521	0.167	0.3881	0.0038	0.7	2.5764	0.0255	0.128	0.0034	0.4645	0.0291	0.13	53.2	5.7	88.2	0.065	2114	17.9	2093	22	2071	46.5	101	102
PB-38	29.1	0.6665	0.0289	0.0831	0.0009	0.55	12.0315	0.1355	0.0582	0.0027	0.0686	0.0079	0.53	27.8	41.5	280.8	0.148	515	5.6	519	18	536	98.6	99	96
PB-38	60.1	1.0443	0.0318	0.1161	0.0012	0.95	8.6142	0.0927	0.0652	0.0022	0.0706	0.0081	1.33	62.7	52.5	405.1	0.13	708	7.2	726	16	782	71.3	97	90
PB-38	12.1	0.7439	0.0375	0.0924	0.0013	0.37	10.8247	0.1525	0.0584	0.0034	0.0678	0.013	1.3	20.2	-	193.5	-	570	7.7	565	22	545	124.3	100	104
PB-38	78.1	0.8221	0.0387	0.0984	0.0017	0.32	10.1603	0.1746	0.0606	0.0034	0.0728	0.0144	1.53	21	43.1	181.6	0.237	605	9.9	609	22	624	118.8	99	96
PB-38	64.1	0.8429	0.0575	0.0999	0.0016	0.21	10.0117	0.1583	0.0612	0.0047	0.2166	0.0231	2.68	11.8	6.7	93.2	0.072	614	9.3	621	32	646	171.6	98	94
PB-38	33.1	0.8931	0.0336	0.1071	0.0012	0.99	9.3357	0.1004	0.0605	0.002	0.0508	0.0311	0.53	56.9	15.5	527.6	0.029	656	6.6	648	17	620	68.2	101	105
PB-38	54.1	1.16	0.0425	0.1304	0.0017	0.67	7.6709	0.0974	0.0645	0.0026	0.0725	0.0084	0.04	26.6	12.8	165.5	0.077	790	9.4	782	20	759	84.5	101	104
PB-38	71.1	1.3351	0.0834	0.1446	0.0022	0.06	6.9156	0.1071	0.067	0.0049	0.4443	0.0351	1.33	17.6	32	80.1	0.399	871	12.6	861	36	837	146.8	101	104
PB-38	35.1	1.3273	0.0473	0.1457	0.0015	0.68	6.8625	0.0709	0.0661	0.0024	0.2313	0.0095	0.48	48.8	108.3	264.1	0.41	877	8.5	858	21	808	76.9	102	108
PB-38	86.1	2.2037	0.0566	0.197	0.0021	0.99	5.0761	0.0549	0.0811	0.0024	0.1224	0.0084	0.78	119	32.3	452.8	0.071	1159	11.5	1182	18	1225	57.0	98	94
PB-38	55.1	1.4315	0.0435	0.1492	0.0016	0.62	6.7031	0.0737	0.0696	0.0023	0.1342	0.0107	0.37	39.6	30.1	217.4	0.139	896	9.2	902	18	916	67.9	99	97
PB-38	41.1	1.5702	0.0622	0.1597	0.0017	0.38	6.2602	0.0675	0.0713	0.0029	0.1769	0.0084	1.02	27.2	-	133	-	955	9.6	959	24	966	83.7	99	98
PB-38	48.1	1.7514	0.0486	0.1726	0.0015	0.83	5.7933	0.0495	0.0736	0.002	0.1313	0.0052	0.23	64	18.4	300.7	0.061	1027	8.1	1028	18	1030	56.5	99	99
PB-38	10.1	1.7984	0.0566	0.1753	0.002	0.51	5.704	0.0635	0.0744	0.0027	0.0855	0.0058	0.15	38.1	5.4	184.7	0.029	1041	10.7	1045	21	1052	72.9	99	98
PB-38	59.1	1.811	0.0719	0.179	0.0026	0.93	5.5877	0.0808	0.0734	0.0032	0.1801	0.0107	0.84	26.9	3.2	101.9	0.031	1061	14.0	1050	26	1025	88.7	101	103
PB-38	32.1	1.8458	0.153	0.1808	0.0039	0.66	5.5301	0.1205	0.074	0.0067	0.1665	0.0237	1.72	9.7	14.3	44.6	0.321	1072	21.4	1062	50	1042	166.3	100	102
PB-38	7.1	1.9457	0.104	0.1914	0.0032	0.33	5.2241	0.0881	0.0737	0.0046	0.0241	0.0169	0.66	19.3	32.5	85.8	0.379	1129	17.4	1097	34	1034	119.6	102	109
PB-38	11.1	2.8572	0.0621	0.2417	0.0021	0.9	4.1382	0.0361	0.0858	0.002	0.1	0.0043	0.79	90.2	138.1	322.9	0.428	1395	11.0	1371	16	1333	46.1	101	104

PB-38	45.1	17.5054	0.4114	0.5912	0.0055	1	1.6916	0.0158	0.2148	0.0049	0.2136	0.0232	0.41	75	7.2	78	0.092	2994	22.4	2963	23	2942	36.3	101	101
PB-38	95.1	18.588	0.4915	0.594	0.0096	0.01	1.6834	0.0272	0.2269	0.0071	0.1135	0.0152	0.6	15.7	4.7	17	0.28	3006	38.9	3021	26	3031	50.4	99	99
PB-38	85.1	14.2797	0.4068	0.5413	0.0092	0.49	1.8475	0.0315	0.1913	0.0065	0.3052	0.0216	0.63	37.8	-	48.3	-	2789	38.5	2769	27	2754	55.9	100	101
PB-38	83.1	10.2015	0.1939	0.457	0.0043	0.98	2.1883	0.0207	0.1619	0.0035	0.1136	0.0107	0.17	120	-	204.3	-	2426	19.4	2453	19	2476	36.3	98	97
PB-38	25.1	10.6518	0.2592	0.4729	0.0045	0.62	2.1145	0.0203	0.1634	0.004	0.6537	0.0109	0.21	84	62.5	97	0.644	2496	19.9	2493	23	2491	40.9	100	100
PB-38	94.1	4.8969	0.1061	0.3144	0.0031	0.2	3.1809	0.0309	0.113	0.0027	0.1358	0.0132	0.78	18.9	17	48.3	0.352	1762	15.0	1802	19	1848	42.8	97	95
PB-38	44.1	4.5694	0.0989	0.3148	0.0023	0.01	3.1764	0.0231	0.1053	0.0021	0.1943	0.0032	0.08	164	-	388.8	-	1764	11.2	1744	18	1719	36.9	101	102
PB-38	22.1	5.4432	0.1091	0.3257	0.0026	0.69	3.0705	0.0248	0.1212	0.0026	0.0406	0.0033	0.6	87.6	3.9	194	0.02	1817	12.7	1892	18	1974	37.8	96	92
PB-38	50.1	5.1398	0.1177	0.3264	0.0032	0.81	3.0638	0.0298	0.1142	0.0027	0.4132	0.0049	0.46	84.8	38.1	161	0.237	1821	15.4	1843	19	1867	43.0	98	97
PB-38	87.1	5.4019	0.1452	0.3306	0.0042	0.74	3.0251	0.0383	0.1185	0.0036	0.2655	0.0058	0.1	69.1	3.8	145.5	0.026	1841	20.3	1885	23	1934	54.4	97	95
PB-38	56.1	5.0659	0.1476	0.3309	0.0042	0.88	3.0222	0.0386	0.111	0.0036	0.1549	0.0068	1.26	33	13.6	87.4	0.156	1843	20.5	1830	25	1817	57.7	100	101
PB-38	18.1	6.9491	0.1913	0.3935	0.0044	0.94	2.5415	0.0285	0.1281	0.0037	0.5135	0.0174	0.14	64.3	-	98	-	2139	20.3	2105	24	2072	51.0	101	103
PB-38	17.1	7.2563	0.1596	0.4058	0.0037	0.9	2.464	0.0223	0.1297	0.003	0.1728	0.022	0.28	71.2	32.5	135.4	0.24	2196	17.0	2144	20	2094	41.3	102	104
PB-38	65.1	0.2185	0.0364	0.0393	0.001	0.16	25.4591	0.6412	0.0404	0.007	0.6134	0.0496	5.14	11.3	62.2	161.3	0.386	248	6.1	201	30	0	67.1	123	####
PB-38	36.1	0.2922	0.0134	0.0407	0.0005	0.51	24.576	0.2742	0.0521	0.0026	0.2321	0.0174	0.75	34.8	215.4	637.8	0.338	257	2.8	260	11	289	112.5	98	88
PB-38	62.1	0.2521	0.0373	0.0407	0.001	0.15	24.5607	0.5851	0.0449	0.0078	0.2623	0.0431	2.8	7.4	-	132.6	-	257	6.0	228	29	0	236.1	112	####
PB-38	28.1	0.3082	0.0186	0.0419	0.0006	0.01	23.846	0.3261	0.0533	0.0035	0.1657	0.0126	0.67	17.1	37.4	324.2	0.115	265	3.5	273	15	341	148.6	97	77
PB-38	96.1	0.3116	0.0225	0.0423	0.0009	0.42	23.6337	0.4984	0.0534	0.0045	0.2109	0.0148	1.34	20.4	22.1	382.2	0.058	267	5.5	275	17	346	184.8	96	77
PB-38	90.1	0.2846	0.0316	0.0424	0.0012	0.25	23.5758	0.6655	0.0487	0.0066	0.3126	0.0329	1.3	13.6	5.1	235.1	0.022	268	7.4	254	25	132	222.2	105	202
PB-38	58.1	0.3354	0.0334	0.0426	0.0012	0.68	23.4473	0.6603	0.057	0.0068	0.242	0.0578	1.93	8.2	14.8	128.1	0.115	269	7.4	294	27	493	253.4	91	54
PB-38	13.1	0.6621	0.0394	0.0809	0.0012	0.42	12.3592	0.1795	0.0594	0.0039	0.2214	0.0133	0.42	21.6	-	199.4	-	502	7.0	516	25	580	155.8	97	86
PB-38	24.1	0.6754	0.0545	0.0823	0.0015	0.63	12.1528	0.2226	0.0595	0.0054	0.2349	0.0164	0.5	14.1	36.5	125.4	0.291	510	9.0	524	34	586	207.9	97	86
PB-38	38.1	0.8329	0.0381	0.0977	0.0011	0.21	10.236	0.1163	0.0618	0.003	0.1327	0.0102	1.05	20	55.7	166	0.336	601	6.5	615	21	669	108.3	97	89
PB-38	40.1	0.8819	0.0877	0.101	0.0021	0.34	9.8989	0.2085	0.0633	0.007	0.2047	0.0254	1.65	8.3	140.8	62	2.272	620	12.5	642	48	719	247.2	96	86
PB-38	6.1	0.8125	0.0541	0.1021	0.0018	0.51	9.7981	0.1733	0.0577	0.0045	0.0795	0.0213	1.21	17.4	53.8	143.9	0.374	627	10.6	604	30	520	169.7	103	120
PB-38	77.1	0.8152	0.034	0.1024	0.0015	0.21	9.7658	0.1462	0.0577	0.0028	0.218	0.0129	0.45	32.1	70.3	236.6	0.297	628	9.0	605	19	520	106.6	103	120
PB-38	49.1	0.8714	0.0564	0.1129	0.0022	0.21	8.8573	0.1745	0.056	0.004	0.475	0.0407	0.01	20	50.1	105.8	0.473	690	12.8	636	32	452	152.7	108	152
PB-38	57.1	1.3987	0.0879	0.1577	0.003	0.18	6.3398	0.1213	0.0643	0.0048	0.18	0.0406	1.82	19	37.5	88.5	0.424	944	16.8	888	34	752	123.2	106	125
PB-38	79.1	1.8828	0.1336	0.1728	0.0052	0.17	5.7864	0.1726	0.079	0.0068	0.2161	0.0317	1.87	13.4	3.5	60.3	0.059	1028	28.2	1075	45	1173	179.6	95	87
PB-39	36.1	0.6605	0.0335	0.0829	0.0013	0.06	12.0697	0.1957	0.0578	0.0033	0.1841	0.0092	0.15	32	17	315	0.05	513	8	515	21	523	129	99	98
PB-39	80.1	0.6735	0.0515	0.0843	0.0024	0.01	11.8573	0.3313	0.0579	0.0046	0.0904	0.0153	0.23	24	19	242	0.08	522	14	523	31	527	174	99	99
PB-39	32.1	0.6874	0.0305	0.0869	0.0013	0.15	11.5087	0.1696	0.0574	0.0028	0.1430	0.0085	0.59	35	-	338	-	537	8	531	18	506	109	101	106
PB-39	63.1	0.7112	0.0370	0.0871	0.0016	0.24	11.4867	0.2175	0.0592	0.0030	0.0946	0.0058	0.63	38	29	370	0.08	538	10	546	22	576	110	98	93
PB-39	38.1	0.6969	0.0407	0.0873	0.0016	0.59	11.4595	0.2065	0.0579	0.0037	0.0904	0.0074	0.37	26	23	265	0.09	539	9	537	24	527	137	100	102
PB-39	34.1	0.7079	0.0302	0.0885	0.0013	0.42	11.2953	0.1628	0.0580	0.0027	0.1078	0.0068	0.53	38	34	353	0.10	547	8	544	18	530	103	100	103
PB-39	82.1	0.7312	0.0389	0.0892	0.0021	0.49	11.2081	0.2600	0.0594	0.0031	0.0372	0.0080	0.32	32	29	329	0.09	551	12	557	23	583	118	98	94
PB-39	57.1	0.7306	0.0419	0.0904	0.0018	0.91	11.0640	0.2199	0.0586	0.0034	0.2108	0.0186	0.50	65	304	619	0.49	558	11	557	24	553	120	100	100
PB-38	98.1	0.7332	0.0318	0.0910	0.0010	0.18	10.9919	0.1195	0.0585	0.0027	0.1150	0.0067	0.28	59	28	545	0.05	561	6	558	19	547	99	100	102
PB-39	75.1	0.8156	0.0508	0.0966	0.0019	0.76	10.3559	0.2075	0.0613	0.0044	0.1825	0.0136	0.89	23	24	195	0.12	594	11	606	28	648	148	98	91
PB-39	1.1	0.8162	0.0512	0.0989	0.0022	0.75	10.1145	0.2288	0.0599	0.0042	0.1174	0.0852	0.63	18	30	168	0.18	608	13	606	29	599	148	100	101
PB-39	45.1	0.8123	0.0338	0.0989	0.0013	0.01	10.1084	0.1357	0.0596	0.0027	0.0288	0.0064	0.30	52	61	477	0.13	608	8	604	19	587	98	100	103
PB-39	48.1	0.8115	0.0630	0.0990	0.0021	0.01	10.1030	0.2129	0.0595	0.0052	0.4307	0.0167	0.80	22	69	151	0.46	608	12	603	35	584	186	100	104
PB-39	59.1	0.8340	0.0533	0.0998	0.0022	0.43	10.0227	0.2179	0.0606	0.0041	0.1945	0.0130	0.26	37	84	299	0.28	613	13	616	30	626	146	99	97
PB-38	93.1	0.8338	0.0402	0.1006	0.0012	0.35	9.9428	0.1171	0.0601	0.0030	0.2055	0.0082	0.38	44	38	348	0.11	618	7	616	22	608	107	100	101
PB-39	41.1	0.8394	0.0577	0.1009	0.0021	0.01	9.9113	0.2066	0.0603	0.0049	0.1127	0.0157	0.65	26	10	236	0.04	620	12	619	33	616	176	100	100
PB-39	72.1	0.8723	0.0581	0.1019	0.0022	0.72	9.8117	0.2134	0.0621	0.0047	0.1207	0.0238	0.94	36	-	292	-	626	13	637	32	677	169	98	92
PB-38	100.1	0.8501	0.0275	0.1029	0.0010	0.58	9.7182	0.0897	0.0599	0.0020	0.1326	0.0105	0.21	94	24	782	0.03	631	6	625	15	601	72	101	105
PB-39	16.1	0.8689	0.0263	0.1038	0.0008	0.83	9.6354	0.0788	0.0607	0.0020	0.0926	0.0054	0.24	64	2	520	0.00	637	5	635	14	629	70	100	101
PB-39	16.1	0.8689	0.0263	0.1038	0.0008	0.83	9.6354	0.0788	0.0607	0.0020	0.0926	0.0054	0.24	64	2	520	0.00	637	5	635	14	629	70	100	101
PB-39	66.1	0.9125	0.0925	0.1049	0.0034	0.11	9.5362	0.3048	0.0631	0.0071	0.1162	0.0258	1.96	16	5	129	0.04	643	20	658	50	712	240	97	90
PB-39	81.1	0.9106	0.0353	0.1058	0.0021	0.56	9.4486	0.1906	0.0624	0.0022	0.1182	0.0050	0.21	51	76	409	0.19	649	13	657	19	688	79	98	94
PB-38	99.1	0.8911	0.0509	0.1062	0.0014	0.49	9.4171	0.1232	0.0609	0.0037	0.2039	0.0167	1.09	27	16	200	0.08	651	8	647	27	634	131	100	102
PB-39	84.1	0.9197	0.0517	0.1080	0.0026	0.58	9.2608	0.2214	0.0618	0.0035	0.1198	0.0107	0.40	28	108	217	0.50	661	15	662	27	666	119	99	99
PB-39	68.1	0.8971	0.0826	0.1083	0.0030	0.12	9.2350	0.2572	0.0601	0.0067	0.1047	0.0199	1.02	13	32	99	0.33	663	18	650	43	607	224	101	109
PB-39	77.1	1.0874	0.0392	0.1236	0.0016	0.53	8.0904	0.1053	0.0638	0.0025	0.0845	0.0048	1.81	44	-	306	-	751	9	747	19	735	81	100	102
PB-39	60.1	1.1392	0.0736	0.1245	0.0029	0.41	8.0353	0.1845	0.0664	0.0044	0.0491	0.0110	0.46	29	14	215	0.07	756	16	772	35	819	138	97	92
PB-39	9.1	1.1373	0.0596	0.1269	0.0026	0.01	7.8787	0.1636	0.0650	0.0037	0.0639	0.0080	0.41	26	2	179	0.01	770	15	771	29	774	119	99	99
PB-38	94.1	1.1782	0.0403	0.1321	0.0013	0.79	7.5709	0.0738	0.0647	0.0023	0.1373	0.0079	0.40	62	24	395	0.06	800	7	791	19	764	74	101	104
PB-39	78.1	1.2611	0.0917	0.1342	0.0034	0.24	7.4491	0.1874	0.0681	0.0059	0.1794	0.0156	0.83	15	73	92	0.79	812	19	828	43	873	201	98	93
PB-39	15.1	1.2835	0.0674	0.1415	0.0016	0.15	7.0664	0.0813	0.0658	0.0038	0.0828	0.0113	0.94	20	8	116	0.07	853	9	838	29	799	114	101	106
PB-39	15.1	1.2835	0.0674	0.1415	0.0016	0.15	7.0664	0.0813	0.0658	0.0038	0.0828	0.0113	0.94	20	8	116	0.07	853	9	838	29	799	114	101	106

PB-39	89.1	1.3712	0.1463	0.1425	0.0055	0.14	7.0153	0.2690	0.0698	0.0084	0.2525	0.0366	1.78	12	64	60	1.08	859	31	877	62	922	237	97	93
PB-39	85.1	1.3713	0.0439	0.1429	0.0027	0.86	6.9977	0.1322	0.0696	0.0018	0.1444	0.0043	0.11	90	105	521	0.20	861	15	877	19	917	55	98	93
PB-39	70.1	1.3721	0.1050	0.1467	0.0038	0.25	6.8159	0.1770	0.0678	0.0059	0.0747	0.0227	1.09	14	25	88	0.28	883	21	877	44	863	181	100	102
PB-39	90.1	1.4663	0.0702	0.1495	0.0035	0.34	6.6872	0.1556	0.0711	0.0033	0.2570	0.0284	0.16	36	29	186	0.15	898	20	917	29	961	99	98	93
PB-39	52.1	1.4977	0.0614	0.1514	0.0022	0.83	6.6067	0.0953	0.0718	0.0033	0.1765	0.0307	2.18	48	74	255	0.29	909	12	930	26	979	94	97	92
PB-39	73.1	1.6756	0.0964	0.1641	0.0035	0.13	6.0921	0.1316	0.0740	0.0050	0.3469	0.0217	0.37	22	25	95	0.27	980	20	999	38	1043	151	98	93
PB-39	79.1	1.7197	0.1090	0.1697	0.0047	0.15	5.8917	0.1642	0.0735	0.0048	0.1632	0.0164	0.46	25	8	120	0.07	1011	26	1016	41	1027	136	99	98
PB-39	65.1	1.7395	0.0627	0.1705	0.0027	0.31	5.8654	0.0926	0.0740	0.0023	0.1296	0.0045	0.64	83	35	414	0.09	1015	15	1023	23	1042	64	99	97
PB-38	101.1	1.8307	0.1117	0.1748	0.0027	0.39	5.7210	0.0877	0.0760	0.0050	0.2039	0.0132	1.57	22	-	102	-	1039	15	1057	40	1094	131	98	94
PB-39	17.1	1.8557	0.0489	0.1784	0.0014	0.82	5.6045	0.0448	0.0754	0.0021	0.1242	0.0056	0.18	56	2	261	0.01	1058	8	1066	18	1080	57	99	98
PB-39	17.1	1.8557	0.0489	0.1784	0.0014	0.82	5.6045	0.0448	0.0754	0.0021	0.1242	0.0056	0.18	56	2	261	0.01	1058	8	1066	18	1080	57	99	98
PB-39	88.1	1.8711	0.0609	0.1789	0.0035	0.18	5.5908	0.1078	0.0759	0.0021	0.0642	0.0045	0.13	75	25	360	0.07	1061	19	1071	22	1092	56	99	97
PB-39	5.1	4.2838	0.1112	0.2952	0.0044	0.53	3.3874	0.0502	0.1052	0.0025	0.1487	0.0019	0.02	142	39	372	0.10	1668	22	1690	22	1719	44	98	97
PB-39	42.1	4.3674	0.1870	0.2982	0.0058	0.20	3.3532	0.0657	0.1062	0.0052	0.2198	0.0171	0.30	23	14	58	0.25	1683	29	1706	35	1735	89	98	96
PB-39	67.1	4.3222	0.1338	0.2984	0.0042	0.15	3.3518	0.0468	0.1051	0.0036	0.1677	0.0106	1.28	35	19	92	0.21	1683	21	1698	25	1716	61	99	98
PB-39	37.1	4.4099	0.0965	0.3013	0.0032	0.01	3.3195	0.0347	0.1062	0.0024	0.1478	0.0040	0.17	129	7	340	0.02	1698	16	1714	18	1735	41	99	97
PB-39	7.1	4.7035	0.1454	0.3034	0.0052	0.92	3.2958	0.0564	0.1124	0.0034	0.2014	0.0040	0.36	71	25	159	0.16	1708	26	1768	26	1839	54	96	92
PB-39	64.1	4.5328	0.1473	0.3077	0.0048	0.85	3.2503	0.0512	0.1069	0.0030	0.1945	0.0045	2.42	86	145	223	0.65	1729	24	1737	27	1746	52	99	99
PB-38	95.1	5.2247	0.1771	0.3331	0.0038	0.53	3.0017	0.0344	0.1137	0.0041	0.3035	0.0125	0.23	56	14	118	0.12	1854	19	1857	29	1860	66	99	99
PB-39	33.1	5.1606	0.1050	0.3361	0.0033	0.45	2.9754	0.0294	0.1114	0.0023	0.1037	0.0122	0.24	210	65	529	0.12	1868	16	1846	17	1822	37	101	102
PB-39	10.1	5.5957	0.1497	0.3426	0.0053	0.77	2.9185	0.0452	0.1184	0.0030	0.6008	0.0050	0.22	139	77	230	0.33	1899	25	1915	23	1933	45	99	98
PB-39	31.1	5.5324	0.1210	0.3438	0.0037	0.96	2.9085	0.0310	0.1167	0.0025	0.1547	0.0040	0.64	146	26	302	0.09	1905	17	1906	19	1906	39	99	99
PB-39	69.1	5.7411	0.1478	0.3476	0.0042	0.86	2.8765	0.0345	0.1198	0.0032	0.1142	0.0075	0.05	93	-	208	-	1923	20	1938	22	1953	47	99	98
PB-39	35.1	5.8134	0.1648	0.3536	0.0049	0.78	2.8284	0.0395	0.1193	0.0038	0.2802	0.0072	1.52	51	32	103	0.31	1952	24	1948	25	1945	57	100	100
PB-39	8.1	7.1426	0.2400	0.3881	0.0076	0.37	2.5766	0.0502	0.1335	0.0047	0.1063	0.0058	0.19	38	7	78	0.09	2114	35	2129	30	2144	61	99	98
PB-39	51.1	6.6716	0.3120	0.3885	0.0085	0.29	2.5738	0.0563	0.1245	0.0068	0.2117	0.0200	0.40	29	25	56	0.46	2116	40	2069	42	2022	98	102	104
PB-39	54.1	7.0728	0.1809	0.3934	0.0046	0.63	2.5419	0.0298	0.1304	0.0035	0.2478	0.0040	0.12	99	47	187	0.25	2139	21	2121	23	2103	47	100	101
PB-39	74.1	0.3214	0.0455	0.0448	0.0017	0.75	22.3153	0.8266	0.0520	0.0090	0.1121	0.0468	1.65	21	23	422	0.05	283	10	283	36	286	214	99	98
PB-39	39.1	0.9408	0.0431	0.1102	0.0017	0.55	9.0715	0.1414	0.0619	0.0032	0.1983	0.0103	0.32	39	44	298	0.15	674	10	673	23	671	112	100	100
PB-39	83.1	1.0283	0.0315	0.1166	0.0021	0.65	8.5733	0.1565	0.0639	0.0016	0.0478	0.0025	0.13	95	44	722	0.06	711	12	718	16	740	53	99	96
PB-39	71.1	1.0278	0.0403	0.1197	0.0016	0.01	8.3514	0.1145	0.0623	0.0026	0.2773	0.0104	0.39	47	1	297	0.00	729	10	718	20	683	90	101	106
PB-39	11.1	0.6077	0.0235	0.0784	0.0013	0.01	12.7483	0.2128	0.0562	0.0022	0.0116	0.0040	0.42	52	-	610	-	487	8	482	15	460	86	100	105
PB-39	50.1	1.4440	0.0467	0.1521	0.0018	0.25	6.5767	0.0778	0.0689	0.0024	0.0366	0.0049	0.11	77	40	467	0.09	913	10	907	19	895	71	100	101
PB-39	4.1	1.6116	0.0507	0.1626	0.0026	0.32	6.1517	0.0972	0.0719	0.0022	0.1037	0.0043	0.12	78	41	396	0.10	971	14	975	20	983	62	99	98
PB-38	97.1	3.7069	0.1502	0.2719	0.0034	0.55	3.6774	0.0466	0.0989	0.0042	0.1868	0.0116	0.61	35	11	98	0.12	1551	17	1573	32	1603	81	98	96
PB-39	86.1	9.5480	0.2367	0.4373	0.0078	0.57	2.2868	0.0409	0.1584	0.0030	0.1351	0.0056	0.11	143	20	260	0.08	2339	35	2392	23	2438	32	97	95
PB-39	44.1	11.5158	0.2664	0.4778	0.0050	0.30	2.0930	0.0221	0.1748	0.0040	0.2378	0.0091	0.25	53	54	80	0.68	2518	22	2566	21	2604	38	98	96
PB-39	2.1	10.4993	0.2571	0.4806	0.0072	0.97	2.0808	0.0311	0.1584	0.0037	0.1538	0.0235	0.84	126	73	194	0.38	2530	32	2480	24	2439	40	102	103
PB-39	62.1	13.2868	0.3728	0.4971	0.0075	0.92	2.0118	0.0303	0.1939	0.0045	0.1147	0.0032	0.10	109	158	173	0.91	2601	32	2700	27	2775	38	96	93
PB-38	91.1	15.9719	0.4124	0.5365	0.0055	0.92	1.8640	0.0190	0.2159	0.0056	0.0998	0.0051	0.47	85	46	120	0.38	2769	23	2875	24	2951	41	96	93
PB-39	18.1	15.4608	0.2942	0.5509	0.0042	0.01	1.8153	0.0138	0.2036	0.0040	0.2420	0.0113	0.48	17	18	22	0.82	2829	18	2844	18	2855	32	99	99
PB-39	49.1	14.9996	0.3392	0.5734	0.0059	0.43	1.7441	0.0181	0.1897	0.0042	0.1396	0.0039	0.27	208	50	279	0.18	2922	24	2815	21	2740	35	103	106
PB-39	6.1	20.0625	0.6414	0.5940	0.0135	0.27	1.6835	0.0382	0.2450	0.0083	0.2189	0.0107	0.45	32	35	37	0.94	3006	55	3094	31	3153	54	97	95
PB-39	43.1	17.2358	0.4321	0.6080	0.0077	0.82	1.6448	0.0209	0.2056	0.0053	0.2571	0.0076	0.27	32	20	36	0.55	3062	31	2948	25	2871	43	103	106
PB-39	55.1	0.7641	0.0710	0.0936	0.0026	0.30	10.6871	0.2981	0.0592	0.0061	0.0908	0.0254	1.06	23	44	213	0.21	577	15	576	41	575	213	100	100
PB-39	47.1	0.8471	0.0494	0.0976	0.0017	0.50	10.2486	0.1831	0.0630	0.0041	0.0890	0.0109	2.08	21	-	189	-	600	10	623	28	707	154	96	84
PB-39	46.1	0.8565	0.1423	0.0992	0.0043	0.01	10.0850	0.4352	0.0626	0.0118	0.2084	0.0363	1.28	8	18	63	0.29	610	25	628	81	696	358	97	87
PB-39	40.1	0.9477	0.0747	0.1064	0.0026	0.26	9.3960	0.2323	0.0646	0.0059	0.0632	0.0257	1.14	12	17	106	0.16	652	15	677	40	761	206	96	85
PB-39	53.1	1.0281	0.0364	0.1145	0.0014	0.78	8.7343	0.1078	0.0651	0.0025	0.0175	0.0060	0.15	47	36	371	0.10	699	8	718	18	778	81	97	89
PB-39	56.1	1.6449	0.0749	0.1515	0.0030	0.99	6.6021	0.1293	0.0788	0.0032	0.0229	0.0045	1.80	70	107	305	0.35	909	16	988	27	1166	80	92	77
PB-39	14.1	1.7153	0.1373	0.1601	0.0029	0.19	6.2479	0.1129	0.0777	0.0068	0.3508	0.0313	0.46	11	20	49	0.41	957	16	1014	54	1140	189	94	83
PB-39	14.1	1.7153	0.1373	0.1601	0.0029	0.19	6.2479	0.1129	0.0777	0.0068	0.3508	0.0313	0.46	11	20	49	0.41	957	16	1014	54	1140	189	94	83
PB-38	92.1	3.8078	0.1003	0.2627	0.0024	0.99	3.8063	0.0345	0.1051	0.0029	0.0845	0.0040	2.07	127	33	335	0.10	1504	12	1594	22	1716	50	94	87
PB-39	61.1	11.8964	0.3256	0.4530	0.0065	0.43	2.2076	0.0316	0.1905	0.0041	0.1072	0.0024	0.05	122	65	211	0.31	2409	29	2596	26	2746	36	92	87
PB-39	3.1	0.7656	0.1049	0.0964	0.0037	0.41	10.3704	0.3973	0.0576	0.0085	0.2827	0.0287	1.06	12	2	80	0.02	593	22	577	55	514	309	102	115
PB-39	87.1	0.7083	0.0525	0.0911	0.0024	0.21	10.9758	0.2948	0.0564	0.0044	0.0922	0.0159	1.98	20	12	191	0.06	562	15	544	32	468	169	103	120
PB-38	96.1	0.6373	0.0737	0.0829	0.0017	0.27	12.0664	0.2475	0.0558	0.0072	0.2738	0.0236	1.66	12	16	111	0.14	513	10	501	46	443	278	102	115
PB-39	12.1	0.5704	0.0488	0.0785	0.0021	0.38	12.7400	0.3360	0.0527	0.0050	0.4770	0.0233	0.36	26	72	205	0.35	487	12	458	32	316	207	106	154
PB-39	13.1	0.6423	0.0288	0.0788	0.0008	0.10	12.6936	0.1278	0.0591	0.0029	0.2079	0.0130	0.27	29	16	293	0.06	489	5	504	18	572	115	97	85
PB-39	13.1	0.6423	0.0288	0.0788	0.0008	0.10	12.6936	0.1278	0.0591	0.0029	0.2079	0.0130	0.27	29	16	293	0.06	489	5	504	18	572	115	97	85
PB-39	58.1	0.6976	0.1507	0.0817	0.0050	0.01	12.2346	0.7522	0.0619	0.0156	0.5601	0.0948	0.79	11	120	95	1.27	507	30	537	99	671	433	94	75

PB-38	96.1	0.3504	0.0457	0.0501	0.0011	0.01	19.9523	0.4217	0.0507	0.0074	0.1767	0.0264	8.40	22	57	329	0.17	315	7	305	35	228	250	103	138
PB-39	76.1	0.2696	0.0544	0.0409	0.0019	0.01	24.4267	1.1544	0.0478	0.0113	0.6102	0.0635	2.94	8	104	122	0.85	259	12	242	43	87	252	106	295
PB-40	53.1	0.6119	0.0397	0.0779	0.0009	0.16	12.8442	0.1546	0.0570	0.0039	0.2090	0.0174	0.00	11	59	103	0.57	0.483	0.006	0.485	0.025	0.492	0.145	99	
PB-40	39.1	0.6138	0.0326	0.0795	0.0008	0.21	12.5763	0.1311	0.0560	0.0031	0.1674	0.0207	2.19	17	80	177	0.45	0.493	0.005	0.486	0.021	0.452	0.119	101	
PB-40	6.1	0.6142	0.0254	0.0811	0.0006	0.19	12.3335	0.0880	0.0549	0.0022	0.2776	0.0101	0.98	20	124	182	0.68	0.503	0.003	0.486	0.016	0.410	0.090	103	
PB-40	34.1	0.6164	0.0330	0.0812	0.0012	0.28	12.3158	0.1862	0.0551	0.0032	0.2883	0.0172	0.00	15	107	131	0.81	0.503	0.007	0.488	0.020	0.415	0.125	103	
PB-40	59.1	0.6437	0.0209	0.0815	0.0007	0.55	12.2703	0.1034	0.0573	0.0019	0.0779	0.0054	3.37	57	209	600	0.35	0.505	0.004	0.505	0.013	0.502	0.072	100	
PB-40	70.1	0.6481	0.0251	0.0819	0.0008	0.45	12.2124	0.1223	0.0574	0.0023	0.3035	0.0106	1.16	22	274	185	1.48	0.507	0.005	0.507	0.015	0.507	0.086	100	
PB-40	17.1	0.6755	0.0366	0.0831	0.0006	0.42	12.0321	0.0828	0.0589	0.0032	0.3192	0.0119	0.00	19	121	167	0.72	0.515	0.003	0.524	0.022	0.565	0.119	98	
PB-40	90.1	0.6609	0.0234	0.0833	0.0009	0.41	11.9989	0.1321	0.0575	0.0020	0.0602	0.0055	0.26	40	62	426	0.15	0.516	0.005	0.515	0.014	0.511	0.077	100	
PB-40	77.1	0.6856	0.0280	0.0859	0.0008	0.74	11.6460	0.1076	0.0579	0.0022	0.0712	0.0068	2.51	56	111	553	0.20	0.531	0.005	0.530	0.017	0.526	0.085	100	
PB-40	94.1	0.6367	0.0375	0.0859	0.0009	0.30	11.6349	0.1282	0.0537	0.0031	0.1575	0.0156	0.47	13	50	119	0.42	0.532	0.006	0.500	0.023	0.360	0.121	106	
PB-40	92.1	0.6820	0.0288	0.0865	0.0009	0.82	11.5592	0.1222	0.0572	0.0023	0.1956	0.0213	0.31	44	275	417	0.66	0.535	0.005	0.528	0.017	0.498	0.086	101	
PB-40	12.1	0.6930	0.0197	0.0867	0.0007	0.74	11.5349	0.0918	0.0580	0.0015	0.2852	0.0040	0.00	87	477	717	0.67	0.536	0.004	0.535	0.012	0.529	0.058	100	
PB-40	11.1	0.7065	0.0221	0.0872	0.0007	0.60	11.4663	0.0916	0.0588	0.0018	0.2435	0.0046	0.00	47	241	411	0.59	0.539	0.004	0.543	0.013	0.558	0.067	99	
PB-40	19.1	0.7103	0.0221	0.0884	0.0007	0.56	11.3137	0.0933	0.0583	0.0017	0.0161	0.0034	0.10	35	13	360	0.04	0.546	0.004	0.545	0.013	0.540	0.066	100	
PB-40	1.1	0.7450	0.0342	0.0886	0.0009	0.38	11.2813	0.1205	0.0610	0.0029	0.2101	0.0146	2.21	10	49	92	0.53	0.548	0.006	0.565	0.020	0.638	0.109	96	
PB-40	2.1	0.7170	0.0213	0.0888	0.0006	0.42	11.2550	0.0771	0.0585	0.0017	0.0489	0.0066	0.02	27	39	277	0.14	0.549	0.004	0.549	0.013	0.550	0.065	99	
PB-40	50.1	0.7300	0.0658	0.0892	0.0007	0.44	11.2051	0.0930	0.0593	0.0054	0.9162	0.0581	2.83	11	139	61	2.29	0.551	0.004	0.557	0.039	0.579	0.193	99	
PB-40	91.1	0.7208	0.0215	0.0893	0.0010	0.69	11.2008	0.1250	0.0586	0.0017	0.1718	0.0037	0.52	53	215	478	0.45	0.551	0.006	0.551	0.013	0.551	0.064	100	
PB-40	8.1	0.7624	0.0325	0.0894	0.0007	0.20	11.1844	0.0845	0.0618	0.0025	0.1341	0.0085	1.10	20	61	184	0.33	0.552	0.004	0.575	0.019	0.669	0.090	95	
PB-40	55.1	0.7368	0.0240	0.0901	0.0008	0.86	11.1013	0.0952	0.0593	0.0020	0.0304	0.0054	5.53	75	69	751	0.09	0.556	0.005	0.561	0.014	0.579	0.072	99	
PB-40	48.1	0.7196	0.0327	0.0905	0.0009	0.75	11.0496	0.1073	0.0577	0.0025	0.1719	0.0248	6.37	28	182	250	0.73	0.558	0.005	0.550	0.019	0.517	0.089	101	
PB-40	43.1	0.7297	0.0196	0.0906	0.0008	0.73	11.0318	0.0936	0.0584	0.0014	0.0230	0.0028	0.11	68	50	707	0.07	0.559	0.005	0.556	0.011	0.544	0.055	100	
PB-40	23.1	0.7476	0.0215	0.0914	0.0007	0.61	10.9376	0.0877	0.0593	0.0016	0.0901	0.0024	0.20	68	135	660	0.21	0.564	0.004	0.567	0.013	0.578	0.060	99	
PB-40	83.1	0.7230	0.0291	0.0918	0.0009	0.65	10.8945	0.1113	0.0571	0.0022	0.3519	0.0068	1.36	42	457	333	1.37	0.566	0.006	0.552	0.017	0.496	0.083	102	
PB-40	9.1	0.7621	0.0253	0.0922	0.0008	0.37	10.8479	0.0950	0.0600	0.0019	0.0827	0.0065	0.00	24	48	229	0.21	0.568	0.005	0.575	0.015	0.602	0.071	98	
PB-40	46.1	0.7654	0.0247	0.0922	0.0008	0.37	10.8505	0.0927	0.0602	0.0019	0.0877	0.0087	0.32	38	73	359	0.21	0.568	0.005	0.577	0.014	0.612	0.068	98	
PB-40	76.1	0.7558	0.0319	0.0922	0.0009	0.41	10.8475	0.1034	0.0595	0.0023	0.0968	0.0051	0.25	40	114	360	0.32	0.568	0.005	0.572	0.018	0.584	0.086	99	
PB-40	52.1	0.7867	0.0345	0.0939	0.0008	0.59	10.6478	0.0871	0.0608	0.0027	0.0934	0.0170	0.00	12	35	106	0.33	0.579	0.005	0.589	0.020	0.630	0.100	98	
PB-40	57.1	0.7953	0.0254	0.0941	0.0008	0.53	10.6314	0.0917	0.0613	0.0020	0.0898	0.0041	0.00	43	95	385	0.25	0.580	0.005	0.594	0.014	0.650	0.070	97	
PB-40	65.1	0.7745	0.0227	0.0941	0.0006	0.51	10.6292	0.0733	0.0597	0.0016	0.0545	0.0042	0.68	54	71	507	0.14	0.580	0.004	0.582	0.013	0.593	0.062	99	
PB-40	86.1	0.7847	0.0264	0.0941	0.0011	0.80	10.6274	0.1212	0.0605	0.0020	0.1081	0.0034	0.04	43	107	391	0.27	0.580	0.006	0.588	0.015	0.621	0.069	98	
PB-40	96.1	0.7977	0.0347	0.0941	0.0010	0.52	10.6242	0.1087	0.0615	0.0025	0.3357	0.0110	0.00	25	176	192	0.92	0.580	0.006	0.596	0.020	0.656	0.094	97	
PB-40	29.1	0.8030	0.0378	0.0959	0.0010	0.33	10.4305	0.1054	0.0607	0.0028	0.0308	0.0052	0.30	34	25	319	0.08	0.590	0.006	0.599	0.021	0.630	0.099	98	
PB-40	4.1	0.7555	0.0492	0.0973	0.0008	0.43	10.2798	0.0844	0.0563	0.0036	0.6180	0.0203	0.24	17	150	106	1.43	0.598	0.005	0.571	0.029	0.465	0.141	104	
PB-40	16.1	0.8194	0.0402	0.0972	0.0012	0.03	10.2917	0.1267	0.0612	0.0032	0.1149	0.0137	0.00	10	28	86	0.33	0.598	0.007	0.608	0.022	0.645	0.115	98	
PB-40	28.1	0.8294	0.0486	0.0972	0.0012	0.33	10.2863	0.1264	0.0619	0.0036	0.0823	0.0145	0.00	13	27	114	0.24	0.598	0.007	0.613	0.028	0.670	0.130	97	
PB-40	10.1	0.8108	0.0267	0.0977	0.0008	0.27	10.2309	0.0838	0.0602	0.0019	0.0644	0.0031	0.00	46	66	412	0.16	0.601	0.005	0.603	0.015	0.609	0.067	99	
PB-40	22	0.8180	0.0245	0.0980	0.0008	0.57	10.2074	0.0830	0.0606	0.0017	0.5034	0.0042	0.00	89	698	565	1.24	0.602	0.005	0.607	0.014	0.623	0.063	99	
PB-40	47.1	0.8263	0.0268	0.1000	0.0010	0.51	10.0019	0.0972	0.0599	0.0019	0.0692	0.0048	0.56	29	59	245	0.24	0.614	0.006	0.612	0.015	0.601	0.068	100	
PB-40	49.1	0.8160	0.0401	0.0999	0.0008	0.25	10.0132	0.0827	0.0593	0.0029	0.1182	0.0098	1.04	18	55	142	0.39	0.614	0.005	0.606	0.022	0.577	0.107	101	
PB-40	40.1	0.8302	0.0293	0.1010	0.0007	0.66	9.9003	0.0721	0.0596	0.0020	0.0909	0.0041	0.00	41	96	360	0.27	0.620	0.004	0.614	0.016	0.590	0.074	101	
PB-40	37	0.8103	0.0554	0.1015	0.0012	0.01	9.8559	0.1173	0.0579	0.0040	0.0794	0.0171	0.00	10	26	82	0.31	0.623	0.007	0.603	0.032	0.527	0.154	103	
PB-40	64.1	0.7704	0.0481	0.1017	0.0010	0.31	9.8289	0.0953	0.0549	0.0034	0.2597	0.0396	1.40	12	53	87	0.61	0.625	0.006	0.580	0.028	0.409	0.136	107	
PB-40	62.1	0.8265	0.0329	0.1024	0.0007	0.28	9.7609	0.0650	0.0585	0.0022	0.2860	0.0101	1.54	36	166	253	0.66	0.629	0.004	0.612	0.018	0.549	0.081	102	
PB-40	32	0.8161	0.0370	0.1027	0.0011	0.38	9.7360	0.1004	0.0576	0.0026	0.0807	0.0051	0.36	26	45	220	0.21	0.630	0.006	0.606	0.021	0.516	0.097	104	
PB-40	73.1	0.8598	0.0328	0.1028	0.0010	0.54	9.7241	0.0973	0.0606	0.0022	0.0430	0.0045	0.51	35	48	301	0.16	0.631	0.006	0.630	0.018	0.626	0.077	100	
PB-40	85.1	0.8536	0.0267	0.1030	0.0012	0.50	9.7046	0.1098	0.0601	0.0019	0.1474	0.0031	1.56	51	296	408	0.73	0.632	0.007	0.627	0.014	0.607	0.065	100	
PB-40	61.1	0.8682	0.0378	0.1032	0.0008	0.56	9.6886	0.0709	0.0610	0.0025	0.2055	0.0224	0.42	13	44	102	0.43	0.633	0.004	0.635	0.020	0.639	0.087	99	
PB-40	41.1	0.9119	0.1015	0.1040	0.0016	0.44	9.6190	0.1467	0.0636	0.0078	0.1248	0.0402	0.68	5	14	41	0.35	0.638	0.009	0.658	0.055	0.729	0.238	96	
PB-40	33.1	0.8943	0.0285	0.1051	0.0012	0.57	9.5112	0.1050	0.0617	0.0020	0.0815	0.0054	0.14	33	67	278	0.24	0.644	0.007	0.649	0.015	0.663	0.071	99	
PB-40	15.1	0.8792	0.0400	0.1066	0.0008	0.48	9.3813	0.0730	0.0598	0.0027	0.2509	0.0111	0.00	22	90	152	0.59	0.653	0.005	0.641	0.021	0.597	0.095	101	
PB-40	5.1	0.8824	0.0316	0.1081	0.0008	0.07	9.2465	0.0696	0.0592	0.0021	0.6973	0.0195	0.00	30	266	164	1.62	0.662	0.005	0.642	0.017	0.574	0.075	103	
PB-40	63.1	0.9173	0.0444	0.1096	0.0010	0.50	9.1261	0.0857	0.0607	0.0029	0.1335	0.0127	0.33	15	34	109	0.31	0.670	0.006	0.661	0.023	0.629	0.101	101	
PB-40	21.1	0.9648	0.0370	0.1100	0.0010	0.24	9.0905	0.0785	0.0636	0.0024	0.2384	0.0078	0.37	31	119	211	0.57	0.673	0.006	0.686	0.019	0.729	0.080	98	
PB-40	88.1	0.9492	0.0399	0.1126	0.0013	0.44	8.8782	0.1031	0.0611	0.0025	0.1036	0.0142	0.74	23	45	167	0.27	0.688	0.008	0.678	0.021	0.643	0.087	101	
PB-40	82.1	0.9656	0.0328	0.1145	0.0012	0.58	8.7350	0.0894	0.0612	0.0020	0.1205	0.0053	1.51	44	201	348	0.58	0.699	0.007	0.686	0.017	0.645	0.071	101	
PB-40	80	1.0341	0.0359	0.1196	0.0012	0.71	8.3592	0.0809	0.0627	0.0020	0.0629	0.0033	0.06	88	93	658	0.14	0.728	0.007	0.721	0.018	0.698	0.069	101	
PB-40	72	1.0776	0.0294	0.1222	0.0010	0.88	8.1852	0.0663	0.0640	0.0017	0.0681	0.0025	0.38	93	137	641	0.21	0.743	0.006	0.742	0.014	0.741	0.057	100	
PB-40	30	1.0362	0.0806	0.1225	0.0014	0.34	8.1601	0.0941	0.0613	0.0047	0.1390	0.0185	5.01	12	39	78	0.51	0.745	0.008	0.722	0.040	0.651	0.168	103	

PB-40	26.1	1.1155	0.0736	0.1249	0.0016	0.42	8.0071	0.1014	0.0648	0.0043	0.1027	0.0150	2.86	13	51	86	0.60	0.759	0.009	0.761	0.035	0.767	0.147	99	
PB-40	58	1.0310	0.0760	0.1254	0.0017	0.13	7.9754	0.1073	0.0596	0.0048	0.5368	0.0271	2.10	9	73	43	1.70	0.761	0.010	0.719	0.036	0.590	0.156	105	
PB-40	36.1	1.1727	0.0455	0.1281	0.0014	0.24	7.8037	0.0876	0.0664	0.0026	0.2321	0.0108	0.35	24	89	136	0.65	0.777	0.008	0.788	0.021	0.818	0.081	98	
PB-40	3.1	1.1188	0.0488	0.1291	0.0012	0.53	7.7431	0.0734	0.0628	0.0029	0.0615	0.0121	0.00	16	17	105	0.16	0.783	0.007	0.762	0.023	0.703	0.094	102	
PB-40	13	1.3931	0.0472	0.1455	0.0011	0.41	6.8731	0.0529	0.0694	0.0023	0.2024	0.0103	0.00	17	55	93	0.60	0.876	0.006	0.886	0.020	0.912	0.070	98	
PB-40	45.1	1.3788	0.0602	0.1471	0.0014	0.35	6.7983	0.0648	0.0680	0.0029	0.2629	0.0105	1.14	32	192	163	1.18	0.885	0.008	0.880	0.026	0.868	0.087	100	
PB-40	71.1	1.4767	0.0533	0.1552	0.0014	0.77	6.4452	0.0564	0.0690	0.0025	0.1898	0.0043	0.00	50	128	250	0.52	0.930	0.008	0.921	0.022	0.900	0.072	100	
PB-40	42	1.5714	0.0502	0.1598	0.0012	0.65	6.2593	0.0459	0.0713	0.0022	0.1225	0.0057	0.43	48	90	256	0.35	0.955	0.007	0.959	0.020	0.967	0.062	99	
PB-40	31.1	1.5922	0.1129	0.1628	0.0024	0.62	6.1408	0.0907	0.0709	0.0050	0.1482	0.0165	1.62	11	21	53	0.39	0.973	0.013	0.967	0.042	0.955	0.136	100	
PB-40	25	1.7137	0.0810	0.1637	0.0019	0.35	6.1078	0.0694	0.0759	0.0035	0.1197	0.0100	2.65	19	29	94	0.31	0.977	0.010	1.014	0.030	1.093	0.093	96	
PB-40	93	1.7026	0.0536	0.1699	0.0018	0.60	5.8844	0.0638	0.0727	0.0021	0.1069	0.0024	0.69	121	279	640	0.44	1.012	0.010	1.010	0.020	1.005	0.058	100	
PB-40	84	1.7188	0.0876	0.1716	0.0022	0.71	5.8262	0.0738	0.0726	0.0037	0.0916	0.0125	0.15	34	51	166	0.31	1.021	0.012	1.016	0.033	1.004	0.100	100	
PB-40	68.1	1.8476	0.1085	0.1729	0.0023	0.59	5.7823	0.0779	0.0775	0.0048	0.0918	0.0137	4.39	11	16	51	0.31	1.028	0.013	1.063	0.039	1.134	0.125	96	
PB-40	24.1	1.8606	0.0531	0.1786	0.0015	0.58	5.5991	0.0475	0.0756	0.0021	0.1277	0.0053	0.00	35	50	164	0.30	1.059	0.008	1.067	0.019	1.083	0.055	99	
PB-40	51	1.9152	0.1144	0.1787	0.0016	0.22	5.5964	0.0486	0.0777	0.0046	0.0705	0.0195	2.13	8	8	36	0.22	1.060	0.008	1.086	0.041	1.140	0.124	97	
PB-40	14.1	1.9533	0.0525	0.1882	0.0013	0.46	5.3133	0.0380	0.0753	0.0020	0.2905	0.0063	0.05	55	143	214	0.67	1.112	0.007	1.100	0.018	1.076	0.052	101	
PB-40	75	1.9739	0.0782	0.1895	0.0018	0.67	5.2778	0.0498	0.0756	0.0028	0.1790	0.0033	0.52	72	248	302	0.82	1.119	0.010	1.107	0.027	1.083	0.075	101	
PB-40	74	2.5028	0.1298	0.2158	0.0022	0.58	4.6329	0.0482	0.0841	0.0041	0.2298	0.0114	0.81	18	38	64	0.59	1.260	0.012	1.273	0.037	1.295	0.093	98	
PB-40	66.1	3.1720	0.0909	0.2389	0.0016	0.84	4.1866	0.0288	0.0963	0.0025	0.3319	0.0061	0.13	52	131	152	0.86	1.381	0.009	1.450	0.022	1.554	0.048	95	
PB-40	20.1	3.0766	0.0811	0.2504	0.0020	0.17	3.9936	0.0319	0.0891	0.0022	0.1329	0.0022	0.00	119	128	386	0.33	1.441	0.010	1.427	0.020	1.407	0.047	100	
PB-40	27.1	3.8336	0.1747	0.2735	0.0030	0.61	3.6558	0.0404	0.1016	0.0044	0.1184	0.0115	1.69	20	22	59	0.38	1.559	0.015	1.600	0.037	1.654	0.081	97	
PB-40	38.1	5.1116	0.1374	0.3255	0.0025	0.71	3.0718	0.0239	0.1139	0.0030	0.2269	0.0044	0.00	69	107	169	0.64	1.817	0.012	1.838	0.023	1.862	0.048	98	
PB-40	35.1	5.1888	0.1858	0.3267	0.0037	0.63	3.0610	0.0351	0.1152	0.0041	0.4575	0.0094	0.33	38	95	75	1.26	1.822	0.018	1.851	0.031	1.883	0.063	98	
PB-40	78	5.1355	0.1882	0.3281	0.0031	0.90	3.0478	0.0289	0.1135	0.0038	0.1660	0.0052	0.02	59	68	133	0.52	1.829	0.015	1.842	0.031	1.856	0.062	99	
PB-40	44.1	5.9057	0.1613	0.3413	0.0032	0.25	2.9302	0.0272	0.1255	0.0032	0.1670	0.0049	0.00	48	51	113	0.45	1.893	0.015	1.962	0.024	2.036	0.046	96	
PB-40	7.1	5.6789	0.1467	0.3420	0.0027	0.67	2.9238	0.0231	0.1204	0.0028	0.1726	0.0030	0.56	64	92	149	0.62	1.896	0.013	1.928	0.022	1.962	0.042	98	
PB-40	89.1	5.8068	0.1919	0.3521	0.0042	0.84	2.8401	0.0340	0.1196	0.0038	0.4159	0.0087	0.25	54	110	97	1.13	1.945	0.020	1.947	0.029	1.950	0.056	99	
PB-40	67.1	5.9435	0.1672	0.3549	0.0031	0.95	2.8177	0.0249	0.1215	0.0034	0.1453	0.0112	0.89	63	114	126	0.90	1.958	0.015	1.968	0.024	1.978	0.049	99	
PB-40	56	6.3703	0.1840	0.3583	0.0034	0.49	2.7911	0.0264	0.1290	0.0039	0.1689	0.0042	0.17	58	65	124	0.53	1.974	0.016	2.028	0.025	2.084	0.052	97	
PB-40	79.1	6.7071	0.2319	0.3818	0.0037	0.79	2.6194	0.0256	0.1274	0.0040	0.1348	0.0060	0.68	47	31	97	0.32	2.085	0.017	2.074	0.030	2.063	0.055	100	
PB-40	81.1	10.7221	0.3207	0.4693	0.0046	0.71	2.1307	0.0209	0.1657	0.0045	0.0922	0.0034	0.30	88	176	147	1.20	2.481	0.020	2.499	0.028	2.515	0.046	99	
PB-40	54.1	11.7811	0.2664	0.4799	0.0038	0.91	2.0839	0.0167	0.1781	0.0042	0.1490	0.0057	0.12	101	95	158	0.60	2.527	0.017	2.587	0.021	2.635	0.039	97	
PB-40	18	11.8895	0.2971	0.4992	0.0036	0.40	2.0033	0.0146	0.1727	0.0042	0.2284	0.0027	0.00	90	68	128	0.54	2.610	0.016	2.596	0.023	2.584	0.040	100	
PB-40	60	0.6397	0.0363	0.0808	0.0009	0.47	12.3771	0.1374	0.0574	0.0034	0.3047	0.0390	21.15	20	259	157	1.66	0.501	0.005	0.502	0.022	0.508	0.126	99	
PB-40	69.1	0.3761	0.0958	0.0840	0.0010	0.21	11.9064	0.1397	0.0325	0.0082	0.1155	0.0457	11.59	4	16	38	0.42	0.520	0.006	0.324	0.061	0.000	0.217	160	
PB-40	95	0.6507	0.0421	0.0930	0.0014	0.36	10.7486	0.1603	0.0507	0.0034	0.1204	0.0186	0.55	12	36	98	0.37	0.573	0.008	0.509	0.026	0.228	0.123	112	
PB-40	87.1	0.9710	0.0964	0.1059	0.0015	0.33	9.4417	0.1346	0.0665	0.0066	0.2311	0.0289	11.06	7	40	48	0.83	0.649	0.009	0.689	0.050	0.822	0.212	94	
PB-41	60.1	0.7652	0.0408	0.0940	0.0016	0.35	10.6399	0.1829	0.0591	0.0035	0.0785	0.0212	2.01	13	-	129	-	579	10	577	23	569	129	100	101
PB-41	19.1	0.7689	0.0454	0.0948	0.0016	0.01	10.5489	0.1835	0.0588	0.0040	0.1465	0.0133	0.55	16	-	141	-	584	10	579	26	561	147	100	104
PB-41	34.1	0.7733	0.0280	0.0949	0.0012	0.63	10.5386	0.1285	0.0591	0.0024	0.0680	0.0075	0.77	36	12	331	0.04	584	7	582	16	571	88	100	102
PB-41	27.1	0.8083	0.0352	0.0977	0.0014	0.51	10.2337	0.1464	0.0600	0.0030	0.2679	0.0098	0.29	33	65	250	0.26	601	8	602	20	604	108	99	99
PB-41	23.1	0.8200	0.0444	0.0984	0.0016	0.36	10.1650	0.1681	0.0605	0.0038	0.1172	0.0388	0.6	17	15	137	0.11	605	10	608	25	620	136	99	97
PB-41	46.1	0.8202	0.0372	0.0992	0.0012	0.29	10.0820	0.1222	0.0600	0.0030	0.0049	0.0078	0.42	35	43	321	0.14	610	7	608	21	603	110	100	101
PB-41	10.1	0.8306	0.0332	0.0997	0.0012	0.47	10.0341	0.1234	0.0604	0.0027	0.0938	0.0078	0.44	28	165	241	0.68	612	7	614	19	620	99	99	98
PB-41	61.1	0.8330	0.0354	0.1006	0.0013	0.56	9.9380	0.1245	0.0600	0.0027	0.0960	0.0046	0.23	36	54	308	0.18	618	7	615	19	605	96	100	102
PB-41	45.1	0.8259	0.0274	0.1009	0.0009	0.19	9.9066	0.0917	0.0593	0.0022	0.1076	0.0051	0.36	64	86	536	0.16	620	6	611	15	580	80	101	106
PB-41	50.1	0.8993	0.0501	0.1041	0.0020	0.18	9.6078	0.1857	0.0627	0.0038	0.0434	0.0173	0.19	16	39	134	0.29	638	12	651	28	697	156	97	91
PB-41	47.1	0.8946	0.0935	0.1044	0.0028	0.73	9.5810	0.2570	0.0622	0.0079	0.2801	0.0313	1.11	13	44	97	0.45	640	16	649	50	680	249	98	94
PB-41	3.1	0.8826	0.0279	0.1051	0.0011	0.83	9.5120	0.0966	0.0609	0.0021	0.0983	0.0122	0.25	53	87	430	0.20	644	6	642	15	635	78	100	101
PB-41	62.1	0.9042	0.0778	0.1078	0.0024	0.01	9.2753	0.2080	0.0608	0.0061	0.0904	0.0176	3.34	13	30	102	0.29	660	14	654	41	633	205	100	104
PB-41	77.1	0.9144	0.0425	0.1089	0.0014	0.42	9.1794	0.1160	0.0609	0.0032	0.0136	0.0122	0.65	35	-	300	-	667	8	659	22	635	111	101	104
PB-41	25.1	0.9191	0.0972	0.1100	0.0036	0.62	9.0949	0.2940	0.0606	0.0082	0.0976	0.0368	2.53	10	11	77	0.15	673	21	662	54	626	301	101	107
PB-41	13.1	0.9356	0.0355	0.1102	0.0014	0.54	9.0735	0.1155	0.0616	0.0026	0.0638	0.0073	0.51	30	1	236	0.00	674	8	671	19	659	91	100	102
PB-41	35.1	1.7691	0.1318	0.1731	0.0048	0.09	5.7779	0.1588	0.0741	0.0066	0.1206	0.0255	1.35	11	44	50	0.89	1029	26	1034	48	1045	183	99	98
PB-41	38.1	1.7436	0.0807	0.1766	0.0024	0.33	5.6626	0.0779	0.0716	0.0038	0.1161	0.0094	0.26	29	23	136	0.17	1048	13	1025	30	975	108	102	107
PB-41	74.1	1.8180	0.0923	0.1782	0.0028	0.39	5.6117	0.0883	0.0740	0.0043	0.2230	0.0264	0.61	30	22	132	0.17	1057	15	1052	33	1041	121	100	101
PB-41	90.1	1.8467	0.0734	0.1783	0.0027	0.48	5.6089	0.0862	0.0751	0.0034	0.1854	0.0104	0.45	29	2	129	0.01	1058	15	1062	27	1072	93	99	98
PB-41	83.1	1.7720	0.0373	0.1784	0.0013	0.83	5.6039	0.0410	0.0720	0.0016	0.0829	0.0042	0.22	198	64	970	0.07	1059	7	1035	14	987	44	102	107
PB-41	16.1	1.7692	0.0970	0.1787	0.0034	0.01	5.5958	0.1050	0.0718	0.0047	0.1988	0.0196	1.68	20	40	85	0.47	1060	18	1034	35	980	127	102	108
PB-41	73.1	1.8483	0.0743	0.1826	0.0023	0.01	5.4775	0.0694	0.0734	0.0033	0.1856	0.0075	0.28	40	6	175	0.04	1081	13	1063	27	1026	91	101	105
PB-41	85.1	4.4472	0.0954	0.3057	0.0032	0.63	3.2707	0.0340	0.1055	0.0024	0.1380	0.0044	0.14	97	23	251	0.09	1720	16	1721	18	1723	42	99	99

PB-41	43.1	4.4919	0.1705	0.3060	0.0044	0.59	3.2677	0.0469	0.1065	0.0047	0.2459	0.0286	0.36	37	29	90	0.33	1721	22	1730	31	1740	80	99	98
PB-41	5.1	4.5170	0.0949	0.3083	0.0026	0.71	3.2441	0.0278	0.1063	0.0023	0.1350	0.0032	0.12	92	188	232	0.81	1732	13	1734	17	1737	40	99	99
PB-41	9.1	4.5192	0.0944	0.3095	0.0026	0.80	3.2311	0.0274	0.1059	0.0023	0.1747	0.0040	0.24	87	163	220	0.74	1738	13	1735	17	1730	40	100	100
PB-41	87.1	4.6148	0.1021	0.3099	0.0033	0.71	3.2271	0.0348	0.1080	0.0026	0.2224	0.0118	0.1	73	4	176	0.02	1740	17	1752	19	1766	45	99	98
PB-41	18.1	4.5929	0.1397	0.3125	0.0045	0.19	3.2002	0.0457	0.1066	0.0036	0.2218	0.0102	0.37	30	16	71	0.22	1753	22	1748	26	1742	64	100	100
PB-41	6.1	5.8271	0.1406	0.3513	0.0037	0.47	2.8468	0.0299	0.1203	0.0032	0.2483	0.0049	0.19	51	26	103	0.25	1941	18	1951	21	1961	46	99	98
PB-41	55.1	5.7929	0.1296	0.3521	0.0038	0.95	2.8399	0.0305	0.1193	0.0026	0.1463	0.0100	0.26	92	41	204	0.20	1945	18	1945	19	1946	40	99	99
PB-41	71.1	5.9272	0.1305	0.3584	0.0033	0.87	2.7905	0.0257	0.1200	0.0026	0.0564	0.0023	0.34	133	13	311	0.04	1974	16	1965	19	1956	39	100	100
PB-41	80.1	6.0103	0.1892	0.3635	0.0049	0.64	2.7510	0.0369	0.1199	0.0041	0.1964	0.0271	0.23	38	60	84	0.72	1999	23	1977	28	1955	64	101	102
PB-41	52.1	5.9454	0.1165	0.3649	0.0032	0.37	2.7408	0.0239	0.1182	0.0022	0.0120	0.0024	0.09	140	21	351	0.06	2005	15	1968	17	1929	34	101	103
PB-41	8.1	11.7373	0.2484	0.4941	0.0053	0.98	2.0238	0.0215	0.1723	0.0040	0.1431	0.0114	0.14	66	64	102	0.63	2589	23	2584	20	2580	39	100	100
PB-41	92.1	12.2697	0.2583	0.5086	0.0060	0.32	1.9661	0.0234	0.1750	0.0041	0.1453	0.0096	0.34	32	4	47	0.09	2651	26	2625	20	2606	38	100	101
PB-41	88.1	12.5641	0.2248	0.5126	0.0049	0.62	1.9510	0.0185	0.1778	0.0033	0.0850	0.0095	0.12	92	12	159	0.08	2668	21	2648	17	2632	32	100	101
PB-41	89.1	0.8505	0.0193	0.1027	0.0010	0.12	9.7339	0.0916	0.0600	0.0015	0.0639	0.0021	0.1	118	28	998	0.03	630	6	625	11	605	52	100	104
PB-41	39.1	0.8932	0.1561	0.1065	0.0046	0.49	9.3908	0.4061	0.0608	0.0119	0.1243	0.0399	1.53	6	16	48	0.34	652	27	648	84	634	405	100	102
PB-41	72.1	0.7476	0.0489	0.0925	0.0016	0.46	10.8056	0.1906	0.0586	0.0043	0.2575	0.0148	0.89	20	77	161	0.48	571	10	567	28	552	155	100	103
PB-41	51.1	0.7582	0.0356	0.0928	0.0014	0.19	10.7751	0.1680	0.0593	0.0031	0.2436	0.0112	0.56	23	35	192	0.18	572	9	573	20	576	112	99	99
PB-41	17.1	0.9656	0.0551	0.1116	0.0020	0.50	8.9637	0.1600	0.0628	0.0041	0.0829	0.0116	0.86	14	4	105	0.04	682	12	686	29	701	145	99	97
PB-41	81.1	0.7054	0.0190	0.0882	0.0007	0.37	11.3387	0.0941	0.0580	0.0017	0.0029	0.0018	0.29	77	45	811	0.06	545	4	542	11	530	64	100	102
PB-41	32.1	0.7125	0.0271	0.0899	0.0011	0.24	11.1281	0.1387	0.0575	0.0025	0.0393	0.0066	0.34	32	58	316	0.18	555	7	546	16	511	94	101	108
PB-41	93.1	1.0646	0.0525	0.1205	0.0020	0.71	8.2965	0.1383	0.0641	0.0037	0.1126	0.0121	0.9	21	33	153	0.22	734	12	736	26	744	125	99	98
PB-41	41.1	1.0843	0.0537	0.1231	0.0017	0.46	8.1245	0.1105	0.0639	0.0037	0.1354	0.0109	0.91	28	62	189	0.33	748	10	746	27	738	124	100	101
PB-41	36.1	1.1219	0.0510	0.1274	0.0020	0.28	7.8468	0.1217	0.0638	0.0035	0.1633	0.0116	1.03	23	47	145	0.32	773	11	764	24	737	112	101	104
PB-41	49.1	1.1596	0.0281	0.1293	0.0013	0.15	7.7369	0.0749	0.0651	0.0016	0.1151	0.0037	0.08	85	33	552	0.06	784	7	782	13	777	51	100	100
PB-41	21.1	1.5665	0.1261	0.1630	0.0042	0.75	6.1360	0.1587	0.0697	0.0066	0.1829	0.0222	1.33	11	38	50	0.77	973	23	957	47	920	184	101	105
PB-41	66.1	1.6703	0.0438	0.1671	0.0016	0.91	5.9860	0.0568	0.0725	0.0019	0.1041	0.0066	0.49	111	40	526	0.08	996	9	997	17	1000	54	99	99
PB-41	24.1	1.7520	0.1064	0.1683	0.0036	0.65	5.9401	0.1270	0.0755	0.0054	0.2399	0.0190	1.58	20	7	96	0.07	1003	20	1028	40	1081	146	97	92
PB-41	2.1	0.6925	0.0358	0.0849	0.0013	0.32	11.7830	0.1805	0.0592	0.0035	0.1478	0.0140	0.31	19	43	176	0.24	525	8	534	22	574	138	98	91
PB-41	20.1	1.4181	0.0461	0.1496	0.0018	0.52	6.6839	0.0798	0.0687	0.0024	0.2544	0.0183	0.5	37	2	179	0.01	899	10	897	20	891	75	100	100
PB-41	42.1	1.5252	0.1200	0.1522	0.0035	0.01	6.5685	0.1515	0.0727	0.0067	0.2898	0.0153	0.72	13	22	62	0.36	914	20	941	49	1005	200	97	90
PB-41	95.1	1.4808	0.0844	0.1549	0.0031	0.17	6.4543	0.1273	0.0693	0.0047	0.3019	0.0148	0.35	21	18	98	0.18	929	17	923	35	908	140	100	102
PB-41	59.1	2.0790	0.0642	0.1952	0.0025	0.73	5.1220	0.0656	0.0772	0.0024	0.1647	0.0065	0.39	42	11	177	0.06	1150	13	1142	21	1127	63	100	101
PB-41	37.1	2.2463	0.1063	0.2057	0.0031	0.62	4.8613	0.0726	0.0792	0.0044	0.1842	0.0101	0.96	26	11	100	0.11	1206	16	1196	33	1177	108	100	102
PB-41	78.1	2.2141	0.0442	0.2068	0.0015	0.01	4.8348	0.0342	0.0776	0.0016	0.0987	0.0029	0.1	171	99	697	0.14	1212	8	1186	14	1138	40	102	106
PB-41	94.1	4.8590	0.0881	0.3176	0.0028	0.05	3.1486	0.0282	0.1110	0.0021	0.1944	0.0023	0.14	156	36	370	0.10	1778	14	1795	16	1815	35	99	97
PB-41	63.1	4.7881	0.2472	0.3233	0.0071	0.35	3.0928	0.0678	0.1074	0.0062	0.2276	0.0183	1.13	16	29	39	0.75	1806	35	1783	43	1756	107	101	102
PB-41	79.1	4.1750	0.1029	0.2914	0.0034	0.61	3.4312	0.0404	0.1039	0.0029	0.1256	0.0043	0.36	68	29	187	0.16	1649	17	1669	20	1695	50	98	97
PB-41	15.1	4.8563	0.1777	0.3327	0.0056	0.44	3.0062	0.0507	0.1059	0.0044	0.1549	0.0174	0.38	35	16	82	0.19	1851	27	1795	30	1730	75	103	107
PB-41	57.1	3.8338	0.3480	0.2827	0.0121	0.01	3.5370	0.1517	0.0983	0.0106	0.3408	0.0648	2.04	7	19	18	1.07	1605	61	1600	71	1593	195	100	100
PB-41	31.1	6.7024	0.2927	0.3792	0.0093	0.52	2.6368	0.0647	0.1282	0.0073	0.2905	0.0257	0.55	16	-	27	-	2073	44	2073	39	2073	102	99	99
PB-41	86.1	6.5152	0.1217	0.3808	0.0036	0.99	2.6258	0.0249	0.1241	0.0025	0.0781	0.0174	0.13	155	25	312	0.08	2080	17	2048	17	2016	36	101	103
PB-41	12.1	6.6754	0.1460	0.3818	0.0037	0.77	2.6193	0.0252	0.1268	0.0030	0.2113	0.0094	0.12	100	71	196	0.36	2085	17	2069	19	2054	41	100	101
PB-41	40.1	7.1248	0.1608	0.3984	0.0034	0.54	2.5099	0.0212	0.1297	0.0031	0.1228	0.0032	0.11	107	16	207	0.08	2162	16	2127	20	2094	43	101	103
PB-41	33.1	8.4307	0.1435	0.4512	0.0035	0.54	2.2164	0.0172	0.1355	0.0024	0.2132	0.0152	0.12	150	-	278	-	2401	16	2279	15	2171	31	105	110
PB-41	30.1	0.2787	0.0192	0.0394	0.0008	0.01	25.4011	0.4879	0.0513	0.0040	0.2687	0.0187	1.62	21	23	395	0.06	249	5	250	15	256	159	99	97
PB-41	11.1	0.3180	0.0174	0.0445	0.0006	0.60	22.4914	0.3252	0.0519	0.0032	0.1096	0.0076	0.92	24	202	461	0.44	280	4	280	13	280	141	100	100
PB-41	56.1	8.4097	0.1674	0.4024	0.0038	0.01	2.4849	0.0237	0.1516	0.0028	0.0521	0.0057	0.3	72	-	133	-	2180	17	2276	18	2364	32	95	92
PB-41	1.1	10.3274	0.3780	0.4704	0.0099	0.96	2.1256	0.0448	0.1592	0.0070	0.3173	0.0228	4.53	16	243	38	6.33	2486	44	2465	35	2447	77	100	101
PB-41	68.1	15.8002	0.4393	0.5370	0.0081	0.89	1.8620	0.0280	0.2134	0.0061	0.1489	0.0255	0.16	77	-	103	-	2771	34	2865	26	2931	45	96	94
PB-41	22.1	14.2405	0.2542	0.5385	0.0054	0.64	1.8571	0.0185	0.1918	0.0034	0.2769	0.0092	0.07	74	13	90	0.14	2777	23	2766	17	2758	29	100	100
PB-41	61.1	13.8518	0.3240	0.5401	0.0069	0.85	1.8516	0.0235	0.1860	0.0048	0.0533	0.0155	0.27	38	4	58	0.07	2784	29	2740	25	2707	45	101	102
PB-41	58.1	15.0173	0.3336	0.5411	0.0067	0.96	1.8479	0.0229	0.2013	0.0044	0.1854	0.0128	0.37	59	-	86	-	2788	28	2816	21	2837	36	99	98
PB-41	4.1	21.5701	0.4174	0.5977	0.0059	0.01	1.6731	0.0164	0.2617	0.0052	0.1102	0.0035	0.16	65	35	77	0.46	3021	24	3165	19	3257	31	95	92
PB-41	79.1	0.3371	0.0508	0.0459	0.0015	0.20	21.8032	0.6935	0.0533	0.0092	0.2910	0.0363	3.15	8	-	122	-	289	9	295	39	342	296	98	84
PB-41	54.1	0.3452	0.0211	0.0471	0.0009	0.40	21.2468	0.3928	0.0532	0.0038	0.1631	0.0254	0.54	16	36	284	0.13	297	5	301	17	337	157	98	87
PB-41	65.1	0.6376	0.0437	0.0834	0.0015	0.38	11.9912	0.2094	0.0555	0.0043	0.1866	0.0174	0.58	20	63	186	0.34	516	9	501	27	431	162	103	119
PB-41	64.1	0.6509	0.0663	0.0845	0.0021	0.76	11.8295	0.2938	0.0558	0.0064	0.3399	0.0247	1.15	20	32	170	0.19	523	13	509	41	446	199	102	117
PB-41	67.1	0.7075	0.0353	0.0905	0.0013	0.76	11.0537	0.1549	0.0567	0.0031	0.2062	0.0088	0.45	35	27	287	0.09	558	8	543	21	481	124	102	116
PB-41	75.1	0.7005	0.0468	0.0909	0.0015	0.08	11.0056	0.1798	0.0559	0.0042	0.1701	0.0269	1.02	21	49	178	0.28	561	9	539	28	449	159	103	124
PB-41	28.1	0.7312	0.0831	0.0926	0.0030	0.07	10.7981	0.3540	0.0573	0.0078	0.9342	0.1840	1.76	12	81	57	1.42	571	18	557	47	502	270	102	113
PB-41	26.1	0.8167	0.0522	0.0940	0.0020	0.01	10.6424	0.2228	0.0630	0.0049	0.2718	0.0263	1.01	16	41	126	0.33	579	12	606	30	710	170	95	81

PB-41	76.1	0.7327	0.0957	0.0944	0.0028	0.70	10.5933	0.3116	0.0563	0.0086	0.2077	0.0243	0.72	9	19	69	0.27	582	16	558	56	464	310	104	125
PB-41	53.1	0.7392	0.0553	0.0951	0.0021	0.23	10.5167	0.2377	0.0564	0.0050	0.1230	0.0330	2.87	12	3	112	0.03	586	13	562	32	468	182	104	125
PB-41	29.1	0.8574	0.1083	0.0967	0.0039	0.54	10.3441	0.4183	0.0643	0.0101	0.2196	0.0433	1.71	7	52	56	0.93	595	23	629	59	752	315	94	79
PB-41	96.1	0.8768	0.0457	0.1070	0.0018	0.12	9.3479	0.1546	0.0594	0.0036	0.2665	0.0096	0.93	27	33	194	0.17	655	10	639	25	583	125	102	112
PB-41	70.1	0.8557	0.0960	0.1071	0.0030	0.43	9.3413	0.2608	0.0580	0.0076	0.0764	0.0354	2.12	12	26	95	0.27	656	17	628	53	529	265	104	123
PB-41	7.1	0.8870	0.0499	0.1078	0.0018	0.44	9.2773	0.1530	0.0597	0.0039	0.0893	0.0138	0.31	17	43	130	0.33	660	10	645	27	592	145	102	111
PB-41	48.1	0.9033	0.1031	0.1094	0.0031	0.09	9.1398	0.2560	0.0599	0.0079	0.4730	0.0243	0.71	14	2	79	0.03	669	18	654	55	599	290	102	111
PB-41	44.1	0.9161	0.0656	0.1126	0.0020	0.90	8.8848	0.1614	0.0590	0.0049	0.0221	0.0176	3.63	11	19	65	0.30	688	12	660	35	568	179	104	120
PB-41	82.1	0.9574	0.0684	0.1146	0.0021	0.01	8.7265	0.1594	0.0606	0.0049	0.1653	0.0133	0.66	18	72	129	0.56	699	12	682	35	625	173	102	111
PB-41	14.1	1.0170	0.0719	0.1246	0.0025	0.01	8.0273	0.1621	0.0592	0.0049	0.3016	0.0150	4.33	14	3	79	0.03	757	14	712	35	575	167	106	131
PB-41	84.1	9.2356	0.1710	0.4081	0.0031	0.90	2.4505	0.0188	0.1641	0.0031	0.0781	0.0057	0.00	-16	21	-30	-0.71	2206	14	2362	17	2499	32	93	88
PB -44	81.1	0.2557	0.0212	0.0343	0.0006	0.65	29.1551	0.5343	0.0541	0.0045	1.6067	0.1848	1.72	45	1541	323.4	4.766	217	4	231	17	374	176	94	
PB -44	66.1	0.2668	0.0901	0.0387	0.0022	0.01	25.8527	1.4471	0.05	0.0189	0.2547	0.0961	5.55	2.6	38.9	47.8	0.814	245	13	240	70	196	508	101	
PB -44	41.1	0.2901	0.029	0.0397	0.0008	0.08	25.1651	0.4832	0.0529	0.0058	0.2166	0.027	3.86	10.1	174	191.1	0.911	251	5	259	23	326	203	97	
PB -44	88.1	0.2816	0.0255	0.0401	0.0008	0.57	24.9574	0.4785	0.051	0.0053	0.197	0.0209	0.66	12.1	170.7	225.4	0.757	253	5	252	20	240	207	100	
PB -44	67.1	0.2816	0.0332	0.0403	0.0009	0.84	24.7906	0.5495	0.0506	0.0067	0.1743	0.0265	1.68	21.3	215.9	339.4	0.636	255	6	252	27	224	213	101	
PB -44	26.1	0.2752	0.0388	0.0404	0.0009	0.02	24.7722	0.5529	0.0494	0.0076	0.2682	0.0346	2.23	5.5	66.6	96.1	0.692	255	6	247	32	169	270	103	
PB -44	3.1	0.2896	0.0329	0.041	0.0008	0.25	24.3746	0.5045	0.0512	0.0066	0.2224	0.034	1.23	6.4	85.9	114.5	0.751	259	5	258	27	250	236	100	
PB -44	10.1	0.2917	0.0303	0.0414	0.0008	0.47	24.166	0.4571	0.0511	0.006	0.3549	0.0217	1.5	10.1	158.1	169.5	0.933	261	5	260	24	246	235	100	
PB -44	73.1	0.2956	0.0187	0.0414	0.0006	0.51	24.1319	0.3428	0.0517	0.0036	0.339	0.0208	0.48	29	434.9	464.4	0.937	262	4	263	15	274	161	99	
PB -44	4.1	0.3293	0.0302	0.0429	0.0008	0.47	23.2914	0.4339	0.0556	0.0058	0.2502	0.0207	3.17	10.8	133.1	193.2	0.689	271	5	289	24	438	203	93	
PB -44	53.1	0.4473	0.0198	0.0601	0.0008	0.2	16.6368	0.2188	0.054	0.0026	0.2227	0.0093	0.28	30.1	210	364.4	0.576	376	5	375	14	370	104	100	
PB -44	52.1	0.5812	0.0253	0.0734	0.001	0.4	13.6297	0.1822	0.0574	0.0028	0.0551	0.0087	0.17	25	40.3	278	0.145	456	6	465	16	509	109	98	
PB -44	5.1	0.6113	0.0231	0.0772	0.0008	0.61	12.9488	0.1312	0.0574	0.0024	0.1805	0.0064	0.57	28.5	130.6	285.9	0.457	480	5	484	15	507	92	99	
PB -44	21.1	0.6158	0.0328	0.078	0.001	0.69	12.8158	0.1642	0.0572	0.0033	0.2188	0.0112	0.48	15.1	99.1	141.3	0.701	484	6	487	21	501	124	99	
PB -44	11.1	0.5964	0.0688	0.0794	0.0017	0.36	12.5877	0.2681	0.0544	0.0071	0.8096	0.0314	1.25	8	103.2	52.6	1.962	493	10	475	42	390	269	103	
PB -44	85.1	0.6414	0.0423	0.0827	0.0013	0.21	12.095	0.1963	0.0563	0.0042	0.0583	0.0131	0.43	15.3	24.2	154.6	0.157	512	8	503	26	463	163	101	
PB -44	49.1	0.6812	0.0269	0.0834	0.0011	0.43	11.9929	0.1526	0.0593	0.0026	0.0807	0.0087	0.63	29.2	69.5	288.4	0.241	516	6	528	16	577	98	97	
PB -44	36.1	0.6768	0.0389	0.0856	0.0011	0.17	11.6859	0.1469	0.0574	0.0036	0.1268	0.0275	0.06	19.3	57.5	177.7	0.324	529	6	525	24	505	150	100	
PB -44	6.1	0.6402	0.0642	0.0858	0.0016	0.01	11.6517	0.2205	0.0541	0.0062	0.1699	0.0255	2.56	8.3	38.8	74.9	0.519	531	10	502	39	375	233	105	
PB -44	28.1	0.7005	0.0939	0.0861	0.0021	0.6	11.6158	0.2793	0.059	0.0089	0.1664	0.0339	0.88	5.6	21.1	47.8	0.442	532	12	539	57	568	314	98	
PB -44	19.1	0.7002	0.0863	0.0875	0.0022	0.01	11.4251	0.29	0.058	0.0082	0.2092	0.0391	0.66	6	29.4	51.9	0.566	541	13	539	51	531	282	100	
PB -44	42.1	0.6941	0.0477	0.0879	0.0013	0.4	11.3814	0.1683	0.0573	0.0043	0.3167	0.0138	0.39	17.7	106.2	137.1	0.774	543	8	535	27	503	146	101	
PB -44	30.1	0.6949	0.0475	0.0879	0.0012	0.41	11.3756	0.1575	0.0573	0.0043	0.3175	0.0138	0.4	16.4	98.6	126.7	0.778	543	7	536	27	504	148	101	
PB -44	22.1	0.7786	0.0663	0.0896	0.0018	0.16	11.1567	0.2204	0.063	0.006	0.1161	0.0232	1.49	7.1	18.2	58.1	0.313	553	11	585	38	708	205	94	
PB -44	69.1	0.7214	0.1214	0.0903	0.003	0.13	11.0697	0.3727	0.0579	0.0109	0.3214	0.0577	0.94	5.8	41.2	42.6	0.967	558	18	552	70	527	374	101	
PB -44	83.1	0.7261	0.024	0.0905	0.0009	0.49	11.052	0.1117	0.0582	0.0021	0.0129	0.0061	0.23	44.8	14.8	424.7	0.035	558	5	554	14	538	77	100	
PB -44	93.1	0.7345	0.0534	0.0916	0.0016	0.53	10.9208	0.1915	0.0582	0.0048	0.0797	0.0135	1.45	13.2	27.1	117.1	0.231	565	10	559	31	537	175	101	
PB -44	61.1	0.7464	0.0259	0.0929	0.001	0.65	10.7677	0.1119	0.0583	0.002	0.2444	0.0054	0.05	55.4	272.2	421.8	0.645	573	6	566	15	541	75	101	
PB -44	24.1	0.7459	0.047	0.093	0.0014	0.73	10.7582	0.1578	0.0582	0.004	0.1511	0.0161	0.46	11.2	39.8	89.8	0.443	573	8	566	27	537	151	101	
PB -44	7.1	0.7276	0.0856	0.0938	0.0021	0.32	10.6596	0.2382	0.0562	0.0077	0.7074	0.0359	1.06	9.3	100.9	52.5	1.923	578	12	555	52	462	283	104	
PB -44	70.1	0.8418	0.1105	0.0939	0.0028	0.01	10.6468	0.3145	0.065	0.0101	0.2309	0.0368	1.48	6.6	29.5	52.6	0.56	579	16	620	63	775	332	93	
PB -44	77.1	0.7789	0.0445	0.0944	0.0014	0.57	10.5986	0.1526	0.0599	0.0038	0.1773	0.0084	1.18	19.9	90.3	159.5	0.566	581	8	585	25	599	135	99	
PB -44	82.1	0.7625	0.0504	0.095	0.0015	0.72	10.5216	0.166	0.0582	0.0041	0.1001	0.0117	0.53	15.4	49.7	124.5	0.399	585	9	576	29	537	158	101	
PB -44	51.1	0.8245	0.0777	0.0956	0.0023	0.54	10.4653	0.2543	0.0626	0.0068	0.1473	0.0357	0.68	11.2	51.5	87.9	0.586	588	14	611	45	694	245	96	
PB -44	64.1	0.7941	0.0546	0.0968	0.0016	0.11	10.3283	0.1731	0.0595	0.0045	0.2068	0.0143	0.58	13.8	61.5	105.3	0.584	596	10	594	32	585	176	100	
PB -44	33.1	0.7696	0.0757	0.0974	0.0018	0.58	10.2671	0.1897	0.0573	0.0062	0.438	0.022	0.65	9.8	77.3	60.8	1.271	599	11	580	42	504	222	103	
PB -44	56.1	0.8453	0.0527	0.0984	0.0017	0.11	10.1624	0.1803	0.0623	0.0044	0.0914	0.0141	0.31	13.6	27.8	113.4	0.245	605	10	622	30	685	167	97	
PB -44	39.1	0.81	0.0497	0.1	0.0014	0.44	10.0023	0.1409	0.0588	0.0039	0.2115	0.0185	0.23	16.9	90.2	121.3	0.743	614	8	602	28	558	145	101	
PB -44	72.1	0.8487	0.0921	0.101	0.0024	0.25	9.8996	0.2369	0.0609	0.0073	0.4001	0.0428	0.62	8.5	62.2	52.9	1.176	620	14	624	49	637	250	99	
PB -44	59.1	0.878	0.0571	0.1031	0.0019	0.02	9.7025	0.1748	0.0618	0.0045	0.0954	0.0144	0.75	14	31.5	112	0.281	632	11	640	31	667	157	98	
PB -44	58.1	0.8685	0.0998	0.104	0.0029	0.42	9.6144	0.2668	0.0606	0.008	0.2785	0.0331	1.09	9.6	47.4	61.1	0.777	638	17	635	55	624	278	100	
PB -44	23.1	0.8923	0.0497	0.1068	0.0014	0.43	9.36	0.125	0.0606	0.0038	0.0693	0.0166	0.13	14.9	15.2	117.4	0.129	654	8	648	26	624	127	101	
PB -44	80.1	0.9115	0.0316	0.1071	0.0011	0.43	9.3362	0.0978	0.0617	0.0023	0.0956	0.0076	0.22	41.4	86.8	317.8	0.273	656	7	658	17	665	80	99	
PB -44	78.1	0.9955	0.0654	0.1134	0.0019	0.75	8.8164	0.1462	0.0637	0.0047	0.0416	0.0232	0.23	15.7	31.1	107.5	0.289	693	11	702	34	730	158	98	
PB -44	17.1	1.0565	0.0421	0.1244	0.0013	0.43	8.0409	0.0872	0.0616	0.0027	0.1669	0.0284	0.25	17.5	37.2	118.2	0.315	756	8	732	21	661	93	103	
PB -44	9.1	1.1697	0.1583	0.1413	0.0037	0.24	7.0759	0.1852	0.06	0.009	0.2504	0.0323	0	5.9	19.8	29.2	0.679	852	21	787	71	605	291	108	
PB -44	35.1	1.5345	0.1242	0.1498	0.0029	0.56	6.6738	0.1285	0.0743	0.0067	0.2782	0.0265	1.39	7.9	25	36.4	0.687	900	16	944	52	1049	197	95	
PB -44	18.1	1.5176	0.1258	0.159	0.0033	0.49	6.2878	0.1286	0.0692	0.0067	0.2073	0.0415	0.86	7.9	18.6	35.1	0.531	951	18	938	50	905	190	101	
PB -44	71.1	1.6241	0.1242	0.1641	0.0033	0.78	6.0938	0.1219	0.0718	0.006	0.5207	0.0227	0.34	14.1	77.5	50	1.55	980	18	980	45	980	168	99	
PB -44	55.1	1.5118	0.1147	0.1642	0.0035	0.47	6.0915	0.1288	0.0668	0.0058	0.3115	0.0227	0.23	11.7	39	45.5	0.857	980	19	935	45	831	164	104	

PB -44	76.1	1.7217	0.0801	0.1708	0.0023	0.7	5.8535	0.0797	0.0731	0.0038	0.19	0.0095	0.92	23.3	52.7	104.3	0.505	1017	13	1017	29	1017	99	100	
PB -44	48.1	1.7296	0.0477	0.1709	0.0015	0.76	5.8509	0.0504	0.0734	0.002	0.2612	0.0054	0.38	66.6	219.5	273.6	0.802	1017	8	1020	18	1025	56	99	
PB -44	44.1	1.7184	0.0559	0.172	0.0017	0.92	5.8129	0.0561	0.0724	0.0024	0.039	0.0064	0.39	49.6	29.9	256.7	0.117	1023	9	1015	21	999	67	100	
PB -44	92.1	1.765	0.0608	0.1729	0.0021	0.34	5.7832	0.0695	0.074	0.0027	0.166	0.0071	0.7	34.7	77.4	151.8	0.51	1028	11	1033	22	1042	74	99	
PB -44	63.1	1.7375	0.0781	0.1729	0.0023	0.12	5.7829	0.0771	0.0729	0.0035	0.2384	0.0091	0.42	25	66.4	102.6	0.648	1028	13	1023	29	1011	95	100	
PB -44	12.1	1.8077	0.0966	0.1729	0.0025	0.58	5.7824	0.0839	0.0758	0.0046	0.2091	0.0129	0.63	13.1	34.2	58.3	0.587	1028	14	1048	35	1090	123	98	
PB -44	47.1	1.7792	0.1009	0.1739	0.0026	0.33	5.7507	0.0868	0.0742	0.0046	0.5009	0.0164	0.75	16.6	76	55.3	1.373	1034	14	1038	37	1047	126	99	
PB -44	37.1	1.7637	0.0509	0.1749	0.0016	0.61	5.7179	0.0509	0.0731	0.0021	0.1358	0.015	0.25	48.7	89.7	214.6	0.418	1039	9	1032	19	1018	59	100	
PB -44	62.1	1.693	0.1454	0.1765	0.0038	0.29	5.6665	0.1221	0.0696	0.0066	0.1259	0.0219	0.39	9.7	14.9	40.9	0.364	1048	21	1006	54	916	182	104	
PB -44	27.1	1.8538	0.2028	0.1773	0.0043	0.32	5.6417	0.1376	0.0759	0.0094	0.2549	0.0359	3.34	6.1	17.8	25.2	0.705	1052	24	1065	68	1091	246	98	
PB -44	65.1	1.8019	0.0693	0.1778	0.0021	0.38	5.6243	0.0667	0.0735	0.0029	0.1165	0.0053	0.61	30.8	50.3	137.8	0.365	1055	12	1046	25	1028	80	100	
PB -44	31.1	1.9071	0.0911	0.1812	0.0023	0.21	5.5177	0.0694	0.0763	0.004	0.2392	0.0215	0.72	17.1	45.2	67.3	0.672	1074	13	1084	32	1103	105	99	
PB -44	43.1	1.9227	0.0938	0.1813	0.0024	0.15	5.5169	0.0742	0.0769	0.0041	0.2387	0.0215	0.69	18.6	48.7	72.8	0.669	1074	13	1089	33	1119	105	98	
PB -44	8.1	1.8655	0.0884	0.1822	0.0024	0.01	5.4883	0.0718	0.0743	0.004	0.1505	0.012	0.65	15.4	26.7	66.3	0.403	1079	13	1069	31	1048	108	100	
PB -44	95.1	1.8735	0.0596	0.1854	0.0021	0.42	5.395	0.0616	0.0733	0.0025	0.1525	0.0087	0.22	50	84.2	208.6	0.404	1096	12	1072	21	1022	67	102	
PB -44	84.1	1.9755	0.1395	0.1942	0.0038	0.32	5.1485	0.0995	0.0738	0.0059	0.126	0.021	0.46	12.2	32.7	50.9	0.642	1144	20	1107	48	1035	159	103	
PB -44	79.1	2.2158	0.1073	0.2032	0.003	0.77	4.9214	0.0728	0.0791	0.0043	0.4802	0.0152	0.41	24	107.2	71.7	1.494	1193	16	1186	34	1174	104	100	
PB -44	90.1	2.2729	0.0681	0.2036	0.0023	0.61	4.912	0.0556	0.081	0.0026	0.2819	0.0059	0.28	46	139.5	154.2	0.904	1195	12	1204	21	1221	63	99	
PB -44	1.1	2.3043	0.1633	0.2102	0.0039	0.01	4.7572	0.0888	0.0795	0.0067	0.1869	0.0205	1.45	6.7	11.7	24.6	0.477	1230	21	1214	50	1185	160	101	
PB -44	45.1	2.7542	0.1637	0.2332	0.004	0.26	4.2885	0.0736	0.0857	0.0056	0.2256	0.0205	1.17	12.5	22.9	39.1	0.585	1351	21	1343	45	1331	132	100	
PB -44	29.1	3.24	0.3352	0.2346	0.0071	0.18	4.2623	0.1289	0.1002	0.0122	0.1412	0.0545	2.55	4.6	5.6	14.6	0.388	1359	37	1467	96	1627	273	92	
PB -44	2.1	2.8592	0.1558	0.2368	0.0038	0.01	4.2228	0.0683	0.0876	0.0054	0.4021	0.0201	2.38	10.6	31.6	28.8	1.097	1370	20	1371	41	1373	120	99	
PB -44	68.1	3.0363	0.2123	0.245	0.0052	0.01	4.0815	0.0869	0.0899	0.0072	0.2188	0.0203	2.29	9.6	26.6	28.5	0.933	1413	27	1417	53	1423	151	99	
PB -44	54.1	4.2052	0.1381	0.2917	0.004	0.06	3.4285	0.0466	0.1046	0.0038	0.1097	0.0063	0.15	27.2	23.2	72	0.322	1650	20	1675	27	1707	68	98	
PB -44	86.1	4.2274	0.4703	0.297	0.0115	0.39	3.3673	0.1301	0.1032	0.0131	0.8098	0.0478	1.88	7.3	29.7	12.1	2.443	1676	57	1679	87	1683	227	99	
PB -44	38.1	4.5306	0.1382	0.3055	0.0032	0.44	3.273	0.0344	0.1075	0.0034	0.1956	0.0068	0.09	31.1	36	72.2	0.499	1719	16	1737	25	1758	58	98	
PB -44	25.1	4.6567	0.8726	0.3086	0.0173	0.38	3.2407	0.1816	0.1094	0.0245	0.2419	0.0985	3.66	2.2	3.3	4.9	0.66	1734	86	1760	179	1790	488	98	
PB -44	60.1	4.8154	0.1595	0.317	0.0044	0.6	3.1549	0.0436	0.1102	0.004	0.124	0.011	0.37	27.4	28.7	63.6	0.452	1775	22	1788	28	1802	67	99	
PB -44	20.1	5.1807	0.119	0.3338	0.0028	0.96	2.9954	0.0255	0.1125	0.0025	0.2008	0.0047	0.6	75.8	90.6	171.7	0.528	1857	14	1849	19	1841	40	100	
PB -44	50.1	5.7002	0.1388	0.3433	0.0037	0.41	2.9132	0.0316	0.1204	0.0031	0.1995	0.0041	0.26	62	67.1	127.3	0.527	1902	18	1931	21	1963	46	98	
PB -44	13.1	5.4974	0.1194	0.3553	0.0029	0.51	2.8147	0.0227	0.1122	0.0025	0.2071	0.0057	0.22	69.7	82.4	147.2	0.56	1960	14	1900	19	1836	40	103	
PB -44	15.1	6.3578	0.1441	0.3676	0.0031	0.36	2.7203	0.0231	0.1254	0.0029	0.3584	0.0089	0.15	54.5	101.4	95.1	1.066	2018	15	2027	20	2035	40	99	
PB -44	40.1	6.6434	0.1415	0.3778	0.0029	0.43	2.6469	0.0201	0.1275	0.0025	0.0701	0.0023	0.19	65.3	33.1	142.8	0.232	2066	14	2065	19	2064	35	100	
PB -44	75.1	6.5916	0.1527	0.393	0.0037	0.95	2.5449	0.0236	0.1217	0.0029	0.0135	0.0038	0.28	108	9.5	234.6	0.04	2137	17	2058	20	1981	41	103	
PB -44	46.1	6.985	0.175	0.3936	0.0036	0.64	2.541	0.0233	0.1287	0.0032	0.1236	0.0047	0.1	57.5	47.3	110.3	0.429	2139	17	2110	22	2081	44	101	
PB -44	96.1	11.45	0.2591	0.4618	0.0051	0.98	2.1654	0.0241	0.1798	0.0044	0.1636	0.016	0.15	53.6	42.9	76.2	0.564	2448	23	2561	22	2651	40	95	
PB -44	16.1	14.3981	0.3581	0.5337	0.0058	0.93	1.8737	0.0203	0.1957	0.0051	0.5535	0.0161	0.3	32.8	60.8	31.1	1.954	2757	24	2776	23	2790	43	99	
PB -44	94.1	20.2157	0.5837	0.5744	0.0098	0.87	1.7409	0.0298	0.2552	0.008	0.0791	0.0147	0.22	20.6	7.4	22.3	0.33	2926	39	3102	28	3218	49	94	
PB -44	87.1	0.3673	0.1321	0.0398	0.003	0.35	25.0967	1.8808	0.0668	0.0286	0.3839	0.1016	4.82	2.1	30.6	35.7	0.858	252	19	318	100	833	702	79	
PB -44	57.1	0.2429	0.1513	0.0409	0.0038	0.8	24.4343	2.2716	0.0431	0.0307	0.2055	0.1325	8.05	1.4	31.2	25.8	1.209	259	24	221	120	0	560	117	
PB -44	32.1	0.2685	0.0392	0.0426	0.0009	0.32	23.479	0.4939	0.0457	0.0073	0.2841	0.037	2.79	7.2	96.3	121.4	0.793	269	6	242	30	0	233	111	
PB -44	34.1	0.7076	0.1894	0.0785	0.0037	0.22	12.7347	0.6053	0.0654	0.0188	0.2429	0.083	16.09	2.2	14.7	23	0.64	487	22	543	107	786	513	89	
PB -44	89.1	0.7367	0.1575	0.0801	0.0038	0.24	12.4829	0.5943	0.0667	0.0171	0.5336	0.0747	2.81	4.2	41.1	29.6	1.387	497	23	561	96	828	485	88	
PB -44	74.1	2.4748	0.4994	0.2016	0.0117	0.48	4.961	0.2884	0.089	0.0226	0.2755	0.0845	15.18	2.8	13.3	10.4	1.283	1184	63	1265	153	1405	466	93	
PB -44	91.1	3.9047	0.104	0.2458	0.0028	0.99	4.0683	0.0463	0.1152	0.0029	0.1348	0.0098	0.77	101	86.2	197.9	0.436	1417	14	1615	20	1883	47	87	
PB -44	14.1	5.6778	0.1148	0.3088	0.0024	0.65	3.2388	0.0249	0.1334	0.0026	0.1866	0.0108	1.69	26.3	11.4	44.2	0.257	1735	12	1928	18	2143	35	89	
PB -47	7.1	0.2801	0.0246	0.0383	0.0016	0.63	26.1016	1.0915	0.053	0.0039	0.2294	0.0151	1.56	15.3	161.8	295.3	0.548	242.4	9.9	250.7	19.2	329.7	152.3	96	
PB -47	66.1	0.4245	0.0495	0.0585	0.002	0.32	17.1009	0.5945	0.0526	0.0063	0.1312	0.0194	1.48	8.8	42.3	113.5	0.373	366.4	12.4	359.3	34.6	313.7	256.3	101	
PB -47	19.1	0.4388	0.02	0.0596	0.0007	0.61	16.7808	0.2081	0.0534	0.0026	0.2294	0.0182	2.74	19.5	198.9	236.3	0.842	373.1	4.5	369.4	13.9	346.2	96.1	101	
PB -47	54.1	0.5986	0.0326	0.0781	0.0014	0.2	12.812	0.2249	0.0556	0.0036	0.2081	0.0189	1.51	9.3	51.1	86.1	0.593	484.5	8.2	476.3	19.9	437.3	130.8	101	
PB -47	42.1	0.6483	0.0342	0.0798	0.001	0.88	12.5255	0.1529	0.0589	0.0033	0.2597	0.0196	2.79	48.2	466.4	383.1	1.217	495.2	5.8	507.4	20.7	563.3	121.2	97	
PB -47	84.1	0.6227	0.0309	0.0807	0.0011	0.19	12.3867	0.1637	0.0559	0.003	0.1839	0.0117	0.18	21.3	116.5	195	0.597	500.5	6.4	491.5	19.5	450	119	101	
PB -47	52.1	0.6363	0.0175	0.0811	0.0008	0.65	12.3293	0.1197	0.0569	0.0017	0.0605	0.0091	0.22	27.9	55.9	290.3	0.192	502.7	4.7	500	10.8	487.7	68	100	
PB -47	49.1	0.7343	0.0474	0.0863	0.002	0.14	11.5897	0.2655	0.0617	0.005	0.1475	0.0317	5.25	5.8	25.9	53.2	0.486	533.5	11.7	559.1	27.5	664.7	164.3	95	
PB -47	50.1	0.6847	0.0248	0.0869	0.0011	0.37	11.502	0.1429	0.0571	0.0024	0.0382	0.0095	0.47	17.2	21.2	166.4	0.127	537.4	6.4	529.6	14.7	496.1	87.5	101	
PB -47	85.1	0.6786	0.0271	0.0871	0.0009	0.07	11.4848	0.1198	0.0565	0.0024	0.0281	0.0076	0.87	25.5	19.4	255.4	0.076	538.2	5.4	525.9	16.1	473	87.5	102	
PB -47	61.1	0.7065	0.2178	0.0886	0.0062	0.49	11.288	0.7899	0.0578	0.0201	0.2763	0.065	2.06	3.8	22.3	27.4	0.812	547.2	36.7	542.7	128.4	523.7	512.2	100	
PB -47	1.1	0.7673	0.0708	0.09	0.0042	0.21	11.1132	0.5139	0.0618	0.0049	0.7208	0.0214	0.68	14.1	142.2	77.6	1.833	555.4	24.6	578.2	41	668.8	179.3	96	
PB -47	82.1	0.7923	0.0938	0.0915	0.0037	0.24	10.9263	0.4367	0.0628	0.0075	0.0454	0.0198	1.11	7.6	9.7	70.8	0.137	564.5	21.6	592.4	53.8	700.9	272.2	95	
PB -47	21.1	0.7599	0.0478	0.0918	0.0015	0.75	10.8894	0.1795	0.06	0.0041	0.2315	0.0237	0.31	8.9	40.8	67.8	0.602	566.4	8.9	574	28.4	604.1	155.9	98	
PB -47	58.1	0.7633	0.0206	0.0923	0.0009	0.97	10.8389	0.1042	0.06	0.002	0.4422	0.0378	4.77	59.7	945.9	408.4	2.316	568.9	5.3	575.9	12.4	603.6	74.2	98	

PB -47	13.1	0.7521	0.0393	0.0939	0.0013	0.11	10.6516	0.1489	0.0581	0.0032	0.3667	0.0154	0.61	13.6	98.5	95.5	1.032	578.5	7.7	569.4	22.3	533.6	115.4	101	
PB -47	29.1	0.7751	0.0394	0.0942	0.0012	0.95	10.6176	0.1369	0.0597	0.0031	0.1616	0.0179	3.74	43.5	132.5	363.9	0.364	580.2	7.2	582.7	22.9	592.2	113.7	99	
PB -47	31.1	0.7976	0.0477	0.0942	0.0014	0.35	10.6155	0.1571	0.0614	0.0037	0.128	0.0124	1.76	14.7	68.3	113.4	0.602	580.3	8.2	595.4	26.7	653.4	135	97	
PB -47	43.1	0.7942	0.0448	0.0948	0.0012	0.38	10.548	0.1377	0.0608	0.0038	0.1853	0.0157	0.7	14.5	58.1	115.6	0.503	583.9	7.3	593.6	25.3	630.7	135.3	98	
PB -47	80.1	0.8074	0.0639	0.0964	0.0031	0.43	10.3706	0.3324	0.0607	0.0047	0.0158	0.0098	0.34	13.4	5.8	120.2	0.048	593.4	18.2	601	36.3	629.6	173.8	98	
PB -47	3.1	0.7919	0.0656	0.0975	0.0041	0.55	10.2586	0.4308	0.0589	0.0041	0.3651	0.0165	3.54	15.4	105.6	99.5	1.061	599.6	24.1	592.3	36.8	564.1	149.1	101	
PB -47	73.1	0.8271	0.0422	0.0984	0.0027	0.68	10.1629	0.2814	0.061	0.0026	0.0616	0.009	0.44	46	77.1	402.3	0.192	605	16	612	23.5	637.9	91.5	98	
PB -47	78.1	0.8298	0.0571	0.099	0.003	0.65	10.0969	0.3062	0.0608	0.004	0.2214	0.0092	0	23.2	109.8	171.6	0.64	608.8	17.6	613.5	32	631.1	139.3	99	
PB -47	22.1	0.8482	0.0272	0.1004	0.0011	0.78	9.9569	0.1088	0.0613	0.002	0.1445	0.006	2	31.2	96.6	251.2	0.385	616.9	6.4	623.7	15.1	648.1	71.1	98	
PB -47	74.1	0.8422	0.0603	0.1007	0.0032	0.76	9.9299	0.3144	0.0607	0.004	0.1366	0.0144	0.46	18.5	56.2	143.7	0.391	618.5	18.7	620.4	33.4	627.1	142.6	99	
PB -47	25.1	0.8775	0.0884	0.1014	0.0021	0.55	9.8638	0.2022	0.0628	0.0066	0.1296	0.0216	1.38	8.2	23.2	64	0.362	622.5	12.1	639.6	46.1	700.7	227.6	97	
PB -47	40.1	0.8503	0.0394	0.1022	0.0011	0.57	9.7844	0.1073	0.0603	0.0031	0.1006	0.0073	0.43	19.3	43.8	155.5	0.282	627.3	6.6	624.8	21.3	615.7	104.6	100	
PB -47	53.1	0.8534	0.0201	0.1026	0.0009	0.32	9.7422	0.0832	0.0603	0.0016	0.0753	0.0042	0.35	42.4	79.3	344	0.23	629.9	5.1	626.5	11	614.4	54.8	100	
PB -47	70.1	0.8728	0.0396	0.1033	0.0025	0.25	9.6848	0.2344	0.0613	0.0025	0.0539	0.0064	0.2	43.3	51.1	331.8	0.154	633.5	14.6	637.1	21.2	649.9	83.9	99	
PB -47	20.1	0.8605	0.0264	0.1034	0.0011	0.3	9.6745	0.1031	0.0604	0.0018	0.0732	0.0058	0.25	42.8	67.7	348	0.194	634.1	6.4	630.4	14.3	617	64.3	100	
PB -47	67.1	0.8829	0.041	0.1035	0.0026	0.97	9.6629	0.2427	0.0619	0.0023	0.0266	0.0154	0.09	62.4	13.8	538.8	0.026	634.8	15.1	642.5	20.7	669.7	70.6	98	
PB -47	36.1	0.8811	0.0305	0.1049	0.0009	0.43	9.5337	0.0843	0.0609	0.0022	0.0706	0.0076	0.4	36.5	52.8	289.9	0.182	643	5.4	641.6	16.5	636.6	79.8	100	
PB -47	12.1	0.8988	0.0552	0.1057	0.004	0.23	9.4615	0.3611	0.0617	0.0029	0.147	0.0071	0.17	21.7	53.8	156.9	0.343	647.7	23.5	651.1	29.9	662.8	105.4	99	
PB -47	17.1	0.9259	0.0525	0.1072	0.0017	0.37	9.3318	0.1449	0.0627	0.0037	0.2272	0.0207	0.85	8.8	31.9	57.6	0.554	656.2	9.7	665.5	27.4	696.9	130.1	98	
PB -47	51.1	0.9142	0.0282	0.1072	0.0012	0.65	9.3297	0.1055	0.0619	0.0022	0.3605	0.0155	0.52	23.8	158.1	142.4	1.11	656.4	7.1	659.3	15	669.3	79.3	99	
PB -47	45.1	1.0242	0.0933	0.108	0.0024	0.46	9.2598	0.2034	0.0688	0.0073	0.2234	0.0253	1.63	6.8	31.3	45.8	0.684	661.1	13.8	716	49	892.3	232.6	92	
PB -47	37.1	1.0173	0.1176	0.1083	0.0029	0.49	9.2338	0.2496	0.0681	0.0092	0.2509	0.0301	1.09	6.2	23.9	38.1	0.626	662.9	17	712.5	58.2	872.4	282.2	93	
PB -47	95.1	0.9926	0.0708	0.1092	0.0023	0.11	9.157	0.1908	0.0659	0.0054	0.1449	0.0232	0.74	8.3	24.9	59.1	0.421	668.1	13.2	700.1	36.4	804	176.9	95	
PB -47	93.1	0.9722	0.0417	0.1101	0.0014	0.16	9.083	0.1126	0.064	0.003	0.1652	0.0128	0.58	20.6	79	141.7	0.558	673.3	7.9	689.6	21.9	743	103.1	97	
PB -47	56.1	0.8685	0.038	0.113	0.0017	0.29	8.8524	0.1311	0.0558	0.0028	0.0984	0.0153	1.5	12.4	46.1	88.8	0.518	689.9	9.7	634.7	20.1	442.8	106.1	108	
PB -47	48.1	1.0605	0.0567	0.115	0.0023	0.31	8.6971	0.1774	0.0669	0.0044	0.1481	0.0253	0.61	8.5	20.7	54.3	0.382	701.6	13.6	734.1	27.8	834.5	132.8	95	
PB -47	34.1	1.0509	0.0923	0.116	0.0022	0.25	8.6189	0.1667	0.0657	0.0061	0.122	0.0253	1.62	8.7	21	63.4	0.33	707.6	13	729.3	46.5	796.7	206.9	97	
PB -47	4.1	1.0084	0.0824	0.1163	0.005	0.43	8.6007	0.3702	0.0629	0.0043	0.1288	0.0152	1.1	11.9	25.4	78.2	0.325	709.1	28.9	708.1	41.4	704.9	142.7	100	
PB -47	2.1	0.9752	0.1407	0.1243	0.0066	0.7	8.0482	0.4246	0.0569	0.0077	0.1796	0.0321	6.31	5.5	12.6	30.7	0.409	755	37.7	691.1	69.8	488.6	283.9	109	
PB -47	72.1	1.0291	0.1039	0.1248	0.0045	0.56	8.0118	0.2914	0.0598	0.006	0.2211	0.0228	1.02	12.6	52.6	80.8	0.652	758.2	26	718.5	52	596.3	208.3	105	
PB -47	44.1	1.1714	0.0516	0.13	0.0014	0.01	7.6917	0.0858	0.0653	0.0031	0.1327	0.0129	0.62	20.3	42.9	122.2	0.352	787.9	8.3	787.3	24.3	785.6	103.2	100	
PB -47	57.1	1.1976	0.0454	0.1332	0.0019	0.65	7.5049	0.1052	0.0652	0.0029	0.181	0.0249	1.03	15.6	60.8	84.8	0.717	806.4	10.6	799.5	20.5	780.3	95.3	100	
PB -47	27.1	1.2247	0.0641	0.134	0.0019	0.52	7.4615	0.1051	0.0663	0.0034	0.0346	0.007	0.9	16.5	22.1	106.1	0.209	810.8	10.7	811.9	28.6	815.1	108.8	99	
PB -47	8.1	1.3723	0.1194	0.1454	0.0064	0.39	6.8796	0.3035	0.0685	0.0051	0.1921	0.0212	1.08	12	28.1	57.2	0.492	874.9	36.2	877.1	49.6	882.9	148.7	99	
PB -47	55.1	1.4069	0.0414	0.1466	0.0017	0.93	6.8191	0.0771	0.0696	0.0023	0.1037	0.0154	1.95	26.8	49.5	154.6	0.32	882.1	9.3	891.8	16.9	916	65.1	98	
PB -47	89.1	1.6796	0.1955	0.1508	0.0062	0.19	6.6311	0.2722	0.0808	0.0113	0.4826	0.0556	1.51	5	26.6	18.9	1.405	905.5	34.7	1001	75.1	1216	294.8	90	
PB -47	11.1	1.4849	0.1124	0.1548	0.0063	0.26	6.4596	0.2647	0.0696	0.0044	0.2221	0.0186	0.68	15	37.2	70	0.531	927.9	35.5	924.2	44.7	915.6	119.9	100	
PB -47	71.1	1.5311	0.117	0.1572	0.0049	0.24	6.3613	0.1998	0.0706	0.0055	0.2071	0.0149	1.55	12.2	51.4	55.8	0.922	941.2	27.6	942.9	47.1	946.9	159.9	99	
PB -47	86.1	1.5767	0.0647	0.162	0.002	0.27	6.1733	0.0758	0.0706	0.0031	0.2474	0.0095	0.63	24.8	83.8	106.9	0.784	967.8	11	961.1	25.1	945.7	86.7	100	
PB -47	60.1	1.6478	0.0648	0.1634	0.0038	0.47	6.1211	0.1414	0.0732	0.0025	0.0647	0.0054	0.69	37.3	30.9	187.5	0.165	975.5	20.9	988.7	24.6	1018	69.4	98	
PB -47	62.1	1.6084	0.0835	0.1634	0.0043	0.24	6.1183	0.1596	0.0714	0.0034	0.2838	0.0083	0.34	28.3	101.8	115	0.885	975.9	23.6	973.5	32	968.1	96.3	100	
PB -47	10.1	1.6071	0.0748	0.1643	0.0057	0.17	6.0865	0.2116	0.0709	0.002	0.1029	0.0036	0.38	59.8	71.3	285.9	0.249	980.6	31.6	973	28.8	955.8	56.8	100	
PB -47	76.1	1.7316	0.0766	0.1684	0.0046	0.26	5.9375	0.1614	0.0746	0.0026	0.0617	0.0039	0.32	51.4	52.8	248.5	0.213	1003	25.3	1020	28.5	1057	71.3	98	
PB -47	92.1	1.69	0.0486	0.1691	0.0014	0.57	5.9126	0.0489	0.0725	0.002	0.1251	0.0028	0.15	66.4	118.2	314.5	0.376	1007	7.7	1005	18	999.3	56.1	100	
PB -47	69.1	1.8225	0.1261	0.1704	0.0053	0.36	5.8691	0.1817	0.0776	0.0055	0.1405	0.0127	0.28	12.4	22.3	54.4	0.411	1014	29	1054	47.1	1136	149.2	96	
PB -47	83.1	1.7381	0.0741	0.1711	0.0047	0.97	5.8438	0.1609	0.0737	0.0023	0.0686	0.0029	0.14	68.9	66.7	327.2	0.204	1018	25.7	1023	26.8	1032	64.5	99	
PB -47	15.1	1.7942	0.062	0.1738	0.0021	0.01	5.754	0.0689	0.0749	0.0026	0.1203	0.0075	0.59	21.6	27.6	97.3	0.284	1033	11.4	1043	22.6	1065	71.3	99	
PB -47	81.1	1.8643	0.1364	0.1747	0.0059	0.34	5.7257	0.193	0.0774	0.0055	0.1413	0.0126	0.3	12.5	22.7	55.2	0.411	1038	32.3	1069	50.1	1132	150.3	97	
PB -47	24.1	1.729	0.1015	0.1759	0.0027	0.29	5.6835	0.0881	0.0713	0.0043	0.2556	0.0125	0.8	16.4	80.2	65.5	1.224	1045	14.9	1019	37.8	965.2	125.1	102	
PB -47	79.1	1.9398	0.1179	0.1802	0.0056	0.07	5.5491	0.1717	0.0781	0.0043	0.2547	0.0129	1.15	23.4	85.7	95.9	0.894	1068	30.4	1095	40.5	1149	108.7	97	
PB -47	18.1	1.9597	0.0562	0.1884	0.002	0.95	5.3091	0.0575	0.0755	0.0022	0.0327	0.0066	0.66	33	13	155.4	0.084	1113	11.1	1102	19.6	1081	58.1	100	
PB -47	64.1	2.1533	0.1769	0.2031	0.0067	0.69	4.9244	0.163	0.0769	0.0069	0.161	0.0216	3.48	12.3	28.1	45.8	0.614	1192	36.4	1166	58.3	1119	177.3	102	
PB -47	38.1	2.1172	0.1869	0.2061	0.0047	0.72	4.8512	0.1095	0.0745	0.0076	0.1413	0.0294	0.66	9	22.8	33.6	0.679	1208	24.9	1154	59.7	1055	197.1	104	
PB -47	75.1	3.6777	0.2131	0.2716	0.0086	0.04	3.6821	0.1164	0.0982	0.0051	0.2105	0.0117	0.34	19.5	33.9	52.2	0.649	1549	43.6	1567	45.5	1591	94.6	98	
PB -47	68.1	4.0192	0.1435	0.2752	0.0064	0.72	3.6342	0.085	0.1059	0.0032	0.1407	0.0033	0.14	57.9	70.2	151.5	0.464	1567	32.5	1638	29	1731	54.4	95	
PB -47	26.1	4.4763	0.2774	0.2951	0.0058	0.43	3.3892	0.0662	0.11	0.0076	0.1481	0.0218	1.74	9.4	9.5	23.3	0.406	1667	28.9	1727	52.5	1800	125.6	96	
PB -47	46.1	4.7347	0.1679	0.312	0.0038	0.01	3.2054	0.0386	0.1101	0.0044	0.1958	0.0097	1.65	18.2	39.5	42.2	0.938	1750	18.5	1773	30.3	1801	73.6	98	
PB -47	47.1	5.0361	0.1291	0.3365	0.0028	0.65	2.9715	0.0247	0.1085	0.0029	0.1378	0.0116	0.2	47.2	89.4	107	0.836	1870	13.5	1825	21.7	1775	48.9	102	
PB -47	5.1	5.1011	0.3314	0.3385	0.015	0.5	2.9546	0.1307	0.1093	0.0053	0.3192	0.0323	1.68	16.6	37.2	33.6	1.106	1879	71.9	1836	54.7	1788	90.5	102	
PB -47	39.1	5.9817	0.1359	0.3472	0.0026	0.13	2.8804	0.0214	0.125	0.0028	0.0944	0.0026	0.17	68.5	43.1	148.4	0.29	1921	12.3	1973	19.5	2028	40.4	97	
PB -47	63.1	6.3823	0.2329	0.3515	0.0086	0.81	2.8446	0.0695	0.1317	0.0041	0.1344	0.0051	0.65	59.8	61.8	119.3	0.518	1942	40.9	2030	31.6	2120	53.7	95	

PB -47	91.1	5.7479	0.163	0.3517	0.0034	0.73	2.8436	0.0278	0.1185	0.0034	0.1859	0.0099	0.35	39.9	63.2	80.4	0.785	1943	16.4	1939	24.5	1934	51.3	100	
PB -47	23.1	6.1489	0.1528	0.3519	0.0037	0.01	2.8414	0.0299	0.1267	0.003	0.206	0.0051	0	53.8	67.3	105.3	0.639	1944	17.6	1997	21.7	2053	42	97	
PB -47	32.1	6.3986	0.2548	0.3555	0.0053	0.73	2.8133	0.0422	0.1306	0.0053	0.1031	0.0143	0.74	16.4	9.8	35.4	0.277	1961	25.4	2032	34.9	2106	71.8	96	
PB -47	87.1	6.4503	0.1515	0.3574	0.0026	0.96	2.7982	0.0202	0.1309	0.003	0.1757	0.003	0.17	139	173.1	283.4	0.611	1970	12.3	2039	20.9	2110	39.8	96	
PB -47	88.1	6.3773	0.1855	0.3604	0.0038	0.69	2.7749	0.0292	0.1283	0.0038	0.1975	0.0074	0.21	35.2	50.9	70.4	0.723	1984	18	2029	25.7	2075	52.8	97	
PB -47	33.1	6.2015	0.1759	0.3614	0.0042	0.61	2.7668	0.0318	0.1244	0.0034	0.1025	0.0043	0.27	39.2	24	82.9	0.289	1989	19.6	2005	24.7	2021	48.3	99	
PB -47	59.1	6.2688	0.1304	0.3673	0.0034	0.5	2.7228	0.0251	0.1238	0.0028	0.4763	0.006	0.14	52.8	114.3	82.1	1.392	2017	15.9	2014	18.1	2012	39.8	100	
PB -47	90.1	7.3805	0.181	0.4015	0.0031	0.94	2.4904	0.0194	0.1333	0.0032	0.2259	0.0055	0.32	107	160.7	193.1	0.832	2176	14.4	2159	22	2142	41.6	100	
PB -47	28.1	7.5796	0.1858	0.4019	0.0043	0.37	2.4879	0.0265	0.1368	0.0032	0.0137	0.0037	0.58	55	10.3	116	0.089	2178	19.7	2183	22.1	2187	39.7	99	
PB -47	94.1	9.6668	0.229	0.463	0.0035	0.86	2.16	0.0165	0.1514	0.0035	0.2501	0.0079	0.1	103	128.9	153.7	0.839	2453	15.7	2404	22.2	2362	39.9	102	
PB -47	9.1	11.064	0.4827	0.4698	0.0169	0.01	2.1287	0.0765	0.1708	0.0041	0.2322	0.0043	0.15	49.2	44.1	68.2	0.646	2483	74	2529	39.9	2566	39.8	98	
PB -47	35.1	11.4021	0.3223	0.5108	0.0062	0.76	1.9578	0.0237	0.1619	0.0045	0.2258	0.0057	0.11	41.4	65.1	55.7	1.169	2660	26.4	2557	26.3	2476	45.9	104	
PB -47	6.1	13.3752	0.6919	0.5133	0.0214	0.01	1.948	0.0813	0.189	0.0065	0.2385	0.0127	0.87	17.9	14.5	22.6	0.641	2671	91.5	2707	48.8	2733	55.8	98	
PB -47	65.1	16.5989	0.5121	0.56	0.0129	0.49	1.7857	0.0412	0.215	0.0051	0.1452	0.0047	0.52	42.7	25.6	50.4	0.509	2867	53.3	2912	29.5	2943	39	98	
PB -47	77.1	16.6174	0.5996	0.5616	0.0151	0.54	1.7806	0.0478	0.2146	0.0055	0.1454	0.0047	0.5	43.1	26.1	51.2	0.51	2873	62.2	2913	34.6	2941	41.6	98	
PB -47	30.1	20.4586	0.5311	0.6161	0.0075	0.39	1.623	0.0197	0.2408	0.0059	0.0204	0.0045	1.67	14.1	1.7	18.2	0.094	3095	29.9	3113	25.3	3125	39.4	99	
PB -47	14.2	25.9881	0.6223	0.6295	0.0073	0.54	1.5886	0.0185	0.2994	0.007	0.1366	0.0291	0.52	30	7.7	34.6	0.222	3148	29.3	3346	24.1	3467	36.5	94	
PB -47	14.1	26.6352	0.6539	0.6445	0.0079	0.96	1.5516	0.0191	0.2997	0.0073	0.1987	0.0519	1.13	33.6	13	38	0.342	3207	31.4	3370	24.8	3469	38	95	
PB -47	16.1	0.6736	0.1425	0.0987	0.0035	0.67	10.1355	0.3631	0.0495	0.0114	0.3236	0.055	3.65	2.5	14.8	16.5	0.898	606.6	20.7	522.9	83.5	172.5	337.9	115	
PB -50	40.1	0.2893	0.0187	0.0411	0.0008	0.3	24.3049	0.4662	0.051	0.0035	0.1791	0.0179	0.2	20	173	359	0.48	260	5	258	15	241	147	100	
PB -50	20.1	0.3075	0.0405	0.0434	0.0009	0.67	23.0362	0.4882	0.0514	0.0073	0.0859	0.0254	1.9	10	66	171	0.39	274	6	272	32	258	267	100	
PB -50	86.1	0.4262	0.0184	0.0582	0.0006	0.57	17.1694	0.1777	0.0531	0.0025	0.1578	0.0051	2.6	51	343	670	0.51	365	4	361	13	332	106	101	
PB -50	55.1	0.7125	0.041	0.0851	0.0017	0.44	11.7514	0.2402	0.0607	0.0036	0.3325	0.0182	2.4	14	114	116	0.98	527	10	546	25	629	136	96	
PB -50	52.1	0.7274	0.0559	0.0853	0.0021	0.07	11.7234	0.2854	0.0619	0.0052	0.2449	0.0279	0.8	12	71	97	0.73	528	12	555	33	669	182	95	
PB -50	2.1	0.7716	0.1747	0.0878	0.0035	0.59	11.3943	0.4596	0.0638	0.0151	0.355	0.0804	0.9	4	24	27	0.88	542	21	581	100	734	467	93	
PB -50	81.1	0.7105	0.0309	0.0886	0.0011	0.46	11.2844	0.1378	0.0581	0.0026	0.0013	0.0023	0.1	36	2	360	0.01	547	6	545	18	535	95	100	
PB -50	93.1	0.7231	0.0766	0.0898	0.002	0.4	11.1376	0.2424	0.0584	0.0069	0.2673	0.025	1.2	11	69	83	0.83	554	12	553	45	545	251	100	
PB -50	8.1	0.696	0.0503	0.0908	0.0013	0.14	11.0079	0.1542	0.0556	0.0043	0.3948	0.018	1.5	16	109	116	0.94	561	8	536	31	435	168	104	
PB -50	96.1	0.7101	0.048	0.0913	0.0013	0.01	10.9518	0.1603	0.0564	0.0041	0.2427	0.0103	0.9	19	113	151	0.75	563	8	545	28	468	157	103	
PB -50	63.1	0.7542	0.039	0.0916	0.0012	0.59	10.9213	0.1442	0.0597	0.0034	0.164	0.012	0.3	25	94	215	0.44	565	7	571	23	594	121	98	
PB -50	60.1	0.7669	0.0283	0.0921	0.0015	0.01	10.8611	0.1738	0.0604	0.0021	0.2356	0.0077	0.1	42	203	333	0.61	568	9	578	16	618	78	98	
PB -50	43.1	0.7355	0.0613	0.0921	0.0022	0.39	10.8556	0.2597	0.0579	0.0054	0.1854	0.0198	0.3	11	44	91	0.48	568	13	560	36	526	201	101	
PB -50	83.1	0.7034	0.0587	0.0929	0.0018	0.35	10.7597	0.2063	0.0549	0.0051	0.1754	0.0159	2.7	15	66	121	0.55	573	11	541	34	408	192	105	
PB -50	90.1	0.7901	0.0559	0.0935	0.0015	0.45	10.6975	0.1727	0.0613	0.0048	0.3296	0.0125	1.0	16	120	118	1.01	576	9	591	32	650	168	97	
PB -50	73.1	0.782	0.0534	0.0937	0.0017	0.17	10.6721	0.188	0.0605	0.0044	0.1217	0.0113	0.9	14	44	123	0.35	577	10	587	30	622	165	98	
PB -50	51.1	0.7623	0.0437	0.0938	0.0019	0.26	10.662	0.2158	0.0589	0.0035	0.1687	0.0173	0.7	14	55	111	0.50	578	11	575	26	565	133	100	
PB -50	58.1	0.7883	0.0315	0.0943	0.0016	0.18	10.6021	0.1768	0.0606	0.0024	0.1908	0.0055	0.3	30	134	236	0.57	581	9	590	18	626	84	98	
PB -50	9.1	0.8701	0.2062	0.0944	0.004	0.13	10.593	0.4519	0.0669	0.0181	0.1842	0.0891	3.0	3	11	23	0.48	582	24	636	116	833	453	91	
PB -50	11.1	0.7873	0.0358	0.0968	0.001	0.88	10.3273	0.1086	0.059	0.0027	0.0263	0.0071	0.8	26	20	210	0.10	596	6	590	20	566	102	101	
PB -50	61.1	0.8069	0.0784	0.0969	0.0021	0.55	10.3222	0.2255	0.0604	0.0064	0.1773	0.0221	0.7	10	47	73	0.65	596	12	601	44	618	232	99	
PB -50	72.1	0.8057	0.0335	0.0971	0.0011	0.44	10.3013	0.1171	0.0602	0.0026	0.0886	0.0045	0.6	37	86	309	0.28	597	7	600	19	611	96	99	
PB -50	29.1	0.7971	0.0545	0.0974	0.0017	0.52	10.2705	0.1749	0.0594	0.0046	0.124	0.0147	1.2	22	70	171	0.41	599	10	595	31	581	172	100	
PB -50	22.1	0.7993	0.0578	0.0975	0.0015	0.43	10.2614	0.1573	0.0595	0.0047	0.2594	0.0127	0.4	18	79	134	0.59	600	9	596	33	585	173	100	
PB -50	64.1	0.8028	0.0338	0.0977	0.0011	0.94	10.235	0.1168	0.0596	0.0027	0.0633	0.0046	5.0	46	118	419	0.28	601	7	598	19	589	97	100	
PB -50	88.1	0.8172	0.1259	0.0979	0.003	0.28	10.2184	0.3169	0.0606	0.0107	0.3593	0.039	3.7	6	52	44	1.20	602	18	607	69	624	356	99	
PB -50	41.1	0.8301	0.0511	0.0982	0.002	0.28	10.1786	0.2034	0.0613	0.004	0.0545	0.0083	0.7	17	32	133	0.24	604	12	614	28	649	134	98	
PB -50	75.1	0.8283	0.0355	0.0983	0.0012	0.57	10.1703	0.1247	0.0611	0.0027	0.0644	0.005	0.4	34	51	293	0.18	605	7	613	20	643	95	98	
PB -50	26.1	0.8201	0.0765	0.0988	0.0022	0.03	10.1264	0.2255	0.0602	0.0064	0.4466	0.0243	1.0	12	89	75	1.19	607	13	608	44	612	234	99	
PB -50	82.1	0.8435	0.0578	0.0993	0.0018	0.16	10.0712	0.1787	0.0616	0.0046	0.0656	0.0279	2.7	13	20	113	0.18	610	10	621	32	661	161	98	
PB -50	27.1	0.7751	0.0894	0.1016	0.0024	0.19	9.8404	0.2365	0.0553	0.0075	0.2833	0.0286	0.2	9	47	57	0.83	624	14	583	48	425	271	107	
PB -50	5.1	0.8719	0.0456	0.1043	0.0012	0.14	9.5832	0.1102	0.0606	0.0034	0.0479	0.0125	0.8	17	17	142	0.12	640	7	637	25	625	120	100	
PB -50	80.1	0.8904	0.039	0.1052	0.0013	0.6	9.509	0.1194	0.0614	0.0027	0.0768	0.0065	0.3	34	68	271	0.25	645	8	647	21	653	96	99	
PB -50	6.1	0.9385	0.0519	0.1091	0.0014	0.59	9.1623	0.1152	0.0624	0.0036	0.2116	0.0137	0.0	19	104	130	0.80	668	8	672	28	687	143	99	
PB -50	78.1	0.9184	0.066	0.1097	0.002	0.24	9.1173	0.169	0.0607	0.0048	0.0286	0.0127	0.5	13	12	96	0.12	671	12	662	35	630	165	101	
PB -50	39.1	0.9075	0.0841	0.1099	0.0029	0.37	9.1009	0.238	0.0599	0.006	0.1911	0.0259	1.8	10	33	69	0.47	672	17	656	44	600	204	102	
PB -50	31.1	0.969	0.0741	0.1105	0.0022	0.38	9.0481	0.1801	0.0636	0.0054	0.1032	0.0172	0.7	12	35	79	0.44	676	13	688	39	728	196	98	
PB -50	91.1	0.9645	0.0323	0.1105	0.001	0.42	9.0468	0.0851	0.0633	0.0022	0.074	0.0041	0.1	54	100	406	0.25	676	6	686	17	718	75	98	
PB -50	85.1	0.9409	0.0719	0.1136	0.0019	0.05	8.8025	0.1487	0.0601	0.0051	0.0782	0.0183	0.4	13	26	101	0.25	694	11	673	37	606	179	103	
PB -50	87.1	1.0351	0.0512	0.1174	0.0015	0.04	8.5197	0.1055	0.064	0.0034	0.0973	0.0104	0.4	25	52	178	0.30	715	8	722	25	740	110	99	
PB -50	48.1	1.0634	0.1011	0.119	0.0033	0.16	8.4052	0.2318	0.0648	0.0072	0.129	0.0282	0.6	9	16	56	0.29	725	19	736	51	769	227	98	
PB -50	1.1	1.0508	0.0718	0.1195	0.0017	0.36	8.3713	0.1217	0.0638	0.0047	0.4082	0.0205	0.6	15	70	77	0.91	727	10	729	36	735	162	99	

PB -50	89.1	1.0665	0.1072	0.1199	0.0027	0.87	8.3432	0.1859	0.0645	0.0076	0.1489	0.023	3.0	9	26	53	0.49	730	16	737	53	759	246	99	
PB -50	65.1	1.102	0.0732	0.1235	0.002	0.33	8.0961	0.1338	0.0647	0.0048	0.2218	0.0118	0.7	15	65	91	0.71	751	12	754	35	765	153	99	
PB -50	30.1	1.1186	0.0927	0.125	0.0027	0.61	8.0009	0.1705	0.0649	0.0061	0.221	0.0204	0.5	10	32	58	0.56	759	15	762	45	772	207	99	
PB -50	33.1	1.3442	0.3016	0.1286	0.0075	0.3	7.7745	0.4537	0.0758	0.0198	0.192	0.0648	3.0	3	8	17	0.45	780	43	865	132	1090	529	90	
PB -50	62.1	1.1041	0.1325	0.1336	0.0033	0.45	7.4834	0.1876	0.0599	0.0083	0.2002	0.0279	3.1	8	31	44	0.70	809	19	755	60	601	266	107	
PB -50	19.1	1.4115	0.0906	0.148	0.0022	0.01	6.7588	0.1022	0.0692	0.0048	0.1156	0.0136	0.6	17	30	89	0.34	890	13	894	38	904	147	99	
PB -50	17.1	1.3752	0.063	0.1506	0.0018	0.61	6.638	0.0787	0.0662	0.0032	0.1347	0.0065	0.2	42	66	209	0.31	905	10	878	27	813	102	102	
PB -50	57.1	1.4829	0.0444	0.153	0.0023	0.61	6.5341	0.0975	0.0703	0.0019	0.0997	0.0042	0.1	67	99	351	0.28	918	13	923	18	936	57	99	
PB -50	34.1	1.5961	0.2026	0.1559	0.0054	0.01	6.4134	0.2212	0.0742	0.0107	0.1608	0.042	0.6	5	10	26	0.37	934	30	969	77	1048	289	96	
PB -50	15.1	1.4467	0.0981	0.156	0.0024	0.52	6.412	0.0974	0.0673	0.0051	0.2041	0.0153	1.6	18	59	88	0.67	934	13	909	41	846	152	102	
PB -50	4.1	1.5504	0.1222	0.1561	0.0028	0.39	6.4048	0.1146	0.072	0.0061	0.1906	0.0193	3.8	9	22	46	0.48	935	16	951	49	987	181	98	
PB -50	95.1	1.6135	0.0562	0.1616	0.0016	0.38	6.1891	0.0614	0.0724	0.0025	0.1117	0.0044	0.3	47	86	229	0.38	966	9	976	21	998	70	98	
PB -50	7.1	1.6418	0.1271	0.1624	0.0028	0.59	6.1585	0.1071	0.0733	0.0063	0.1082	0.0246	2.1	9	13	45	0.29	970	16	986	50	1023	181	98	
PB -50	69.1	1.6786	0.0697	0.167	0.002	0.56	5.9884	0.0724	0.0729	0.0032	0.2376	0.0127	0.5	34	106	149	0.71	996	11	1001	26	1011	90	99	
PB -50	66.1	1.7343	0.1043	0.1698	0.0028	0.23	5.8897	0.0965	0.0741	0.005	0.1193	0.0107	1.9	16	30	68	0.44	1011	15	1021	39	1044	135	98	
PB -50	68.1	1.7239	0.0945	0.1719	0.0026	0.67	5.8185	0.0875	0.0727	0.0044	0.2998	0.0143	0.6	21	72	86	0.84	1022	14	1018	35	1007	122	100	
PB -50	32.1	1.7511	0.0682	0.1722	0.0021	0.34	5.8056	0.0711	0.0737	0.0031	0.0842	0.0066	0.3	32	30	150	0.20	1025	12	1028	25	1034	85	99	
PB -50	70.1	1.7056	0.1925	0.174	0.0048	0.46	5.7461	0.1588	0.0711	0.0095	0.2128	0.0339	0.6	6	16	28	0.56	1034	26	1011	72	960	254	102	
PB -50	14.1	1.773	0.0952	0.1748	0.0024	0.69	5.7209	0.0784	0.0736	0.0043	0.2099	0.0106	0.4	24	54	98	0.55	1039	13	1036	35	1030	119	100	
PB -50	10.1	1.7825	0.116	0.1806	0.0027	0.78	5.5376	0.0837	0.0716	0.0049	0.2211	0.0272	0.3	18	41	69	0.60	1070	15	1039	41	974	136	102	
PB -50	37.1	1.8607	0.1164	0.1822	0.0041	0.63	5.4897	0.1235	0.0741	0.005	0.2328	0.0117	4.7	14	37	58	0.64	1079	22	1067	41	1044	134	101	
PB -50	45.1	4.2154	0.1229	0.2888	0.0044	0.87	3.4632	0.0528	0.1059	0.003	0.196	0.0056	0.3	51	102	121	0.84	1635	22	1677	24	1730	52	97	
PB -50	16.1	3.9351	0.2417	0.2902	0.0051	0.71	3.4455	0.0601	0.0983	0.0067	0.2698	0.0152	0.5	20	37	44	0.84	1643	25	1621	50	1593	126	101	
PB -50	24.1	3.9459	0.1232	0.3001	0.0031	0.82	3.3326	0.034	0.0954	0.0031	0.2241	0.0058	0.1	82	123	192	0.64	1692	15	1623	25	1536	60	104	
PB -50	71.1	4.4848	0.1496	0.3013	0.0035	0.53	3.3185	0.0385	0.1079	0.0038	0.158	0.0074	0.0	39	49	95	0.51	1698	17	1728	28	1765	65	98	
PB -50	25.1	4.2837	0.4935	0.3062	0.0125	0.5	3.266	0.1335	0.1015	0.0136	0.4448	0.0368	0.6	6	13	12	1.11	1722	61	1690	90	1651	243	101	
PB -50	84.1	4.4621	0.2034	0.3069	0.005	0.22	3.2586	0.0536	0.1055	0.0052	0.2026	0.0161	0.7	22	34	52	0.66	1725	25	1724	38	1722	89	100	
PB -50	44.1	4.4476	0.1237	0.3101	0.0046	0.96	3.2243	0.0477	0.104	0.0027	0.0869	0.009	1.0	50	56	156	0.36	1741	22	1721	23	1697	48	101	
PB -50	12.1	4.7831	0.1481	0.3277	0.0033	0.3	3.0517	0.031	0.1059	0.0035	0.2832	0.0074	0.0	34	55	71	0.77	1827	16	1782	27	1729	61	102	
PB -50	74.1	5.7254	0.1559	0.3283	0.0033	0.52	3.0463	0.0302	0.1265	0.0032	0.1596	0.0102	0.1	70	70	162	0.43	1830	16	1935	24	2050	46	94	
PB -50	59.1	6.0072	0.1674	0.3477	0.0052	0.32	2.8762	0.0427	0.1253	0.0031	0.1142	0.0022	0.0	88	67	194	0.34	1924	25	1977	24	2033	43	97	
PB -50	21.1	5.8431	0.1998	0.3543	0.0041	0.77	2.8223	0.033	0.1196	0.0042	0.2536	0.01	0.1	45	60	81	0.75	1955	20	1953	30	1950	64	100	
PB -50	76.1	6.5197	0.2045	0.3562	0.0042	0.77	2.8075	0.0335	0.1328	0.0042	0.0712	0.0141	0.1	34	23	75	0.31	1964	20	2049	28	2135	55	95	
PB -50	67.1	6.11	0.2115	0.3586	0.0045	0.5	2.789	0.0353	0.1236	0.0047	0.3309	0.0074	0.3	36	69	63	1.10	1975	22	1992	30	2009	66	99	
PB -50	77.1	6.2769	0.1894	0.3633	0.0041	0.52	2.7529	0.0308	0.1253	0.0037	0.1532	0.0157	0.2	45	43	93	0.46	1998	19	2015	26	2033	53	99	
PB -50	47.1	6.8446	0.1643	0.367	0.0051	0.25	2.7251	0.0376	0.1353	0.0029	0.1331	0.0032	0.1	55	41	114	0.36	2015	24	2092	22	2168	39	96	
PB -50	54.1	6.6125	0.246	0.3698	0.0072	0.65	2.704	0.0528	0.1297	0.0048	0.1384	0.0117	0.8	20	16	40	0.40	2029	34	2061	33	2094	64	98	
PB -50	28.1	6.4131	0.1616	0.3828	0.0038	0.95	2.6126	0.0259	0.1215	0.0033	0.1108	0.0147	0.2	124	120	238	0.50	2089	18	2034	23	1979	48	102	
PB -50	35.1	6.8175	0.4006	0.3831	0.0095	0.59	2.61	0.0644	0.1291	0.0087	0.2835	0.0424	0.6	12	13	20	0.63	2091	44	2088	51	2085	117	100	
PB -50	53.1	6.9366	0.3289	0.3865	0.0096	0.39	2.5872	0.0642	0.1302	0.0065	0.2321	0.0191	1.3	11	13	20	0.66	2107	45	2103	43	2100	90	100	
PB -50	18.1	7.3265	0.2258	0.3976	0.0044	0.67	2.515	0.0276	0.1336	0.0042	0.1752	0.0058	0.3	54	42	93	0.45	2158	20	2152	28	2146	56	100	
PB -50	49.1	7.5117	0.2652	0.3982	0.0075	0.49	2.5112	0.047	0.1368	0.0047	0.2074	0.0084	1.2	22	25	39	0.62	2161	34	2174	32	2187	59	99	
PB -50	13.1	7.7455	0.2156	0.4119	0.0041	0.89	2.4277	0.0243	0.1364	0.0038	0.1915	0.0065	0.0	92	96	151	0.63	2224	19	2202	25	2182	49	100	
PB -50	38.1	7.9045	0.2364	0.4197	0.0069	0.85	2.3828	0.0392	0.1366	0.0041	0.1539	0.0062	0.1	36	26	61	0.43	2259	31	2220	27	2185	52	101	
PB -50	50.1	9.14	0.297	0.4222	0.0075	0.81	2.3686	0.0423	0.157	0.0048	0.1941	0.0093	0.3	30	29	47	0.61	2270	34	2352	30	2424	51	96	
PB -50	3.1	11.6681	0.2651	0.4719	0.0041	0.46	2.1189	0.0184	0.1793	0.004	0.0662	0.0049	0.6	44	13	74	0.17	2492	18	2578	21	2647	37	96	
PB -50	56.1	10.9426	0.3091	0.4762	0.0075	0.51	2.0998	0.0329	0.1666	0.0043	0.1137	0.0036	0.3	55	33	84	0.39	2511	33	2518	26	2524	43	99	
PB -50	79.1	12.1615	0.354	0.4819	0.0057	0.33	2.0751	0.0243	0.183	0.0052	0.2847	0.0062	0.2	55	77	74	1.04	2536	25	2617	27	2681	47	96	
PB -50	94.1	14.387	0.3384	0.5203	0.0045	0.45	1.922	0.0166	0.2006	0.0045	0.2165	0.0086	0.1	76	78	96	0.81	2700	19	2776	23	2831	38	97	
PB -50	92.1	0.1152	0.0778	0.0244	0.0018	0.27	41.0267	3.0228	0.0343	0.0264	0.3048	0.1014	4.2	2	75	67	1.12	155	11	111	63	0	368	140	
PB -50	46.1	0.1471	0.0606	0.0247	0.0016	0.26	40.4132	2.5974	0.0431	0.021	0.2531	0.0704	4.9	3	42	76	0.56	158	10	139	52	0	471	113	
PB -50	36.1	0.7855	0.1279	0.0821	0.0033	0.08	12.1768	0.4917	0.0694	0.0131	0.394	0.0526	1.4	5	39	42	0.92	509	20	589	77	910	417	86	
PB -50	23.1	0.8191	0.164	0.0873	0.0033	0.29	11.4494	0.4287	0.068	0.0145	0.1334	0.0546	0.4	5	14	41	0.34	540	19	608	97	869	402	88	
PB -50	42.1	1.085	0.2111	0.0887	0.0057	0.45	11.2793	0.7292	0.0888	0.021	0.3618	0.0778	5.6	3	17	22	0.80	548	34	746	124	1399	544	73	
PB-51	6.1	0.7968	0.0441	0.0969	0.0016	0.4	10.3189	0.1655	0.0596	0.0037	0.2831	0.0108	0.04	15	65	107	0.61	596	9	595	25	590	136	100	
PB-51	5.1	0.8491	0.0591	0.0979	0.0019	0.45	10.2195	0.2031	0.0629	0.005	0.1081	0.0171	0.44	8	15	70	0.218	602	11	624	34	706	183	96	
PB-51	12.1	0.8078	0.0761	0.098	0.0024	0.01	10.1995	0.2481	0.0598	0.0064	0.0954	0.0292	1.06	6	8	46	0.179	603	14	601	43	595	214	100	
PB-51	3.1	0.7939	0.0409	0.099	0.0016	0.83	10.1025	0.1582	0.0582	0.0029	0.6492	0.0145	0.17	27	251	160	1.574	609	9	593	22	536	110	102	
PB-51	9.1	0.8679	0.0969	0.1014	0.0029	0.08	9.8659	0.2781	0.0621	0.008	0.1249	0.0226	1.36	5	9	36	0.25	622	17	634	50	678	259	98	
PB-51	7.1	0.8154	0.0377	0.1029	0.0014	0.53	9.7161	0.1361	0.0575	0.0028	0.28	0.0122	0.10	21	103	158	0.652	632	8	606	21	509	109	104	
PB-51	2.1	0.8322	0.0967	0.1032	0.003	0.49	9.6859	0.2772	0.0585	0.0074	0.7705	0.0281	0.28	9	95	49	1.953	633	17	615	53	547	233	103	

PB-51	13.1	0.8566	0.0434	0.1042	0.0013	0.09	9.6005	0.1171	0.0596	0.0032	0.0755	0.0116	1.35	19	24	156	0.153	639	7	628	24	591	111	101	
PB-51	8.1	0.8379	0.1168	0.1048	0.0036	0.25	9.5397	0.33	0.058	0.0091	0.2261	0.0508	0.54	6	20	39	0.516	643	21	618	76	529	289	103	
PB-51	18.1	1.6962	0.0829	0.165	0.0022	0.76	6.0597	0.0821	0.0745	0.0036	0.1388	0.01	0.71	12	17	53	0.312	985	12	1007	31	1056	103	97	
PB-51	23.2	1.876	0.1731	0.1677	0.0036	0.57	5.9632	0.128	0.0811	0.0082	0.135	0.0261	1.77	6	7	24	0.286	999	20	1073	64	1225	218	93	
PB-51	19.1	1.6686	0.085	0.1704	0.0023	0.34	5.8689	0.0793	0.071	0.0037	0.1958	0.0153	0.91	14	29	62	0.467	1014	13	997	32	958	105	101	
PB-51	23.1	1.6492	0.15	0.1566	0.0033	0.71	6.3862	0.1352	0.0764	0.0066	0.1357	0.0281	0.00	6	12	26	0.443	938	19	989	57	1105	194	94	
PB-51	14.1	0.7163	0.0328	0.0896	0.0011	0.65	11.1589	0.1319	0.058	0.0027	0.1516	0.0083	0.50	20	63	177	0.356	553	6	549	20	529	108	100	
PB-51	16.1	1.379	0.0701	0.1437	0.002	0.3	6.959	0.0947	0.0696	0.0036	0.0964	0.0091	0.23	13	16	71	0.228	866	11	880	30	917	110	98	
PB-51	21.1	2.6268	0.1154	0.2274	0.0031	0.57	4.398	0.0593	0.0838	0.0037	0.172	0.0107	1.14	18	40	57	0.705	1321	16	1308	32	1288	88	100	
PB-51	4.1	4.2484	0.1294	0.2827	0.0039	0.95	3.5376	0.0485	0.109	0.0036	0.1445	0.0075	0.44	19	22	49	0.443	1605	20	1683	26	1783	63	95	
PB-51	22.1	4.1759	0.1284	0.2974	0.0035	0.91	3.3628	0.0394	0.1018	0.0031	0.0651	0.0084	0.15	28	15	82	0.188	1678	17	1669	25	1658	56	100	
PB-51	10.1	5.0722	0.1645	0.3408	0.0049	0.66	2.9345	0.0419	0.108	0.0038	0.1931	0.0123	0.63	17	25	36	0.701	1890	24	1832	28	1765	65	103	
PB-51	17.1	5.2065	0.1083	0.3646	0.0034	0.51	2.7429	0.0258	0.1036	0.002	0.1327	0.0027	0.25	57	52	129	0.403	2004	16	1854	18	1689	34	108	
PB-51	20.1	6.3736	0.1461	0.3829	0.004	0.91	2.6119	0.0272	0.1207	0.0025	0.0469	0.0038	0.23	65	25	143	0.173	2090	18	2029	20	1967	37	103	
PB-51	11.1	6.9978	0.2272	0.3855	0.0061	0.17	2.5939	0.0411	0.1316	0.0046	0.1564	0.0097	0.50	14	11	27	0.395	2102	28	2111	29	2120	63	99	
PB-51	15.1	11.577	0.2605	0.4881	0.0054	0.01	2.0487	0.0226	0.172	0.0035	0.1221	0.0078	1.00	24	11	37	0.298	2563	23	2571	21	2577	35	99	
PB-51	1.1	1.2485	0.2457	0.1332	0.0067	0.79	7.5077	0.3794	0.068	0.0162	0.2738	0.0539	10.00	2	9	12	0.714	806	38	823	116	868	457	97	
PB-56	63.1	0.7993	0.0279	0.0945	0.0009	0.38	10.5841	0.1024	0.0614	0.0024	0.2057	0.0073	0.92	18.1	81.5	144.8	0.563	582	5.4	596.4	15.7	651.8	81.8	97	
PB-56	72.1	0.7711	0.0596	0.0945	0.0017	0.28	10.5835	0.1912	0.0592	0.0052	0.1799	0.026	0.51	6.8	27.1	55.2	0.49	582	10.1	580.4	34.3	573.9	182.2	100	
PB-56	91.1	0.8105	0.0533	0.0955	0.0017	0.77	10.4726	0.1882	0.0616	0.0041	0.1681	0.0093	1.14	14.2	69.1	112.5	0.614	587.9	10.1	602.8	30.4	659	143.6	97	
PB-56	64.1	0.8522	0.0404	0.0959	0.0012	0.06	10.4263	0.1322	0.0644	0.0034	0.1728	0.0166	1.12	10.7	48	83.3	0.576	590.4	7.2	625.9	22.2	756.2	122.4	94	
PB-56	78.1	0.829	0.0492	0.0963	0.0013	0.11	10.3852	0.1432	0.0624	0.0039	1.9323	0.0333	1.3	17	341.5	55.3	6.18	592.6	7.8	613.1	27.9	689.3	144.1	96	
PB-56	29.1	0.749	0.0495	0.0968	0.0011	0.45	10.333	0.1143	0.0561	0.0038	0.1674	0.0184	0.35	12.6	45.5	97.3	0.468	595.5	6.3	567.7	28.7	457.7	151.7	104	
PB-56	21.1	0.7861	0.0293	0.0977	0.0008	0.23	10.2306	0.0855	0.0583	0.0023	0.3587	0.0296	0.21	32	228.2	217.4	1.05	601.2	4.8	589	16.7	542.2	87.3	102	
PB-56	14.1	0.8024	0.0791	0.0978	0.0018	0.03	10.2257	0.1837	0.0595	0.0067	0.4329	0.0194	2.68	7.4	51.2	46.2	1.108	601.5	10.3	598.2	43.3	585.7	223.2	100	
PB-56	28.1	0.8564	0.0477	0.0981	0.001	0.64	10.1938	0.1087	0.0633	0.0038	0.1537	0.0138	0	11.5	38.5	91.3	0.422	603.3	6.2	628.2	28	719	144.9	96	
PB-56	46.1	0.8773	0.0522	0.0982	0.0012	0.19	10.181	0.1246	0.0648	0.0042	0.1259	0.0164	0.92	9.1	24.1	73.3	0.329	604	7	639.5	28.9	767.1	139.5	94	
PB-56	17.1	0.8497	0.0393	0.0988	0.001	0.14	10.1257	0.1024	0.0624	0.0031	0.148	0.0077	0.52	15.9	46.2	123.8	0.373	607.1	5.9	624.5	21.6	688	107.6	97	
PB-56	54.1	0.8323	0.0574	0.1003	0.0014	0.43	9.9739	0.1426	0.0602	0.0046	0.1783	0.0123	0.75	10.7	48.4	88.1	0.549	615.9	8.4	614.9	32.2	610.9	165.1	100	
PB-56	10.1	0.8991	0.0852	0.1044	0.0019	0.47	9.5782	0.1737	0.0625	0.0066	0.1423	0.0212	2.96	6.2	18.3	44.8	0.407	640.2	11.1	651.3	46.2	689.9	223.7	98	
PB-56	59.1	0.8722	0.141	0.0967	0.0031	0.24	10.3367	0.326	0.0654	0.0122	0.233	0.0408	3.63	4.8	22.1	38.1	0.58	595.3	17.9	636.8	76.5	786.9	395.9	93	
PB-56	38.1	0.9059	0.1982	0.1049	0.0036	0.53	9.5369	0.3284	0.0627	0.0154	0.3943	0.0545	4.5	2.3	15.4	15.2	1.011	642.8	21	654.9	103.5	696.7	468.4	98	
PB-56	85.1	0.9599	0.0556	0.1117	0.0019	0.46	8.9543	0.1555	0.0623	0.0035	0.1666	0.01	0.76	17	61.3	116	0.528	682.5	11.2	683.2	28.4	685.8	119.2	99	
PB-56	79.1	1.0563	0.0675	0.1129	0.0017	0.01	8.8592	0.1358	0.0679	0.0047	0.541	0.063	0.25	9.6	74.6	52	1.433	689.4	10	732	33.1	864.5	152.7	94	
PB-56	39.1	1.0171	0.0493	0.1159	0.0012	0.67	8.6277	0.0902	0.0636	0.0033	0.246	0.0118	0.78	16.4	66.3	100.1	0.663	707	7	712.5	25.1	729.9	110.3	99	
PB-56	35.1	1.0298	0.0472	0.1164	0.0011	0.91	8.5935	0.082	0.0642	0.0029	0.0645	0.0111	0.57	14.6	19.6	99.9	0.196	709.6	6.4	718.8	23.6	747.6	97.9	98	
PB-56	89.1	1.001	0.0661	0.1186	0.0021	0.39	8.4343	0.1524	0.0612	0.004	0.1349	0.0109	0.51	14.6	35.6	100.4	0.354	722.3	12.4	704.3	32.9	647.5	132.9	102	
PB-56	5.1	1.0804	0.0823	0.1212	0.0019	0.76	8.2518	0.1288	0.0647	0.0054	0.2685	0.0197	0.52	8.8	32.7	49	0.668	737.4	10.9	743.8	39.3	763.2	171	99	
PB-56	73.1	1.7363	0.0695	0.1695	0.0019	0.55	5.8997	0.067	0.0743	0.0031	0.1712	0.0103	0.26	12.7	32.5	55.4	0.586	1009	10.6	1022	26	1049	83.7	98	
PB-56	84.1	1.7369	0.0934	0.17	0.0025	0.17	5.8807	0.0869	0.0741	0.0042	0.2006	0.0185	0.98	9.1	24.2	39.2	0.619	1012	13.8	1022	35.4	1044	114.1	99	
PB-56	22.1	1.7725	0.0716	0.1705	0.0018	0.59	5.8661	0.0603	0.0754	0.0034	0.0679	0.0136	0.37	13.8	12.6	66.4	0.189	1015	9.7	1035	27.8	1080	98	97	
PB-56	57.1	1.7355	0.0415	0.1709	0.0012	0.16	5.8498	0.0411	0.0736	0.0019	0.1804	0.0038	0.51	39.5	94.1	175.5	0.536	1017	6.6	1022	15.3	1031	50.9	99	
PB-56	7.1	1.7136	0.0841	0.1718	0.002	0.01	5.8209	0.0687	0.0723	0.0038	0.3654	0.0434	1.81	9.9	29.3	39.2	0.746	1022	11.1	1014	30.8	995.7	104.2	100	
PB-56	11.1	1.7923	0.0975	0.1732	0.0023	0.48	5.7722	0.0766	0.075	0.0045	0.2359	0.0104	0.63	11.7	35.6	48.4	0.735	1030	12.6	1043	35.1	1069	117.1	98	
PB-56	45.1	1.8839	0.113	0.1758	0.0024	0.59	5.6886	0.0785	0.0777	0.0051	0.3229	0.0185	0.28	9.9	36.4	38.7	0.939	1044	13.3	1075	40.1	1140	131.8	97	
PB-56	55.1	1.8544	0.0623	0.1759	0.0016	0.63	5.6855	0.0527	0.0765	0.0028	0.1907	0.0059	0.19	20.8	51.4	85.9	0.599	1045	8.9	1065	22.2	1107	73.4	98	
PB-56	4.1	1.8709	0.0666	0.1795	0.0017	0.94	5.5704	0.0523	0.0756	0.0028	0.117	0.0226	1.05	13.4	17.4	60.1	0.29	1064	9.2	1071	23.8	1084	75.7	99	
PB-56	93.1	1.9321	0.1754	0.1827	0.0043	0.28	5.4749	0.1299	0.0767	0.0072	0.3732	0.0233	4.22	8.2	36.3	31.3	1.16	1081	23.6	1092	61.8	1114	197.3	99	
PB-56	92.1	1.7789	0.1266	0.167	0.0034	0.21	5.9863	0.1224	0.0772	0.0057	0.1376	0.0167	1.03	10.1	18.5	47.9	0.387	995.8	18.9	1038	46.6	1127	151.8	95	
PB-56	37.1	4.6481	0.1264	0.3117	0.0027	0.77	3.2084	0.0275	0.1082	0.0032	0.1872	0.0086	0.12	28.6	34.2	64.4	0.53	1749	13.2	1758	23	1769	52.9	99	
PB-56	3.1	4.7429	0.1788	0.313	0.0038	0.3	3.1947	0.0388	0.1099	0.0045	0.1859	0.0125	1.45	14.1	19.1	32.6	0.586	1756	18.6	1775	31.8	1798	75.3	98	
PB-56	94.1	4.7833	0.1939	0.3228	0.0055	0.01	3.0978	0.0524	0.1075	0.0041	0.1955	0.0056	1.42	23.6	52.3	53.7	0.974	1803	26.6	1782	33.8	1757	69.1	101	
PB-56	12.1	4.5104	0.1456	0.3017	0.0031	0.85	3.315	0.0345	0.1084	0.0037	0.2204	0.0097	0.63	18.5	28.9	45	0.642	1700	15.5	1733	26.4	1773	62.4	98	
PB-56	74.1	6.7858	0.4263	0.387	0.0097	0.26	2.5843	0.0648	0.1272	0.0086	0.5619	0.033	1.73	6.2	14.6	9	1.633	2109	45.1	2084	54.8	2059	114.5	101	
PB-56	44.1	6.8892	0.3143	0.3874	0.0059	0.33	2.5813	0.0395	0.129	0.0064	0.2905	0.0171	0.37	10.1	14.5	17.3	0.839	2111	27.6	2097	41.3	2084	89.3	100	
PB-56	88.1	6.7616	0.1959	0.39	0.0057	0.91	2.564	0.0374	0.1257	0.0032	0.105	0.005	0.66	69.9	57.6	146	0.394	2123	26.4	2081	26.1	2039	45.2	102	
PB-56	20.1	6.8319	0.1599	0.3909	0.0032	0.61	2.558	0.0208	0.1267	0.0031	0.2738	0.0132	0.91	32.5	44.4	56.1	0.791	2127	14.7	2090	21.2	2053	44.4	101	
PB-56	30.1	6.9238	0.1871	0.3911	0.0034	0.68	2.557	0.0221	0.1284	0.0035	0.2275	0.0082	0.28	22.8	33.9	40.9	0.828	2128	15.7	2102	23.8	2076	48.2	101	
PB-56	65.1	6.8142	0.117	0.3946	0.0026	0.62	2.5345	0.0169	0.1253	0.0022	0.134	0.0041	0.5	53.9	49.3	106.6	0.463	2144	12.2	2088	15.2	2032	31.1	102	
PB-56	9.1	1.1494	0.0858	0.1261	0.002	0.93	7.9303	0.1257	0.0661	0.0053	0.1228	0.0132	1.52	9.7	23.8	63.7	0.374	765.6	11.4	777	40.3	809.9	165.5	98	
PB-56	33.1	1.1525	0.0428	0.1296	0.0011	0.67	7.7146	0.0653	0.0645	0.0025	0.0519	0.0083	0.77	21.8	17.9	140.1	0.128	785.7	6.3	778.4	20.6	757.6	82.1	100	

PB-56	19.1	1.1688	0.0736	0.1304	0.0017	0.25	7.6714	0.1015	0.065	0.0045	0.1916	0.0141	0.41	10.1	30	56.3	0.533	789.9	9.8	786.1	34	775.4	141.9	100	
PB-56	87.1	1.3057	0.1102	0.1452	0.003	0.37	6.8858	0.1437	0.0652	0.0056	0.1827	0.0142	2.42	8.8	25.6	45.9	0.557	874.2	17.1	848.2	48.6	781.1	179.5	103	
PB-56	32.1	0.9788	0.0629	0.1109	0.0013	0.55	9.0157	0.1046	0.064	0.0043	0.2743	0.0141	0.3	12.3	60.2	80.6	0.748	678.1	7.4	693	31.6	741.6	145	97	
PB-56	96.1	0.9058	0.0391	0.1077	0.0017	0.58	9.2815	0.1459	0.061	0.0024	0.1345	0.1074	1.23	39.6	352.8	257.9	1.368	659.6	9.8	654.8	20.8	638.3	88.6	100	
PB-56	56.1	0.7217	0.0229	0.087	0.0007	0.01	11.4993	0.0909	0.0602	0.002	0.1371	0.0101	0.71	24.7	90.7	227.7	0.398	537.5	4.1	551.7	13.5	610.4	73.4	97	
PB-56	86.1	0.6644	0.0342	0.0818	0.0014	0.94	12.2265	0.2077	0.0589	0.0028	0.1789	0.0096	1.72	36.7	153.6	282.3	0.544	506.8	8.3	517.3	20.9	563.9	104.6	97	
PB-56	50.1	0.5973	0.04	0.0744	0.001	0.53	13.4456	0.1788	0.0582	0.0043	0.1749	0.0105	2.62	9.6	50.8	100.4	0.506	462.5	5.9	475.5	24.5	539.1	158.6	97	
PB-56	71.1	0.9075	0.0414	0.1038	0.0013	0.84	9.6343	0.1169	0.0634	0.0033	0.1244	0.0176	1.32	12.8	36.4	108.5	0.335	636.6	7.4	655.7	22.2	722.1	109.4	97	
PB-56	66.1	0.9309	0.0364	0.1053	0.0011	0.4	9.4964	0.1026	0.0641	0.0028	0.1595	0.0121	0.32	14.7	46.2	105.8	0.436	645.4	6.6	668.1	19.4	745.5	94.7	96	
PB-56	81.1	0.9636	0.0686	0.1074	0.0018	0.44	9.3108	0.1522	0.0651	0.0051	0.192	0.0244	2.28	5.9	22.4	41.1	0.545	657.6	10.2	685.2	37	776.6	167.9	95	
PB-56	48.1	0.7711	0.0441	0.0912	0.001	0.01	10.9652	0.1254	0.0613	0.0038	0.1675	0.0127	0.68	9.9	40.4	80.9	0.5	562.6	6.2	580.4	25.4	650.7	138.6	96	
PB-56	31.1	0.603	0.0405	0.0792	0.0009	0.41	12.6306	0.1393	0.0552	0.0039	0.1423	0.0195	0.3	10	51.4	95.3	0.539	491.2	5.2	479.2	25.5	422	153	102	
PB-56	41.1	1.9501	0.1257	0.1908	0.0027	0.4	5.2415	0.0737	0.0741	0.0052	0.428	0.0141	1.09	12.1	47.1	40	1.179	1126	14.5	1099	41.9	1045	134.1	102	
PB-56	27.1	1.6711	0.0889	0.1619	0.0018	0.14	6.1768	0.0679	0.0749	0.0042	0.1584	0.0145	2.57	10.5	20.9	50.1	0.418	967.3	9.9	997.6	33	1065	107.2	96	
PB-56	67.1	1.9038	0.1114	0.1859	0.0032	0.48	5.3791	0.0913	0.0743	0.0052	0.1876	0.0148	0.05	6	14.3	23.4	0.608	1099	17.1	1082	40.1	1049	144.8	101	
PB-56	47.1	1.8942	0.0592	0.185	0.0015	0.35	5.4058	0.0443	0.0743	0.0025	0.2342	0.0073	0.56	28.7	83.9	112.8	0.744	1094	8.3	1079	20.8	1049	67	101	
PB-56	40.1	1.9127	0.1069	0.1841	0.0023	0.01	5.4315	0.0686	0.0753	0.0046	0.1486	0.0121	0.9	9.8	15.8	40.5	0.39	1089	12.7	1086	36.5	1078	117.2	100	
PB-56	80.1	1.9676	0.0953	0.1828	0.0025	0.49	5.47	0.0758	0.0781	0.004	0.3123	0.0223	0.8	9.6	31.1	36.7	0.847	1082	13.8	1105	33.8	1148	105.3	97	
PB-56	58.1	1.5829	0.0542	0.1603	0.0015	0.63	6.2375	0.0567	0.0716	0.0027	0.3006	0.0488	0.21	23.8	89.1	102.1	0.873	958.6	8.1	963.5	21.4	974.9	76.5	99	
PB-56	8.1	1.5926	0.196	0.1626	0.0041	0.47	6.1483	0.1563	0.071	0.0098	0.2154	0.0343	3.04	4.5	10.3	18.7	0.549	971.5	22.9	967.3	75.8	957.9	270.2	100	
PB-56	53.1	1.8916	0.071	0.1815	0.0018	0.75	5.5111	0.0551	0.0756	0.0031	0.2185	0.0076	2.24	18.8	56.2	77.4	0.726	1075	9.9	1078	24.7	1085	80.7	99	
PB-56	76.1	2.059	0.0659	0.1953	0.0019	0.7	5.1201	0.0502	0.0765	0.0024	0.1346	0.0081	1.42	18.9	36.6	77.2	0.474	1150	10.3	1135	21.5	1107	62.4	101	
PB-56	2.1	2.904	0.2839	0.2376	0.0061	0.44	4.2096	0.1087	0.0887	0.0099	0.2808	0.0447	1.31	5	11.5	13.9	0.827	1374	32	1383	74.6	1397	222.9	99	
PB-56	62.1	2.7398	0.0694	0.2409	0.002	0.95	4.1507	0.0351	0.0825	0.0023	0.153	0.0206	2.07	20	28.2	78.2	0.361	1392	10.6	1339	18.9	1257	55.9	103	
PB-56	75.1	3.9162	0.1864	0.2823	0.0044	0.31	3.5427	0.0555	0.1006	0.005	0.2416	0.014	0.52	7.2	12.8	18.1	0.706	1603	22.2	1617	36.7	1636	89	99	
PB-56	25.1	3.9114	0.081	0.2878	0.0019	0.53	3.4746	0.0233	0.0986	0.002	0.055	0.0037	0.87	43.2	22.3	119	0.187	1631	9.7	1616	16.8	1597	37.9	100	
PB-56	69.1	5.6619	0.1447	0.3513	0.0036	0.2	2.8465	0.0288	0.1169	0.0033	0.1775	0.0088	1.54	15.9	18.8	31.6	0.596	1941	16.9	1926	21.9	1909	50.2	100	
PB-56	77.1	5.1289	0.1315	0.3385	0.0032	0.8	2.9541	0.0281	0.1099	0.0027	0.275	0.0064	0.27	26.9	50.1	56.1	0.893	1880	15.5	1841	21.7	1798	44.7	102	
PB-56	82.1	5.2158	0.1715	0.3317	0.004	0.11	3.0151	0.0366	0.1141	0.0038	0.2766	0.0105	0.44	13.2	24	26.7	0.899	1846	19.4	1855	27.5	1865	58.4	99	
PB-56	90.1	5.4249	0.1867	0.3471	0.0055	0.85	2.8811	0.046	0.1134	0.0034	0.3438	0.0065	0.14	45.9	93.8	87.9	1.067	1921	26.4	1889	28.4	1854	52.9	101	
PB-56	26.1	6.233	0.1789	0.3612	0.0032	0.8	2.7687	0.0246	0.1252	0.0037	0.2878	0.0068	0.28	20.5	37	37.4	0.99	1988	15.2	2009	25.1	2031	52	98	
PB-56	70.1	6.2709	0.1425	0.3631	0.0033	0.19	2.754	0.0252	0.1253	0.0031	0.2183	0.0058	0.22	20.8	32.7	40.8	0.802	1997	15.7	2014	20	2032	44.1	99	
PB-56	23.1	0.2845	0.0215	0.0386	0.0005	0.21	25.8798	0.3467	0.0534	0.0044	0.1882	0.0119	1.07	10	107.9	192.3	0.561	244.4	3.2	254.2	17.1	346	182.1	96	
PB-56	52.1	0.2915	0.0164	0.0406	0.0005	0.62	24.6298	0.2731	0.0521	0.0031	0.1649	0.013	0.11	17.6	145.2	339.7	0.427	256.6	2.8	259.8	12.8	288.7	136.9	98	
PB-56	51.1	0.3459	0.0692	0.0458	0.0015	0.01	21.8418	0.7226	0.0548	0.0117	0.2802	0.0413	1.56	3.5	44.4	52.6	0.844	288.6	9.3	301.6	51.2	403.8	399.7	95	
PB-56	15.1	0.1819	0.0501	0.0294	0.001	0.06	34.019	1.1778	0.0449	0.0136	0.2217	0.0546	4.54	2.6	33.7	64.8	0.52	186.8	6.4	169.7	42	0	349.8	110	
PB-56	24.1	9.141	0.2567	0.4345	0.0047	0.4	2.3013	0.0249	0.1526	0.0047	0.2015	0.0077	0.14	19.6	18.6	31.8	0.586	2326	21.2	2352	26.6	2375	53.8	98	
PB-56	68.1	10.9663	0.2156	0.4589	0.0039	0.67	2.1789	0.0187	0.1733	0.0037	0.2698	0.0082	0.68	34.9	48.6	50.6	0.961	2435	17.5	2520	18.2	2590	34.8	96	
PB-56	49.1	10.8639	0.2162	0.4939	0.0039	0.71	2.0245	0.0161	0.1595	0.0033	0.142	0.0037	0.18	37.9	25.7	58.1	0.443	2588	16.9	2512	18.4	2451	35.2	103	
PB-56	13.1	13.4463	0.3248	0.5317	0.0052	0.86	1.8807	0.0184	0.1834	0.0047	0.1632	0.0077	0.28	23.1	14	29.7	0.471	2749	21.9	2712	22.8	2684	42.3	101	
PB-56	18.1	16.9465	0.3467	0.5958	0.0049	0.61	1.6785	0.0139	0.2063	0.0043	0.1632	0.0068	0.78	36.5	26.7	41.7	0.639	3013	20	2932	19.7	2877	34	102	
PB-56	1.1	8.3925	0.3143	0.4356	0.0062	0.71	2.2959	0.0329	0.1397	0.0053	0.2666	0.0183	0.22	15.7	21.3	24.7	0.861	2331	27.5	2274	33	2224	68.3	102	
PB-56	95.1	7.3518	0.2721	0.3912	0.0067	0.04	2.5566	0.0437	0.1363	0.0048	0.146	0.0069	0.75	23.2	20.2	44.5	0.455	2128	30.9	2155	33.3	2181	60.2	98	
PB-56	83.1	7.1166	0.1358	0.3828	0.0029	0.67	2.6125	0.0195	0.1348	0.0023	0.1367	0.0042	0.22	56.1	53.7	107.6	0.499	2089	13.4	2126	17	2162	30	98	
PB-56	34.1	7.9599	0.2743	0.4212	0.0046	0.85	2.3742	0.026	0.1371	0.0046	0.2021	0.0117	1.22	15.6	16.8	26.5	0.636	2266	20.6	2227	29.3	2190	57.6	101	
PB-56	60.1	0.3394	0.0284	0.0419	0.0007	0.32	23.8612	0.386	0.0587	0.0053	0.2925	0.0351	4.77	9.3	142.2	155.6	0.914	264.7	4.2	296.7	21.3	557.4	197.1	89	
PB-56	61.1	0.883	0.0754	0.0891	0.002	0.14	11.2216	0.2553	0.0719	0.0072	0.2197	0.0396	2.6	4.9	21.1	41.2	0.512	550.3	12	642.6	40.9	982.2	221.8	85	
PB-56	36.1	0.9914	0.0942	0.1011	0.0017	0.69	9.8942	0.1621	0.0711	0.0072	0.02	0.0219	1.6	4.6	0.2	38.4	0.006	620.7	9.7	699.4	49	961.5	233.1	88	
PB-56	16.1	0.998	0.1897	0.1024	0.0039	0.31	9.7622	0.3708	0.0707	0.015	0.2392	0.044	2.03	2.4	10.2	16.9	0.601	628.7	22.6	702.8	95.8	947.6	459.8	89	
PB-56	43.1	1.0164	0.098	0.1043	0.0019	0.17	9.5913	0.1746	0.0707	0.0077	0.1404	0.0252	1.27	5	17	37.5	0.452	639.3	11.1	712.1	48.4	948.9	227.2	89	
PB-56	42.1	0.3126	0.0503	0.0462	0.001	0.36	21.642	0.4597	0.0491	0.0089	0.1431	0.0317	7.52	3.9	29.6	66.1	0.448	291.2	6.1	276.2	38.3	151.2	279.7	105	
PB-56	6.1	13.7601	0.5494	0.5246	0.0097	0.13	1.9062	0.0354	0.1902	0.0083	0.3843	0.0222	11.89	9.9	13	11.2	1.167	2719	41.3	2733	38.6	2744	76.2	99	
PB -59	48.1	0.6209	0.0715	0.0805	0.0017	0.68	12.4197	0.257	0.0559	0.0068	0.2963	0.0337	1.37	10.5	91.5	87.2	1.048	499.2	9.9	490.4	42.3	449.5	229	101	
PB -59	81.1	0.7037	0.0754	0.0824	0.0018	0.33	12.1331	0.2668	0.0619	0.0073	0.2338	0.0309	2.35	7.3	60.4	62	0.973	510.5	10.8	541	47.1	671.6	261.6	94	
PB -59	49.1	0.6544	0.0476	0.0827	0.0015	0.38	12.0974	0.225	0.0574	0.0046	0.163	0.0462	4.58	12.1	81.3	113.8	0.714	512	9.2	511.2	29.2	507.4	173.5	100	
PB -59	84.1	0.7135	0.0359	0.0834	0.001	0.41	11.9939	0.1488	0.0621	0.0033	0.7111	0.0473	0.64	20.4	239.9	148.7	1.613	516.2	6.1	546.8	21.9	676.3	128.1	94	
PB -59	85.1	0.6957	0.0541	0.084	0.0013	0.65	11.9092	0.185	0.0601	0.0052	0.2348	0.0113	2.55	10.4	76.5	94	0.814	519.8	7.8	536.2	32.6	606.9	191.4	96	
PB -59	30.1	0.6888	0.0394	0.0841	0.0012	0.45	11.8874	0.1668	0.0594	0.0037	0.2258	0.0172	1.1	12.8	61	110.4	0.552	520.7	7	532.1	23.7	581.2	138.4	97	
PB -59	5.1	0.6364	0.0934	0.0853	0.0018	0.69	11.7176	0.2516	0.0541	0.0085	0.1283	0.0365	2.24	5.4	17.2	49.7	0.347	527.9	10.9	500.1	55.9	374.5	315.1	105	
PB -59	80.1	0.7087	0.0473	0.0867	0.0013	0.66	11.5326	0.1677	0.0593	0.0042	0.1958	0.0131	2.28	13.2	81.7	119.2	0.686	536.1	7.5	543.9	27.7	577.2	155.9	98	
PB -59	51.1	0.7936	0.0455	0.0995	0.0016	0.36	10.0481	0.1627	0.0578	0.0036	0.2786	0.0226	0.8	15.9	85.2	117.9	0.722	611.6	9.4	593.2	25.5	523.6	130.7	103	

PB -59	32.1	0.8679	0.0521	0.1004	0.0015	0.13	9.9651	0.1523	0.0627	0.0041	0.288	0.0427	1.98	10.1	51.7	74.7	0.693	616.5	9	634.4	28.8	699	154.9	97	
PB -59	76.1	0.8446	0.0643	0.101	0.0017	0.48	9.9027	0.166	0.0607	0.005	0.2205	0.0213	1.34	15.2	93.1	113	0.823	620.2	9.9	621.7	37.2	627.1	177.1	99	
PB -59	26.1	0.8806	0.0391	0.1012	0.0012	0.03	9.8814	0.1163	0.0631	0.003	0.2083	0.01	0.34	16.4	70	122.5	0.571	621.4	7	641.3	21.1	712	100.1	96	
PB -59	3.1	0.8317	0.0901	0.103	0.0018	0.5	9.7128	0.1718	0.0586	0.0069	0.4081	0.0296	2.08	8.5	62	52.9	1.171	631.7	10.6	614.6	48.7	552	246.8	102	
PB -59	54.1	0.8989	0.0636	0.1033	0.002	0.3	9.6799	0.1899	0.0631	0.0048	0.0181	0.0149	0.45	10.8	3.3	91.3	0.036	633.8	11.8	651.1	34.9	711.8	172.6	97	
PB -59	1.1	0.9331	0.1004	0.1048	0.002	0.42	9.5382	0.1827	0.0646	0.0075	0.1765	0.0321	1.29	5.9	18.3	42.8	0.427	642.7	11.7	669.3	54	759.7	262.1	96	
PB -59	18.1	0.8777	0.0377	0.1059	0.001	0.06	9.442	0.0933	0.0601	0.0027	0.1406	0.0092	0.67	36	90.5	263.4	0.344	648.9	6.1	639.8	20.3	607.5	92.7	101	
PB -59	52.1	0.889	0.0467	0.1061	0.0017	0.13	9.4225	0.1476	0.0607	0.0034	0.091	0.009	0.71	16.6	39.9	128.7	0.31	650.2	9.7	645.8	25.1	630.4	121.8	100	
PB -59	19.1	0.9314	0.0378	0.1068	0.001	0.16	9.3649	0.0917	0.0633	0.0026	0.2858	0.006	0.18	41.7	210	271.2	0.774	654	6.1	668.4	19.9	717.1	89	97	
PB -59	42.1	0.8864	0.06	0.1082	0.0017	0.53	9.2457	0.1426	0.0594	0.0041	0.2773	0.0119	0.94	16.2	83.6	109.9	0.76	662	9.7	644.4	31.5	583.3	143.6	102	
PB -59	70.1	0.8917	0.0343	0.1083	0.0012	0.79	9.2355	0.1065	0.0597	0.0025	0.1562	0.0069	0.82	35.6	141.8	254.5	0.557	662.7	7.3	647.3	18.5	593.7	90.7	102	
PB -59	20.1	0.9773	0.1056	0.1096	0.0022	0.01	9.1214	0.1793	0.0647	0.0076	0.7531	0.0241	0.29	13.3	117.8	62.4	1.887	670.6	12.5	692.2	54.4	763.1	254.3	96	
PB -59	71.1	0.9616	0.0514	0.1107	0.0016	0.6	9.034	0.1328	0.063	0.0037	0.2896	0.012	0.28	15.6	87.3	97.8	0.892	676.8	9.4	684.1	26.2	708.4	121.8	98	
PB -59	29.1	1.0144	0.0752	0.1118	0.0021	0.44	8.9416	0.169	0.0658	0.0055	0.5637	0.0351	0.59	9.4	75.3	49.2	1.53	683.4	12.3	711.1	39.3	799.6	179.3	96	
PB -59	79.1	0.9516	0.0535	0.1143	0.0015	0.01	8.7516	0.1135	0.0604	0.0037	0.2082	0.0207	1.3	15	94.2	105.4	0.894	697.5	8.6	678.9	28.2	618	131.2	102	
PB -59	69.1	0.9644	0.0387	0.1147	0.0014	0.54	8.7149	0.1044	0.061	0.0026	0.1278	0.0102	0.29	31	102.7	228	0.45	700.2	7.9	685.5	20.1	637.6	93.6	102	
PB -59	21.1	1.4648	0.1601	0.1606	0.0033	0.63	6.226	0.1272	0.0661	0.008	0.0814	0.025	0.98	7.3	10.9	35.2	0.309	960.2	18.2	916	67	810.9	242.6	104	
PB -59	15.1	1.6835	0.0993	0.163	0.0022	0.81	6.1332	0.082	0.0749	0.0047	0.1393	0.0171	0.57	17.6	31.2	82.9	0.377	973.7	12.1	1002	36.6	1065	124.5	97	
PB -59	12.1	1.6454	0.1218	0.1636	0.0025	0.59	6.1128	0.0926	0.0729	0.0059	0.1763	0.0144	1.07	10.4	23	47.4	0.484	976.7	13.7	987.8	47.8	1012	175.5	98	
PB -59	65.1	1.6934	0.0493	0.1686	0.0017	0.93	5.9319	0.0613	0.0729	0.0022	0.0932	0.0074	0.21	43	61.1	204.6	0.298	1004	9.6	1006	18.2	1010	60.1	99	
PB -59	23.1	1.7197	0.0707	0.1694	0.0018	0.55	5.9039	0.0617	0.0736	0.0031	0.2373	0.0169	1.27	25.8	90.7	109.7	0.826	1009	9.8	1016	26.7	1032	87.9	99	
PB -59	88.1	1.9574	0.1682	0.1796	0.0036	0.7	5.5694	0.1112	0.0791	0.0075	0.1329	0.0214	2.96	6.1	12.2	28.6	0.427	1065	19.6	1101	58.6	1174	196.6	96	
PB -59	90.1	1.8695	0.0613	0.1825	0.0019	0.94	5.4804	0.0572	0.0743	0.0026	0.3078	0.073	0	36.9	110.3	144.9	0.761	1081	10.4	1070	22.3	1050	72.9	100	
PB -59	61.1	1.8585	0.0536	0.1841	0.0019	0.85	5.4321	0.056	0.0732	0.0022	0.0369	0.0061	0.51	42.5	34.5	187.3	0.184	1089	10.3	1066	19.1	1020	62.7	102	
PB -59	46.1	4.3366	0.0963	0.2998	0.0029	0.97	3.3352	0.0319	0.1049	0.0022	0.2453	0.033	0.21	62.4	111.1	154.7	0.718	1691	14.3	1700	18.6	1713	38.4	99	
PB -59	92.1	4.5238	0.1116	0.3067	0.003	0.83	3.2609	0.0316	0.107	0.0028	0.2486	0.0045	0.02	46.4	91.3	103	0.886	1724	14.7	1735	20.7	1749	48	99	
PB -59	82.1	4.485	0.1125	0.309	0.0027	0.96	3.2363	0.0282	0.1053	0.0029	0.1929	0.0162	0.43	61.8	115.1	144.2	0.798	1736	13.4	1728	22.2	1719	50.1	100	
PB -59	55.1	5.7783	0.1371	0.3486	0.0041	0.82	2.8682	0.0338	0.1202	0.0027	0.2431	0.0048	0.48	66.5	174.7	133.5	1.308	1928	19.6	1943	20.1	1959	40.3	99	
PB -59	47.1	5.8245	0.15	0.3489	0.0038	0.76	2.8661	0.0315	0.1211	0.0029	0.3713	0.0367	0.43	49.9	136.6	90.3	1.512	1929	18.3	1950	22.4	1972	43.3	98	
PB -59	77.1	5.932	0.1456	0.355	0.0031	0.52	2.817	0.0248	0.1212	0.003	0.2908	0.0167	0.23	55.9	113.3	105.4	1.075	1958	14.9	1966	21.4	1974	44	99	
PB -59	38.1	0.8451	0.1019	0.1005	0.0023	0.27	9.9467	0.2289	0.061	0.0079	0.3175	0.0244	1.84	6.4	45.3	44.5	1.018	617.5	13.5	622	56	638.1	283.5	99	
PB -59	24.1	0.7711	0.11	0.1035	0.0022	0.63	9.6641	0.2071	0.054	0.0082	0.3321	0.0358	4.27	7	52.3	46.7	1.119	634.7	12.9	580.4	60.7	373	297.2	109	
PB -59	66.1	0.8599	0.0948	0.1038	0.0026	0.26	9.6362	0.2398	0.0601	0.0076	0.1476	0.028	1.29	5.8	20	41.3	0.484	636.5	15.1	630	50.2	607	251.7	101	
PB -59	4.1	0.7402	0.0375	0.0949	0.0009	0.61	10.5339	0.1051	0.0565	0.003	0.2316	0.0077	0.18	23.5	120.9	176.5	0.685	584.6	5.6	562.5	21.3	473.9	110.2	103	
PB -59	56.1	0.8011	0.0421	0.0962	0.0015	0.62	10.3926	0.1636	0.0604	0.0033	0.1069	0.0108	1	14.6	42.6	115	0.371	592.2	8.9	597.4	23.4	617.3	117.1	99	
PB -59	93.1	0.7848	0.0373	0.0963	0.0011	0.71	10.3819	0.121	0.0591	0.0029	0.153	0.0084	0.96	23.7	107.5	199	0.54	592.8	6.6	588.2	20.8	570.4	106.7	100	
PB -59	6.1	0.8273	0.0516	0.0968	0.0012	0.31	10.3264	0.1243	0.062	0.0041	0.0913	0.0134	1.89	12.8	27.6	108.3	0.255	595.9	6.9	612.1	28.5	672.6	141	97	
PB -59	27.1	0.8445	0.0245	0.0981	0.0008	0.04	10.1979	0.0872	0.0625	0.0018	0.0292	0.005	0.08	36.3	19.1	317.2	0.06	603	4.9	621.6	13.6	689.9	64.5	97	
PB -59	72.1	0.7908	0.0407	0.0993	0.0014	0.57	10.0721	0.1382	0.0578	0.0032	0.1779	0.0181	3.48	16.3	85.9	126.2	0.681	610.2	8	591.6	23	521	118.2	103	
PB -59	7.1	0.7931	0.0506	0.0994	0.0012	0.71	10.0577	0.1187	0.0579	0.0038	0.11	0.0171	0.74	16.3	42.3	130.5	0.325	611	6.9	592.9	28.3	524.2	143.8	103	
PB -59	13.1	0.9815	0.1521	0.1025	0.0029	0.61	9.7578	0.2773	0.0695	0.0119	0.3815	0.0511	2.6	5.2	33.3	33.7	0.986	628.9	17	694.4	82.4	912.4	348.2	90	
PB -59	16.1	0.8727	0.1779	0.0981	0.0033	0.57	10.1915	0.341	0.0645	0.0138	0.4479	0.0312	0.48	6.7	45.7	43.1	1.061	603.4	19.2	637.1	93.4	758.4	420.3	94	
PB -59	8.1	0.7064	0.075	0.0932	0.0016	0.62	10.7323	0.1788	0.055	0.0063	0.5508	0.0221	0.32	11.6	96.3	67.8	1.419	574.3	9.1	542.6	44.3	411.7	234.9	105	
PB -59	39.1	1.0605	0.0345	0.1202	0.0013	0.25	8.3172	0.0874	0.064	0.002	0.2424	0.0075	0.51	37.2	209.4	227.1	0.922	731.9	7.3	734	16.9	740.6	65.6	99	
PB -59	67.1	1.1192	0.0889	0.1207	0.0025	0.52	8.2869	0.1711	0.0673	0.006	0.5037	0.0347	0.77	12.9	102.8	64.5	1.595	734.4	14.3	762.6	40.2	846	170.6	96	
PB -59	87.1	1.1127	0.1075	0.1311	0.0023	0.19	7.6283	0.1367	0.0616	0.0065	0.169	0.0316	3.69	11.2	30.1	66.6	0.452	794.1	13.4	759.5	49.5	658.9	195.9	104	
PB -59	78.1	1.1828	0.0652	0.1314	0.0018	0.01	7.6101	0.1022	0.0653	0.0038	0.1417	0.0097	0.9	13.6	38.7	81.1	0.478	795.9	10	792.6	30.4	783.5	127.1	100	
PB -59	73.1	1.272	0.0771	0.1366	0.002	0.72	7.3219	0.1078	0.0675	0.0046	0.2027	0.0199	0.42	12.5	46.1	64.6	0.713	825.3	11.5	833.3	35.4	854.6	141.2	99	
PB -59	14.1	6.3419	0.1964	0.3611	0.0037	0.74	2.769	0.0285	0.1274	0.004	0.2626	0.0133	0.38	44.6	60	84.9	0.706	1988	17.5	2024	27	2062	54.7	98	
PB -59	34.1	6.1165	0.1825	0.3638	0.004	0.58	2.7488	0.0302	0.1219	0.0038	0.5548	0.0227	0.67	25	78.9	39.3	2.009	2000	18.8	1993	25.6	1985	55.8	100	
PB -59	35.1	6.3152	0.1292	0.3682	0.0027	0.79	2.7161	0.0196	0.1244	0.0025	0.0447	0.015	0.5	56.6	23.4	132.5	0.177	2021	12.6	2021	18.2	2020	36.5	100	
PB -59	83.1	6.8098	0.1789	0.3694	0.0036	0.88	2.7072	0.0263	0.1337	0.0036	0.1265	0.0167	0.22	50.8	61.2	110.2	0.556	2027	16.8	2087	23.2	2147	46.5	97	
PB -59	10.1	6.7101	0.2785	0.381	0.0049	0.77	2.6246	0.0339	0.1277	0.0056	0.3706	0.0136	1.62	16.1	38.7	27.1	1.427	2081	23	2074	35.7	2067	76.1	100	
PB -59	31.1	6.3832	0.2072	0.3827	0.0046	0.25	2.6128	0.0313	0.121	0.0042	0.4679	0.0127	0.06	29.2	72.2	47.2	1.528	2089	21.4	2030	27.9	1970	61	102	
PB -59	41.1	6.554	0.1295	0.3828	0.0035	0.55	2.6124	0.0242	0.1242	0.0022	0.3581	0.0089	1.37	79.7	187.3	127.4	1.47	2089	16.5	2053	18.1	2017	32.3	101	
PB -59	68.1	7.1163	0.246	0.3837	0.0058	0.17	2.6063	0.0395	0.1345	0.0051	0.1813	0.0074	0.23	16.2	17.8	29.8	0.599	2094	27	2126	30.5	2158	66.9	98	
PB -59	57.1	6.9696	0.1763	0.3873	0.0049	0.33	2.5822	0.0325	0.1305	0.0033	0.1483	0.0064	0.17	42.3	40.6	78.5	0.517	2110	22.6	2108	22	2105	43	100	
PB -59	58.1	6.9918	0.1449	0.3976	0.0043	0.64	2.5149	0.0271	0.1275	0.0025	0.1205	0.0023	0.3	93.1	87.6	177.8	0.493	2158	19.8	2110	18.4	2064	34.8	102	
PB -59	96.1	7.4628	0.1927	0.399	0.0043	0.86	2.5064	0.0268	0.1357	0.0037	0.17	0.0127	0.87	35.3	34.3	63.5	0.54	2164	19.7	2169	23.2	2173	47.3	99	
PB -59	44.1	5.0618	0.125	0.3221	0.0034	0.07	3.1046	0.0325	0.114	0.0026	0.1081	0.0051	0.68	44.5	61.8	106.4	0.581	1800	16.4	1830	20.9	1864	41.4	98	
PB -59	17.1	5.2921	0.1382	0.3349	0.0029	0.09	2.9861	0.0258	0.1146	0.0029	0.1055	0.0031	0.44	53.9	33.9	122.2	0.277	1862	13.9	1868	22.3	1874	46.6	99	

PB -59	9.1	6.0849	0.1778	0.3448	0.0032	0.01	2.8999	0.0272	0.128	0.0039	0.3073	0.0059	0.74	32.4	59.6	62.4	0.955	1910	15.5	1988	25.4	2070	53.1	96	
PB -59	59.1	5.3182	0.125	0.3449	0.004	0.88	2.8996	0.0337	0.1118	0.0026	0.2057	0.0139	0.78	55.1	90.1	117.7	0.765	1910	19.2	1872	20.5	1830	42.7	102	
PB -59	37.1	6.6493	0.1865	0.4045	0.0048	0.97	2.4721	0.0292	0.1192	0.0032	0.7932	0.0909	0.6	58.5	320.3	82.3	3.891	2190	21.8	2066	24.8	1945	47.4	105	
PB -59	94.1	5.3045	0.1074	0.3153	0.0029	0.99	3.1712	0.0288	0.122	0.0023	0.0999	0.0263	0.81	172	192.6	326.2	0.59	1767	13.7	1870	16	1986	33.9	94	
PB -59	91.1	4.6428	0.0965	0.3181	0.0028	0.79	3.1438	0.0272	0.1059	0.0023	0.3339	0.0486	0	145	457.9	281.4	1.627	1780	13.5	1757	17.5	1729	39.9	101	
PB -59	64.1	1.3874	0.0589	0.1458	0.0019	0.66	6.8594	0.091	0.069	0.0031	0.1483	0.0101	0.33	29.1	83.9	155.1	0.541	877.3	10.9	883.6	25.1	899.4	94.9	99	
PB -59	53.1	2.0671	0.1251	0.1959	0.0038	0.3	5.104	0.099	0.0765	0.0052	0.2413	0.0127	1.6	11.4	35.2	39.9	0.881	1153	20.5	1138	41.4	1109	131.1	101	
PB -59	74.1	2.6537	0.0651	0.2254	0.0018	0.01	4.4364	0.0359	0.0854	0.0021	0.1045	0.0026	0.05	67.5	80.4	236.9	0.339	1310	9.6	1316	18.1	1324	47.4	99	
PB -59	95.1	3.4114	0.0892	0.2584	0.0025	0.96	3.8695	0.038	0.0957	0.0027	0.1433	0.0053	0.21	64	78.9	167.9	0.47	1482	12.9	1507	20.5	1543	52.1	98	
PB -59	36.1	3.2698	0.0749	0.2642	0.002	0.87	3.7856	0.0289	0.0898	0.002	0.3628	0.02	0.79	83.4	245.2	213.2	1.15	1511	10.3	1474	17.7	1421	42.7	102	
PB -59	62.1	3.7796	0.2159	0.2783	0.0058	0.38	3.5938	0.0744	0.0985	0.0064	0.1805	0.022	3.35	8.8	13.8	23.9	0.577	1583	29	1588	46.5	1596	126.4	99	
PB -59	22.1	4.0141	0.1369	0.2973	0.0031	0.81	3.363	0.0349	0.0979	0.0033	0.269	0.0252	0.23	54	144.7	122.4	1.182	1678	15.2	1637	27.6	1585	64.5	102	
PB -59	25.1	0.3022	0.0319	0.0405	0.0009	0.69	24.7082	0.5504	0.0541	0.0066	0.5018	0.0296	2.19	7.2	148.7	113.8	1.306	255.8	5.6	268.1	25.4	377.3	231.6	95	
PB -59	33.1	0.3539	0.0187	0.0459	0.0006	0.47	21.7817	0.2772	0.0559	0.0032	0.2192	0.0189	1.36	16.1	217	269.8	0.804	289.4	3.6	307.6	14	448.7	131.3	94	
PB -59	86.1	0.4348	0.0291	0.0565	0.0008	0.24	17.7105	0.2424	0.0558	0.0041	0.1857	0.0203	0.94	14.3	152.5	188	0.811	354.1	4.7	366.6	21.2	446.2	167.5	96	
PB -59	2.1	10.4882	0.2373	0.45	0.0034	0.91	2.2221	0.017	0.169	0.0037	0.1388	0.003	0.09	56.8	41.7	94.5	0.441	2395	15.3	2479	20.5	2548	35.4	96	
PB -59	63.1	10.8762	0.2173	0.4547	0.004	0.29	2.1991	0.0195	0.1735	0.0035	0.1194	0.0038	0.32	55.7	42.6	85.4	0.498	2416	17.9	2513	18.8	2591	34	96	
PB -59	60.1	13.2828	0.2589	0.5547	0.0059	0.63	1.8027	0.0192	0.1737	0.0031	0.1377	0.0027	0.46	91.5	75.7	125.1	0.605	2845	24.5	2700	18.3	2593	30.6	105	
PB -59	89.1	14.6631	0.2581	0.5582	0.0046	0.97	1.7914	0.0147	0.1905	0.0035	0.0573	0.0074	0.17	145	77.6	196.2	0.396	2859	19.1	2794	17.4	2747	30.8	102	
PB -59	43.1	0.3552	0.0432	0.0433	0.001	0.03	23.0861	0.5225	0.0595	0.0078	0.3384	0.0245	0.95	7.9	216.2	125.5	1.722	273.4	6.1	308.7	33.7	584.7	251.1	88	
PB -59	50.1	0.6729	0.0951	0.097	0.0026	0.28	10.3071	0.281	0.0503	0.0078	0.1426	0.0307	3.04	5.7	41.5	46.6	0.892	596.9	15.6	522.5	52.9	209	271.1	114	
PB -59	45.1	0.651	0.0248	0.0785	0.0008	0.99	12.7446	0.1298	0.0602	0.0031	0.1483	0.0519	9.19	29.6	420.9	294.7	1.428	487	4.8	509.1	17.4	609.9	109.6	95	
PB -59	75.1	0.6797	0.231	0.0961	0.005	0.46	10.4051	0.5418	0.0513	0.0186	0.3501	0.0792	11.53	2.1	19.3	15.9	1.213	591.6	29.4	526.6	134.4	254	487.4	112	
PB -59	40.1	0.8961	0.0594	0.1053	0.0016	0.67	9.4982	0.1476	0.0617	0.0042	0.1883	0.0221	7.34	12.2	108.3	93.4	1.159	645.3	9.5	649.7	31.5	664.8	149.3	99	
PB -59	28.1	6.0183	0.3951	0.3752	0.0093	0.17	2.665	0.0662	0.1163	0.0093	0.3518	0.033	37.5	6.1	21	10.4	2.024	2054	43.8	1979	55.1	1901	135.3	103	
PB -59	11.1	7.8875	0.3376	0.448	0.0062	0.79	2.2322	0.0308	0.1277	0.0058	0.207	0.012	7.66	12.2	29.1	21.1	1.38	2386	27.5	2218	38.8	2067	81.4	107	

ANEXO V – DADOS DIAGÊNESE

Sample	Total Points	Components (%)			Porosity (%)					Contacts (%)					
		Quartz	Feldspars	Lithics	Primary	Moldic	Intragranular	Total	IGV	Flot	Point	Linear	Concave-convex	Sutured	Total
RB-00	300	59.92	22.96	17.12	0	0	0.333333	0.33	22.0	0.4	19.3	48.8	26.2	5.4	100.0
RB-03	356	64.47	21.71	13.82	16.0	0.3	4.8	21.1	23.6	0.2	28.4	42.9	21.3	7.2	100.0
RB-06	303	65.20	25.11	9.69	4.6	1.0	5.6	11.2	31.7	1.3	31.5	30.6	30.0	6.7	100.0
RB-07	300	64.13	27.80	8.07	9.3	1.0	3.0	13.3	29.7	0.7	35.5	34.5	23.2	6.2	100.0
RB-11	303	56.60	36.60	6.81	3.6	0.0	0.3	4.0	15.2	0.0	15.9	17.6	44.9	21.7	100.0
RB-13	304	72.84	20.99	6.17	14.1	0.7	3.0	17.8	24.0	0.0	22.0	29.1	40.3	8.6	100.0
RB-20	300	68.97	22.84	8.19	14.3	1.3	2.3	18.0	26.3	0.2	23.6	36.5	29.6	10.1	100.0
RB-21	204	67.86	24.60	7.54	12.0	1.3	3.3	16.7	22.3	0.1	17.6	38.1	34.7	9.4	100.0
RB-33	204	66.26	21.95	11.79	0.7	0.7	0.0	1.3	21.3	0.6	32.4	36.8	25.7	4.4	100.0
RB-34	204	66.39	23.95	9.66	14.7	0.3	1.6	16.6	27.7	0.0	25.2	41.8	29.3	3.7	100.0
RB-45	300	68.75	23.75	7.50	10.2	0.7	3.3	14.2	25.7	0.1	17.5	44.4	36.7	1.3	100.0
RB-46	303	64.77	24.24	10.98	2.3	0.0	4.6	6.9	19.8	0.0	13.0	48.8	32.7	5.5	100.0
RB-48	300	66.22	27.56	6.22	7.8	0.3	1.6	9.8	26.5	0.2	16.2	47.0	34.4	2.3	100.0
RB-49	300	60.43	27.70	11.87	7.7	1.3	1.3	10.3	17.7	0.1	11.1	41.9	41.8	5.0	100.0
RB-55	300	62.10	21.34	16.56	7.6	0.3	2.7	10.6	14.0	0.0	5.3	33.7	33.3	27.7	100.0
RB-60	204	53.94	33.86	12.20	14.3	1.0	2.3	17.7	24.7	0.0	17.1	52.4	26.4	4.1	100.0
RB-63	321	78.22	16.00	5.78	4.0	2.2	1.2	7.5	30.5	1.3	18.3	66.0	14.3	0.0	100.0
RB-64	310	57.86	35.00	7.14	0.0	0.0	1.6	1.6	12.9	0.0	2.5	28.1	49.8	19.7	100.0
RB-65	300	65.38	25.38	9.23	14.0	1.0	1.7	16.7	19.0	0.3	7.6	46.6	44.6	0.8	100.0
RB-69	305	66.20	21.95	11.85	13.8	0.3	1.6	15.7	16.7	0.3	7.7	51.6	39.3	1.1	100.0
RB-71	312	67.62	23.84	8.54	10.9	0.3	1.6	12.8	17.6	0.0	4.6	52.7	34.3	8.4	100.0
Mean		64.83	25.26	9.91					22.3	0.3	17.7	41.4	33.0	7.6	100.0

Sample	Cements (Counts)										
	Zeolite	Quartz	Calcite	Smectite	Ilite	Albite	Chlorite	Iron Oxide	Gypsum	Dolomite	Total
RB-00	0	1	0	0	0	0	5	3	0	56	65
RB-03	0	0	2	5	0	0	0	2	0	0	9
RB-06	0	0	0	6	0	0	0	0	0	56	62
RB-07	0	0	36	11	0	2	0	0	0	0	49
RB-11	0	24	0	7	0	0	1	2	0	0	34
RB-13	0	0	0	19	0	0	0	0	0	0	19
RB-20	0	0	19	5	0	0	0	1	0	0	25
RB-21	0	0	0	16	0	0	0	1	0	0	17
RB-33	0	0	0	0	0	0	60	0	0	0	60
RB-34	1	0	29	4	0	0	0	0	0	0	34
RB-45	6	0	22	5	0	0	0	0	2	0	35
RB-46	0	1	35	3	0	0	0	0	0	0	39
RB-48	0	24	19	8	0	0	0	0	0	0	51
RB-49	0	3	6	12	0	1	0	0	0	0	22
RB-55	0	4	0	5	0	0	0	1	0	0	10
RB-60	0	1	2	15	0	1	0	2	0	0	21
RB-63	26	5	43	0	0	0	0	0	0	0	74
RB-64	0	5	24	0	0	0	0	2	0	4	35
RB-65	0	3	2	0	0	1	0	1	0	0	7
RB-69	0	0	0	0	0	3	0	0	0	0	3
RB-71	3	0	4	0	0	7	0	0	1	0	15

Grain-size (%)						
Silt	Very fine sand	Fine sand	medium sand	coarse sand	very coarse sand	Sorting
10.14	16.22	27.03	24.32	18.24	4.05	1.65
4.11	8.90	21.92	28.08	33.56	3.42	1.20
8.63	16.55	13.67	39.57	18.71	2.88	1.56
9.15	23.24	30.99	27.46	7.75	1.41	1.42
3.75	9.38	32.50	46.25	8.13	0.00	0.93
3.27	32.03	41.83	16.34	6.54	0.00	0.98
2.80	15.38	13.29	31.47	32.87	4.20	1.27
9.62	29.49	30.77	28.21	1.92	0.00	1.30
16.88	27.27	11.04	14.94	29.87	0.00	1.92
8.16	24.49	17.01	21.09	27.89	1.36	1.61
3.29	29.61	42.76	15.79	8.55	0.00	1.03
4.52	22.58	32.26	30.32	10.32	0.00	1.10
4.26	45.39	24.11	16.31	9.93	0.00	1.12
7.41	33.95	17.90	20.37	19.14	1.23	1.51
1.14	3.43	11.43	13.71	68.00	2.29	0.89
0.65	5.81	20.65	51.61	19.35	1.94	0.92
2.19	5.84	28.47	32.12	31.39	0.00	1.06
5.23	11.63	47.09	34.88	1.16	0.00	0.88
3.75	11.25	51.25	28.75	5.00	0.00	0.84
1.16	1.16	9.30	41.86	46.51	0.00	0.78
1.20	2.41	16.87	32.53	45.78	1.20	0.92

ANEXO VI - DADOS PETROFÍSICA

Sample	Well-core	Depth (m)	Ultrasonic acoustic velocity																	
			Heigh (mm)											P-wave arrival time			S-wave arrival time		P-wave velocity (kms^{-1})	S-wave velocity (kms^{-1})
			1	2	3	4	5	6	7	8	9	10	Mean	Δt1	Δt2	Δt3	Δt1	Δt2		
RB 1	TG-27	1.25	25.98	26.86	25.70	26.56	25.46	25.93	26.62	25.28	26.45	26.48	26.13	4.78	4.68		7.38	7.33	5.52	3.55
RB 2		1.9	44.92	44.93	45.04	44.94	44.78	44.80	44.88	44.92	45.03	44.89	44.91	13.63	13.93		18.63	18.83	3.26	2.40
RB 3		2.9	44.04	43.49	43.50	42.96	42.76	43.45	43.58	43.44	43.56	43.71	43.45	13.53	12.73		15.93	15.63	3.31	2.75
RB 4		3.9	47.45	46.67	46.45	46.14	46.52	47.06	47.43	48.79	47.82	47.68	47.2	13.68	13.73		16.23	16.93	3.44	2.85
RB 5		4.9	45.59	45.43	45.28	45.34	45.30	45.24	45.20	45.25	45.28	45.36	45.33	13.48	12.58		14.23	14.23	3.48	3.19
RB 0		51	46.04	45.92	45.61	45.21	45.32	46.06	45.98	46.02	45.97	44.95	45.71	10.57	10.53		12.93	13.23	4.33	3.49
RB 6		97.2	66.27	66.45	66.88	66.22	66.24	66.12	66.27	66.20	66.38	66.30	66.33	14.38	14.38		22.43	21.03	4.61	3.05
RB 7		97.7	48.28	48.54	48.38	48.14	48.00	48.35	48.34	48.31	48.27	48.01	48.26	18.13	16.08	15.39	23.03	20.63	3.07	2.21
RB 8		98.3	39.79	40.02	39.80	39.68	39.82	39.68	39.92	39.88	39.67	39.84	39.81	17.13	15.33		23.83	24.23	2.45	1.66
RB 9		98.55	47.79	47.75	47.87	47.40	47.54	47.77	47.73	47.07	47.53	47.73	47.62	18.58	14.13	16.08	18.73	17.33	3.15	2.64
RB 10		99	52.47	51.84	52.36	52.15	52.23	51.95	51.98	51.92	52.45	52.35	52.17	8.33	16.43	17.43	24.23	26.63	3.08	2.05
RB 11	TG-100	223	44.78	44.73	44.82	44.88	45.62	44.86	44.95	44.82	44.79	44.68	44.89	9.43	9.23		11.23	11.68	4.81	3.92
RB 12		223.5	51.78	51.72	51.89	51.72	51.76	51.99	51.81	52.22	51.68	52.03	51.86	14.03	14.13		20.43	20.33	3.68	2.54
RB 13		224.5	47.66	47.47	47.10	46.98	47.03	47.21	47.19	47.80	47.61	47.08	47.31	15.03	14.53		19.33	18.73	3.20	2.49
RB 14		228.5	50.44	50.11	50.38	50.62	50.22	49.98	50.52	49.89	50.55	50.11	50.28	14.63	16.63	14.33	17.63	17.33	3.47	2.88
RB 15		232.4	39.59	39.46	39.21	39.46	39.45	39.41	39.05	39.50	39.42	39.63	39.42	14.23	12.53		17.83	18.13	2.95	2.19
RB 16		236.4	50.84	50.63	50.90	50.86	50.72	51.33	51.27	51.19	50.88	51.14	50.98	16.73	16.13		19.53	20.98	3.10	2.52
RB 17		240.4	41.66	40.27	41.99	41.88	42.07	42.09	41.89	41.51	41.95	41.66	41.7	15.43	12.73		17.63	18.33	2.96	2.32
RB 18		246.25	47.34	47.20	47.64	47.25	47.01	47.43	47.40	47.11	47.08	47.52	47.3	14.98	14.63		22.23	24.03	3.19	2.04
RB 19		252.6	30.77	30.51	29.92	29.11	29.67	30.85	29.93	30.04	30.74	30.84	30.24	8.93	9.55		13.13	12.63	3.27	2.35
RB 20		259.5	48.92	48.57	48.72	49.08	48.90	48.75	48.83	48.82	49.14	48.99	48.87	12.68	12.63		17.43	15.53	3.86	2.97
RB 21		268.5	33.70	33.34	33.38	33.95	33.65	33.03	33.11	33.08	33.48	33.84	33.46	10.73	9.93		14.93	14.63	3.24	2.26
RB 22		277.95	38.07	38.12	37.93	38.05	37.97	38.13	38.17	38.04	37.75	38.03	38.03	12.78	12.13		17.13	17.03	3.05	2.23
RB 23		286.7	46.93	46.92	46.85	46.88	46.79	46.44	46.63	46.52	46.72	46.89	46.76	16.03	14.88		17.03	17.23	3.03	2.73
RB 24		297.8	48.63	49.11	48.40	48.74	49.17	49.09	48.82	48.60	47.81	48.83	48.72	15.23	15.43		24.43	22.23	3.18	2.09
RB 25		305.1	39.34	39.56	39.42	39.79	39.51	39.42	39.77	39.88	39.78	39.61	39.61	13.68	11.73	12.13	18.33	16.33	3.32	2.29
RB 26		312.8	50.64	50.28	50.57	50.23	50.24	50.43	50.30	50.25	50.15	50.21	50.33	17.13	16.33		20.03	17.03	3.01	2.72
RB 27		316.85	49.58	48.64	49.72	48.68	48.65	49.09	49.39	49.25	49.01	49.07	49.11	16.83	16.18		24.03	24.83	2.98	2.01
RB 28		286.35	51.50	51.46	51.54	51.27	51.26	51.04	51.68	51.12	51.37	51.41	51.37	21.53	17.93	16.45	23.32	23.23	2.99	2.21

RB 29		284.35	48.63	49.03	48.83	48.47	48.91	48.81	48.75	48.70	48.74	48.96	48.78	16.48	15.73		20.23	20.63	3.03	2.39
RB 30		281.9	51.34	51.61	51.47	51.91	51.37	51.35	51.28	51.35	51.19	51.50	51.44	17.23	15.28	15.68	19.73	19.43	3.32	2.63
RB 31		281	44.36	44.40	43.72	44.18	44.22	44.44	44.03	44.42	44.22	44.30	44.23	13.88	14.08		18.43	19.93	3.16	2.31
RB 32		280.1	47.10	47.23	47.22	47.42	47.28	47.13	46.84	46.56	46.48	46.60	46.99	11.18	11.31		13.33	13.23	4.18	3.54
RB 33		275.15	48.94	48.74	48.61	48.59	48.60	49.02	48.87	49.07	48.63	48.72	48.78	10.23	10.11		14.63	14.73	4.80	3.32
RB 34		274.5	47.71	47.51	47.61	47.72	47.64	47.93	47.90	47.68	47.42	47.51	47.66	13.23	12.83		15.33	15.93	3.66	3.05
RB 35		273.7	46.34	46.07	46.90	46.29	46.25	46.42	46.57	46.22	46.16	45.96	46.32	20.63	15.93	15.93	21.13	20.53	2.91	2.22
RB 36		272.3	45.93	46.20	46.04	46.11	46.01	45.96	45.74	45.68	45.63	46.06	45.94	19.03	16.68	15.88	18.33	20.58	2.82	2.36
RB 37	TG-179	268.1	48.55	49.23	48.63	48.58	48.67	49.08	49.26	48.25	49.27	48.33	48.79	20.93	15.63	16.38	23.03	20.43	3.05	2.24
RB 38		265.2	49.99	49.80	49.86	49.43	49.47	49.37	49.68	49.48	49.66	49.91	49.67	17.23	15.98		18.13	20.03	2.99	2.60
RB 39		262.6	50.60	50.65	50.48	50.85	50.57	50.52	50.99	50.83	51.28	50.74	50.75	21.23	15.68	16.03	17.83	19.73	3.20	2.70
RB 40		258.1	49.10	49.49	50.56	50.79	50.90	50.57	50.31	49.30	49.35	49.03	49.94	20.23	16.43	16.58	20.93	21.68	2.71	2.34
RB 41		253.2	49.97	50.46	50.40	49.94	50.12	49.94	49.97	50.04	50.00	50.41	50.13	15.33	14.48		17.78	18.28	3.36	2.78
RB 42		250.2	48.64	48.62	48.47	48.73	48.45	48.47	48.39	48.64	48.51	48.49	48.54	16.63	14.83		18.13	18.53	3.09	2.65
RB 43		247.05	45.87	46.00	46.24	46.58	45.91	46.06	46.09	46.32	45.85	46.02	46.09	15.73	14.08		16.53	17.93	3.09	2.68
RB 44		242.45	44.52	44.91	44.68	44.70	44.51	44.63	44.46	44.61	44.55	44.91	44.65	14.03	12.48		16.03	15.73	3.37	2.81
RB 45		241.25	46.62	46.11	46.04	46.05	46.24	45.25	46.12	46.21	45.81	46.14	46.06	15.63	13.93		19.63	19.03	3.12	2.38
RB 46		237.2	47.39	47.72	47.81	47.49	47.30	47.75	47.23	47.62	47.77	47.88	47.6	10.53	10.39		14.33	14.93	4.55	3.25
RB 47		298.15	50.18	49.14	49.52	49.46	49.60	49.80	49.24	49.28	49.13	49.29	49.46	18.63	13.93	14.11	19.43	18.13	3.53	2.63
RB 48		298.4	46.13	46.03	46.17	46.27	45.94	45.95	46.28	45.91	46.28	46.39	46.14	10.03	10.09		14.63	14.83	4.59	3.13
RB 49		299.4	40.29	39.85	40.68	40.25	39.79	40.33	40.94	40.85	40.14	40.31	40.34	9.48	9.43		15.33	14.03	4.27	2.75
RB 50		300.85	46.70	46.15	46.60	47.06	46.98	46.68	46.52	46.55	46.54	46.99	46.68	12.28	11.68		15.13	16.03	3.90	3.00
RB 51		302.15	47.14	47.02	47.15	46.81	46.96	46.70	47.26	47.03	47.07	47.01	47.02	12.57	11.73		13.93	13.53	3.87	3.42
RB 52		305.05	47.01	46.78	46.76	46.41	46.62	46.70	47.13	46.95	46.92	47.00	46.83	13.23	12.03		16.63	14.83	3.71	2.98
RB 53		308.6	48.53	48.46	48.48	48.73	48.54	48.84	48.61	48.72	48.35	48.80	48.61	14.63	14.03		17.13	15.73	3.39	2.96
RB 54	TG-227	312.5	46.77	46.78	46.63	46.85	46.58	46.71	46.86	46.87	46.59	46.80	46.74	12.28	11.73		16.53	14.33	3.89	3.03
RB 55		317.1	46.26	46.22	46.83	46.87	47.12	46.89	46.36	46.54	46.49	46.45	46.6	11.48	11.13		13.63	13.73	4.12	3.41
RB 56		319.4	47.83	47.79	47.95	47.92	48.01	47.84	47.54	47.84	47.87	47.77	47.84	11.48	10.85		16.83	1.83	4.28	5.13
RB 57		325.2	41.32	41.34	41.27	41.10	41.29	41.35	41.14	41.24	41.23	41.12	41.24	11.53	10.83		17.33	16.33	3.69	2.45
RB 58		331.65	47.54	47.33	47.57	47.43	47.08	47.96	47.90	47.55	47.70	47.45	47.55	12.88	12.53		16.93	16.63	3.74	2.83
RB 59		335.85	47.84	48.61	48.72	48.32	48.57	47.75	48.66	48.64	48.02	48.57	48.37	13.18	13.33		16.83	17.53	3.65	2.82
RB 60		340.3	47.64	47.76	47.79	47.75	47.88	47.87	47.67	47.94	47.66	47.85	47.78	14.73	13.78		24.43	22.43	3.35	2.04
RB 61			16.49	16.05	16.49	16.60	15.55	17.27	16.69	16.38	15.85	15.75	16.31	7.78	6.35				2.31	

RB 62	CBM-100UF		43.89	43.55	43.17	43.88	43.54	43.96	43.97	43.89	43.04	43.84	43.67	27.93	23.13				1.71	
RB 63			34.40	35.41	35.40	34.81	34.32	33.31	33.08	33.70	34.17	34.45	34.31	19.13	16.53	16.28			2.09	
RB 64			51.43	51.76	51.89	51.91	52.32	52.05	52.41	52.74	52.27	51.70	52.05	10.93	10.03		15.83	14.83	4.97	3.39
RB 65			34.49	34.54	33.42	32.95	31.30	31.98	33.95	34.84	35.02	33.16	33.57	8.63	8.78		11.53	11.33	3.86	2.94
RB 66			36.68	36.51	36.21	36.61	36.62	36.74	36.93	36.74	36.83	36.46	36.63	10.39	9.03		14.33	14.83	3.77	2.51
RB 67			44.56	43.80	42.54	44.26	43.52	42.96	42.64	43.32	44.43	42.74	43.48	11.78	11.07		13.73	13.33	3.81	3.21
RB 68			56.25	56.95	57.82	59.36	59.42	59.06	57.39	57.07	56.53	56.33	57.62	16.33	15.48		18.23	18.13	3.62	3.17
RB 69			28.72	28.54	28.58	28.85	28.94	28.84	28.21	28.38	28.09	27.90	28.51	9.28	7.18		11.53	11.43	3.46	2.48
RB 70			44.29	41.78	44.02	43.10	43.33	41.20	44.18	41.27	44.31	44.45	43.19	10.73	10.09		14.23	13.83	4.15	3.08
RB 71			34.55	34.44	34.79	35.01	35.80	36.32	36.57	35.89	35.20	34.77	35.33	8.48	8.83		11.03	12.63	4.08	2.99

Sample	Well-core	Depth (m)	Porosity Experiment						
			Dry mass (g)	Submerged mass (g)	Satured masss (g)	Bulk volume	Pore volume	Porosity	Density
RB 1	TG-27	1.25	50.45	29.35	50.50	21.15	0.05	0.24	2.39
RB 2		1.9	52.10	31.81	55.33	23.52	3.23	13.73	2.22
RB 3		2.9	35.26	26.50	37.76	11.26	2.50	22.20	3.13
RB 4		3.9	54.56	34.03	58.86	24.83	4.30	17.32	2.20
RB 5		4.9	56.21	35.50	59.39	23.89	3.18	13.31	2.35
RB 0		51	61.55	37.05	62.14	25.09	0.59	2.35	2.45
RB 6		97.2	51.81	31.66	53.45	21.79	1.64	7.53	2.38
RB 7		97.7	28.47	15.29	30.03	14.74	1.56	10.58	1.93
RB 8		98.3	29.42	18.39	29.74	11.35	0.32	2.82	2.59
RB 9		98.55	27.92	16.25	28.58	12.33	0.66	5.35	2.26
RB 10		99	29.69	19.55	31.67	12.12	1.98	16.34	2.45
RB 11	TG-100	223	44.35	23.19	44.76	21.57	0.41	1.90	2.06
RB 12		223.5	45.48	23.80	46.23	22.43	0.75	3.34	2.03
RB 13		224.5	37.28	22.97	39.70	16.73	2.42	14.47	2.23
RB 14		228.5	42.09	26.73	43.75	17.02	1.66	9.75	2.47
RB 15		232.4	34.30	18.54	35.33	16.79	1.03	6.13	2.04
RB 16		236.4	43.97	26.10	45.30	19.20	1.33	6.93	2.29
RB 17		240.4	30.63	16.71	32.16	15.45	1.53	9.90	1.98
RB 18		246.25	39.80	23.05	41.89	18.84	2.09	11.09	2.11
RB 19		252.6	27.88	15.55	29.37	13.82	1.49	10.78	2.02
RB 20		259.5	58.79	35.90	62.06	26.16	3.27	12.50	2.25
RB 21		268.5	30.18	17.39	30.83	13.44	0.65	4.84	2.25
RB 22		277.95	34.21	22.51	34.55	12.04	0.34	2.82	2.84
RB 23		286.7	35.85	22.99	36.56	13.57	0.71	5.23	2.64
RB 24		297.8	43.05	25.72	43.97	18.25	0.92	5.04	2.36
RB 25		305.1	35.74	21.95	37.53	15.58	1.79	11.49	2.29
RB 26		312.8	38.88	23.63	40.38	16.75	1.50	8.96	2.32
RB 27		316.85	37.82	21.27	38.67	17.40	0.85	4.89	2.17
RB 28		286.35	44.79	28.27	47.93	19.66	3.14	15.97	2.28

RB 29		284.35	44.60	24.81	47.20	22.39	2.60	11.61	1.99
RB 30		281.9	51.85	28.71	54.54	25.83	2.69	10.41	2.01
RB 31		281	40.12	20.11	40.22	20.11	0.10	0.50	2.00
RB 32		280.1	48.15	28.25	48.14	19.89	-0.01	0.00	2.42
RB 33		275.15	47.64	30.31	47.42	17.11	-0.22	0.00	2.78
RB 34		274.5	42.41	27.40	44.58	17.18	2.17	12.63	2.47
RB 35		273.7	42.75	26.66	44.51	17.85	1.76	9.86	2.39
RB 36		272.3	42.20	22.18	44.38	22.20	2.18	9.82	1.90
RB 37	TG-179	268.1	44.13	27.47	46.27	18.80	2.14	11.38	2.35
RB 38		265.2	45.15	27.11	46.24	19.13	1.09	5.70	2.36
RB 39		262.6	41.98	24.38	43.33	18.95	1.35	7.12	2.22
RB 40		258.1	45.55	27.60	48.67	21.07	3.12	14.81	2.16
RB 41		253.2	42.67	24.10	45.16	21.06	2.49	11.82	2.03
RB 42		250.2	42.82	26.85	44.75	17.90	1.93	10.78	2.39
RB 43		247.05	38.50	27.26	40.04	12.78	1.54	12.05	3.01
RB 44		242.45	36.38	19.78	38.49	18.71	2.11	11.28	1.94
RB 45		241.25	40.37	25.07	43.53	18.46	3.16	17.12	2.19
RB 46		237.2	43.54	21.79	43.38	21.59	-0.16	-0.74	2.02
RB 47		298.15	42.10	23.62	43.30	19.68	1.20	6.10	2.14
RB 48		298.4	44.24	25.74	47.33	21.59	3.09	14.31	2.05
RB 49		299.4	38.30	22.35	39.20	16.85	0.90	5.34	2.27
RB 50		300.85	40.06	25.02	43.00	17.98	2.94	16.35	2.23
RB 51		302.15	42.16	26.25	44.04	17.79	1.88	10.57	2.37
RB 52		305.05	39.30	24.74	41.03	16.29	1.73	10.62	2.41
RB 53	TG-227	308.6	39.73	24.69	42.62	17.93	2.89	16.12	2.22
RB 54		312.5	42.27	24.89	44.25	19.36	1.98	10.23	2.18
RB 55		317.1	42.23	26.27	42.16	15.89	-0.07	0.00	2.66
RB 56		319.4	40.35	26.10	41.97	15.87	1.62	10.21	2.54
RB 57		325.2	33.56	26.39	36.07	9.68	2.51	25.93	3.47
RB 58		331.65	40.18	23.15	42.01	18.86	1.83	9.70	2.13
RB 59		335.85	42.37	26.15	44.85	18.70	2.48	13.26	2.27
RB 60		340.3	46.08	28.79	49.51	20.72	3.43	16.55	2.22
RB 61									

RB 62	CBM-100UF								
RB 63									
RB 64			66.40	40.20	68.09	27.89	1.69	6.06	2.38
RB 65			36.42	21.95	38.26	16.31	1.84	11.28	2.23
RB 66			124.57	76.74	134.28	57.54	9.71	16.88	2.16
RB 67			157.28	89.95	165.70	75.75	8.42	11.12	2.08
RB 68			185.47	112.66	198.75	86.09	13.28	15.43	2.15
RB 69			31.30	17.36	33.55	16.19	2.25	13.90	1.93
RB 70			149.60	92.11	157.97	65.86	8.37	12.71	2.27
RB 71			131.68	77.95	138.79	60.84	7.11	11.69	2.16

ANEXO I

Título da Dissertação/Tese:

"*CONTROLES DE PROVENIÊNCIA E QUALIDADE DE RESERVATÓRIO DA FORMAÇÃO BOTUCATU, CRETÁCEO DA BACIA DO PARANÁ*"

Área de Concentração: Estratigrafia

Autor: **Gabriel Bertolini**

Orientadora: Profa. Dra. Juliana Charão Marques

Examinador: Prof. Dr. Marcus Vinicius Dorneles Remus

Data: 30 abril de 2020

Conceito: A (Excelente)

PARECER:

A tese de doutorado, apresentada na forma de três artigos científicos integrados, aborda um tema muito importante e de grande relevância cientifica: o deserto do Botucatu, sua proveniência e qualidade dos potenciais reservatórios. Importante destacar a vasta área geográfica de amostragem abrangida pela tese. Isto produz maior robustez a obra. O manuscrito possui boa redação está bem estruturado e as ilustrações são adequadas. Os três artigos são apresentados de forma elegante e estruturada e mostram objetividade nos problemas abordados e nas principais conclusões. Um dos pontos altos da tese consiste em ilustrações contendo mapas geológicos e diversos parâmetros sedimentológicos integrados de modo a sintetizar as principais conclusões dos artigos. Importante destacar que os sedimentos da unidade Botucatu apresentam predominância na fração areia fina > areia muito fina. Desta forma, julga-se importante estudar de forma integrada as duas frações (areia fina-areia muito fina) pois considera-se que as informações de proveniência, incluindo suíte de minerais pesados e suas relações e variações, seriam potencialmente mais completas. De qualquer forma, a escolha da fração areia-muito fina unicamente, não compromete as principais conclusões e o mérito da tese. A proposta da origem policíclica dos sedimentos do Botucatu está bem muito bem embasada. Isto fica demonstrado, especialmente pelos índices elevados do parâmetro ZTR, composição essencialmente quartzosa dos sedimentos analisados e idades dos zircões detríticos. Uma questão universal, que na verdade não é exclusiva e nem um problema da tese, diz respeito ao número de grãos de zircões detríticos analisados. Creio que poderia acrescentar um paragrafo discutindo e validando o número de grãos analisados e o possivel efeito disto no trend proposto na figura 6, pg. 100. Alguns pontos que podem melhorar a obra, envolvem a inclusão de diversas referencias bibliográficas de autores que abordaram estudos sedimentológicos e petrográficos, incluindo minerais pesados da unidade Botucatu (ex. Carvalho, 1954, Paraguassu, 1968, Wu & Caetano-

Chang, 1992, etc.). Importante também revisar a lista de referencias que possui citações fora da ordem alfabética e de formatação. Outro aspecto que considero necessário revisar, são pequenas, mas diversas correções na ortografia e pequenos erros de concordância em algumas frases. Assinalei estes pontos no manuscrito em pdf que está disponível para o autor. Algumas figuras merecem também pequena revisão, especialmente na legenda (ex.: Fig. 1 pg 88; Fig. 11 pg 113). Estas observações são pontos menores e não comprometem a alta qualidade da Tese. Considero esta tese uma obra importante, onde os resultados e conclusões trazem avanços científicos consideráveis, ampliando o conhecimento da proveniência e qualidade dos reservatórios da unidade Botucatu. **Finalizando, julgo a qualidade da Tese Excelente e atribuo nota A para a obra.**

Assinatura: Data: 30/04/2020

Ciente do Orientador:

Ciente do Aluno: